Novel Radiochemistry for Positron Emission Tomography Imaging

Osman Tack

A thesis submitted to the board of the faculty of Physical Sciences in partial fulfilment of the requirements for the degree of Doctor of Philosophy at the University of Oxford



St John's College Trinity Term 2020

Author's Declaration

The work presented in this thesis was conducted at the Chemistry Research Laboratory at the University of Oxford under the supervision of Professor Véronique Gouverneur, unless otherwise specified. All the work is my own, except where otherwise stated, and has not been submitted for any other degree at this or any other university.



Osman Tack

June 2020

Acknowledgements

First acknowledgements must go to my supervisor Veronique for giving me positions in her group for my Part II during my undergraduate studies, a summer project and a PhD. I thank her for financial support and for helping award a BBSRC studentship. She has passed on much wisdom and insight into the world of academic research and the minds of academics, for which I am truly grateful.

Many thanks go to Jan Passchier for being an exemplary supervisor during my collaboration at Invicro, London. As well as being a fountain of knowledge, I could not have asked for a more friendly and caring supervisor. I am grateful to Giulia Boscutti for guiding me during my stay at Invicro, Christophe Plisson and Mickael Huiban for sharing their expertise, Sharon Ashworth for helping me through my first *in vivo* PET experiments, Prem Kubinski for being so friendly and knowledgeable about cyclotrons, Sac-Pham Tang and David Bonsall for sharing their expertise on biological experiments and finally Zhen Fan and the Invicro Boston imaging team for their help reconstructing my first PET image.

I am hugely grateful to the members of the VG group both past and present for making my time an enjoyable learning experience. I thank Lukas Pfeifer for being my unfailing guide in introducing me to many of the laboratory and psychological techniques needed to tackle working in an organic research lab. His friendliness and authoritative skills both personally and professionally have been inspirational. Thanks go to Tanatorn Khotavivattana for introducing me to projects to do with difluorocarbene and radiochemistry with such kind willingness, Tom Wilson for hilarious times in the hot lab and for the most invaluable contributions to the Langlois project from beginning to end, Florian Guibbal for helping to complete the final manuscript and for patiently sharing his invaluable knowledge on

automation and biological experiments, and Mateusz Imiołek for his help in dealing with proteins and MS/MS analysis. Thanks go to Michael Tilby and the Willis group for their advice in implementing amine-SO_2 adducts as sources of sulfur dioxide.

Huge thanks go to Francesco Ibba and Zijun Chen for being wonderful friends, Jeroen Sap for his humble kindness, amazing magic tricks and for keeping me company on night shifts, Paolo di Ricci for being an knowledgeable, funny and strong character, Giulia Roagna, Anna Chiara Vicini and Silvia Venturi for their unparalleled kindness and positivity, Janis Veliks, Gregor Cremosnik, Nicholas Taylor, and Enrico Emer for being so approachable and sharing their deep knowledge. Thank you Anna Spearing-Ewyn for reading my thesis and being a wonderful friend and Chemistry buddy during my entire time at Oxford.

Finally, thank you Razia for making me so happy and for all your love. Thank you to my parents for their unconditional love and support throughout my PhD and when writing my thesis at home. I hope to continue to make them proud.

Abstract:

Novel Radiochemistry for Positron Emission Tomography Imaging

This thesis describes the development of novel radiochemistry using fluorine-18 and its subsequent application in conducting Positron Emission Tomography (PET) imaging *in vivo*. Publication of this work: *J. Am. Chem. Soc.* **2020**, 142 (3), 1180 – 1185.

Chapter 1 introduces PET imaging and fluorine-18 radiochemistry, including an overview of the general considerations made in these areas. An extensive review of the library of radiolabelled fluorinating reagents available and the range of methods for radiolabelling peptides with fluorine-18 are described. The literature for synthesis and application of sodium trifluoromethanesulfinate, also known as the Langlois reagent, is also reviewed.

Chapter 2 describes the validation of a novel synthetic route for forming the Langlois reagent from sources of fluoride, difluorocarbene and sulfur dioxide. Successful synthesis of the Langlois reagent was achieved by employing potassium or caesium fluoride, a phase transfer catalyst, difluoromethylenephosphobetaine (PDFA), and DABCO-bis(sulfur dioxide) (DABSO) or a sulfur dioxide adduct of *N*-methylmorpholine (NMM-SO_2).

This chemical strategy was successfully translated into a radiochemical setting using [^{18}F]fluoride by extensive optimisation in stages. The identity of the [^{18}F]Langlois reagent was confirmed analytically and a procedure was developed for its purification and isolation. Processes and reaction conditions were subsequently re-optimised to develop an automated radiosynthesis and improve the molar activity.

Chapter 3 explores the application of the [^{18}F]Langlois reagent in labelling tyrosine and tryptophan amino acids and residues in unprotected peptides. In contrast to literature

methods that generally employ large excesses of Langlois reagent, new reaction conditions were developed for reacting the Langlois reagent in substoichiometric amounts. Key to this was the addition of stoichiometric amounts of metal salts, allowing successful radiochemical translation of the reaction. A number of dipeptides and biologically active peptides were labelled using this method including human insulin, the largest unmodified peptide to date that has been labelled directly with fluorine-18. The procedure for labelling tyrosine and tryptophan containing peptides was also automated.

An *in vitro* competition binding study, using the tryptophan-containing peptide octreotide, was used to demonstrate that installing the trifluoromethyl group directly onto the active site of a peptide does not have a large inhibiting effect on its activity. This led us to further investigate the practical utility of this automated radiosynthesis by carrying out an *in vivo* PET imaging study on naïve rats using octreotide labelled with fluorine-18. The activity and molar activity of the final dose were improved such that a coherent PET signal for the tracer could be observed in naïve rats. The pharmacokinetics of labelled octreotide were in agreement with literature analogues, however further studies and improvements to molar activity are required in order for this method to find use in oncological or neurological studies.

These results are proof of concept that labelling the Langlois reagent provides a new way of studying peptides using PET imaging, which may find applications in drug development or for diagnostic imaging in the future.

Abbreviations and Acronyms

α	alpha radioactive decay; alpha
Å	angstrom
$(aa)_n$	amino acid sequence
Ac	acetyl
AF	ammonium formate
aq.	aqueous
Au	absorbance unit
AY	activity yield
β+	positron; beta
BINAP	2,2′-bis(diphenylphosphino)-1,1′-binaphthalene
Bn	benzyl
Boc	*tert*-butyloxycarbonyl
bp	boiling point
Bq	becquerel
°C	degrees Celcius
c(RGDfC)	cyclo(-Arg-Gly-Asp-D-Phe-Cys)
c(RGDyK)	cyclo(-Arg-Gly-Asp-D-Tyr-Lys)
CT	computed tomography
Cy	cyclohexyl
δ	chemical shift (ppm)
Δ	heat
d	deuteron
DABCO	1,4-diazabicyclo[2.2.2]octane
DABSO	DABCO-bis(sulfur dioxide)
DAST	diethylaminosulfur trifluoride
Deoxo-Fluor	bis(2-methoxyethyl)aminosulfur trifluoride
DBN	1,5-diazabicyclo[4.3.0]non-5-ene
DBU	1,8-diazabicycloundec-7-ene
DCE	dichloroethane
DCM	dichloromethane

DIPEA	*N*,*N*-diisopropylethylamine
DMA	*N*,*N*-dimethylacetamide
DMAP	4-dimethylaminopyridine
DMF	*N*,*N*-dimethylformamide
DMI	1,3-dimethyl-2-imidazolidinone
DMPU	*N*,*N*′-dimethylpropyleneurea
DMSO	dimethylsulfoxide
DMTMM	4-(4,6-dimethoxy-1,3,5-triazin-2-yl)-4-methylmorpholinium chloride
DOPA	dihydroxyphenylalanine
DPEPhos	bis[(2-diphenylphosphino)phenyl] ether
DPPF	1,1′-bis(diphenylphosphino)ferrocene
DTT	dithiothreitol
e^-	electron
ee	enantiomeric excess
EI	electrospray ionization
equiv.	equivalent
ESF	ethenesulfonylfluoride
ESI	electrospray ionisation
Et	ethyl
eV	electron volts
FA	formic acid
FA01010	(4*R*,5*S*)-4-amino-5-methylheptanoic acid
FACPC	(*R*,*S*) anti-1-amino-2-fluorocyclopentyl-1-carboxylic acid
FBA	4-fluorobenzoic acid
FBABM	*N*-{4-[(4-fluorobenzylidene)aminooxy]butyl}maleimide
FDG	2-deoxy-2-fluoro-D-glucose
FMISO	fluoromisonidazole
FMOC	fluorenylmethoxycarbonyl
γ	gamma radioactive decay
g	gram
h	hour
HPLC	high performance liquid chromatography
HRMS	high-resolution mass spectroscopy

Hz	hertz
i-Pr	*iso*-propyl
IC_{50}	half maximal inhibitory concentration
IR	infrared spectroscopy
J	joule
J	scalar coupling constant
JohnPhos	(2-biphenyl)di-tert-butylphosphine
K_{222}	4,7,13,16,21,24-hexaoxa-1,10-diaza-bicyclo[8.8.8]-hexacosane
K_i	inhibitory constant
Kryptofix	4,7,13,16,21,24-hexaoxa-1,10-diaza-bicyclo[8.8.8]-hexacosane
L	litre
LC	liquid chromatography
LG	leaving group
LUMO	lowest unoccupied molecular orbital
m-	meta-
M	molar; metal
MA	molar activity
m-CPBA	*meta*-chloroperoxy-benzoic acid
Me	methyl
MeCN	acetonitrile
min	minute
mol	mole
M.P.	melting point
MRI	magnetic resonance imaging
MS	mass spectrometry
MTBD	7-methyl-1,5,7-triazabicyclo[4.4.0]dec-5-ene
MTBE	methyl *tert*-butyl ether
MTM	4-methylthiomorpholine 1,1-dioxide
m/*z*	mass-to-charge ratio
n	neutron
n	number of runs
NaDT	sodium decatungstate
Nap	napthyl

NFSi	*N*-fluorobenzenesulfonimide
NHC	*N*-heterocyclic carbine
NMM	*N*-methylmorpholine
NMM-SO_2	sulfur dioxide adduct of *N*-methylmorpholine
NMP	*N*-methyl-2-pyrrolidone
NMR	nuclear magnetic resonance
Nu	nucleophile
σ-	ortho-
Oxone	potassium peroxymonosulfate
ρ-	para-
p	proton
PBS	phosphate-buffered saline
PDFA	difluoromethylenephosphobetaine
PET	positron emission tomography
Ph	phenyl
PIDA	(diacetoxyiodo)benzene
PMP	1,2,2,6,6-pentamethylpiperidine
ppm	parts per million
PTC	phase transfer catalyst
PyFluor	2-pyridinesulfonyl fluoride
QMA	quaternary methyl ammonium
RCP	radiochemical purity
RCY	radiochemical yield
rt	room temperature
s	second
SAR	structure-activity relationship
salen	*N*,*N*'-ethylenebis(salicylimine)
Selectfluor I	1-chloromethyl-4-fluoro-1,4-diazoniabicyclo[2.2.2]octane bis(tetrafluoroborate)
Selectfluor II	1-Fluoro-4-methyl-1,4-diazoniabicyclo[2.2.2]octanebis(tetrafluoroborate)
SFB	*N*-succinimidyl-4-fluorobenzoate
SPhos	2-dicyclohexylphosphino-2′,6′-dimethoxybiphenyl
Sta	statine

Su	succinimide
SUV	standardised uptake value
Synfluor	*N*,*N*'-difluoro-2,2'-bipyridinium bis(tetrafluoroborate)
T	temperature
TBAF	tetrabutylammonium fluoride
$TBAHCO_3$	tetrabutylammonium bicarbonate
TBHP	*tert*-butyl hydroperoxide
t-Bu	*tert*-butyl
*t*BuBrettPhos	2-(di-tert-butylphosphino)-2′,4′,6′- triisopropyl-3,6-dimethoxy-1,1′-biphenyl
TMAF	tetramethylammonium fluoride
TMEDA	tetramethylethylenediamine
TMP	tetramesitylporphyrin
Tf	triflyl
Tf_2O	trifluoromethanesulfonic anhydride
TFA	trifluoroacetic acid
THF	tetrahydrofuran
TLC	thin layer chromatography
TMS	tetramethylsilyl
Tol	toluene
TPFPP	tetrakis(pentafluorophenyl)porphyrin
TREAT-HF	triethylamine trishydrofluoride
Ts	tosyl
UV	ultraviolet
ν	wavenumbers (cm^{-1})
V	volt
WAX	weak anion exchange
X	halogen
XantPhos	4,5-bis(diphenylphosphino)-9,9-dimethylxanthene
XPhos	2-dicyclohexylphosphino-2′,4′,6′-triisopropylbiphenyl

Table of Contents

Author's Declaration i

Acknowledgements ii

Abstract: Novel Radiochemistry for Positron Emission Tomography Imaging iv

Abbreviations and Acronyms vi

Table of Contents xi

Chapter 1: Introduction 1

1.1 Positron Emission Tomography Imaging 1

1.2 Radiochemistry Using Fluorine-18 5

1.3 Commercial Fluorinating Reagents 14

1.3.1 Nucleophilic Fluorinating Reagents 14

1.3.2 Electrophilic Fluorinating Reagents 16

1.4 [^{18}F]Fluorinating Reagents 18

1.4.1 Production of [^{18}F]Fluorinating Reagents Directly from a Cyclotron 18

1.4.2 Methods for Producing Nucleophilic [^{18}F]Fluorinating Reagents 20

1.4.3 Methods for Producing Electrophilic [^{18}F]Fluorinating Reagents 25

1.5 Methods for Labelling Other Fluorinated Motifs using [^{18}F]Fluorinating Reagents 42

1.6 Strategies for Labelling Peptides with Fluorine-18 53

1.7 Synthesis and Application of Sodium Trifluoromethanesulfinate: the Langlois Reagent 60

1.8 References 69

Chapter 2: Radiolabelling the Langlois Reagent with Fluorine-18 77

2.1 Development of a Novel Strategy for Synthesising the Langlois Reagent 77

2.2 Radiolabelling the Langlois Reagent and Mechanistic Insights 85

2.3 Purification and Isolation of the Langlois Reagent 101

2.4 Purification and Isolation of the [^{18}F]Langlois Reagent 106

2.5 Development of Conditions Amenable to Automated Radiolabelling of the Langlois Reagent 119

2.6 Automated Radiosynthesis of the [^{18}F]Langlois Reagent 129

2.7 References 135

Chapter 3: Radiolabelling Peptides using the [^{18}F]Langlois Reagent 137

3.1 Trifluoromethylation of Amino Acids and Peptides with the Langlois Reagent.....137
3.1.1 Literature Precedent.....137
3.1.2 Trifluoromethylation of Tyrosine and Tryptophan with Substoichiometric Langlois Reagent.....144
3.1.3 Synthesis and Isolation of Trifluoromethylated Amino Acid and Peptide References.....155
3.2 Radiolabelling Tyrosine and Tryptophan using the [^{18}F]Langlois Reagent.....159
3.3 Radiolabelling Peptides using the [^{18}F]Langlois Reagent.....165
3.4 Automated Radiolabelling of Peptides using the [^{18}F]Langlois Reagent.....176
3.5 *In Vivo* study for Octreotide Radiolabelled with the [^{18}F]Langlois Reagent.....182
3.6 References.....187
Chapter 4: Experimental Data.....189
4.1 General Experimental Information.....189
4.2 Experimental Procedures and Compound Characterisations.....191
4.3 Reaction Screening for Synthesis of the Langlois Reagent.....273
4.4 Radiochemistry at the University of Oxford.....274
4.4.1 General Experimental Details.....274
4.4.2 Radiosynthesis of [^{18}F]Langlois Reagent.....276
4.4.3 [^{18}F]Trifluoromethylation of Amino Acids and Peptides.....283
4.5 Automated Radiosynthesis at Invicro.....324
4.5.1 General Experimental Details.....324
4.5.2 Automated Radiosynthesis of [^{18}F]Langlois Reagent and Octreotide[Trp(2-$CF_2{}^{18}F$)].....326
4.5.3 Automated Radiosynthesis of [^{18}F]Langlois Reagent and c(RGDyK)[Tyr(3-$CF_2{}^{18}F$)].....333
4.6 Cell Uptake Experiments.....337
4.7 *In Vivo* Naïve Rat Model.....342
4.8 References.....344

Chapter 1: Introduction

1.1 Positron Emission Tomography Imaging

Positron Emission Tomography (PET) is a powerful non-invasive nuclear imaging technique that delineates injected radioactive substances *in vivo*. PET provides quantitative temporal and three-dimensional spatial data, and can be used in conjunction with *ex vivo* analysis, autoradiography and structural imaging techniques such as Computed Tomography (CT) or Magnetic Resonance Imaging (MRI).[1,2] Using these methods, whole-body and brain imaging studies enable investigations into biodistribution, kinetics, specific binding to tissues, and metabolism of any molecule tagged with a specific radionuclide.[3]

PET studies allow examination of biochemical processes which aids in assessing the efficacy of therapeutic interventions and serves as a valuable diagnostic tool in oncology, cardiology and neurology. Molecular imaging techniques such as PET may be used to discern whether drug molecules reach a tissue of interest in potentially pharmacologically active concentrations, determine the level of build-up in non-target tissues, and make an assessment of blood-brain barrier penetration.[4]

PET studies of receptor occupancy examine displacement of a radiotracer by a drug candidate at varying concentrations which can guide the drug dosage. Similarly, PET can quantitatively determine therapeutic effectiveness of a drug candidate by imaging a radiotracer associated with the specific biological pathways, receptor expression or cell proliferation. These studies make PET an invaluable tool in drug discovery for early validation of potential drug candidates.

A major advancement in the field of imaging came with the advent of small animal PET scanners which connected preclinical research with human applications in the clinic.[5] This made it possible to assess similarities between animal species and humans in order to design useful and efficient preclinical studies.

Radionuclides used in PET imaging produce a positron (β^+) upon nuclear decay (Figure 1.1). The positron travels a short distance (2 – 3 mm) before annihilating with an electron, causing two γ-photons to be emitted 180° from each other. This pair of γ-photons are detected by scintillation detectors surrounding the subject.[4] This is used to determine the original point of annihilation and thus an approximate location of the positron-emitting radionuclide.

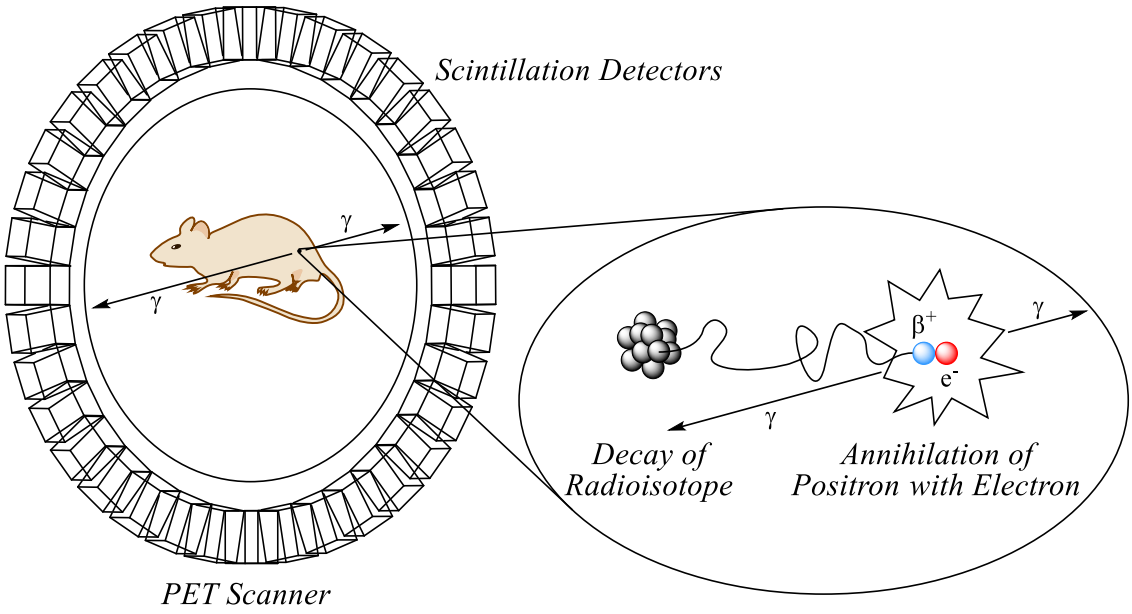


Figure 1.1: Nuclear decay of a positron-emitting radiotracer during a PET scan *in vivo*

Several radionuclides are used in PET imaging, each displaying a variety of properties that must be considered when designing a radiotracer (Table 1.1). Replacing natural elements such as carbon-12 and fluorine-19 with the corresponding positron-emitting radionuclides (carbon-11 and fluorine-18) has negligible effect on a molecule's biological activity.

Incorporation of metal radionuclides, such as ^{64}Cu and ^{68}Ga, requires installation of bulky metal chelators which may affect the molecular interactions. PET scanners are sensitive enough to detect radiotracer concentrations that are low enough to not have any pharmacological effect.[4]

Table 1.1: Properties of positron-emitting radionuclides

Radionuclide	Nuclear Reaction for Radionuclide Production	Half-Life (min)	Proportion of Decay as β^+	Maximum β^+ Energy (MeV)	Decay Product
^{11}C	^{14}N(p,α)^{11}C	20.3	99%	0.97	^{11}B
^{13}N	^{16}O(p,α)^{13}N	10.0	100%	1.20	^{13}C
^{15}O	^{15}N(d,n)^{15}O	2.04	100%	1.74	^{15}N
^{18}F	^{18}O(p,n)^{18}F	110	97%	0.64	^{18}O
^{64}Cu	^{64}Ni(d,n)^{64}Cu	762	19%	0.66	^{64}Ni
^{68}Ga	^{68}Ge Generator	68.1	89%	1.90	^{68}Zn

As a useful guideline for developing new radiotracers, the time between radionuclide production and injection of the radiotracer should not exceed three half-lives, although it is important to consider any *in vitro* or *in vivo* incubation times required before data collection.[6] This limitation imposes restrictions on the molecular and biological targets that can be used for PET imaging when employing short-lived radionuclides. The half-life of the radionuclide must be appropriate for the biological process being studied, for example oxygen-15 is useful for imaging biological processes with a short half-life such as cerebral blood flow.[7]

Low energy β^+ particles travel shorter distances before annihilation, therefore radionuclides with lower maximum β^+ energies will give PET images with intrinsically higher resolution. Fluorine-18 has a favourable combination of the lowest maximum β^+ energy, a high

proportion of decay as β^+, and a reasonably long half-life. This allows fluorine-18 to be used in facilities that may not have direct access to a cyclotron whilst giving relatively high resolution PET images.

There are many other challenges associated with PET imaging such as optimising PET scanner and detector design to improve spatial and temporal aspects of resolution and sensitivity. This allows imaging of small tissues of interest, such as in early tumour detection, or in imaging biological targets present in low quantities.[3] Optimisation of image reconstruction algorithms, corrections and calibrations enable PET images to convey quantitative data. This includes corrections for photon scattering, attenuation, and the partial volume effect – a complex field of research where activity concentrations are underestimated in small regions. Many algorithms are available for reconstructing 2D and 3D images that balance spatial resolution with image noise and artefacts.

Another challenge in PET imaging is keeping the subject immobile throughout the entire study. In animal studies this is primarily achieved using controlled levels of anaesthetics such as isoflurane and Propofol, although these are known to induce significant effects on central nervous, cardiovascular and respiratory systems, which may impact the results.[8] Awake animal imaging studies and motion correction have been investigated although maintenance of stress levels is a pervading problem.[9]

One of the most prominent challenges to the widespread use of PET imaging is the limited range of accessible radiochemical methods. This restricts the set of radiotracers that can be used in PET imaging, stunting the development of new molecular probes for imaging biological targets. Developing innovative and accessible radiochemical methods that provide

access to structurally diverse radiotracers is therefore highly sought after in accelerating the progress of PET imaging research.

1.2 Radiochemistry Using Fluorine-18

Organofluorine compounds are rarely found in nature and there is no radioactive isotope of hydrogen that can be used *in vivo* that emits radiation detectable from outside a body. Hydrogen atoms within target molecules are often replaced with fluorine-18 because of its favourable properties (Table 1.2).[10]

Table 1.2: Properties of hydrogen, oxygen and fluorine

X	Van der Waal's Radius (Å)	Pauling Electronegativity	$C(sp^3)$-X Bond Length (Å)[a]	$C(sp^2)$-X Bond Length (Å)	C-X Bond Dissociation Energy (kJ mol^{-1})
H	1.20	2.2	1.09	1.08	339
O	1.52	3.4	1.43	1.33	1077
F	1.47	4.0	1.40	1.34	514

[a] Primary and secondary $C(sp^3)$.

Fluorine has a Van der Waal's radius of 1.47 Å, which is in between hydrogen (1.20 Å) and oxygen (1.52 Å), and has a Pauling electronegativity of 4.0 leading to highly polarised C-F bonds. When attached to a drug molecule, fluorinated motifs typically alter a molecule's lipophilicity favourably, particularly for drugs that have to cross the blood-brain barrier.[11] Additionally, different fluorinated motifs can induce modulations in conformation, pK_a of proximal functional groups, hydrogen bonding, and electrostatic interactions. A molecule's affinity for biological targets can be tuned by altering these properties.[14] This explains the rise of fluorine incorporation in pharmaceutical and agrochemical molecules from 2% in

1970 to 25% in 2011.[12] About 40% of new molecules that entered phase III clinical trials in 2012 and 2013 contained fluorine.[13]

Metabolism of drug molecules *in vivo* is often undesired because the molecule can be destroyed before inducing its desired effect. Common metabolic pathways include oxidation of R-H or demethylation of R-O-Me groups by P450 enzymes.[14] Introducing C-F bonds at metabolic sites of drug molecule may prolong a drug's biological half-life because the C-F bond dissociation energy is greater than that of the C-H bond. In addition, the rare occurrence of fluorine in nature means the C-F bond is naturally resistant to metabolism by P450 enzymes.

Conversely, introduction of fluorine into molecules may affect the physiochemical properties in a way that has adverse effects on the compound's biological properties. This could lead to lower binding selectivity, affinity or poorer metabolic stability. For example, substitution of a fluorine group σ- to the hydroxyl group of a phenol will increase its reactivity as a nucleophile, making it more susceptible to metabolic attack such as methylation.[15] Therefore it is important to assess the positive and negative changes that fluorination may induce on a molecule's pharmacological activity.

To incorporate the unnatural radionuclide fluorine-18 into molecules of interest, it is generated artificially. Fluorine-18 is most commonly produced in the form of [^{18}F]fluoride and is generated in a cyclotron by bombardment of ^{18}O-enriched water with a high energy proton beam resulting in the ^{18}O(p,n)^{18}F nuclear reaction (Figure 1.2).[16,17]

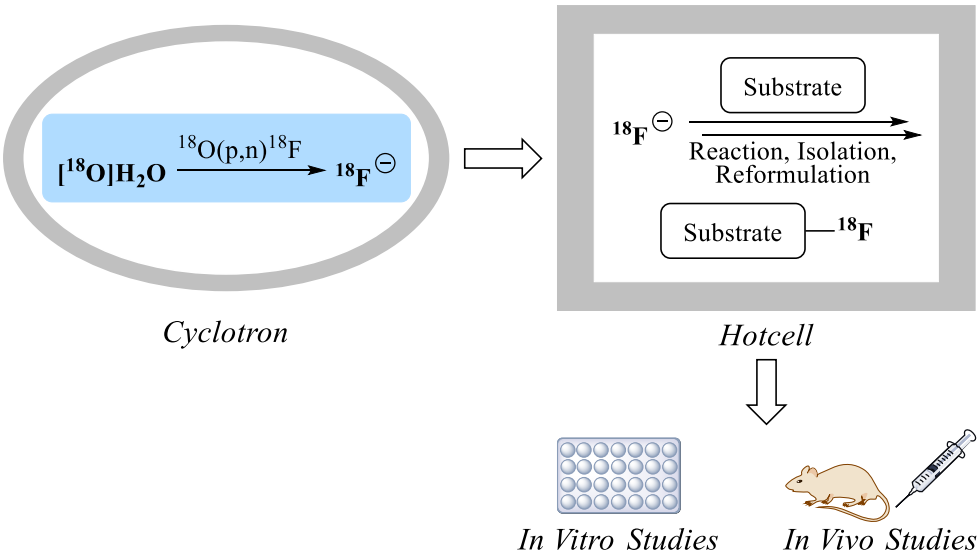


Figure 1.2 Typical sequence for generation of [^{18}F]fluoride, synthesis of a radiotracer, and subsequent biological studies

The solution of [^{18}F]fluoride in [^{18}O]H_2O is delivered from the cyclotron to a lead-shielded hotcell; the metal counterion at this stage is from the target chamber material in the cyclotron.[18] A procedure is followed for radiolabelling, isolating and reformulating a target radiotracer, before transporting to research labs or the clinic for carrying out *in vitro* or *in vivo* studies.

There are several innate challenges when conducting radiochemical reactions using [^{18}F]fluoride. It is important to streamline radiosynthetic experimental design for operational simplicity and efficiency because of the limiting half-life of fluorine-18. This implies that the number and length of manipulations that can be carried out are limited once fluorine-18 has been generated.

Fluorine-18 is typically only introduced into molecules in the last stage of synthesis. This means it is common to have a relatively lengthy chemical synthesis for constructing an appropriate substrate with a reactive functional group to aid efficient radiosynthesis. The

radiochemistry implemented must be versatile enough to pinpoint the reactive site whilst keeping the rest of the molecule intact, which is particularly an issue for larger molecules such as peptides and proteins. It is therefore highly desirable to develop radiosynthetic procedures that incorporate the radionuclide directly onto the native drug or ligand without the need for constructing additional reactive functional groups or protecting groups. Other constraints in carrying out radiochemical reactions include the use of water-miscible reaction solvents to aid purification procedures, short reaction times, and practical feasibility since complex setups limit a reaction's reliability and accessibility.

[^{18}F]Fluoride is produced in picomolar quantities which poses unique challenges to conducting radiochemical reactions.[19] This is in contrast to non-radioactive fluorination reactions which often employ super-stoichiometric amounts of fluoride to achieve high conversions. When such minute quantities of [^{18}F]fluoride are used, other undesirable side effects may occur. For example, [^{18}F]fluoride reacting or affixing with glass, lines and connections used in transfer ultimately lead to significant decreases in the final yield. Therefore, importance is placed on using plastic materials such as polyether ether ketone instead of borosilicate glassware, which contains boron and aluminium compounds known to bind irreversibly to [^{18}F]fluoride.[20]

Developing efficient methods for isolating radiotracers is of paramount importance as this often takes up a majority of the overall synthesis time. Standard laboratory methods for purification used in chemical laboratories are too incompatible with radiochemical reaction designs. Traditional reaction work-up and separation of organic and inorganic phases, flash column chromatography, and vacuum assisted concentration or distillation of solvents or compounds are too cumbersome for purifying tiny quantities of radiotracers. Instead, purification may be streamlined by employing a wide range of commercially available

cartridges and columns that contain silica-based reverse phase, normal phase and ion exchange phases. An understanding of the molecular interactions that take place between the radiotracer and the purification medium is key to achieving efficient purification and isolation of the desired compound.

The following sequence is the standard procedure for carrying out radiochemical reactions starting from [^{18}F]fluoride in [^{18}O]H_2O: [^{18}F]fluoride trapping, elution, azeotropic drying, addition of reagents, reaction, purification and isolation of the radiolabelled compound (Figure 1.3).

The free energy of solvation of fluoride ions in aqueous solution is calculated as -104.3 kJ mol^{-1}.[21] This high value means that the solution of [^{18}F]fluoride in [^{18}O]H_2O obtained from the cyclotron is highly solvated and weakly nucleophilic, making it unsuitable for carrying out reactions.[22] Therefore, the first step is to separate [^{18}F]fluoride from [^{18}O]H_2O by using a silica-based Quaternary Methyl Ammonium (QMA) cartridge. This acts as a solid-phase support for anion exchange, trapping [^{18}F]fluoride onto the cartridge whilst allowing the [^{18}O]H_2O to wash through. The fluoride is commonly eluted with an aqueous acetonitrile solution of an alkali metal base, such as potassium/caesium carbonate, hydrogen carbonate, oxalate or hydroxide. Crown ether phase transfer catalysts (PTCs), such as Kryptofix® (K_{222}), are used to facilitate [^{18}F]fluoride solubilisation into organic solvents, enabling chemical reactions to take place.

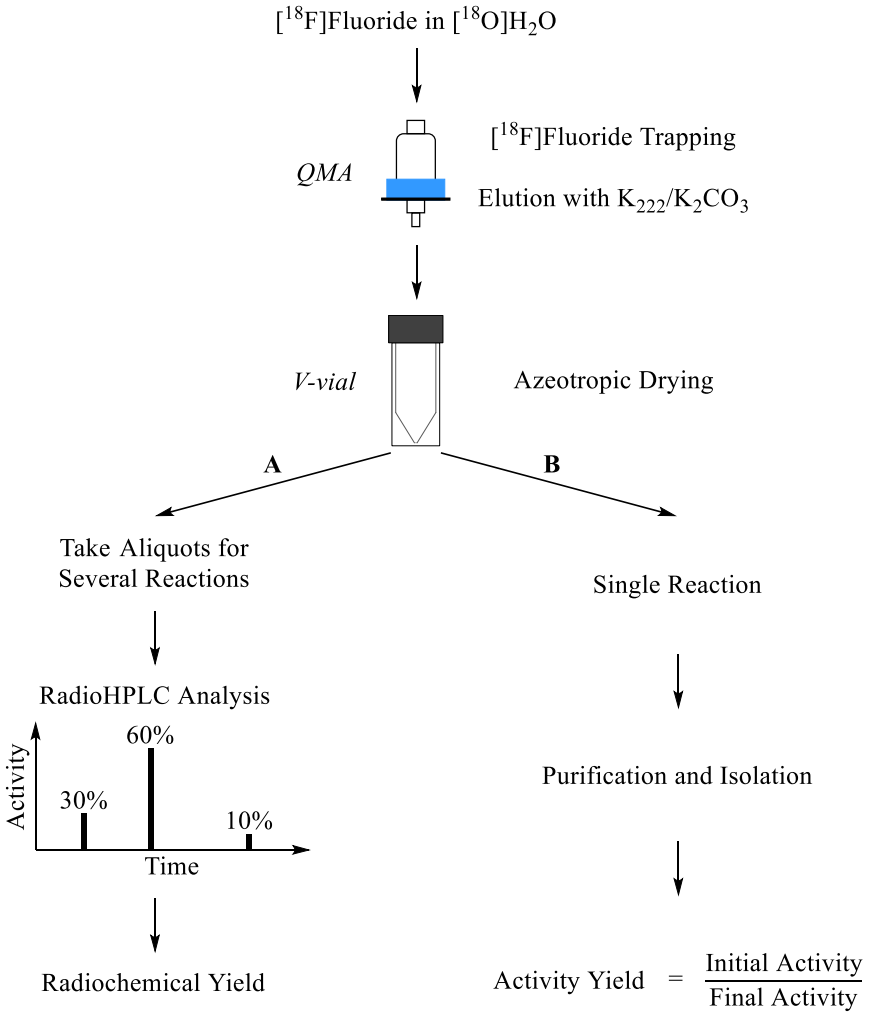


Figure 1.3 Procedure for carrying out radiochemical reactions using [^{18}F]fluoride in A) aliquots or B) for a single reaction

Other customised elution methods have been explored.[23] For example, ammonium salts such as tetraethyl ammonium salts accommodate both functionalities by eluting [^{18}F]fluoride and solubilising it in organic solvents. The large free energy of solvation for fluoride juxtaposed with the practical constraints inherent in carrying out radiochemical reactions implies that the [^{18}F]fluoride often cannot be dried sufficiently for use in very water-sensitive chemistry.

In the early stages of reaction development it is more efficient to redissolve [^{18}F]fluoride after azeotropic drying and take aliquots as required (Figure 1.3, A). This allows several

reactions to be performed from one batch of [^{18}F]fluoride. A disadvantage of this method is that these reactions are a misrepresentation of the conditions used when carrying out only one reaction from a single batch of [^{18}F]fluoride (Figure 1.3, B). This is due to lower concentrations of base, PTC and cyclotron impurities present in the reaction, and when using larger amounts of activity, decreases in yield are often observed because of radiolysis. In addition, the reaction yields are calculated by radio-HPLC analysis so activity losses through purification procedures, decay, affixation to the reaction vial, and evaporation of volatile radioactive side products are not taken into account. These reasons explain why using aliquots of [^{18}F]fluoride often leads to an overestimated yield.

Carrying out radiochemical reactions using aliquots of [^{18}F]fluoride provides information on the relative effect of altering variables such as reaction temperature, time and reagent stoichiometry. The efficiency of labelling the desired product starting from [^{18}F]fluoride is calculated as the Radiochemical Yield (RCY). The reaction is quenched with an aqueous solution to dissolve unreacted [^{18}F]fluoride and an aliquot is taken for analysis by radio-HPLC. The RCY is the measured activity of labelled product as a percentage of the unreacted [^{18}F]fluoride and other labelled side products. The RCY is decay corrected which indicates the chemical efficiency but ignores the time taken to carry out the radiosynthetic procedures.

When determining the efficiency of purification and isolation procedures, reactions are carried out using a single batch of [^{18}F]fluoride and the Activity Yield (AY) is used. This is calculated by comparing the starting activity with the activity of the purified product. AY is not corrected for decay and is used to analyse overall synthesis efficiency. Comparing RCY with AY and stating the overall synthesis time gives a clear indication of activity losses incurred through technical manipulations and their duration.

Molar Activity (MA), measured in GBq μmol^{-1}, is calculated as the activity of isolated radiolabelled product divided by the mass of unlabelled product, typically measured using HPLC analysis. It is often important to consider this property of a radiotracer when carrying out PET imaging because it is a measure of the ratio between the amount of labelled and unlabelled compound. If a radiotracer is chemically pure, the molar activity is the ratio between a compound containing radioactive fluorine-18 and its natural fluorine-19 analogue, which may be increased by increasing the activity of radiolabelled compound and decreasing the moles of its non-radioactive analogue.

When an *in vivo* PET study is conducted, a mixture of labelled and unlabelled compounds is injected into the subject which distributes around the body and may bind to the target receptor, known as specific binding. Non-specific binding also occurs and is defined as binding to sites other than the target, such as proteins or cell membranes. If there is a large excess of unlabelled compound, the target receptor will become mostly unavailable for binding with the labelled compound, resulting in a weakened PET signal. Because there is always a large excess of non-specific binding sites available, the majority of the labelled compound will bind to these sites, and is observed as noise in a PET image. Therefore, a greater ratio between the labelled and unlabelled compound, equal to a higher molar activity, leads to a higher signal to noise ratio in the final PET image.

Part of radiotracer design involves developing a radiosynthesis that minimises the level of unlabelled product and maximises the labelled product in order to obtain a high enough molar activity. It is therefore important to identify and prevent any source of fluorine-19 release, such as through nucleophilic substitution or decomposition of fluorinated motifs. Intentional addition of fluorine-19 sources, known as carrier addition, is undesirable but

unavoidable for some processes. In this case it is important to be aware that the administered dose of unlabelled product is below the toxicity threshold.

When developing new reactions, radiosyntheses are often carried out manually, employing the use of tongs and/or a glove box in order to carry out reactions by hand. This facilitates multiple reaction condition screening (10 – 25 MBq) from one production of [^{18}F]fluoride. Radiosyntheses in commercial settings are automated whereby all manipulations are carried out remotely employing syringe pumps and compressed gases inside a lead-shielded hotcell. This allows much higher levels of radioactivity to be employed with lower exposure levels to the radiochemist.

Automation allows a method to become more widely accessible due to the commercial availability of automated modules, however significant changes have to be made in order to make most radiosyntheses amenable to automation. Setups must be designed to allow transfer of all compounds and reaction mixtures as solutions, and even simple steps such as stirring, putting a reaction mixture under inert atmosphere or bubbling air through the mixture are not trivial; in some automated setups this may not be possible.

Additional challenges include preventing line blockages as a result of precipitate forming, manipulating small volumes to facilitate purification and reduce the amount of unlabelled products, and keeping reagents localised over a small area otherwise affixation to the reaction vial wall may prevent participation in the reaction. The entire experimental design must be thoroughly planned and set up correctly before production of radionuclides as issues cannot often be fixed during the radiosynthesis. This means designing and constructing the right setup is time-consuming but necessary.

1.3 Commercial Fluorinating Reagents

1.3.1 Nucleophilic Fluorinating Reagents

The attraction of late-stage fluorination for synthesising medicinal targets has led to the development of a number of reagents with increasingly greater selectivity and accessibility. The first of a set of early fluorinating reagents is hydrofluoric acid (Figure 1.4). Despite this reagent's high utility and abundance, its low boiling point, hazardous nature and the community's desire for highly selective fluorination technologies led to the development of many other commercially available fluorinating reagents.[24]

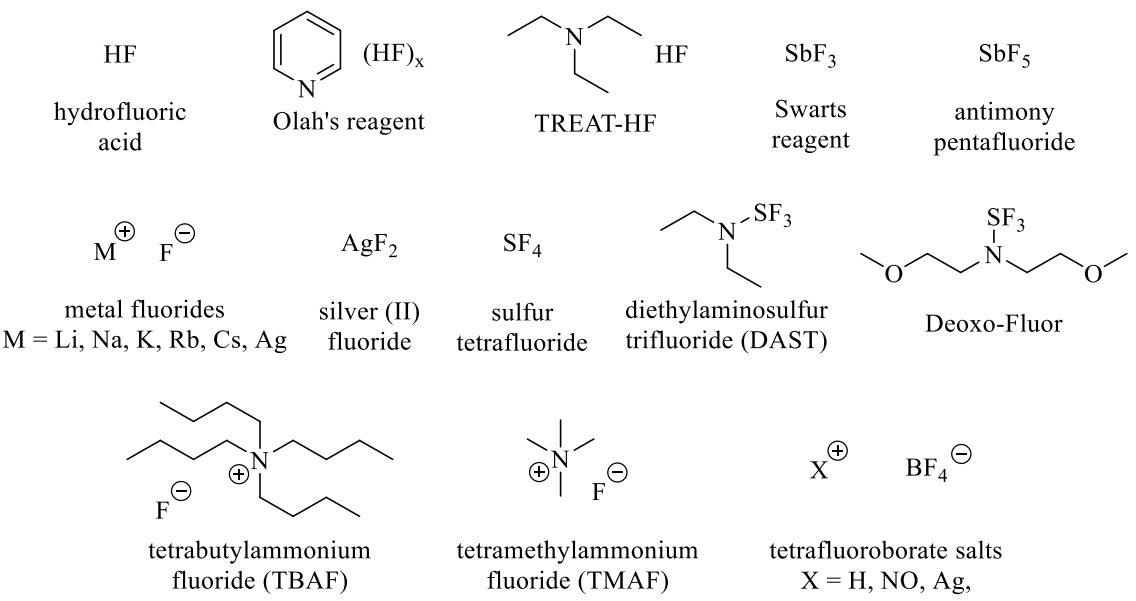


Figure 1.4 Commercial nucleophilic fluorinating reagents

By taking advantage of the propensity for HF to form hydrogen bonds, HF complexation with oxygen and nitrogen containing compounds was explored. Novel complexes were isolated that possess the favourable property of not releasing HF upon heating, thus allowing their use in synthesis without the need for specialised equipment or precautions. The HF complex with pyridine, known as Olah's reagent, reportedly always contains a small amount

of “free” reactive hydrogen fluoride in equilibrium with the pyridinium polyhydrogen fluoride complex, essentially acting as a source of anhydrous HF whilst allowing heating up to 60 ºC without loss.[25,26] Similarly, the HF complex with triethylamine, TREAT-HF, was introduced with the distinct advantage of being compatible with borosilicate glassware without causing corrosion.[27]

Classical metal fluoride salts can be used in carrying out nucleophilic fluorination reactions under the right conditions. Antimony trifluoride, known as the Swarts reagent, is employed in combination with antimony pentachloride or chlorine gas to form the active species antimony trifluorodichloride *in situ* and has been successfully applied to fluorination of chlorinated hydrocarbons.[28] Antimony pentafluoride shows even greater potency as a fluorinating reagent reacting violently with many compounds, notably forming one of the strongest known acids, fluoroantimonic acid, when mixed with HF.

Challenges associated with classical nucleophilic fluorination stem from the readiness for fluoride to form hydrogen bonds. This leads to high kinetic barriers in forming C-F bonds. Alkali metal fluorides are highly hygroscopic, preferring to be encapsulated by water molecules. In comparison to antimony fluorides, lithium fluoride is a very stable salt insoluble in most solvents resulting in low reactivity, hence there are few examples demonstrating its utility as a fluorinating reagent. Fluorination is more effective as the size and electropositivity of the alkali metal cation increases, hence potassium and caesium fluoride have greater application in organofluorine chemistry, particularly when combined with phase transfer catalysts to aid solubility in organic solvents. Silver(I) fluoride is capable of mediating various transformations including addition to double bonds, fluorodesulfurisation, and fluorination of aryl and alkyl halides facilitated by the

halogenophilic nature of silver.[29] In addition, silver(II) fluoride was explored by Hartwig for the selective C-H fluorination of pyridines and diazines.[30]

This desire to further improve the solubility and reactivity of fluoride in organic solvents prompted the development of fluoride reagents containing organic, lipophilic counter ions such as tetrabutylammonium fluoride (TBAF) and tetramethylammonium fluoride (TMAF).[31,32] These reagents are highly accessible, reactive, soluble in organic solvents, and can be partially dried, or fully dried in the case of TMAF.

Advances in deoxygenative fluorination of carbonyls and alcohols came with the advent of the classical reagent sulfur tetrafluoride, which selectively targets the C-O bond because of the strong affinity of the sulfur atom for oxygen over fluorine.[33,34] Gaseous sulfur tetrafluoride releases HF and SO_2 upon contact with moisture. Amine-sulfur trifluoride compounds, such as DAST and Deoxo-Fluor, are significantly less hazardous liquids and can be used in a range of transformations.[35]

A number of synthetically relevant examples of fluoride transfer have been demonstrated from tetrafluoroborate salts and the commercial reagent boron trifluoride.[36,37] Aryl fluorides have been conveniently prepared from the Balz-Schiemann reaction starting from tetrafluoroborate salts of aryl diazonium compounds. Alkyl fluorides may be formed from the reaction between boron trifluoride or tetrafluoroborate salts and a wide range of electrophiles.

1.3.2 Electrophilic Fluorinating Reagents

Electrophilic fluorinating reagents can be synthesised, despite the fact that fluorine is the most electronegative element, provided that good leaving groups and inductively electron

withdrawing groups are employed (Figure 1.5). Traditionally, fluorine gas was used as the main source of "F^+" in fluorination of double bonds and electron-rich C-H bonds.[38] Despite fluorine gas being highly reactive, causing explosions and fires, and releasing HF when in contact with moisture, it is highly useful in the manufacture of perfluorinated compounds.[39]

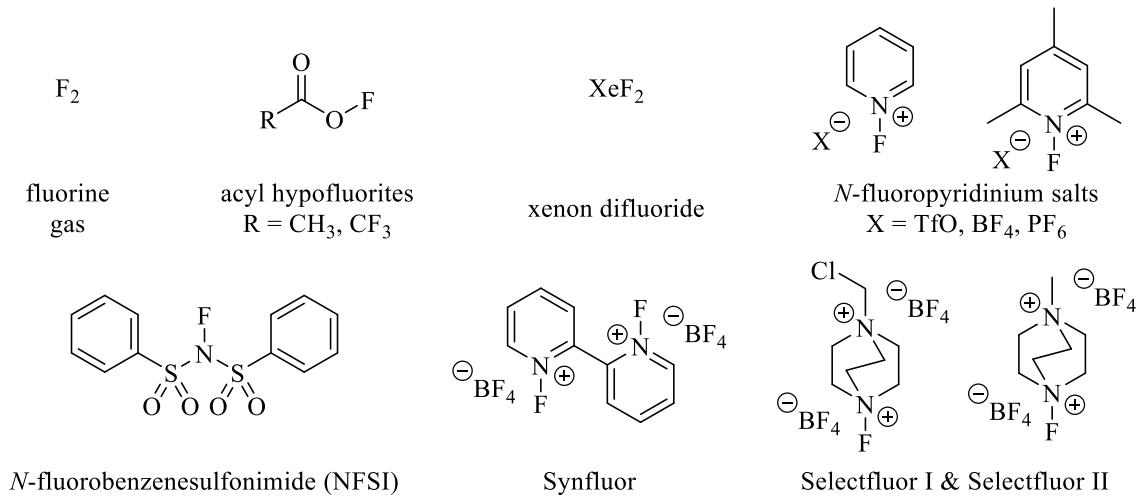


Figure 1.5 Commercially available electrophilic fluorinating reagents

Trifluoromethyl hypofluorite, synthesised from fluorine gas and carbon monoxide, was sometimes used instead of fluorine gas.[40] Electrophilic fluorinating reagents such as hypofluorites, particularly acyl hypofluorites, are slightly safer alternatives to F_2, but toxicity and selectivity is still problematic. Alternatively, xenon difluoride is a synthetically valuable solid reagent that can be transferred in air without precautions. It is highly dangerous under certain conditions, for example the presence of HF leads to explosive autocatalytic decomposition.[41]

The field of electrophilic fluorine chemistry was revolutionised by the invention of reagents bearing an N-F bond, which often possess greater stability, selectivity and are much easier to handle than traditional electrophilic reagents.[42] The most versatile reagents, Synfluor, Selectfluor I & II, *N*-fluoropyridinium salts, and *N*-fluorobenzenesulfonamides, are

commercially prepared from the reaction between the corresponding amine and fluorine gas, and their relative kinetic reactivity has been experimentally determined.[43,44] A number of asymmetric electrophilic N-F reagents have also been developed, advancing the field of enantioselective fluorination.[45]

1.4 [^{18}F]Fluorinating Reagents

1.4.1 Production of [^{18}F]Fluorinating Reagents Directly from a Cyclotron

In contrast to the range of commercial fluorinating reagents that are available, nucleophilic [^{18}F]fluoride and electrophilic [^{18}F]F_2 are primarily the only two sources of fluorine-18 that can be produced from a cyclotron. [^{18}F]Fluoride is typically produced from the $^{18}O(p,n)^{18}F$ reaction of [^{18}O]H_2O and there are a number of ways to generate [^{18}F]F_2 (Table 1.3). Pharmaceuticals radiolabelled with fluorine-18 are most frequently produced starting from nucleophilic [^{18}F]fluoride because of the higher molar activity and ease of technical handling.

Table 1.3 Cyclotron production of fluorine-18[46–49]

^{18}F Product	^{18}F Precursor	Nuclear Reaction	Final Activity (GBq)	Molar Activity (GBq μmol^{-1})
[^{18}F]F_2	[^{20}Ne]Ne + F_2	$^{20}Ne(d,\alpha)^{18}F$	9.3	0.11
[^{18}F]F_2	[^{18}O]O_2 + F_2	$^{18}O(p,n)^{18}F$	13	1.3
[^{18}F]F_2 *via* [^{18}F]CH_3F from [^{18}F]F^-	[^{18}O]H_2O	$^{18}O(p,n)^{18}F$	7.5	55
[^{18}F]F^-	[^{18}O]H_2O	$^{18}O(p,n)^{18}F$	37	5200

One method for producing [^{18}F]F_2 is from irradiating a mixture of neon and fluorine with deuterons.[46] The ^{18}F generated exchanges with F_2 to form a mixture of ^{18}F-F in F_2.

In a second method, irradiation of $[^{18}O]O_2$ produces ^{18}F which deposits on the cyclotron target walls. This is then removed as $[^{18}F]F_2$ after a second irradiation and flushing with fluorine gas.[47] Production of $[^{18}F]F_2$ from the bombardment of $[^{18}O]O_2$ gives a higher molar activity but requires a more complicated setup.

A third method involves vicarious production of $[^{18}F]F_2$ by using $[^{18}O]H_2O$ to generate $[^{18}F]$fluoride which reacts with methyl iodide to form $[^{18}F]CH_3F$.[48] After purification by gas chromatography, the $[^{18}F]CH_3F$ is atomised by a high-voltage electrical discharge in the presence of fluorine gas and induce isotope exchange to form $[^{18}F]F_2$.

$[^{18}F]$Fluoride generated from the $^{18}O(p,n)^{18}F$ reaction of $[^{18}O]H_2O$ has a high molar activity because high levels of activity and low quantities of fluoride are obtained.[48] Conversely, $[^{18}F]F_2$ is obtained in lower levels of activity because a gaseous target is used and there is a low recovery efficiency of $[^{18}F]F_2$ from the cyclotron. An external supply of fluorine gas is used as a carrier to transport $[^{18}F]F_2$ from the cyclotron resulting in a dramatic reduction in molar activity. For all three possible methods of $[^{18}F]F_2$ production, an increase in the amount of carrier gas increases the recovery, and therefore the yield, but decreases the molar activity due to the greater amount of unlabelled F_2 present. In addition, the RCY of subsequent fluorination reactions can only reach a theoretical maximum of 50% due to the presence of one fluorine-18 and one fluorine-19 atom in each radiolabelled diatomic fluorine molecule.

Traces of nitrogen, carbon dioxide or carbon tetrafluoride gases in the cyclotron target result in the production of $[^{18}F]NF_3$ and $[^{18}F]CF_4$, at the expense of $[^{18}F]F_2$.[49] Although these compounds are chemically inert, the amount of useful $[^{18}F]F_2$ activity is decreased.

In an effort to expand the available radiochemical space beyond these two fluorine-18 labelled reagents, new protocols were developed for convenient preparation and isolation of

radiolabelled fluorinating reagents. These studies have enabled new transformations that expand the library of imaging probes, and provide novel strategies that address some of the limitations associated with conventional fluorine-18 radiochemistry.

One of the earliest reported methods is for labelling hydrofluoric acid with fluorine-18, but this has found limited application in modern times. Anhydrous [^{18}F]HF has been formed from bombardment of O_2 gas mixed with a small quantity of HF to initiate isotope exchange in the $^{16}O(\alpha,p\ n)^{18}F$ or $^{16}O(^{3}He,p)^{18}F$ reaction.[50] An alternative method involves the irradiation of a solid target such as Li_2CO_3 dissolved in H_2SO_4 containing trace amounts of H_2SiF_6. The $^{6}Li(n,\alpha)t$ reaction of Li generates tritium which subsequently converts oxygen-16 to fluorine-18 *via* the $^{16}O(t,n)^{18}F$ reaction.[50] This method requires addition of hydrofluoric acid to form carrier added [^{18}F]HF.

The challenge of synthesising non-carrier added [^{18}F]HF was overcome by irradiating a mixture of hydrogen and neon-20 with deuterons in the $^{20}Ne(d,\alpha)^{18}F$ reaction, or of neon-20 to form neon-18 in the reaction $^{20}Ne(^{3}He,\alpha\ n)^{18}Ne$.[46,51] Neon-18 has a half-life of 1.5 seconds decaying by electron capture to fluorine-18. A number of reactions using [^{18}F]HF have been explored forming [^{18}F]NOF, [^{18}F]ClF, [^{18}F]BrF_3, [^{18}F]IF_5, [^{18}F]SbF_5 and [^{18}F]BrF_5, mainly through isotopic exchange, however none of these have found further application.[52] A potentially useful application of [^{18}F]HF has been in the labelling of diethylaminosulphur trifluoride (DAST).[53]

1.4.2 Methods for Producing Nucleophilic [^{18}F]Fluorinating Reagents

Once [^{18}F]fluoride has been trapped on a QMA, a variety of reagents may be added to elute [^{18}F]fluoride paired with different counter ions. Classically, various combinations of alkali metal inorganic bases and PTCs have been employed, however not all reactions are

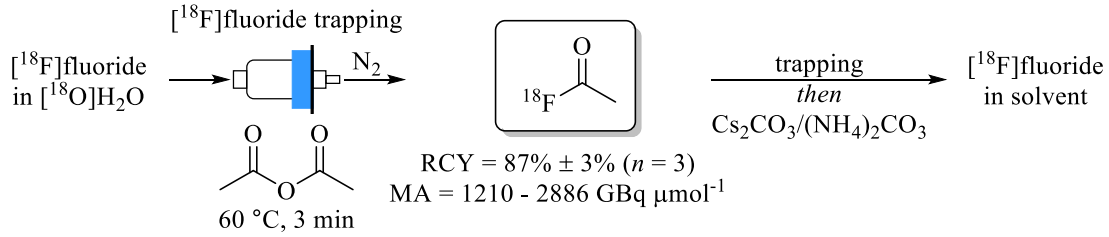
compatible with these conditions. Carbonate is notably detrimental to copper-mediated fluorination of certain heterocyclic and aromatic boronic esters.[54] To solve this problem, various protocols for eluting [^{18}F]fluoride have been investigated.[55] Organic bases such as DMAP or pyridine triflate are viable alternatives to carbonate and PTCs for eluting [^{18}F]fluoride, and that correct cartridge preconditioning enables a wider range of bases to be implemented.

After eluting [^{18}F]fluoride, it may be used in nucleophilic substitution of alkyl substrates by employing a good leaving group such as acetates and sulfonates. Nucleophilic aromatic substitution may also be carried out with leaving groups such as halogens, $-NO_2$ or $-NMe_3^+$. Incorporating fluorine-18 into most electron-deficient aromatic compounds proceeds smoothly in the presence of [^{18}F]KF/K_{222} when dissolved in solvents such as DMF, DMA or DMSO at temperatures of around 140 ºC, or with microwave heating, for 5 – 15 mins.[56] Many electron-rich analogues of these substrates remain unreactive under these conditions, although this problem has partially been solved by employing substrates charged with iodonium salts.[57]

In some cases, [^{18}F]fluoride may be eluted with the reagents that are used in the subsequent reaction. For example, [^{18}F]fluoride has been eluted from a QMA cartridge with a solution of a manganese porphyrin tosylate complex or silver tosylate, which then facilitates radical C-H fluorination reactions.[58,59] A ruthenium complex combined with a phenolic substrate and a chloroimidazolium chloride has also proved to be a successful eluent.[60] The eluted mixture was heated to initiate deoxyfluorination of the phenol substrate to afford [^{18}F]aryl fluorides.

An original strategy for carrying out fluorination that curtails the need for extraneous additives is to employ the aqueous solution of [^{18}F]fluoride received from the cyclotron directly in a reaction. This has been achieved by combining aryl nickel complexes with this aqueous solution in acetonitrile for aryl fluorinations.[61] Microliter quantities of the [^{18}F]fluoride solution are used which limits the maximum amount of activity because a solution of approximately 2 mL of [^{18}F]fluoride is normally obtained from the cyclotron.

[^{18}F]Fluoride has been converted into other organic reagents for specifically acting as a latent source of [^{18}F]fluoride for water sensitive reactions. One such reagent is [^{18}F]acetyl fluoride. This has been synthesised by trapping [^{18}F]fluoride on an ion-exchange cartridge, followed by heating with acetic anhydride, before eluting gaseous [^{18}F]acetyl fluoride under nitrogen flow (Scheme 1.1).[62] The [^{18}F]acetyl fluoride may then be re-dissolved in organic solvent, trapped on a weak anion exchange (WAX) cartridge or condensed in a cooling trap. This affords the isolated product in a final RCY of 87% ± 3% (n = 3), obtaining molar activities of up to 2886 GBq μmol^{-1}.

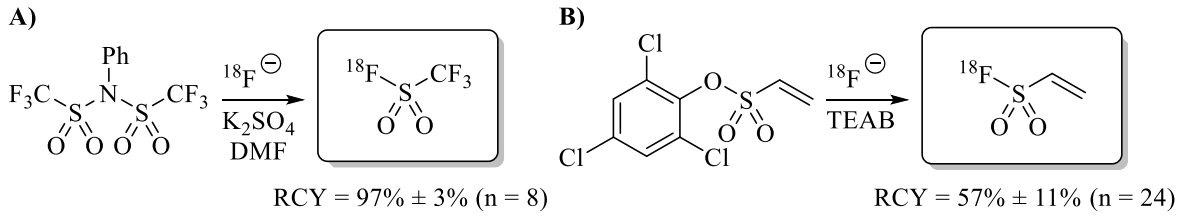


Scheme 1.1 Radiosynthesis of [^{18}F]acetyl fluoride

The gaseous nature of [^{18}F]acetyl fluoride at room temperature also enables efficient transfer through tubing. Elution efficiency is high when implementing a WAX cartridge, allowing the reagent to be concentrated in less than 0.1 mL of solvent, an important advantage when carrying out microfluidic reactions. However, the disadvantage of this application is the

added complexity of introducing dedicated systems for generating and distributing [^{18}F]acetyl fluoride. Additionally, the [^{18}F]acetyl fluoride is converted to the [^{18}F]fluoride ion by a base such as caesium or ammonium carbonate.

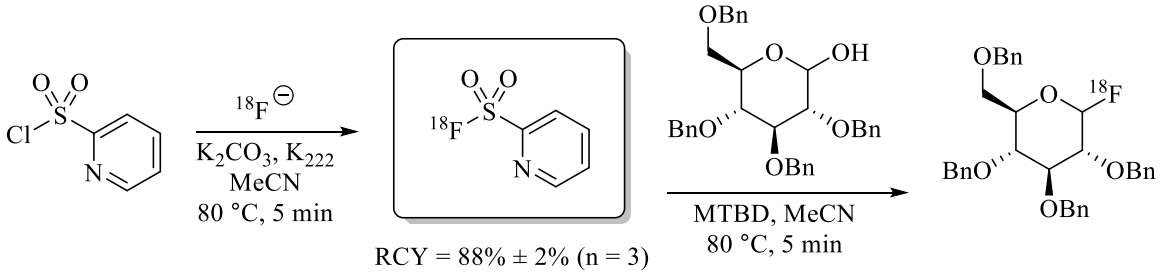
A similar procedure has been developed for generating gaseous [^{18}F]triflyl fluoride from phenyl triflimide in a RCY of 97% ± 3% (n = 8) with a time frame shorter than standard azeotropic drying (Scheme 1.2, A).[63] In comparison to [^{18}F]acetyl fluoride, a wider range and smaller concentration of elution bases/PTCs could be employed in the final step converting the reagent to dry [^{18}F]fluoride. In another procedure, 2,4,6-trichlorophenylethenesulfonate was employed to afford [^{18}F]ethenesulfonylfluoride ([^{18}F]ESF), a liquid at room temperature, in RCY of 57% ± 11% (n = 24) (Scheme 1.2, B).[64] The compound remains stable when trapped on a cartridge, facilitating transport of the compound, which can then be eluted and converted to [^{18}F]fluoride with tetraethylammonium bicarbonate as required.



Scheme 1.2 Radiosynthesis of A) [^{18}F]triflyl fluoride; B) [^{18}F]ESF

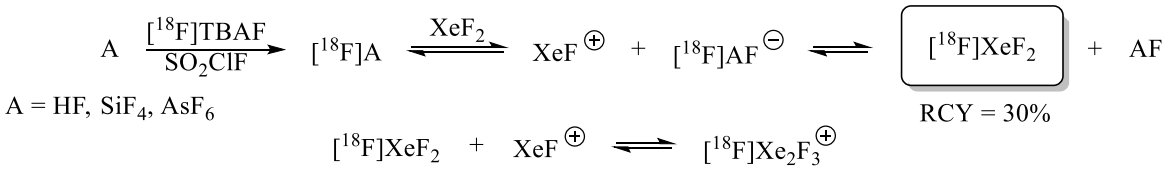
In order to obviate this conversion step back to [^{18}F]fluoride, new fluorinating reagents were radiolabelled with the aim of being employed in one-pot reactions. The goal of this strategy was to improve radiolabelling efficiency and widen the extent of transformations beyond that of [^{18}F]fluoride. This concept was explored by M. K. Nielsen and co-workers in labelling 2-pyridinesulfonyl fluoride (PyFluor) under no-carrier-added conditions giving a RCY of 88% ± 2% (n = 3) (Scheme 1.3).[65] The synthesis was inspired by previous investigations into

stability of sulfonyl fluorides and their radiolabelling starting from [^{18}F]fluoride and sulfonyl chlorides.[66] The application of [^{18}F]PyFluor was demonstrated by radiolabelling a protected sugar using a strong base 7-methyl-1,5,7-triazabicyclo[4.4.0]dec-5-ene (MTBD) in a proof of concept deoxy-radiofluorination reaction.



Scheme 1.3 Radiosynthesis and application of [^{18}F]PyFluor

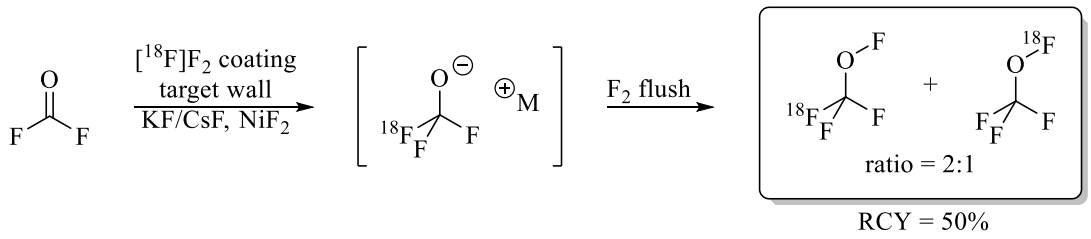
Xenon difluoride has been labelled with fluorine-18 *via* isotopic exchange using an activated form of [^{18}F]fluoride (Scheme 1.4).[67] No exchange was observed between xenon difluoride and [^{18}F]fluoride, therefore a mixture of [^{18}F]TBAF and sulfuryl chloride fluoride was added to HF, SiF_4 or AsF_6 producing carrier-added [^{18}F]HF, [^{18}F]SiF_4 or [^{18}F]AsF_6. To this mixture was added xenon difluoride affording [^{18}F]xenon difluoride in 30% RCY. Unreacted reagents were subsequently removed by vacuum to give isolated [^{18}F]xenon difluoride. The mechanism of this reaction proceeds *via* fluoride exchange between the well-established xenon species XeF^+ and $Xe_2F_3^+$ in equilibrium.



Scheme 1.4 Radiosynthesis of [^{18}F]xenon difluoride by isotopic exchange

1.4.3 Methods for Producing Electrophilic [^{18}F]Fluorinating Reagents

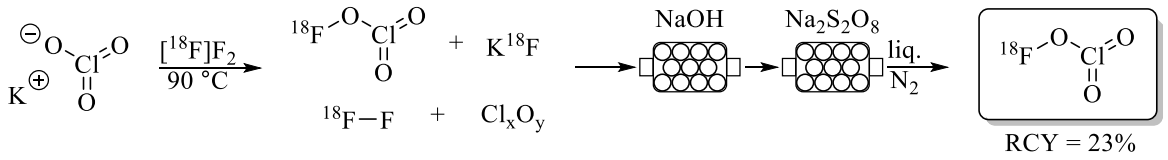
Despite the fact that [^{18}F]F_2 is not an ideal radiolabelling agent, it has been used to radiolabel a number of electrophilic reagents that possess greater selectivity. Some of the earliest radiolabelled fluorinating reagents were small, highly reactive molecules containing O-F bonds. Such a reagent is gaseous [^{18}F]trifluoromethyl hypofluorite which has been formed from the reaction between carbonyl fluoride and potassium or caesium fluoride in the presence of [^{18}F]F_2, generated from the ^{20}Ne(d,α)^{18}F reaction (Scheme 1.5).[68] Initially, the walls of a nickel cyclotron target were coated with nickel difluoride and potassium or caesium fluoride. The chamber was filled with neon gas and bombarded to form [^{18}F]F_2 which adhered to the target walls. The target was evacuated and carbonyl fluoride combined with fluorine gas was added to form [^{18}F]trifluoromethyl hypofluorite *via* the trifluoromethoxide ion in 50% RCY. Although [^{18}F]trifluoromethyl hypofluorite has a boiling point of -95 ºC, it is stable in glass and can even be in contact with water for days without apparent reaction.



Scheme 1.5 Radiosynthesis of [^{18}F]trifluoromethyl hypofluorite

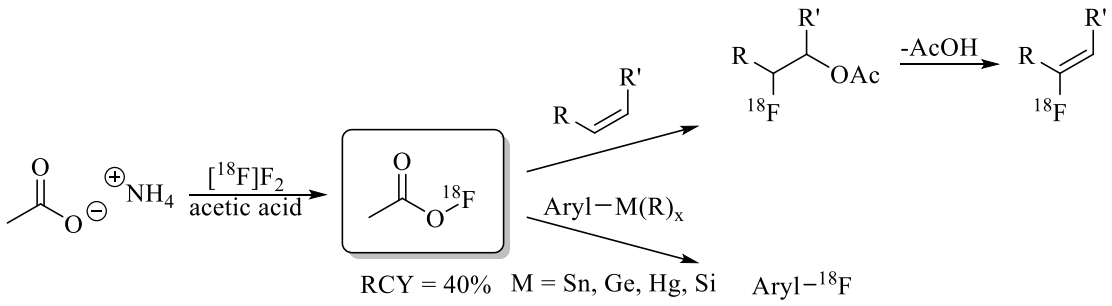
[^{18}F]Perchloryl fluoride has been synthesised by passing [^{18}F]F_2 over potassium chlorate at 90 ºC (Scheme 1.6).[69] The gaseous products were passed through a column of solid sodium hydroxide and sodium thiosulfate, to remove unreacted F_2 or any chlorine oxides, before isolating [^{18}F]perchloryl fluoride in 23% RCY by condensing with liquid nitrogen. Analysis

was carried out using gas chromatography and [^{18}F]aryl fluorides were prepared in 1% – 8% overall RCYs from reaction with aryl lithium precursors. A non-carrier added synthesis of [^{18}F]perchloryl fluoride starting from [^{18}F]fluoride has been reported, however the investigation concluded that the procedures were unreliable, very low RCYs were obtained and a majority of experiments failed.[70]



Scheme 1.6 Radiosynthesis of [^{18}F]perchloryl fluoride

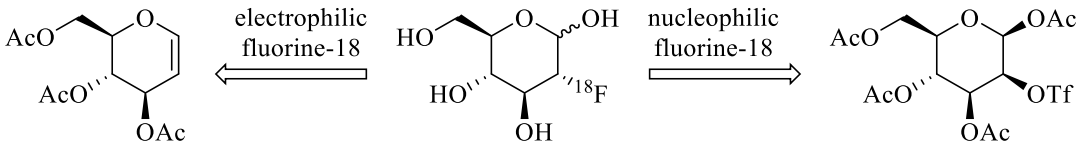
[^{18}F]Acetyl hypofluorite is a more accessible fluorinating reagent than [^{18}F]F_2 due to greater selectivity and ease of handling. It adds to aromatics and olefins, such as in the formation of 6-[^{18}F]fluoro-L-DOPA, and can be used to perform fluoro-demetallation of tin, germanium, mercury and silicon compounds.[71,72,73] [^{18}F]acetyl hypofluorite is a liquid at room temperature and has been synthesised from the reaction between [^{18}F]F_2 and ammonium acetate (Scheme 1.7).[74] [^{18}F]F_2 was bubbled through a solution of ammonium acetate in glacial acetic acid affording [^{18}F]acetyl hypofluorite in 40% RCY which was used immediately for subsequent reactions. Exchanging the cation for alkali metals was explored but with no improvement in RCY.



Scheme 1.7 Radiosynthesis and application of [^{18}F]acetyl hypofluorite

The addition of [^{18}F]acetyl hypofluorite to double bonds in sugars is a strategy that has been implemented when labelling clinically relevant molecules such as 2-deoxy-2-[^{18}F]fluoro-D-glucose ([^{18}F]FDG). In contrast, [^{18}F]FDG synthesis employing [^{18}F]trifluoromethyl hypofluorite or [^{18}F]perchloryl fluoride has not been reported. [^{18}F]FDG, mediated by [^{18}F]acetyl hypofluorite, was afforded in a higher RCY than with [^{18}F]F_2, 24% RCY compared to 8% and a molar activity of 0.025 GBq μmol^{-1} compared to 0.032 GBq μmol^{-1} (Table 1.4).[75,76,77] [^{18}F]acetyl hypofluorite demonstrated a higher selectivity in generating [^{18}F]FDG in 98% RCP, whereas [^{18}F]F_2 afforded a three-to-one mixture with the mannose derivative.

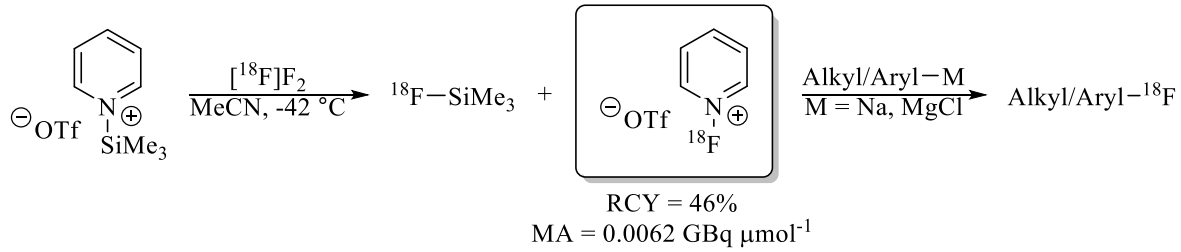
Table 1.4 Properties of fluorine-18 sources and their utility in forming [^{18}F]FDG[74–78]



Source of Fluorine-18	Reagent Properties	RCY	Molar Activity (GBq μmol^{-1})	Synthesis Time (min)
[^{18}F]F_2	bp = -188 ºC; toxic; strong oxidiser; generates HF upon contact with moisture; special apparatus required	8%	0.032	110
[^{18}F]CF_3OF	bp = -97 ºC; highly toxic; strong oxidiser; stable in water and glass	-	-	-
[^{18}F]$FClO_3$	bp = -47 ºC; highly toxic; strong oxidiser; highly explosive upon contact with organics	-	-	-
[^{18}F]AcOF	bp = 53 ºC; unstable at rt; explosive when concentrated	24%	0.025	60
[^{18}F]XeF_2	solid at rt; strong oxidiser; contamination and moisture may cause explosion or release of HF	15%	-	60
[^{18}F]TBAF	solid at rt; reacts with strong acids to form HF	58%	>94	70

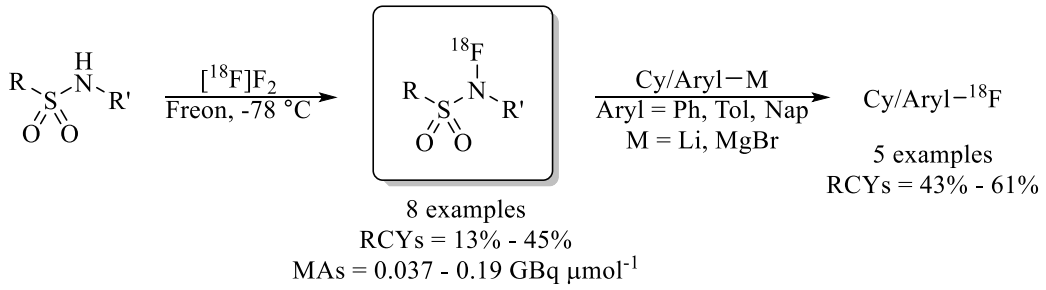
The application of [^{18}F]xenon difluoride to synthesise [^{18}F]FDG has been reported although molar activity was not recorded and the method has not been explored further.[78] The synthesis of [^{18}F]FDG only became highly valuable clinically with the discovery of a method employing nucleophilic substitution, utilising the reaction between mannose triflate and [^{18}F]TBAF. This afforded RCYs as high as 58% and very high molar activities were obtained due to almost undetectable amounts of unlabelled product.[79]

In the search for radiolabelled electrophilic fluorinating reagents possessing greater selectivity, a milestone was reached by labelling various N-F reagents with fluorine-18. In comparison to O-F reagents, N-F reagents are not hygroscopic and they possess higher levels of stability whilst retaining reactivity. *N*-Fluoropyridinium triflate was first labelled with fluorine-18 by the reaction between a trimethylsilane precursor and [^{18}F]F_2 in acetonitrile at -42 ºC (Scheme 1.8).[80] Evaporation of the solvent, precipitation and filtration afforded solid *N*-[^{18}F]fluoropyridinium triflate in 46% RCY. Iodometric titration was used to calculate molar activity giving 0.0062 GBq μmol^{-1} since conventional TLC or HPLC methods failed, and mass spectrometry and ^{19}F NMR spectroscopy were used to confirm the identity after the sample had decayed. Initial investigations demonstrated a reactivity with aryl and alkyl Grignards and sodium substrates. The analogue 1-fluoro-2-pyridone has also been radiolabelled in 37% RCY and 0.004 GBq μmol^{-1}.[81]



Scheme 1.8 Radiosynthesis of *N*-[^{18}F]fluoropyridinium triflate

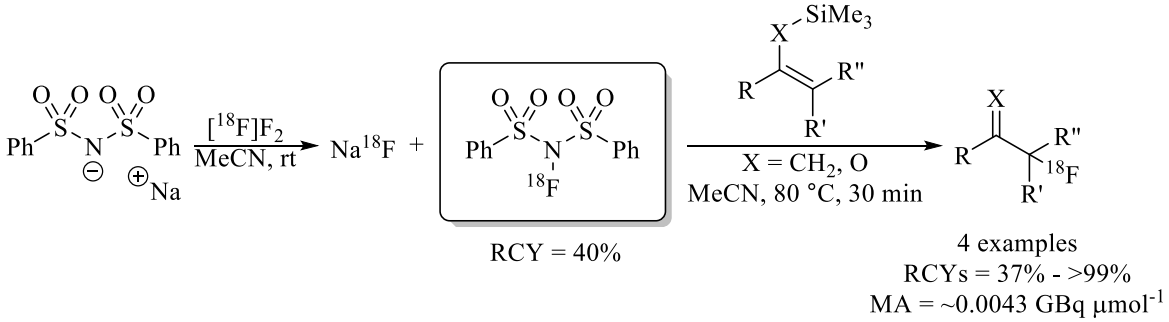
N-Fluoro-*N*-alkylsulfonamides were labelled with fluorine-18 by bubbling $[^{18}F]F_2$ into a solution of the respective sulfonamide in Freon at -78 ºC (Scheme 1.9).[82] Evaporation at room temperature afforded the *N*-[^{18}F]fluoro-*N*-alkylsulfonamide compounds in at least 90% RCP which were generally stable under HPLC and TLC conditions, an advantageous property over *N*-[^{18}F]fluoropyridinium compounds. A number of alkylsulfonamides were synthesised using this method achieving RCYs up to 45% and molar activities up to 0.19 GBq μmol^{-1} when synthesising *N*-[^{18}F]fluoro-*endo*-norbornyl-*p*-tolylsulfonamide. Subsequent investigations into reactivity demonstrated that *N*-[^{18}F]fluoro-*N*-alkylsulfonamides were somewhat efficient in labelling organometallic compounds such as alkyl or aryl lithium or Grignard substrates in up to 61% RCY.



Scheme 1.9 Radiosynthesis and application of *N*-[^{18}F]fluoro-*N*-alkylsulfonamides

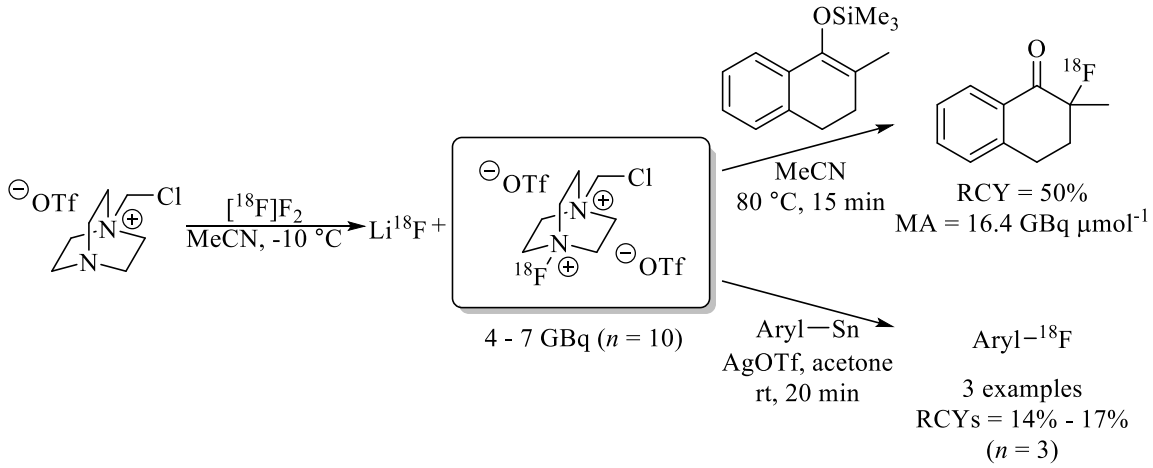
In comparison to *N*-fluoropyridinium compounds, *N*-fluorobenzenesulfonimide (NFSi) possesses much greater reactivity and has been widely used in the pharmaceutical industry due to its favourable combination of high reactivity and ease of synthesis.[43,83] The formation of *N*-[^{18}F]fluorobenzenesulfonimide ([^{18}F]NFSi) was achieved by bubbling $[^{18}F]F_2$ into an aqueous acetonitrile solution of the sodium salt of dibenzenesulfonamide (Scheme 1.10).[84] Evaporation at 110 ºC afforded a one-to-one mixture of [^{18}F]NFSi and [^{18}F]sodium fluoride, as identified by radio-HPLC analysis. The residue was redissolved in acetonitrile for use without further purification affording [^{18}F]NFSi in a RCY of 40% and a total synthesis time

of 30 minutes. Proof of principle reactivity was demonstrated using allyl silanes and silyl enol ethers to produce labelled allylic fluorides and α-fluorinated ketones in 37% – >99% RCYs with an approximate molar activity of 0.0043 GBq μmol^{-1}.



Scheme 1.10 Radiosynthesis and application of [^{18}F]NFSi

The emergence of [^{18}F]Selectfluor represented a major advancement in labelled electrophilic fluorination reagents because Selectfluor is easy to handle, stable and has superior reactivity, demonstrating a wide substrate scope.[85,86] [^{18}F]Selectfluor bis(triflate) was chosen as the target in the radiosynthesis, in preference to the bis(tetrafluoroborate) salt, to avoid isotope exchange. [^{18}F]F_2 was bubbled through an acetonitrile solution of 1-chloro-methyl-4-aza-1-azoniabicyclo[2.2.2]octane triflate and lithium triflate at -10 ºC (Scheme 1.11). [^{18}F]Selectfluor bis(triflate) was formed instantly and dried at 80 ºC before reformulating for use in further reactions, giving a total synthesis time of 25 minutes. The RCY and molar activity could not be measured because [^{18}F]Selectfluor retains poorly on HPLC columns, preventing separation from [^{18}F]lithium fluoride. The reaction between [^{18}F]Selectfluor and a silyl enol ether was examined with the resultant product being afforded in 50% RCY and 16.4 GBq μmol^{-1}. Generating [^{18}F]Selectfluor from [^{18}F]F_2 is therefore assumed to be >99% efficient, according to the theoretical maximum RCY of 50% when employing ^{18}F-F. High molar activity was achieved by deriving [^{18}F]F_2 from [^{18}F]fluoride.

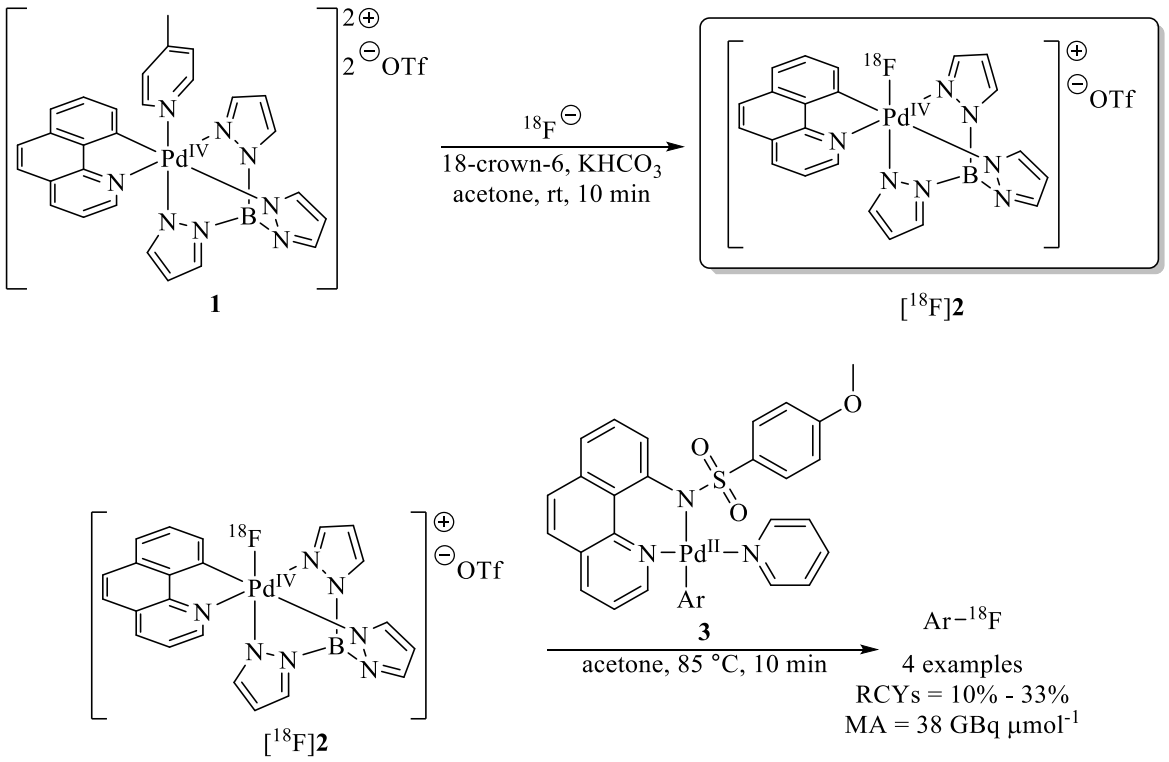


Scheme 1.11 Radiosynthesis and application of [^{18}F]Selectfluor bis(triflate)

This evolution in labelling electrophilic fluorinating reagents with fluorine-18 has demonstrated that the radiosynthesis of stable, reactive, selective and easy to handle reagents is possible. However the major limitations of these methods demonstrate a lack of accessible syntheses, low AYs and/or low molar activities, thus limiting their acceptance by the wider PET imaging community. This can be explained in part by the fundamental limitations inherent in [^{18}F]F_2 production, hence attention in the last 10 years has been focussed on employing high molar activity [^{18}F]fluoride to generate electrophilic fluorinating reagents labelled with fluorine-18.

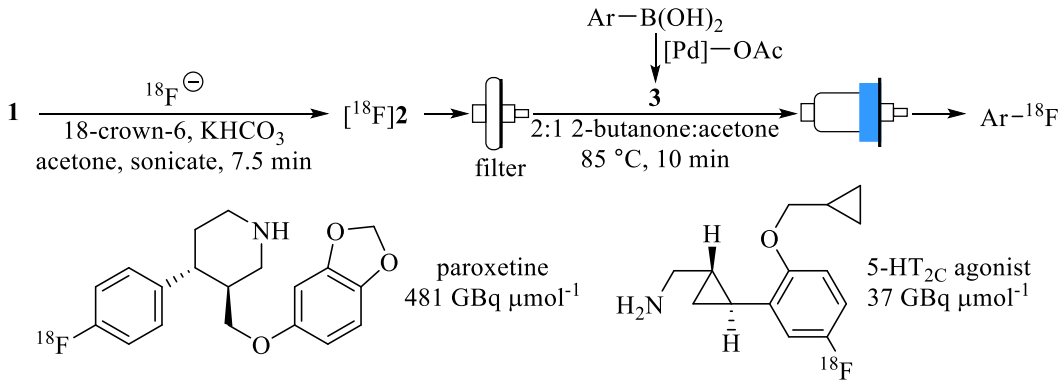
The first successful high molar activity electrophilic fluorination was reported in 2011 where a palladium-based electrophilic fluorinating reagent [^{18}F]**2**, derived from [^{18}F]fluoride, enabled late-stage fluorination of conventionally inaccessible PET tracers (Scheme 1.12).[87] The palladium centre in complex **1** carries three positive charges so favourably accepts [^{18}F]fluoride to form complex [^{18}F]**2** which is stable to water and heat. Palladium is an example of a late transition metal which, upon reduction from a high to low oxidation state such as Pd^{IV} to Pd^{II}, can transfer a ligand to a nucleophile. Hence, reduction of palladium in complex [^{18}F]**2** allows transfer of fluorine-18, acting as an electrophilic fluorinating

reagent.[88] To prevent unwanted C-F reductive elimination or nucleophilic attack at Pd, caused by the highly polarising nature of fluorine, benzo[*h*]quinolyl and tetrapyrazole borate ligands were employed. The only LUMO available for nucleophilic attack is that of the Pd-F sigma antibonding orbital because these ligands block any other trajectory. An arylboronate substrate and a palladium acetate precursor were reacted to form Pd^{II} complex **3**. Subsequent addition to complex [^{18}F]**2** initiated transposition of ^{18}F *via* reductive elimination of an intermediate Pd^{IV} complex, affording the labelled aryl fluoride product. To demonstrate clinical applicability of this method, four example compounds of PET radiotracers were labelled in 10% – 33% RCY with one measurement of molar activity yielding 38 GBq μmol^{-1}.



Scheme 1.12 Radiosynthesis and application of a palladium-based electrophilic fluorinating reagent starting from [^{18}F]fluoride

The clinical relevance of this method was advanced in a follow-up report using complex [^{18}F]**2** to label the two radiotracers paroxetine and a 5-HT$_{2C}$ agonist with fluorine-18 achieving high levels of activity with an automated procedure (Scheme 1.13).[89] A two-step automated procedure was developed starting from the formation of palladium complex [^{18}F]**2** followed by filtration and reaction with preformed aryl-palladium complex **3** to afford the final compound. Paroxetine and the 5-HT$_{2C}$ agonist were labelled with a molar activity of 481 GBq μmol^{-1} and 37 GBq μmol^{-1} and were both subsequently used in non-human primate PET imaging studies.

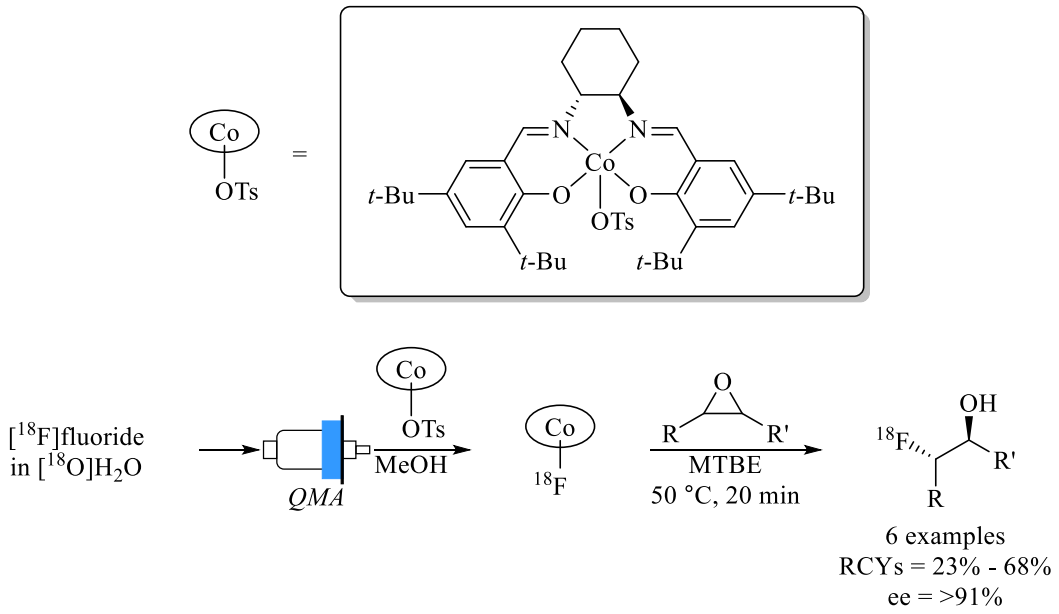


Scheme 1.13 Automation procedure using palladium-based electrophilic fluorinating reagent for PET studies of two radiotracers

This palladium based electrophilic fluorinating reagent showcases the development of a novel fluorinating reagent that enables radiolabelling of electron rich and electron deficient compounds containing a variety of functional groups. These transformations are otherwise challenging if conventional fluorination techniques were employed. Developing an automated synthesis and carrying out PET studies are ways of demonstrating real-world applicability. However, there are limitations to the scope and feasibility of this method. Currently the method does not tolerate nucleophilic or basic functional groups such as tertiary alkyl amines, although pyridine substituents are tolerated. Substrate synthesis and

radiolabelling of complex **3** is difficult to achieve when it contains substituents other than the hydrogen atom σ- to the site of palladium coordination. Additionally, knowledge of practical organometallic chemistry is required for synthesising the palladium-complexed substrates, limiting its recognition as a commercially viable method by the PET imaging community.

The precedent set by labelling an electrophilic reagent containing a transition metal-fluorine complex was followed by investigations into the production of other metal-fluorine complex reagents from high molar activity [^{18}F]fluoride. A chiral (salen)CoF complex was labelled with fluorine-18 and used to carry out enantioselective late-stage fluorination of epoxides under mild conditions forming [^{18}F]fluorohydrins, a motif found in radiotracers and the rare natural product 4-fluorothreonine (Scheme 1.14).[90]

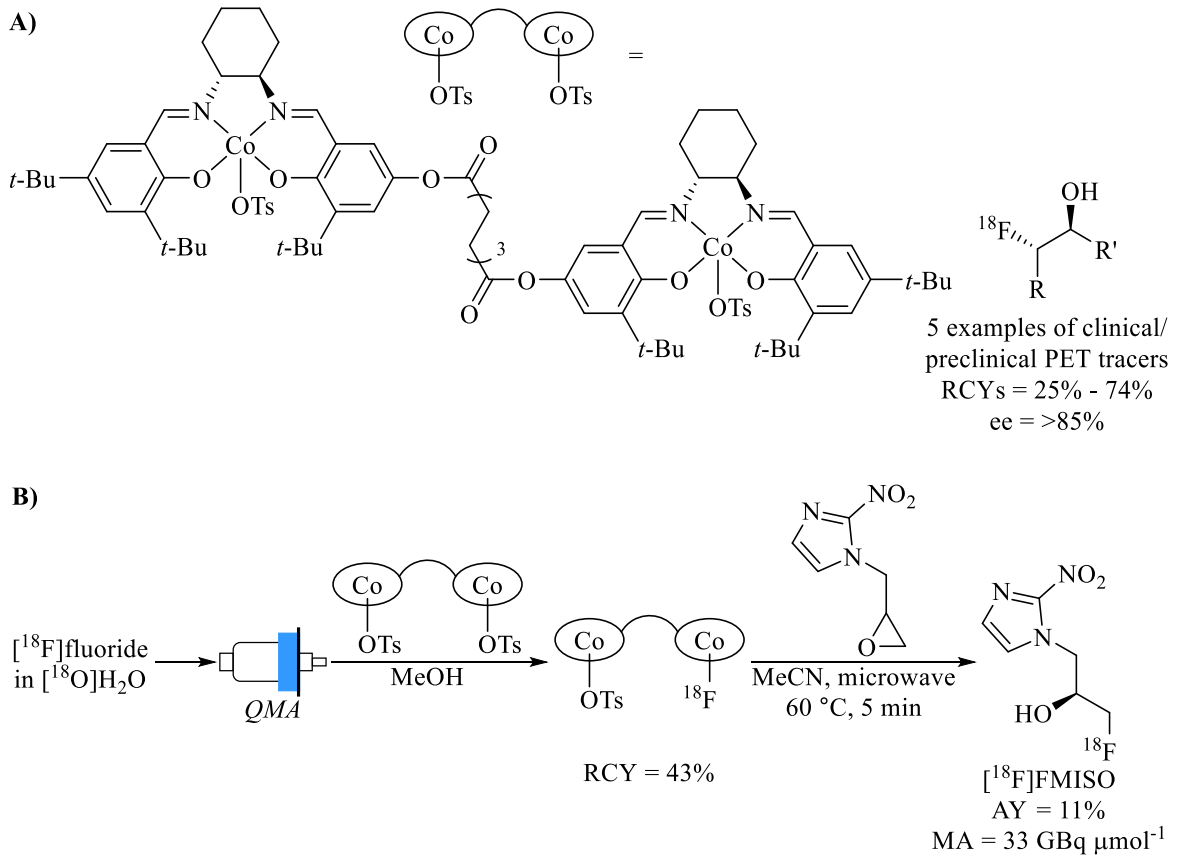


Scheme 1.14 Radiosynthesis and application of [^{18}F](salen)CoF

The synthesis of [^{18}F](salen)CoF was facilitated by eluting [^{18}F]fluoride trapped on a QMA with (salen)CoOTs in methanol. After evaporating to dryness and adding the epoxide

substrate in methyl *tert*-butyl ether (MTBE), the reaction mixture was heated at 50 ºC for 20 minutes to afford [^{18}F]fluorohydrins. Six examples were reported affording 23% – 68% RCYs (n = 3) with >91% enantiomeric excess (ee).

This strategy was made more compatible with Lewis basic nitrogen functionalities, prevalent among bioactive substrates, through dimerization of the metal complex which increased the rate of fluorination by intramolecular reaction (Scheme 1.15, A). The proposed mechanism involves coordination of one cobalt centre with the epoxide oxygen whilst [^{18}F]fluoride is delivered by the other cobalt centre.[91] Five examples of clinical or preclinical PET tracers were radiolabelled in 25% – 74% RCY with >85% ee.

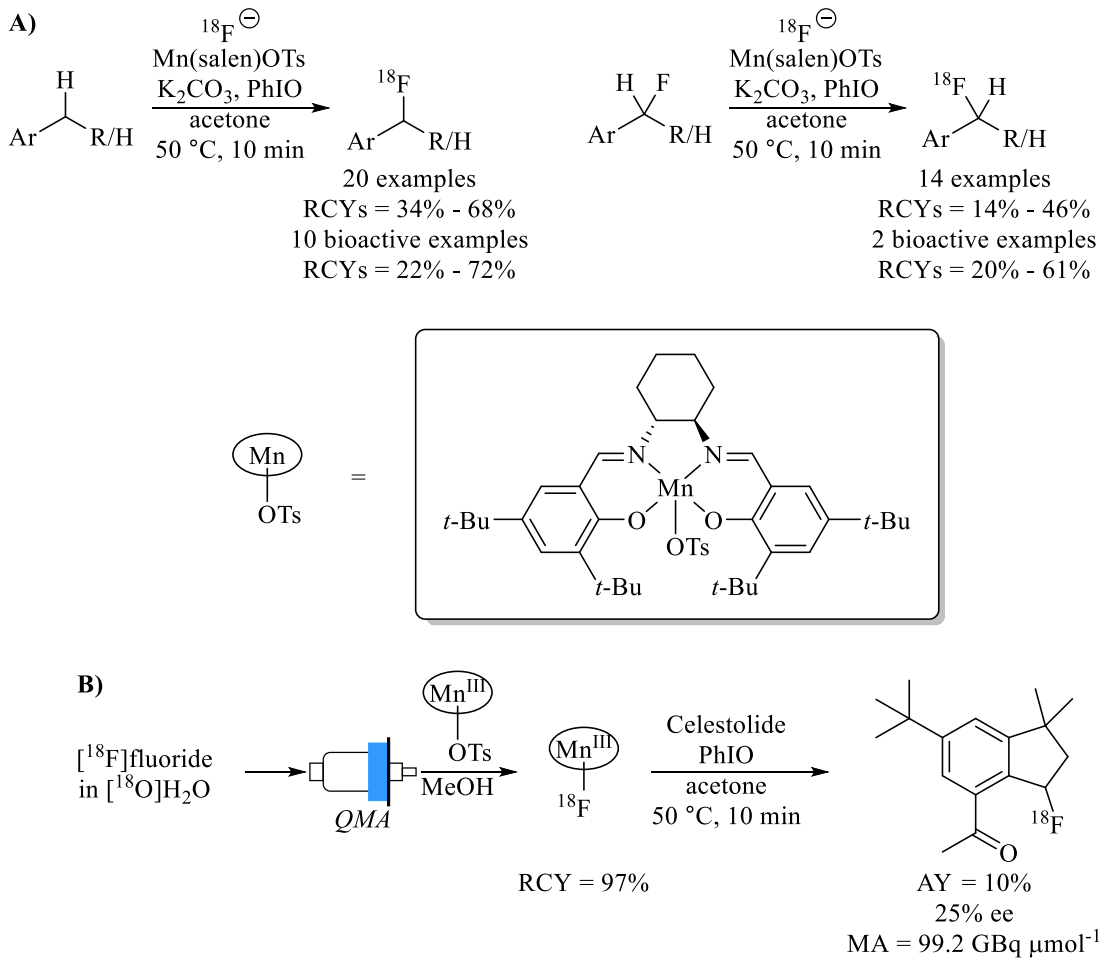


Scheme 1.15 A) Radiosynthesis of PET tracers using a dimeric cobalt catalyst;

B) automated procedure for labelling [^{18}F]FMISO

This method was improved to make it more amenable to automation and, by extension, ready for use in PET imaging studies (Scheme 1.15, B). [^{18}F]fluoride trapped on a QMA was eluted in 43% RCY by the dimeric cobalt catalyst before introducing microwave heating in the presence of the substrate for 5 minutes at 50 ºC. Filtration was followed by isolation of the product by HPLC. Using this procedure, the hypoxia imaging agent [^{18}F]FMISO was isolated with an activity yield of 11% and molar activity of 33 GBq μmol^{-1}. This method is limited by the required usage of protecting groups to label molecules containing Lewis basic groups. Other limitations include the use of a microwave reactor in the automation procedure, poor [^{18}F]fluoride elution efficiency with the dimeric catalyst and formation of large amount of precipitate after reaction quenching. This makes purification by HPLC difficult without manual intervention.

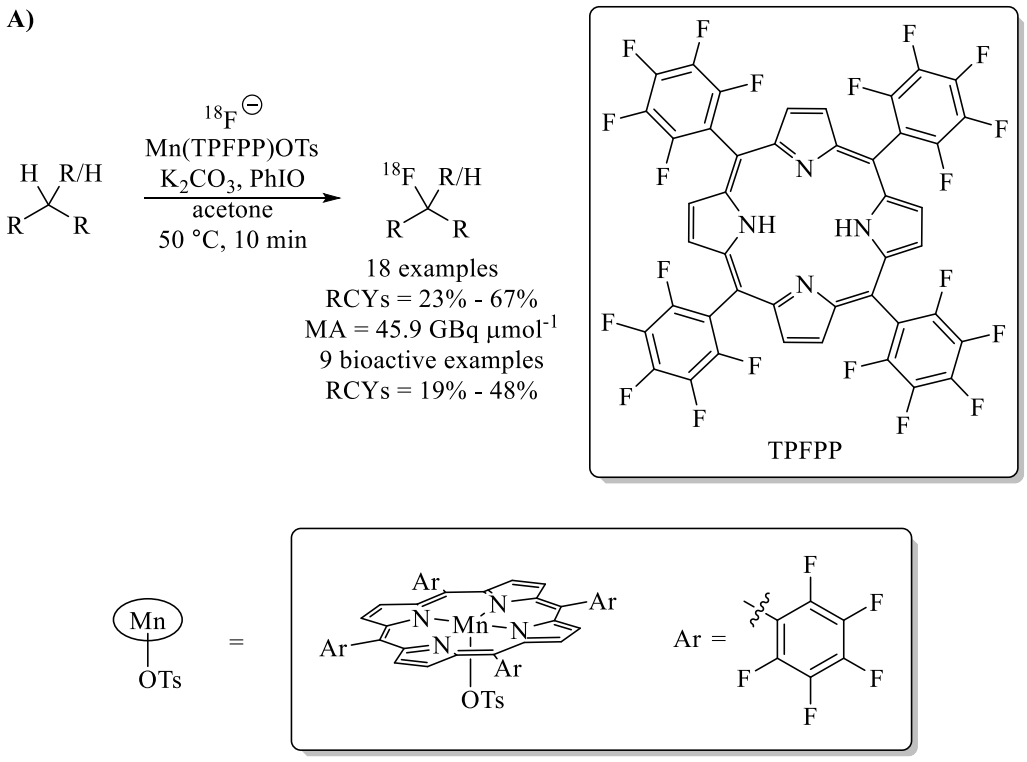
A similar experimental design was implemented for labelling a manganese-fluorine reagent with fluorine-18, allowing selective radical fluorination of C-H bonds in bioactive molecules. [^{18}F]Mn(salen)F was generated *in situ* through the introduction of [^{18}F]fluoride and Mn(salen)OTs.[92] Complex-mediated fluorination of benzylic C-H bonds was performed in acetone at 50 ºC by addition of iodosylbenzene (Scheme 1.16, A). This method was made amenable to automation by eluting [^{18}F]fluoride trapped on a QMA as [^{18}F]Mn(salen)F by using a methanolic solution of Mn(salen)OTs (Scheme 1.16, B). The ensuing reaction with Celestolide afforded the labelled product in 10% AY, 25% ee, and the molar activity calculated at the end of bombardment was 99.2 GBq μmol^{-1}.

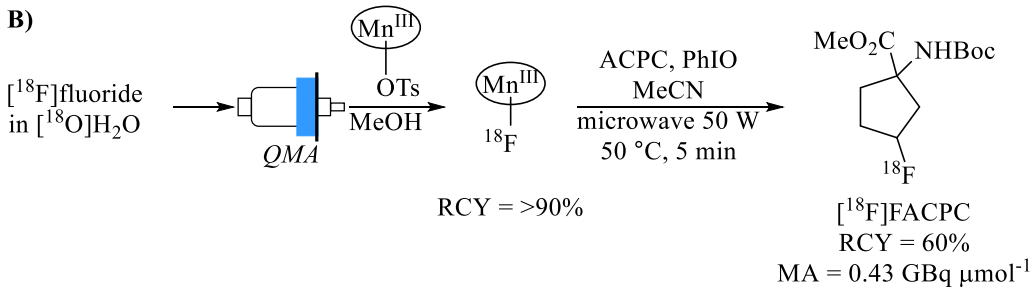


Scheme 1.16 A) Radiosynthesis of benzyl fluorides using [^{18}F]Mn(salen)F formed *in situ*; B) automated method for forming [^{18}F]Mn(salen)F and labelling Celestolid

Iodosylbenzene is used as an oxidant and the proposed mechanism involves formation of an intermediate I-F compound *in situ* which subsequently fluorinates the manganese catalyst. However, oxidation of the manganese catalyst followed by an oxygen-rebound mechanism leads to competing oxidation of the substrate thus limiting the yield. A large amount of precipitate is formed during reaction quenching and iodosylbenzene was added in solid form to the reaction mixture, which prevent automating the synthesis, thus limiting the applicability of the method. Additionally, the method currently has little application in enantioselective fluorination due to the low ees obtained.

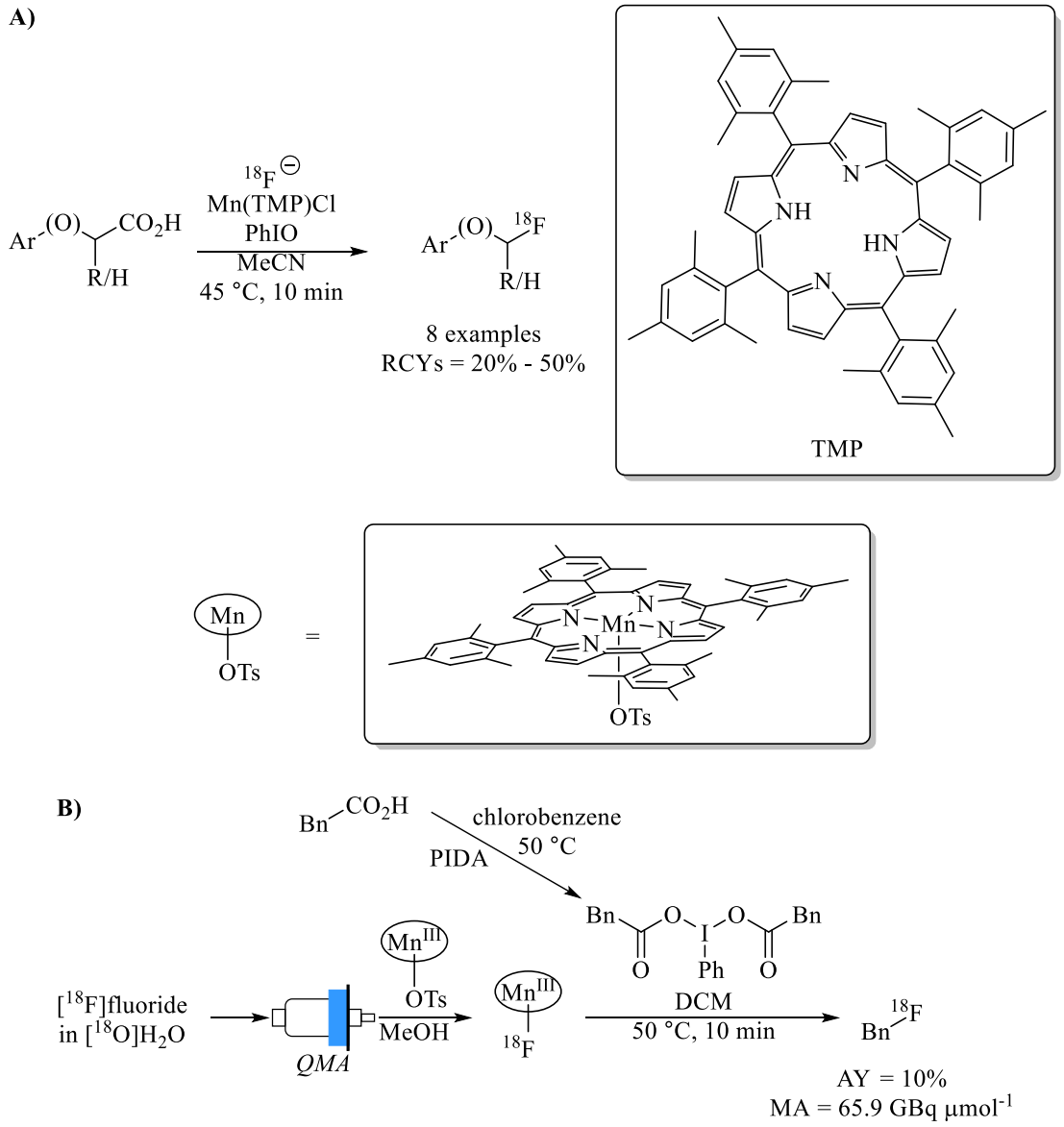
The reactivity of this manganese-fluorine complex was redefined by altering the ligand, and thus widening the substrate scope. A porphyrin ligand was adopted for carrying out fluorination of remote, unactivated C-H bonds.[93] C-H sites of alkanes were labelled with fluorine-18 by addition of [^{18}F]fluoride, iodosylbenzene and porphyrin-ligated manganese tosylate in acetone at 50 ºC (Scheme 1.17, A).[94] Tetrakis(pentafluorophenyl)porphyrin (TPFPP) was chosen as the optimal ligand due to the favourable steric and electronic properties it can induce on the manganese centre. The method was made more amenable to automation by elution of [^{18}F]fluoride from the QMA in >90% RCY using Mn(TPFPP)OTs, and by microwave reaction affording the labelled amino acid transporter [^{18}F]FACPC in 60% RCY with a molar activity of 0.43 GBq μmol^{-1} (Scheme 1.17, B). Synthesis of a model compound using a larger amount of activity gave a molar activity of 45.9 GBq μmol^{-1} calculated at the end of bombardment.





Scheme 1.17 A) Radiosynthesis of alkyl fluorides using [^{18}F]Mn(TPFPP)F formed *in situ*; B) method for forming [^{18}F]Mn(TPFPP)F and labelling FACPC

The reactivity could be altered by further ligand modification. Employing a tetramesitylporphyrin (TMP) ligand enabled the first decarboxylative [^{18}F]fluorination reaction of benzyl and aryloxy carboxylic acids starting from [^{18}F]fluoride (Scheme 1.18, A).[95] A number of carboxylic acids were fluorinated in 20% – 50% RCY by combining [^{18}F]fluoride with Mn(TMP)Cl and iodosylbenzene. This methodology of decarboxylative [^{18}F]fluorination has been employed for the convenient preparation of difluoromethylarenes and difluoromethoxyarenes labelled with fluorine-18.[96] To demonstrate real-world applicability, [^{18}F]benzyl fluoride was produced and isolated using conditions more amenable to automation (Scheme 1.18, B). The proposed iodine(III) carboxylate intermediate was formed beforehand by reaction of iodosobenzene diacetate (PIDA) with substrate, which could then be added as a solution. [^{18}F]fluoride was eluted from a QMA as [^{18}F]Mn(TMP)F and subsequent fluorination of the iodine(III) carboxylate intermediate afforded [^{18}F]benzyl fluoride in 10% AY with a molar activity of 65.9 GBq μmol^{-1} calculated at the end of bombardment.

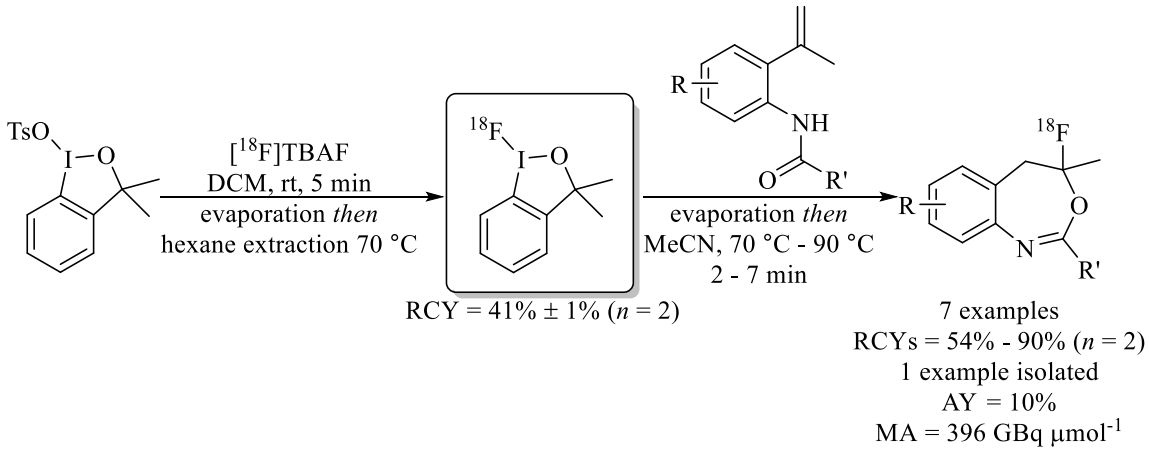


Scheme 1.18 A) Radiosynthesis of benzyl and aryloxy fluorides using [^{18}F]Mn(TMP)F formed *in situ*; B) method for forming [^{18}F]Mn(TMP)F and labelling [^{18}F]benzyl fluoride

Methodologies for labelling organic selective electrophilic fluorinating reagents from [^{18}F]fluoride have been designed to avoid the use of organometallic chemistry and synthesis of complex ligands. One example of this is the radiosynthesis of [^{18}F]fluoro-benziodoxole.[97] Fluoro-benziodoxole is a safe, stable and easy to handle reagent and is an apotheosis of the recent discoveries into applications of I-F reagents in organofluorine chemistry.[98] The wide reaction scope of [^{18}F]fluoro-benziodoxole addresses *gem*-difluorinations, oxyfluorinations,

fluorocyclisations, and other unprecedented fluorination-rearrangement and/or -cyclisation cascade reactions.

A report on the reaction of [^{18}F]TBAF with tosyl-benziodoxole in dichloromethane at room temperature for 5 minutes afforded [^{18}F]fluoro-benziodoxole in 41% ± 1% (n = 2) RCY (Scheme 1.19).[97] [^{18}F]fluoro-benziodoxole is unstable on silica so could not be analysed or isolated by TLC or HPLC. This obstruction to the purification of [^{18}F]fluoro-benziodoxole was overcome by concentrating the crude solution and extracting with hexane at 70 ºC. The RCY was increased significantly by increasing the extraction temperature with hexane above 40 ºC. The RCP was assumed to be 100% since neither TBAF, tosyl-benziodoxole nor the inorganic side products formed in the reaction are soluble in hexane. HRMS and ^{19}F NMR spectroscopic analyses of a decayed sample were carried out to confirm product isolation. A control experiment using these same conditions omitted the tosyl-benziodoxole reagent, revealing that only 7% of [^{18}F]TBAF activity is carried over by hexane extraction.



Scheme 1.19 Radiosynthesis of [^{18}F]fluoro-benziodoxole with application in fluorocyclisation reactions and oxyfluorination reactions of diazoketones

After extraction of [^{18}F]fluoro-benziodoxole, the hexane solution was added to the target substrate dissolved in acetonitrile, the mixture concentrated, and the residue redissolved in

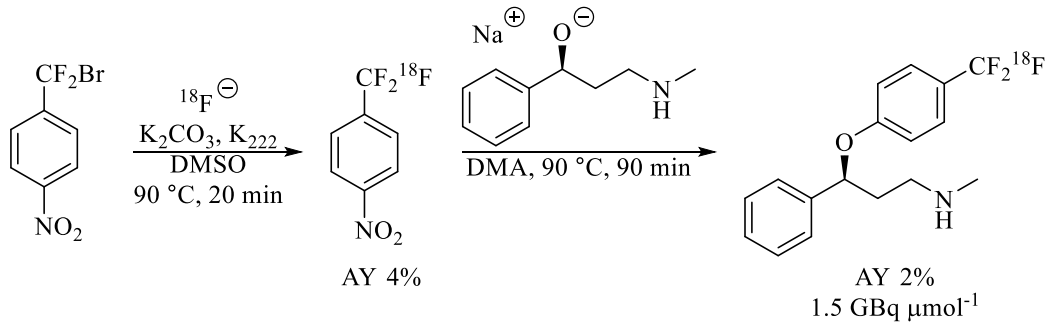
acetonitrile followed by heating. Seven examples of fluorocyclisation reactions were reported affording 54% – 90% (n = 2) RCYs. In a one-pot reaction, a product was isolated with an AY of 10%, a synthesis time of two hours and a molar activity of 396 GBq μmol^{-1}. To date, the method has not been automated. This may be attributed to the difficulty in performing phase separation and multiple evaporation procedures under automation conditions. However, the substrate scope has since been extended to [^{18}F]oxyfluorination of diazoketones by employing rhodium reagents as a means of activation.[99]

1.5 Methods for Labelling Other Fluorinated Motifs using [^{18}F]Fluorinating Reagents

Several highly important fluorinated motifs other than "-F" have been incorporated into biologically active drugs and radiotracers on account of their unique physicochemical properties and the favourable biological properties they can induce on a molecule.[100,101,102] These motifs include the trifluoromethyl "-CF_3", difluoromethyl "-CF_2H/R", trifluoromethylthio "-SCF_3", trifluoromethoxy "-OCF_3, and pentafluorosulfanyl "-SF_5" groups.

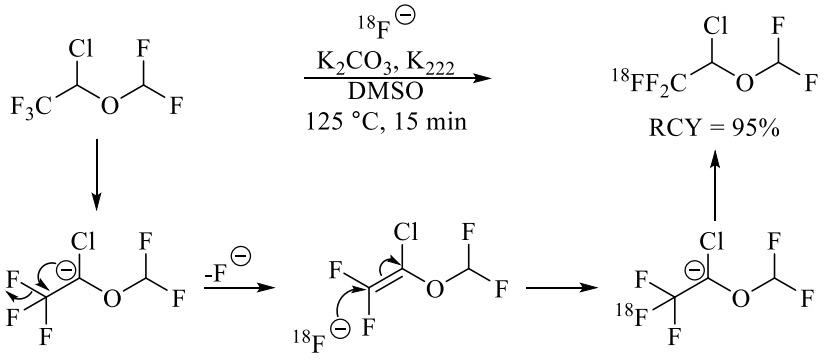
Since different fluorinated motifs introduce unique attributes onto molecules, many novel labelling strategies have been explored in order to radiolabel these motifs with the aim of expanding the toolkit of fluorine-18 technologies used for PET imaging. Various fluorinated motifs have been labelled through construction of a functionalised group, attached to the target molecule, followed by reaction with [^{18}F]fluoride. This was first achieved by halogen exchange, including isotope exchange with fluorine-19. For example, the trifluoromethyl group of Fluoxetine has been labelled with fluorine-18 in 4% AY by reaction of [^{18}F]fluoride, Kryptofix and potassium carbonate with 1-nitro-4-(bromodifluoromethyl)-

benzene in DMSO at 90 ºC (Scheme 1.20).[103] Subsequent nucleophilic displacement of the nitro group with an alkoxide precursor in DMA at 90 ºC for 90 minutes afforded [^{18}F]Fluoxetine in 2% AY and 1.5 GBq μmol^{-1} with a total synthesis time of 180 minutes.



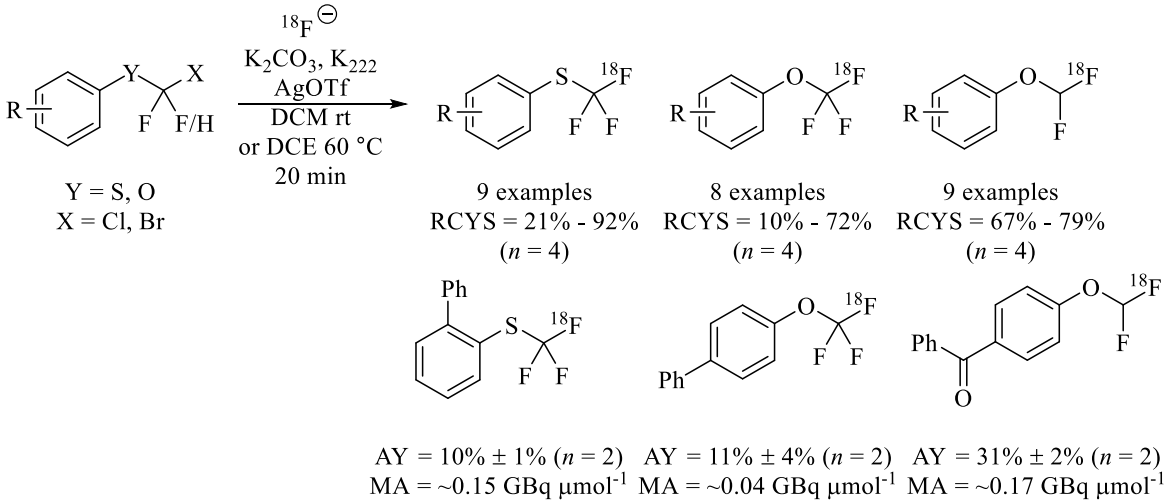
Scheme 1.20 Radiosynthesis of [^{18}F]Fluoxetine by halogen exchange

Isotope exchange has also been used to label inhalation anaesthetics, such as isoflurane (Scheme 1.21). [^{18}F]Fluoride, Kryptofix and potassium carbonate were combined with isoflurane in DMSO at 125 ºC for 15 minutes to initiate isotope exchange. The trifluoromethyl group of isoflurane increases the acidity of the adjacent proton, thus assisting isotope exchange and leading to higher fluorine-18 incorporation.[104] Due to the release of fluorine-19, a low molar activity is always obtained when carrying out isotope exchange reactions.



Scheme 1.21 Radiosynthesis of [^{18}F]isoflurane by isotope exchange

The most successful implementation of halogen exchange reactions can be seen in the labelling of aryl -$OCHF_2$, -OCF_3 and -SCF_3 derivatives. Corresponding motifs were labelled starting from the bromo- or chloro- precursors by combining [^{18}F]fluoride with silver triflate (Scheme 1.22).[105] Only electron rich substrates gave high RCYs and the loss of fluoride from the cationic intermediate resulted in a low molar activity. Additionally, precursor synthesis is not straightforward and it is very difficult or impossible to isolate the product from its precursor, especially for larger complex molecules.



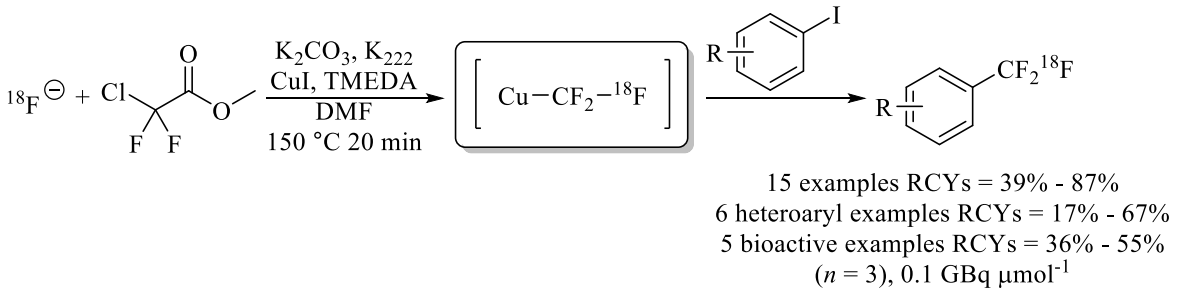
Scheme 1.22 Silver-mediated halogen exchange with [^{18}F]fluoride

Despite these advances in halogen exchange reactions, construction of fluorinated motifs by nucleophilic substitution remains an unresolved problem because of the negative effects α-fluorine substituents impose on a substitution centre. Fluorine has an electron withdrawing effect, destabilising the partial positive charge that forms at the centre during nucleophilic substitution, and there is electrostatic repulsion of incoming nucleophiles with the lone pairs on fluorine which hinders their approach.[106]

Constructing and radiolabelling complex prefunctionalised substrates is not an efficient or very successful strategy when labelling fluorinated motifs. An alternative strategy is to

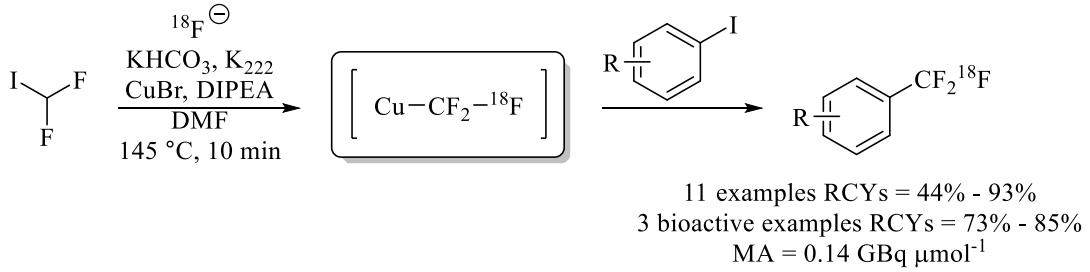
directly install the fluorinated motif, pre-labelled with fluorine-18, onto the target molecule. Ideally this is carried out in a one-pot reaction that use reactive functional groups easy to install onto substrates, such as halogens, hydroxyls and boronates, or by exploiting innate reactivity of the substrate, such as reacting with native C-H bonds. Two approaches to this strategy entail combining various reagents to form a reactive fluorinated intermediate *in situ*, or a prior synthesis and isolation of radiolabelled fluorinating reagents that then allow late-stage introduction of fluorinated motifs onto a variety of substrates.

An example of this first approach can be seen in labelling the trifluoromethyl group *via* copper-mediated trifluoromethylation of aryl iodides with [^{18}F]$CuCF_3$, formed *in situ* by combining [^{18}F]fluoride, difluorocarbene and copper(I) iodide (Scheme 1.23).[107] High temperature and iodide were used to activate methyl chlorodifluoroacetate to release difluorocarbene, carbon dioxide, methyl iodide and chloride. Reaction with [^{18}F]fluoride and $Cu^{(I)}$ generated [^{18}F]$CuCF_3$ which was stabilised using the ligand tetramethylethylenediamine (TMEDA) and DMF as the solvent. Subsequent coupling reactions with iodide substrates led to the formation of trifluoromethylated arenes and heteroarenes labelled with fluorine-18 in good RCYs. Disadvantages of this method include harsh labelling conditions, difficulty in isolating the final product and a low molar activity of 0.1 GBq μmol^{-1}.



Scheme 1.23 Radiosynthesis and application of [^{18}F]$CuCF_3$ formed *in situ* from [^{18}F]fluoride, difluorocarbene and copper(I) iodide

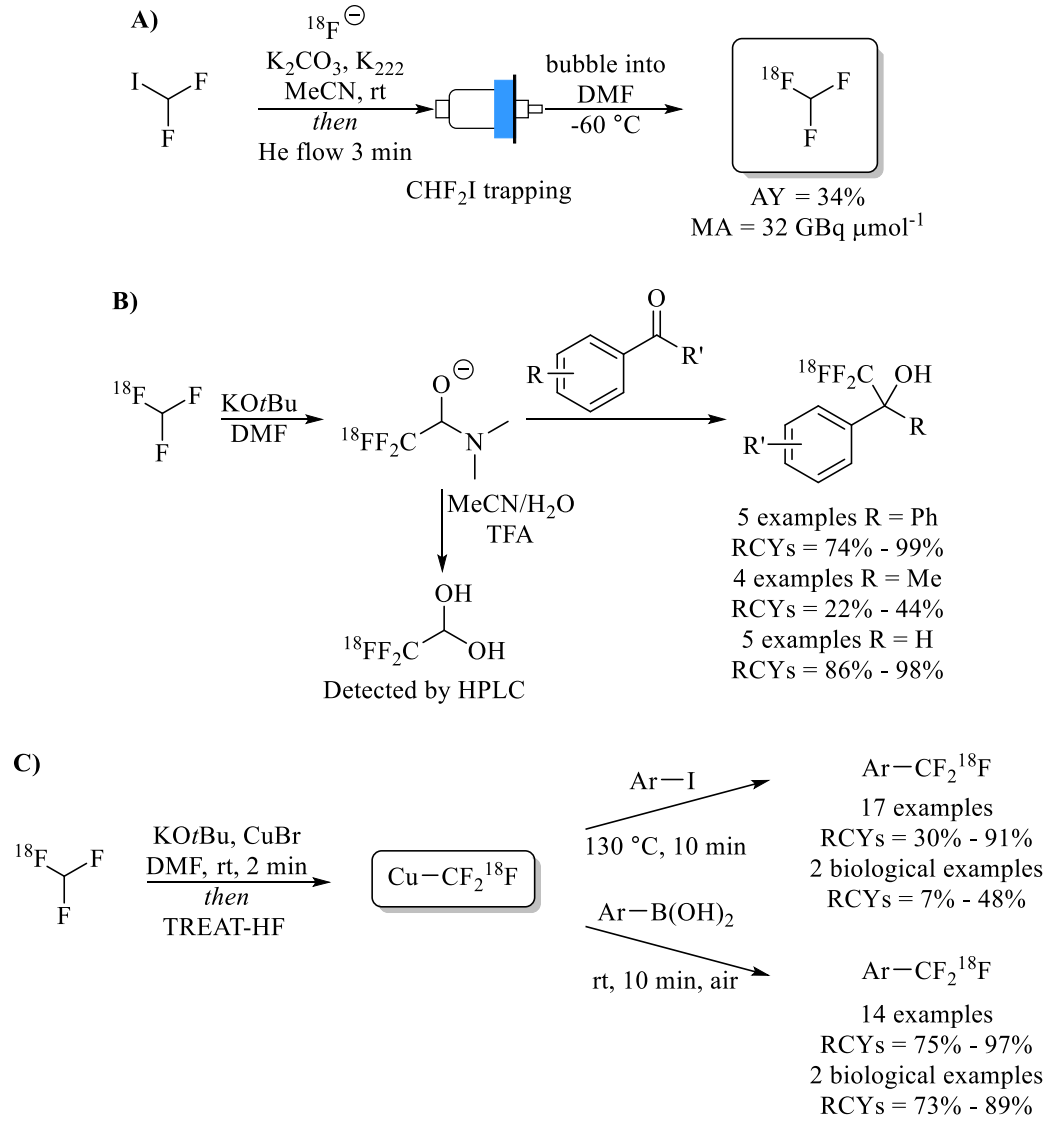
A similar radiosynthesis of [^{18}F]$CuCF_3$ was developed using modified conditions (Scheme 1.24).[108] The reaction of difluoro(iodo)methane with potassium hydrogen carbonate and Kryptofix in DMF at 145 ºC led to the release of hydrogen iodide and generation of difluorocarbene *in situ*. [^{18}F]$CuCF_3$ was formed *in situ* by reaction with [^{18}F]fluoride and copper(I) bromide with the ligand *N*,*N*-diisopropylethylamine (DIPEA) and DMF as solvent to increase stability. Aryl iodides were trifluoromethylated to afford trifluoromethyl arenes labelled with fluorine-18 in 44% – 93% RCYs with a measured molar activity of 0.14 GBq μmol^{-1}.



Scheme 1.24 Radiosynthesis and application of [^{18}F]$CuCF_3$ *in situ* starting from [^{18}F]fluoride, difluoro(iodo)methane and copper(I) bromide

Labelling gaseous fluoroform with fluorine-18 widened the substrate scope and molar activity for trifluoromethylation reactions. The reaction of [^{18}F]fluoride with difluoro(iodo)methane in the presence of Kryptofix and potassium carbonate in acetonitrile afforded [^{18}F]fluoroform (Scheme 1.25, A).[109] This was separated from difluoro(iodo)methane by passing the gaseous mixture through a QMA and condensing purified [^{18}F]fluoroform in DMF at -60 ºC or THF at -100 ºC in 88% or 96% trapping efficiency. Deprotonation of fluoroform with a base such as potassium *tert*-butoxide generally leads to decomposition into fluoride and difluorocarbene without the presence of a stabilising agent.[110] In this case, [^{18}F]fluoroform was deprotonated and stabilised by

reversible formation of an adduct with DMF (Scheme 1.25, B), which was either hydrated in acidic HPLC eluent to form the [^{18}F]fluoral hydrate for characterisation by HPLC, or was employed in nucleophilic addition with various electrophiles such as aldehydes and ketones.

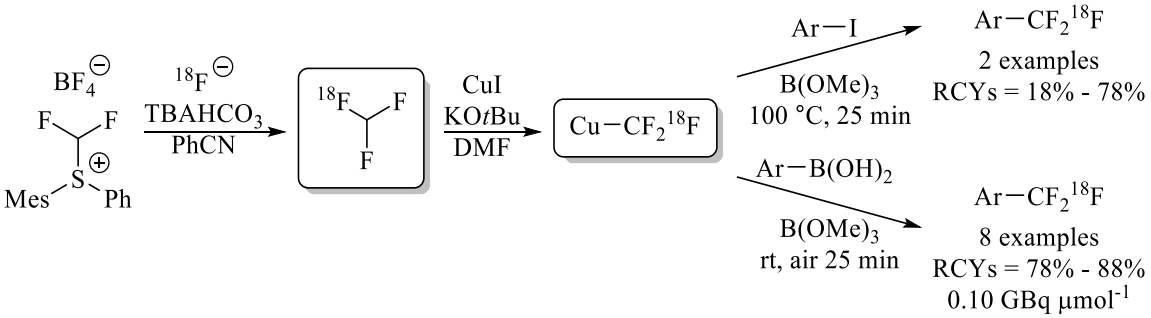


Scheme 1.25 Radiosynthesis, analysis and application of [^{18}F]fluoroform from difluoro(iodo)methane

Following extensive investigations into stability and reactivity of the trifluoromethyl anion, [^{18}F]$CuCF_3$ was formed and isolated from [^{18}F]fluoroform using copper(I) bromide (Scheme 1.25, C).[111,112,113] Addition of a stabilising agent such as TREAT-HF was essential in

isolating [^{18}F]$CuCF_3$ as this instigates precipitation of potassium ions as potassium fluoride, which would otherwise extract fluoride from [^{18}F]$CuCF_3$ leading to isotope exchange and decomposition.[111] Heating [^{18}F]$CuCF_3$ with aryl iodides in DMF afforded labelled trifluoromethyl arenes in good yields. Thermally unstable substrates were successfully labelled through reaction with arylboronic acids at room temperature in air.

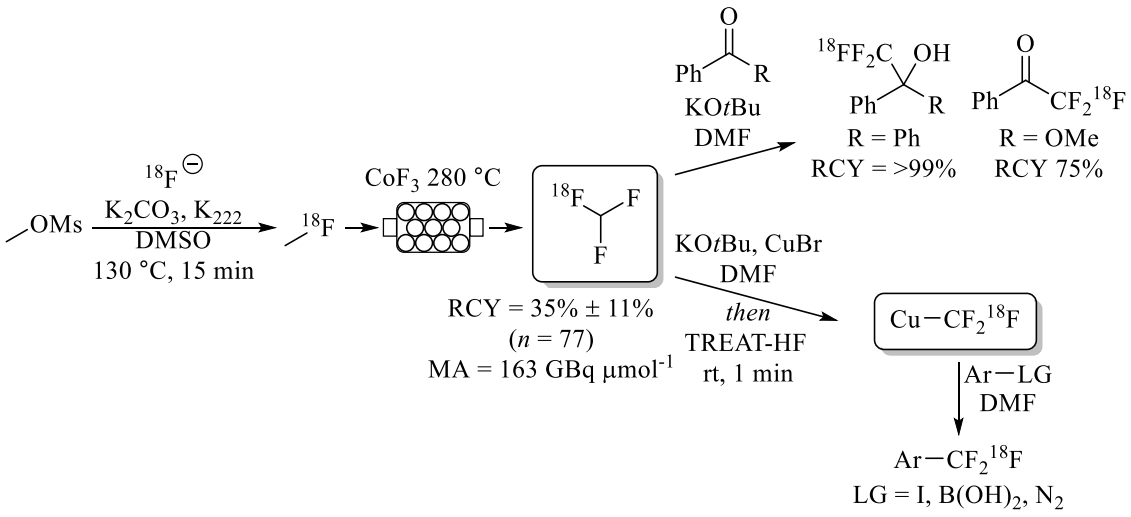
This method was not automated because difluoro(iodo)methane has a boiling point of 22 ºC, so this reagent was replaced by a difluoromethyl sulfonium salt (Scheme 1.26).[114] This allowed instant production of [^{18}F]fluoroform from a stable solid reagent which could be bubbling directly into a solution of copper(I) *tert*-butoxide generated *in situ* to form [^{18}F]$CuCF_3$. Reactions with aryl iodides and arylboronic acids afforded good yields, however the use of this new difluorocarbene reagent gave a high amount of unlabelled product, leading to a final molar activity of only 0.10 GBq μmol^{-1}. This method has also found use in labelling trifluoromethylthio- and trifluoromethylseleno- arenes from disulfides and diselenides.[115]



Scheme 1.26 Radiosynthesis and application of [^{18}F]fluoroform and [^{18}F]$CuCF_3$ from a solid difluorocarbene reagent

A novel strategy has been developed more recently for automated production of [^{18}F]fluoroform by treating methyl mesylate with [^{18}F]fluoride to form the gas

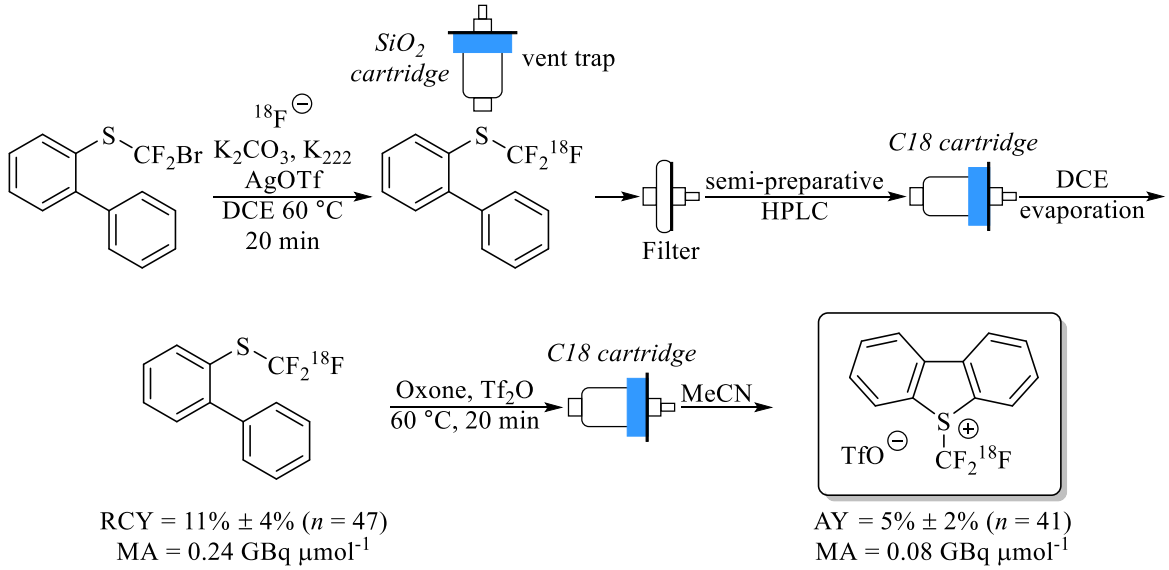
[^{18}F]fluoromethane (Scheme 1.27).[116] This was purified by gas chromatography, or by passing through an acetonitrile/dry ice condenser, and was collected using liquid argon. In the next step, the [^{18}F]fluoromethane was passed through a cobalt(III) trifluoride column heated to 280 ºC generating [^{18}F]fluoroform in 35% ± 11% (*n* = 77) AY and 98% ± 3% RCP. The maximum molar activity achieved was 163 GBq μmol^{-1} when starting with a [^{18}F]fluoride molar activity of 336 GBq μmol^{-1}. Proof of principle reactivity was demonstrated on a variety of substrates, such as a non-enolizable ketone, aryl esters, iodoarenes, arylboronic acids, and aryldiazonium salts, either by using [^{18}F]fluoroform or [^{18}F]$CuCF_3$ formed *in situ* from addition of potassium *tert*-butoxide and copper(I) bromide in DMF.



Scheme 1.27 Radiosynthesis and application of [^{18}F]fluoroform and [^{18}F]$CuCF_3$ from methyl mesylate

The electrophilic trifluoromethylating reagent commonly referred to as the Umemoto reagent has been labelled with fluorine-18 using a two-step process involving silver mediated halogen exchange followed by oxidative cyclisation (Scheme 1.28).[117] Fluorination of the brominated precursor in dichloroethane (DCE) at 60 ºC afforded the

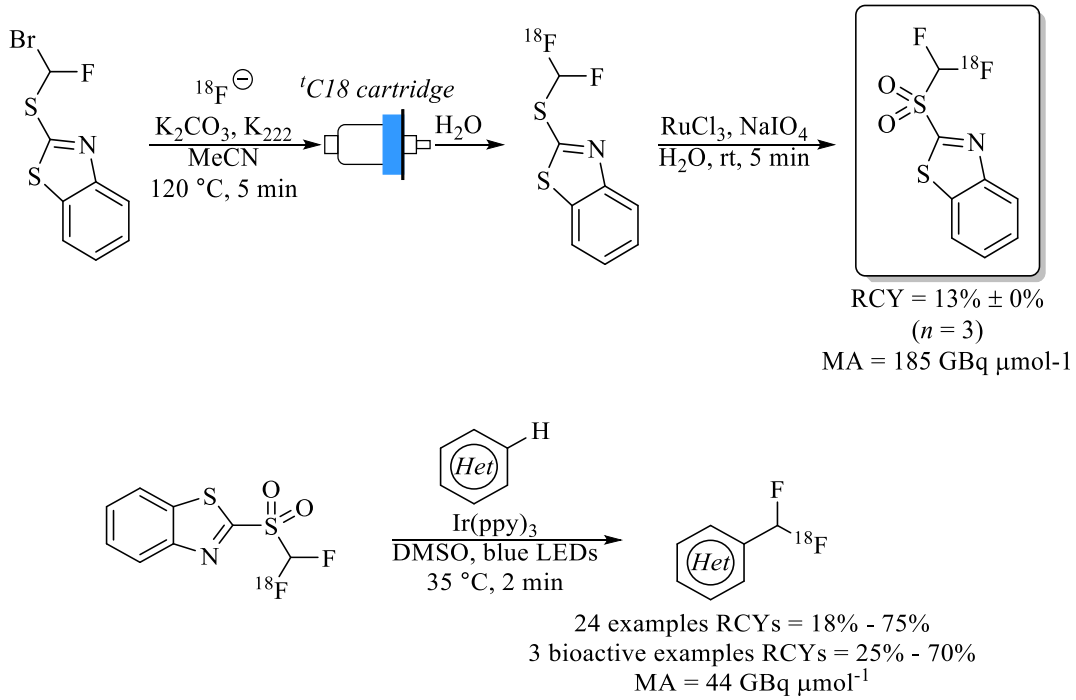
[^{18}F]trifluoromethylthiolated biphenyl compound in 11% ± 4% RCY (n = 47) and with a molar activity of 0.24 GBq μmol^{-1}. Solvent was evaporated using a vent charged with a SepPak SiO_2 cartridge to trap the volatile product. After eluting the trapped activity back into the reaction vial, filtration and semi-preparative HPLC led to product isolation. The product fraction in HPLC eluent was reformulated in dichloroethane using another SepPak C18 cartridge before reacting with potassium peroxymonosulfate (Oxone®) and triflic anhydride at 60 ºC. This facilitated oxidative cyclisation to the Umemoto reagent, isolated using another SepPak C18 cartridge and eluted with acetonitrile in 5% ± 2% AY (n = 41) with a molar activity of 0.08 GBq μmol^{-1}. The entire procedure has a synthesis time of several hours, is difficult to carry out, is highly sensitive to the quality of triflic anhydride used, has not been automated and is highly irreproducible.



Scheme 1.28 Radiosynthesis and application of the Umemoto reagent labelled with fluorine-18

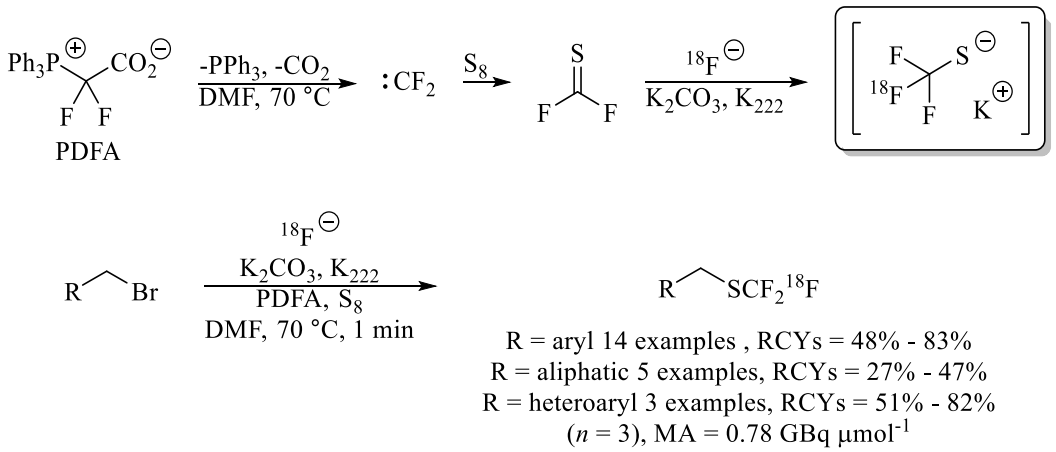
In contrast to the trifluoromethyl group, the difluoromethyl group "-CF_2H" currently makes less of an appearance in the pharmaceuticals although it can impart enhanced biological activity due to its unique property as a hydrogen bond donor.[118]

To date only one difluoromethylation reagent has been labelled with fluorine-18 (Scheme 1.29).[119] An initial study into radical difluoromethylation revealed that a number of difluoromethyl sulfones could be activated using photoredox catalysis.[120] An automated procedure was developed for labelling a difluoromethyl sulfone with fluorine-18 by halogen exchange of the bromofluoromethyl sulfide, before oxidising with sodium periodate and ruthenium(III) trichloride, affording the sulfone in 13% ± 0% RCY (n = 3) and with a molar activity of 185 GBq μmol^{-1}.



Scheme 1.29 Radiosynthesis and application of a radical difluoromethylation reagent labelled with fluorine-18

As with the difluoromethyl group, there is one reported instance of the labelled trifluoromethylthio group "-SCF3" being directly introduced onto molecules (Scheme 1.30).[121,122] When difluoromethylenephosphobetaine (PDFA) was heated to 70 ºC in DMF, difluorocarbene was released *in situ*. In the presence of elemental sulfur, difluorothiophosgene was formed which could undergo nucleophilic attack by [^{18}F]fluoride to form the [^{18}F]trifluoromethylthiolate anion. The presence of aryl bromides, heteroaryl bromides, aliphatic bromides or α-bromocarbonyls allowed this one-pot reaction to afford [^{18}F]trifluoromethylthiolation with a molar activity of 0.78 GBq μmol^{-1}.



Scheme 1.30 Radiosynthesis and *in situ* application of the [^{18}F]trifluoromethylthiolate anion

Labelling fluorinated motifs with fluorine-18 and incorporating them into molecules is challenging and a limited number of procedures have been developed, hence their use in drugs and radiotracers is also limited. However, the unique and valuable attributes that fluorinated motifs can impart onto molecules means that they cannot be ignored by the radiochemical community. Future perspectives on reagent labelling should observe the factors that enhance accessibility across PET imaging centres. Ideally, methods should be efficient, highly accessible, employ commercially available reagents, not require preparation

of precursors by installing prefunctionalised motifs, and should not require specialised equipment, such as for condensing gases. An important step in allowing real-world applicability is demonstrating that the method is amenable to automation, ideally showing that the reaction can be scaled up using large amounts of activity.

1.6 Strategies for Labelling Peptides with Fluorine-18

Peptides have quickly developed in the last 25 years as useful tools in diagnostic imaging and radiotherapy, since they can display excellent binding specificities. Their low molecular weight allows for rapid clearance from the blood and non-target tissue, which would lead to an increase in signal-to-noise ratio in a PET study. However, their low metabolic stability is often a major concern. The majority of peptide radiolabelling employs various radioactive metals such as ^{99m}Tc, ^{68}Ga, and ^{177}Lu. Peptide labelling by direct introduction of [^{18}F]fluoride has remained limited due to the incompatibility of classical fluorination reaction conditions.

Two strategies exist for labelling peptides with fluorine-18.[123] First is the direct incorporation of fluorine-18 or labelled fluorinated motifs, where their naturally occurring functional groups are exploited. Conditions associated with classical fluorination reactions can generally not be applied to peptides and proteins due to their poor stability at high temperatures and incompatibility with solvents other than water and DMSO. The variety of functional groups present in large peptides and proteins imposes an additional challenge to developing reactions with high selectivity. This means that many direct methods to date employ protecting groups or require prior incorporation of highly reactive artificial functional groups during peptide synthesis.

The second alternative strategy for labelling peptides is indirect incorporation of fluorinated motifs *via* prosthetics. This is carried out by synthesising small molecules labelled with fluorine-18 and introducing this prosthetic into the peptide. This strategy usually involves simple, high yielding chemical reactions on accessible building blocks, referred to as "click" chemistry, and has been applied in the indirect labelling of many peptides with fluorine-18. These indirect approaches generally require several synthetic steps and structure-activity relationship (SAR) studies which must be carried out for each proposed peptide analogue in order to develop an effective radiotracer with comparable affinities and specificities to the native peptide. Issues have arisen when labelling molecular targets this way, such as insufficient molar activities, extensive purification procedures, and low *in vivo* stability due to defluoridation.[124,125,126]

The most common prosthetic groups used for labelling peptides with fluorine-18 take advantage of the reactivity of thiols and amine groups inherent in amino acids, such as in cysteine and lysine, by using acylation, alkylation, amidation, imidation, oxime and hydrazine formation.[127]

[^{18}F]*N*-succinimidyl-4-fluorobenzoate ([^{18}F]SFB) and its derivative [^{18}F]4-fluorobenzoic acid ([^{18}F]FBA) are the most commonly used prosthetic groups in fluorine-18 radiochemistry for attachment to the amine group of lysine (Figure 1.6). [^{18}F]4-fluorobenzaldehyde can be attached to artificially installed hydroxylamine or hydrazine functional groups, forming oximes or hydrazones. The thiol group of cysteine can be labelled with the maleimide [^{18}F]FBABM or other maleimide derivatives. Prosthetic groups labelled with fluorine-18 containing α-halo ketones have been used, since they can be installed through alkylation reactions. Selectivity for sulfur, oxygen or nitrogen containing groups is often achieved through moderation of the reaction pH.

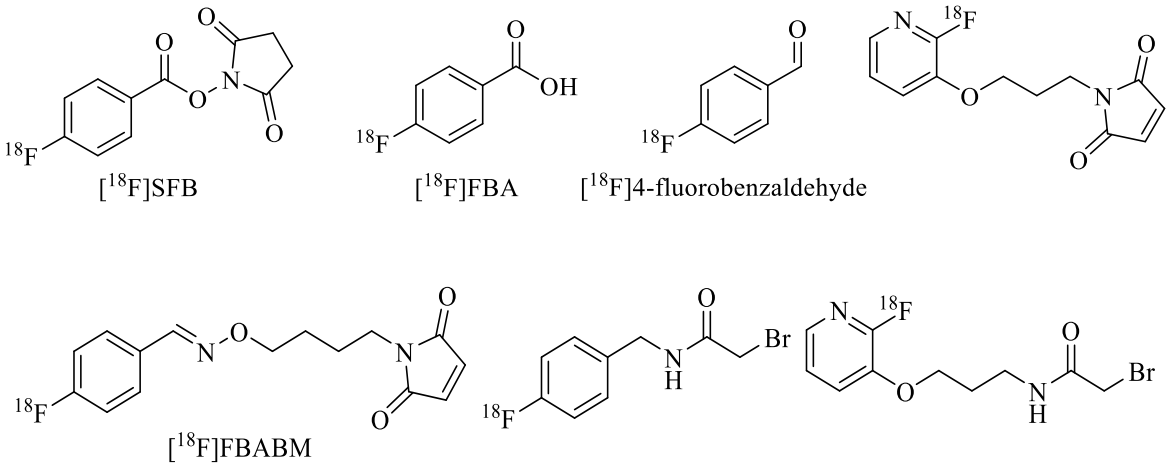
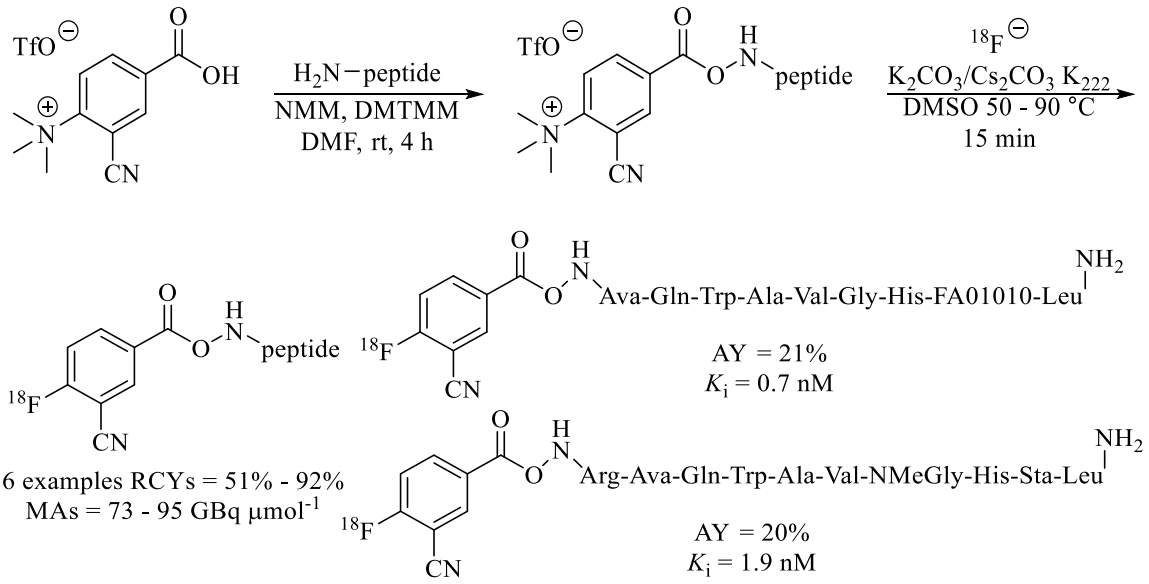


Figure 1.6 Commonly used prosthetic groups labelled with fluorine-18

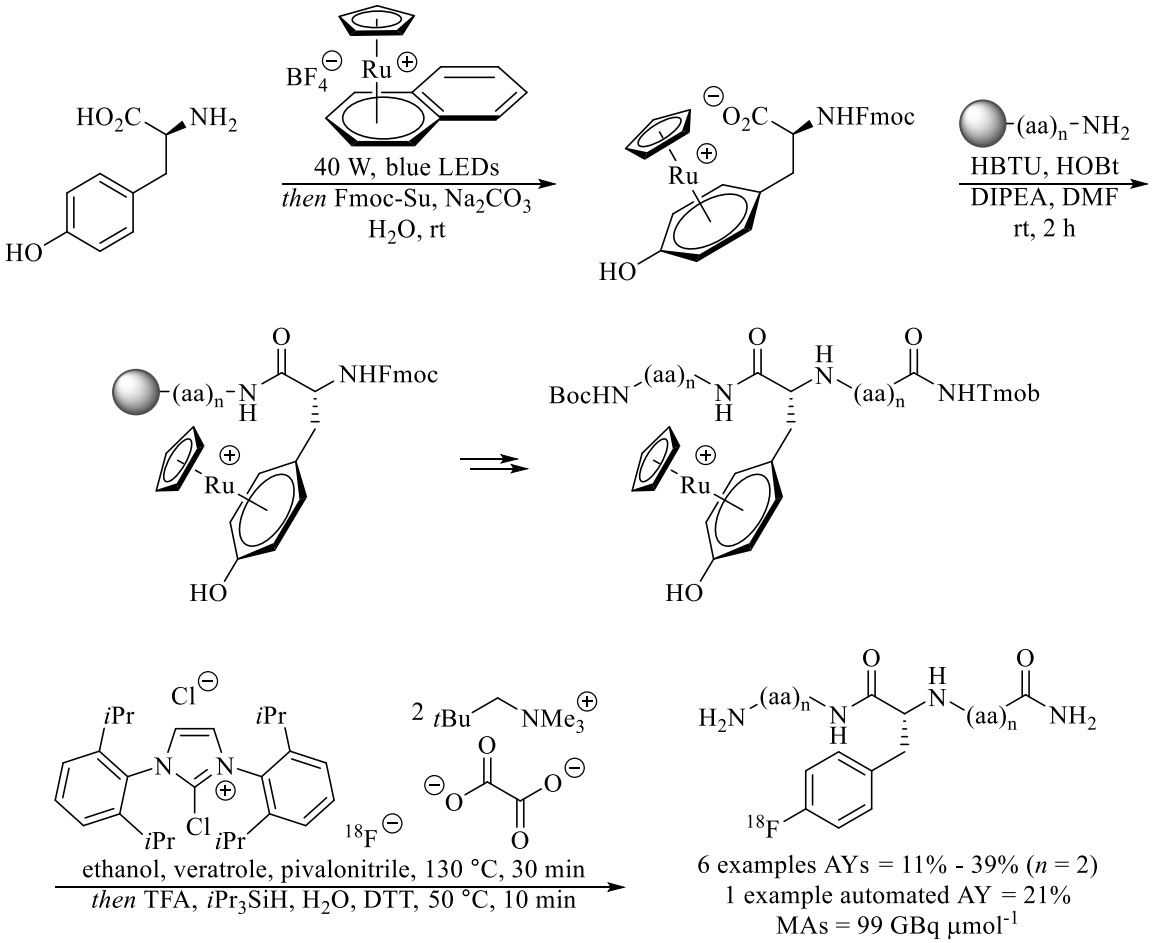
The first report to successfully radiolabel peptides with fluorine-18 describes the synthesis of an amino acid modified with a quaternary ammonium functional group. This was subsequently incorporated into the synthesis of a peptide. This prefunctionalised peptide acted as the precursor for one-step radiofluorination *via* nucleophilic aromatic substitution starting from [^{18}F]fluoride (Scheme 1.31).[128] Fluorination of quaternary ammonium arenes typically require reaction temperatures above 100 ºC, however many peptides are not stable at these temperatures. Therefore, fluorination was facilitated by attaching electron withdrawing substituents, such as the nitrile group, *σ*- to the ammonium leaving group. This allowed reduction of the reaction temperature to 50 ºC.

This method enabled labelling of six examples of peptides in 51% – 92% RCYs, giving molar activities of 73 – 95 GBq μmol^{-1}. Two bombesin peptides were isolated in 20% and 21% AYs and were used for *in vitro* binding assays. Inhibitory constant (K_i) values of 0.7 nM and 1.9 nM were obtained, comparable to the K_i value of 0.06 nM obtained using an established radioligand analogue radiolabelled with iodine-125. This demonstrated that the biological activities of the two target compounds were retained upon direct fluorination.



Scheme 1.31 Radiosynthesis of prefunctionalised peptides from aromatic nucleophilic substitution using [^{18}F]fluoride. FA01010 = (4R,5S)-4-amino-5-methylheptanoic acid; Sta = statine; NMeGly = sarcosine

Another method for labelling prefunctionalised peptides with [^{18}F]fluoride involves fluorination of tyrosine residues activated with ruthenium complexes (Scheme 1.32).[129] Modified tyrosine was incorporated into peptides using a resin-bound synthesis. The resultant ruthenium-complexed peptides were stable and no degradation or side reactions were observed during synthesis. A mixture of reagents in reaction solvent were used to elute [^{18}F]fluoride with addition of bis(trimethylneopentylammonium) oxalate key to high elution efficiency. No special precautions towards air or moisture were taken, however the reaction was carried out at 130 ºC for 30 min, limiting this methodology only to highly thermally stable peptides. Six examples of protected peptides were labelled and deprotected to give AYs of 11% – 39% (n = 2). This method was fully automated using a model substrate affording an AY of 21% with a molar activity of 99 GBq μmol^{-1}.

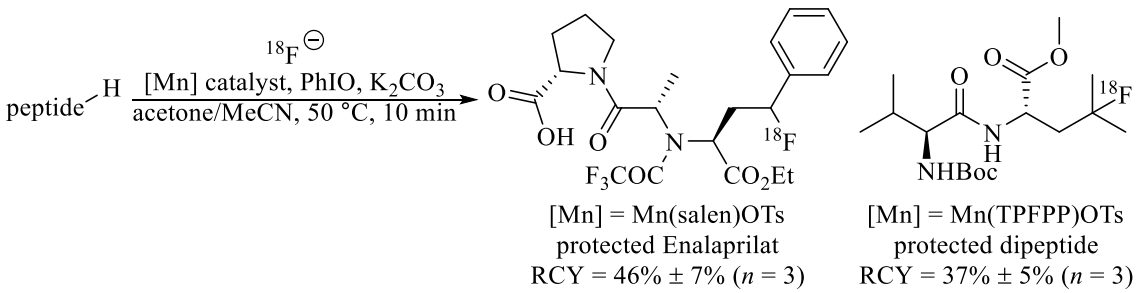


Scheme 1.32 Radiolabelling peptides prefunctionalised with a ruthenium complex using [^{18}F]fluoride. $(aa)_n$ = amino acid sequence; Su = succinimide.

Other methods for labelling prefunctionalised peptides with fluorine-18 include the formation of Si-^{18}F, B-^{18}F and Al-^{18}F bonds.[130,131,132] SAR studies of several modified analogues are usually required in order to obtain radiotracers with similar binding affinities. Synthesis of peptides containing chelators are required when forming Al-^{18}F bonds.

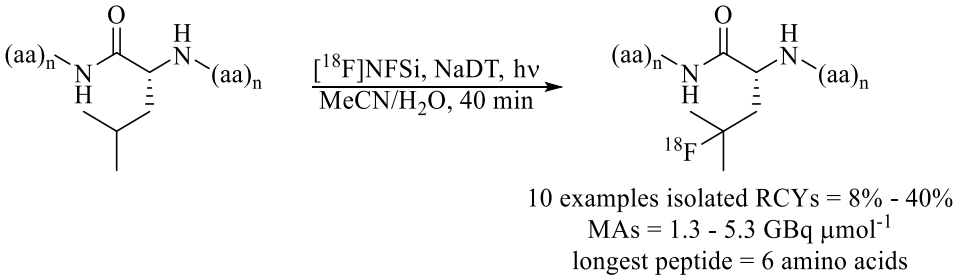
There are only a handful of examples that describe using radiolabelled fluorinating reagents to label protected or unprotected peptides with fluorine-18. Manganese catalysed C-H fluorination methodology has been used to label two small molecule protected peptides (Scheme 1.33).[58,92a] Protected Enalaprilat, the metabolite of ACE inhibitor Enalapril, was

labelled in 47% ± 7% (*n* = 3) RCY by employing the [^{18}F]Mn(salen)F reagent, and protected dipeptide Val-Leu was labelled using the [^{18}F]Mn(TPFPP)F reagent in 37% ± 5% (*n* = 3) RCY. The severely limited substrate scope suggests the technology is unsuitable for labelling longer peptides.



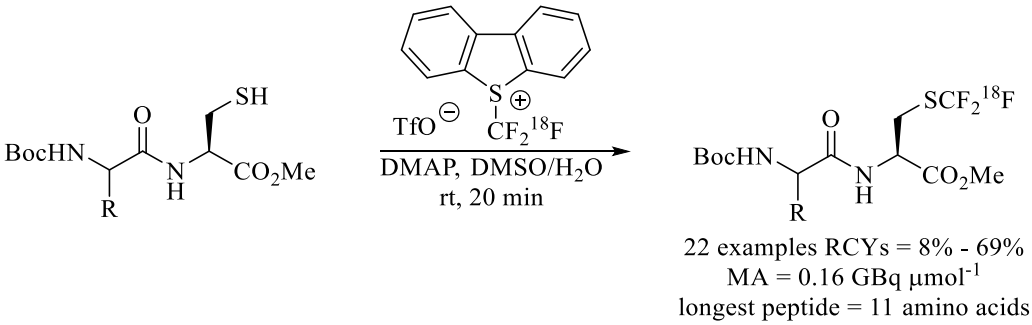
Scheme 1.33 Radiolabelling protected Enalaprilat and a dipeptide using manganese-fluorine reagents

[^{18}F]NFSi has been used for C-H fluorination of unprotected leucine and peptides containing leucine under aqueous conditions.[133] Mild reaction conditions were achieved using photochemical activation of [^{18}F]NFSi with sodium decatungstate (NaDT) as the photocatalyst (Scheme 1.34). Ten examples of native peptides were isolated in 8% – 40% RCYs with molar activities of 1.3 – 5.3 GBq μmol^{-1}. Disadvantages of this method include the use of specialised equipment for synthesising [^{18}F]NFSi and for subsequent photochemical reactions. Low molar activities were achieved, and the longest peptide labelled was only six amino acids in length.



Scheme 1.34 Radiolabelling native peptides using photoactivated [^{18}F]NFSi

Cysteine residues of protected peptides have been radiolabelled using the Umemoto reagent labelled with fluorine-18 (Scheme 1.35).[117] Electrophilic [^{18}F]trifluoromethylation of cysteine-containing peptides, protected with Boc and methyl ester groups, was conducted by addition of 4-dimethylaminopyridine (DMAP) in aqueous DMSO. Twenty-two examples of [^{18}F]trifluoromethylthiolated products were afforded in 8% – 69% RCYs with a measured molar activity of 0.16 GBq μmol^{-1}. The *in vivo* stability of the [^{18}F]trifluoromethylthio motif was investigated by obtaining biodistribution and dynamic PET images of [^{18}F]trifluoromethylthiolated cyclic peptide cRGDfC in naïve CBA mice. A high clearance rate suggested metabolism of the fluorinated motif to [^{18}F]fluoride did not occur. For using this method for further imaging studies, the molar activity would have to be improved.



Scheme 1.35 Radiolabelling cysteine residues in protected peptides using the Umemoto reagent labelled with fluorine-18

Radiolabelled fluorinating reagents show potential in helping develop new and accessible approaches to labelling peptides directly with fluorine-18 or with fluorinated motifs containing fluorine-18. The limitations of current procedures demonstrate that future methods should aim to achieve higher functional group tolerance and greater selectivity for native target sites present in peptides, pointing towards labelling larger molecules with fluorine-18. Highly desirable methods employ mild conditions avoiding the need for specialised equipment, thus enabling accessibility across PET centres and compatibility with sensitive substrates. Direct introduction of labelled motifs has the distinct advantage over indirect methods as procedures are simplified obviating the need for lengthy precursor synthesis. Current state of the art fluorinating reagents display versatile functionality allowing multiple transformations to take place selectively depending on the reaction conditions employed. Therefore, labelling these reagents would prove highly valuable for advancing the frontiers of peptide imaging.

1.7 Synthesis and Application of Sodium Trifluoromethanesulfinate: the Langlois Reagent

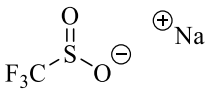
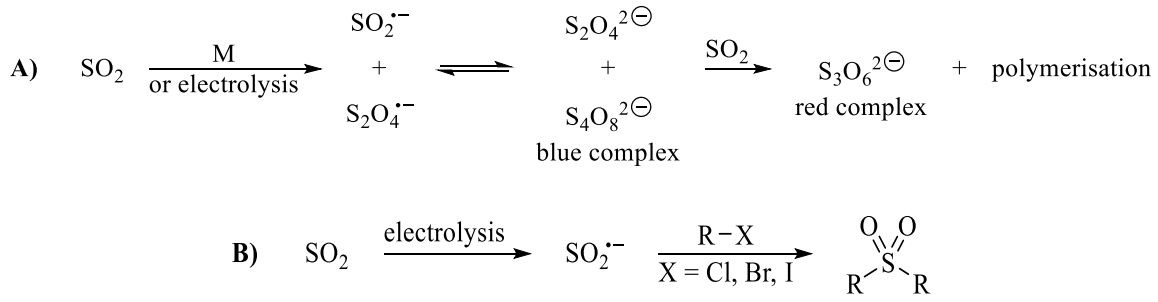


Figure 1.7 The Langlois reagent

Sodium trifluoromethanesulfinate, known as the Langlois reagent, is a highly versatile fluorinating reagent (Figure 1.7).[134] It has been employed in installing several fluorinated motifs including the trifluoromethyl "-CF_3", trifluoromethylthio "-SCF_3", trifluoromethyl sulfoxide "-$SOCF_3$", and trifluoromethyl sulfone "-SO_2CF_3" groups onto a wide array of compounds by choosing reaction conditions accordingly. The first industrial scale isolation

and characterisation of the Langlois reagent resulted from the collision between two areas of study; the first investigating the behaviour of sulfur dioxide solutions in the presence of metals and other adducts, and the second studying the utility of bromotrifluoromethane in the formation of trifluoromethyl anions and radicals.[135,136]

It has been observed that many elemental forms of transition and non-transition metals are solubilised by mixtures of sulfur dioxide and dimethyl sulfoxide, despite being insoluble in the two separate compounds. When sulfur dioxide is dissolved in non-protic solvents such as DMSO and DMF, it reacts with metals, metal sulfites and metal oxides to form various metal dithionites, sulfates, disulfates and pyrosulfates. The mechanism of this reaction involves reduction of sulfur dioxide by a metal, or by electrolysis, to the $SO_2^{\bullet-}$ and $S_2O_4^{\bullet-}$ radical anions which are in equilibrium with their anionic dimers (Scheme 1.36, A).

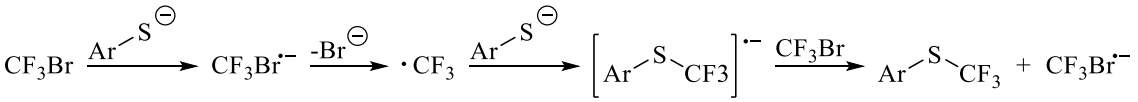


Scheme 1.36 Reduction of sulfur dioxide by metals or electrolysis A) forming the $SO_2^{\bullet-}$ and $S_2O_4^{\bullet-}$ radical anions and B) reaction with electrophiles to form sulfones

The dimer of the latter species, $S_4O_8^{2-}$, is responsible for the observation of a characteristic blue colour, and further addition of SO_2 to these species leads to formation of $S_3O_6^{2-}$, which has a characteristic red colour.[137] Further polymerisation is dependent on the coordinating ability of the solvent and the metal.[138] Amide solvents such as DMF and propylene carbonate bind more strongly to SO_2 compared to acetonitrile so polymerisation is slower, and DMSO strongly coordinates to SO_2 to form an adduct. Electrophiles such as alkyl halides undergo

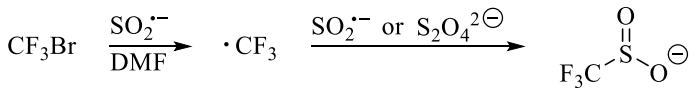
nucleophilic substitution in the presence of the $SO_2^{\bullet-}$ radical anion to form sulfones (Scheme 1.36, B).[139]

Investigations into the reactivity of bromotrifluoromethane revealed that trifluoromethylation of nucleophiles occurs through a radical mechanism (Scheme 1.37).[136] Addition of bromotrifluoromethane to potassium sulfides under pressure led to the formation of trifluoromethylated sulfides, which was supressed in the presence of radical inhibitors.



Scheme 1.37 Mechanism for formation and reaction of trifluoromethyl radicals from bromotrifluoromethane

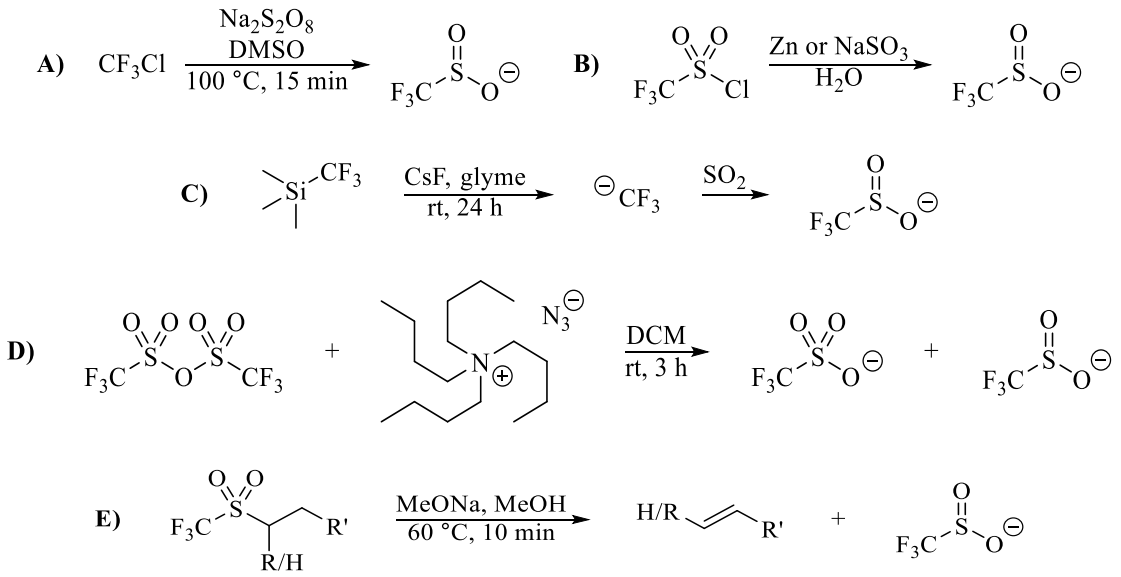
The convergence of these two areas of research led to the discovery that sulfur dioxide radical anions may be used to activate bromotrifluoromethane in forming trifluoromethyl radicals (Scheme 1.38).[140] In the absence of any reactive substrates, this radical continues to react with another sulfur dioxide radical anion, or its anionic dimer, to form the stable salt trifluoromethanesulfinate.



Scheme 1.38 Synthesis of trifluoromethanesulfinate from bromotrifluoromethane

Since this discovery, a number of syntheses have been proposed for producing the trifluoromethanesulfinate salt (Scheme 1.39). Instead of using sulfur dioxide gas, the trifluoromethanesulfinate salt has been synthesised from chlorotrifluoromethane using sodium persulfate in DMSO at 100 ºC for 15 minutes (Scheme 1.39, A).[141] Alternatively, the reduction of trifluoromethanesulfonyl chloride with zinc or sodium sulfite in water has

led to the formation of the trifluoromethanesulfinate salt (Scheme 1.39, B).[142,143] (Trifluoromethyl)trimethylsilane, when activated with caesium fluoride, releases trifluoromethyl anions in solution which, in the presence of equimolar amounts of sulfur dioxide dissolved in glyme, produces the trifluoromethanesulfinate salt in almost quantitative yields (Scheme 1.39, C).[144]



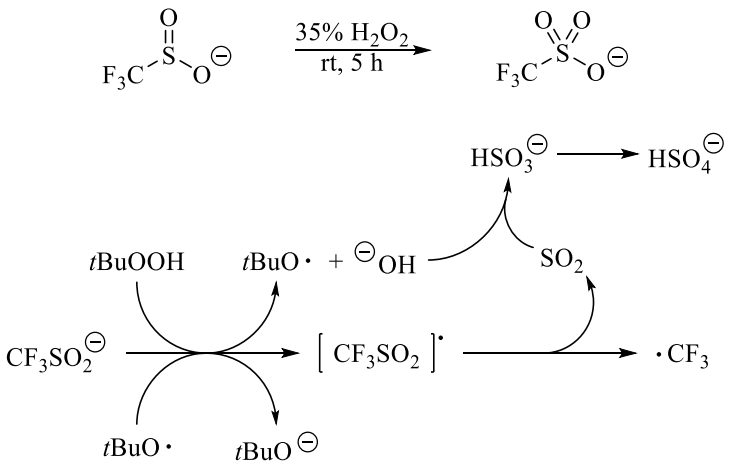
Scheme 1.39 Alternative syntheses of trifluoromethanesulfinate

Environmentally friendly synthetic routes have been explored to avoid using ozone-depleting bromotrifluoromethane and other halogenated fluorocarbons. The reaction between tetrabutylammonium azide and triflic anhydride produce a one-to-one mixture of the trifluoromethanesulfinate and trifluoromethanesulfonate salt (Scheme 1.39, D).[145] The β-elimination of aliphatic triflones has led to the synthesis of triflinate salts, although the synthesis of the precursors is time consuming (Scheme 1.39, E).[146,147]

Reactions for generating the Langlois reagent often require gaseous or volatile reagents so purification is carried out by evaporating excess reagents. Nevertheless, a patented procedure is described for extracting the Langlois reagent from organic and inorganic impurities.[148] A

mixture of Langlois reagent, water, DMF and various inorganic salts was first extracted with dichloromethane to remove organic compounds before the aqueous phase was concentrated to dryness. The residue was dissolved in ethyl acetate, the insoluble inorganic salts filtered and the solvent evaporated to afford purified Langlois reagent.

The trifluoromethanesulfinate salt is oxidised to its sulfonate by oxygen transfer using hydrogen peroxide.[140] Oxygen transfer can be avoided by employing other oxidisers, such as *tert*-butyl hydroperoxide, di-*tert*-butyl peroxide, dinitrogen tetroxide, cerium ammonium nitrate, sodium persulfate, cumyl hydroperoxide, dicumyl peroxide and sodium hypochlorite. Instead, these reagents act as single-electron oxidisers, delivering the $CF_3SO_2^{\bullet}$ radical *in situ* (Scheme 1.40).



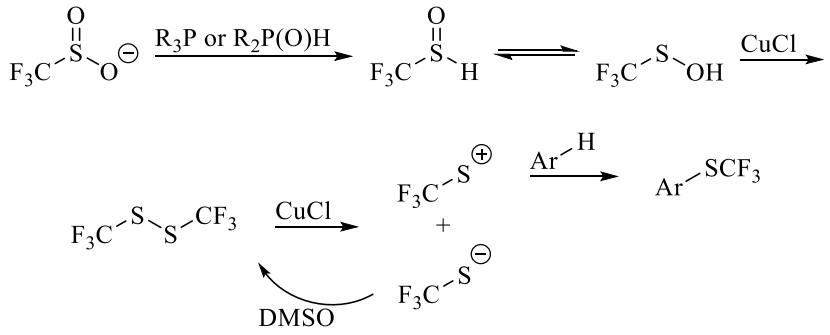
Scheme 1.40 The reaction of trifluoromethanesulfinate with oxidants in oxygen transfer or single-electron transfer

Tert-butyl hydroperoxide is the most efficient reagent for generating the $CF_3SO_2^{\bullet}$ radical and the initiation step is thought to involve activation of *tert*-butyl hydroperoxide by trace metals to initially generate a *tert*-butoxyl radical and hydroxide anion.[149] Presence of a metal species is very important in facilitating the production of *tert*-butoxyl radicals.[150] The $CF_3SO_2^{\bullet}$

radical is known to be unstable, quickly dissociating to sulfur dioxide and the trifluoromethyl radical.[151]

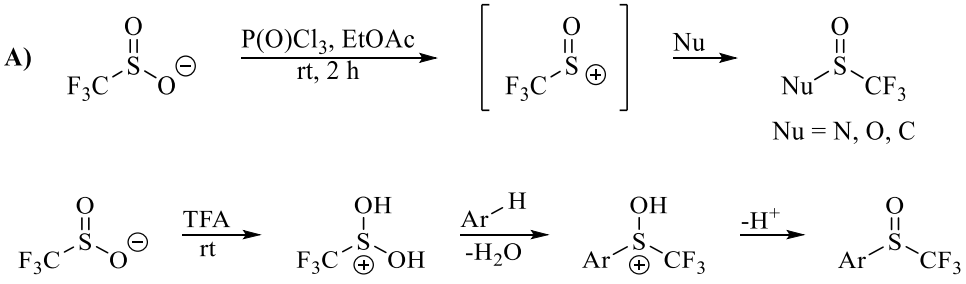
This method for generating trifluoromethyl radicals has found application in a variety of transformations with a wide range of substrates.[134,149,152,153] Trifluoromethylation of aryl or vinyl boronic acids, trifluoroborates or diazonium compounds has been investigated, as well as C-H activation of heterocyclic compounds. A wide range of alkenes have been trifluoromethylated in the presence of halides, carbon- or oxygen-containing nucleophiles using a number of organic, inorganic or metal activators. Additionally, recent advances have been made in photochemical activation of the Langlois reagent.[154]

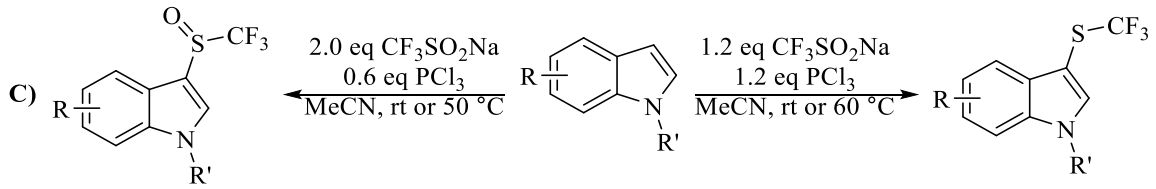
The Langlois reagent has allowed installation of the trifluoromethylthio group on arenes and on the 2- position of indoles (Scheme 1.41).[155] The mechanism is initiated by reduction to $CF_3S(O)H$ by addition of phosphine reagents in a range of solvents, which subsequently collapses to CF_3SOH.[156] CF_3SOH is unstable, decomposing to the CF_3S^+ cation which may react with a nucleophilic substrate, or may be further reduced to CF_3SSCF_3 in the presence of a copper(I) salt.[142] CF_3SSCF_3 acts as a stable electrophilic trifluoromethylthiolating reagent through dissociation by copper insertion. The SCF_3^- anion produced may be recycled back to CF_3SSCF_3 in the presence of an oxidant, such as DMSO.[157] Many of these fluorinated sulfurous species are stable enough to be observed by ^{19}F NMR spectroscopy.



Scheme 1.41 Mechanism for trifluoromethylthiolation using the Langlois reagent

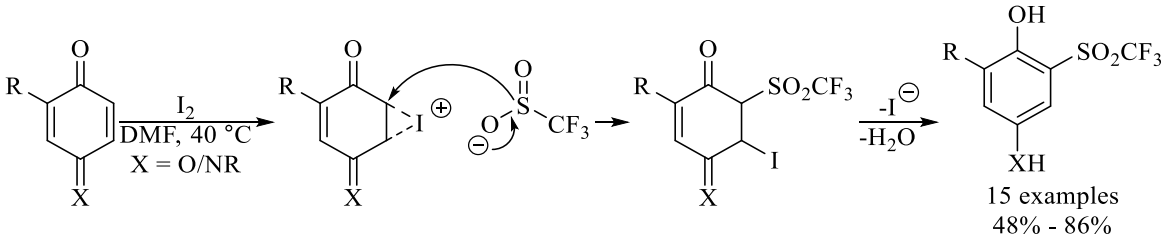
Phosphorus oxychloride is an efficient reagent for reducing the Langlois reagent to the trifluoromethylsulfinyl cation ($CF_3S(O)^+$), which reacts with amine, alcohol and carbon nucleophiles (Scheme 1.42, A).[158] Another method for carrying out trifluoromethylsulfinylation of arenes using the Langlois reagent involves the addition of triflic acid or triflic anhydride in dichloromethane (Scheme 1.42, B).[159] Double protonation of the Langlois reagent occurs forming an unstable form of sulfinic acid which participates in aromatic electrophilic substitution to form trifluoromethylsulfinyl arenes. This method has found utility in the synthesis of highly reactive forms of the Umemoto reagent.[160] Recent studies have shown that PCl_3 may also be employed for trifluoromethylsulfinylation or trifluoromethylthiolation depending on the stoichiometry and reaction temperature (Scheme 1.42, C).[161]





Scheme 1.42 Methods and mechanisms for trifluoromethylsulfinylation using the Langlois reagent

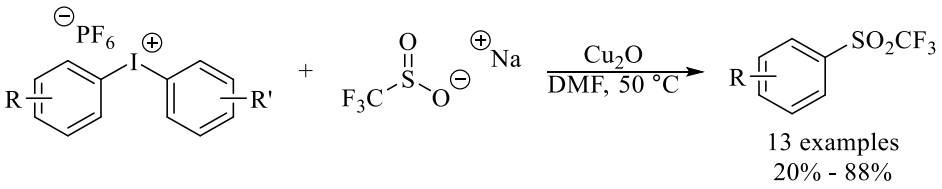
The trifluoromethyl sulfone (-SO_2CF_3) group has been introduced on a series of 1,4-benzoquinones using iodine under mild conditions to afford aryl trifluoromethyl sulfones in good yields (Scheme 1.43).[162] The mechanism of the reaction is proposed to occur *via* an iodonium ion intermediate formed between iodine and the substrate, which is attacked by the trifluoromethanesulfinate ion at the sulfur atom. The desired product is formed after subsequent elimination, dehydration and aromatisation.



Scheme 1.43 Mechanism for forming aryl trifluoromethyl sulfones from the Langlois reagent

A copper-catalysed coupling reaction between aryl iodonium salts and the Langlois reagent has been developed, allowing a more generally applicable method for forming aryl trifluoromethyl sulfones (Scheme 1.44).[163] Following several reports of Cu- and Pd-catalysed reactions for forming aryl sulfones, the transformation was achieved by combining aryl iodonium salts, the Langlois reagent and copper(I) oxide in DMF at 50 °C. Although the substrate scope reported only covered a limited array of small molecules, a model reaction

was spiked with a variety of compounds containing functional groups commonly found in larger complex molecules. Through this experimental design, a number of functional groups were found to be compatible with the method. The scope has since been extended to aryl and heteroaryl diazonium compounds, chlorides and triflates.[164,165]



Scheme 1.44 Copper-catalysed formation of aryl trifluoromethyl sulfones from the Langlois reagent

The Langlois reagent is a highly versatile fluorinating reagent that if labelled with fluorine-18 could be an invaluable asset for the radiochemical and PET imaging communities.

The aim of this thesis is to report our development of a unique and elegant radiosynthesis of the [^{18}F]Langlois reagent, and to demonstrate an initial appraisal of the reagent's real-world application in accelerating the discovery of peptides as imaging agents.

1.8 References

[1] L. Champion *et al*. *Eur. J. Med. Mol. Imaging* **2013**, 40, 1206 – 1213.

[2] L. Ceriani *et al*. *J. Clin. Endocrinol. Metab.* **2013**, 98 (6), 2208 – 2209.

[3] C. Kuntner & D. Stout *Front. Phys.* **2014**, 2, Article 12.

[4] P. M. Mathews *et al*. *Br. J. Clin. Pharmacol.* **2011**, 73 (2), 175 – 186.

[5] S. R. Cherry & S. S. Gambhir *ILAR J.* **2001**, 42 (3), 219 – 232.

[6] P. W. Miller, N. J. Long, R. Vilar & A. D. Gee *Angew. Chem. Int. Ed.* **2008**, 47, 8998 – 9033.

[7] A. R. Braun *et al. Brain* **1997**, 120, 1173 – 1197.

[8] a) A. Gjedde & M. Rasmussen *J. Neurochem.* **1980**, 35, 1382 – 1387. b) J. C. LaManna & S. L. Harik *J. Cereb. Blood Flow Metab.* **1986**, 6, 717 – 723. c) S. Momosaki *et al. Synapse* **2004**, 54, 207 – 213.

[9] a) S. Momosaki *et al. Synapse* **2004**, 54, 207 – 213. b) V. W. Pike *et al. J. Nucl. Med.* **2009**, 50, 749 – 756. c) H. Onoe *et al. J. Nucl. Med.* **2010**, 51, 1068 – 1075. d) T. Sugita *et al. Nucl. Med. Commun.* **2018**, 39, 753 – 760. e) M. Palner *et al. EJNMMI Res.* **2016**, 6, 80 – 91.

[10] W. M. Haynes *CRC Handbook of Chemistry and Physics 97th Ed.* CRC Press, **2016 – 2017**.

[11] A. Bondi *J. Phys. Chem.* **1964**, 68 (3), 441 – 451.

[12] J. Wang *et al. Chem. Rev.* **2014**, 114, 2432 – 2506.

[13] Y. Zhou *et al. Chem. Rev.* **2016**, 116, 422 – 518.

[14] S. Purser, P. R. Moore, S. Swallow & V. Gouverneur *Chem. Soc. Rev.* **2008**, 37, 320 – 330.

[15] B. K. Park, N. R. Kitteringham & P. M. O'Neill *Annu. Rev. Pharmacol. Toxicol.* **2001**, 41, 443 – 470.

[16] C. S. Levin *Eur. J. Mol. Imaging* **2005**, 32, S325 – S345.

[17] M. R. Kilbourn, J. T. Hood & M. T. Welch *Int. J. Appl. Radiat. Isot.* **1984**, 35 (7), 599 – 602.

[18] M. A. Avila-Rodriguez, J. S. Wilson & S. A. McQuarrie *Appl. Radiat. Isot.* **2008**, 66, 1775 – 1780.

[19] O. Jacobsen, D. O. Kiesewetter & X. Chen *Bioconjug. Chem.* **2015**, 26, 1 – 18.

[20] Patent **2012** US20120229804 A1.

[21] C. Zhan & D. A. Dixon *J. Phys. Chem. A* **2004**, 108, 2020 – 2029.

[22] M. R. C. Gerstenberger & A. Haas *Angew. Chem. Int. Ed.* **1981**, 20 (8), 647 – 667.

[23] A. V. Mossine *et al*. *Sci. Rep.* **2017**, 7, Article 233.

[24] a) G. A. Olah, J. G. Shih & G. K. S. Prakash *J. Fluor. Chem.* **1986**, 33, 377 – 396. b) J. A. Wilkinson *Chem. Rev.* **1992**, 92, 404 – 519. c) T. Liang, C. N. Neumann & T. Ritter *Angew. Chem. Int. Ed.* **2013**, 52, 8214 – 8264. d) P. A. Champagne *et al. Chem. Rev.* **2015**, 115, 9073 – 9174. e) C. N. Neumann & T. Ritter *Angew. Chem. Int. Ed.* **2015**, 54, 3216 – 3221. f) D. E. Yerien, S. Bonesi & A. Postigo *Org. Biomol. Chem.* **2016**, 14, 8398 – 8427.

[25] F. Wang *Olah's Reagent Fluorination for Preparing Alkyl Fluorides* in *Fluorination* Springer Nature Singapore **2018**.

[26] G. A. Olah, M. Nojima & I. Kerekes *Synthesis* **1973**, 12, 779 – 780.

[27] M. A. McClinton *Aldrichimica Acta* **1995**, 28 (2), 31 – 35.

[28] F. Swarts *Bull. Acad. Roy. Belg*. **1892**, 3 (24), 474 – 484.

[29] a) T. Khotavivattana *et al. Angew. Chem.* **2015**, 127, 10129 – 10133. b) V. Koch, A. Hafner & S. Bräse *Silver-Mediated Fluorination, Perfluoroalkylation, and Trifluoromethylthiolation Reactions* in *Silver Catalysis in Organic Synthesis* John Wiley & Sons **2018**, 271 – 330.

[30] P. S. Fier & J. F. Hartwig *Science* **2013**, 342 (6161), 956 – 960.

[31] H. Sun & S. G. DiMagno *TBAF Fluorination for Preparing Alkyl Fluorides* in *Fluorination* Springer Nature Singapore **2018**.

[32] H. Sun & S. G. DiMagno *J. Am. Chem. Soc.* **2005**, 127, 2050 – 2051.

[33] M. Hu & J. Hu *SF_4 Deoxofluorination* in *Fluorination* Springer Nature Singapore **2018**.

[34] a) W. C. Smith *et al. J. Am. Chem. Soc.* **1959**, 81, 3165 – 3166. b) C. Ni, M. Hu & J. Hu *Chem. Rev.* **2015**, 115, 765 – 825.

[35] M. Hudlicky *Fluorinations with Diethylaminosulfur Trifluoride and Related Aminosulfurans* in *Organic Reactions* John Wiley & Sons **1988**, 35, 513 – 637.

[36] A. J. Cresswell *et al. Chem. Rev.* **2015**, 115, 566 – 611.

[37] a) C. Ding *et al. BF_3 Fluorination for Preparing Alkyl Fluorides* in *Fluorination* Springer Nature Singapore **2018**. b) S. G. Davies & P. M. Roberts *Tetrafluoroborate Salt Fluorination for Preparing Alkyl Fluorides* in *Fluorination* Springer Nature Singapore **2018**.

[38] D. H. R. Barton *et al. J. Am. Chem. Soc.* **1976**, 98, 3036 – 3037.

[39] T. Okazoe *Perfluorination with F_2* in *Fluorination* Springer Nature Singapore **2018**.

[40] G. Cady, S. I. Khayat & K. S. Wilson *Trifluoromethyl Hypofluorite* in *Inorganic Synthesis* McGraw-Hill Book Company **1966**.

[41] M. A. Tius *Tetrahedron* **1995**, 51, 6605 – 6634.

[42] S. D. Taylor, C. C. Kotoris & G. Hum *Tetrahedron* **1999**, 55, 12431 – 12477.

[43] G. S. Lal, G. P. Pez & R. G. Syvret *Chem. Rev.* **1996**, 96, 1737 – 1755.

[44] N. Rozatian *et al. Chem. Sci.* **2018**, 9, 8692 – 8702.

[45] a) K. Muñiz *Angew. Chem. Int. Ed.* **2001**, 40, 1653 – 1656. b) N. Shibata *et al. J. Fluor. Chem.* **2007**, 128, 469 – 483. c) J. Ma & D. Cahard *Chem. Rev.* **2008**, 108, PR1 – PR43. d) D. Cahard *et al. Chem. Soc. Rev.* **2010**, 39, 558 – 568.

[46] G. Blessing *et al. Appl. Radiat. Isot.* **1986**, 37 (11), 1135 – 1139.

[47] R. Chirakal *et al. Nucl. Med. Biol.* **1995**, 22 (1), 111 – 116.

[48] J. Bergman & O. Solin *Nucl. Med. Biol.* **1997**, 24, 677 – 683.

[49] G. T. Bida *et al. J. Nucl. Med.* **1980**, 21, 758 – 762.

[50] T. Nozaki *et al. Int. J. Appl. Radiat. Isot.* **1968**, 19, 27 – 32.

[51] a) C. Crouzel & D. Comar *Int. J. Appl. Radiat. Isot.* **1978**, 29, 407 – 408. b) J. R. Dahl *et al. Int. J. Appl. Radiat. Isot.* **1983**, 34, 693 – 700.

[52] R. M. Lambrecht, R. Neirinckx & A. P. Wolf *Int. J. Appl. Radiat. Isot.* **1978**, 29, 175 – 183.

[53] M. G. Straatmann & M. J. Welch *J. Nucl. Med.* **1977**, 18, 151 – 158.

[54] a) B. D. Zlatopolskly *et al. Chem. Eur. J.* **2015**, 21, 5972 – 5979. b) A. V. Mossine *et al. Sci. Rep.* **2017**, 7, Article 233.

[55] X. Zhang, F. Basuli & R. E. Swenson *J. Label. Compd. Radiopharm.* **2019**, 62, 139 – 145.

[56] a) D. R. Hwang *et al. J. Chem. Soc., Chem. Commun.* **1987**, 1799 – 1801. b) R. Gail & H. H. Coenen *Appl. Radiat. Isot.* **1994**, 45 (1), 105 – 111. c) M. Karramkam *et al. J. Label. Compd. Radiopharm.* **2003**, 46, 979 – 992.

[57] a) V. Pike & F. I. Aigbirhio *J. Label. Compd. Radiopharm.* **1995**, 37, 120 – 122. b) T. L. Ross *et al. J. Am. Chem. Soc.* **2007**, 129, 8018 – 8025.

[58] W. Liu *et al. Chem. Sci.* **2018**, 9, 1168 – 1172.

[59] S. J. Lee *et al. Chem. Commun.* **2019**, 55, 2976 – 2979.

[60] M. H. Beyzavi *et al. ACS Cent. Sci.* **2017**, 3, 944 – 948.

[61] E. Lee, J. M, Hooker & T. Ritter *J. Am. Chem. Soc.* **2012**, 134, 17456 – 17458.

[62] H. Jiang, S. G. DiMagno & T. R. DeGrado *J. Fluor. Chem.* **2015**, 180, 181 – 185.

[63] A. Pees *et al. Chem. Commun.* **2018**, 54, 10179 – 10182.

[64] B. Zhang *et al. Chem. Eur. J.* **2019**, 25, 7613 – 7617.

[65] M. K. Nielson *et al. J. Am. Chem. Soc.* **2015**, 137, 9671 – 9674.

[66] L. Matesic *et al. J. Org. Chem.* **2013**, 78, 11262 – 11270.

[67] G. Schrobilgen *et al. J. Chem. Soc., Chem. Commun.* **1981**, 4, 198 – 199.

[68] R. D. Neirinckx, R. M. Lambrecht & A. P. Wolf *Int. J. Appl. Radiat. Isot.* **1978**, 29, 323 – 327.

[69] R. E. Ehrenkaufer & R. R. MacGregor *Int. J. Appl. Radiat. Isot.* **1983**, 34 (3), 613 – 615.

[70] A. Hiller *et al. Appl. Radiat. Isot.* **2008**, 66 (2), 152 – 157.

[71] M. J. Adam *et al. J. Nucl. Med.* **1986**, 27, 1462 – 1466.

[72] R. Chirakal *et al. Int. J. Appl. Radiat. Isot.* **1984**, 35 (7), 651 – 653.

[73] a) M. J. Adam *et al. J. Fluor. Chem.* **1984**, 25, 329 – 337. b) G. W. M. Visser *et al. J. Chem. Soc., Chem. Commun.* **1984**, 655 – 656. c) M. Speranza *et al. J. Fluor. Chem.* **1985**, 30, 97 – 107. d) H. H. Coenen & S. M. Moelein *J. Fluor. Chem.* **1987**, 36, 63 – 75.

[74] C. Shuie *et al. J. Nucl. Med.* **1982**, 23, 899 – 903.

[75] M. Diksic & D. Jolly *Int. J. Appl. Radiat. Isot.* **1983**, 34 (6), 893 – 896.

[76] T. Ido *et al. J. Label. Compd. Radiopharm.* **1978**, 14, 175 – 183.

[77] J. S. Fowler & T. Ido *Semin. Nucl. Med.* **2002**, 32 (1), 6 – 12.

[78] C. Shiue, K. To & A. P. Wolf *J. Label. Compd. Radiopharm.* **1983**, 20, 157 – 162.

[79] a) B. H. Mock, M. T. Vavrek & G. K. Mulholland *Nucl. Med. Biol.* **1996**, 23, 497 – 501. b) M. Yuasa, H. Yoshida & T. Hara *Appl. Radiat. Isot.* **1997**, 48, 201 – 205.

[80] F. Oberdorfer, E. Hofmann & W. Maier-Borst *J. Label. Compd. Radiopharm.* **1988**, 25, 999 – 1005.

[81] F. Oberdorfer, E. Hofmann & W. Maier-Borst *Appl. Radiat. Isot.* **1988**, 39 (7), 685 – 688.

[82] N. Satyamurthy *et al. Appl. Radiat. Isot.* **1990**, 41 (8), 733 – 738.

[83] a) E. Differding & H. Ofner *Synlett* **1991**, 3, 187 – 189. b) D. L. Boger, S. R. Brunette & R. M. Garbaccio *J. Org. Chem.* **2001**, 66, 5163 – 5173.

[84] H. Teare *et al. Chem. Commun.* **2007**, 2330 – 2332.

[85] H. Teare *et al. Angew. Chem. Int. Ed.* **2010**, 49, 6821 – 6824.

[86] a) P. T. Nyffeler *et al. Angew. Chem. Int. Ed.* **2005**, 44, 192 – 212. b) S. Stavber *Molecules* **2011**, 16 (8), 6432 – 6464.

[87] E. Lee *et al. Science* **2011**, 334 (6056), 639 – 642.

[88] S. S. Stahl, J. A. Labinger & J. E. Bercaw *Angew. Chem. Int. Ed.* **1998**, 37, 2180 – 2192.

[89] A. D. Kamlet *et al. PLoS One* **2013**, 8 (3), e59187.

[90] T. J. A. Graham *et al. J. Am. Chem. Soc.* **2014**, 136, 5291 – 5294.

[91] S. H. Liang & N. Vasdev *Angew. Chem. Int. Ed.* **2014**, 53, 11416 – 11418.

[92] a) X. Huang *et al. J. Am. Chem. Soc.* **2014**, 136, 6842 – 6845. b) Patent **2015**, WO134467A1.

[93] W. Liu *et al. Science* **2012**, 337 (6100), 1322 – 1325.

[94] W. Liu *et al. Chem. Sci.* **2018**, 9, 1168 – 1172.

[95] X. Huang *et al. Angew. Chem. Int. Ed.* **2015**, 54, 5241 – 5245.

[96] J. B. I. Sap *et al. Chem. Sci.* **2019**, 10, 3237 – 3241.

[97] a) B. Yang *et al. Chem. Commun.* **2017**, 53, 3497 – 3500. b) M. A. C. González *et al. Chem. Commun.* **2018**, 54, 4286 – 4289.

[98] a) N. O. Ilchenko, B. O. A. Tasch & K. J. Szabó *Angew. Chem. Int. Ed.* **2014**, 53, 12897 – 12901. b) G. C. Geary, E. G. Hope & A. M. Stuart *Angew. Chem. Int. Ed.* **2015**, 54, 14911 – 14914. c) G. C. Geary *et al. Chem. Commun.* **2013**, 49, 9263 – 9265. d) W. Yuan & K. J. Szabó *Angew. Chem. Int. Ed.* **2015**, 54, 8533 – 8537. e) N. O. Ilchenko, M. A. Cortés & K. J. Szabó *ACS Catal.* **2016**, 6, 447 – 450. f) W. Yuan, L. Ariksson & K. J. Szabó *Angew. Chem. Int. Ed.* **2016**, 55, 8410 – 8415. g) A. Ulmer *et al. Chem. Eur. J.* **2016**, 22, 3660 – 3664. h) S. V. Kohlhepp & T. Gulder *Chem. Soc. Rev.* **2016**, 45, 6270 – 6288. i) N. O. Ilchenko *et al. Chem. Sci.* **2017**, 8, 1056 – 1061. j) C. Brunner *et al. Eur. J. Org. Chem.* **2018**, 2615 – 2621.

[99] M. A. Cortés *et al. Chem. Commun.* **2019**, 55, 13358 – 13361.

[100] N. A. Meanwell *J. Med. Chem.* **2018**, 61, 5822 – 5880.

[101] H. Böhm *et al. ChemBioChem* **2004**, 5, 637 – 643.

[102] T. Yamazaki, T. Taguchi & I. Ojima *Unique Properties of Fluorine and their Relevance to Medicinal Chemistry and Chemical Biology* in *Fluorine in Medicinal Chemistry and Chemical Biology* John Wiley & Sons **2009**.

[103] M. K. Das & J. Mukherjee *Appl. Radiat. Isot.* **1993**, 44 (5), 835 – 842.

[104] M. R. Satter *et al. Appl. Radiat. Isot.* **1994**, 45 (11), 1093 – 1100.

[105] T. Khotavivattana *et al. Angew. Chem. Int. Ed.* **2015**, 54, 9991 – 9995.

[106] H. Martinez *et al. J. Fluor. Chem.* **2012**, 135, 167 – 175.

[107] M. Huiban *et al. Nat. Chem.* **2013**, 5, 941 – 944.

[108] T. Rühl *et al. Chem. Commun.* **2014**, 50, 6056 – 6059.

[109] D. Born *et al. Chem. Commun.* **2013**, 49, 4018 – 4020.

[110] J. Russell & N. Roques *Tetrahedron* **1998**, 54, 13771 – 13782.

[111] A. Zanardi *et al. J. Am. Chem. Soc.* **2011**, 133, 20901 – 20913.

[112] a) O. A. Tomashenko & V. V. Grushin *Chem. Rev.* **2011**, 111, 4475 – 4521. b) A. Lishchynskyi *et al. J. Org. Chem.* **2013**, 78, 11126 – 11146. c) A. I. Konovalov, A. Lishchynskyi & V. V. Grushin *J. Am. Chem. Soc.* **2014**, 136, 13410 – 13425.

[113] D. Born *et al. Angew. Chem. Int. Ed.* **2014**, 53, 11046 – 11050.

[114] P. Ivashkin *et al. Chem. Eur. J.* **2014**, 20, 9514 – 9518.

[115] E. Carbonnel *et al. Chem. Commun.* **2017**, 53, 5706 – 5709.

[116] B. Y. Yang *et al. Sci. Rep.* **2019**, 9, Article 14835.

[117] S. Verhoog *et al. J. Am. Chem. Soc.* **2018**, 140, 1572 – 1575.

[118] J. A. Erickson & J. I. McLoughlin *J. Org. Chem.* **1995**, 60, 1626 – 1631.

[119] L. Trump *et al. Angew. Chem. Int. Ed.* **2019**, 58, 13149 – 13154.

[120] J. Rong *et al. Angew. Chem. Int. Ed.* **2016**, 55, 2743 – 2747.

[121] J. Zheng *et al. Angew. Chem. Int. Ed.* **2015**, 54, 13236 – 13240.

[122] J. Zheng *et al. Angew. Chem. Int. Ed.* **2017**, 56, 3196 – 3200.

[123] a) S. M. Okarvi *Eur. J. Nucl. Med. Mol. Imaging* **2001**, 28 (7), 929 – 938. b) O. Jacobsen & X. Chen *Curr. Top. Med. Chem* **2010**, 10, 1048 – 1059. c) S. Richter & F. Wuest *Molecules* **2014**, 19, 20536 – 20556. d) H. S. Krishnan *et al. Chem. Eur. J.* **2017**, 23, 15553 – 15577. e) I. M. Jackson *et al. Semin. Nucl. Med.* **2017**, 47 (5), 493 – 523. f) O. Morris *et al. J. Label. Compd. Radiopharm.* **2019**, 62, 4 – 23.

[124] H. Wester K. Kamacher & G. Stöcklin *Nucl. Med. Biol.* **1996**, 23 (3), 365 – 372.

[125] a) L. W. Herman *et al. Nucl. Med. Biol.* **1994**, 21 (7), 1005 – 1010. b) Y. Shai *et al. Biochemistry* **1989**, 28 (11), 4801 – 4806.

[126] a) L. Lang & W. C. Eckelman *Appl. Radiat. Isot.* **1994**, 45 (12), 1155 – 1163. b) L. Lang & W. C. Eckelman *Appl. Radiat. Isot.* **1997**, 48 (2), 169 – 173.

[127] a) X. Chen *et al. Nucl. Med. Biol.* **2004**, 31 (2), 179 – 189. b) Z. Wu *et al. Eur. J. Nucl. Med. Mol. Imaging* **2007**, 34 (11), 1823 – 1831. c) X. Li *et al. Bioconjug. Chem.* **2008**, 19, 1684 – 1688. d) M. Namavari *et al. Bioconjug. Chem.* **2009**, 20, 432 – 436.

[128] J. Becaud *et al. Bioconjug. Chem.* **2009**, 20, 2254 – 2261.

[129] J. Rickmeier & T. Ritter *Angew. Chem. Int. Ed.* **2018**, 57, 14207 – 14211.

[130] C. Wängler *et al. Appl. Sci.* **2012**, 2, 277 – 302.

[131] D. M. Perrin *Acc. Chem. Res.* **2016**, 49, 1333 – 1343.

[132] W. J. McBride *et al. Bioconjug. Chem.* **2010**, 21, 1331 – 1340.

[133] a) M. B. Nodwell *et al. J. Am. Chem. Soc.* **2017**, 139, 3595 – 3598. b) Z. Yuan *et al. Angew. Chem. Int. Ed.* **2018**, 57, 12733 – 12736.

[134] B. R. Langlois *Once Upon a Time was the Langlois Reagent: A "Sleeping Beauty"* in *Modern Synthesis Processes and Reactivity of Fluorinated Compounds* Elsevier **2016**.

[135] a) W. D. Harrison, J. B. Gill & D. C. Goodall *J. Chem. Soc., Chem. Commun.* **1976**, 540 – 541. b) W. D. Harrison, J. B. Gill & D. C. Goodall *J. Chem. Soc., Dalton Trans.* **1978**, 1431 – 1433. c) W. D. Harrison, J. B. Gill & D. C. Goodall *J. Chem. Soc., Dalton Trans.* **1979**, 847 – 850. d) J. B. Gill, D. C. Goodall & W. D. Harrison *Hydrometallurgy* **1981**, 6, 347 – 351. e) N. K. Graham, J. B. Gill & D. C. Goodall *J. Chem. Soc., Dalton Trans.* **1983**, 1363 – 1365. f) W. D. Harrison, J. B. Gill & D. C. Goodall *Polyhedron* **1983**, 2 (3), 153 – 156. g) N. K. Graham, J. B. Gill & D. C. Goodall *Aust. J. Chem.* **1983**, 36, 1991 – 1995. h) D. C. Goodall *Food Chem.* **1984**, 15, 93 – 111. i) B. Jeffreys, J. B. Gill & D. C. Goodall *J. Chem. Soc., Dalton Trans.* **1985**, 99 – 100. j) J. B. Gill *et al. J. Chem. Soc., Dalton Trans.* **1986**, 2597 – 2602. k) J. B. Gill, D. C. Goodall & B. Jeffreys *J. Chem. Soc., Dalton Trans.* **1986**, 2603 – 2605. l) J. B. Gill, D. C. Goodall & W. D. Harrison *J. Chem. Soc., Dalton Trans.* **1987**, 2995 – 2997.

[136] a) I. Rico, D. Cantacuzene & C. Wakselman *J. Org. Chem.* **1983**, 48, 1979 – 1982. b) C. Wakselman & M. Tordeaux *J. Chem. Soc., Chem. Commun.* **1984**, 793 – 794. c) C. Wakselman & M. Tordeaux *J. Org. Chem.* **1985**, 50, 4047 – 4051. d) C. Francèse, M. Tordeaux & C. Wakselman *J. Chem. Soc., Chem. Commun.* **1987**, 642 – 643. e) C. Wakselman & M. Tordeaux *J. Chem. Soc., Chem. Commun.* **1987**, 1701 – 1702. f) C. Francèse, M. Tordeaux & C. Wakselman *Tetrahedron Lett.* **1988**, 29, 1029 – 1030. g) M. Tordeaux, C. Francèse & C. Wakselman *J. Fluor. Chem.* **1989**, 43, 27 – 34. h) M. Tordeaux, B. Langlois & C. Wakselman *J. Chem. Soc., Perkin Trans. 1* **1990**, 2293 – 2299. i) C. Wakselman *et al. J. Chem. Soc., Chem. Commun.* **1991**, 993 – 994. j) J. Clave *et al. J. Chem. Soc., Perkin Trans. 1* **1992**, 3371 – 3375.

[137] E. Potteau, E. Levillain & J. Lelieur *New J. Chem.* **1999**, 23, 1117 – 1124.

[138] a) R. G. Rinker & S. Lynn *J. Phys. Chem.* **1968**, 72, 4706 – 4707. b) R. P. Martin & D. T. Sawyer *Inorg. Chem.* **1972**, 11, 2644 – 2647. c) C. L. Gardner & D. T. Fouchard *J. Electrochem. Soc.* **1981**, 128, 2337 – 2345. d) C. L. Gardner & D. T. Fouchard *J. Electrochem. Soc.* **1981**, 128, 2345 – 2350. e) D. Knittel *J. Electroanal. Chem.* **1985**, 195, 345 – 356.

[139] D. Knittel & B. Kastening *J. Appl. Electrochem.* **1973**, 3, 291 – 296.

[140] M. Tordeaux, B. Langlois & C. Wakselman *J. Org. Chem.* **1989**, 54, 2452 – 2453.

[141] H. Cao & Q. Chen *J. Fluor. Chem.* **2007**, 128, 1187 – 1190.

[142] R. N. Hazeldine & J. M. Kidd *J. Chem. Soc.* **1955**, 2901 – 2910.

[143] Patent **2011** WO108622 A1

[144] R. P. Singh & J. M. Shreeve *Chem. Commun.* **2002**, 1818 – 1819.

[145] J. B. Hendrickson, D. A. Judelson & T. Chancellor *Synthesis* **1984**, 4, 320 – 322.

[146] B. R. Langlois *et al. J. Fluor. Chem.* **2007**, 128, 851 – 856.

[147] J. B. Hendrickson, A. Giga & J. Wareing *J. Am. Chem. Soc.* **1974**, 96, 2275 – 2276.

[148] Patent **1990** CA2015793 A1.

[149] Y. Ji *et al. Proc. Natl. Acad. Sci. U. S. A.* **2011**, 108 (35), 14411 – 14415.

[150] K. B. Sharpless & T. R. Verhoeven *Aldrichimica Acta* **1979**, 12 (4), 63 – 74.

[151] D. Gonbeau *et al. Chem. Phys.* **1989**, 135, 85 – 89.

[152] C. Zhang *Adv. Synth. Catal.* **2014**, 356, 2895 – 2906.

[153] H. Guyon, H. Chachignon & D. Cahard *Beilstein J. Org. Chem.* **2017**, 13, 2764 – 2799.

[154] Q. Lefebvre *Synlett* **2017**, 28, 19 – 23.

[155] a) L. Jiang *et al. Angew. Chem. Int. Ed.* **2015**, 54, 14965 – 14969. b) Y. Yang *et al. Chem. Eur. J.* **2016**, 22, 858 – 863. c) M. Bu *et al. Org. Chem. Front.* **2017**, 4, 266 – 270. d) X. Zhao *et al. J. Org. Chem.* **2017**, 82, 9175 – 9181. e) Q. Yan *et al. Adv. Synth. Catal.* **2017**, 359, 2471 – 2480.

[156] Z. Huang *et al. Org. Lett.* **2015**, 17, 1094 – 1097.

[157] T. Wallace *J. Am. Chem. Soc.* **1964**, 86, 2018 – 2021.

[158] a) T. Billard, A. Greiner & B. R. Langlois *Tetrahedron* **1999**, 55, 7243 – 7250. b) S. Roussel *et al. Synlett* **2004**, 12, 2119 – 2122. c) Z. Liu & R. C. Larock *J. Am. Chem. Soc.* **2005**, 127, 13112 – 13113. d) C. S. Richards-Taylor *et al. J. Org. Chem.* **2017**, 82, 9898 – 9904.

[159] C. Wakselman *et al. Synlett* **2001**, 4, 550 – 552.

[160] a) E. Magnier *et al. Angew. Chem. Int. Ed.* **2006**, 45, 1279 – 1282. b) T. Okazaki, K. K. Laali & A. S. Reddy *J. Fluor. Chem.* **2014**, 165, 91 – 95. c) T. Umemoto *et al. J. Org. Chem.* **2017**, 82, 7708 – 7719.

[161] a) X. Zhao *et al. J. Org. Chem.* **2017**, 82, 9175 – 9181. b) D. Sun *et al. Eur. J. Org. Chem.* **2017**, 3505 – 3511.

[162] S. Yue *et al. J. Fluor. Chem* **2019**, 228, 109410 – 109415.

[163] S. C. Cullen, S. Shekhar & N. K. Nere *J. Org. Chem.* **2013**, 78, 12194 – 12201.

[164] K. Zhang, X. Xu & F. Qing *J. Org. Chem.* **2015**, 80, 7658 – 7665.

[165] a) S. K. Aithagani *et al. RSC Adv.* **2014**, 4, 50208 – 50211. b) L. A. Smyth *et al. J. Org. Chem.* **2016**, 81, 1285 – 1294.

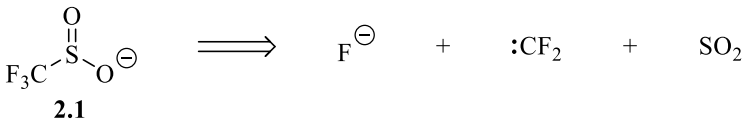
Chapter 2: Radiolabelling the Langlois Reagent with Fluorine-18

Here we report a novel synthesis of the Langlois reagent starting from fluoride. We discuss the modifications required to adapt the chemistry to a radiochemical setting, and subsequently to full automation.

2.1 Development of a Novel Strategy for Synthesising the Langlois Reagent

To accomplish a successful radiosynthesis of the Langlois reagent labelled with fluorine-18, it was necessary to develop a novel synthetic route. To achieve this, many vital validatory studies were carried out employing fluoride in the absence of any radioisotopes. These studies were carried out with the aim of providing insight into which reaction conditions and reagents would be compatible in generating the trifluoromethylsulfinate anion, and therefore amenable to radiosynthesis.

Current approaches to synthesising the Langlois reagent employ toxic, gaseous reagents such as sulfur dioxide, or require multistep syntheses of precursors. None have attempted to carry out a synthesis starting from nucleophilic or electrophilic fluoride. We envisaged a multicomponent one-step approach that combines fluoride, a difluorocarbene source and a source of sulfur dioxide to form trifluoromethanesulfinate **2.1** (Scheme 2.1).

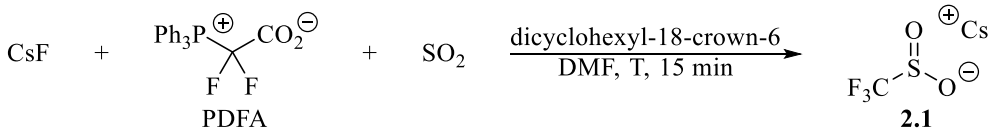


2.1

Scheme 2.1 Proposed one-step approach towards synthesising trifluoromethanesulfinate **2.1** from nucleophilic fluoride

In order to combine these three components while minimising side reactions, a suitable difluorocarbene precursor was selected. A plethora of difluorocarbene reagents have been discovered, each with differing modes of activation, either through nucleophilic/basic attack or thermal decomposition. Additionally, each reagent allows a unique range of reactions to take place. During initial investigations, we elected to heat caesium fluoride in a saturated solution of sulfur dioxide in DMF with difluoromethylenephosphobetaine (PDFA), which upon thermal activation releases triphenylphosphine, carbon dioxide and difluorocarbene (Table 2.1, Entry 1). Dicyclohexyl-18-crown-6 was chosen as an appropriate phase transfer catalyst (PTC) for facilitating solvation of caesium fluoride in organic solvents.

Table 2.1 Novel synthesis of trifluoromethanesulfinate **2.1** from fluoride, PDFA and sulfur dioxide[a]



Entry	T (°C)	Additive	^{19}F NMR Yield 2.1 (%)[b]
1	100	-	0
2	100	DABCO (0.1 mmol)	0
3	120	-	7

[a] General conditions: caesium fluoride (0.1 mmol), dicyclohexyl-18-crown-6 (0.1 mmol), PDFA (0.2 mmol) and SO_2 saturated in DMF (0.5 mL) at T for 15 min.
[b] Relative to 0.1 mmol $PhCF_3$ internal standard.

The crude reaction mixture was dissolved in deuterated DMSO and analysed by ^{19}F NMR spectroscopy using α,α,α-trifluorotoluene as an internal standard. However, no trifluoromethanesulfinate product **2.1** was observed at δ -88.6. Amines such as 1,4-diazabicyclo[2.2. 2]octane (DABCO) are known to form adducts with sulfur dioxide in

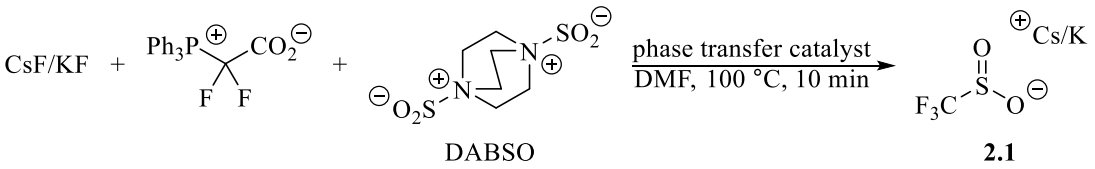
solution, however addition of one equivalent of DABCO had no effect (Table 2.1, Entry 2).[1] A ^{19}F NMR yield of 7% was obtained after increasing the reaction temperature to 120 ºC, giving evidence that the approach laid out in Scheme 2.1 is a viable strategy.

In order to improve the reaction yield, a range of alternative reaction variables were explored. These included sulfur dioxide sources, fluoride sources, solvent, reaction time and temperature.

DABCO-bis(sulfur dioxide) (DABSO) is the adduct formed between DABCO and sulfur dioxide; it is a commercially available reagent that is an efficient, safe and effective alternative to using sulfur dioxide. So far it has only found application in sulfonamide and sulfamide preparation.[2] Since DABSO is a solid that can be weighed out in air, it may be employed in supplying reactions with a controllable source of sulfur dioxide *in situ*, without the need for special setups and precautions.

By employing DABSO instead of sulfur dioxide, trifluoromethanesulfinate **2.1** was afforded in 43% yield (Table 2.2, Entry 1). Under these conditions, altering the ring size of the PTC had little effect on the yield (Table 2.2, Entries 2 – 4). A similar yield of 46% was obtained when employing potassium fluoride with Kryptofix (Table 2.2, Entry 5) suggesting that the two metal fluoride/PTC systems are interchangeable.

Table 2.2 Forming **2.1** with various fluoride/PTC systems when applying DABSO as a source of SO_2[a]

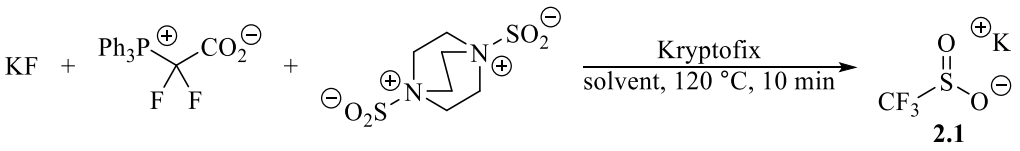


Entry	Fluoride Source	Phase Transfer Catalyst	^{19}F NMR Yield 2.1 (%)[b]
1	CsF	dicyclohexyl-18-crown-6	43
2	CsF	dibenzo-24-crown-8	42
3	CsF	dibenzo-30-crown-10	37
4	CsF	15-crown-5	38
5	KF	Kryptofix	45

[a] General conditions: fluoride source (0.1 mmol), PTC (0.1 mmol), PDFA (0.2 mmol) and DABSO (0.1 mmol) in DMF (0.5 mL) at 100 ºC for 10 min.
[b] Relative to 0.1 mmol $PhCF_3$ internal standard.

To investigate the effect of solvent on the reaction, a number of anhydrous solvents were examined using the potassium fluoride, Kryptofix, PDFA and DABSO system (Table 2.3). When translating reactions to radiochemistry, it is important to know which classes of solvents are compatible or not in order to streamline reaction screening. The ideal solvent in a radiochemical reaction should be water-miscible to aid subsequent purification steps by HPLC or cartridges.

Table 2.3 Solvent compatibility for formation of **2.1**[a]



2.1

Entry	Solvent	^{19}F NMR Yield 2.1 (%)[b]
1	**amide solvents**: DMF, DMA, DMI, NMP, DMPU	22 – 46
2	propylene carbonate	31
3	sulfolane	34
4	DMSO	0
5	**ether solvents**: diglyme, 1,4-dioxane	48 – 55
6	ethylene glycol	0
7	**apolar solvents**: σ-xylene, chlorobenzene, toluene, decalin	22 – 47
8	α,α,α-trifluorotoluene	64[c]

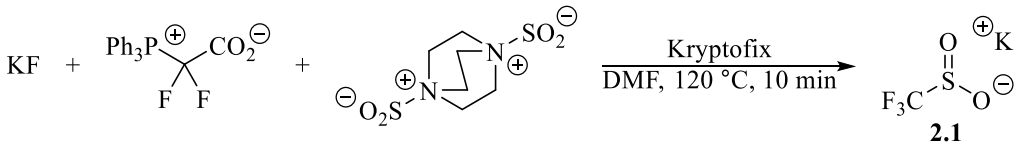
[a] General conditions: potassium fluoride (0.1 mmol), Kryptofix (0.1 mmol), PDFA (0.2 mmol) and DABSO (0.1 mmol) in solvent (0.5 mL) at 120 ºC for 10 min.
[b] Relative to 0.1 mmol $PhCF_3$ internal standard.
[c] Relative to 0.1 mmol TFA internal standard.

Employing polar aprotic and apolar solvents generally furnished **2.1** in moderate yields. Amide solvents afforded yields ranging 22% – 46% (Table 2.3, Entry 1), propylene carbonate 31% (Table 2.3, Entry 2), sulfolane 34% (Table 2.3, Entry 3), ether solvents ranging 48% – 55% (Table 2.3, Entry 5) and apolar solvents ranging 22% – 47% (Table 2.3, Entry 7). No product was observed with DMSO (Table 2.3, Entry 4), which may be due to the strong 1:1 adduct that forms between DMSO and sulfur dioxide.[3] No result was obtained when employing ethylene glycol (Table 2.3, Entry 6), suggesting protic solvents are incompatible with this reaction. α,α,α-Trifluorotoluene afforded **2.1** in the highest yield of

64% which may be due to solvent fuelling the reaction by acting as a fluoride source through decomposition under the reaction conditions.

The effects of altering temperature, time, presence of moisture and additives on the yield of **2.1** were examined (Table 2.4). The yield was lowered when the reaction temperature was decreased from 120 ºC to 100 ºC or 85 ºC (Table 2.4, Entries 1 – 3). Formation of **2.1** was markedly supressed at 150 ºC (Table 2.4, Entry 4).

Table 2.4 Limiting reaction constraints for formation of **2.1**[a]



Entry	Deviation from Conditions	^{19}F NMR Yield 2.1 (%)[b]
1	-	46
2	reaction temperature: 85 ºC	31
3	reaction temperature: 100 ºC	39
4	reaction temperature: 150 ºC	7
5	reaction time: 60 min	12
6	no Kryptofix	9
7	additive: DABCO (0.1 mmol)	19
8	additive: H_2O (0.2 mmol)	<1

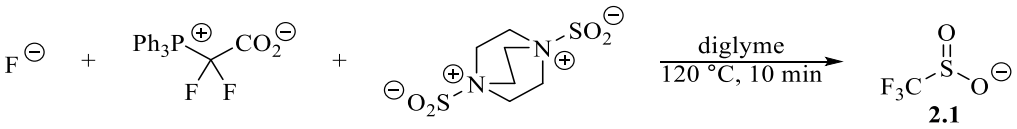
[a] General conditions: potassium fluoride (0.1 mmol), Kryptofix (0.1 mmol), PDFA (0.2 mmol) and DABSO (0.1 mmol) in DMF (0.5 mL) at 120 ºC for 10 min.
[b] Relative to 0.1 mmol $PhCF_3$ internal standard.

Increasing the reaction time to 60 minutes had a significantly detrimental effect on the yield (Table 2.4, Entry 5) compared to standard conditions of 10 minutes (Table 2.4, Entry 1),

suggesting that the Langlois reagent undergoes side reactions over time under these conditions, such as reduction by triphenylphosphine.[4] Withholding Kryptofix saw a drop in yield to 9% suggesting that a PTC is essential for dissolving potassium fluoride in DMF in order for reaction to take place (Table 2.4, Entry 6). Significant decreases in yield were brought about by adding one equivalent of DABCO or two equivalents of water, suggesting the reaction can be quenched by these reagents (Table 2.4, Entries 7 & 8).

We investigated the compatibility of various fluoride sources in order to expedite radiochemical screening. The fluoride sources chosen reflected those used for radiochemical reactions (Table 2.5).

Table 2.5 Fluoride source compatibility for formation of **2.1**[a]



2.1

Entry	Fluoride Source	^{19}F NMR Yield 2.1 (%)[b]
1	KF/Kryptofix	55
2	RbF	12
3	AgF	6
4	CuF_2	2
5	TBAF 1 M in THF	<1
6	$TBAF.3H_2O$	<1

[a] General conditions: fluoride source (0.1 mmol), PDFA (0.2 mmol) and DABSO (0.1 mmol) in diglyme (0.5 mL) at 120 °C for 10 min.
[b] Relative to 0.1 mmol $PhCF_3$ internal standard.

Optimal results were obtained with potassium fluoride and Kryptofix, affording **2.1** in 55% yield (Table 2.5, Entry 1), whereas rubidium, silver or copper(II) fluoride gave poorer yields (Table 2.5, Entries 2 – 4). TBAF was employed either as the trihydrate or in solution with THF, however only trace amounts of **2.1** were observed (Table 2.5, Entries 5 & 6). These results indicate the importance of fluoride solubility for reaction to take place, however ammonium PTCs are incompatible.

To confirm the identity of **2.1**, a crude reaction using exemplary conditions (Table 2.5, Entry 1) was spiked with commercially available Langlois reagent and ^{19}F NMR spectroscopic analysis was carried out (Figure 2.1). A corresponding increase in integration for the suspected trifluoromethanesulfinate signal occurred at δ -88.6, thus helping to confirm the product identity.

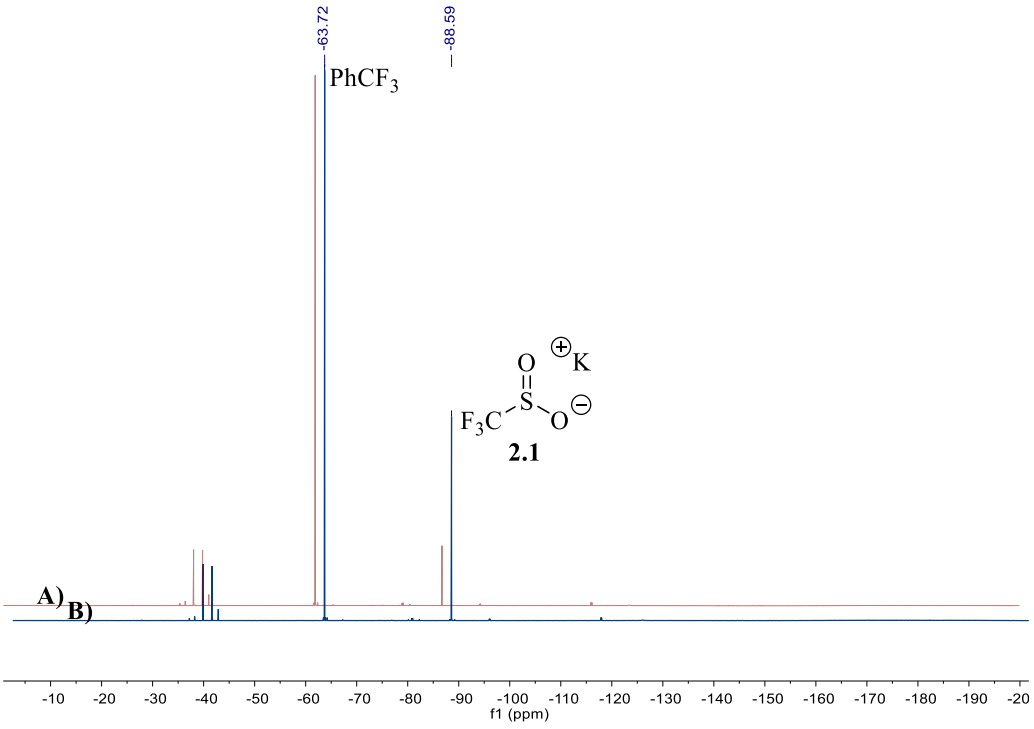


Figure 2.1 ^{19}F NMR spectra of the A) crude reaction B) crude reaction spiked with commercial Langlois reagent

There is more than one possible counterion of trifluoromethanesulfinate present in the crude reaction mixture, however there was no appreciable deviation in chemical shift in the ^{19}F NMR spectra from commercially available sodium trifluoromethanesulfinate. This observation is concurrent with literature which reports a maximum deviation of 0.5 ppm between sodium, potassium and silver salts of trifluoromethanesulfinate.[5] Larger deviations of more than 2 ppm have been observed with ammonium counterions.[6] Therefore it is assumed that a potassium (or caesium) cation is the counterion and not an ammonium compound.

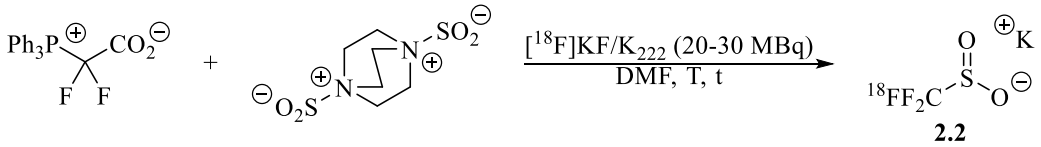
In conclusion, a novel synthetic route was validated for synthesising the Langlois reagent in a three-component reaction. After investigating the reaction parameters, successful synthesis of the Langlois reagent was achieved by employing fluoride solubilised by a PTC, PDFA as a thermally activated difluorocarbene source, and the commercial reagent DABSO. The reaction could be carried out in most polar aprotic and apolar solvents, at a reaction temperature of 120 ºC to afford optimal yields.

2.2 Radiolabelling the Langlois Reagent and Mechanistic Insights

Having identified optimal conditions for synthesising the trifluoromethanesulfinate ion from the fluoride ion, we set about translating this reaction to label the Langlois reagent with fluorine-18 (Table 2.6). Successful formation of the radiolabelled Langlois reagent was observed in trace amounts by adding aliquots of potassium [^{18}F]fluoride and Kryptofix in DMF (10 – 50 μL) to PDFA (0.08 mmol) and DABSO (0.04 mmol) in DMF (300 μL) before heating to 100 ºC for 10 minutes (Table 2.6, Entry 1). No substantial improvements were made to the RCY by increasing the reaction time to 20 minutes (Table 2.6, Entry 2),

decreasing the amount of NMM-SO_2 to 0.02 mmol (Table 2.6, Entry 3), or decreasing the reaction temperature to 80 ºC (Table 2.6, Entry 4).

Table 2.6 Radiolabelling the Langlois reagent using DABSO[a]



2.2

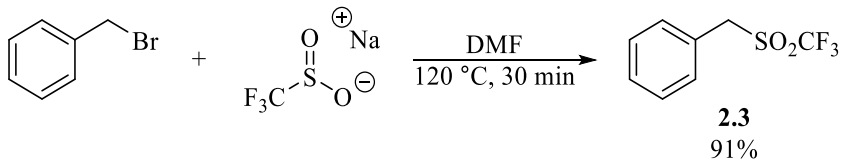
Entry	DABSO (mmol)	t (min)	T (ºC)	RCY 2.2 (%, *n* = 2)
1	0.04	10	100	1 ± 1
2	0.04	20	100	2 ± 0
3	0.02	20	100	4 ± 3
4	0.02	20	80	3 ± 3

[a] General conditions: [^{18}F]KF/K_{222} (20 – 30 MBq in 10 – 50 μL DMF), PDFA (0.08 mmol) and DABSO in DMF (300 μL) at T for t. Crude quenched with water and RCY measured by radio-HPLC.

The radio-HPLC of the radiochemical reaction was compared with a UV spectrum of commercially available Langlois reagent, detectable at 220 nm, establishing the identity of **2.2** at a retention time of 5.5 minutes (see Chapter 4: Experimental Data for details). ESI-MS of this suspected peak was collected and analysed (*m/z* calculated for $CF_3SO_2^-$, 133.0; found, 133.1; see Chapter 4: Experimental Data for details). Although MS detectors are not sensitive enough to identify radiolabelled compounds, present in picomolar quantities, a calibration curve for the unlabelled compound revealed it was generated in micromolar quantities and the molar activity was 0.01 GBq μmol^{-1}, sufficient for analysis by ESI-MS.

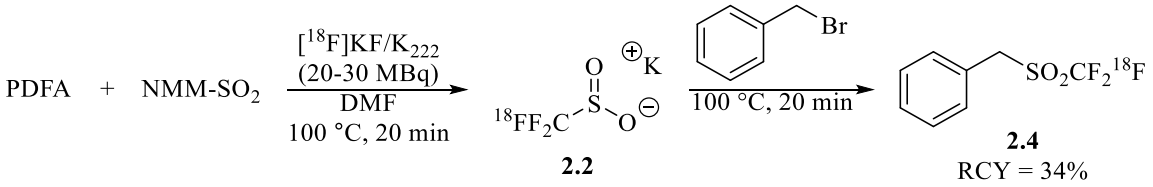
To further validate the identity of radiolabelled Langlois reagent **2.2**, it was converted into an organic compound with better retention on HPLC columns. To test reaction conditions

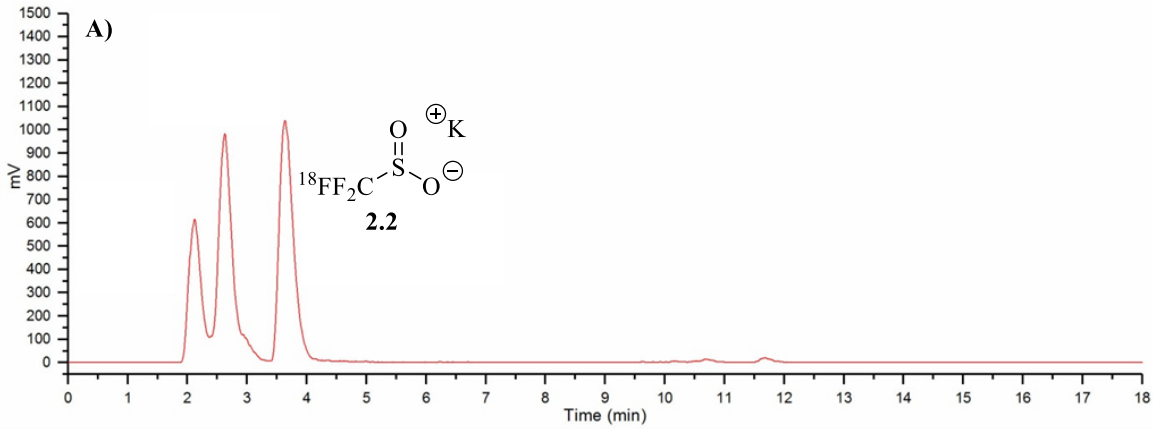
for this, a non-radiochemical reaction was carried out between the Langlois reagent **2.1** and benzyl bromide. The product of this nucleophilic substitution, **2.3**, was isolated in 91% yield (Scheme 2.2) and used as a HPLC reference for the analogous radiochemical reaction.



Scheme 2.2 Nucleophilic substitution reaction between the Langlois reagent and benzyl bromide to form **2.3**

To test this reaction in a radiochemical setting, **2.2** was synthesised and benzyl bromide was added to the crude reaction mixture before heating to 100 ºC (Figure 2.2). The product of nucleophilic substitution **2.4** was identified by radio-HPLC in 34% RCY suggesting **2.2** was indeed formed during the initial reaction.





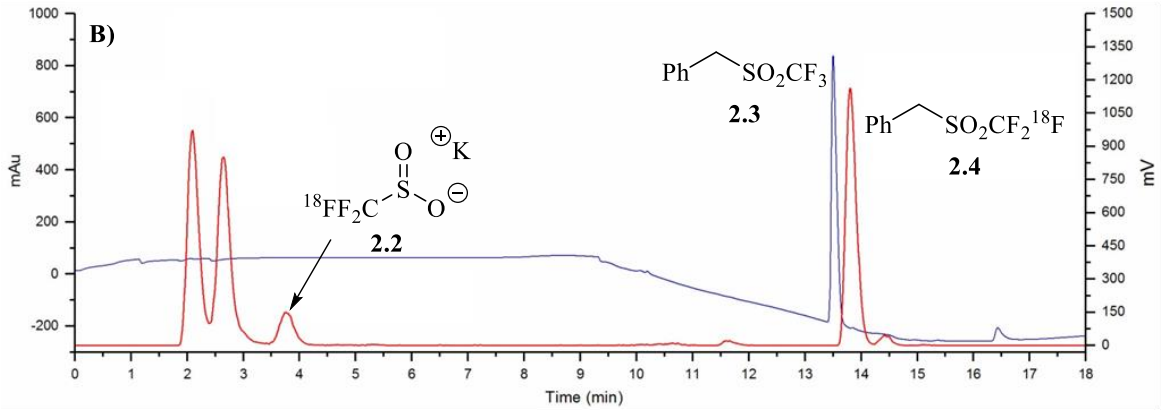
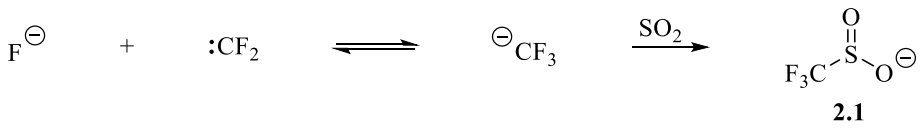


Figure 2.2 Reaction between **2.2** and benzyl bromide with radio-HPLC analysis A) before the reaction B) after the reaction with overlay of UV trace of authentic reference **2.3**

In order to improve the RCY of **2.2**, analysis of the non-radiochemical reaction mixture was examined to provide insight into possible reaction mechanisms. One proposed mechanism involves nucleophilic attack of difluorocarbene by fluoride to form the trifluoromethyl anion. This is analogous to the reported formation of $CuCF_3$ from difluorocarbene, fluoride and a copper(I) salt.[7] This trifluoromethyl anion proceeds to react with sulfur dioxide, released in solution upon heating DABSO, to form trifluoromethanesulfinate (Scheme 2.3).



Scheme 2.3 Potential reaction mechanism for generating trifluoromethanesulfinate *via* the trifluoromethyl anion

This mechanism does not account for the observed large difference in yields when employing DABSO (Table 2.2, Entry 1) or a saturated solution of sulfur dioxide, with or without the presence of DABCO (Table 2.1). Additionally, formation of the trifluoromethyl anion is known to be highly unstable in the presence of group one metals, which decomposes

to difluorocarbene and fluoride even at very low temperatures.[8] Therefore, under the specified conditions, formation of **2.1** may not proceed *via* the trifluoromethyl anion.

To identify alternative reaction mechanisms, we assigned all products observed by ^{19}F NMR spectroscopic analysis of the crude reaction mixture (Figure 2.3). The observation of a singlet peak at 38.3 ppm corresponds to the fluorosulfate anion **2.5**.[9] This provides evidence that fluoride and sulfur dioxide may react under these conditions to form the fluorosulfite anion (FSO_2^-). FSO_2^- subsequently disproportionates to the fluorosulfate anion (FSO_3^-) in the presence of sulfur dioxide, a mechanism supported by the literature.[10] Alternatively, the fluorosulfite anion rapidly hydrolyses to form bifluoride, disulfite and sulfur dioxide in the presence of moisture.

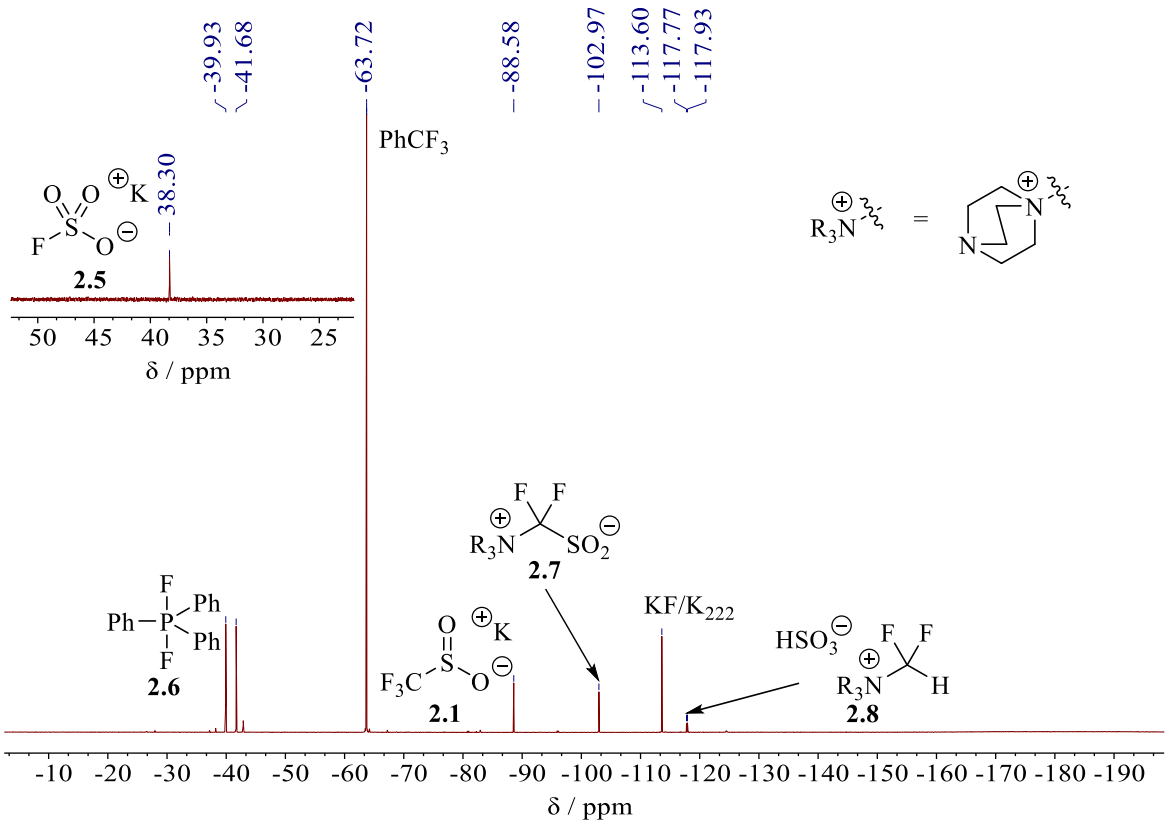
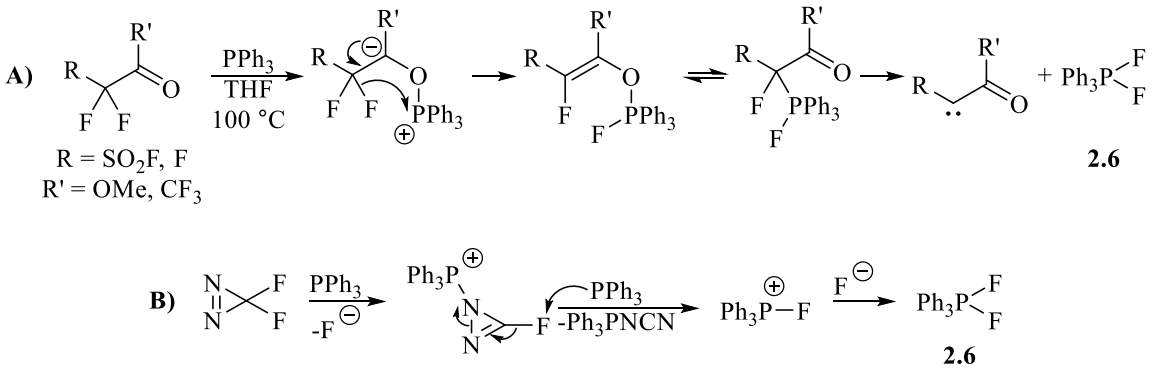


Figure 2.3 ^{19}F NMR spectrum of crude reaction mixture between KF/K_{222}, PDFA, and DABSO heated in DMF

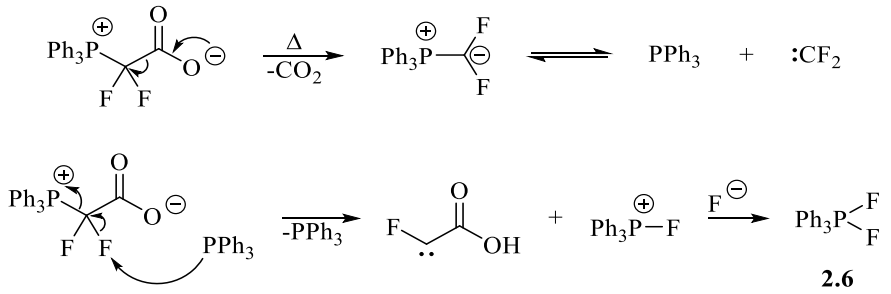
The doublet observed at -40.8 ppm corresponds to difluorotriphenylphosphorane **2.6**, which has been observed in the literature for a reaction between triphenyl phosphine and a difluorocarbene reagent.[11] The reaction mechanism proposed in the literature involves initial P-O bond formation between triphenyl phosphine and the carbonyl group followed by double transfer of fluorine by the difluorocarbene reagent methyl 2,2-difluoro-2-(fluorosulfonyl)acetate to phosphorus (Scheme 2.4, A). This same mechanism has also been suggested for the reaction between triphenylphosphine and hexafluoroacetone.[12] An alternative mechanism is proposed for the reaction between triphenylphosphine and the difluorocarbene reagent difluorodiazomethane (Scheme 2.4, B).[13]



Scheme 2.4 Formation of difluorotriphenylphosphorane **2.6** from triphenylphosphine and various difluorocarbene reagents

Following on from these literature reports, we proposed the following mechanism for forming difluorotriphenylphosphorane **2.6** from PDFA (Scheme 2.5). It is well know that difluorocarbene in the presence of triphenylphosphine forms a phosphonium ylide reversibly.[14] This phosphobetaine intermediate possesses unique reactivity over difluorocarbene which has mainly found utility in Wittig-type reactions.[15] Triphenylphosphine, produced from thermal activation of PDFA, may abstract fluorine from another PDFA molecule by nucleophilic attack, with triphenylphosphine as a leaving group.

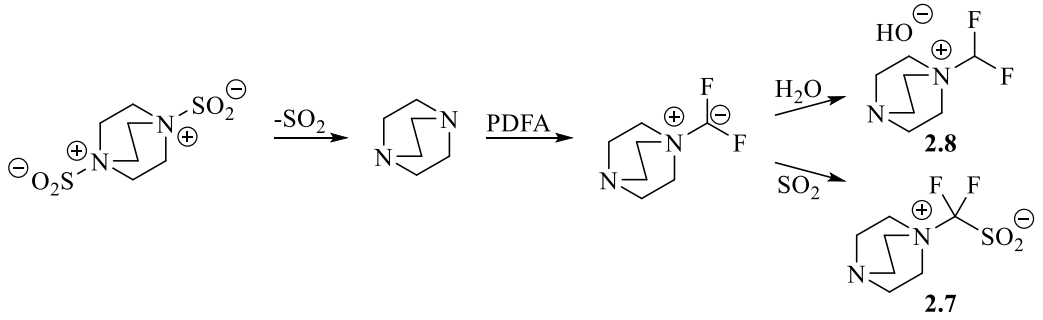
The resultant fluorotriphenylphosphonium cation is then susceptible to nucleophilic attack by fluoride affording difluorotriphenylphosphorane.



Scheme 2.5 Proposed mechanism for the formation of difluorotriphenylphosphorane **2.6** from PDFA

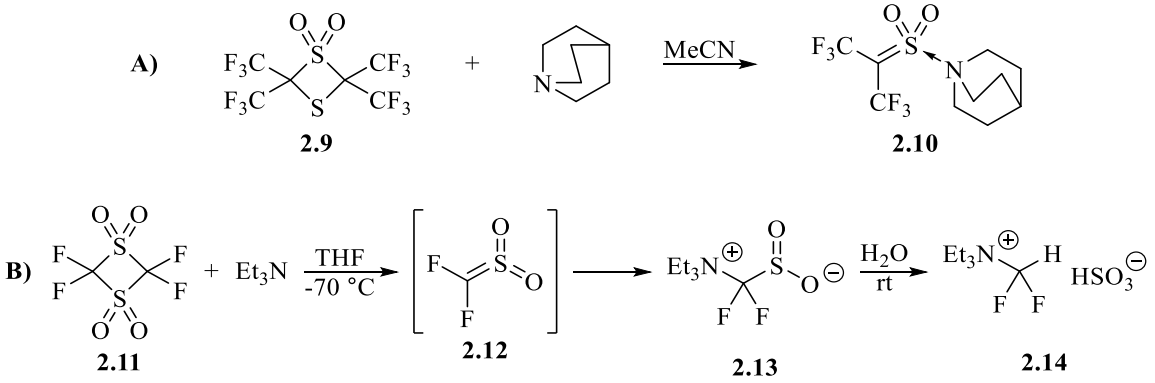
The singlet and doublet observed at δ -103.0 and -117.8 of the ^{19}F NMR spectrum belong to the difluoromethylsulfinate and difluoromethyl compounds of DABCO (**2.7** and **2.8**). The doublet signal at δ -117.8 has a coupling constant of 58.5 Hz which is in agreement with the literature and characteristic of difluoromethyl amines.[16] In addition, these two signals shifted accordingly when other amine-SO_2 adducts were employed, for example, reacting the *N*-methylmorpholine-SO_2 adduct gave rise to a singlet and doublet observed at δ -101.29 and -114.51.

The appearance of these amine products provides some insight into the reaction mechanism. The difluoromethylated product **2.8** may have been produced by the reaction between difluorocarbene and DABCO followed by protonation during work-up (Scheme 2.6). This type of reaction has been reported using a number of amines and difluorocarbene sources.[17] Instead of protonation, subsequent reaction with sulfur dioxide may afford the difluoromethylsulfinate product **2.7**. Capture of sulfur dioxide by carbon nucleophiles has previously been reported, mainly through using alkyl Grignard and alkali metal compounds.[18]



Scheme 2.6 Proposed mechanism for formation of **2.7** and **2.8**

An alternative mechanism for the synthesis of these two compounds is inspired by the work of Sundermeyer *et al.* who synthesised analogous products, using amines quinuclidine and triethylamine, that proceeded *via* sulfene intermediates (Scheme 2.7).[19] The combination of 2,2,4,4-tetrakis(trifluoromethyl)-1,3-dithietane 1,1-dioxide (**2.9**) with quinuclidine in acetonitrile led to precipitation of the bis(trifluoromethyl)sulfene-quinuclidine adduct (**2.10**) (Scheme 2.7, A). X-ray crystallography of the product indicated that quinuclidine donates its pair of electrons to the sulfur atom of the sulfene.

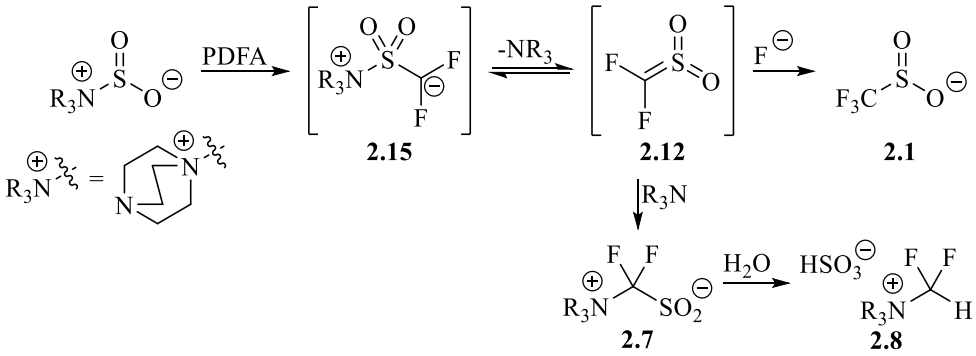


Scheme 2.7 Formation of sulfene adducts with amines

In contrast, the reaction between 2,2,4,4-tetrafluoro-1,3-dithietane 1,1,3,3-tetraoxide **2.11** and triethylamine afforded product **2.13** (Scheme 2.7, B). This was proposed as evidence for the existence of the sulfene intermediate **2.12** which was not isolated. In the presence of

water, **2.13** hydrolysed to **2.14**. The structure of compound **2.13** was elucidated using X-ray crystallography and ^{19}F NMR spectroscopy, giving a characteristic signal of δ -99.6. **2.14** gave a doublet signal at δ -111.2 with a coupling constant of 57.1 Hz, characteristic of difluoromethyl amines.

Compounds **2.5** and **2.6** are DABCO analogues of compounds **2.13** and **2.14** which may suggest a mechanism for their formation involving sulfene intermediate **2.12**. This led us to propose a mechanism starting with nucleophilic attack of difluorocarbene by DABSO (Scheme 2.8). Nucleophilic behaviour of DABSO has been reported with electrophiles such as aluminium trichloride or diazonium compounds.[20] DABCO acts as a leaving group to form sulfene intermediate **2.12** which may undergo nucleophilic attack by fluoride to form **2.1** or by DABCO to form **2.7** which subsequently hydrolyses during work-up to **2.8**.



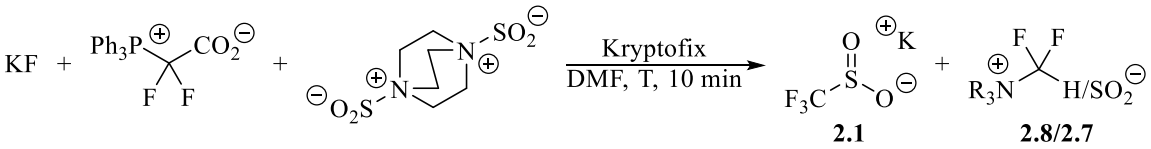
Scheme 2.8 Proposed mechanism for formation of **2.1**, **2.7** and **2.8** *via* sulfene intermediate **2.12**

This mechanism is in accordance with observations made during the reaction between DABSO, PDFA and KF/K_{222} or CsF/dicylcohexyl-18-crown-6 in DMF at 100 ºC. All reagents were combined in a vial with both PDFA and the fluoride ion source remaining as insoluble precipitates. Upon heating, effervescence was observed, which may be attributed to PDFA thermally activating to release carbon dioxide, triphenylphosphine and

difluorocarbene. The ensuing difluorocarbene generated reacted with DABSO to form **2.15**. Once gas release subsided, the mixture contained a white precipitate, suggesting that when all PDFA had reacted, metal fluoride was left suspended as this precipitate. At this point in time, no **2.1**, **2.7** or **2.8** products were observed by ^{19}F NMR spectroscopic analysis of the reaction mixture, which is concurrent with this running hypothesis. Within 5 minutes the white precipitate slowly disappeared and the three aforementioned compounds formed accordingly, as identified by ^{19}F NMR spectroscopy.

The ratio between trifluoromethanesulfinate **2.1** and products **2.7** and **2.8** was dependant on reaction temperature (Table 2.7). At 85 ºC, 20%, 66% and 31% of **2.7**, **2.8** and **2.1** were produced respectively (Table 2.7, Entry 1). Increasing the temperature to 100 ºC saw a decrease in **2.7** and **2.8** but an increase in **2.1** (Table 2.7, Entry 2).

Table 2.7 Temperature-dependant formation of **2.1**, **2.7** and **2.8**[a]



Entry	T (ºC)	^{19}F NMR Yield 2.1 (%)[b]	^{19}F NMR Yield 2.7 (%)[b]	^{19}F NMR Yield 2.8 (%)[b]
1	85	31	20	66
2	100	39	8	36
3	120	46	0	0
4	150	7	0	0

[a] General conditions: potassium fluoride (0.1 mmol), Kryptofix (0.1 mmol), PDFA (0.2 mmol) and DABSO (0.1 mmol) in DMF (0.5 mL) at T for 10 min.
[b] Relative to 0.1 mmol $PhCF_3$ internal standard.

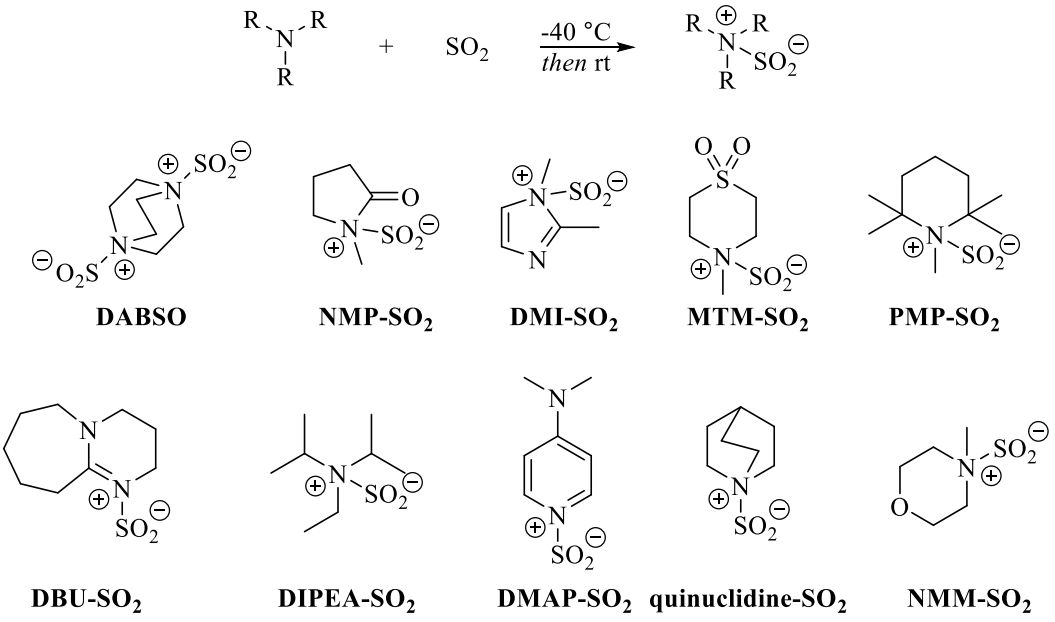
At 120 ºC and 150 ºC, **2.1** was achieved in 46% and 7% yield with no **2.7** or **2.8** being formed (Table 2.7, Entries 3 & 4). This suggests that the pathway to **2.7** and **2.8** is favoured at lower temperatures, but **2.1** is favoured at higher temperatures with a cut-off point at excessively high temperatures.

The proposed mechanism (Scheme 2.8), supported by reaction observations and ^{19}F NMR spectroscopic analysis, suggests that intermediate fluorinated species such as **2.15** or **2.12** exist for a few minutes before reacting with fluoride or DABCO. Therefore the nature of the amine may play a pivotal role in generating these two species and in deciding the rate of competing side reactions.

With this hypothesis in mind we investigated the synthesis and reaction of several amine-sulfur dioxide adducts. Several sulfur dioxide adducts have previously been synthesised with the purpose of studying stability and structure, but only DABSO has found synthetic use.[21,2] Raman and IR spectroscopy have been used to examine the strength of intermolecular forces between sulfur dioxide and various compounds, revealing that many amines are bound weakly, such as *N*-methylaniline, *N*,*N*-dimethylaniline and *N*,*N*-diethylaniline.[22] IR spectroscopic analysis revealed that the degree of non-bonding electron donation by the amine to the anti-bonding orbital of the S-O bond is related to a corresponding change in magnitude of vibrational frequency shift.[22]

Only a handful of substrates possess sterically and electronically favourable characteristics to form isolable solid or liquid adducts. These compounds include sulfur dioxide adducts with trimethylamine, dimethylamine, *ρ*-phenylenediamine, *N*,*N*,*N'*,*N'*-tetramethyl-*ρ*-phenylenediamine, aniline, hydroquinone, alkyl hydrazines, hexamethylenetetramine, quinuclidine, pyridine derivatives and most recently a novel phosphine reagent.[22,23]

We attempted to synthesise a number of amine-SO_2 adducts by condensing sulfur dioxide gas at -40 ºC onto an amine under anhydrous conditions and inert atmosphere. The solution was then brought to room temperature under N_2 gas flow to remove excess sulfur dioxide. Under these conditions, adducts of 1,2-dimethylimidazole (DMI), 4-dimethylaminopyridine (DMAP), quinuclidine, 1,8-diazabicyclo[5.4.0]undec-7-ene (DBU), 1,2,2,6,6-pentamethylpiperidine (PMP), *N*,*N*-diisopropylethylamine (DIPEA), 4-methylthiomorpholine 1,1-dioxide (MTM), *N*-methyl-2-pyrrolidone (NMP), and *N*-methylmorpholine (NMM) were successfully isolated (Scheme 2.9). Factors that hindered isolation of other adducts include low boiling points, high vapour pressures, high sensitivity to moisture, and thermal instability at room temperature.

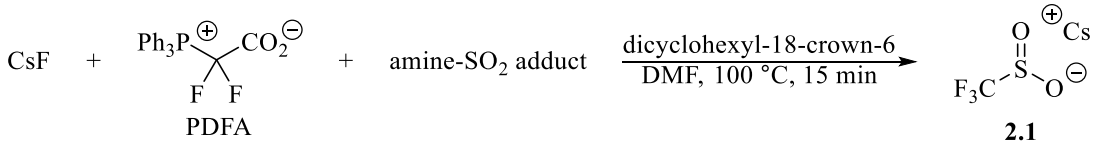


Scheme 2.9 Successful formation of amine-SO_2 adducts

With these amine-SO_2 adducts in hand, we proceeded to test their compatibility for reactions forming trifluoromethanesulfinate **2.1** (Table 2.8). Sulfur dioxide adducts of DBU, DMI, DMAP, DIPEA and NMP did not afford any trifluoromethanesulfinate **2.1** (Table 2.8, Entries 1 – 5). The major product was often fluoroform, supporting the case that the nature

of the amine plays a role in the reaction mechanism. It has been reported that adding nucleophilic bases, such as sodium hydroxide, to the Langlois reagent leads to quantitative release of fluoroform gas.[24] The sulfur dioxide adducts obtained for DBU, DIPEA and NMP were very hygroscopic which may have hampered the reaction. PMP-SO_2 and quiuclidine-SO_2 adducts afforded **2.1** in 3% and 5% respectively (Table 2.8, Entries 6 & 7). 18% and 52% yields were observed when employing MTM-SO_2 and NMM-SO_2 (Table 2.8, Entries 8 & 9).

Table 2.8 Amine-SO_2 adduct screening for formation of **2.1**[a]



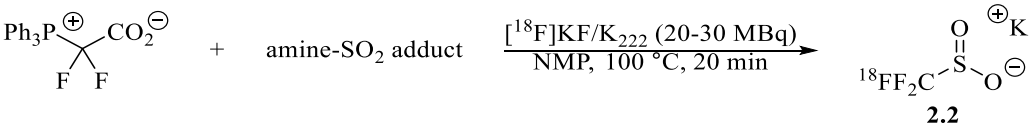
2.1

Entry	Amine-SO_2 Adduct	^{19}F NMR Yield 2.1 (%)[b]
1	DBU-SO_2	0
2	DMI-SO_2	0
3	DMAP-SO_2	0
4	DIPEA-SO_2	0
5	NMP-SO_2	<1
6	PMP-SO_2	3
7	quinuclidine-SO_2	5
8	MTM-SO_2	18
9	NMM-SO_2	52
10	DABSO	43

[a] General conditions: caesium fluoride (0.1 mmol), dicyclohexyl-18-crown-6 (0.1 mmol), PDFA (0.2 mmol) and amine-SO_2 adduct (0.2 mmol) in DMF (0.5 mL) at 100 ºC for 15 min. [b] Relative to 0.1 mmol $PhCF_3$ internal standard.

Following this reaction screening, we proceeded to test amine-SO_2 adducts under radiochemical conditions (Table 2.9). Adducts of MTM, quinuclidine, DMAP and DMI led to small or trace amounts of labelled Langlois reagent **2.2** (Table 2.9, Entries 1 – 4). Employing NMM-SO_2 afforded **2.2** most successfully, giving 16% RCY (Table 2.9, Entry 5).

Table 2.9 Amine-SO_2 adduct screening for formation of **2.2**[a]



2.2

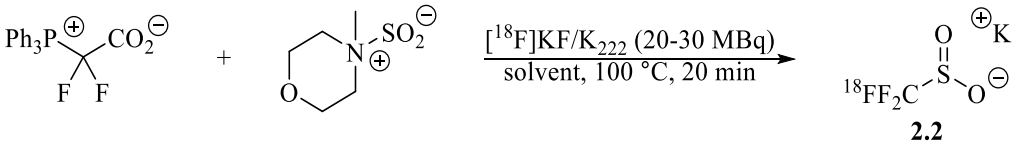
Entry	Amine-SO_2 Adduct	RCY 2.2 (%, *n* = 2)
1	MTM-SO_2	0
2	quinuclidine-SO_2	4 ± 3
3	DMAP-SO_2	5 ± 1
4	DMI-SO_2	6 ± 1
5	NMM-SO_2	16 ± 3
6[b]	DABSO	4 ± 3

[a] General conditions: [^{18}F]KF/K_{222} (20 – 30 MBq in 10 – 50 μL DMF), PDFA (0.08 mmol) and amine-SO_2 adduct (0.02 mmol) in NMP (300 μL) at 100 ºC for 20 min. Crude quenched with water and RCY measured by radio-HPLC.
[b] Reaction solvent DMF

To identify the reaction conditions for achieving optimal yields, various solvents, concentrations, reagent stoichiometries and reaction temperatures were extensively investigated.

Solvent screening revealed that DMI, DMA, DMF and propylene carbonate all afforded **2.2** in similar RCYs of 21% – 24% (Table 2.10, Entries 1 – 4), whereas DMPU, diglyme, 1,4-dioxane and acetonitrile gave lower RCYs of 4% – 12% (Table 2.10, Entries 5 – 8).

Table 2.10 Solvent screening for formation of **2.2**[a]



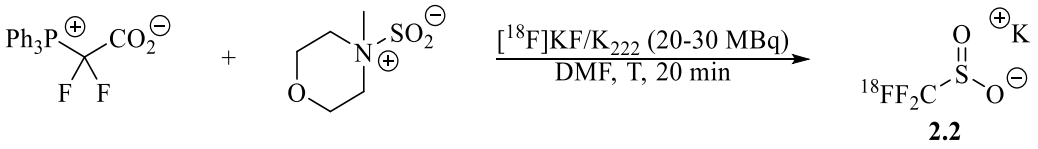
2.2

Entry	Solvent	RCY 2.2 (%, *n* = 2)
1	DMI	21 ± 5
2	DMA	24 ± 10
3	DMF	22 ± 8[b]
4	propylene carbonate	22 ± 6[b]
5	DMPU	12 ± 2
6	diglyme	8 ± 2[b]
7	1,4-dioxane	11 ± 4
8	MeCN	4 ± 0[c]

[a] General conditions: [^{18}F]KF/K_{222} (20 – 30 MBq in 10 – 50 μL DMF), PDFA (0.08 mmol) and NMM-SO_2 (0.02 mmol) in solvent (300 μL) at 100 ºC for 20 min. Crude quenched with water and RCY measured by radio-HPLC.
[b] (*n* = 4). [c] Reaction temperature 80 ºC.

To examine the effect of concentration, the reaction was carried out in increasing volumes of DMF (Table 2.11, Entries 1 –3). Reaction volumes of 600 μL or 900 μL DMF afforded **2.2** in 18% and 14%, however an optimum yield of 22% was obtained by employing 300 μL DMF. Increasing the temperature to 120 ºC had no effect on the yield (Table 2.11, Entry 4).

Table 2.11 Effect of concentration and reaction temperature on formation of **2.2**[a]



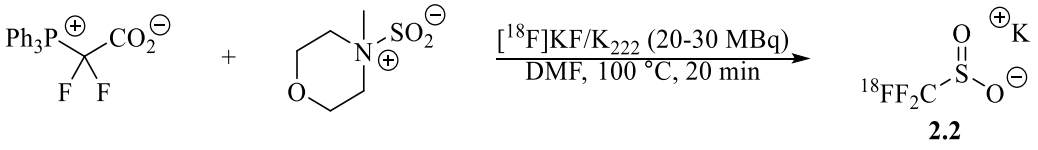
2.2

Entry	T (°C)	Solvent Volume	RCY 2.2 (%, *n* = 2)
1	100	300 μL	22 ± 8[b]
2	100	600 μL	18 ± 4
3	100	900 μL	14 ± 4
4	120	300 μL	22 ± 1

[a] General conditions: [^{18}F]KF/K_{222} (20 – 30 MBq in 10 – 50 μL DMF), PDFA (0.08 mmol) and NMM-SO_2 (0.02 mmol) in DMF at T for 20 min. Crude quenched with water and RCY measured by radio-HPLC. [b] (*n* = 4).

Investigations into varying the stoichiometry of NMM-SO_2 and PDFA identified the ideal ratio to be one-to-four (Table **2.12**). The reaction shut down when the amount of NMM-SO_2 fell outside the range of 0.02 – 0.04 mmol in the presence of 0.08 mmol PDFA (Table **2.12**, Entries 1 – 4). Similarly, the range of PDFA was limited to 0.06 – 0.10 mmol in the presence of 0.02 mmol NMM-SO_2 (Table **2.12**, Entries 2 & 5 – 7).

Table 2.12 Characterising stoichiometry ranges of NMM-SO_2 and PDFA for formation of **2.2**[a]



2.2

Entry	NMM-SO_2 (mmol)	PDFA (mmol)	RCY 2.2 (%, *n* = 2)
1	0.01	0.08	0

2	0.02	0.08	22 ± 8
3	0.04	0.08	19 ± 5[b]
4	0.08	0.08	1 ± 1
5	0.02	0.04	7 ± 4
6	0.02	0.06	14 ± 14
7	0.02	0.10	11 ± 2

[a] General conditions: [^{18}F]KF/K_{222} (20 – 30 MBq in 10 – 50 μL DMF), PDFA and NMM-SO_2 in DMF at 100 ºC for 20 min. Crude quenched with water and RCY measured by radio-HPLC. [b] (n = 4).

In summary, the novel synthetic strategy of combining fluoride, a difluorocarbene reagent and a sulfur dioxide source to synthesise the Langlois reagent was successfully rendered in a radiochemical setting. Identity of the radiolabelled Langlois reagent was confirmed by HPLC analysis, mass spectrometry and subsequent reaction with benzyl bromide. After considering the reaction mechanism, the RCY was optimised by employing NMM-SO_2, a novel amine-SO_2 compound.

2.3 Purification and Isolation of the Langlois Reagent

With conditions in hand for radiolabelling the Langlois reagent with fluorine-18, methods were investigated for purifying and isolating the Langlois reagent from the crude reaction. Attempts to apply a patented purification method, described by B. R. Langlois for purifying the Langlois reagent from organic and inorganic impurities were unsuccessful in separating the Langlois reagent from unreacted fluoride and PTC so was unsuitable for use in a radiochemical setting.[25]

Instead, we predicted that ion-exchange cartridges could be employed as a way of purifying the Langlois reagent from the reaction mixture. Weak Anion Exchange (WAX) cartridges could be used for this as they consist of polymers containing amine functional groups that protonate reversibly to allow trapping and elution of anions (Figure 2.4, A).

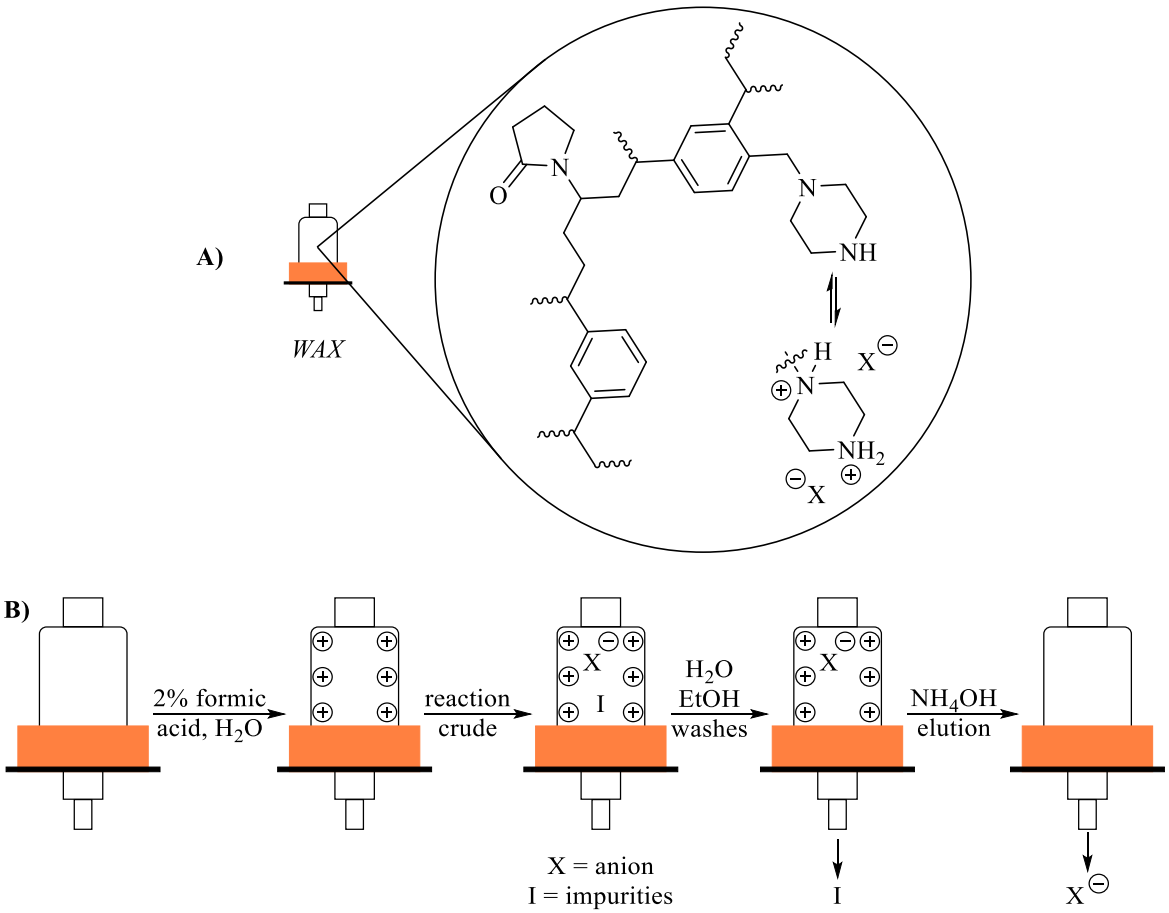
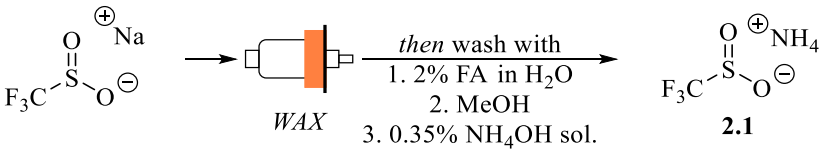


Figure 2.4 A) Amine functional groups in a WAX cartridge trap anions at acidic pH B) procedure for purifying anions from a reaction mixture using a WAX cartridge

These amine functional groups are protonated by passing an acidic solution through the cartridge, followed by addition of the crude mixture to trap the desired anionic compound (Figure 2.4, B). Anionic components remain bound to the solid phase whilst impurities may be removed with aqueous and organic washes. To elute off the product, the cartridge is deactivated by deprotonating the amine functional groups using a basic solution.

Preliminary experiments were carried out using commercially available Langlois reagent to test the retention of the trifluoromethanesulfinate ion on WAX cartridges (Oasis Plus, short cartridge) and to find optimum conditions for elution (Table 2.13). The Langlois reagent was excellently retained when a solution of sodium trifluoromethanesulfinate in water (1 mL, 0.1 M) was loaded onto an activated WAX cartridge and washed with 2% formic acid in water or 100% methanol (Table 2.13, Entries 1 & 2). The product was eluted off almost quantitatively as the ammonium salt by using 0.35% ammonium hydroxide solution in water or methanol (Table 2.13, Entries 3 & 4). The amount of trifluoromethanesulfinate in each elution solution was analysed by ^{19}F NMR spectroscopy and a yield of the isolated compound was obtained by evaporating the solvent *in vacuo*. In conclusion, WAX cartridges are ideal for extracting the Langlois reagent from solution with high efficiency.

Table 2.13 WAX cartridge retention and elution efficiency of commercial Langlois reagent[a]

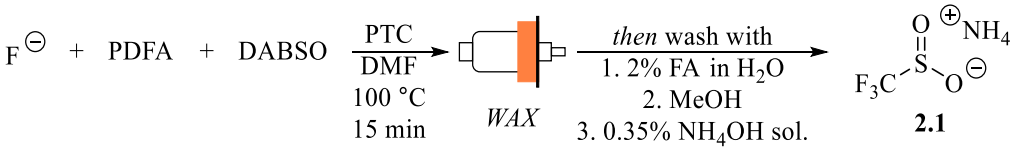


Entry	Elution Solution	^{19}F NMR Yield 2.1 (%)[b]
1	2% formic acid in H_2O	<1
2	MeOH	<1
3	0.35% NH_4OH in H_2O	99 (88)
4	0.35% NH_4OH in MeOH	98 (87)

[a] General conditions: load activated WAX cartridge (Oasis Plus, short) with sodium trifluoromethanesulfinate in water (1 mL, 0.1 M), wash with elution solution (3 mL).
[b] Relative to 0.1 mmol TFA internal standard, isolated yield in parentheses.

After establishing this protocol, we proceeded to purify trifluoromethanesulfinate from crude reaction mixtures (Table **2.14**). A reaction was carried out using PDFA, DABSO and KF/K_{222} or CsF/dicyclohexyl-18-crown-6 in DMF at 100 ºC for 15 minutes. 2% formic acid in water was added and the mixture was loaded onto an activated WAX cartridge. Trifluoromethanesulfinate **2.1** retained well upon loading and washing with 2% formic acid in water or methanol. 0.35% ammonium hydroxide solution in methanol/water was employed to elute **2.1** in 32% and 37% yield for the two respective reactions, as determined by ^{19}F NMR spectroscopy. The product was analytically pure as determined by ESI-MS, ^{1}H, ^{19}F, ^{13}C and ^{31}P NMR spectroscopy. As a comparison, spectroscopic analysis of the crude mixtures revealed ^{19}F NMR yields of 47% and 51% respectively, suggesting the purification method is efficient.

Table 2.14 WAX cartridge retention and elution efficiency of trifluoromethanesulfinate from crude reaction mixtures[a]



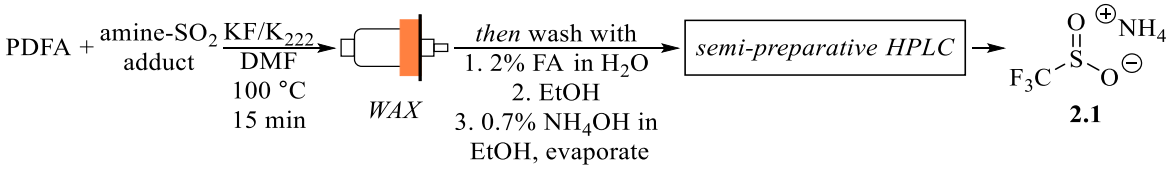
Entry	Fluoride Source	Elution Solution	^{19}F NMR Yield 2.1 (%)[b]
1	KF/K_{222}	Load	11
2		2% formic acid in H_2O	<1
3		MeOH	<1
4		0.35% NH_4OH in MeOH:H_2O 25:75	32
5	CsF/dicyclohexyl-18-crown-6	Load	2
6		2% formic acid in H_2O	<1

7	MeOH	<1
8	0.35% NH_4OH in MeOH:H_2O 25:75	37

[a] General conditions: fluoride source (0.1 mmol), PTC (0.1 mmol), PDFA (0.2 mmol) and DABSO (0.1 mmol) in DMF (0.5 mL) at 100 ºC for 15 min. Load activated WAX cartridge (Oasis Plus, short) with crude reaction mixture diluted with 2% formic acid in water (0.5 mL), wash with elution solution (3 mL).
[b] Relative to 0.1 mmol TFA internal standard.

Next we explored methods for isolating the Langlois reagent using semi-preparative HPLC. Reactions were carried out with KF/K_{222}, PDFA and DABSO or NMM-SO_2 in DMF followed by WAX cartridge purification (Table 2.15). The trifluoromethanesulfinate anion was eluted from the WAX cartridge using 0.7% ammonium hydroxide in ethanol which was then evaporated *in vacuo*. The residue was redissolved in water before isolating **2.1** by semi-preparative HPLC. The Langlois reagent was poorly retained on nearly all HPLC columns tested, except for 100% aqueous stable columns such as the Synergi Hydro-RP or Gemini NX-C18 columns by Phenomenex. Interestingly, better retention was obtained when running an eluent comprising of 95% water and 5% acetonitrile, compared to 100% water, however a higher proportion of acetonitrile led to poorer retention. The HPLC eluent was evaporated azeotropically with acetonitrile to afford isolated **2.1** in 31% and 44% yield when using DABSO or NMM-SO_2 respectively (Table 2.15, Entries 1 & 2).

Table 2.15 Implementation of WAX cartridges and semi-preparative HPLC for purification and isolation of **2.1** from crude reaction mixtures[a]



Entry	Amine-SO_2 Adduct	Yield Isolated 2.1 (%)
1	DABSO	31
2	NMM-SO_2	44

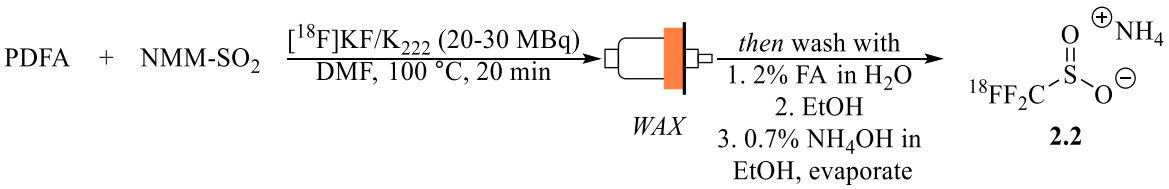
[a] General conditions: potassium fluoride (0.1 mmol), Kryptofix (0.1 mmol), PDFA (0.2 mmol) and DABSO (0.1 mmol) or NMM-SO_2 (0.2 mmol) in DMF (0.5 mL) at 100 ºC for 15 min.

After successfully using WAX cartridges and semi-preparative HPLC in tandem to purify and isolate the Langlois reagent from the reaction mixture, these methods were pursued further in purifying and isolating the Langlois reagent labelled with fluorine-18.

2.4 Purification and Isolation of the [^{18}F]Langlois Reagent

A reaction was carried out with [^{18}F]KF/K_{222} (25.2 MBq aliquot in DMF), PDFA and NMM-SO_2 in DMF at 100 ºC for 20 min, followed by purification of trifluoromethanesulfinate from the reaction mixture using a WAX cartridge (Table 2.16). Starting from 25.2 MBq of [^{18}F]fluoride, 5.0 MBq of activity was eluted from the cartridge containing the radiolabelled ammonium trifluoromethanesulfinate salt with a RCP of 59%, resulting in a non-decay corrected AY of 11%.

Table 2.16 Purification of **2.2** from the crude reaction mixture using a WAX cartridge[a]



Activity at Reaction Start (MBq)	Final Activity (MBq)[b]	RCP 2.2 (%)	AY 2.2 (%)
25.2	5.0	59	11

[a] General conditions: [^{18}F]KF/K$_{222}$ (20 – 30 MBq in 10 – 50 µL DMF), PDFA (0.08 mmol) and NMM-SO$_2$ (0.02 mmol) in DMF (300 µL) at 100 ºC for 20 min.
[b] Activity of mixture eluted from WAX cartridge measured.

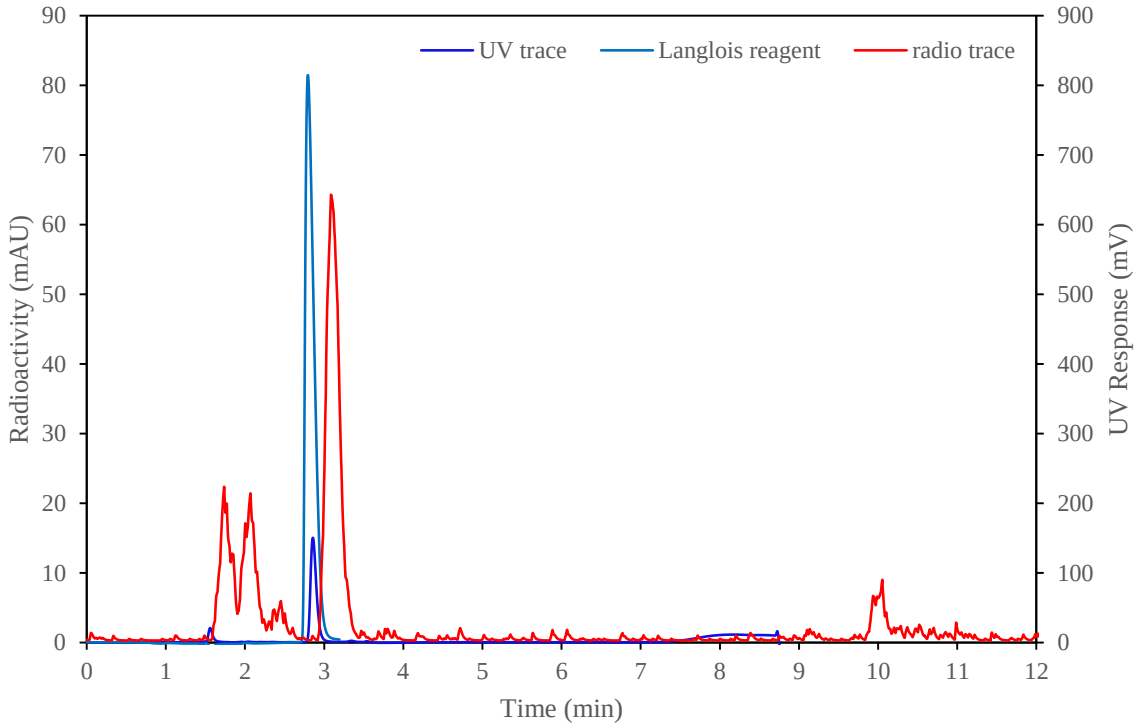


Figure 2.5 Radio-HPLC and UV trace of **2.2** purified using WAX cartridge overlaid with UV of commercial Langlois reagent

The identity and purity of **2.2** after WAX isolation were confirmed using analytical HPLC. The radio-HPLC trace and UV trace of the product eluted from the WAX overlapped with

the UV trace of commercial Langlois reagent (Figure 2.5). A delay between UV and radio traces is observed which corresponds with the distance between the two detectors.

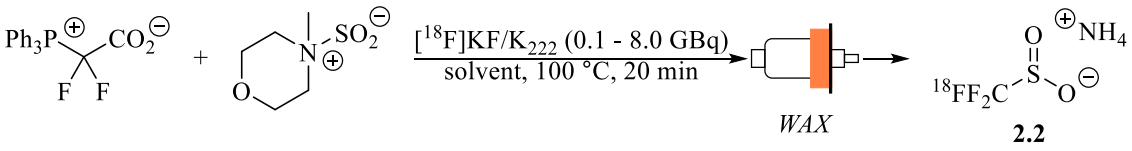
This demonstrates that WAX cartridges may be used to increase the purity of the radiolabelled Langlois reagent **2.2** from ~22% in the crude reaction mixture to 59% RCP. To test the viability of using alumina for purifying the radiolabelled Langlois reagent, we implemented an alumina cartridge in tandem with a WAX cartridge. The RCP of **2.2** only increased from 59% to 71% so alumina cartridges were not pursued further.

A RCP of at least 95% was required to successfully isolate **2.2** and then employ it in subsequent labelling reactions. Since WAX and alumina cartridges could not achieve this, semi-preparative HPLC was investigated for isolating **2.2**.

In general, appreciable losses are incurred during semi-preparative HPLC purification when employing small amounts of activity (<100 MBq). Therefore, larger amounts of activity were required. All radiochemical screening reactions for forming **2.2** described so far have employed 20 – 30 MBq aliquots of [^{18}F]fluoride. Therefore, we proceeded to subject larger amounts of [^{18}F]fluoride (0.1 – 8.0 GBq) to QMA trapping, elution and azeotropic drying before carrying out a single reaction with this entire batch of activity (see Figure 1.3). In addition, this would better emulate the conditions and procedures used in automation and for conducting PET imaging studies.

With this change in protocol in hand, the reaction for forming **2.2** was carried out with a single batch of [^{18}F]fluoride followed by WAX purification of the reaction mixture (Table 2.17).

Table 2.17 Radiosynthesis and purification of **2.2** using WAX cartridges in single batch reactions[a]



Entry	Initial Activity (MBq)	Solvent	RCP 2.2 (%)	RCY 2.2 (%)	AY 2.2 (%)
1	489	DMF	61	7	4
2	276	DMF	57	7	5
3	231	propylene carbonate	0	0	0
4	894	1:1 propylene carbonate/DMF	0	0	0
5	894	6:1 propylene carbonate/DMF (350 µL)	22	3	2

[a] General conditions: [^{18}F]KF/K_{222} (0.1 – 8.0 GBq), PDFA (0.08 mmol) and NMM-SO_2 (0.03 mmol) in solvent (300 µL) at 110 ºC for 20 min. [^{18}F]KF/K_{222} was dissolved in solvent at 100 ºC for 2 min before transferring to a V-vial containing reagents.

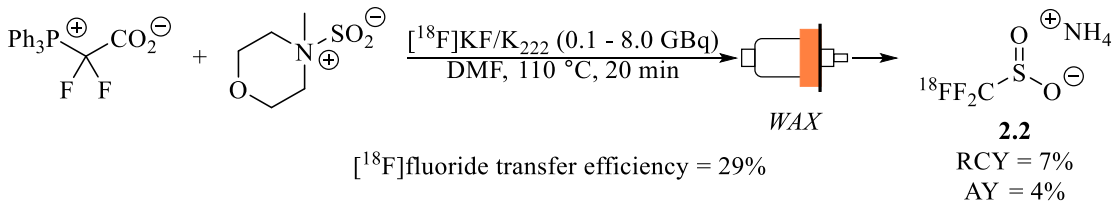
In comparison to carrying out the same reaction using aliquots of [^{18}F]fluoride for several small scale reactions, a difference in RCY was immediately apparent. The RCY dropped to 7% when starting from 489 MBq or 276 MBq of [^{18}F]fluoride (Table 2.17, Entries 1 & 2). Possible reasons for this include increased amounts of Kryptofix/potassium carbonate and cyclotron impurities that hinder the reaction to form **2.2**, or decomposition of **2.2** by radiolysis due to the increased amount of activity.

Surprisingly, no **2.2** was observed when the reaction was carried out using propylene carbonate or a one-to-one mixture of DMF and propylene carbonate (Table 2.17, Entries 3 & 4). During small scale reactions using [^{18}F]fluoride aliquots, a RCY of 22% was obtained when employing propylene carbonate in the presence of 10 – 50 µL DMF (Table 2.10, Entry

4). To emulate this, a single batch reaction was carried out using a six-to-one mixture of propylene carbonate and DMF, which afforded **2.2** in 3% RCY and 2% AY.

To explain these reductions in yield, activity measurements were taken at various points in the radiosynthesis, first with DMF as the reaction solvent (Table 2.18). No unusual amounts of activity were lost as a result of QMA elution, azeotropic drying, or as volatile release during the reaction.

Table 2.18 Measurements of activity during radiosynthesis of **2.2** using DMF as reaction solvent[a]



[^{18}F]fluoride transfer efficiency = 29%

2.2
RCY = 7%
AY = 4%

Procedure Step	Activity (MBq)[b]
Load [^{18}F]fluoride onto QMA	489
Elute [^{18}F]fluoride off QMA	458
After azeotropic drying	468
Transfer [^{18}F]fluoride in DMF to reaction vial	137
Activity left in drying vial after transfer	306
End of reaction	138
Elute [^{18}F]Langlois reagent off WAX	55

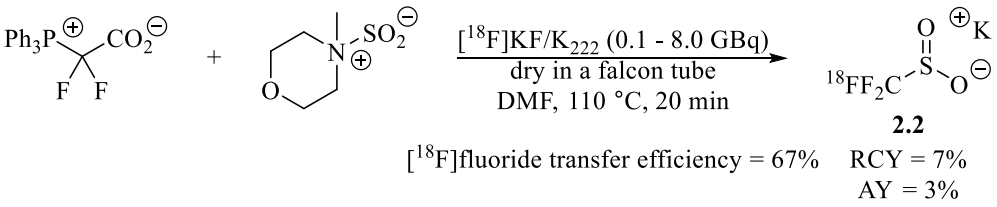
[a] General conditions: [^{18}F]KF/K_{222} (0.1 – 8.0 GBq), PDFA (0.08 mmol) and NMM-SO_2 (0.03 mmol) in DMF (300 μL) at 110 ºC for 20 min. [^{18}F]KF/K_{222} was dissolved in solvent at 100 ºC for 2 min before transferring to a V-vial containing reagents.
[b] Decay corrected to start of synthesis.

Significant amounts of activity were lost when transferring [^{18}F]fluoride from the drying vial to the reaction vial, giving a transfer efficiency of 29% (Table 2.18). When carrying out single batch reactions, dried [^{18}F]fluoride was redissolved in reaction solvent at 100 ºC for 2 minutes before transferring *via* syringe to the reaction vial containing the reagents. This is a major practical difference in procedure compared to using aliquots of [^{18}F]fluoride, as any activity lost in transfer is reflected as a decrease in the yield. Examination of activity before and after transfer showed that a majority remained in the drying vial with ~5% activity lost in the lines and syringe used for transfer.

Boron and aluminium compounds in borosilicate glassware are known to influence [^{18}F]fluoride reactivity by binding irreversibly.[26] Interactions with the glassware may explain why [^{18}F]fluoride transfer efficiency is low since this efficiency did not improve with increased volumes of solvent or by transferring the activity with multiple portions of DMF.

To test this hypothesis we replaced the glass V-vial used for drying [^{18}F]fluoride with a plastic falcon tube and measured [^{18}F]fluoride transfer efficiency (Table 2.19). Transfer efficiency increased from 29% to 67%, supporting this hypothesis, however the RCY remained the same at 7% and an AY of 3% was obtained. This is because low heat transfer using the falcon tube resulted in poor [^{18}F]fluoride drying efficiency compared to using glass drying vials, leading to an impractically long drying period.

Table 2.19 Measurements of activity during radiosynthesis of **2.2** using DMF as reaction solvent and a falcon tube for [^{18}F]fluoride drying[a]



2.2

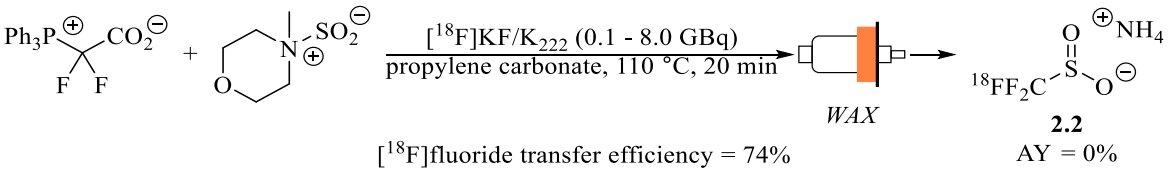
[^{18}F]fluoride transfer efficiency = 67% RCY = 7%
AY = 3%

Procedure Step	Activity (MBq)[b]
Load [^{18}F]fluoride onto QMA	407
Elute [^{18}F]fluoride off QMA	377
After azeotropic drying	329
Transfer [^{18}F]fluoride in DMF to reaction vial	200
Activity left in drying vial after transfer	67

[a] General conditions: [^{18}F]KF/K_{222} (0.1 – 8.0 GBq), PDFA (0.08 mmol) and NMM-SO_2 (0.03 mmol) in DMF (300 μL) at 110 ºC for 20 min.
[^{18}F]KF/K_{222} was dissolved in solvent at 100 ºC for 2 min using a plastic falcon tube before transferring to a V-vial containing reagents. [b] Decay corrected.

A similar assessment was carried out for a reaction using propylene carbonate (Table 2.20). No significant amounts of activity were lost as a result of QMA elution, azeotropic drying, or as volatile release during the reaction. [^{18}F]Fluoride transfer was carried out with 74% efficiency when employing propylene carbonate, however no **2.2** was formed in the reaction.

Table 2.20 Measurements of activity during radiosynthesis of **2.2** using propylene carbonate as reaction solvent[a]



Procedure Step	Activity (MBq)[b]
Load [^{18}F]fluoride onto QMA	231
Elute [^{18}F]fluoride off QMA	232
After azeotropic drying	225
Transfer [^{18}F]fluoride in propylene carbonate to reaction vial	167
Activity left in drying vial after transfer	29
End of reaction	179
Elute [^{18}F]Langlois reagent off WAX	15

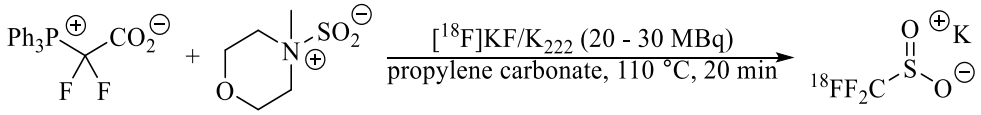
[a] General conditions: [^{18}F]KF/K_{222} (0.1 – 8.0 GBq), PDFA (0.08 mmol) and NMM-SO_2 (0.03 mmol) in propylene carbonate (300 µL) at 110 ºC for 20 min. [^{18}F]KF/K_{222} was dissolved in solvent at 100 ºC for 2 min before transferring to a V-vial containing reagents. [b] Decay corrected.

Since transferring [^{18}F]fluoride from the drying vial to reaction vial proved to be an unsuccessful strategy, we investigated transferring PDFA and NMM-SO_2 reagents to the [^{18}F]fluoride, circumventing any [^{18}F]fluoride transfer step. The main issue with this strategy was that PDFA is insoluble in all solvents except for partial solubility in methanol. Addition of PDFA to the reaction vial prior to elution and azeotropic drying of [^{18}F]fluoride was not possible because PDFA decomposed during azeotropic drying.

A fine suspension of PDFA in reaction solvent could be produced by using a vortex mixer, allowing addition of all reagents to dried [^{18}F]fluoride *via* syringe. Carrying out the reaction

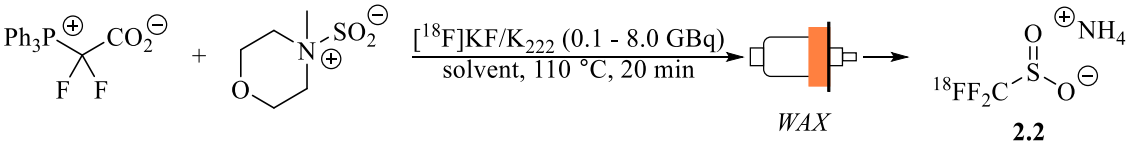
in this manner using aliquots of [^{18}F]fluoride (20 – 30 MBq) afforded **2.2** in 36% RCY (Table 2.21). A corresponding increase was observed in single batch reactions using larger amounts of [^{18}F]fluoride (0.1 – 8.0 GBq) which afforded **2.2** in 9% RCY and 5% AY when using DMF as the reaction solvent (Table 2.21, Entry 1), or 9% RCY and 7% AY when using propylene carbonate (Table 2.21, Entry 2). These results clearly showed that adding PDFA and NMM-SO_2 as a suspension to [^{18}F]fluoride led to higher yields of labelled Langlois reagents.

Table 2.21 Small scale and single batch reactions to form **2.2** by adding reagents as a suspension to [^{18}F]fluoride[a]



2.2

Add [^{18}F]fluoride to reagents: RCY = 22% ± 6% (n = 4)
Add reagent suspension to [^{18}F]fluoride: RCY = 36% ± 2% (n = 2)



2.2

Entry	Solvent	Initial Activity (MBq)	RCP 2.2 (%)	RCY 2.2 (%)	AY 2.2 (%)
1	DMF (300 µL)	554	45	9	5
2	6:1 propylene carbonate/DMF (350 µL)	166	52	9	7

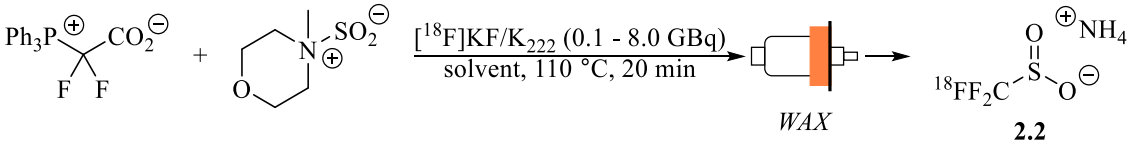
[a] General conditions: [^{18}F]KF/K_{222} (0.1 – 8.0 GBq), PDFA (0.08 mmol) and NMM-SO_2 (0.03 mmol) in solvent at 110 ºC for 20 min. Reagents were added to [^{18}F]KF/K_{222} in DMF as a suspension.

Despite obviating the need to transfer [^{18}F]fluoride to the reaction vial by adding reagents as a suspension to [^{18}F]fluoride, poor RCYs were still obtained in single batch reactions compared to using [^{18}F]fluoride aliquots. This may be explained by increased quantities of

Kryptofix/potassium carbonate and cyclotron impurities present in these reactions that hinder the formation of **2.2**. This may occur *via* quenching of the reagents in a side reaction, for example, carbonate is known to react with difluorocarbene.[27]

To solve this problem the amounts of reagents were increased (Table 2.22). Doubling the quantities of PDFA and NMM-SO_2 to 0.16 mmol and 0.06 mmol in 300 µL DMF led to an RCY of 19% ± 0 (*n* = 2) (Table 2.22, Entry 1). With these quantities of reagents, reducing the solvent volume to 200 µL led to a decrease in RCY to 8%, suggesting that 300 µL is the minimum amount of solvent needed for efficient reaction (Table 2.22, Entry 2). A RCY of 23% was obtained by applying a mixture of propylene carbonate and DMF as the reaction solvent (Table 2.22, Entry 3).

Table 2.22 Radiosynthesis of **2.2** using increased amounts of PDFA and NMM-SO_2[a]



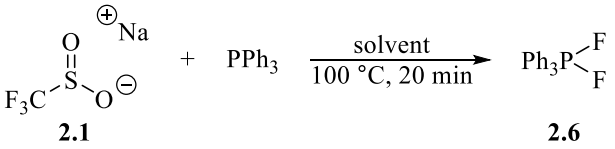
Entry	Initial Activity (MBq)	Solvent	RCY 2.2 (%)	AY 2.2 (%)
1	445 – 543	DMF (300 µL)	19 ± 0 (*n* = 2)	13 ± 0 (*n* = 2)
2	500	DMF (200 µL)	8	5
3	567	6:1 propylene carbonate/DMF (350 µL)	23	16
4[b]	522	DMF (300 µL)	9	6

[a] General conditions: [^{18}F]KF/K_{222} (0.1 – 8.0 GBq), PDFA (0.16 mmol) and NMM-SO_2 (0.06 mmol) in solvent at 110 ºC for 20 min. Reagents were added to [^{18}F]KF/K_{222} in solvent as a suspension. [b] [^{18}F]Fluoride trapped with Waters SepPak Accell Plus QMA Plus Light cartridge (130 mg) activated with Na_2SO_4 solution, and eluted with Kryptofix (0.05 mmol) in H_2O (500 µL)

The reaction was carried out without any carbonate present by employing a SepPak cartridge activated with sulfate instead of carbonate and released [^{18}F]fluoride with a solution of Kryptofix, affording only 9% RCY (Table 2.22, Entry 4).

From these results, reactions using propylene carbonate were more successful when a small amount of DMF was added. To explain this, we examined the stability of the Langlois reagent in the presence of triphenylphosphine using different reaction solvent mixtures at 100 ºC (Table 2.23) and analysed the resultant products by ^{19}F NMR spectroscopy (Figure 2.6).

Table 2.23 Stability of the Langlois reagent with triphenylphosphine[a]



2.1 **2.6**

Entry	Solvent	^{19}F NMR Yield 2.1 (%)[b]	^{19}F NMR Yield 2.6 (%)[b]
1	DMF	91	0
2	1:1 propylene carbonate/DMF	96	0
3	6:1 propylene carbonate/DMF (350 μL)	99	0
4	propylene carbonate	35	54

[a] General conditions: Langlois reagent (0.1 mmol) and triphenylphosphine (0.2 mmol) in DMF (0.5 mL) at 100 ºC for 20 min. [b] Relative to 0.1 mmol $PhCF_3$ internal standard.

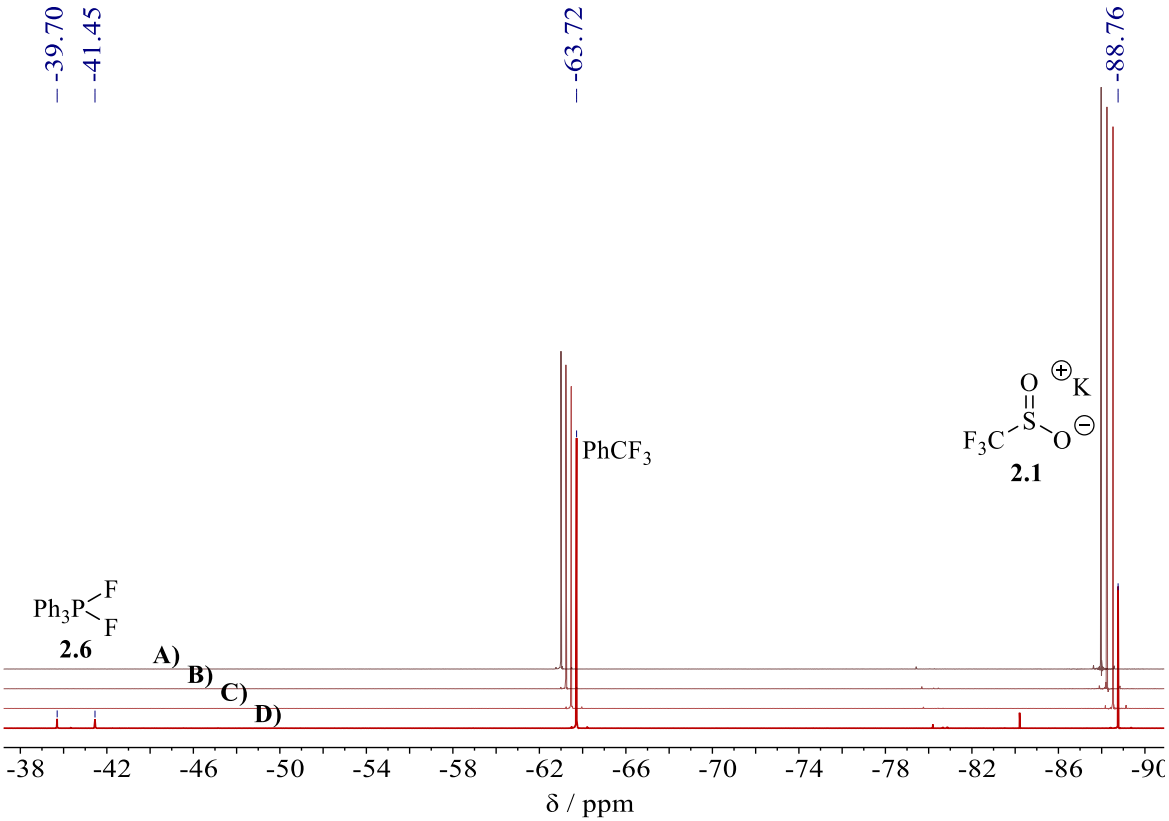


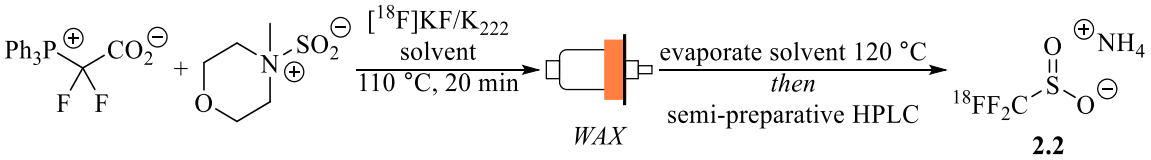
Figure 2.6 ^{19}F NMR spectra for crude reaction mixtures using solvents A) DMF B) 1:1 DMF/propylene carbonate C) 1:6 DMF/propylene carbonate D) propylene carbonate

No decomposition of the Langlois reagent was observed when employing DMF, 1:1 propylene carbonate/DMF and 6:1 propylene carbonate/DMF (Table 2.23, Entries 1 – 3). However, in the presence of 100% propylene carbonate, significant decomposition to difluorotriphenylphosphorane **2.6** was observed. Reduction of the Langlois reagent with triphenylphosphine has been reported in the literature but the effect of solvent was not discussed.[4]

With reaction conditions in hand, we proceeded to carry out semi-preparative HPLC to isolate the radiolabelled Langlois reagent after WAX purification (Table 2.24). The ammonium hydroxide/ethanol solution of **2.2** eluted from the WAX was concentrated to dryness at 120 ºC under nitrogen flow before loading onto the HPLC. This was done to avoid

the presence of small quantities of ethanol which otherwise led to very poor retention of **2.2** on the column. Employing a HPLC eluent of 25 mM ammonium formate in 100% water enabled excellent separation of **2.2**, allowing isolation in >99% RCP. With DMF as the reaction solvent **2.2** was isolated in 16% RCY and 10% AY with a synthesis time of 82 minutes (Table 2.24, Entry 1). Using a mixture of propylene carbonate and DMF afforded **2.2** in 17% ± 2% RCY and 10% ± 1% AY (n = 9) with an average synthesis time of 74 ± 5 minutes (Table 2.24, Entry 2).

Table 2.24 Isolation of **2.2** using semi-preparative HPLC[a]



Entry	Initial Activity (GBq)	Solvent	Synthesis Time (min)	RCY 2.2 (%)	AY 2.2 (%)
1	5.0	DMF (300 µL)	82	16	10
2[b]	2.0 – 10.0	6:1 propylene carbonate/DMF (350 µL)	74 ± 5	17 ± 2	10 ± 1

[a] General conditions: [^{18}F]KF/K$_{222}$, PDFA (0.16 mmol) and NMM-SO$_2$ (0.06 mmol) in solvent at 110 ºC for 20 min.
Reagents were added to [^{18}F]KF/K$_{222}$ in solvent as a suspension. [b] (n = 9)

In conclusion, the [^{18}F]Langlois reagent has been successfully purified from the crude reaction mixture using WAX cartridges starting from 0.1 – 8.0 GBq of activity. Lower RCYs were obtained when carrying out a single reaction using one batch of [^{18}F]fluoride compared to using aliquots of [^{18}F]fluoride. This was solved by doubling the concentration of PDFA and NMM-SO$_2$ allowing isolation of the [^{18}F]Langlois reagent by semi-preparative HPLC. Using propylene carbonate with a small amount of DMF gave more successful results. This

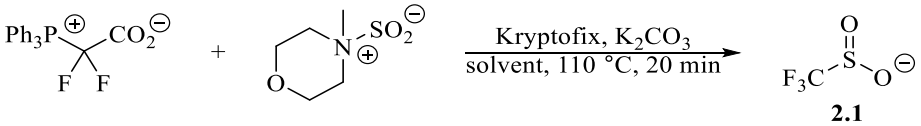
was explained by showing that the Langlois reagent decomposes in the presence of triphenylphosphine in 100% propylene carbonate.

2.5 Development of Conditions Amenable to Automated Radiolabelling of the Langlois Reagent

We have demonstrated the first novel radiosynthesis of the Langlois reagent isolated in a reasonable RCY. To develop real-world applicability of this proof of concept, challenges associated with automating the synthesis were addressed. Our aim focussed on using an automated synthesis of the labelled Langlois reagent to enable PET studies of imaging probes containing labelled fluorinated motifs. In preparation, we made a number of pivotal changes to the radiosynthetic procedures that optimise molar activity and synthesis time.

The molar activity of **2.2** formed from the reaction between [^{18}F]KF/K_{222}, PDFA and NMM-SO_2 was measured as 0.01 GBq μmol^{-1} (see Chapter 4: Experimental Data for details). A molar activity less than 1 GBq μmol^{-1} is generally insufficient for carrying out meaningful PET imaging studies. To demonstrate the cause of this low molar activity, the same reaction conditions used for radiolabelling were repeated in the absence of [^{18}F]fluoride and the resultant products were analysed by ^{19}F NMR spectroscopy (Table 2.25). Trifluoromethanesulfinate **2.1** was formed in 7% – 9% by heating NMM-SO_2 and PDFA (Table 2.25, Entries 1 – 3), suggesting that under the reaction conditions used for radiolabelling, fluoride is released by side reactions. This occurred because difluorocarbene is a highly reactive intermediate that is able to react with many nucleophiles, such as with oxygen carbonyls in DMF, to release fluoride.[28]

Table 2.25 Forming **2.1** in the absence of fluoride from PDFA and NMM-SO_2[a]



2.1

Entry	Solvent	^{19}F NMR Yield 2.1 (%)[b]
1	DMF (300 μL)	8
2	6:1 propylene carbonate/DMF (350 μL)	9
3	propylene carbonate	7

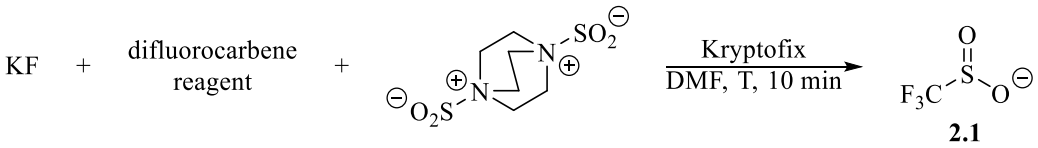
[a] General conditions: PDFA (0.08 mmol), NMM-SO_2 (0.03 mmol), Kryptofix (0.017 mmol) and potassium carbonate (0.007 mmol) in solvent (300 μL) at 110 ºC for 20 min. [b] Relative to 0.1 mmol $PhCF_3$ internal standard.

In addition to poor molar activity, the current method for radiolabelling the Langlois reagent is unsuitable for translating to automation for a number of reasons. Having a short synthesis time is paramount to achieving high enough amounts of activity for injecting into subjects as well as for improving molar activity. This, in addition to the practical restrictions inherent in manipulating everything remotely, meant that purification steps in the radiosynthetic procedure were re-evaluated and detailed procedures were developed for carrying them out successfully.

PDFA must be added as a suspension in reaction solvent which is incompatible with automated setups, where reagents are added remotely as predissolved solutions. This major setback culminated in the discovery of new reaction conditions employing alternate reagents to PDFA that are not only soluble in reaction solvents, but are commercially available, obviating the need to carry out preparatory reagent syntheses.

Forming trifluoromethanesulfinate with difluorocarbene reagents other than PDFA was investigated (Table 2.26). These reagents included fluorosulfonyldifluoroacetic acid, potassium bromodifluoroacetate, diethyl bromodifluoromethylphosphonate, sodium chlorodifluoroacetate, potassium bromodifluoroacetate, methyl chlorodifluoroacetate and methyl fluorosulfonyldifluoroacetate, that are either thermally (Table 2.26, Entry 1 – 4) or nucleophilically activated reagents (Table 2.26, Entries 5 & 6).[7,29] However, none proved successful in forming **2.1** under standard reaction conditions.

Table 2.26 Unsuccessful attempts to replace PDFA with alternate difluorocarbene reagents[a]



Entry	Difluorocarbene Reagent	T (°C)	^{19}F NMR Yield 2.1 (%)[b]
1	$FSO_2CF_2CO_2H$	100	0
2	$ClCF_2CO_2Na$	150	0
3	$BrCF_2CO_2K$	100	0
4	$(EtO)_2P(O)CF_2Br$	100	0
5	$ClCF_2CO_2Me$[c]	150	0
6	$FSO_2CF_2CO_2Me$[c]	100	0

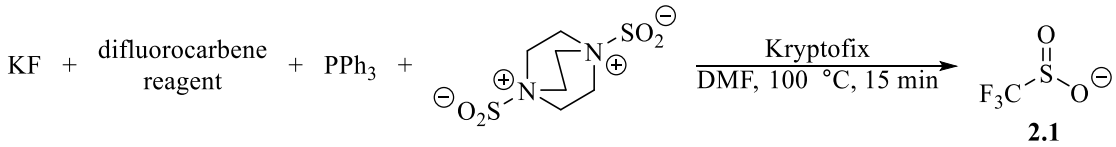
[a] General conditions: potassium fluoride (0.1 mmol), Kryptofix (0.1 mmol), NMM-SO_2 (0.1 mmol), and difluorocarbene reagent (0.2 mmol) in DMF (0.5 mL) at T for 10 min. [b] Relative to 0.1 mmol $PhCF_3$ internal standard.
[c] Potassium iodide (0.1 mmol) added.

Derivatives of PDFA were also synthesised and tested. Pentafluorophenyl, 1-napthyl, 4-fluorophenyl and 4-methoxyphenyl analogues of PDFA afforded **2.1** in trace amount or not

at all. The major products were difluoromethyl and difluoromethylsulfinate compounds **2.7** and **2.8**, suggesting that the phosphine plays a role in the reaction mechanism.

Phosphine additives are important in some transformations involving difluorocarbene, due to the phosphonium ylide formed *in situ*. Therefore, this difluorocarbene/phosphine manifold was examined for forming trifluoromethanesulfinate by screening difluorocarbene reagents in the presence of triphenylphosphine (Table 2.27).

Table 2.27 Screening difluorocarbene reagents in the presence of triphenylphosphine for forming **2.1**[a]



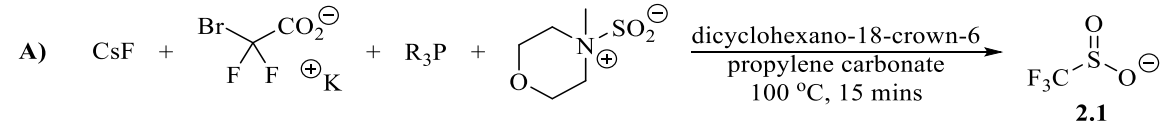
2.1

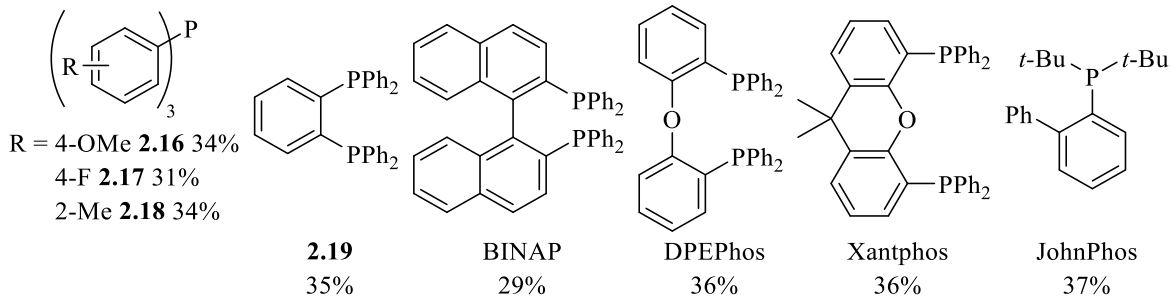
Entry	Difluorocarbene Reagent	^{19}F NMR Yield 2.1 (%)[b]
1	$(EtO)_2P(O)CF_2Br$	<1
2	CF_2Br_2	0
3	$FSO_2CF_2CO_2H$	<1
4	$ClCF_2CO_2Na$	0
5	$BrCF_2CO_2K$	51
6	$ClCF_2CO_2Me$	24
7	$BrCF_2CO_2Me$	34
8	$FSO_2CF_2CO_2Me$	18

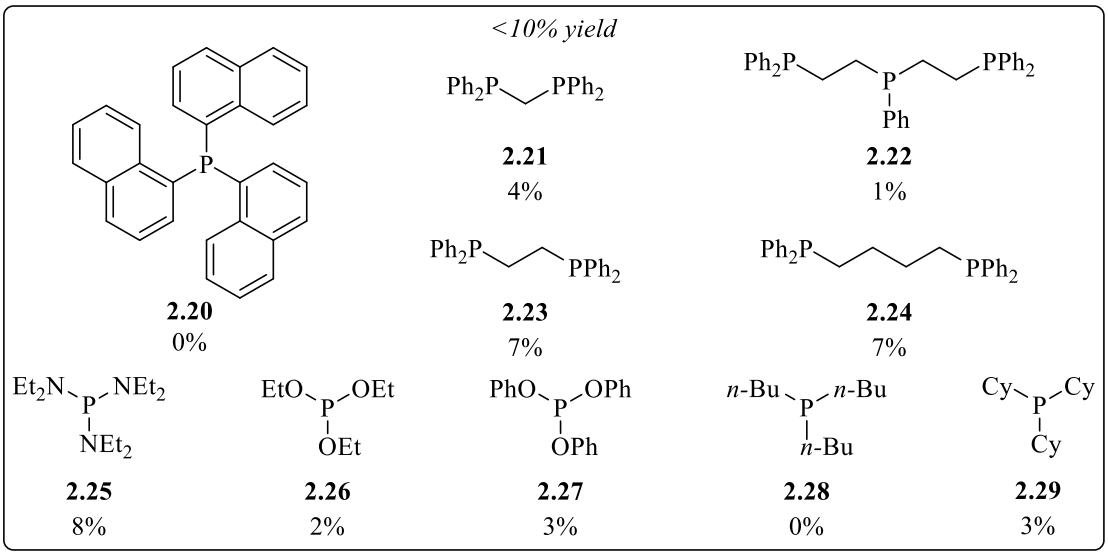
[a] General conditions: potassium fluoride (0.1 mmol), Kryptofix (0.1 mmol), NMM-SO_2 (0.2 mmol), difluorocarbene reagent (0.2 mmol) and triphenylphosphine (0.2 mmol) in DMF (0.5 mL) at 100 ºC for 15 min. [b] Relative to 0.1 mmol $PhCF_3$ internal standard.

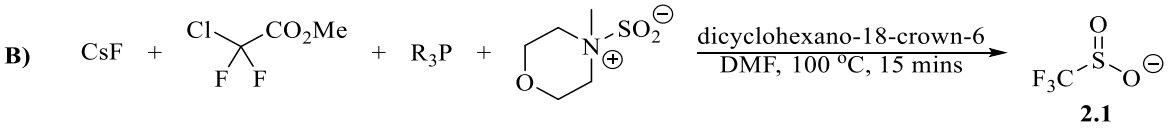
Diethyl bromodifluoromethylphosphonate, dibromodifluoromethane, fluorosulfonyl-difluoroacetic acid and sodium chlorodifluoroacetate afforded **2.1** in only trace amounts or not at all (Table 2.27, Entries 1 – 4). Potassium bromodifluoroacetate, methyl chloro-difluoroacetate, methyl bromodifluoroacetate and methyl fluorosulfonyl-difluoroacetate afforded **2.1** in 51%, 24%, 34% and 18% (Table 2.27, Entries 5 – 8). For methyl acetate difluorocarbene reagents, additives such as potassium iodide were not required since phosphines are known to activate such motifs.[30]

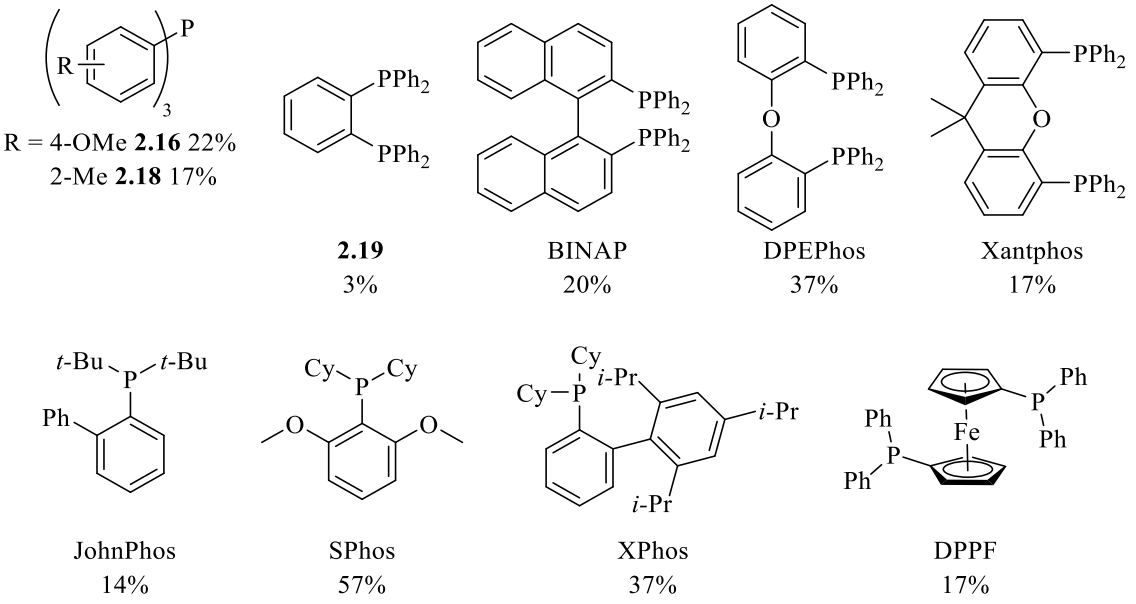
These results underline the value of phosphines in forming **2.1** therefore the scope was extended to other phosphine derivatives (Scheme 2.10). Several mono- and bi-dentate phosphines were found to be compatible when using potassium bromodifluoroacetate, such as **2.16** – **2.19**, BINAP, DPEPhos, XantPhos and JohnPhos which afforded **2.1** in 29% – 39% yield, whereas phosphines **2.20** – **2.29** afforded **2.1** in <10% yield (Scheme 2.10, A). When employing methyl chlorodifluoroacetate, **2.16**, **2.18**, BINAP, DPEPhos, XantPhos, JohnPhos, SPhos, XPhos and DPPF afforded **2.1** in 14% – 57% yield (Scheme 2.10, B). Good yields were obtained when employing electron-rich phosphines.









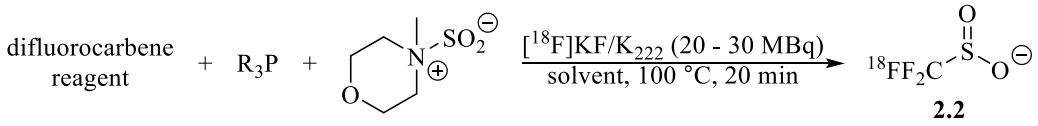


[a] General conditions: caesium fluoride (0.1 mmol), dicyclohexyl-18-crown-6 (0.1 mmol), NMM-SO_2 (0.2 mmol), difluorocarbene reagent (0.4 mmol) and phosphine (0.4 mmol) in solvent (0.5 mL) at 100 °C for 15 min. ^{19}F NMR yield relative to 0.1 mmol $PhCF_3$ standard.

Scheme 2.10 Phosphine screening for forming **2.1** in the presence of A) potassium bromodifluoroacetate B) methyl chlorodifluoroacetate[a]

This difluorocarbene reagent/phosphine manifold was inspected in a radiochemical setting using aliquots of [^{18}F]fluoride (Table 2.28). The reaction between potassium bromodifluoroacetate, triphenylphosphine, NMM-SO_2 and [^{18}F]KF/K_{222} produced the radiolabelled Langlois reagent in 1% or 4% RCY, with propylene carbonate or DMA as solvents respectively (Table 2.28, Entries 1 & 2). The phosphine did not dissolve in propylene carbonate which may explain the lack of product.

Table 2.28 Forming **2.2** using bromodifluoroacetate/phosphine manifold[a]



2.2

Entry	Difluorocarbene Reagent	Phosphine	Solvent	RCY 2.2 (%, *n* = 2)
1	$BrCF_2CO_2K$	PPh_3	propylene carbonate	1 ± 0
2	$BrCF_2CO_2K$	PPh_3	DMA	3 ± 0
3	$BrCF_2CO_2K$	JohnPhos	DMA	15 ± 3
4	$BrCF_2CO_2Me$	JohnPhos	DMF	18 ± 0
5	$ClCF_2CO_2Me$	JohnPhos	DMF	10 ± 1
6[b]	$BrCF_2CO_2Me$	JohnPhos	DMF	24 ± 1
7[b]	$ClCF_2CO_2Me$	JohnPhos	DMF	15 ± 3

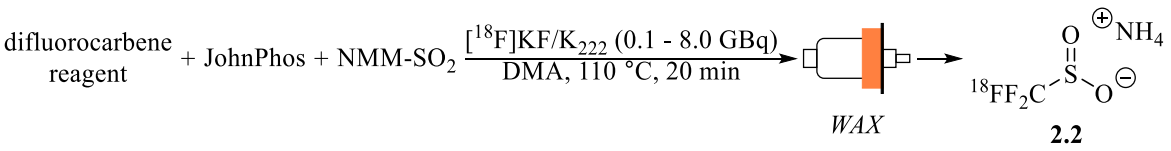
[a] General conditions: [^{18}F]KF/K_{222} (20 – 30 MBq in 10 – 50 μL DMF), NMM-SO_2 (0.03 mmol), difluorocarbene reagent (0.08 mmol) and phosphine (0.08 mmol) in solvent (300 μL) at 100 ºC for 20 min. Reagents were added to [^{18}F]KF/K_{222} in solvent as a suspension. Crude quenched with water and RCY measured by radio-HPLC. [b] NMM-SO_2 (0.06 mmol), difluorocarbene reagent (0.16 mmol) and phosphine (0.16 mmol) added

A higher RCY of 15% was obtained with JohnPhos (Table 2.28, Entry 3), and similar yields of 18% and 10% RCY obtained by employing methyl bromo- or chloro-difluoroacetate

(Table 2.28, Entries 4 & 5). This increased to 24% and 15% after doubling the concentration of all reagents (Table 2.28, Entries 6 & 7).

Single batch reactions were carried out producing **2.2** using these alternative difluorocarbene reagents (Table 2.29). Both potassium and methyl bromodifluoroacetate afforded **2.2** in low RCYs and AYs (Table 2.29, Entries 1 & 2) whereas methyl chlorodifluoroacetate gave **2.2** in 24% RCY and 17% AY (Table 2.29, Entry 3).

Table 2.29 Radiosynthesis and purification of **2.2** using alternate difluorocarbene reagents[a]



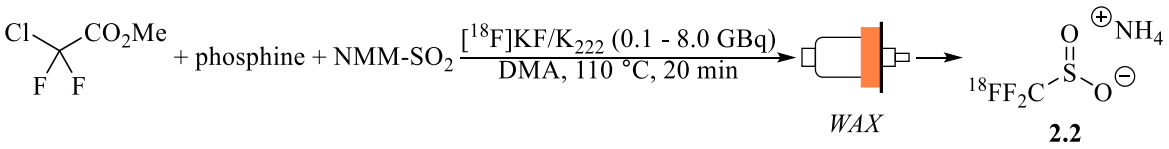
Entry	Initial Activity (MBq)	Difluorocarbene Reagent	RCY 2.2 (%)	AY 2.2 (%)
1	427	$BrCF_2CO_2K$	5	4
2	793	$BrCF_2CO_2Me$	4	3
3	515 – 650	$ClCF_2CO_2Me$	24 ± 1 (n = 2)	17 ± 1 (n = 2)

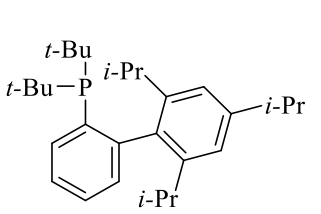
[a] General conditions: [^{18}F]KF/K_{222} (0.1 – 8.0 GBq), NMM-SO_2 (0.06 mmol), difluorocarbene reagent (0.16 mmol) and phosphine (0.16 mmol) in solvent (300 μL) at 110 ºC for 20 min.

We proceeded to screen phosphine reagents under these radiochemical conditions. However, many were insoluble in reaction solvent at room temperature so could not be transferred to the reaction vial. To counteract this issue, a new protocol was devised where phosphine was added to the [^{18}F]fluoride drying vial prior to commencing radiosynthetic procedures. [^{18}F]Fluoride was then eluted and dried in this vial before adding the rest of the reagents.

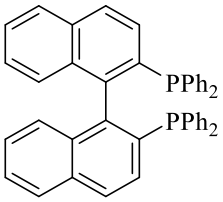
This procedure allowed a number of phosphines to be tested such as *t*BuBrettPhos, BINAP, DPEPhos, XantPhos, JohnPhos, SPhos, tri(σ-tolyl)phosphine and DTBPF (Scheme 2.11).

The highest RCYs were obtained with JohnPhos and tri(σ-tolyl)phosphine. The procedure of loading the [^{18}F]fluoride drying vial with phosphine was unsuitable for an automated procedure because much of the phosphine was left on the side of the vial leading to unreliable results. Thankfully, JohnPhos and tri(σ-tolyl)phosphine were soluble in DMA so could be added as a solution.

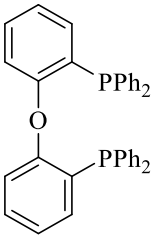




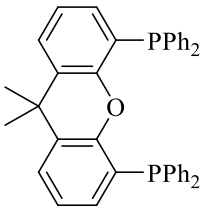
*t*BuBrettPhos
RCY = 21%
AY = 14%



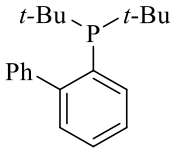
BINAP
RCY = 16%
AY = 11%



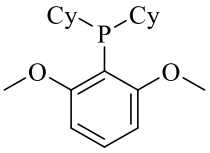
DPEPhos
RCY = 14%
AY = 9%



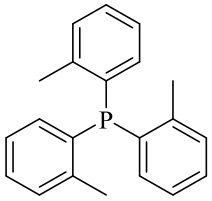
Xantphos
RCY = 10%
AY = 7%



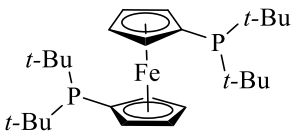
JohnPhos
RCY = 25%
AY = 16%



SPhos
RCY = 19%
AY = 13%



2.18
RCY = 26% ± 4%
AY = 18% ± 3%
(*n* = 2)



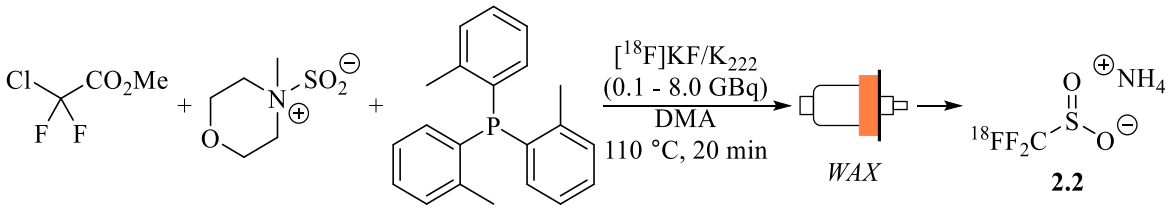
DTBPF
RCY = 7%
AY = 5%

[a] General conditions: [^{18}F]KF/K_{222} (0.1 – 8.0 GBq), NMM-SO_2 (0.06 mmol), methyl chlorodifluoroacetate (0.16 mmol) and phosphine (0.16 mmol) in DMA (300 μL) at 110 ºC for 20 min. Phosphine was added before eluting [^{18}F]fluoride.

Scheme 2.11 Screening phosphine reagents for formation of **2.2** by initially charging the [^{18}F]fluoride drying vial with phosphine[a]

Having identified optimal phosphine and difluorocarbene reagents that could be transferred as solutions, the protocol of adding all reagents dissolved in reaction solvent to [^{18}F]fluoride was tested. (Table 2.30). Under these conditions, labelled trifluoromethanesulfinate was afforded in 16% RCY and 24% AY (Table 2.30, Entry 1). Eluting [^{18}F]fluoride with a mixture of dibenzo-24-crown-8, caesium oxalate and caesium carbonate afforded **2.2** in 6% RCY and 8% AY (Table 2.30, Entry 2). Reducing the reaction time to 10 minutes led to an increase in RCY and AY up to 21% and 27% (Table 2.30, Entry 3).

Table 2.30 Radiosynthesis and purification of **2.2** by adding all reagents in reaction solvent[a]



Entry	Deviation from Conditions	RCY 2.2 (%)	AY 2.2 (%)
1	-	24	16
2	elute [^{18}F]fluoride with dibenzo-24-crown-8 (0.018 mmol), $Cs_2C_2O_4$ (0.006 mmol), $CsCO_3$ (0.77 μmol)	8	6
3	reaction time 10 min	27	21

[a] General conditions: [^{18}F]KF/K_{222} (0.1 – 8.0 GBq), NMM-SO_2 (0.06 mmol), methyl chlorodifluoroacetate (0.16 mmol) and tri(σ-tolyl)phosphine (0.16 mmol) in DMA (300 μL) at 110 ºC for 20 min.

The method for radiolabelling the Langlois reagent with fluorine-18 has been made amenable to automation through implementing commercially available reagents methyl chlorodifluoroacetate and phosphines JohnPhos or tri(σ-tolyl)phosphine, which are all soluble in reaction solvents. These replace PDFA, which requires a two-step synthesis, is not soluble in reaction solvents, and leads to very low molar activities of [^{18}F]Langlois

reagent. This change paves the way for developing an automated synthesis and optimising molar activity.

2.6 Automated Radiosynthesis of the [^{18}F]Langlois Reagent

An automated radiosynthesis of the Langlois reagent labelled with fluorine-18 was developed using a NanoTek® (Advion) platform. For any radiosynthesis with the intention of carrying out PET imaging studies, it is vital to develop efficient purification procedures that minimise synthesis time and maximise molar activity. The final activity must be high enough to obtain a strong PET signal after injecting this activity *in vivo*.

[^{18}F]Fluoride (2 – 50 GBq) generated from a cyclotron was separated from [^{18}O]H_2O by trapping on a QMA using a remotely accessed syringe pump (CE1) (Figure 2.7). Elution and drying steps were then carried out in a reaction vial (R1).

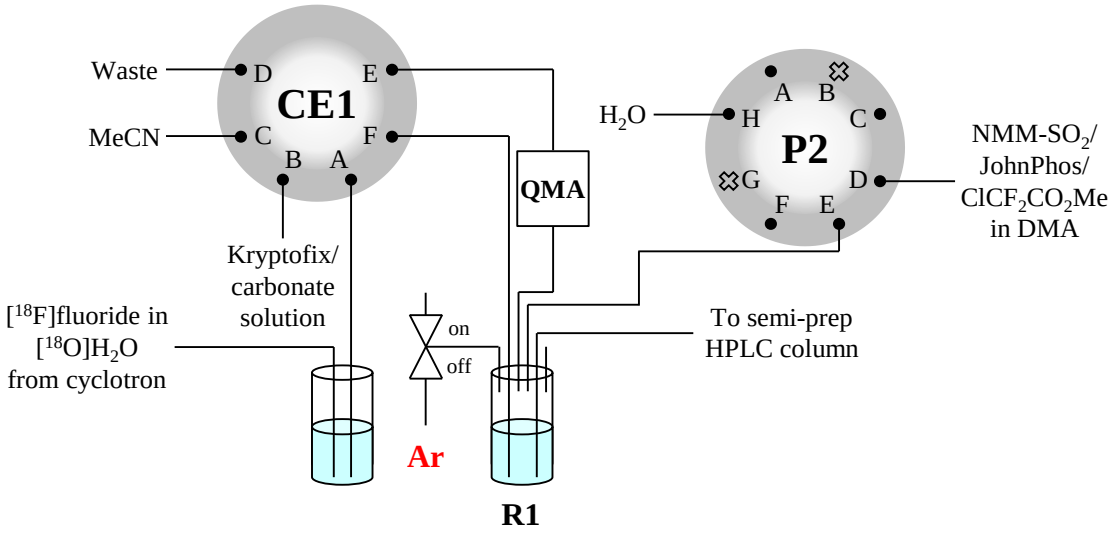


Figure 2.7 Setup for automated synthesis of the radiolabelled Langlois reagent using a NanoTek® (Advion) platform

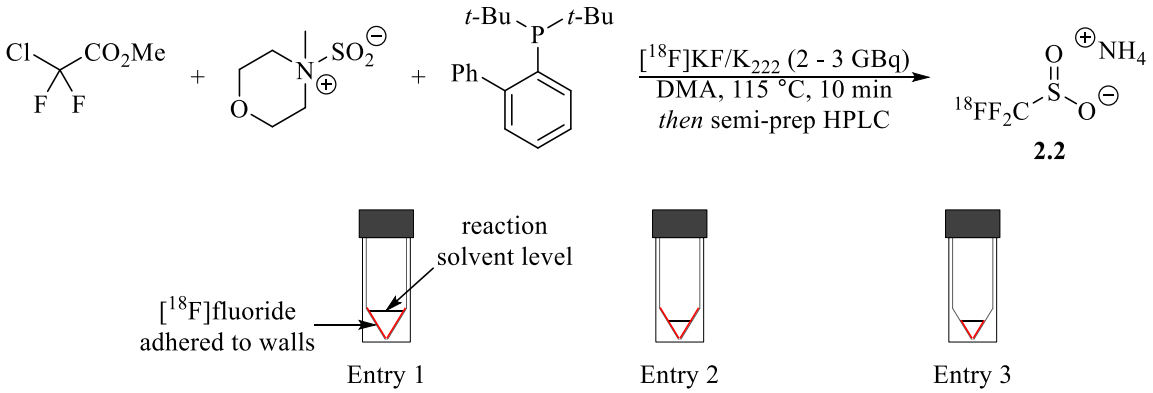
A solution of methyl chlorodifluoroacetate, JohnPhos and NMM-SO_2 in DMA was prepared inside the hot cell before starting radiosynthesis which remained stable for extended periods

and was easily transferred using another syringe pump (P2). JohnPhos was chosen over tri(σ-tolyl)phosphine due to better solubility in reaction solvent.

Initially, [^{18}F]fluoride (2 – 50 GBq) was eluted from the QMA using 3 x 300 μL aliquots of K_{222}/K_2CO_3 solution and azeotropic drying was carried out with 3 x 300 μL aliquots of acetonitrile. Neither stirring or manual intervention was possible, therefore any [^{18}F]fluoride attached to the reaction vial wall above the reaction solvent could not take place in the reaction. One proposed solution to this would be to increase the reaction solvent volume, however such dilution would have adverse effects on the RCY, or the molar activity if the amounts of reagents were correspondingly increased.

In practice, employing a solvent volume of 300 μL led to line blockage when attempting transfer after the reaction (Table 2.31, Entry 1). This was not an issue for a reaction volume of 150 μL, however only 4% RCY was obtained due to [^{18}F]fluoride adhering to the reaction vial wall above the reaction mixture (Table 2.31, Entry 2). To overcome this, [^{18}F]fluoride elution and drying steps were optimised by adjusting solvent volume size, flow rate and vial temperature to prevent [^{18}F]fluoride from splashing and adhering higher up on the vial walls. As a result of this optimisation, the RCY increased to 10% (Table 2.31, Entry 3). Taking dead volume in the lines into account was key to minimising [^{18}F]fluoride elution and MeCN volume by making sure to flush lines at the end of each step in the automation.

Table 2.31 Optimisation of reaction solvent, elution solution and drying solution[a]



Entry	Reaction Solvent	[^{18}F]Fluoride Elution Solution	MeCN for Azeotropic Drying	RCY 2.2 (%)
1[b]	300 µL	3 x 300 µL	3 x 300 µL	-
2	150 µL	3 x 300 µL	3 x 300 µL	4
3	150 µL	6 x 50 µL	3 x 100 µL	10

[a] General conditions for 300 µL reaction: [^{18}F]KF/K_{222} (2 – 3 GBq), NMM-SO_2 (0.06 mmol), methyl chlorodifluoroacetate (0.16 mmol) and JohnPhos (0.16 mmol) in DMA (300 µL) at 115 ºC for 10 min. General conditions for 150 µL reaction: [^{18}F]KF/K_{222} (2 – 3 GBq), NMM-SO_2 (0.028 mmol), methyl chlorodifluoroacetate (0.065 mmol) and JohnPhos (0.065 mmol) in DMA (150 µL) at 115 ºC for 10 min. [b] Line blockage occurred during purification.

A reduction in reaction volume to 150 µL allowed product purification by semi-preparative HPLC directly from the reaction mixture without the need for WAX cartridge purification and solvent evaporation. This simplified the automation setup and reduced the synthesis time from 80 to 40 minutes approximately. A number of parameters were optimised in order to achieve acceptable separation of **2.2** from the reaction solvent without causing line blockage. Parameters considered were HPLC column choice, flow rate, injection volume and HPLC eluent.

By examining the HPLC spectra of Langlois reagent in DMF or DMA under different conditions, we were able to ascertain a procedure for achieving optimal separation and isolation of the Langlois reagent (Figure 2.8).

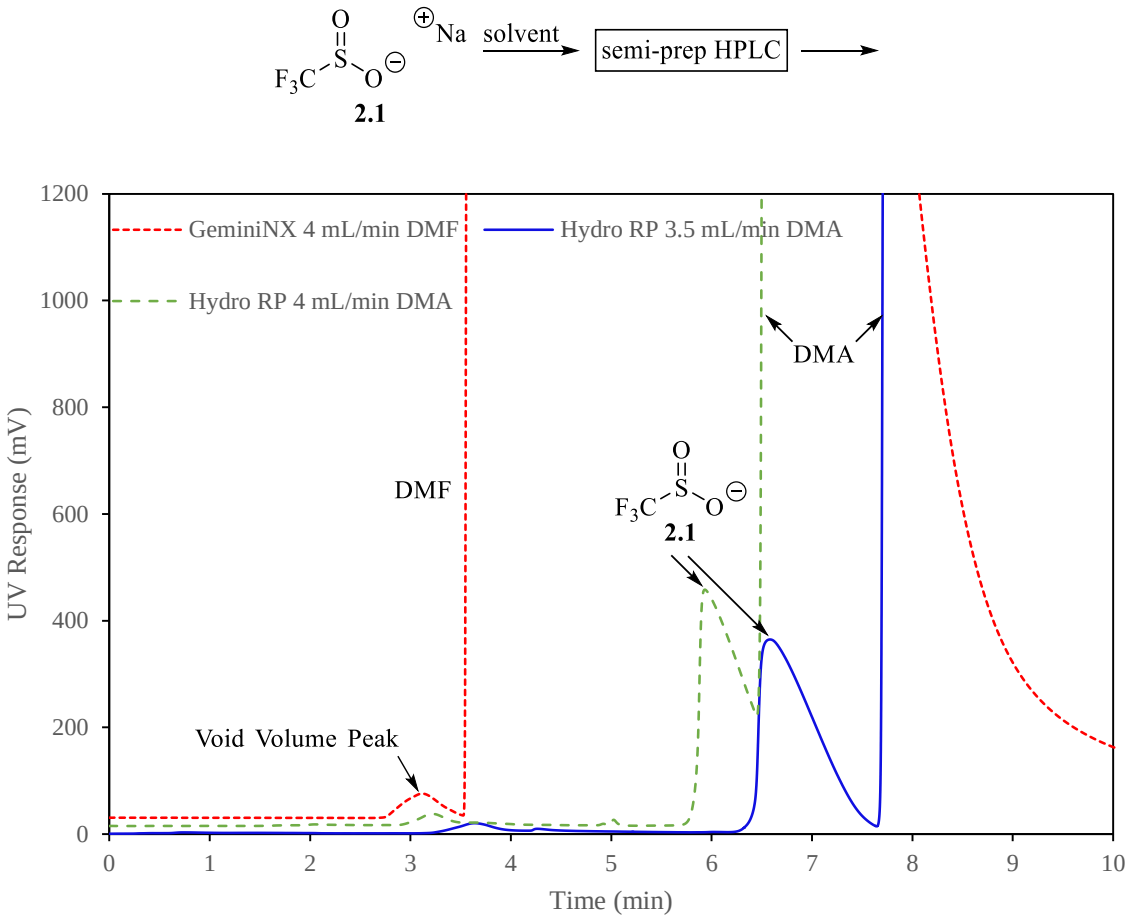


Figure 2.8 Overlaid semi-preparative HPLC spectra of Langlois reagent dissolved in DMF or DMA varying column and flow rate

Employing a Phenomenex Synergi™ Hydro RP semi-preparative column at a flow rate of 3.5 mL/min led to the best separation and using 50 mM aqueous ammonium formate as HPLC eluent helped to achieve minimal peak width. Addition of 1.7 mL HPLC eluent to the reaction mixture with 20-30 seconds of heating before taking up into a 2 mL injection loop provided the most reliable method for injecting the crude reaction mixture without risk of

blocking the lines. DMA was chosen as the ideal reaction solvent because of its superior retention compared to DMF. This method was implemented to successfully isolate the [^{18}F]Langlois reagent (Figure 2.9; see Chapter 4: Experimental Data for details).

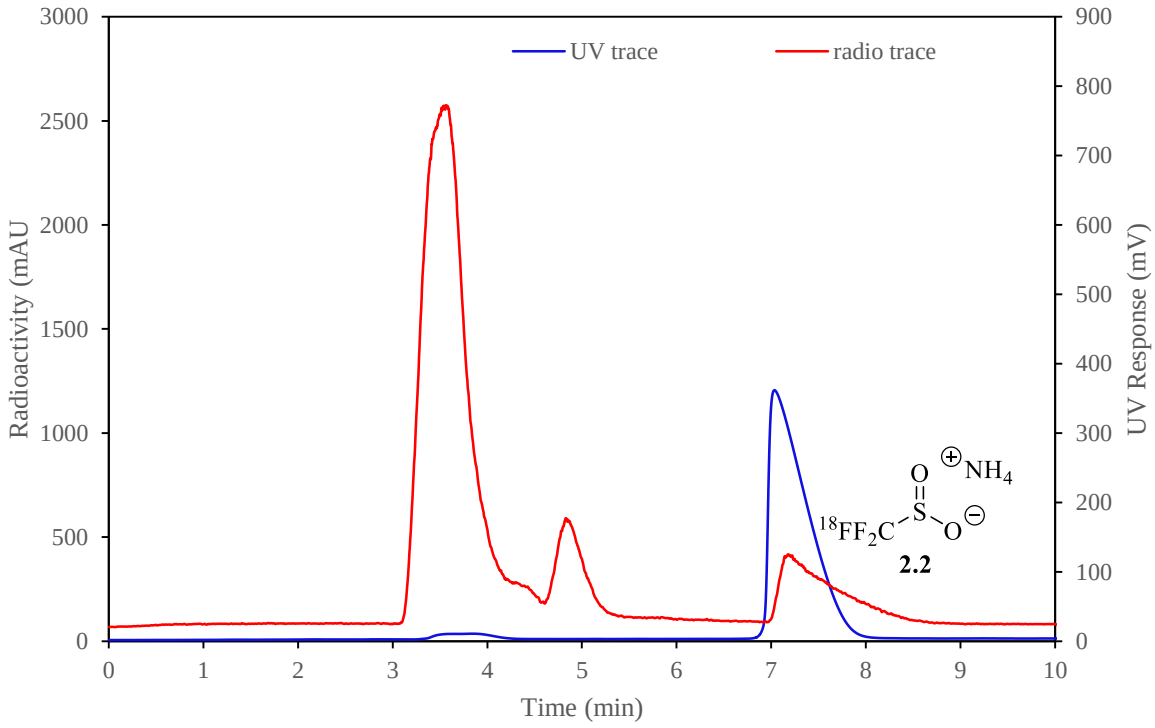
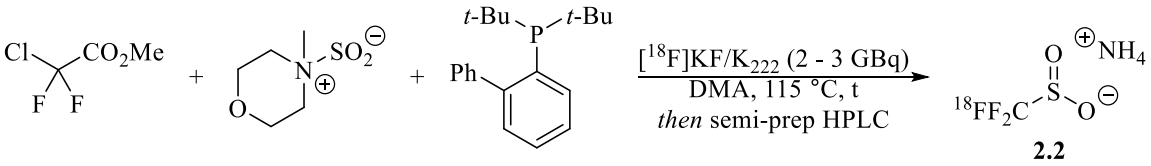


Figure 2.9 Spectra showing separation of **2.2** from a crude radiochemical reaction by semi-preparative HPLC

With an optimal setup and purification procedure in hand, we proceeded to fine tune reaction conditions, optimise molar activity and test reaction scale up (Table 2.32). A reaction time of 15 minutes afforded **2.2** in 7% RCY, 6% AY and 0.085 GBq μmol^{-1} (Table 2.32, Entry 1). Decreasing the reaction solvent to 100 μL led to an increase in molar activity to 0.12 GBq μmol^{-1} because less reagents were added. However a decrease in RCY to 4% suggested a minimum solvent volume of 150 μL was required to get efficient solvation of [^{18}F]fluoride (Table 2.32, Entry 2). Therefore a reaction solvent of 150 μL and reaction time of 10 minutes proved the optimum conditions affording **2.2** in 10% RCY and 8% AY (Table

2.32, Entry 3). Employing these conditions with 40 – 50 GBq of [^{18}F]fluoride led to a molar activity of 1.1 GBq μmol^{-1} (Table 2.32, Entry 4). A decrease in RCY to 7% was observed when employing this large amount of activity, which may be caused by larger concentrations of metals originating from the cyclotron target due to longer bombardment times. The higher levels of these impurities may hinder the reaction forming **2.2**. An additional explanation may be that radiolysis is more prevalent at higher levels of activity.

Table 2.32 Optimisation of reaction solvent, elution solution and drying solution[a]



Entry	Reaction Solvent (μL)	Reaction Time (min)	RCY 2.2 (%)	AY 2.2 (%)	Molar Activity (GBq μmol^{-1})	Synthesis Time (min)
1	150	15	7	6	0.085	45
2	100	10	4	3	0.12	40
3	150	10	10	8	0.10	42
4[b]	150	10	7	6	1.1	38

[a] General conditions for 150 μL reaction: [^{18}F]KF/K_{222} (2 – 3 GBq), NMM-SO_2 (0.028 mmol), methyl chlorodifluoroacetate (0.065 mmol) and JohnPhos (0.065 mmol) in DMA (150 μL) at 115 ºC for t. General conditions for 100 μL reaction: [^{18}F]KF/K_{222} (2 – 3 GBq), NMM-SO_2 (0.019 mmol), methyl chlorodifluoroacetate (0.043 mmol) and JohnPhos (0.047 mmol) in DMA (100 μL) at 115 ºC for 10 min.
[b] Approximately 40 – 50 GBq activity employed.

In conclusion, a fully automated method for labelling the Langlois reagent was successfully achieved by considering a number of reaction and purification parameters. In addition, the RCY, synthesis time and molar activity were optimised. Developing an automated preparation of the [^{18}F]Langlois reagent allows its wider use among PET centres.

2.7 References

[1] P. S. Santos & M. T. S. Mello *J. Mol. Struct.* **1988**, 178, 121 – 133.

[2] H. Woolven *et al. Org. Lett.* **2011**, 13, 4876 – 4878.

[3] J. B. Gill, D. C. Goodall & W. D. Harrison *Hydrometallurgy* **1981**, 6, 347 – 351.

[4] a) L. Jiang *et al. Angew. Chem. Int. Ed.* **2015**, 54, 14965 – 14969. b) Y. Yang *et al. Chem. Eur. J.* **2016**, 22, 858 – 863. c) M. Bu *et al. Org. Chem. Front.* **2017**, 4, 266 – 270. d) X. Zhao *et al. J. Org. Chem.* **2017**, 82, 9175 – 9181. e) Q. Yan *et al. Adv. Synth. Catal.* **2017**, 359, 2471 – 2480.

[5] a) H. W. Roesky & G. Holtschneider *J. Fluor. Chem.* **1976**, 7, 77 – 84. b) B. R. Langlois *et al. J. Fluor. Chem.* **2007**, 128, 851 – 856.

[6] B. A. Shainyan *et al. Russ. J. Org. Chem.* **2004**, 40 (8), 1071 – 1075.

[7] M. Huiban *et al. Nat. Chem.* **2013**, 5, 941 – 944.

[8] A. Zanardi *et al. J. Am. Chem. Soc.* **2011**, 133, 20901 – 20913.

[9] a) R. Gereke, H. Plinta & R. Schmutzler *Z. Anorg. Allg. Chem.* **1997**, 623, 1333 – 1343. b) C. Zhao *et al. Tetrahedron* **2019**, 4648 – 4656.

[10] A. Kornath & F. Neumann *Inorg. Chem.* **1997**, 36, 5570 – 5573.

[11] C. S. Thomoson, H. Martinez & W. R. Dolbier *J. Fluor. Chem.* **2013**, 150, 53 – 59.

[12] F. Ramirez & C. P. Smith *Tetrahedron Lett.* **1966**, 30, 3651 – 3656.

[13] R. A. Mitsch *J. Am. Chem. Soc.* **1967**, 89, 6297 – 6303.

[14] D. J. Burton *et al. J. Org. Chem.* **1983**, 48, 3616 – 3618.

[15] a) D. J. Burton *Chem. Rev.* **1996**, 96, 1641 – 1715. b) J. Zheng *et al. Chem. Commun.* **2013**, 49, 7513 – 7515. c) J. Zheng *et al. Chem. Eur. J.* **2013**, 19, 15261 – 15266. d) X. Deng *et al. Chin. J. Chem.* **2014**, 32, 689 – 693. e) F. Wang *et al. Beilstein J. Org. Chem.* **2014**, 10, 344 – 351. f) Y. Qiao *et al. J. Org. Chem.* **2014**, 79, 7122 – 7131. g) V. V. Levin *et al. Org. Lett.* **2014**, 16, 6256 – 6259. h) X. Deng e*t al. Chem. Commun.* **2015**, 51, 8805 – 8808. i) Y. Liu *et al. Tetrahedron Lett.* **2019**, 60, 1934 – 1937.

[16] S. V. Pasenok *et al. Z. Anorg. Allg. Chem.* **1999**, 625, 834 – 838.

[17] Y. Zafrani *et al. J. Org. Chem.* **2016**, 81, 9180 – 9187.

[18] a) P. Allen *J. Org. Chem.* **1942**, 7, 23 – 30. b) P. Allen, W. R. Rehl & P. E. Fuchs *J. Org. Chem.* **1955**, 20, 1237 – 1239.

[19] a) U. Hartwig *et al. Angew. Chem. Int. Ed. Engl.* **1989**, 28, 221 – 223. b) H. Pritzkow *et al. Angew. Chem.* **1990**, 102, 80 – 81.

[20] a) J. Yu *et al. Org. Chem. Front.* **2017**, 4, 617 – 621. b) T. Wang *et al. Tetrahedron Lett.* **2018**, 59, 1183 – 1187.

[21] E. J. Emmett & M. C. Willis *Asian J. Org, Chem.* **2015**, 4, 602 – 611.

[22] a) A. B. Burg *J. Am. Chem. Soc.* **1943**, 65, 1629 – 1635. b) T. Hata & S. Kinumaki *Nature* **1964**, 203, 1378 – 1379. c) D. L. A. Faria & P. S. Santos *J. Raman Spectrosc.* **1988**, 19, 471 – 478. d) P. S. Santos & P. C. Isolani *Chem. Phys. Lett.* **1979**, 67, 487 – 490. e) J. M. Kanamueller *J. Inorg. Nucl. Chem.* **1971**, 33, 4051 – 4055. f) P. S. Santos & R. Lieder *J. Mol. Struct.* **1986**, 144, 39 – 45. g) Z. Pawelka, G. Maes & T. Z. Huyskens *J. Phys. Chem.* **1981**, 85, 3431 – 3435. h) P. S. Santos & M. T. S. Mello *J. Mol. Struct.* **1988**, 178, 121 – 133.

[23] F. Buß *et al. Dalton Trans.* **2018**, 47, 10420 – 10424.

[24] M. Tordeaux, B. Langlois & C. Wakselman *J. Org. Chem.* **1989**, 54, 2452 – 2453.

[25] Patent **1990** CA2015793 A1.

[26] Patent **2012** US20120229804 A1.

[27] Z. Liu *et al. Chin. Chem. Lett.* **2019**, 30, 714 – 716.

[28] S. Singh *et al. Can. J. Chem.* **2004**, 82, 1249 – 1253.

[29] a) Q. Chen & S. Wu *J. Chem. Soc., Chem. Commun.* **1989**, 705 – 706. b) Z. Zafrani, G. Sod-Moriah & Y. Segall *Tetrahedron* **2009**, 65, 5278 – 5283. c) J. Zheng *et al. Org. Lett.* **2015**, 17, 532 – 535. d) D. L. Orsi, M. R. Yadav & R. A. Altman *Tetrahedron* **2019**, 75, 4325 – 4336.

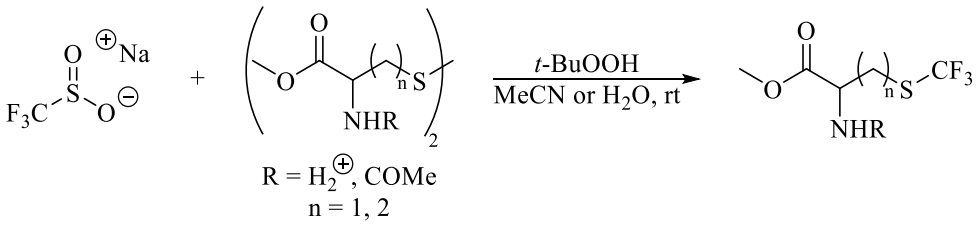
[30] a) N. Rodríguez *et al. Chem. Eur. J.* **2011**, 17, 13688 – 13691. b) G. Niu, P. Huang & G. J. Chuang *Asian J. Org. Chem.* **2016**, 5, 57 – 61.

Chapter 3: Radiolabelling Peptides using the [^{18}F]Langlois Reagent

3.1 Trifluoromethylation of Amino Acids and Peptides with the Langlois Reagent

3.1.1 Literature Precedent

First investigations into reacting the Langlois reagent with amino acid functional groups were reported in 1994.[1] *Tert*-butyl hydroperoxide (TBHP) was used to activate the Langlois reagent to generate trifluoromethyl radicals *in situ*. Reactions with disulfide forms of cysteine and homocysteine derivatives formed the trifluoromethylthiolated products (Scheme 3.1). These trifluoromethylated building blocks were subsequently used in peptide synthesis.[2]

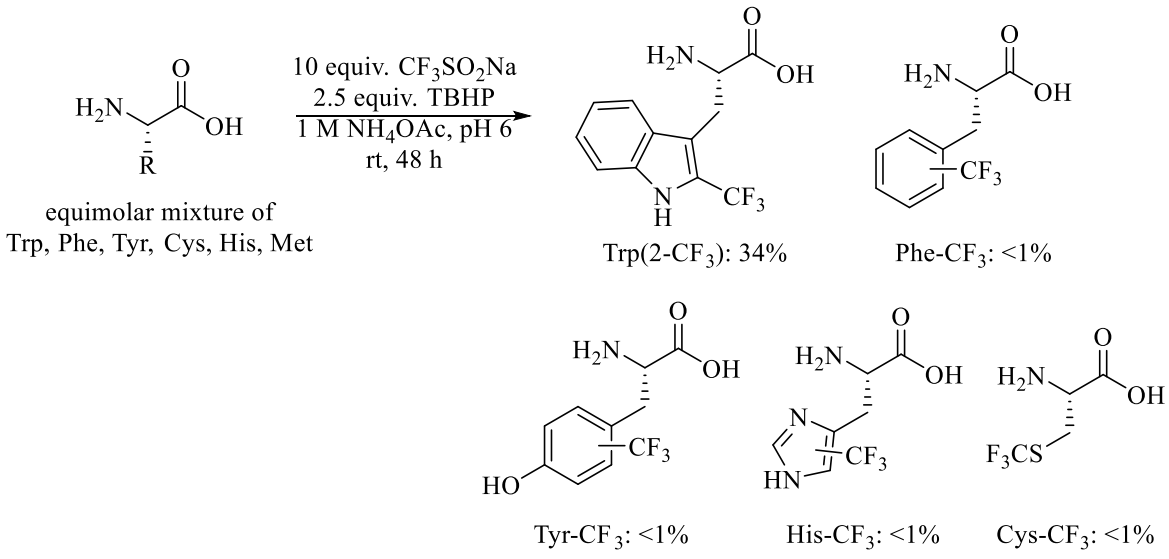


Scheme 3.1 Trifluoromethylation of cysteine and homocysteine derivatives using the Langlois reagent

With the exception of this report from 1994, trifluoromethylation of amino acid residues in peptides using the Langlois reagent has been reported only in the last three years. Applications of these products have focussed mainly utilising the trifluoromethyl group's advantageous properties as a tag for ^{19}F NMR spectroscopic studies.

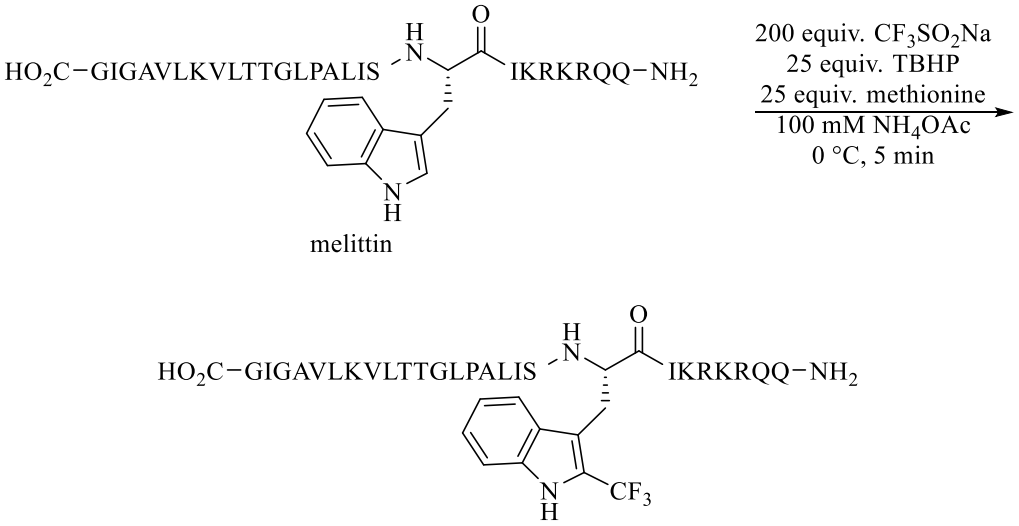
In a comprehensive study by Imiołek *et al.*, reactions of the Langlois reagent with all twenty natural amino acids were examined using *tert*-butyl hydroperoxide as an activator.[3] Reactivity was selective to cysteine and aromatic amino acids tryptophan, tyrosine, phenylalanine and histidine. Reaction yields were greater than 20% with tryptophan, histidine and cysteine, which were improved further by modifying pH. A low yield was obtained using tyrosine due to poor solubility in aqueous reaction solvent. Competitive trifluoromethylation of cysteine disulfides was not observed under the reaction conditions.

A competition assay was carried out using a mixture of equimolar Trp, Phe, Tyr, Cys, His and Met with 10 equivalents of sodium trifluoromethanesulfinate and 2.5 equivalents of *tert*-butyl hydroperoxide (Scheme 3.2). Tryptophan was the most reactive amino acid, trifluoromethylating in 34% ^{19}F NMR yield, with preferential trifluoromethylation at the 2-position. Trifluoromethylation of all other amino acids were observed in trace amounts with mixtures of regioisomers observed for Phe, Tyr and His.



Scheme 3.2 Competition assay for trifluoromethylation of reactive amino acids using excess Langlois reagent

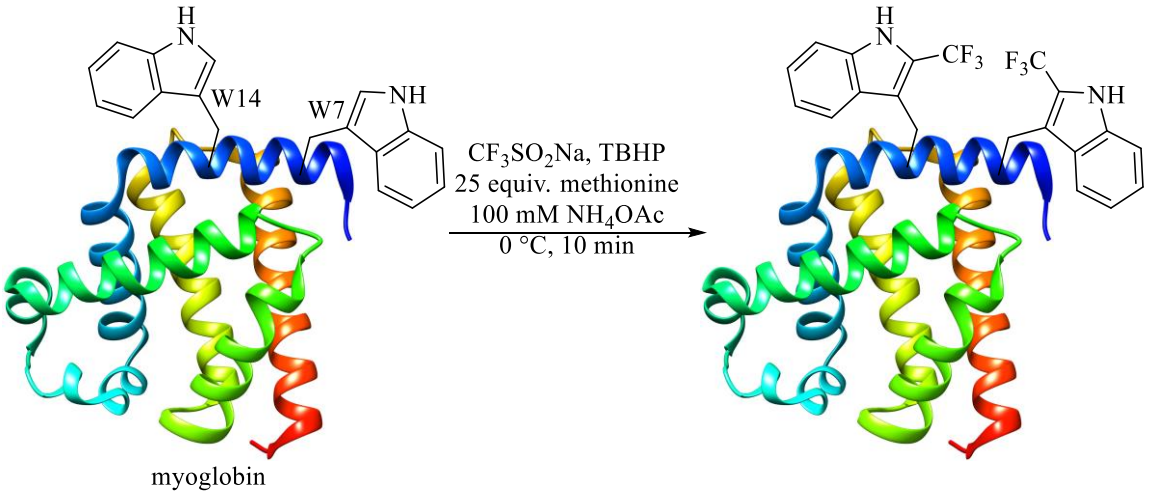
Melittin, a 26 residue peptide with a single Trp, was chosen as a model peptide (Scheme 3.3). To a 50 μM solution of melittin in buffer (100 mM ammonium acetate, pH 6) was added 200 equivalents of Langlois reagent, 25 equivalents of *tert*-butyl hydroperoxide and 25 equivalents of methionine at 0 ºC for 5 minutes. Modification of melittin was confirmed exclusively at Trp by LC-MS/MS analysis. Large excesses of reagents were employed to decrease the reaction time from 48 hours to 5 minutes. Oxidation and dual trifluoromethylation were observed under prolonged reaction conditions.



Scheme 3.3 Trifluoromethylation of melittin using excess Langlois reagent

Myoglobin was chosen as a model protein to test the compatibility of this Langlois/TBHP system. It contains 2 Trp residues as well as 7 Phe, 2 Tyr, 2 Cys and 11 Hisresidues (Table 3.1). Trifluoromethylation occurred exclusively at Trp and predominantly mono-trifluoromethylation was observed when employing 200 equivalents of Langlois reagent with 25 equivalents of *tert*-butyl hydroperoxide (Table 3.1, Entry 1). In contrast, when the equivalents of the Langlois reagent and *tert*-butyl hydroperoxide were increased to 1500 and 50, bis-trifluoromethylated myoglobin was the major product (Table 3.1, Entry 2).

Table 3.1 Mono-trifluoromethylation and bis-trifluoromethylation of myoglobin using excess Langlois reagent



Entry	Langlois Reagent (equiv.)	TBHP (equiv.)	^{19}F NMR Yield myoglobin (%)	^{19}F NMR Yield +1 CF_3 (%)	^{19}F NMR Yield +2 CF_3 (%)
1	200	25	29	53	17
2	1500	50	0	34	41

The relative site exposures for tryptophan in myoglobin were calculated as 29% and 35%, suggesting both sites are poorly accessible areas. However, this did not impede trifluoromethylation of these sites thus underlining the value of using the Langlois reagent to install a trifluoromethyl group as a tag in biological molecules, such as proteins, compared to other methods employing prosthetic groups. Additionally, partial denaturation of the protein was not required.

As proof of concept, a ^{19}F NMR spectroscopic study compared the products before and after trypsin digestion of trifluoromethylated myoglobin to its free amino acid residues. Both sites of tryptophan trifluoromethylation were distinctly observed at δ -58.0 and -68.7 before

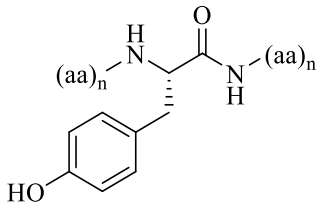
trypsin digestion, which collapsed to one peak at δ -58.8 after digestion. This chemical shift was in agreement with separately synthesised Trp(2-CF_3).

To demonstrate that the Langlois reagent is an excellent choice of reagent for fluorinating large biological molecules, trifluoromethylation studies were extended to substrates pantothenate synthetase (1 Trp, 9 Phe, 7 Tyr and 12 His residues; 319 residues long) and lysozyme (6 Trp, 3 Phe, 8 Cys as disulfides, 3 Tyr and 2 His residues; 129 residues long). As with myoglobin, trifluoromethylation occurred on Trp for both substrates.

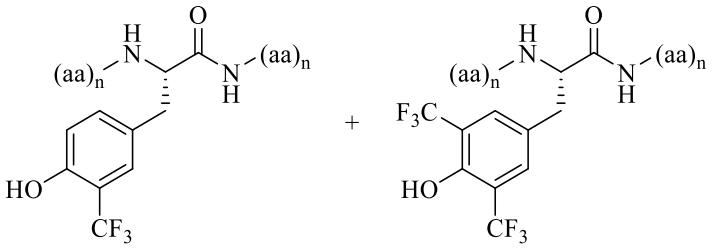
Other reported uses of the Langlois reagent include trifluoromethylation of proteins using laser-initiated activation.[4] Trifluoromethylation was carried out on neuropeptide Y fragment 18-36, myoglobin (153 residues), vitamin K epoxide reductase (283 residues) and beta-lactoglobulin (162 residues) by irradiating an aqueous solution of the protein or peptide with hydrogen peroxide and the Langlois reagent. Modifications were observed on all amino acid residues, except methionine and cysteine, using LC-MS/MS analysis. Addition of hydrogen peroxide and laser irradiation were necessary for reaction to take place. This supported a mechanism involving oxidation of the Langlois reagent to generate trifluoromethyl radicals, initiated by hydroxyl radicals formed from photolysis of H_2O_2.

Trifluoromethylation of tyrosine residues in peptides using photocatalytic conditions is also reported (Scheme 3.4).[5] This reaction was carried out by employing an iridium photocatalyst in combination with blue LEDs in a photoreactor. Peptides up to 51 residues in length were trifluoromethylated, however other residues such as Phe were also trifluoromethylated in up to 26% yield (Scheme 3.4, A). Slight selectivity was observed for the dipeptide Trp-Tyr, giving a trifluoromethylation ratio of 11:18 Tyr:Trp (Scheme 3.4, B).

A)

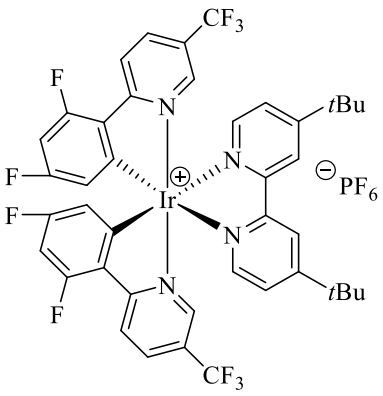


20 equiv. CF_3SO_2Na
15 mol% $Ir[(dFCF_3ppy)_2(dtbpy)](PF_6)$
10% AcOH in MeCN
rt, 20 h, blue LEDs

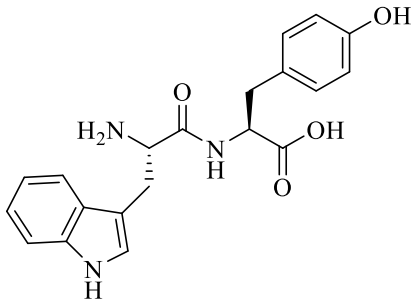


13 examples up to 51 residues long
mono-CF_3: 10% - 47%
ratio of mono-CF_3:bis-CF_3 = 1:0 - 1:1

$Ir[(dFCF_3ppy)_2(dtbpy)](PF_6)$ =

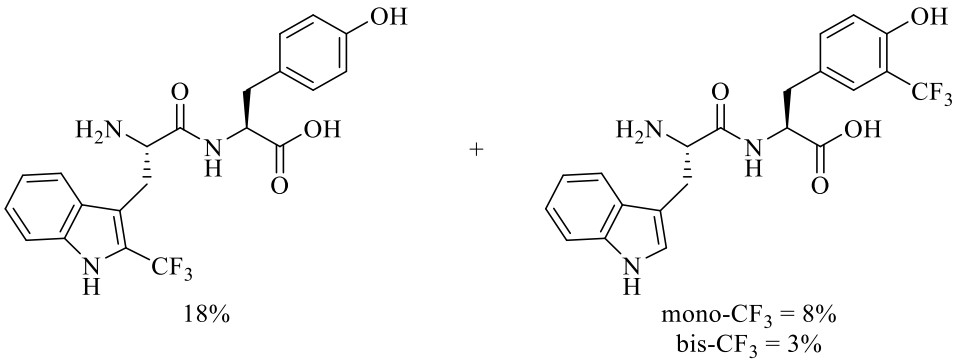


B)



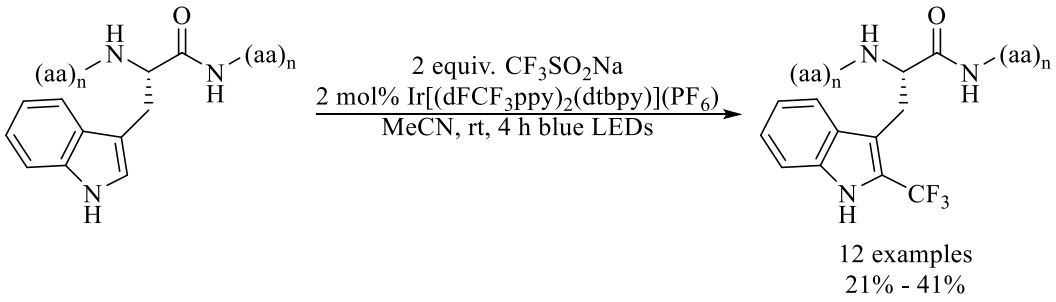
Trp-Tyr

20 equiv. CF_3SO_2Na
15 mol% $Ir[(dFCF_3ppy)_2(dtbpy)](PF_6)$
10% AcOH in MeCN
rt, 20 h, blue LEDs



Scheme 3.4 Trifluoromethylation of tyrosine residues in peptides and tryptophan in Trp-Tyr using the Langlois reagent activated with photocatalytic conditions

Similar photoredox conditions have been reported for trifluoromethylation of tryptophan residues in di- and tri-peptides (Scheme 3.5).[6] Better selectivity for trifluoromethylation of tryptophan was observed in dipeptides with Phe, Tyr, or Cys.



Scheme 3.5 Trifluoromethylation of tryptophan residues in di- and tri-peptides using the Langlois reagent activated with photocatalytic conditions

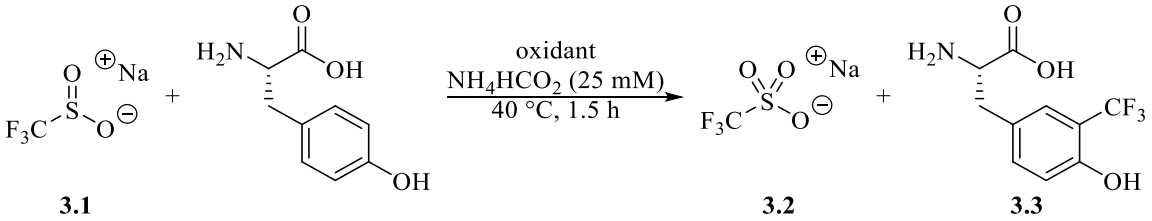
In summary, the literature to date demonstrates utilising the Langlois reagent to trifluoromethylate large biomolecules such as peptides and proteins. This trifluoromethylation has been made possible by generating trifluoromethyl radicals *in situ* using oxidants, laser-initiated activation or photoredox catalysis. The most reactive residues were Trp, Tyr, Cys, Phe and His.

3.1.2 Trifluoromethylation of Tyrosine and Tryptophan with Substoichiometric Langlois Reagent

To date, literature methods for trifluoromethylation of amino acid residues employ large excesses of the Langlois reagent. This is not amenable to radiosynthetic methods. Therefore we set about developing reaction conditions for trifluoromethylation of amino acids and peptides that employ substoichiometric amounts of Langlois reagent.

Initially, trifluoromethylation of tyrosine was examined using 1 equivalent of Langlois reagent, 4 equivalents of oxidant and 8 equivalents of tyrosine (Table 3.2).

Table 3.2 Oxidant screening for trifluoromethylation of tyrosine with the Langlois reagent



3.1 **3.2** **3.3**

Entry	Oxidant	^{19}F NMR Yield 3.1 (%)[b]	^{19}F NMR Yield 3.2 (%)[b]	^{19}F NMR Yield 3.3 (%)[b]
1	TBHP	22	9	0
2	I_2O_5	90	2	<1
3	H_2O_2 (30%)	58	12	0
4	Urea-H_2O_2	59	9	0
5	$NaIO_4$	0	76	0
6	Oxone	0	93	0

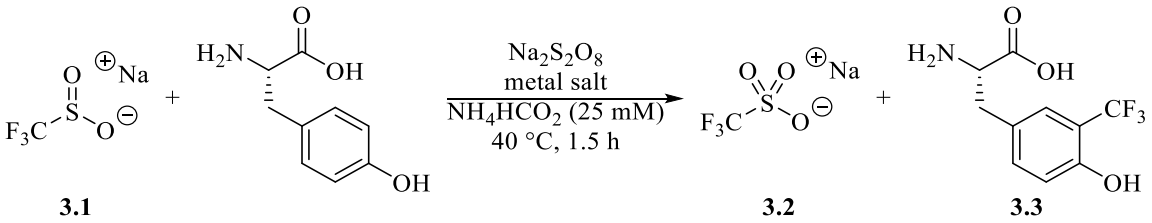
[a] General conditions: Langlois reagent (0.05 mmol), tyrosine (0.4 mmol) and oxidant (0.2 mmol) in ammonium formate (0.5 mL, 25 mM) at 40 ºC for 1.5 h.
[b] Relative to 0.1 mmol TFA internal standard.

Several oxidants were tested, however no trifluoromethylated tyrosine was detected. Instead the Langlois reagent either remained unreacted, was oxidised to triflate, or reacted to form fluoroform depending on the oxidant used. Fluoroform was observed at δ -77.8 by ^{19}F NMR spectroscopy, consistent with literature reports.[7] Additionally, the reaction of the Langlois reagent with *tert*-butyl hydroperoxide in the absence of substrate is known to form fluoroform.[8]

It is known that metal compounds such as copper(II) and iron(III) salts are required for successful reactions between the Langlois reagent and aromatic substrates.[9] Literature methods of trifluoromethylation have employed superstoichiometric amounts of Langlois reagent where addition of metal compounds was not required. This is because trace metals are already present in commercially available Langlois reagent.[8]

Since we were conducting trifluoromethylation reactions using substoichiometric amounts of Langlois reagent, addition of metal salts in stoichiometric amounts was investigated (Table 3.3). No trifluoromethylated tyrosine was observed when adding Mn^{II}, Zn^{II} or Cu^{II} triflate salts (Table 3.3, Entries 1 – 3). A 4% yield was obtained with copper(II) sulfate and 11% with iron(II) or iron(III) salts (Table 3.3, Entries 4 – 6).

Table 3.3 Addition of metal salts for trifluoromethylation of tyrosine using the Langlois reagent



3.1 **3.2** **3.3**

Entry	Metal Salt	^{19}F NMR Yield 3.1 (%)[b]	^{19}F NMR Yield 3.2 (%)[b]	^{19}F NMR Yield 3.3 (%)[b]
1	MnO_2	0	0	0
2	$ZnCl_2$	49	42	<1
3	$Cu(OTf)_2$	80	20	0
4	$CuSO_4$	16	46	4
5	$FeSO_4.7H_2O$	5	30	11
6	$Fe(NO_3)_3.9H_2O$	12	32	11

[a] General conditions: Langlois reagent (0.05 mmol), tyrosine (0.4 mmol), sodium persulfate (0.2 mmol) and metal salt (0.1 mmol) in ammonium formate (0.5 mL, 25 mM) at 40 ºC for 1.5 h. [b] Relative to 0.1 mmol TFA internal standard.

The trifluoromethylated tyrosine product **3.3** was characterised by High Resolution Mass Spectrometry (HRMS) (requires mass = 250.0686 *m/z*; found 250.0684 *m/z*), ^{1}H, ^{19}F and ^{13}C NMR spectroscopy. The chemical shifts for the aromatic region shifted downfield from two signals at δ 6.85 (H-2 & H-6) and 6.50 (H-3 & H-5) for tyrosine to three signals at δ 7.46 (d, *J* = 2.2 Hz, H-2), 7.35 (dd, *J* = 8.4, 2.2 Hz, H-6) and 6.93 (d, *J* = 8.3 Hz, H-5) for L-Tyr(3-CF_3) (**3.3**) (Figure 3.1, A).[10] A chemical shift of δ -61.45 was observed by ^{19}F NMR spectroscopy and a quartet signal was observed by ^{13}C NMR spectroscopy at δ 126.52 with a *J* value of 271.1 Hz corresponding to the carbon of the trifluoromethyl group. These values

were all in agreement with the literature and were consistent with signal patterns observed for other tyrosine derivatives.[5,11]

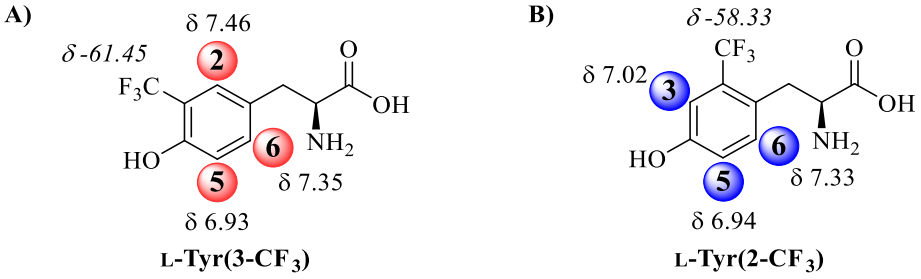
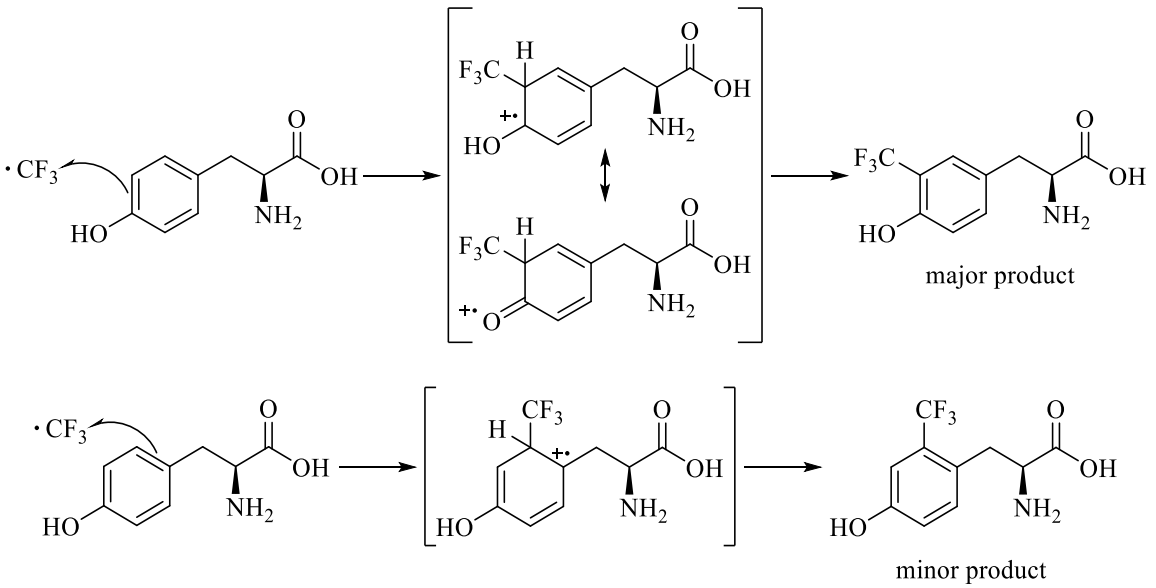


Figure 3.1 Assignments for chemical shifts from ^{1}H and ^{19}F NMR spectroscopy (italics) for A) L-Tyr(3-CF_3) B) L-Tyr(2-CF_3)

Trace amounts of L-Tyr(2-CF_3) were isolated from the reaction and characterised. The chemical shifts for the aromatic region were δ 7.33 (d, J = 8.5 Hz, H-6), 7.02 (d, J = 2.7 Hz, H-3) and 6.94 (dd, J = 8.3, 2.6 Hz, H-5) (Figure 3.1, B). A chemical shift of δ -58.33 was observed by ^{19}F NMR spectroscopy. Assignment of L-Tyr(2-CF_3) and L-Tyr(3-CF_3) was made by comparing the ^{1}H and ^{19}F NMR spectroscopic data for the two compounds and by noting the shielding effect on σ- and ρ- positions to the mesomerically electron-donating hydroxyl group.

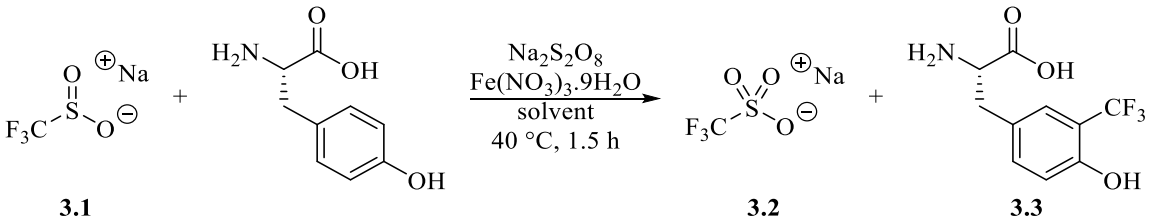
Further evidence for assignment is illustrated by the reaction mechanism which favours formation of L-Tyr(3-CF_3) over L-Tyr(2-CF_3). Initial electron donation of the aromatic ring to the trifluoromethyl radical leads to a radical cation intermediate. When the trifluoromethyl group is installed on the 3- position, this radical cation can be stabilised mesomerically by the hydroxyl group, but only inductively by the alkyl group when on the 2- position (Scheme 3.6).



Scheme 3.6 Reaction mechanism and stabilisation of radical cation intermediate in formation of L-Tyr(3-CF_3) and L-Tyr(2-CF_3)

To optimise the reaction conditions further, a variety of solvent systems were tested (Table 3.4). Optimal results were achieved at pH <4 by employing 10% AcOH solutions (Table 3.4, Entries 6 – 8). Addition of acetonitrile led to lower yields (Table 3.4, Entries 9 & 10).

Table 3.4 Optimisation of solvent for trifluoromethylation of tyrosine using the Langlois reagent



3.1 **3.2** **3.3**

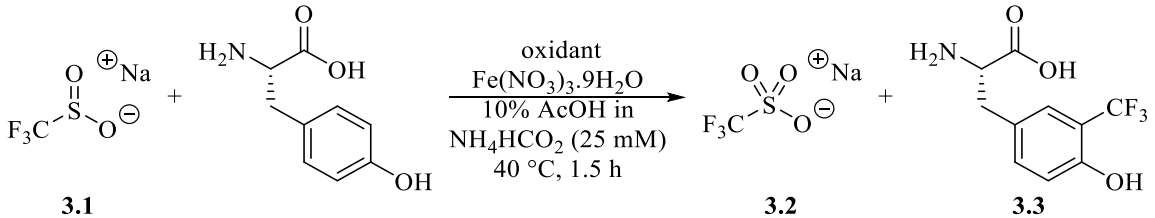
Entry	Solvent	^{19}F NMR Yield 3.1 (%)[b]	^{19}F NMR Yield 3.2 (%)[b]	^{19}F NMR Yield 3.3 (%)[b]
1	NH_4HCO_2 (25 mM)	12	32	11
2	Tris-Buffered Saline	0	13	14

3	NH_4OAc/NH_3 pH 8	22	45	0
4	NH_4OAc/AcOH pH 6	23	41	0
5	NH_4OAc/AcOH pH 4	<1	24	17
6	10% AcOH in NH_4HCO_2 (25 mM)	16	24	28
7	10% AcOH in H_2O	12	36	12
8	10% AcOH in DMSO	0	23	22
9	10% AcOH in 1:1 H_2O:MeCN	10	33	5
10	1:1 H_2O:MeCN	10	30	12

[a] General conditions: Langlois reagent (0.05 mmol), tyrosine (0.4 mmol), sodium persulfate (0.2 mmol) and iron(III) nitrate nonahydrate (0.1 mmol) in solvent (0.5 mL) at 40 ºC for 1.5 h. [b] Relative to 0.1 mmol TFA internal standard.

Oxidant screening revealed sodium and ammonium persulfate afforded trifluoromethylated tyrosine in 28% and 15% yield respectively (Table 3.5, Entries 1 & 2). Employing (diacetoxyiodo)benzene (PIDA) or *meta*-chloroperoxybenzoic acid (*m*CPBA) led to almost quantitative oxidation to triflate **3.2** (Table 3.5, Entries 3 & 4), whereas *tert*-butyl hydroperoxide afforded **3.3** in 30% yield and almost no triflate (Table 3.5, Entry 5).

Table 3.5 Optimisation of oxidants for trifluoromethylation of tyrosine using the Langlois reagent and iron(III) nitrate nonahydrate



3.1 **3.2** **3.3**

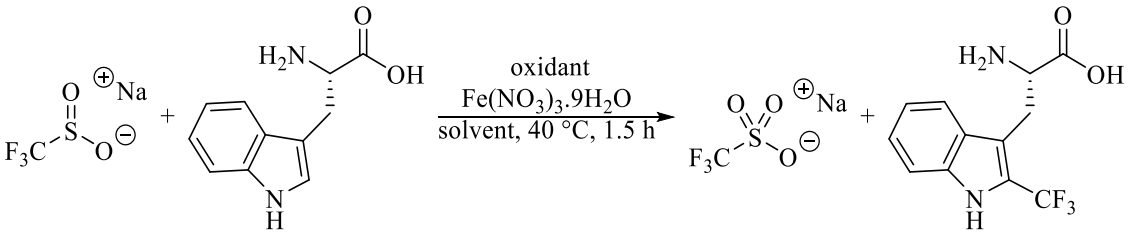
Entry	**Oxidant**	**^{19}F NMR Yield 3.1 (%)[b]**	**^{19}F NMR Yield 3.2 (%)[b]**	**^{19}F NMR Yield 3.3 (%)[b]**
1	$Na_2S_2O_8$	16	24	28

2	$NH_4S_2O_8$	16	29	15
3	PIDA	7	93	0
4	*m*CPBA	0	100	0
5	*t*-BuOOH	0	3	30

[a] General conditions: Langlois reagent (0.05 mmol), tyrosine (0.4 mmol), oxidant (0.2 mmol) and iron(III) nitrate nonahydrate (0.1 mmol) in 10% acetic acid in ammonium formate (0.5 mL, 25 mM) at 40 ºC for 1.5 h. [b] Relative to 0.1 mmol TFA internal standard.

Trifluoromethylation of tryptophan was examined in various solvents and higher yields of trifluoromethylated tryptophan **3.4** were obtained at higher pH (Table 3.6, Entries 1 – 7). An optimal yield of 32% was afforded by employing DMSO (Table 3.6, Entry 8). As with reactions using tyrosine, fluoroform was commonly observed as the side product.

Table 3.6 Optimisation of oxidants and solvent for trifluoromethylation of tryptophan using the Langlois reagent



3.1 **3.2** **3.4**

Entry	Oxidant	Solvent	^{19}F NMR Yield 3.1 (%)[b]	^{19}F NMR Yield 3.2 (%)[b]	^{19}F NMR Yield 3.4 (%)[b]
1	$Na_2S_2O_8$	10% AcOH in NH_4OAc (25 mM)	88	<1	0
2	$Na_2S_2O_8$	NH_4OAc/AcOH pH 4	95	<1	0
3	$Na_2S_2O_8$	NH_4OAc/AcOH pH 6	73	6	4
4	$Na_2S_2O_8$	NH_4OAc/NH_3 pH 8	78	6	4
5	*t*-BuOOH	NH_4OAc/AcOH pH 4	96	<1	0

6	*t*-BuOOH	NH_4OAc/AcOH pH 6	4	4	12
7	*t*-BuOOH	NH_4OAc/NH_3 pH 8	2	5	18
8	*t*-BuOOH	DMSO	0	0	32

[a] General conditions: Langlois reagent (0.05 mmol), tryptophan (0.4 mmol), oxidant (0.2 mmol) and iron(III) nitrate nonahydrate (0.1 mmol) in solvent (0.5 mL, 25 mM) at 40 ºC for 1.5 h. [b] Relative to 0.1 mmol TFA internal standard.

The trifluoromethylated tryptophan product **3.4** was characterised by MS (requires mass = 273.1 *m/z*; found 273.1 *m/z*) along with ^{1}H and ^{19}F NMR spectroscopy. Analyses were in agreement with the literature.[3] The chemical shifts for the aromatic region shifted downfield from five signals at δ 7.56 (d, *J* = 8.0 Hz, H-4), 7.35 (d, *J* = 8.0 Hz, H-7), 7.20 (s, H-2), 7.06 (t, *J* = 7.5 Hz, H-6) and 6.98 (t, *J* = 7.5 Hz, H-5) for tryptophan to four signals at δ 7.76 (d, *J* = 8.1 Hz, 1H), 7.46 (d, *J* = 8.1 Hz, 1H), 7.33 – 7.30 (m, 1H), 7.18 – 7.15 (m, 1H) for L-Trp(2-CF_3) (**3.4**).[12] TOCSY NMR spectroscopy revealed a correlation between all the aromatic protons but none between the indole NH and H-2, as seen in tryptophan (Figure 3.2). This data suggested that the major product had trifluoromethylation at this 2- position with a chemical shift at δ -57.81, as observed by ^{19}F NMR spectroscopy.

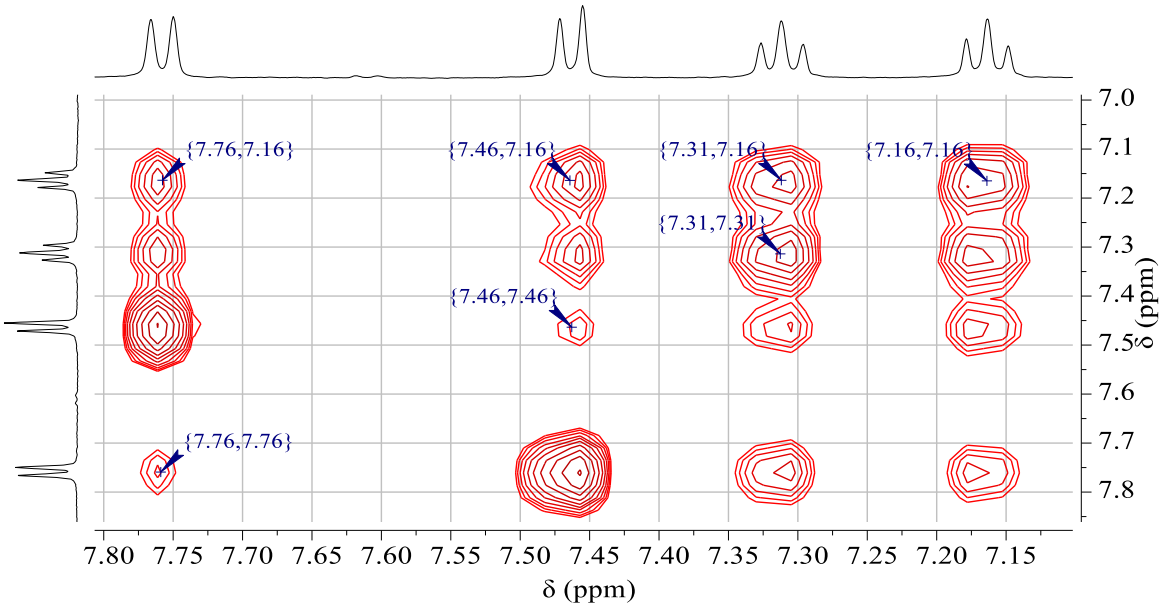


Figure 3.2 Aromatic region of ^{1}H TOCSY NMR spectrum (500 Hz) for Trp(2-CF_3) showing correlation across all aromatic signals suggesting trifluoromethylation occurs mainly at the 2- position

Trace amounts of L-Trp(4-CF_3) and L-Trp(7-CF_3) products were isolated and characterised as a mixture. The aromatic regions displayed chemical shifts of δ 7.74 (d, *J* = 8.1 Hz, 1H), 7.53 (d, *J* = 2.3 Hz, 1H), 7.46 (d, *J* = 7.4 Hz, 1H), 7.28 – 7.25 (m, 1H) and δ 7.88 (d, *J* = 8.0 Hz, 1H), 7.47 (d, *J* = 7.7 Hz, 1H), 7.35 (d, *J* = 2.0 Hz, 1H), 7.21 – 7.18 (m, 1H) respectively. Analysis of the *J* values, COSY and NOESY spectra indicated correlation between H-2 doublet signals at δ 7.53 or 7.35 and the indole NH proton signals at δ 11.73 or 11.43, which suggested that trifluoromethylation did not occur at the 2- position. COSY NMR spectroscopic analysis showed correlation between all the remaining aromatic signals, indicative of trifluoromethylation at the 4- or 7- positions (Figure 3.3).

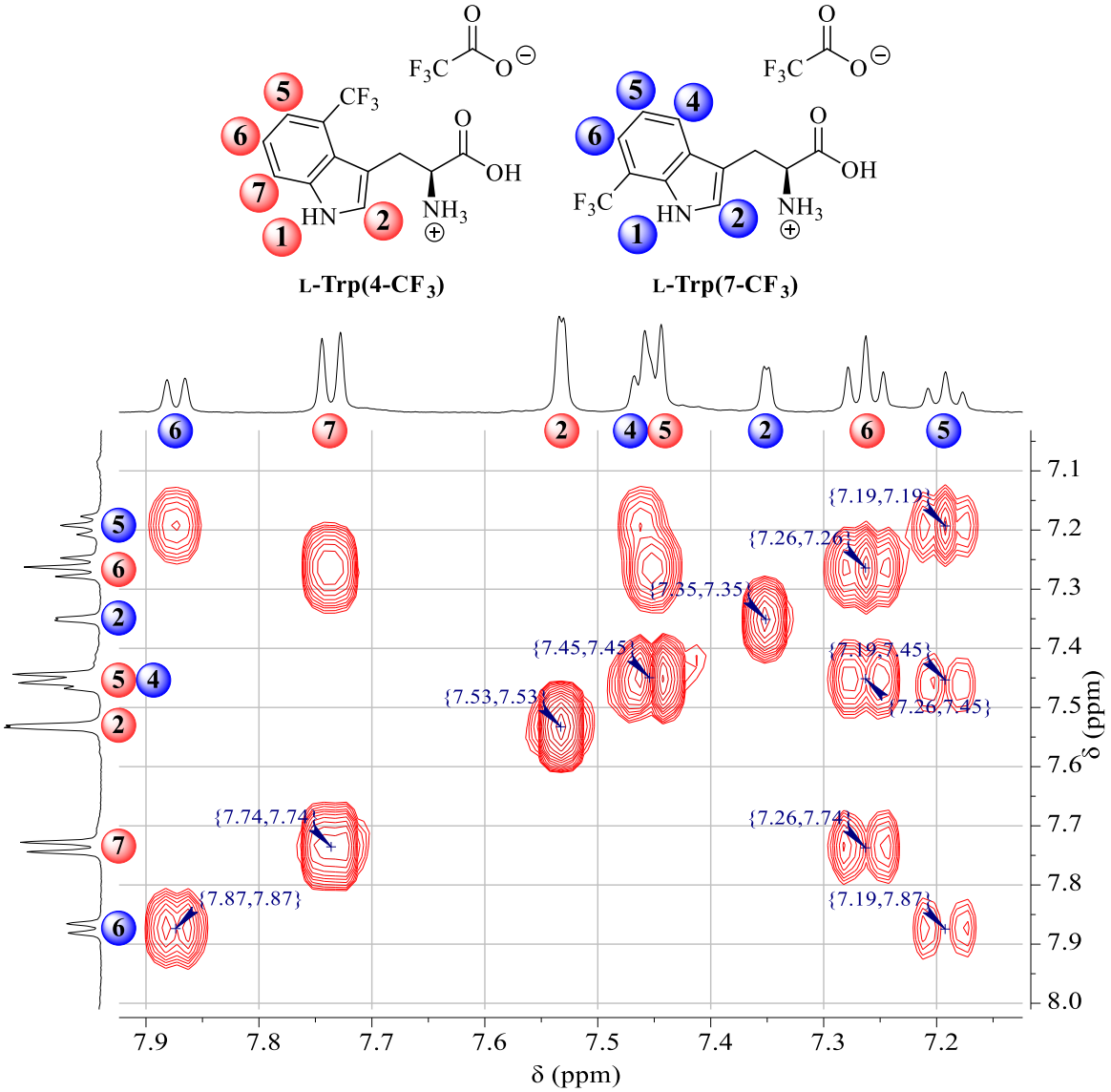


Figure 3.3 ^{1}H COSY NMR spectrum (500 Hz) for a mixture of L-Trp(4-CF_3) and L-Trp(7-CF_3) showing correlations that indicate trifluoromethylation on the 4- or 7- position

These two products were distinguished using NOESY NMR spectroscopy by observing a through-space correlation between the indole NH proton and H-7 at δ 7.74 for only Trp(4-CF_3) and not Trp(7-CF_3) (Figure 3.4). This allowed assignment of L-Trp(4-CF_3) and L-Trp(7-CF_3) as the major and minor products with chemical shifts at δ -57.74 and -61.21 respectively by ^{19}F NMR spectroscopy.

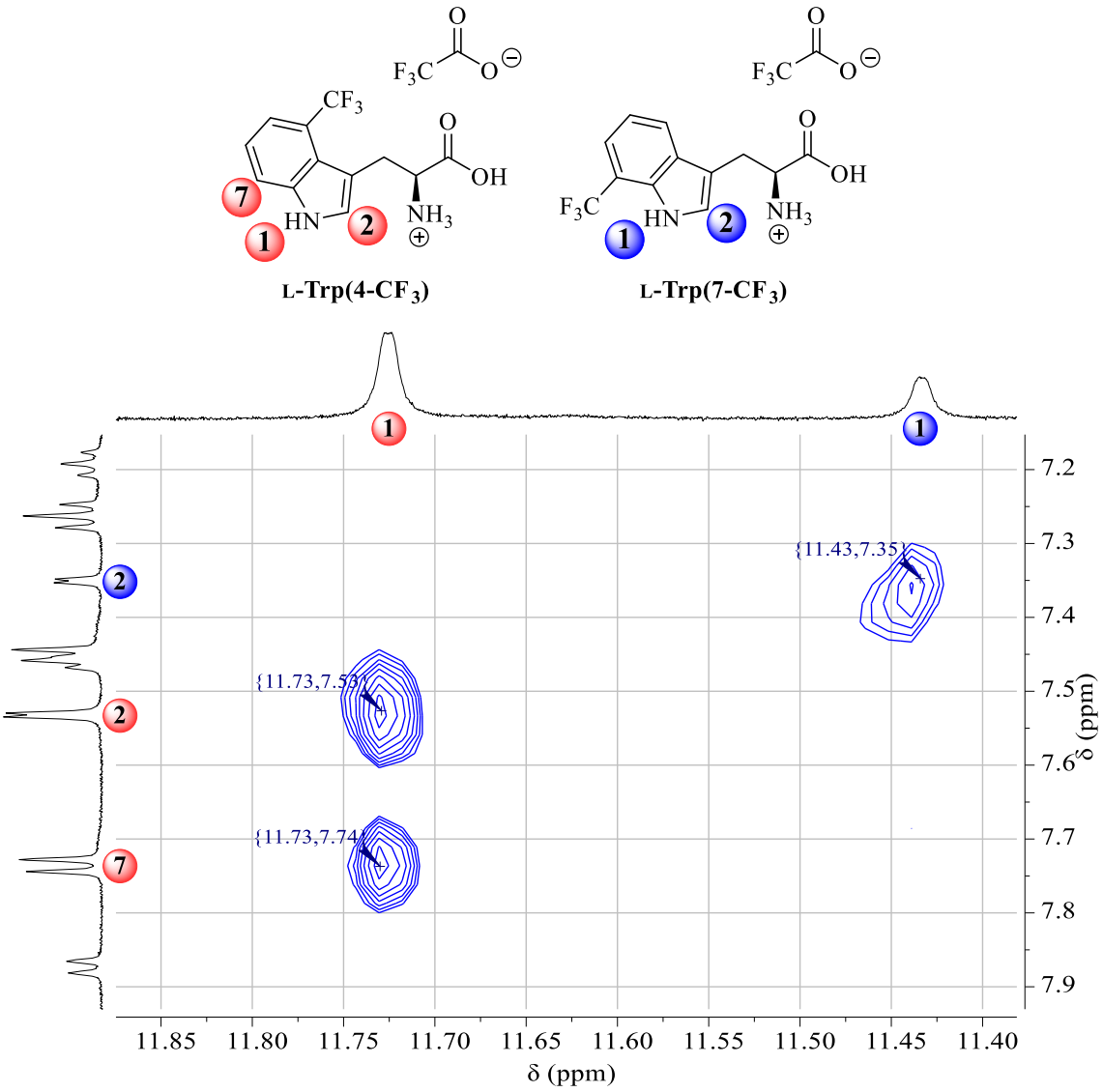


Figure 3.4 ^{1}H NOESY NMR spectrum (500 Hz) for a mixture of L-Trp(4-CF_3) and L-Trp(7-CF_3) showing through-space correlations that distinguish the two products

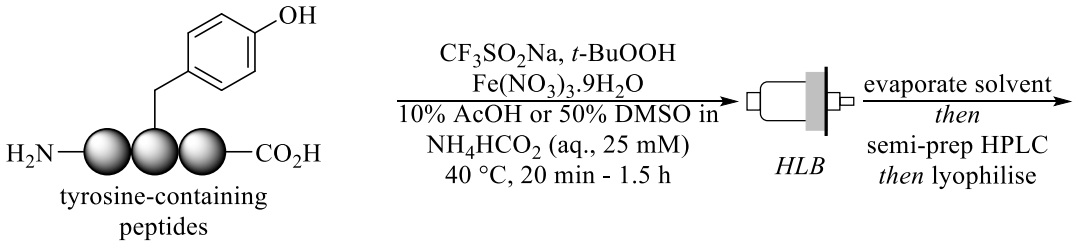
In summary, optimisation of the reaction between amino acids and substoichiometric amounts of Langlois reagent indicated that the addition of a metal compound, such as iron(III) salts, was essential to obtaining trifluoromethylated amino acids. *Tert*-butyl hydroperoxide was the ideal oxidant for this transformation. Best results were obtained using 10% acetic acid in aqueous ammonium formate or DMSO for reactions with tyrosine, and DMSO for tryptophan. Trifluoromethylation occurred mainly at the 3- position of tyrosine

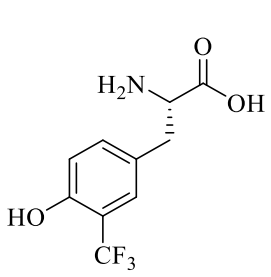
and the 2- position of tryptophan, with trace amounts of trifluoromethylation detected at the 2- position of tyrosine or 4- and 7- position of tryptophan.

3.1.3 Synthesis and Isolation of Trifluoromethylated Amino Acid and Peptide References

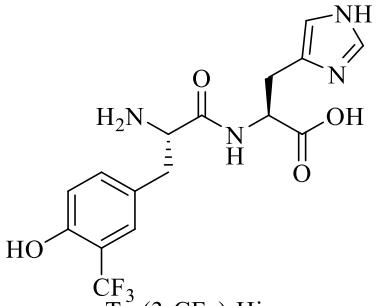
Before translating this reaction into a radiochemical setting, the trifluoromethylated compounds of selected dipeptides and peptides were synthesised for use as HPLC references in radiochemical reactions. Products were isolated by semi-preparative HPLC, identified by mass spectrometry and characterised by spectroscopic analysis (see Chapter 4: Experimental Data for details).

To assess the reactivity of tyrosine in the presence of other residues, dipeptides of Met, His or Phe with Tyr were tested (Scheme 3.7). Trifluoromethylation on Tyr at the 3- position was found as the major product.

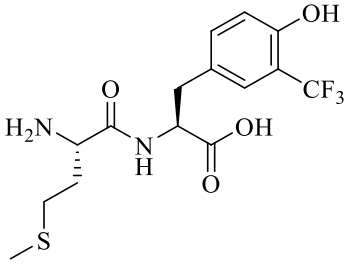




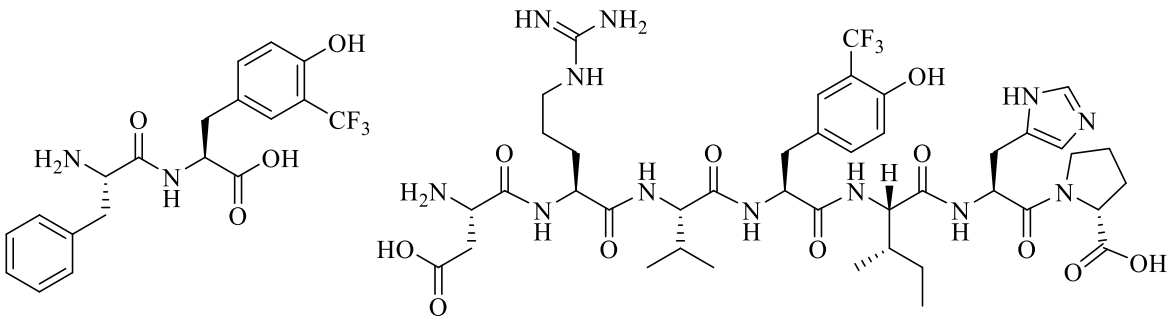
L-Tyr(3-CF_3)
12%

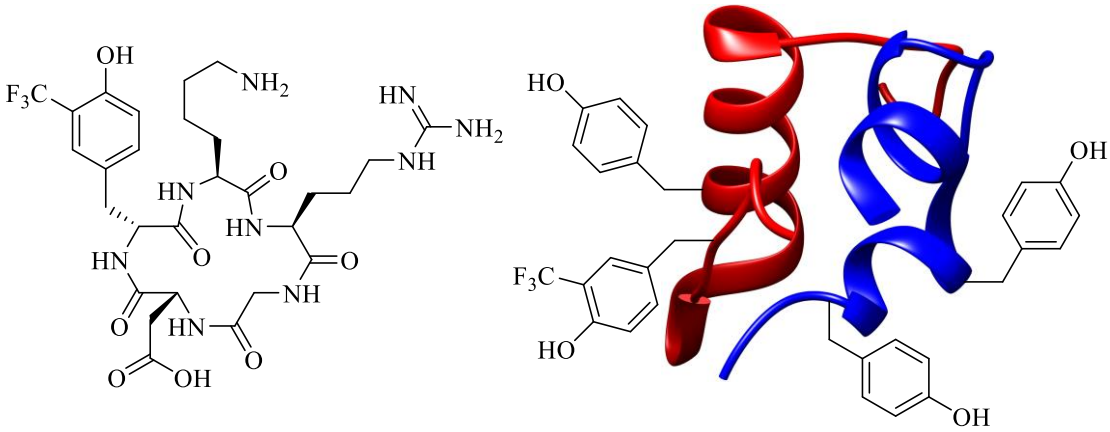


Tyr(3-CF_3)-His
11%



Met-Tyr(3-CF_3)
10%





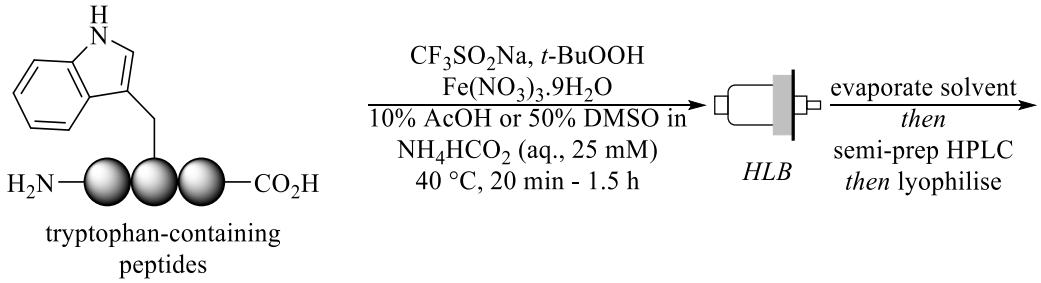
Scheme 3.7 Synthesis of trifluoromethylated references containing tyrosine

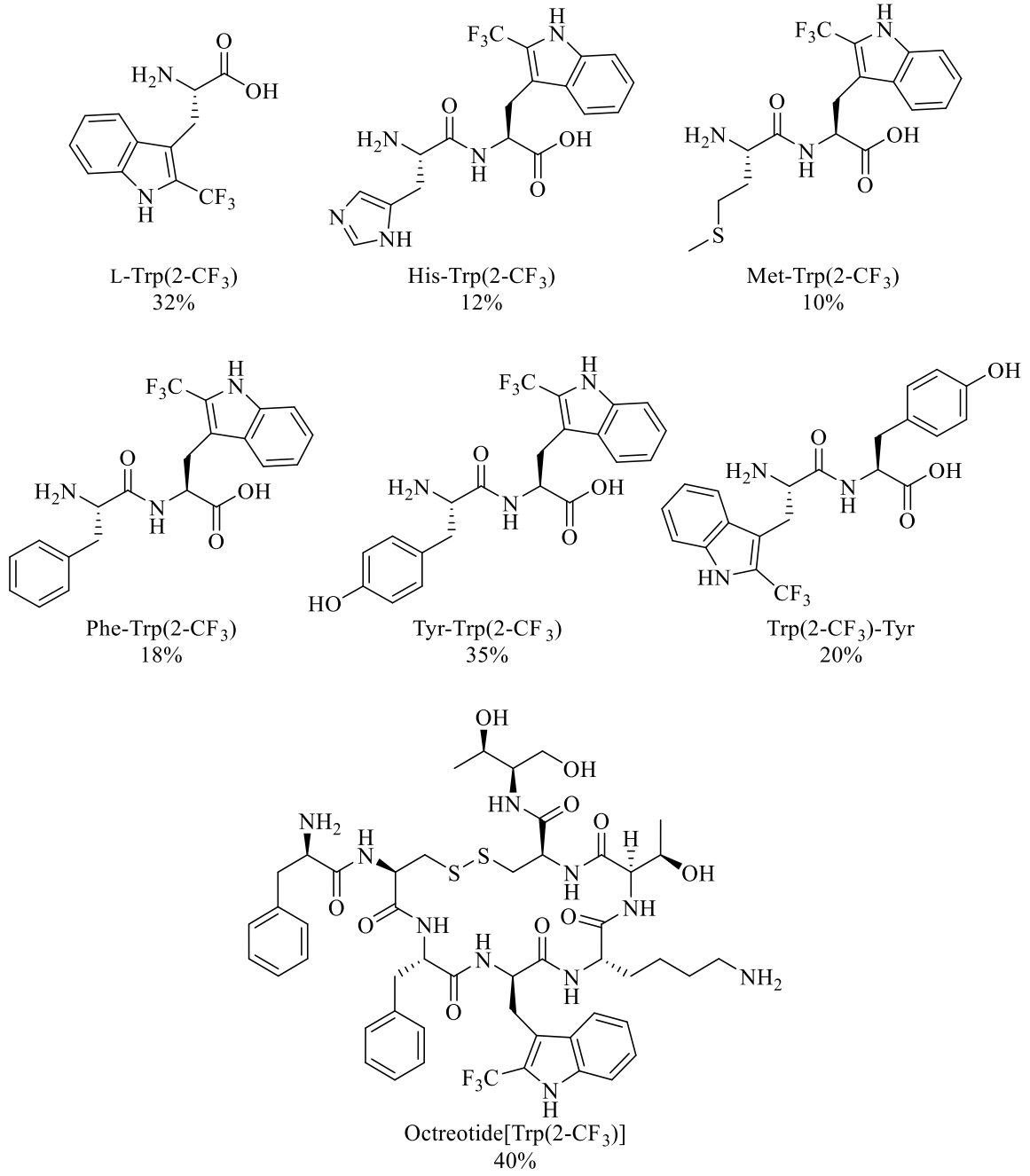
The histidine of Tyr(3-CF_3)-His, phenyl ring of Phe-Tyr(3-CF_3) or methyl of Met-Tyr(3-CF_3) were all intact, as observed by ^{1}H NMR spectroscopy, indicating trifluoromethylation took place solely on Tyr. Additionally, MS/MS analysis showed that trifluoromethylation occurred exclusively on Tyr for these products. HRMS indicated mono-trifluoromethylation occurred for all three substrates. Trace amounts of Tyr(2-CF_3)-His, Phe-Tyr(2-CF_3), Met-Tyr(2-CF_3) or Met(O)-Tyr(3-CF_3) products were also isolated from each reaction, characterised and analysed using the same reasoning for distinguishing L-Tyr(3-CF_3) from L-Tyr(2-CF_3).

The Met-containing products were identified by comparing the chemical shifts of the isolated products to those given in the literature for methionine and partially oxidised methionine. The methyl group of Met-Tyr(3-CF_3) was observed at δ 2.04, compared to Met reported at δ 2.06.[13] The methyl group of Met(O)-Tyr(3-CF_3) was observed at δ 2.55, compared to protected Met(O) reported at δ 2.69.[14] ESI-MS analysis was in agreement with mono-oxidation (requires *m*/*z* = 397.10, found 397.10).

A selection of biologically relevant peptides were chosen as model compounds to demonstrate trifluoromethylation on larger substrates. Angiotensin I/II fragment 1 – 7, a tyrosine-containing peptide displaying anti-inflammatory properties,[15] was trifluoro-methylated and isolated in 36%. c(RGDyK), a ligand of integrin $\alpha_v\beta_3$ receptors,[16] was trifluoromethylated in 20%. All evidence supporting the sites of trifluoromethylation was given by ^{1}H, ^{19}F and 2D NMR spectroscopy, HRMS, and MS/MS analysis (see Chapter 4: Experimental Data for details). Insulin was subjected to trifluoromethylation conditions before separating the products by HPLC and analysing by MS/MS and ^{19}F NMR spectroscopy. CF_3 modification was found only on chain A Tyr-26.

The reactivity of tryptophan-containing dipeptides was also assessed (Scheme 3.8). The histidine of His-Trp(2-CF_3), the methyl of Met-Trp(2-CF_3) or the phenyl ring of Phe-Trp(2-CF_3) were all intact, as observed by ^{1}H NMR spectroscopy, indicating trifluoromethylation took place solely on Trp. Additionally, MS/MS analysis showed that trifluoromethylation occurred exclusively on Trp for these products. HRMS indicated mono-trifluoromethylation occurred for all three substrates. The chemical shift for the methyl of Met-containing products were all δ 2.04 – 2.06, suggesting that Met was not oxidised in any of the products.





Scheme 3.8 Synthesis of trifluoromethylated substrates containing tryptophan

Small amounts of products trifluoromethylated on the 4- or 7- positions were also isolated from each reaction, characterised and analysed using the same reasoning for distinguishing L-Trp(2-CF_3), L-Trp(4-CF_3) and L-Trp(7-CF_3).

In addition, trifluoromethylation of dipeptides Tyr-Trp or Trp-Tyr was carried out and CF_3 incorporation occurred solely on Trp with none observed on Tyr. These results suggest that under these conditions Trp is a more reactive residue than Tyr.

To demonstrate that trifluoromethylation of tryptophan residues is possible for longer peptides, the somatostatin mimic octreotide[17] was trifluoromethylated and isolated in 40% yield. MS/MS and NMR spectroscopic analysis revealed trifluoromethylation occurred at the 2- position of Trp (see Chapter 4: Experimental Data for details).

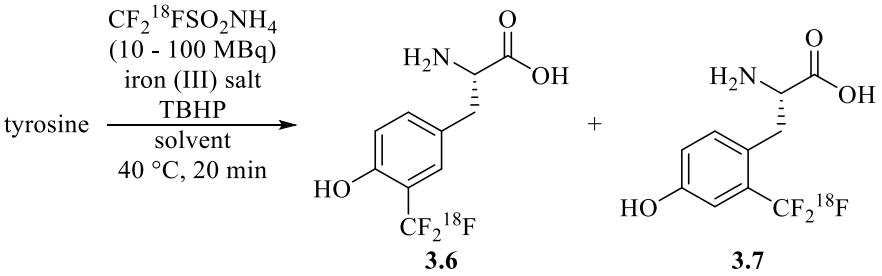
In summary, the reaction conditions developed for trifluoromethylating tyrosine and tryptophan were applied to a number of dipeptides and biologically relevant peptides containing either of these two amino acids. The major products isolated from these reactions were found to contain trifluoromethyl groups on Trp or Tyr residues at the 2- and 3- positions respectively. Little or no trifluoromethylation of His, Phe or Met residues was observed. Competitive trifluoromethylation between Tyr and Trp residues occurred exclusively on Trp.

3.2 Radiolabelling Tyrosine and Tryptophan using the [^{18}F]Langlois Reagent

After optimising reaction conditions for trifluoromethylating amino acid residues with the Langlois reagent, radiochemical reactions were pursued by dispensing aliquots of [^{18}F]Langlois reagent (10 – 100 MBq) in aqueous ammonium formate buffer into vials containing a peptide and iron source. *Tert*-butyl hydroperoxide was then added in solvent

before heating to 40 ºC for 20 minutes. Iron(III) acetylacetonate, iron(III) chloride or iron(III) nitrate nonahydrate were added to the reaction (Table 3.6).

Table 3.6 Radiolabelling tyrosine with the [^{18}F]Langlois reagent and iron(III) salts[a]



Entry	Iron(III) Salt	Solvent	RCY 3.6 (%, *n* = 2)	RCY 3.7 (%, *n* = 2)
1	$Fe(acac)_3$	DMSO in AF (200 µL)	0	0
2	$FeCl_3$	DMSO in AF (200 µL)	7 ± 3	1 ± 0
3	$Fe(NO_3)_3.9H_2O$	DMSO in AF (200 µL)	14 ± 5	2 ± 1
4	$Fe(NO_3)_3.9H_2O$	AcOH in AF (300 µL)	16 ± 4 (*n* = 4)	3 ± 1 (*n* = 4)
5	none	AcOH in AF (300 µL)	0	0

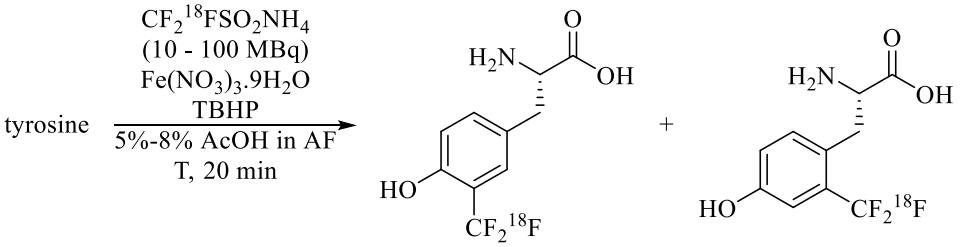
[a] General conditions: [^{18}F]$CF_3SO_2NH_4$ (10 – 100 MBq), tyrosine (0.03 mmol), iron(III) salt (0.06 mmol) and TBHP (0.12 mmol) in 5% – 8% AcOH or 50% – 75% DMSO in ammonium formate (AF) at 40 ºC for 20 min. RCY measured by taking aliquot of crude for radio-HPLC.

Iron(III) nitrate nonahydrate afforded labelled tyrosine in 14% RCY at the 3- position and 2% RCY at the 2-position (Table 3.6, Entry 3). Similar RCYs were obtained with a mixture of acetic acid or DMSO in aqueous ammonium formate (Table 3.6, Entries 3 & 4). No product was observed in the absence of iron(III) salt which emphasises its importance in the reaction (Table 3.6, Entry 5).

The effect of temperature and stoichiometry on labelling tyrosine and tryptophan was studied. Studies with tyrosine revealed that increasing the temperature to 60 ºC led to an

increase in RCY to 49% (Table 3.7, Entry 1). Increasing the amount of tyrosine from 0.03 mmol to 0.06 mmol increased the RCY to 58% but no further increase was observed at 0.12 mmol (Table 3.7, Entries 2 – 4).

Table 3.7 Optimisation of reaction conditions for radiolabelling tyrosine[a]



Entry	Tyrosine (mmol)	T (ºC)	RCY 3.6 (%, *n* = 2)	RCY 3.7 (%, *n* = 2)
1	0.03	40	16 ± 4 (*n* = 4)	3 ± 1 (*n* = 4)
2	0.03	60	49 ± 1	11 ± 1
3	0.06	60	58 ± 3	11 ± 2
4	0.12	60	55 ± 2	12 ± 1

[a] General conditions: [^{18}F]$CF_3SO_2NH_4$ (10 – 100 MBq), tyrosine (0.03 mmol), iron(III) nitrate nonahydrate (0.06 mmol) and TBHP (0.12 mmol) in 5% – 8% AcOH in aqueous ammonium formate (300 μL) at 40 ºC for 20 min. RCY measured by taking aliquot of crude for radio-HPLC.

The radiolabelled products were confirmed by overlaying UV spectra of non-radioactive reference compounds with the radio-HPLC spectrum (Figure 3.5). Products were labelled only on the 3- and 2- positions of tyrosine which were separated by HPLC. All other reactions with tyrosine-containing residues displayed similar spectra with tyrosine labelled on the 2- position appearing first as the minor product of the two.

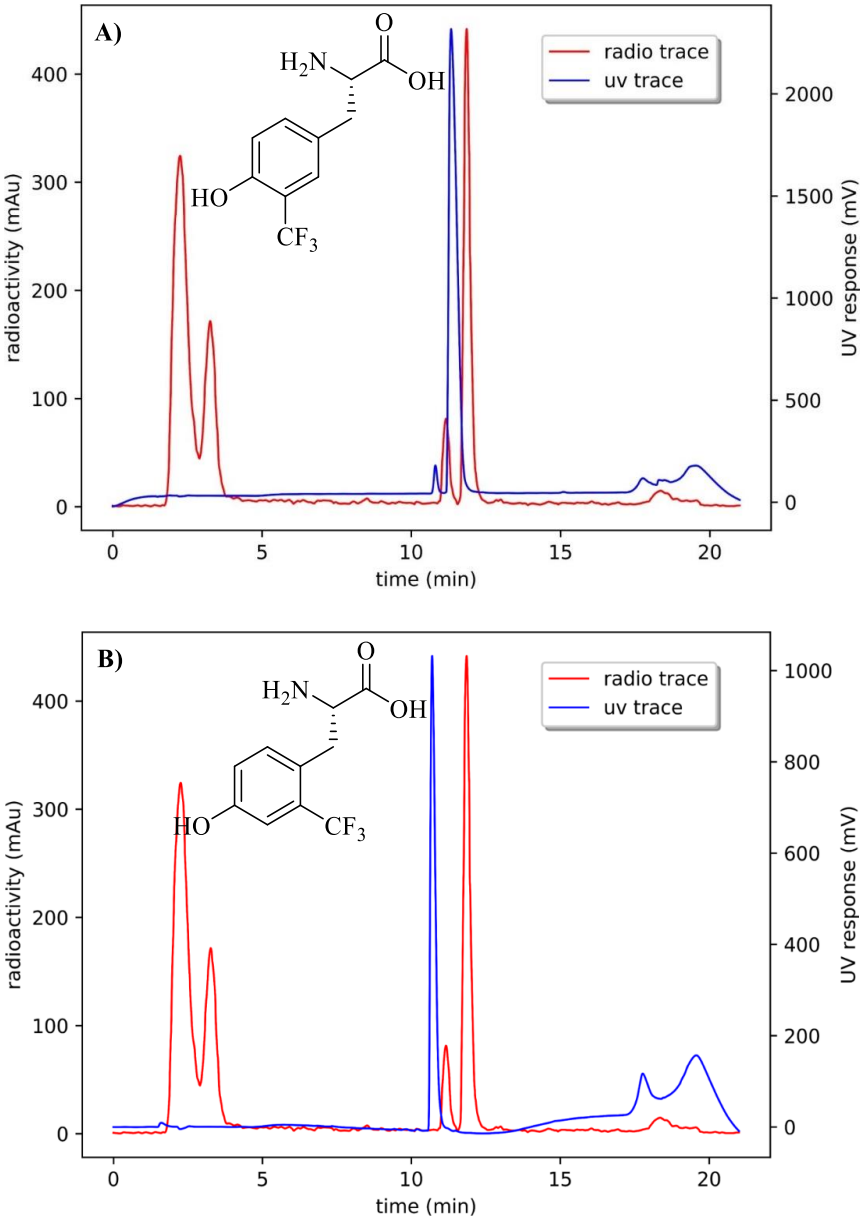
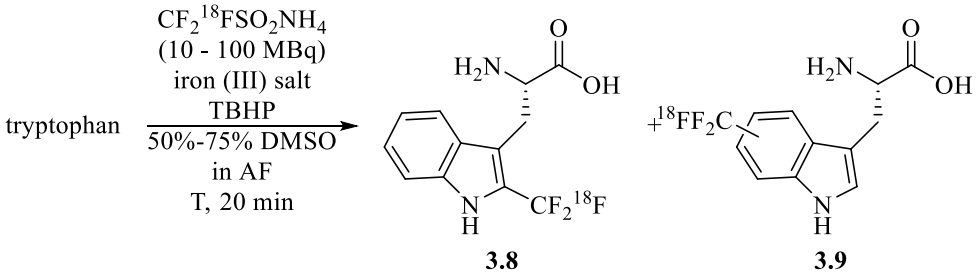


Figure 3.5 Radio-HPLC for reaction between tyrosine and [^{18}F]Langlois reagent overlaid with UV trace of A) Tyr(3-CF_3) B) Tyr(2-CF_3)

Next, conditions were optimised for labelling tryptophan (Table 3.8). As with tyrosine, no product was detected when employing iron(III) acetylacetonate at 40 ºC (Table 3.8, Entry 1). Higher RCYs were obtained with iron(III) chloride or iron(III) nitrate (Table 3.8, Entries 2 & 3), which increased further on heating (Table 3.8, Entry 4).

Table 3.8 Optimisation of reaction conditions for radiolabelling tryptophan using the [^{18}F]Langlois reagent[a]



3.8 **3.9**

Entry	Iron(III) Salt (mmol)	T (ºC)	RCY 3.8 (%, *n* = 2)	RCY 3.9 (%, *n* = 2)
1	$Fe(acac)_3$	40	0	0
2	$FeCl_3$	40	25 ± 11 (*n* = 6)	11 ± 4 (*n* = 6)
3	$Fe(NO_3)_3.9H_2O$	40	22 ± 1	10 ± 1
4[b]	$Fe(NO_3)_3.9H_2O$	60	38 ± 9	13 ± 4

[a] General conditions: [^{18}F]$CF_3SO_2NH_4$ (10 – 100 MBq), tryptophan (0.03 mmol), iron(III) salt (0.06 mmol) and TBHP (0.12 mmol) in 50% – 75% DMSO in aqueous ammonium formate (300 μL) at 40 ºC for 20 min. RCY measured by taking aliquot of crude for radio-HPLC. [b] Reaction solvent 5% – 8% AcOH in aqueous ammonium formate (300 μL)

Major trifluoromethylation of tryptophan occurred at the 2- position with minor products labelled at 4- and 7- positions (Figure 3.6).

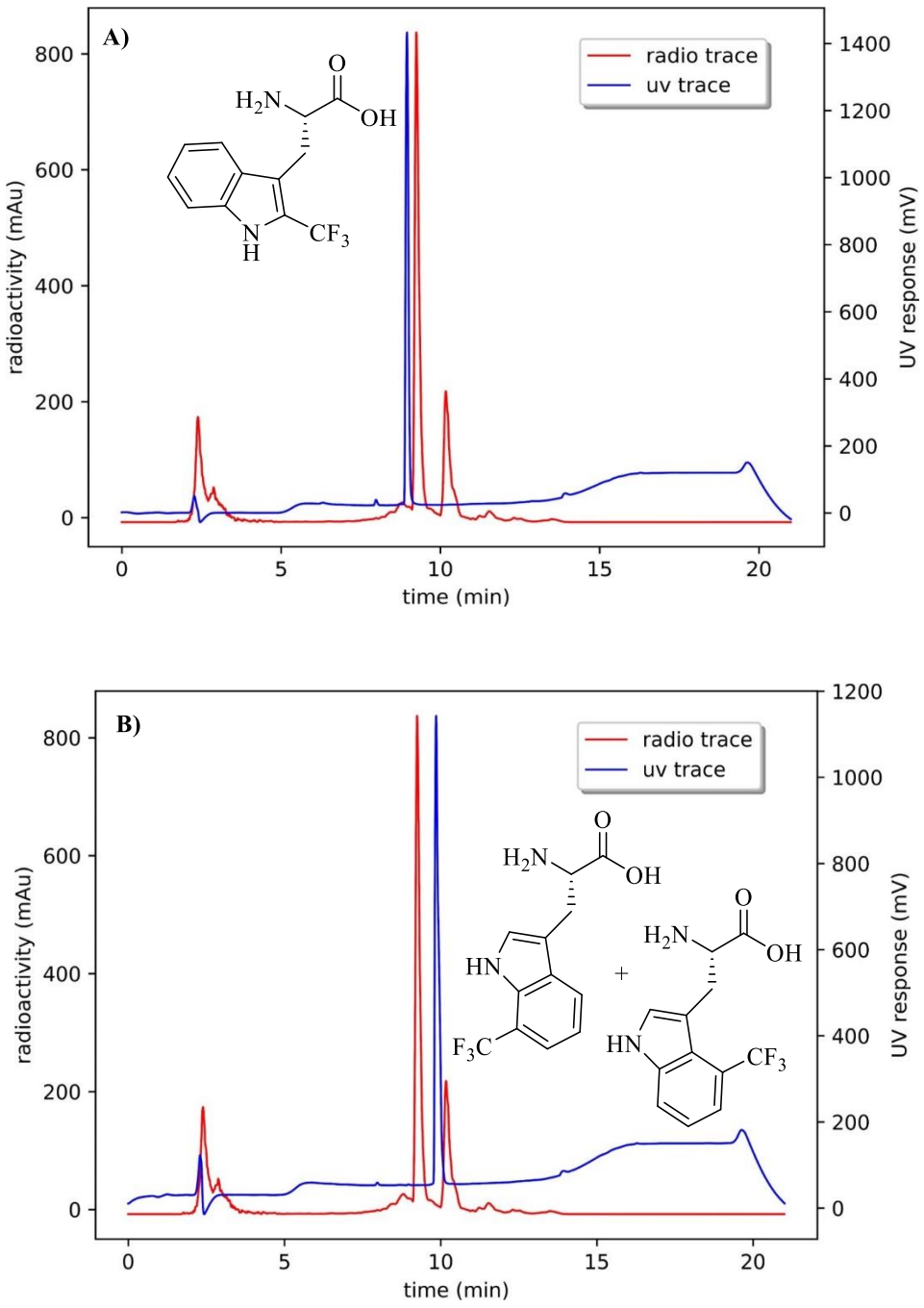


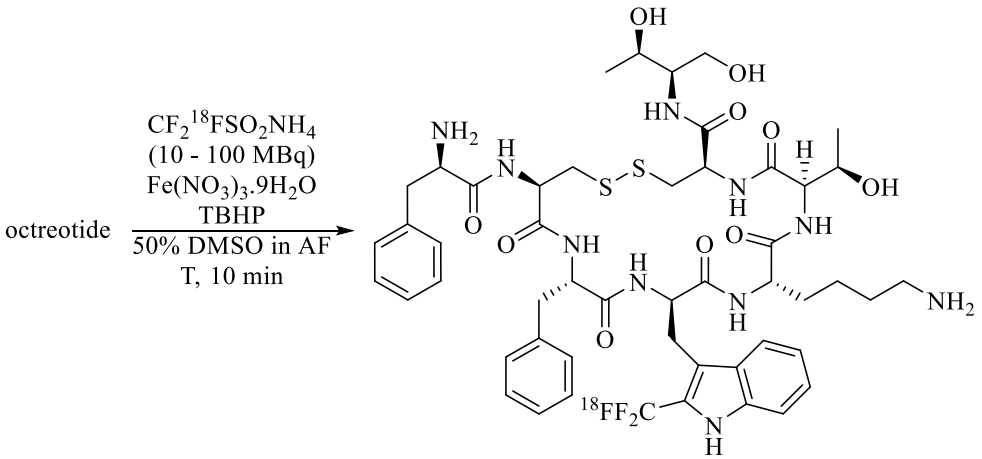
Figure 3.6 Radio-HPLC for reaction between tryptophan and [^{18}F]Langlois reagent overlaid with UV trace of A) Trp(2-CF_3) B) a mixture of Trp(4-CF_3) and Trp(7-CF_3)

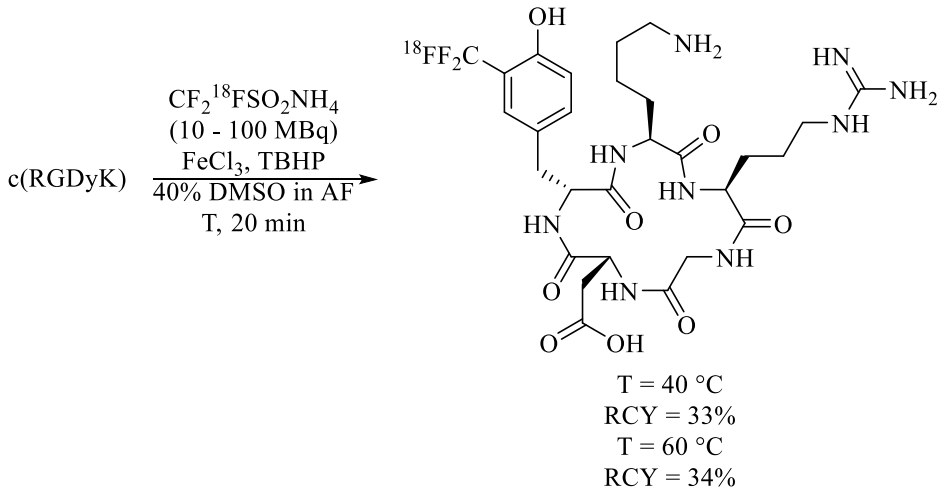
In summary, tyrosine and tryptophan were labelled with the [^{18}F]Langlois reagent forming Tyr(3-$CF_2{}^{18}F$) and Trp(2-$CF_2{}^{18}F$) as the major products. The addition of stoichiometric amounts of iron(III) salts was essential to achieving any reaction. These observations

correlate with reactions employing non-radioactive Langlois reagent. High RCYs were achieved by increasing the reaction temperature to 60 ºC.

3.3 Radiolabelling Peptides using the [^{18}F]Langlois Reagent

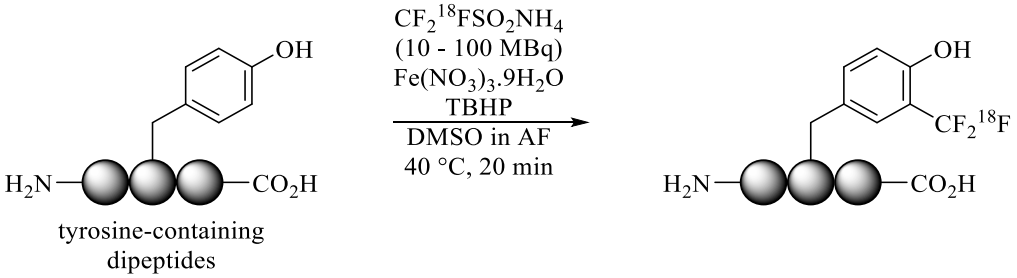
To take radiolabelling one step further from amino acids, peptides containing tyrosine and tryptophan were also examined. Since the thermal stability of peptides is often lower than amino acids, the [^{18}F]Langlois reagent was reacted at 40 ºC and 60 ºC using two model peptides, octreotide and c(RGDyK) (Scheme 3.9). At 40 ºC, octreotide was labelled in 33% RCY, however 0% was obtained at 60 ºC due to decomposition. In contrast, no change in RCY was achieved when reacting c(RGDyK) at 40 ºC or 60 ºC. This demonstrates that, unlike tyrosine or tryptophan, not all peptides are stable or give higher yields above 40 ºC, therefore all subsequent peptide labelling took place at 40 ºC.

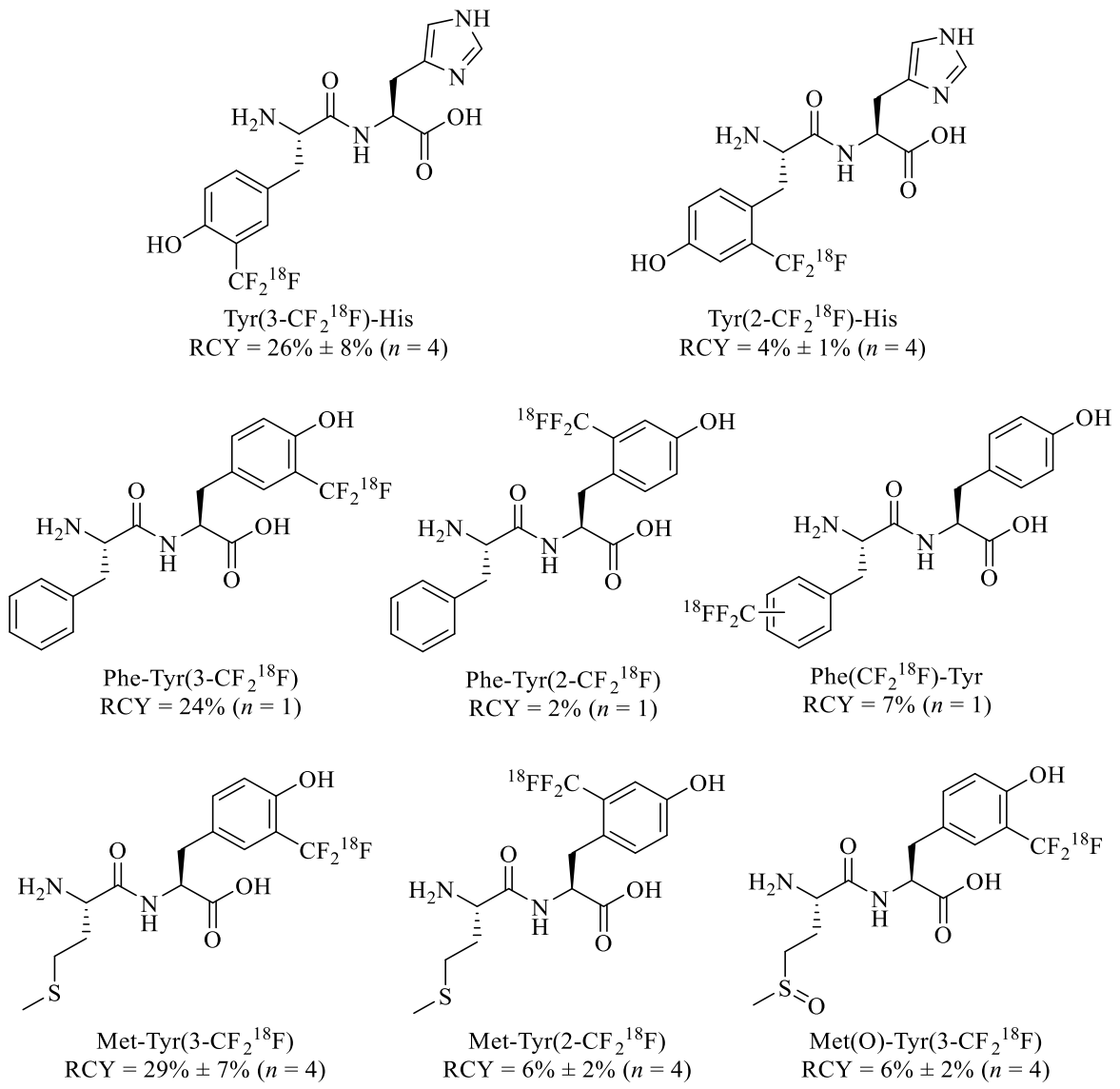




Scheme 3.9 Labelling Tyr- and Trp-containing peptides with the [^{18}F]Langlois reagent at 40 °C or 60 °C

To gain a better understanding of selectivity in radiochemical reactions, dipeptides of Tyr with His, Phe or Met were radiolabelled (Scheme 3.10). Labelling for all three substrates occurred mainly at Tyr with no labelling on His or Met, and minimal amount on Phe, as observed by radio-HPLC (see Chapter 4: Experimental Data for details). Met oxidation was observed in only 6% RCY.

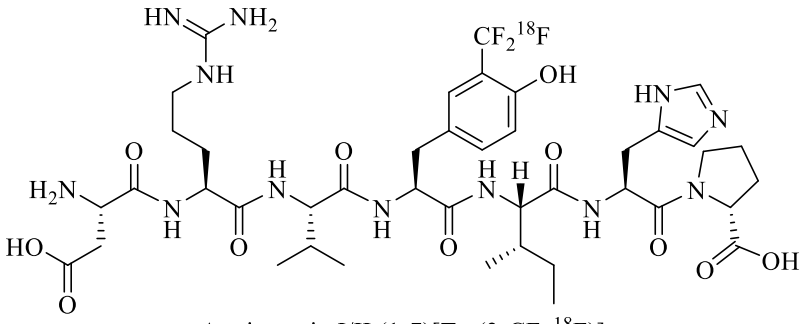




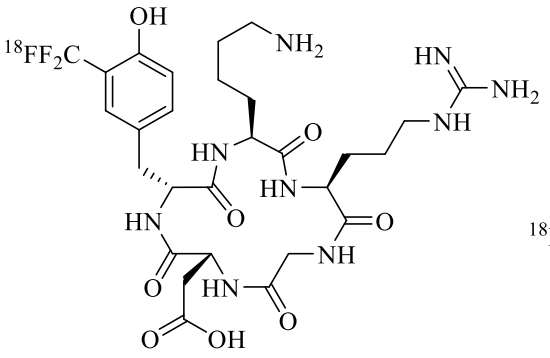
Scheme 3.10 Radiolabelling tyrosine-containing dipeptides with the [^{18}F]Langlois reagent

The scope of substrates was extended to longer and more biologically relevant peptides (Scheme 3.11). Angiotensin I/II fragment 1 – 7 and c(RGDyK) were labelled at tyrosine in 16% and 33% RCY respectively and identified by radio-HPLC using UV overlays of the isolated references (see Chapter 4: Experimental Data for details). The 51 amino acid long human recombinant insulin was successfully labelled in 34% RCY. This constitutes the largest unmodified peptide to date that has been labelled directly with fluorine-18.

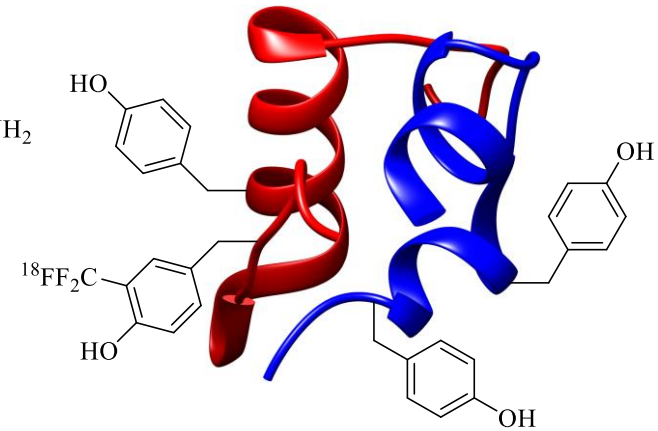




Angiotensin I/II (1-7)[Tyr(3-$CF_2{}^{18}F$)]
RCY = 16% ± 4% (*n* = 3)



c(RGDyK)[Tyr(3-$CF_2{}^{18}F$)]
RCY = 33% ± 1% (*n* = 3)

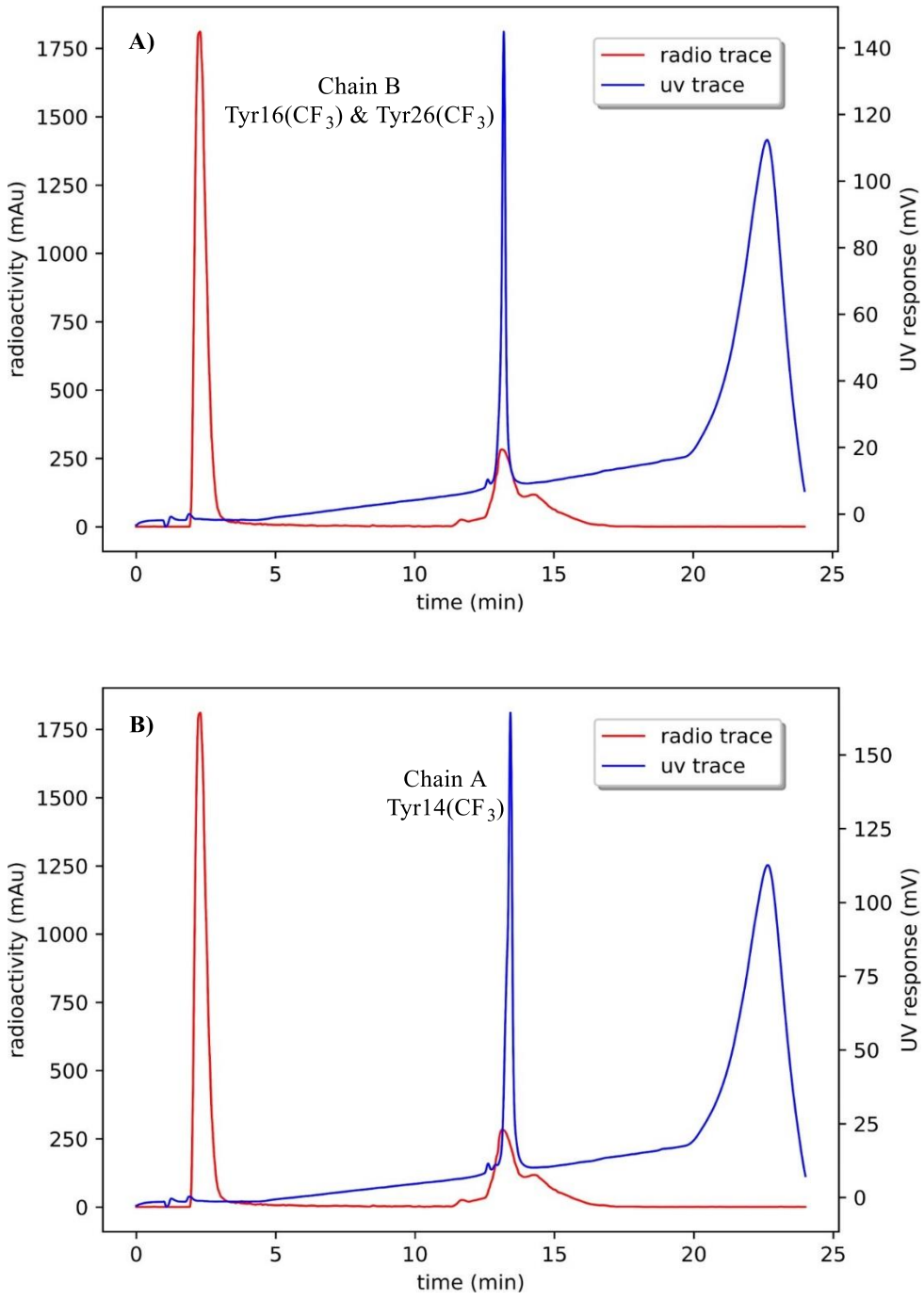


Recombinant Human Insulin[Tyr(3-$CF_2{}^{18}F$)]
RCY = 34% ± 9% (*n* = 7)

Scheme 3.11 Radiolabelling tyrosine-containing peptides with the [^{18}F]Langlois reagent

Identifying the labelling sites on insulin was attempted by overlaying the radio-HPLC with the UV spectra of references trifluoromethylated at each of the four tyrosine sites (Figure 3.7). Three of these references were synthesised and verified by C. W. Kee using a reported procedure.[5] Since UV peaks of all four references overlapped with the peak observed by

radio-HPLC, we were unable to conclude that modification occurred at one specific tyrosine site, even though this was observed in the analogous reaction with the non-radioactive Langlois reagent.



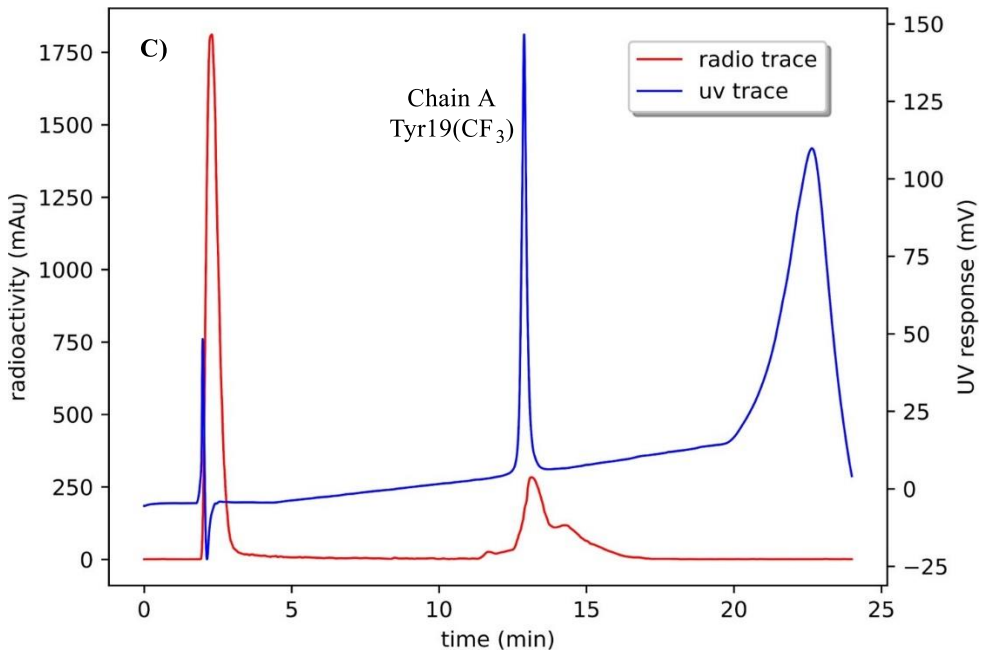
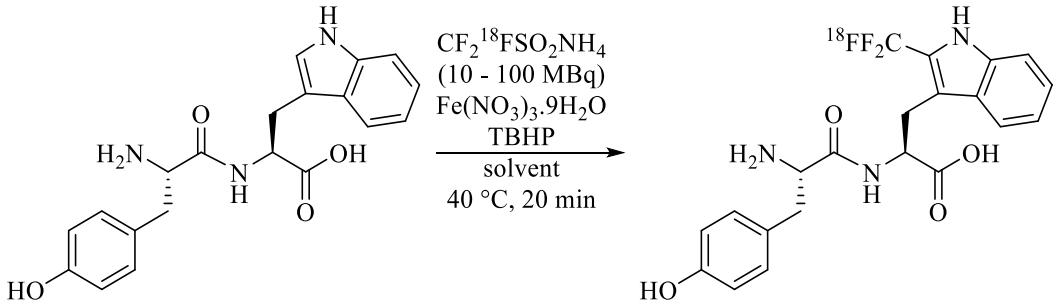


Figure 3.7 Radio-HPLC for reaction between insulin and [^{18}F]Langlois reagent overlaid with UV trace of A) a mixture of chain B insulin[Tyr16(CF_3)] and insulin[Tyr26(CF_3)] B) chain A insulin[Tyr14(CF_3)] C) chain A insulin[Tyr19(CF_3)]

Prior to screening tryptophan-containing substrates, a reaction between Tyr-Trp and the [^{18}F]Langlois reagent was carried out in 100% aqueous ammonium formate. The radio-HPLC and UV spectra of the crude reaction showed complete decomposition into a variety of products suggestive of polymerisation (Figure 3.8, A). This decomposition was not observed when employing DMSO, therefore this solvent system was chosen for all further reactions with tryptophan-containing substrates (Figure 3.8, B).



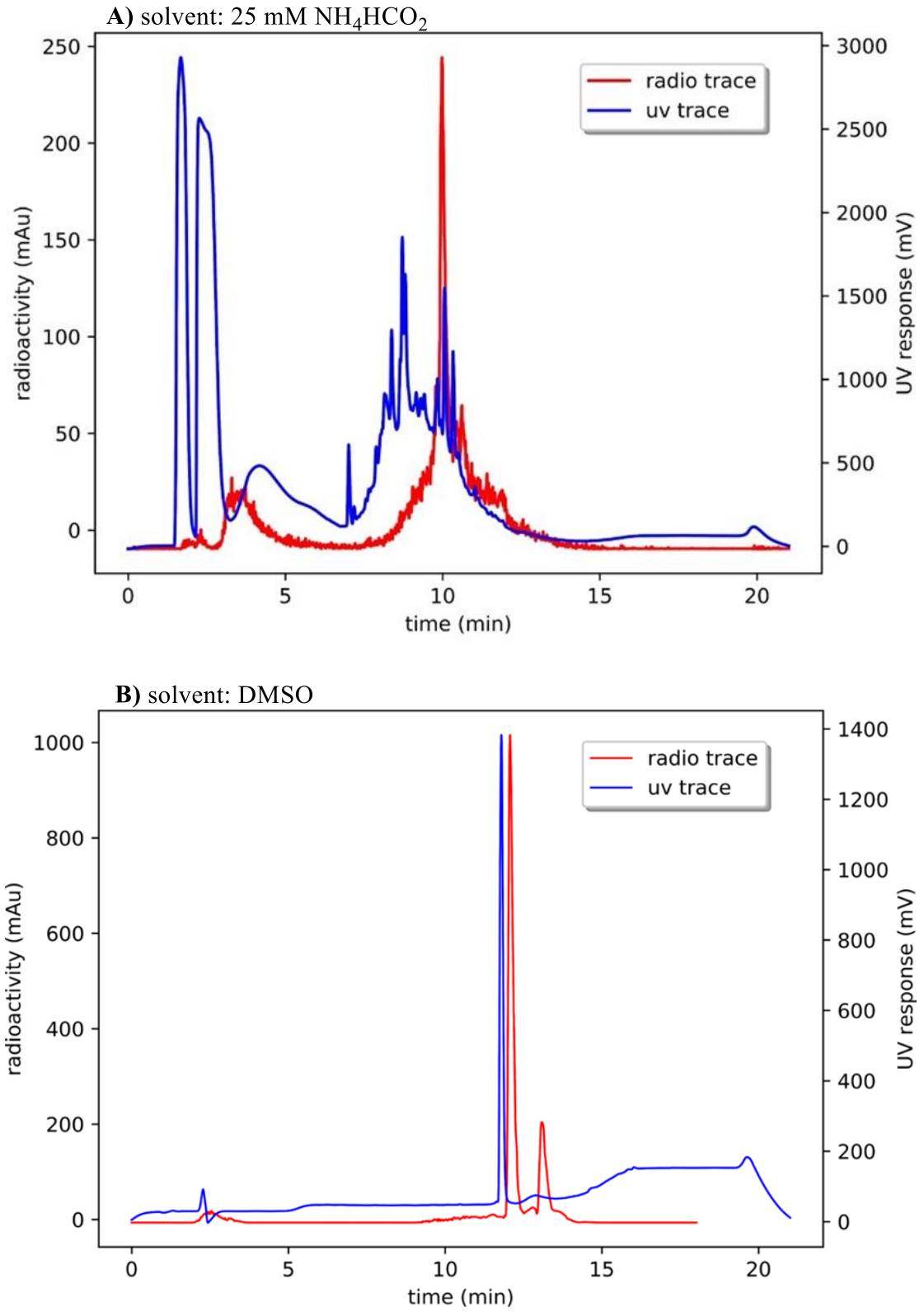
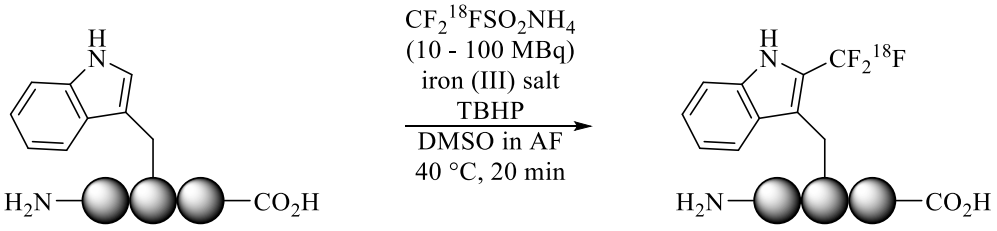
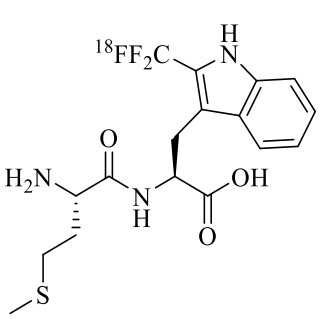


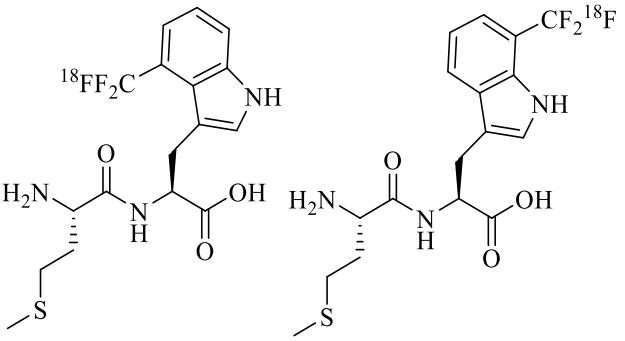
Figure 3.8 HPLC spectra for reaction of TyrTrp with [^{18}F]Langlois reagent in A) aqueous ammonium formate B) DMSO

Dipeptides of Trp with Met, His, Phe or Tyr were examined (Scheme 3.12). Labelling Met-Trp, His-Trp or Phe-Trp was observed only on Trp with labelling on the 2- position as the major product, and on the 4- and 7- positions as the minor products. Met was not oxidised in any of the products. Trifluoromethylation occurred exclusively on Trp for both Trp-Tyr and Tyr-Trp suggesting Trp is the most reactive amino acid residue under these radiochemical conditions.

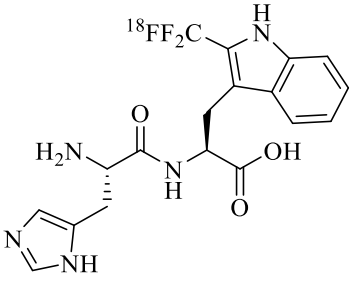




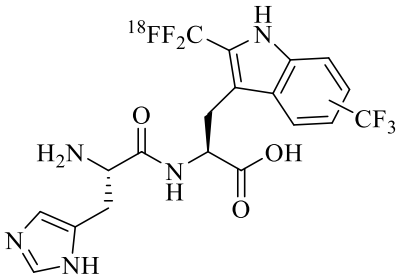
Met-Trp(2-$CF_2{}^{18}F$)
RCY = 39% ± 6% (*n* = 3)

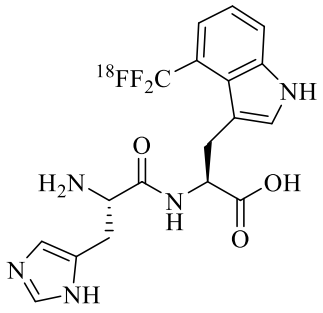
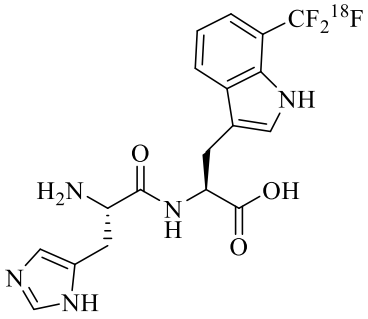


Met-Trp(4-$CF_2{}^{18}F$) & Met-Trp(7-$CF_2{}^{18}F$)
RCY = 14% ± 1% (*n* = 3)

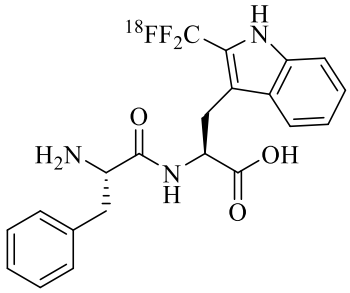


His-Trp(2-$CF_2{}^{18}F$)
RCY = 56% ± 4% (*n* = 3)

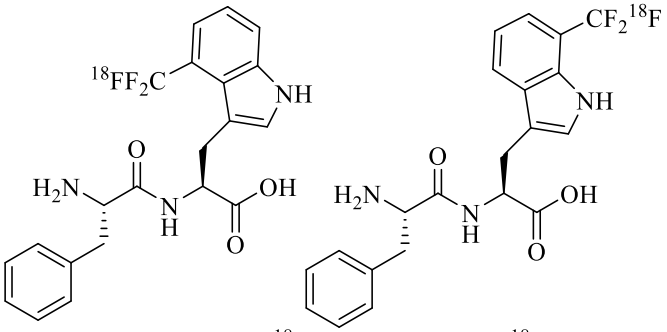


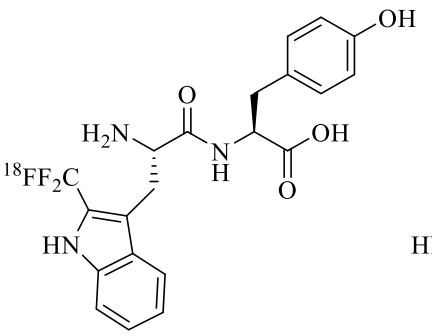
His-Trp(4-$CF_2{}^{18}F$), His-Trp(7-$CF_2{}^{18}F$) & His-Trp($CF_2{}^{18}F$)(CF_3)
RCY = 16% ± 1% (*n* = 3)



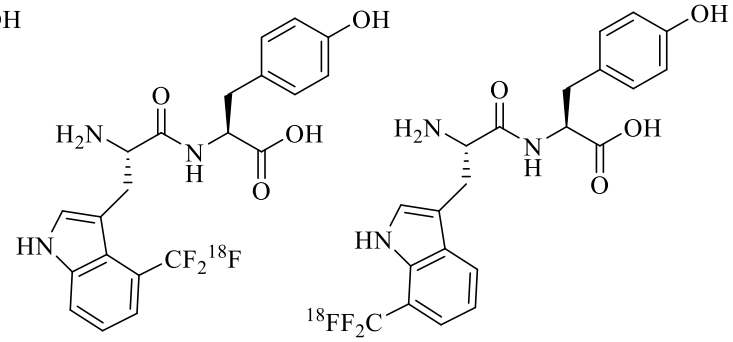
Phe-Trp(2-$CF_2{}^{18}F$)
RCY = 43% ± 10% (*n* = 3)



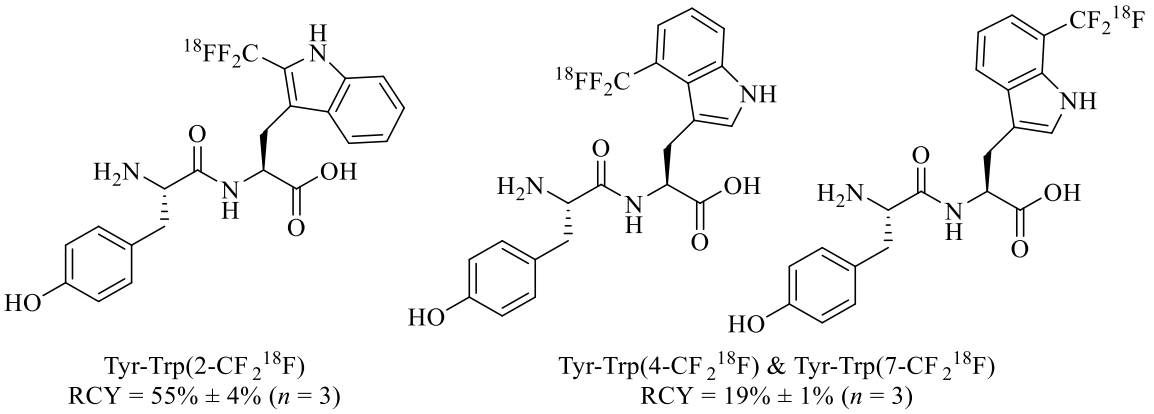
Phe-Trp(4-$CF_2{}^{18}F$) & Phe-Trp(7-$CF_2{}^{18}F$)
RCY = 16% ± 1% (*n* = 3)



Trp(2-$CF_2{}^{18}F$)-Tyr
RCY = 24% ± 3% (*n* = 2)

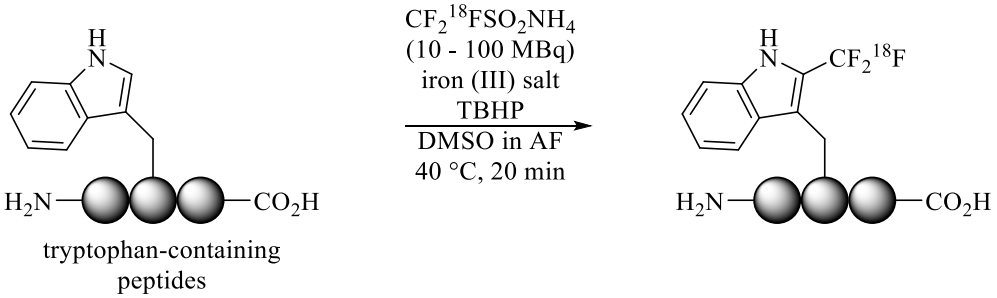


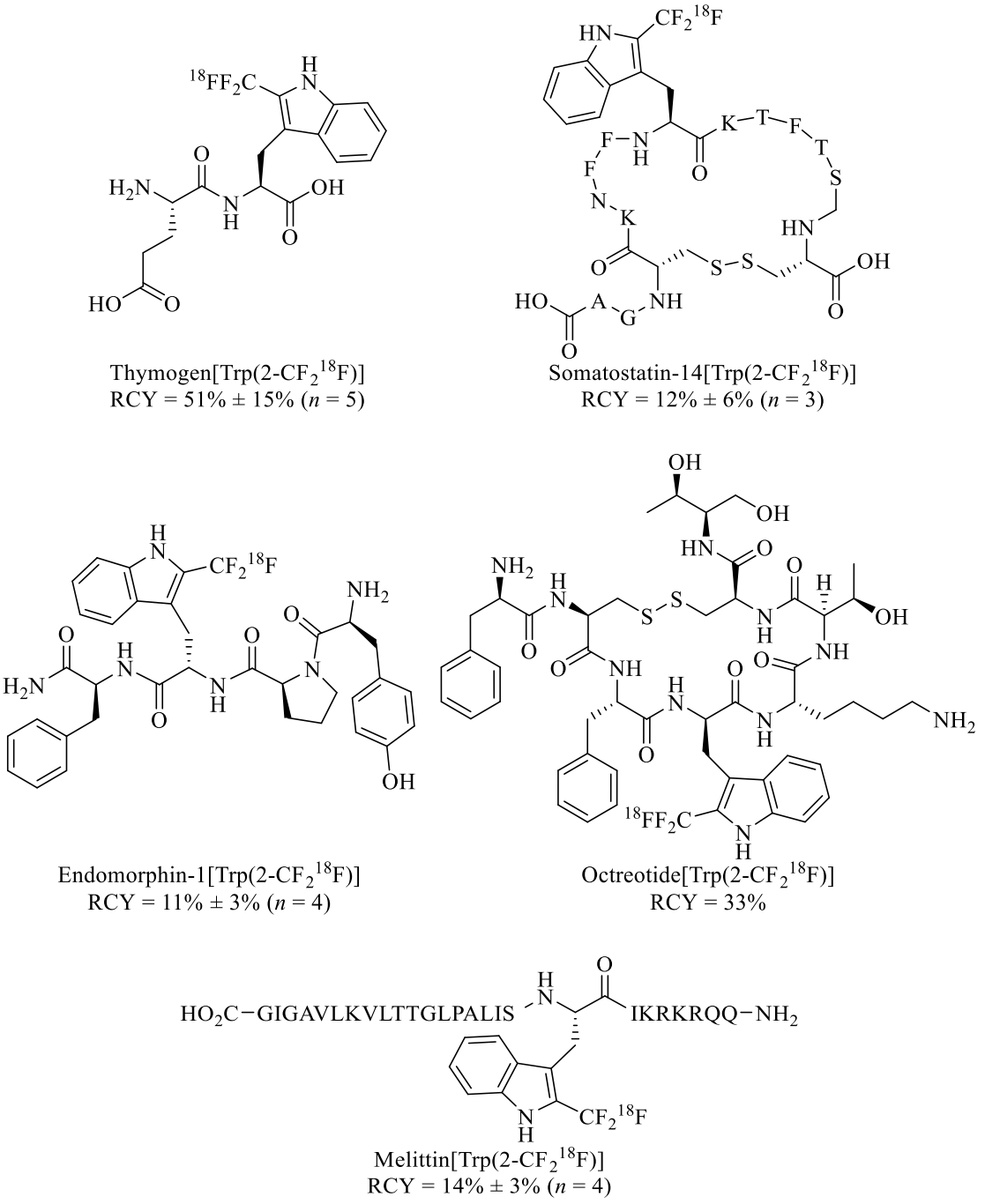
Trp(4-$CF_2{}^{18}F$)-Tyr & Trp(7-$CF_2{}^{18}F$)-Tyr
RCY = 19% ± 1% (*n* = 2)



Scheme 3.12 Radiolabelling tryptophan-containing dipeptides with the [^{18}F]Langlois reagent

Labelling studies were extended further to assess the potential for labelling longer and more biologically relevant peptides containing tryptophan (Scheme 3.13). The immunomodulatory dipeptide thymogen[18] and the cyclic hormone somatostatin-14[19] were labelled in 51% and 12% RCY respectively. Endomorphin-1 is associated with Alzeimer's disease[20] and melittin is a venom peptide,[21] both of which were labelled in 11% RCY and 14% RCY. The octapeptide mimic of somatostatin, octreotide,[17] was labelled in 33% RCY. References for thymogen, somatostatin-14, endomorphin-1 and melittin were synthesised and verified by C. W. Kee.





Scheme 3.13 Radiolabelling tryptophan-containing peptides with the [^{18}F]Langlois reagent

In conclusion, tyrosine and tryptophan residues in a number of dipeptides and biologically relevant peptides were successfully radiolabelled using the [^{18}F]Langlois reagent. Selectivity of labelling was mainly at the 3- position of Tyr and 2- position of Trp residues. Trp proved to be the most reactive residue followed by Tyr, with little or no reactivity at His, Phe and

Met residues. We have demonstrated that the [^{18}F]Langlois reagent allows facile, direct trifluoromethylation of unprotected peptides, including the 51 amino acid long insulin. This is the largest unmodified peptide to date that has been labelled directly with fluorine-18.

3.4 Automated Radiolabelling of Peptides using the [^{18}F]Langlois Reagent

To demonstrate real-world applicability of labelling peptides with the [^{18}F]Langlois reagent, an automated setup was developed for producing labelled peptides that can be used in *in vitro* and *in vivo* PET imaging studies.

After isolating the [^{18}F]Langlois reagent using automated radiosynthesis (see Chapter 4: Experimental Data for details), the reagent was dissolved in 5 – 10 mL of aqueous HPLC eluent. In order to carry out subsequent reactions with peptides, the volume had to be reduced to 300 μL. To do this, various methods of reformulation were assessed.

Initial attempts to reduce the volume of the [^{18}F]Langlois reagent solution involved evaporating the HPLC eluent in aliquots at 150 ºC but at this temperature the reagent evaporated with the eluent. Decreasing the temperature to 120 ºC prevented any appreciable losses of activity, but the extended drying time of 90 minutes was unacceptable for a radiosynthesis using fluorine-18.

To minimise drying time, reformulation into a more volatile solvent was investigated. The [^{18}F]Langlois reagent in HPLC eluent was diluted in 2% formic acid before passing the solution through a WAX cartridge by helium pressure (Figure 3.9). This trapped the [^{18}F]Langlois reagent and removed the HPLC eluent. The [^{18}F]Langlois reagent was eluted into reaction vial 2 (R2) using basic ethanol or acetonitrile solutions, added *via* pump 3 (P3).

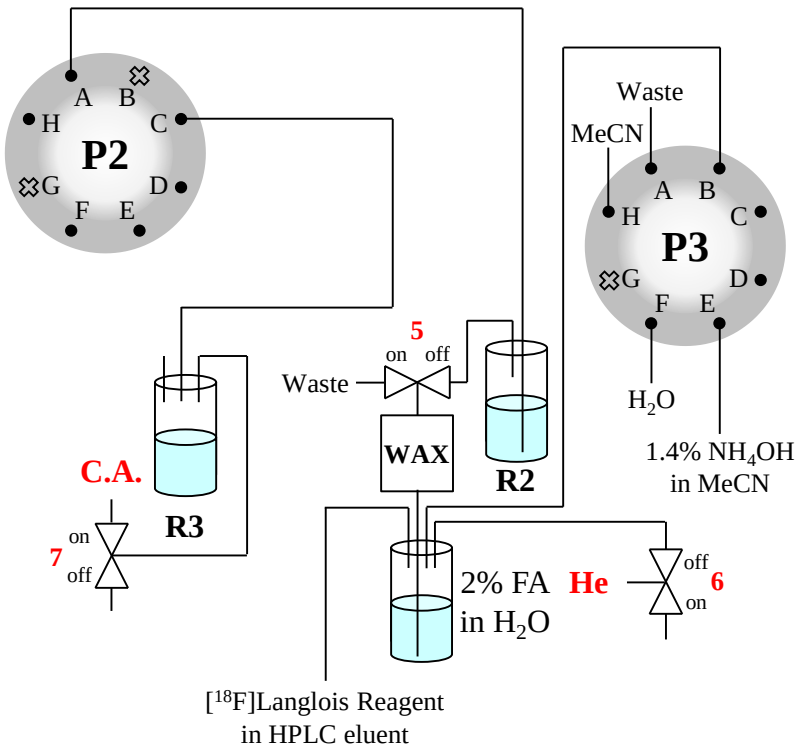


Figure 3.9 Automation setup for reformulating and drying the [^{18}F]Langlois reagent

In order to reduce the drying time, the volume of the basic elution solution was minimised. This was done by adding varying volumes of eluent and measuring the remaining activity using a radiodetector attached to the WAX cartridge. Eluting with 1 mL of 1.4% ammonium hydroxide in acetonitrile gave an elution efficiency of 45%, which increased to 97% when eluting with 2 mL.

To ensure that the [^{18}F]Langlois reagent remained at the bottom of the vial R3 during the drying process, the solution in R2 was added to R3 in 200 µL aliquots using P2. R3 was set at 90 ºC with an air flow to expedite drying. Additionally, the solution of [^{18}F]Langlois reagent in R2 was heated to 70 ºC before taking aliquots for drying, reducing the total drying time to 15 minutes. This is the first reported effective drying procedure carried out using a fully automated set up.

In order to show that the automated setup could be used to label biologically relevant peptides, c(RGDyK) and octreotide were labelled. These two peptides were chosen as examples of peptides containing tyrosine or tryptophan residues. The complete automated setup for synthesis of [^{18}F]Langlois reagent and peptide labelling, including their purification and reformulation, is illustrated (Figure 3.10).

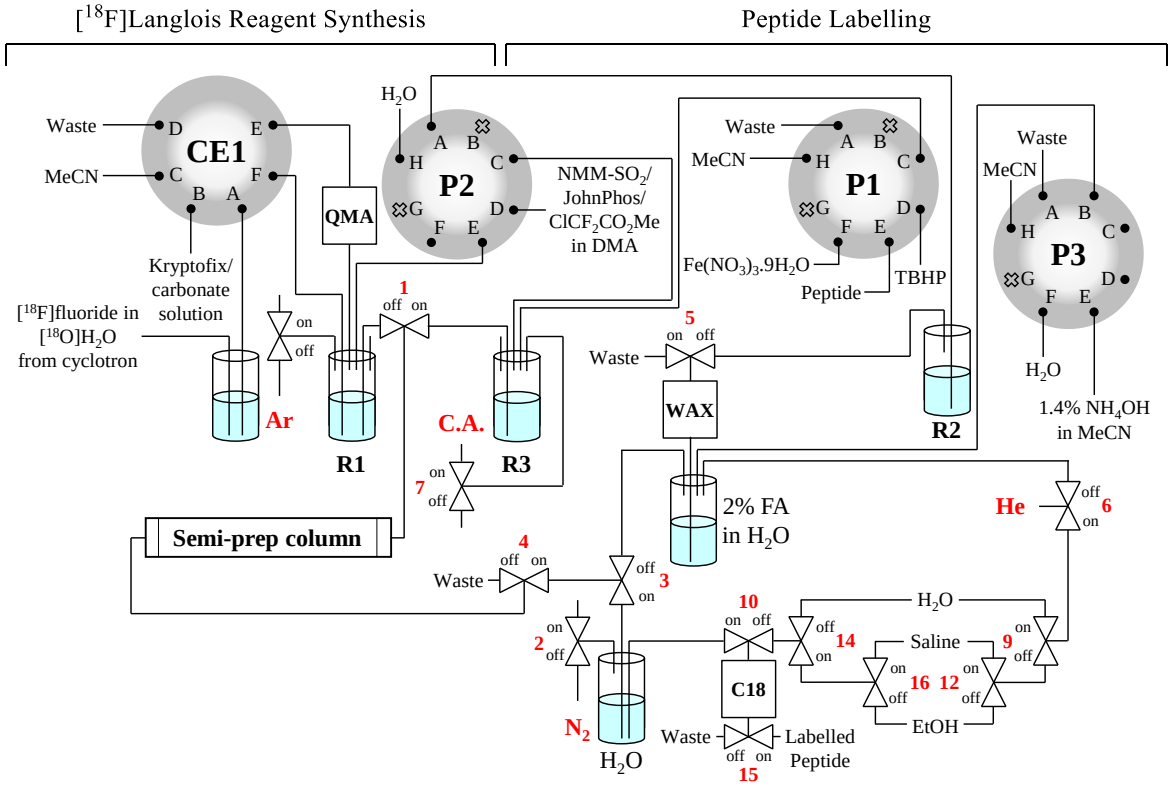


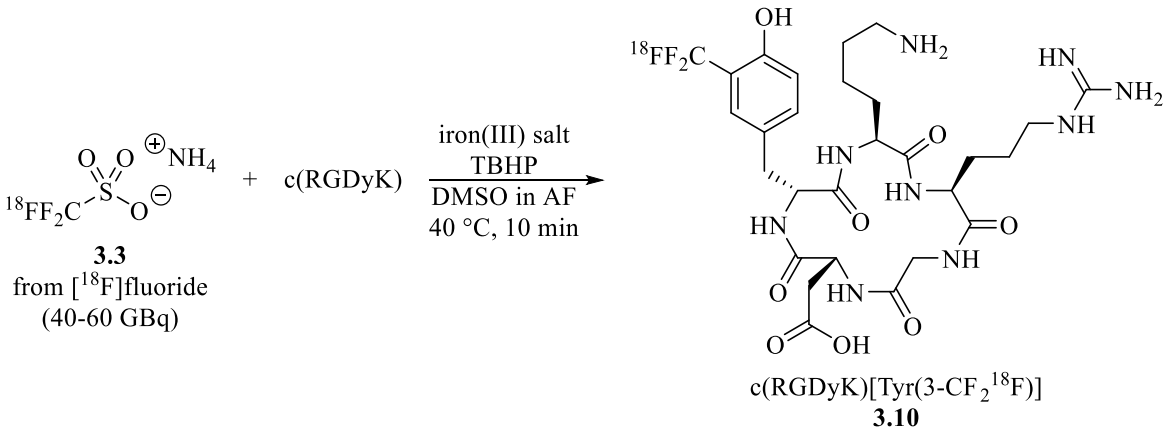
Figure 3.10 Complete automation setup for labelling peptides with the [^{18}F]Langlois reagent

After drying the [^{18}F]Langlois reagent, the peptide and iron(III) nitrate in aqueous ammonium formate were introduced into R3 using P1, followed by *tert*-butyl hydroperoxide in DMSO. In order to mix the two solutions together, air was bubbled through the solution before heating to 40 ºC for 10 minutes.

At the end of the reaction, the labelled peptide was isolated by semi-preparative HPLC and collected in water. The product was trapped on a C18 cartridge to remove the HPLC eluent and then eluted with ethanol or acetonitrile for collection outside the hot cell.

c(RGDyK) was labelled starting from [^{18}F]fluoride generated in a cyclotron using a 55 μA beam for 45 minutes (Table 3.9). Reaction between the peptide, [^{18}F]Langlois reagent, *tert*-butyl hydroperoxide and iron(III) chloride afforded 3.7 MBq of final labelled product (Table 3.9, Entry 1).

Table 3.9 Automated radiolabelling of tyrosine-containing peptide c(RGDyK)[a]

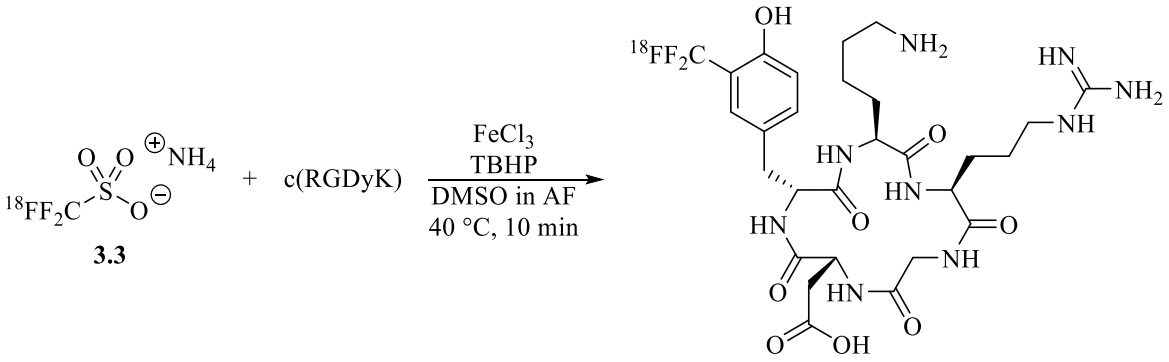


Entry	Cyclotron Beam	Reformulation Cartridge	Iron(III) Salt	Final Dose 3.10 (MBq)	Molar Activity 3.10 (GBq μmol^{-1})	Synthesis Time (min)
1	55 μA 45 min	StrataX	$FeCl_3$	3.7	-	128
2	55 μA 45 min	^{t}C18 SepPak	$FeCl_3$	49.9	0.70	118
3	55 μA 45 min	C18 Classic SepPak Plus	$Fe(NO_3)_3.9H_2O$	99.7	0.76	128
4	55 μA 55 min	C18 Classic SepPak Plus	$Fe(NO_3)_3.9H_2O$	296	0.68	144

[a] General conditions: [^{18}F]$CF_3SO_2NH_4$ from [^{18}F]fluoride (40 – 60 GBq), c(RGDyK) (0.04 mmol), iron(III) salt (0.027 mmol) and TBHP (0.043 mmol) in 50% DMSO in aqueous ammonium formate (150 μL) at 40 ºC for 10 min.

A detector attached to the C18 cartridge used for final reformulation revealed that the product was not retained on a StrataX polymeric cartridge. Retention was improved using a ^{t}C18 SepPak cartridge, giving a final dose of 49.9 MBq (Table 3.9, Entry 2). By using iron(III) nitrate and a C18 Classic SepPak Plus, the final dose was further increased to 99.7 MBq (Table 3.9, Entry 3). Increasing the beam time to 55 minutes afforded a final dose of 296 MBq and a molar activity of 0.68 GBq μmol^{-1} (Table 3.9, Entry 4).

Table 3.10 Activity measurements for reaction between c(RGDyK) and the [^{18}F]Langlois reagent using $FeCl_3$ as the iron(III) salt[a]



3.3

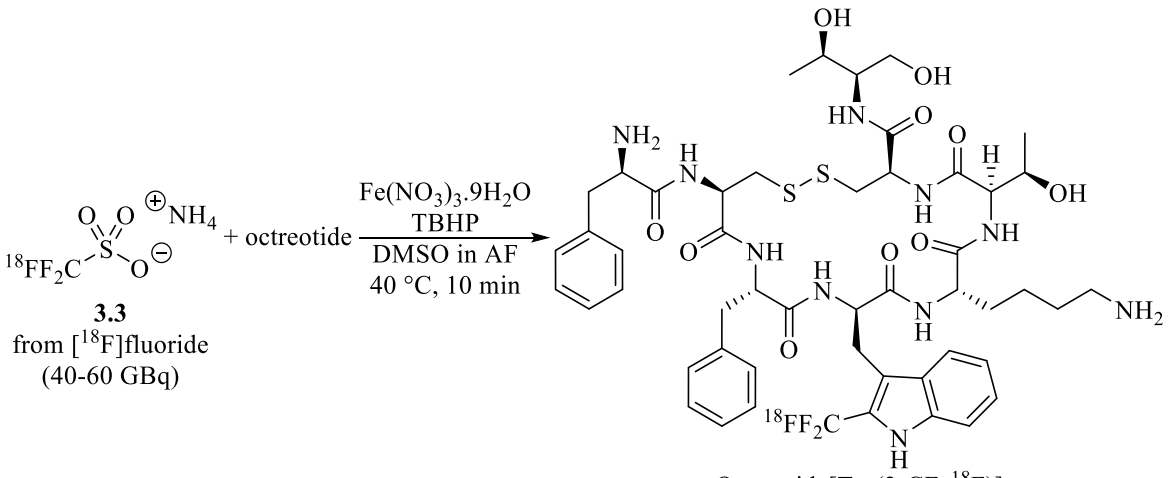
c(RGDyK)[Tyr(3-$CF_2{}^{18}F$)]
3.10

Entry	Procedure Step	Activity (MBq)[b]
1	Reaction on	103
2	Reaction off	77
3	Left in vial after transfer to HPLC loop	38
4	Semi-prep isolation	3.2

[a] General conditions: [^{18}F]$CF_3SO_2NH_4$ from [^{18}F]fluoride, c(RGDyK) (0.04 mmol), iron(III) chloride (0.027 mmol) and TBHP (0.043 mmol) in 50% DMSO in aqueous ammonium formate (150 μL) at 40 ºC for 10 min.
[b] Decay corrected to start of synthesis using [^{18}F]$CF_3SO_2NH_4$.

To investigate why the final dose doubled when employing iron(III) nitrate instead of iron(III) chloride, activity measurements were taken at various stages of the reaction and purification (Table 3.10). Approximately 30% activity was lost during the reaction as volatile side products (Table 3.10, Entries 1 & 2), and only half the activity was transferred to the HPLC loop (Table 3.10, Entries 2 & 3). Washing the vial with DMSO, 10% MeCN in water, or 0.1% TFA in MeCN could not dissolve the radioactive side products, suggesting they are attached to the glass or are insoluble decomposition products. This was not observed when iron(III) nitrate was employed.

Table 3.11 Automated radiolabelling of tryptophan-containing peptide octreotide[a]



3.3
from [^{18}F]fluoride
(40-60 GBq)

Octreotide[Trp(2-$CF_2{}^{18}F$)]
3.11

Entry	Cyclotron Beam	Final Dose 3.11 (MBq)	Molar Activity 3.11 (GBq μmol^{-1})	Synthesis Time (min)
1	55 μA 40 min	36.2	0.25	126
2	55 μA 45 min	69.0	0.37	146
3	55 μA 45 min	68.6	0.22	128

[a] General conditions: [^{18}F]$CF_3SO_2NH_4$ from [^{18}F]fluoride (40 – 60 GBq), octreotide acetate (0.0028 mmol), iron(III) nitrate nonahydrate (0.011 mmol) and TBHP (0.022 mmol) in 50% DMSO in aqueous ammonium formate (150 μL) at 40 ºC for 10 min.

The peptide octreotide was labelled with a final dose of 36.2 MBq starting from [^{18}F]fluoride generated using a cyclotron beam of 55 μA for 40 minutes (Table 3.11, Entry 1). The final dose increased to 68.8 ± 0.3 MBq (n = 2) when the beam time was increased to 45 minutes (Table 3.11, Entries 2 & 3). The molar activity was 0.30 ± 0.1 GBq μmol^{-1} and total synthesis time was 137 ± 13 minutes.

In summary, a complete automated synthesis was developed for formation and reaction of the [^{18}F]Langlois reagent to label two biologically relevant peptides, c(RGDyK) containing a tyrosine residue and octreotide containing a tryptophan residue. This involved optimising an automated method for efficient drying of the [^{18}F]Langlois reagent, labelling the peptide, and reformulating the isolated product ready for *in vivo* injections.

3.5 *In Vivo* study for Octreotide Radiolabelled with the [^{18}F]Langlois Reagent

Octreotide is a mimic of natural somatostatin, a growth hormone-inhibiting hormone involved in regulating the endocrine system.[22] The somatostatin receptor is naturally expressed mainly in the hypothalamus, pancreas and gastrointestinal pathway and octreotide was a pioneering discovery in providing therapy for endocrine disorders such as acromegaly and related tumours. Specifically, octreotide shows similar IC_{50} values as somatostatin for sst_2, the subtype of somatostatin most present in endocrine tumours. A number of radiolabelled analogues of octreotide have since been developed to provide diagnostic imaging of these tumours.[23]

An initial assessment was made to demonstrate the use of this method for labelling peptides with the [^{18}F]Langlois reagent in biological studies using octreotide as a model substrate.

This is because its biological relevance, pharmacokinetics and binding activity are well characterised in the literature, facilitating comparisons.

To assess the effect of the trifluoromethyl group on the activity of octreotide, an *in vitro* competition binding assay was carried out. [^{125}I]DOTA-TATE binding to somatostatin receptors in AR42J cells was measured in the presence of varying concentrations of octreotide or octreotide[Trp(2-CF_3)]. The percentage of [^{125}I]DOTA-TATE bound to AR42J decreased with increasing concentrations of the two octreotide compounds, giving IC_{50} values of 12nM and 140 nM for octreotide and octreotide[Trp(2-CF_3)] respectively (Figure 3.11). The cells, [^{125}I]DOTA-TATE radiolabelling and binding assays were prepared and carried out by Juliette Chupin, Roxana Kashani, Jane K. Sosabowski and Sven Macholl at the Centre for Molecular Oncology, Queen Mary, University of London.

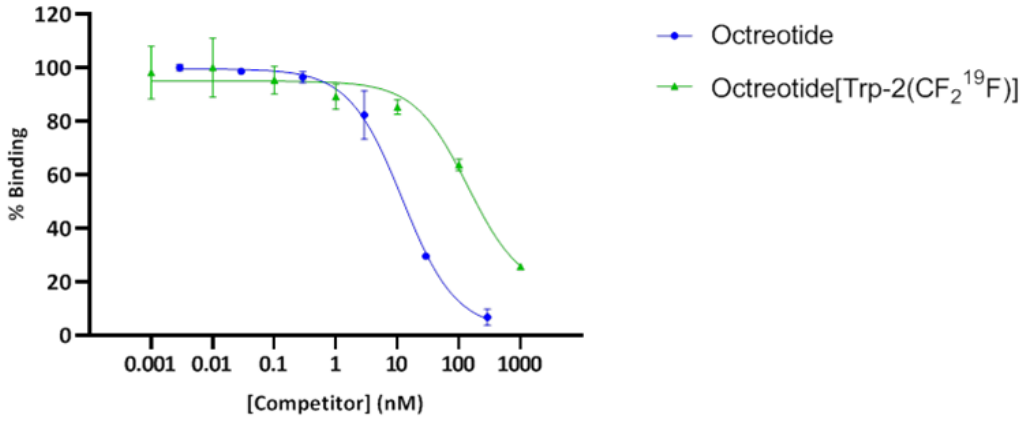


Figure 3.11 *In vitro* competition binding assay in AR42J cells for octreotide and octreotide[Trp(2-CF_3)] using [^{125}I]DOTA-TATE

Trifluoromethylation at Trp on the 2-position of octreotide affected its binding negatively by a factor of approximately ten times. This shows that trifluoromethylation at the

pharmacophore site of octreotide has a hindering effect on its binding to somatostatin receptors in AR42J cells, however binding is not inhibited completely.[24]

Following this, an *in vivo* dynamic PET imaging study was carried out on anaesthetised naïve Sprague-Dawley rats using octreotide[Trp(2-CF_3)] synthesised using the automated procedure.

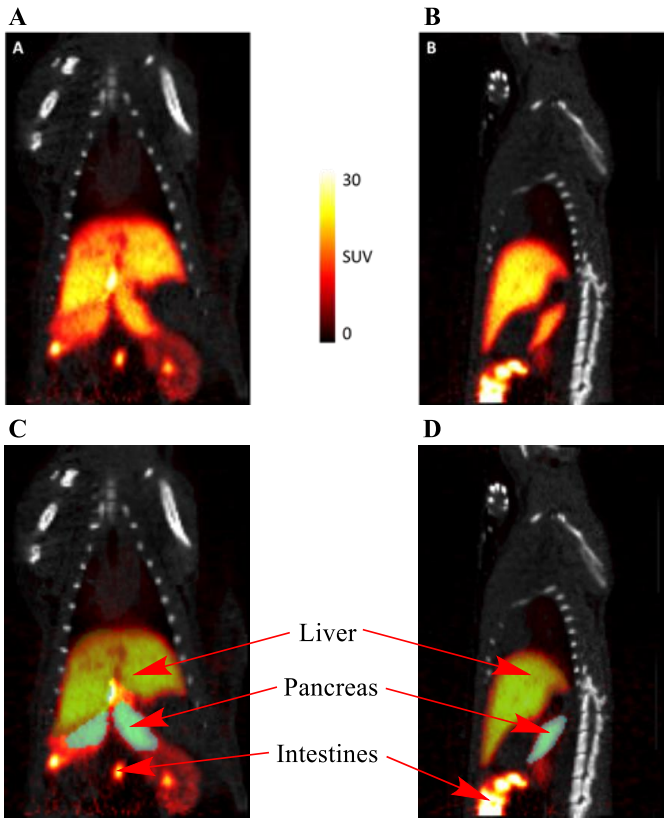


Figure 3.12 Summed (0 – 60 minutes) PET/CT images of Sprague Dawley rat after iv injection of octreotide[Trp-2($CF_2{}^{18}F$)]. A) Transverse view; B) Sagittal view; C) & D) Transverse view & Sagittal view with anatomical atlas overlay for liver and pancreas

After injecting 9.5 MBq of dose with a molar activity of 0.25 MBq μmol^{-1}, its quick distribution across the body was observed. Over the course of 60 minutes, coherent signals across the liver, pancreas, and intestines were seen as the dose accumulated in these organs. A PET image was reconstructed to illustrate the Standardised Uptake Values (SUVs)

summed over the course of the 60 minute period (Figure 3.12). The liver and pancreas were distinguished by overlay using an anatomical atlas.

The animals for this study were supplied and handled in collaboration with Sharon Ashworth, Invicro London. A plot of average SUVs for the liver and pancreas summed over time showed a constant increase after initial injection and distribution (Figure 3.13).

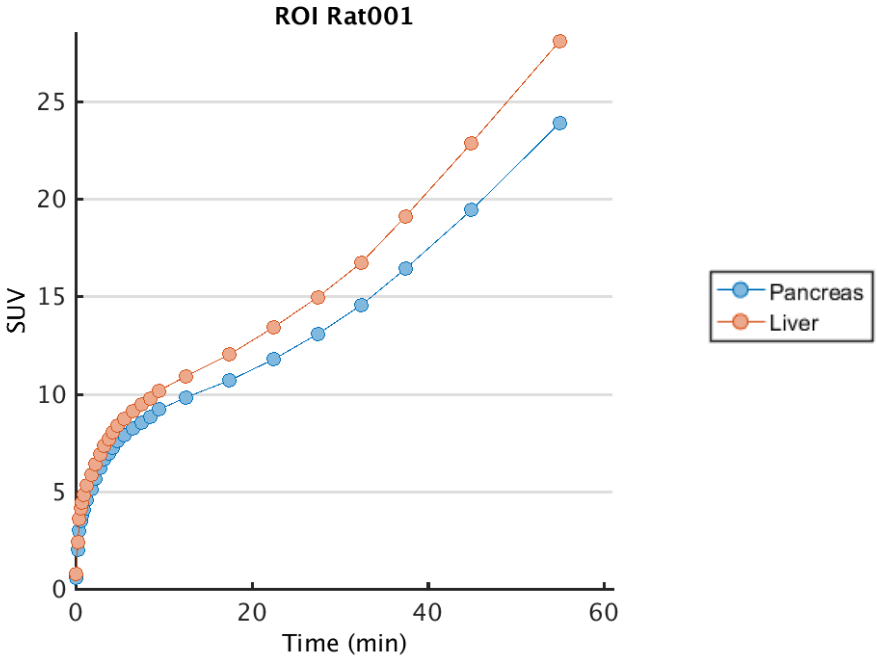


Figure 3.13 Average SUVs for the liver and pancreas summed over 60 min

Although a considerable amount of activity was still present in the liver and pancreas 60 minutes after injection, *ex vivo* biodistribution analysis activity showed clearance from the blood and non-targeted tissues (see Chapter 4: Experimental Data for details). A lack of uptake in bone suggested the trifluoromethyl group remained intact *in vivo*. Any [^{18}F]fluoride released from decomposition would have been rapidly taken up by bone.[25]

This biodistribution profile suggests that excretion occurs *via* the gastrointestinal pathway which is consistent with biodistribution profiles reported for other radiolabelled analogues of octreotide.[26]

The data obtained from this dynamic PET study showed binding occurred in organs that naturally contain somatostatin receptors, such as the liver, pancreas and gastrointestinal pathway. To demonstrate whether binding was specific or non-specific, further experiments, including blocking experiments with octreotide[Trp(2-CF_3)], would have to be carried out.

In conclusion, the biological application of labelling peptides with the [^{18}F]Langlois reagent has been demonstrated by carrying out *in vitro* and *in vivo* PET imaging studies. To extend this application as a diagnostic tool in oncology or neurology, the final doses and molar activities of [^{18}F]Langlois reagent and labelled peptides would have to be improved.

These goals may be achieved through investigations into alternate synthetic routes for labelling the Langlois reagent and by optimising reaction conditions and procedures. Emerging micro-volume technologies such as microfluidics and radiochemical reactions "on a chip" may aid future advancements.[27]

3.6 References

[1] B. Langlois, D. Montègre & N. Roidot *J. Fluor. Chem.* **1994**, 68, 63 – 66.

[2] C. Gadais *et al. Eur. J. Org. Chem.* **2017**, 246 – 251.

[3] M. Imiołek *et al. J. Am. Chem. Soc.* **2018**, 140, 1568 – 1571.

[4] M. Cheng *et al. Angew. Chem. Int. Ed.* **2017**, 56, 14007 – 14010.

[5] N. Ichiishi *et al. Chem. Sci.* **2018**, 9, 4168 – 4175.

[6] B. Ding *et al. Eur. J. Org. Chem.* **2019**, 7596 – 7605.

[7] T. Yang *et al. Org. Lett.* **2020**, 22, 827 – 831.

[8] Y. Ji *et al. Proc. Natl. Acad. Sci. U. S. A.* **2011**, 108 (35), 14411 – 14415.

[9] B. R. Langlois, E. Laurant & N. Roidot *Tetrahedron Lett.* **1991**, 32, 7525 – 7528.

[10] M. S. Refat, S. A. El-Korashy & A. S. Ahmed *J. Mol. Struct.* **2008**, 881, 28 –45.

[11] S. Ozturk *et al. J. Org. Chem.* **2018**, 83, 7309 – 7317.

[12] Y. Fan *et al. Molecules* **2018**, 23, 1361.

[13] D. Kuman, P. Bandyopadhay & N. Suryaprakash *J. Org. Chem.* **2013**, 78, *6*, 2373 – 2378.

[14] C. D. Gabbutt *et al. J. Chem. Soc., Perkin Trans 1* **2002**, 2799 – 2808.

[15] a) K. D. Silveira *et al. J. Immunol.* **2010**, 185, 5569 – 5576. b) A. Z. El-Hashim *et al. Br. J. Pharmacol.* **2012**, 166, 1964 – 1976.

[16] W. Cai *et al. J. Nucl. Med.* **2006**, 47, 1172 – 1180.

[17] E. Pauwels *et al. Eur. J. Nucl. Med. Mol. Imaging* **2019**, 46, 2398 – 2399.

[18] V. I. Deigin *et al. Int. Immunopharmacol.* **2007**, 7, 375 – 382.

[19] W. Vale *et al. Science* **1972**, 176 (4037), 933 –934.

[20] A. Frydman-Marom *et al. ACS Chem. Biol.* **2011**, 6, 1265 – 1276.

[21] H. Raghuraman & A. Chattopadhyay *Biosci. Rep.* **2007**, 27, 189 – 223.

[22] L. Anthony & P. U. Freda *Curr. Med. Res. Opin.* **2009**, 25, 2989 – 2999.

[23] W. A. P. Breeman *et al. Eur. J. Nucl. Med.* **2001**, 28, 1421 – 1429.

[24] a) G. Melacini *et al. J. Med. Chem.* **1997**, 40, 2252 – 2258. b) P. Martin-Gago *et al. Molecules* **2013**, 18, 14564 – 14584.

[25] M. Blau, R. Ganatra & M. A. Bender *Semin. Nucl. Med.* **1972**, 2, 31 – 37.

[26] a) S. Guhkle *et al. Nucl. Med. Biol.* **1994**, 21, 819 – 825. b) C. J. Anderson *et al. J. Nucl. Med.* **1995**, 36, 2315 – 2325. c) H. Wester *et al. Nucl. Med. Biol.* **1997**, 24, 275 – 286.

[27] M. Sergeev *et al. Commun. Chem.* **2018**, 1, Article 10.

Chapter 4: Experimental Data

4.1 General Experimental Information

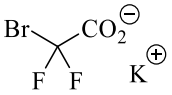
All NMR spectra were recorded on Bruker AVIII HD 400, AVII 500 and AVIII HD 500 spectrometers. ^{1}H and ^{13}C NMR spectra are reported as chemical shifts (δ) in parts per million (ppm) relative to the solvent peak values as given in Gottlieb *et al*.[1] ^{19}F NMR spectra are referenced relative to $CFCl_3$ in $CDCl_3$. If a trifluoroacetate peak is present, it is used as a reference with values in the relevant solvent as given in Rosenau *et al*.[2] Coupling constants (*J*) are reported in units of hertz (Hz). The following abbreviations are used to describe multiplicities: s (singlet), d (doublet), t (triplet), q (quartet), m (multiplet). High Resolution Mass Spectra (HRMS) were recorded on a Bruker MicroTOF spectrometer using positive electrospray ionization (ESI+). Infrared spectra (IR) were recorded either as a neat compound or in a solution using a Bruker Tensor 27 FT-IR spectrometer. Absorptions are reported in wavenumbers (cm^{-1}). Optical rotations were measured on a PerkinElmer Polarimeter model 341 at 25 °C. Data are reported as: $[\alpha]_D^T$, concentration (*c* in g/100 mL), and solvent. Melting points of solids were measured on a Griffin apparatus and are uncorrected. Elemental analysis (CHNS) was carried out using the Vario MICRO Cube analyser that uses a combustion method in pure oxygen. IUPAC names were obtained using Chemdraw Professional software v. 17.1 (Perkin Elmer). Solvents were purchased from Sigma-Aldrich, Honeywell and Fisher. Chemicals were purchased from Acros, Alfa Aesar, Bachem, Fluorochem, Sigma-Aldrich and used as received. Peptides were purchased from Bachem and used as received.

The LC-MS/MS analyses were recorded on Xevo G2 Q-TOF coupled to ACQUITY UPLC H-Class LC system (Waters Corporation). ESI ionization source parameters: capillary 3 kV,

cone voltage 40 V, source temperature 100 °C, desolvation temperature 400 °C and desolvation gas (nitrogen) flow 700 L/h. MS was working at 30,000 (FWHM) resolution. The mass spectrometer operated in data dependent acquisition (DDA) mode with MS survey scan (0.1 s) followed by 0.1 s – 0.5 s MS/MS scans on the three most intense ions. To avoid optimisation of collision conditions broad MS/MS Collision Energy Ramp 15 – 60 V was used. Leucine enkephalin was used as the lock mass standard. MS/MS data was processed using PEAKS Studio software v. 8.0 (Bioinformatics Solutions Inc.) with DeNovo analysis using the following parameters: parent mass error tolerance 10.0 ppm; fragment mass error tolerance 0.02 Da; monoisotopic precursor mass search type. Additional identification in selected cases was accomplished with spectral interpretation software (HighChem Mass Frontier 7.0). Peptide samples (10 – 50 µg/mL) were prepared in (10 – 50%) MeCN:H_2O mixture with 0.1% formic acid or trifluoroacetic acid (TFA). Disulfide containing peptides (insulin, somatostatin) were reduced before LC-MS/MS analysis by mixing with a solution of 1.0 M DTT in 100 mM NH_4OAc buffer (pH 9.0) and incubated for 1 h at room temperature. The final concentration of DTT was 2 mM and basic pH was confirmed with pH indicator strips. Melittin (0.4 µg) sample was digested at 37 °C with porcine trypsin in 50 mM PBS at pH 8.0 overnight with protein to enzyme ratio 1:25. The reduction/digestion was terminated by acidification with 0.2% formic acid. Simulation and comparison of fragmentation spectra for cyclic peptide cyclo(-Arg-Gly-Asp-D-Tyr-Lys)[Tyr(3-CF_3)] was done using mMass software (Version 5.5.0).[3]

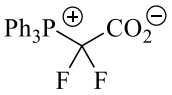
4.2 Experimental Procedures and Compound Characterisations

Potassium 2-bromo-2,2-difluoroacetate



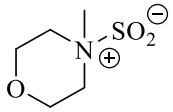
To a solution of potassium hydroxide (5.61 g, 100 mmol) in methanol (90 mL) was added ethyl bromodifluoroacetate (12.8 mL, 100 mmol) before stirring at rt for 12 h. The solvent was evaporated on a rotary evaporator and dried *in vacuo* to obtain a white solid (19.4 g, 91.1 mmol, 91%). Characterisation data is consistent with those reported in the literature.[4] **^{19}F NMR** (377 MHz, Methanol-d_4): δ -58.05; **^{13}C NMR** (101 MHz, Methanol-d_4): δ 164.98 (t, J = 24.9 Hz), 115.22 (t, J = 320.4 Hz).

2,2-Difluoro-2-(triphenylphosphonio)acetate



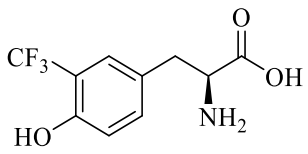
A solution of potassium 2-bromo-2,2-difluoroacetate (2.13 g, 10.0 mmol) and triphenylphosphine (2.62 g, 10.0 mmol) in dry DMF (10 mL) was stirred at rt for 16 h. The mixture was filtered, and the residue was washed with copious amounts of water, acetone and diethyl ether before drying *in vacuo* to obtain a white solid (2.68 g, 7.53 mmol, 75%). Characterisation data is consistent with those reported in the literature.[4] **^{1}H NMR** (400 MHz, Methanol-d_4): δ 7.98 – 7.82 (m, 9H), 7.81 – 7.73 (m, 6H); **^{19}F NMR** (377 MHz, Methanol-d_4): δ -96.04 (d, J = 96.4 Hz); **^{31}P NMR** (162 MHz, Methanol-d_4): δ 27.13 (t, J = 96.8 Hz).

4-Methylmorpholin-4-ium-4-sulfinate



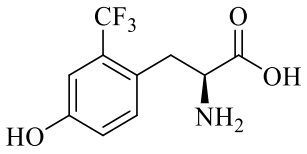
To a dry three neck round-bottom flask containing a magnetic stir bar, with a dry ice/acetone condenser, nitrogen inlet and bubbler attached, was added 4-methylmorpholine (5.94 mL, 50.0 mmol) before cooling with a dry ice/MeCN bath. Sulfur dioxide gas was added until approximately 100 mL had condensed. The dry ice/MeCN bath was replaced with a water bath and the excess sulfur dioxide was evaporated while stirring under a nitrogen stream. The resultant solid was dried overnight over P_2O_5 to obtain a pale yellow solid (7.38 g, 44.7 mmol, 89%). The solid was stored at -20 ºC under an inert atmosphere as it is hygroscopic and slowly decomposes at rt over long periods of time. **^{1}H NMR** (500 MHz, Methanol-d_4): δ 3.94 (t, J = 5.0 Hz, 4H), 3.41 – 3.18 (m, 4H), 2.88 (s, 3H); **^{13}C NMR** (101 MHz, Methanol-d_4): δ 65.03, 54.47, 44.05; **^{15}N NMR** (51 MHz, Methanol-d_4) *observed indirectly from HMBC*: δ 40.62; **IR** (solid): 615.0, 623.8, 644.5, 765.2, 859.8, 893.4, 900.5, 936.8, 996.2, 1028.9, 1044, 1067.2, 1088.2, 1112.9, 1156.5, 1181.6, 1198.3, 1280.4, 1313.4, 1370.6, 1460.0, 2866.2, 2966.5, 3026.1; **M.P.**: 40 °C; **Elemental analysis**: calculated for $C_5H_{11}NO_3S$: C 36.35%, H 6.71%, N 8.48%, O 29.05%, S 19.41% found C 35.32%, H 6.88%, N 8.14%, O 31.03%, S 18.64%.

(*S*)-2-Amino-3-(4-hydroxy-3-(trifluoromethyl)phenyl)propanoic acid



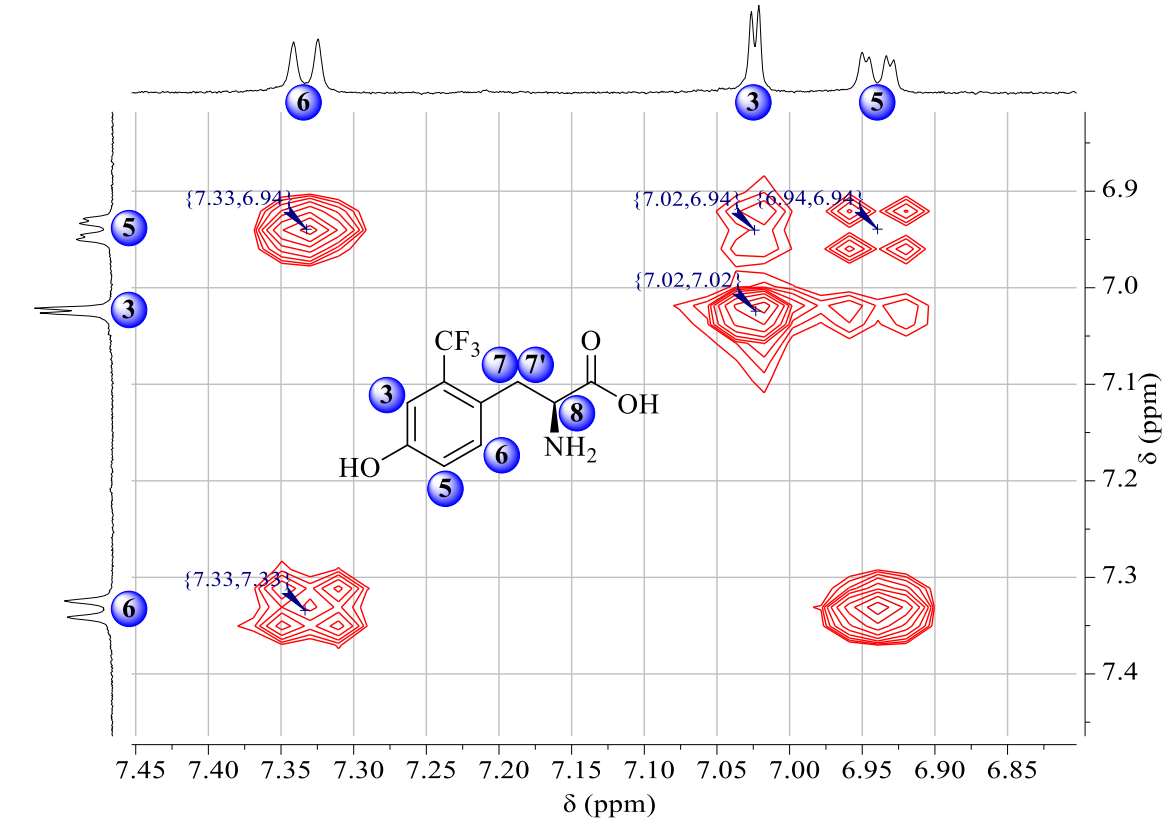
To a mixture of L-tyrosine (18.1 mg, 0.1 mmol), sodium trifluoromethanesulfinate (15.6 mg, 0.1 mmol), and iron(III) nitrate nonahydrate (40.4 mg, 0.1 mmol) in 1:9 AcOH:25 mM aqueous NH_4HCO_2 (1 mL) was added *tert*-butyl hydroperoxide solution (27.7 μL, 0.2 mmol, 70% in H_2O) before stirring at 40 ºC for 20 min. The solution was taken up in H_2O (10 mL) and added to an Oasis HLB Plus cartridge (Waters, part # 186000132, activated with 2 mL MeOH, 10 mL H_2O) before eluting the crude product with MeOH (5 mL). The MeOH was evaporated, the desired product was isolated using reverse phase preparative HPLC and lyophilised to obtain a white solid (3.0 mg, 0.012 mmol, 12%). **Reverse phase HPLC details**: Phenomenex Synergi^{TM} 4 μm Hydro RP 80 Å, 250 x 10 mm, flow rate = 4 mL/min, column temperature = 40 °C, eluent = 5% MeCN (0.1% TFA) and 95% H_2O (0.1% TFA) for 7 min then increase linearly to 40% MeCN (0.1% TFA) at 19 min, retention time = 14.8 min; **^{1}H NMR** (400 MHz, Methanol-d_4): δ 7.46 (d, *J* = 2.2 Hz, 1H), 7.35 (dd, *J* = 8.4, 2.2 Hz, 1H), 6.93 (d, *J* = 8.3 Hz, 1H), 3.76 (dd, *J* = 8.2, 4.6 Hz, 1H), 3.23 (dd, *J* = 14.7, 4.5 Hz, 1H), 3.00 (dd, *J* = 14.7, 8.2 Hz, 1H), *carboxylic acid OH and amine NH_2 were not observed*; **^{13}C NMR** (101 MHz, Methanol-d_4): δ 173.52, 156.56, 135.33, 128.78 (q, *J* = 5.1 Hz), 127.45, 126.52 (q, *J* = 271.1 Hz), 118.30, 118.07 (q, *J* = 30.8 Hz), 57.39, 37.12; **^{19}F NMR** (376 MHz, Methanol-d_4): δ -61.45; **HRMS** (ESI$^+$): for $C_{10}H_{11}F_3NO_3$ $[M+H]^+$ requires *m*/*z* = 250.0686, found 250.0684.

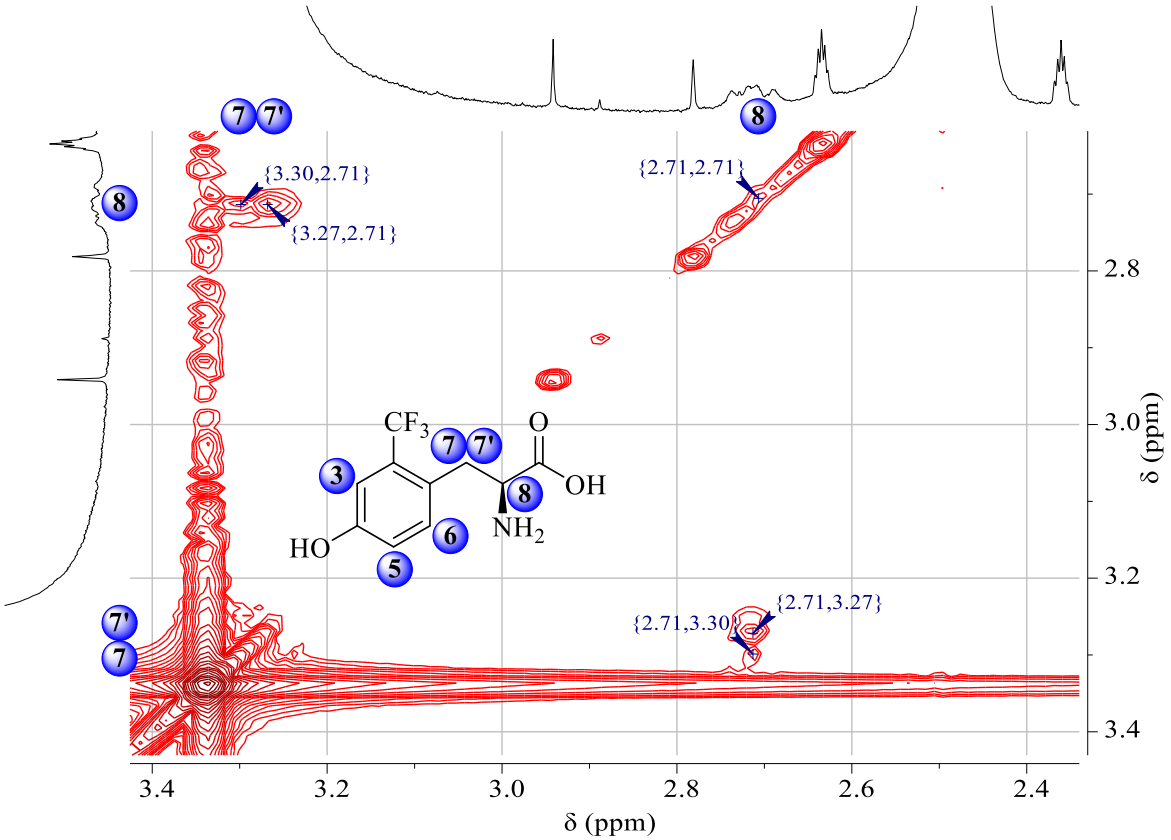
(*S*)-2-Amino-3-(4-hydroxy-2-(trifluoromethyl)phenyl)propanoic acid



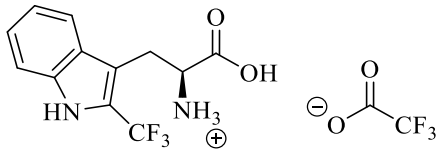
To a mixture of L-tyrosine (18.1 mg, 0.1 mmol), sodium trifluoromethanesulfinate (15.6 mg, 0.1 mmol), and iron(III) nitrate nonahydrate (40.4 mg, 0.1 mmol) in 1:9 AcOH:25 mM aqueous NH_4HCO_2 (1 mL) was added *tert*-butyl hydroperoxide solution (27.7 μL, 0.2 mmol, 70% in H_2O) before stirring at 40 ºC for 20 min. The solution was taken up in H_2O (10 mL) and added to an Oasis HLB Plus cartridge (Waters, part # 186000132, activated with 2 mL MeOH, 10 mL H_2O) before eluting the crude product with MeOH (5 mL). The MeOH was evaporated, the desired product was isolated using reverse phase preparative HPLC and lyophilised to obtain a white solid. **Reverse phase HPLC details**: Phenomenex Synergi^{TM} 4 μm Hydro RP 80 Å, 250 x 10 mm, flow rate = 4 mL/min, column temperature = 40 °C, eluent = 5% MeCN (0.1% TFA) and 95% H_2O (0.1% TFA) for 7 min then increase linearly to 40% MeCN (0.1% TFA) at 19 min, retention time = 13.9 min; **^{1}H NMR** (500 MHz, DMSO-d_6): δ 7.33 (d, *J* = 8.5 Hz, 1H), 7.02 (d, *J* = 2.7 Hz, 1H), 6.94 (dd, *J* = 8.3, 2.6 Hz, 1H), *observed indirectly from COSY since obscured by solvent peak*: 3.30, 3.27, 2.71, *carboxylic acid OH and amine NH_2 were not observed*; **^{19}F NMR** (470 MHz, DMSO-d_6): δ -58.33; **HRMS** (ESI^+): for $C_{10}H_{11}F_3NO_3$ $[M+H]^+$ requires *m*/*z* = 250.0686, found 250.0686.

COSY NMR


{7.33,6.94}
{7.02,6.94}
{6.94,6.94}
{7.02,7.02}
{7.33,7.33}
CF3
O
OH
NH2
HO
7.45 7.40 7.35 7.30 7.25 7.20 7.15 7.10 7.05 7.00 6.95 6.90 6.85
δ (ppm)
6.9 7.0 7.1 7.2 7.3 7.4
δ (ppm)

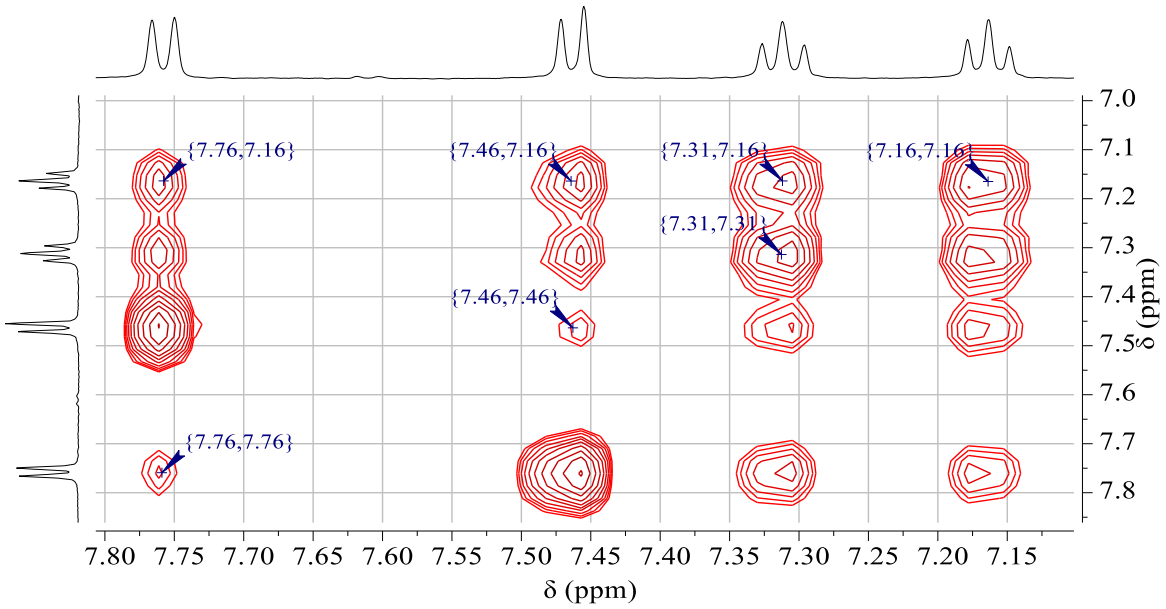

{3.30,2.71}
{3.27,2.71}
{2.71,2.71}
{2.71,3.30}
{2.71,3.27}
CF3
O
OH
NH2
HO
3.4 3.2 3.0 2.8 2.6 2.4
δ (ppm)
2.8 3.0 3.2 3.4
δ (ppm)

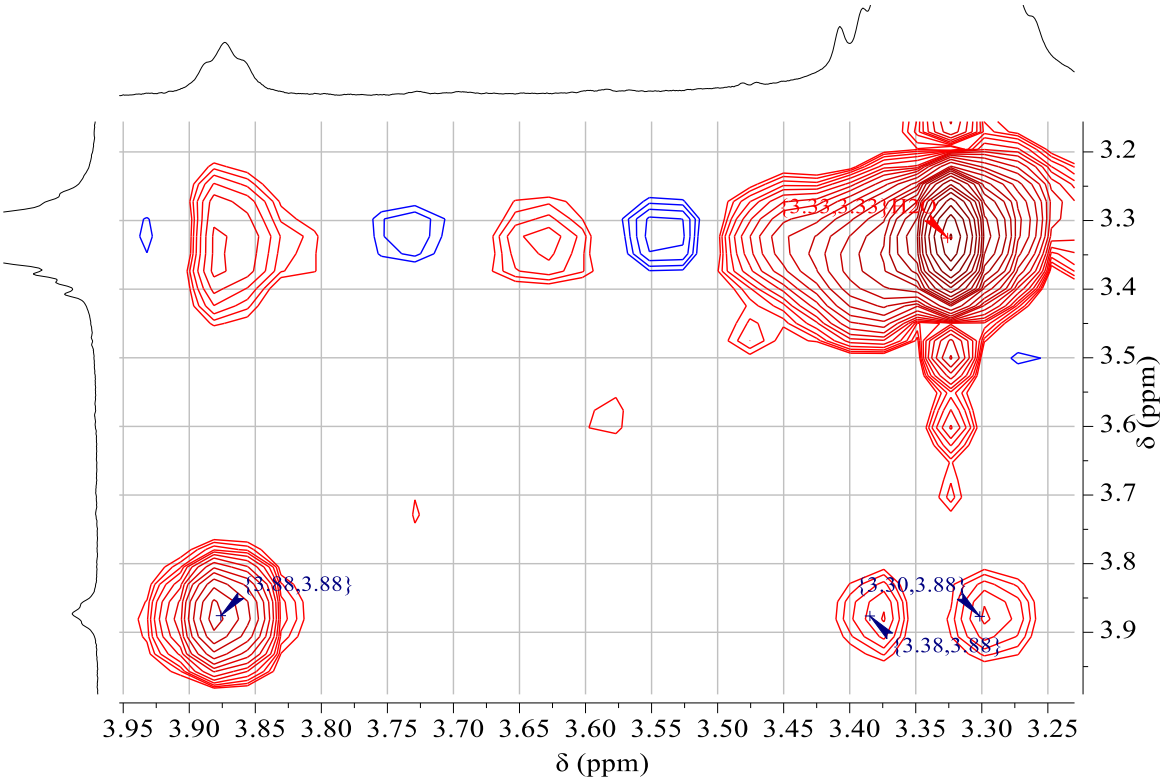
(*S*)-1-Carboxy-2-(2-(trifluoromethyl)-1H-indol-3-yl)ethan-1-aminium 2,2,2-trifluoroacetate



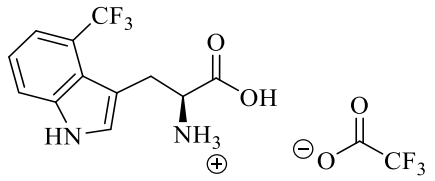
To a mixture of L-tryptophan (20.4 mg, 0.1 mmol), sodium trifluoromethanesulfinate (15.6 mg, 0.1 mmol), and iron(III) nitrate nonahydrate (40.4 mg, 0.1 mmol) in DMSO (1 mL) was added *tert*-butyl hydroperoxide solution (27.7 μL, 0.2 mmol, 70% in H_2O) before stirring at 40 ºC for 20 min. The solution was taken up in H_2O (10 mL) and added to an Oasis HLB Plus cartridge (Waters, part # 186000132, activated with 2 mL MeOH, 10 mL H_2O) before eluting the crude product with MeOH (5 mL). The MeOH was evaporated, the desired product was isolated using reverse phase preparative HPLC and lyophilised to obtain a white solid. Characterisation data is consistent with literature.[5] **Reverse phase HPLC details**: Phenomenex Synergi^{TM} 4 μm Hydro RP 80 Å, 250 x 10 mm, flow rate = 4 mL/min, column temperature = 40 °C, eluent = 20% MeCN (0.1% TFA) and 80% H_2O (0.1% TFA) for 3 min then increase linearly to 27% MeCN (0.1% TFA) at 15 min and hold at 27% MeCN for another 3 min, retention time = 9.4 min; **^{1}H NMR** (500 MHz, DMSO-d_6): δ 12.12 (s, 1H), 8.27 (s, 3H), 7.76 (d, *J* = 8.1 Hz, 1H), 7.46 (d, *J* = 8.1 Hz, 1H), 7.33 – 7.30 (m, 1H), 7.18 – 7.15 (m, 1H), 3.87 (s, 1H), *observed indirectly from TOCSY since obscured by solvent peak*: 3.38, 3.30, *carboxylic acid OH was not observed*; **^{19}F NMR** (471 MHz, DMSO-d_6): δ -57.81, -74.95; **MS** (ESI$^+$): for $C_{12}H_{12}F_3N_2O_2$ $[M+H]^+$ requires *m*/*z* = 273.1, found 273.1.

TOCSY NMR

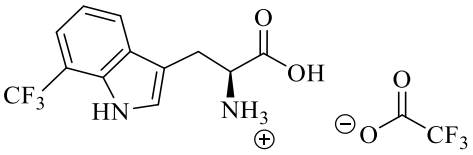

{7.76,7.16}
{7.46,7.16}
{7.31,7.16}
{7.16,7.16}
{7.31,7.31}
{7.46,7.46}
{7.76,7.76}
7.0
7.1
7.2
7.3
7.4
7.5
7.6
7.7
7.8
δ (ppm)
7.80 7.75 7.70 7.65 7.60 7.55 7.50 7.45 7.40 7.35 7.30 7.25 7.20 7.15
δ (ppm)


{3.88,3.88}
{3.30,3.88}
{3.38,3.88}
3.2
3.3
3.4
3.5
3.6
3.7
3.8
3.9
δ (ppm)
3.95 3.90 3.85 3.80 3.75 3.70 3.65 3.60 3.55 3.50 3.45 3.40 3.35 3.30 3.25
δ (ppm)

(*S*)-1-Carboxy-2-(4-(trifluoromethyl)-1H-indol-3-yl)ethan-1-aminium 2,2,2-trifluoroacetate and (*S*)-1-carboxy-2-(7-(trifluoromethyl)-1H-indol-3-yl)ethan-1-aminium 2,2,2-trifluoroacetate



L-Trp(4-CF$_3$)



L-Trp(7-CF$_3$)

To a mixture of L-tryptophan (20.4 mg, 0.1 mmol), sodium trifluoromethanesulfinate (15.6 mg, 0.1 mmol), and iron(III) nitrate nonahydrate (40.4 mg, 0.1 mmol) in DMSO (1 mL) was added *tert*-butyl hydroperoxide solution (27.7 μL, 0.2 mmol, 70% in H_2O) before stirring at 40 ºC for 20 min. The solution was taken up in H_2O (10 mL) and added to an Oasis HLB Plus cartridge (Waters, part # 186000132, activated with 2 mL MeOH, 10 mL H_2O) before eluting the crude with MeOH (5 mL). The MeOH was evaporated, the crude was purified using reverse phase preparative HPLC and lyophilised to obtain a mixture of products in a ratio of 2:1 L-Trp(4-CF_3):L-Trp(7-CF_3). **Reverse phase HPLC details**: Phenomenex Synergi^{TM} 4 μm Hydro RP 80 Å, 250 x 10 mm, flow rate = 4 mL/min; Column temperature = 40 °C, eluent = 20% MeCN (0.1% TFA) and 80% H_2O (0.1% TFA) for 3 min then increase linearly to 27% MeCN (0.1% TFA) at 15 min and hold at 27% MeCN for another 3 min, retention time = 16.2 min.

L-Trp(4-CF$_3$):

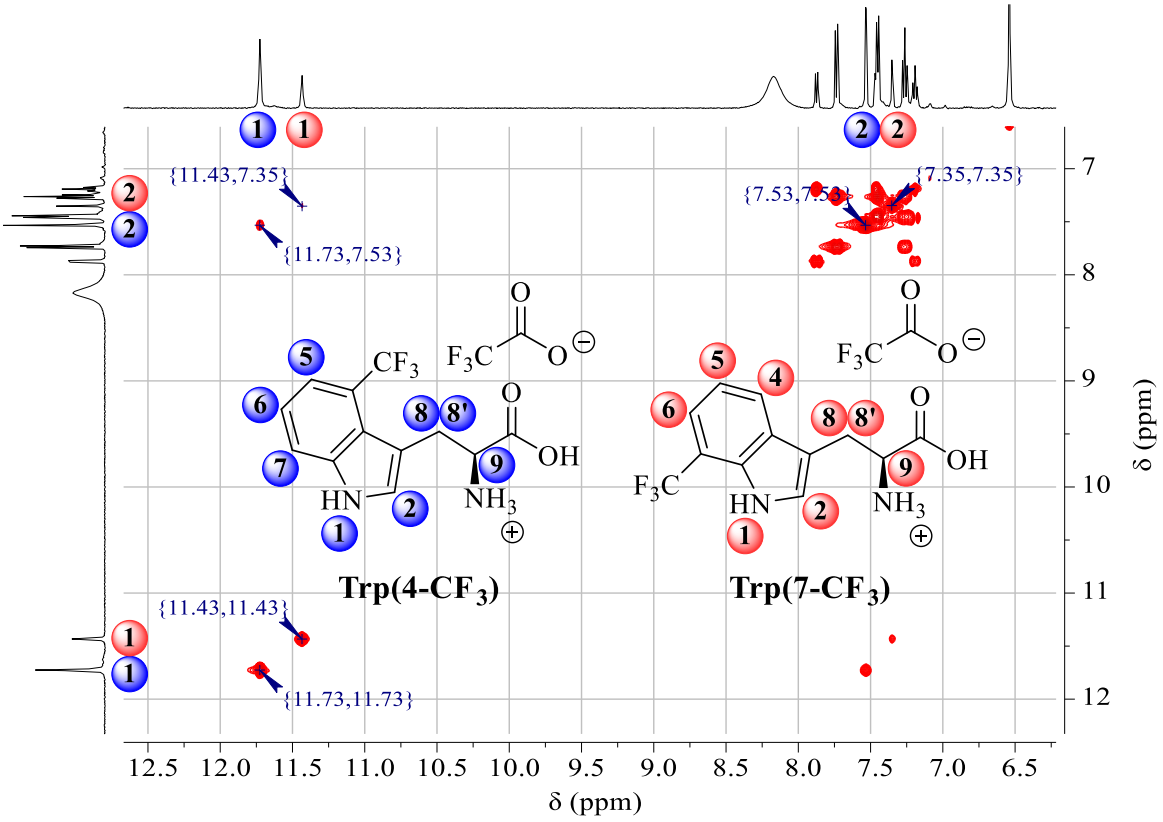
^{1}H NMR (500 MHz, DMSO-d_6): δ 11.73 (d, *J* = 2.3 Hz, 1H), 8.18 (s, 3H), 7.74 (d, *J* = 8.1 Hz, 1H), 7.53 (d, *J* = 2.3 Hz, 1H), 7.46 (d, *J* = 7.4 Hz, 1H), 7.28 – 7.25 (m, 1H), 4.05 – 4.00 (m, 1H), 3.13 (dd, *J* = 15.7, 9.6 Hz, 1H), *observed indirectly from COSY since obscured by*

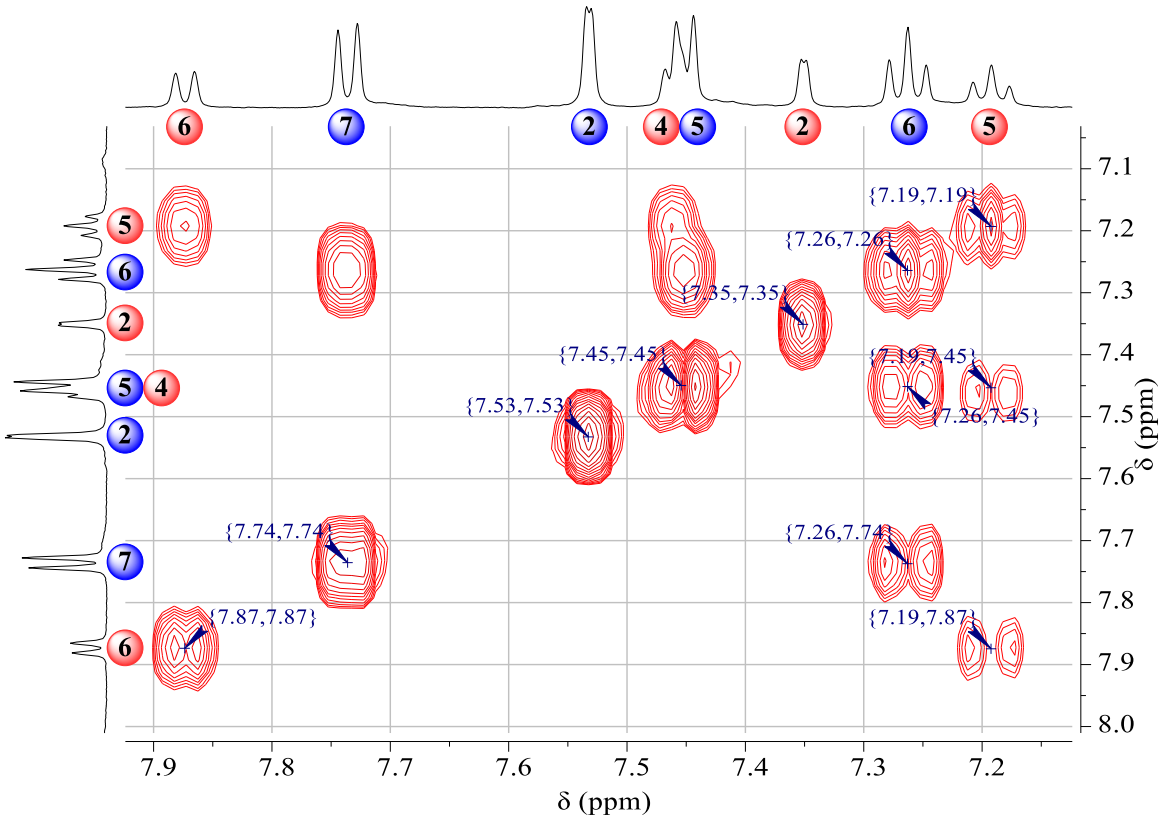
solvent peak: 3.41, *carboxylic acid OH was not observed*; **^{19}F NMR** (471 MHz, DMSO-d_6): δ -57.74, -74.95; **HRMS** (ESI$^+$): for $C_{12}H_{12}F_3N_2O_2$ $[M+H]^+$ requires *m/z* = 273.0845, found 273.0845.

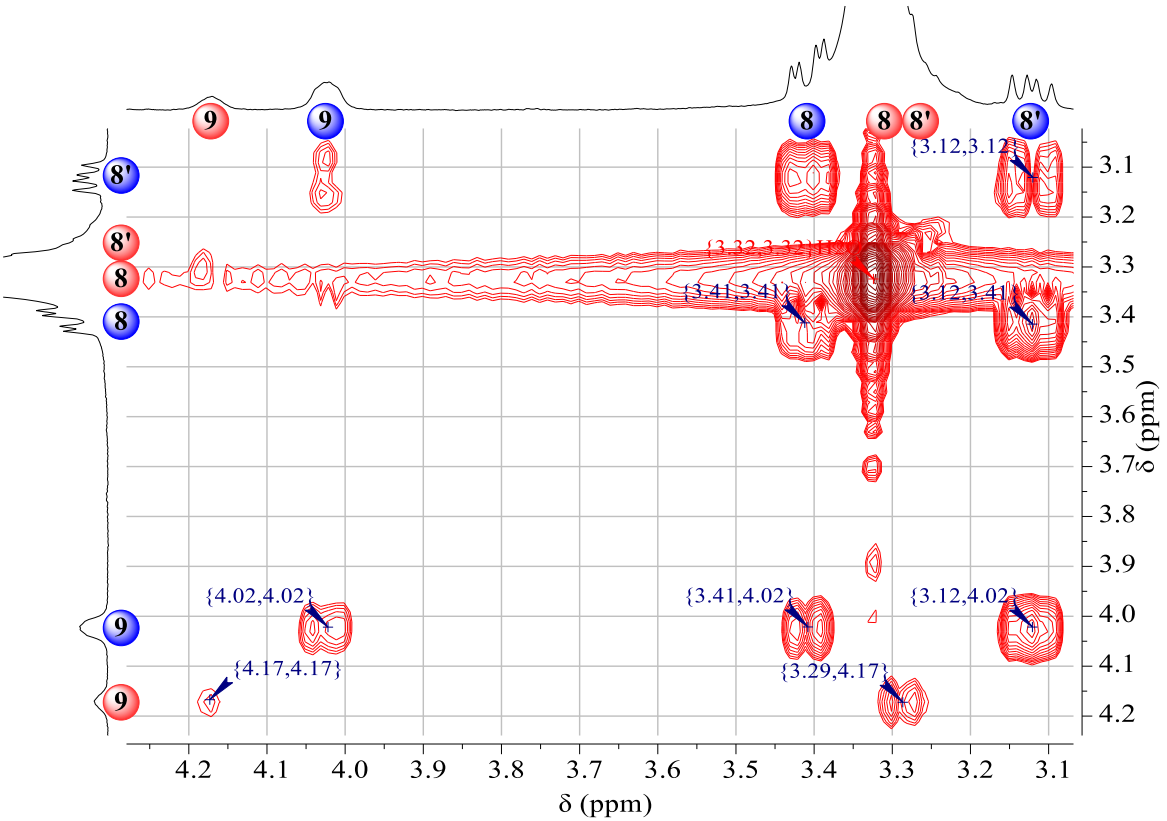
L-Trp(7-CF$_3$):

^{1}H NMR (500 MHz, DMSO-d_6): δ 11.43 (d, *J* = 2.0 Hz, 1H), 8.17 (s, 3H), 7.88 (d, *J* = 8.0 Hz, 1H), 7.47 (d, *J* = 7.7 Hz, 1H), 7.35 (d, *J* = 2.0 Hz, 1H), 7.21 – 7.18 (m, 1H), 4.19 – 4.15 (m, 1H), *observed indirectly from COSY since obscured by solvent peak*: 3.29, *carboxylic acid OH was not observed*; **^{19}F NMR** (471 MHz, DMSO-d_6): δ -61.21, -74.95; **HRMS** (ESI$^+$): for $C_{12}H_{12}F_3N_2O_2$ $[M+H]^+$ requires *m/z* = 273.0845, found 273.0845.

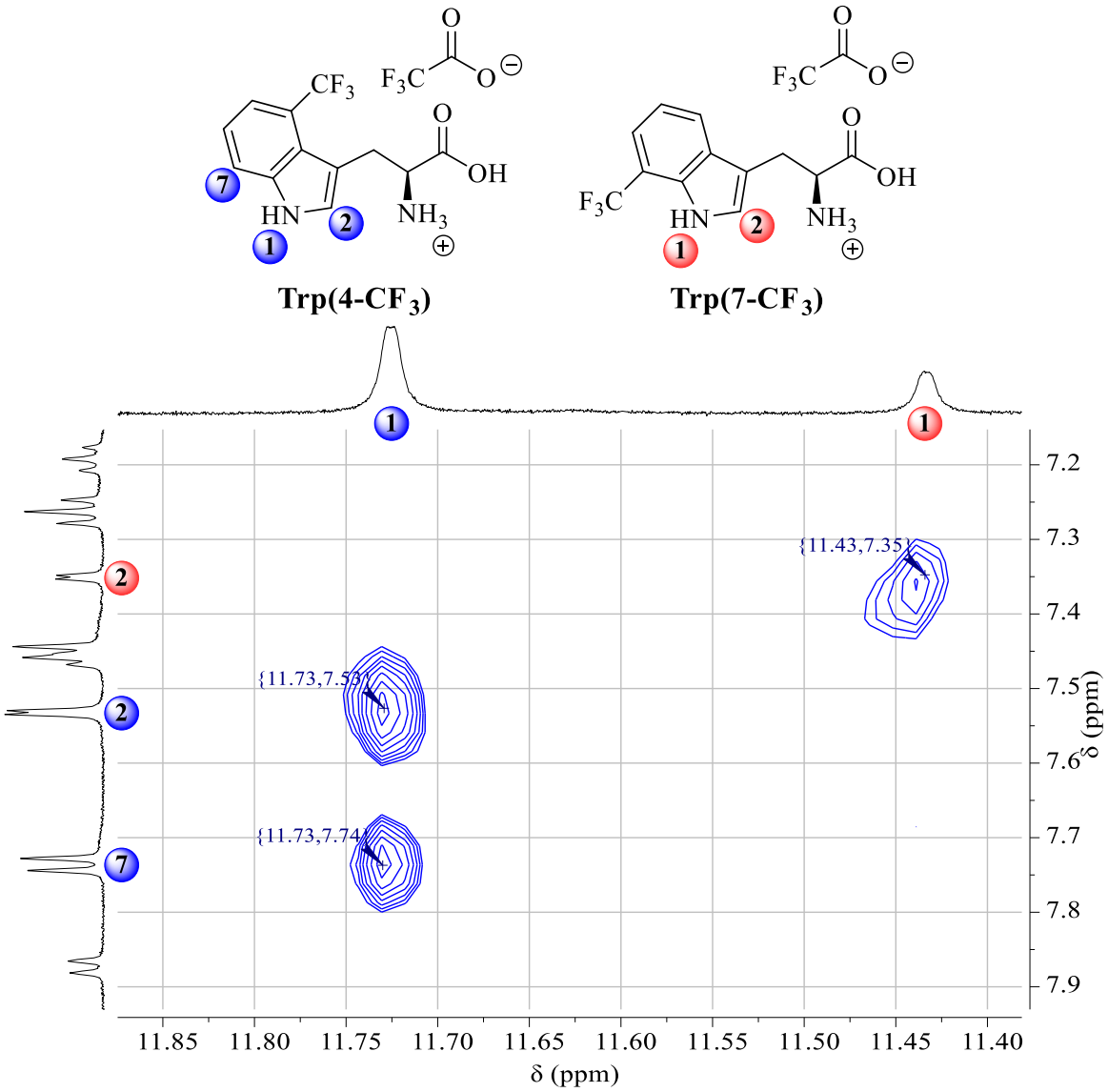
COSY Assignment



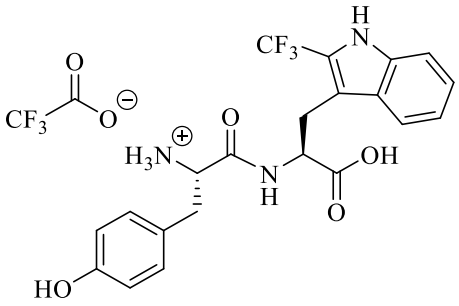

6
7
2
4
5
2
6
5
{7.19,7.19}
{7.26,7.26}
{7.35,7.35}
{7.45,7.45}
{7.53,7.53}
{7.19,7.45}
{7.26,7.45}
{7.74,7.74}
{7.26,7.74}
{7.87,7.87}
{7.19,7.87}
δ (ppm)
δ (ppm)


9
9
8
8
8'
8'
{3.12,3.12}
{3.32,3.32}
{3.41,3.41}
{3.12,3.41}
{4.02,4.02}
{3.41,4.02}
{3.12,4.02}
{4.17,4.17}
{3.29,4.17}
δ (ppm)
δ (ppm)

NOESY Assignment



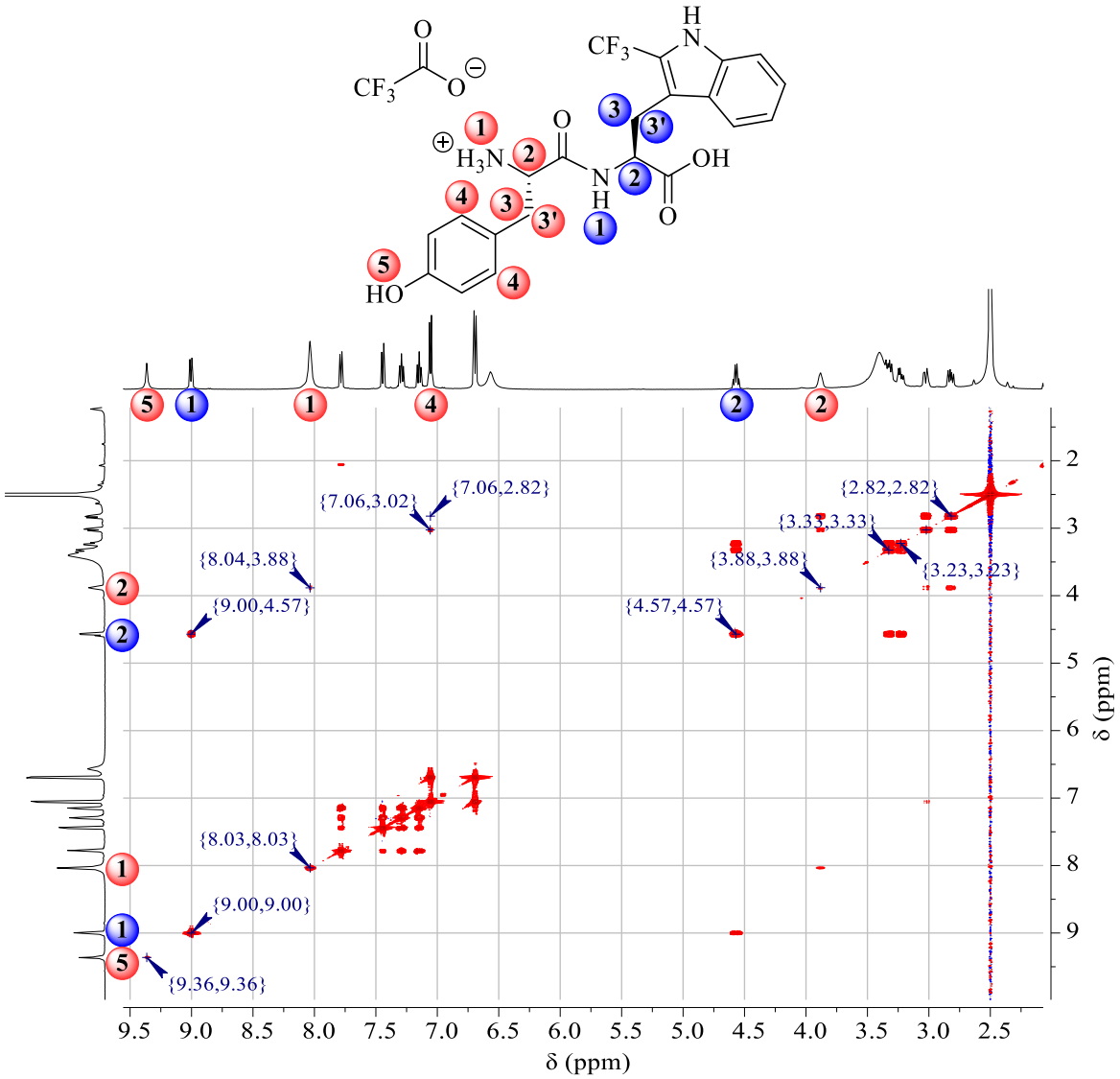
(*S*)-1-(((*S*)-1-Carboxy-2-(2-(trifluoromethyl)-1H-indol-3-yl)ethyl)amino)-3-(4-hydroxyphenyl)-1-oxopropan-2-aminium 2,2,2-trifluoroacetate

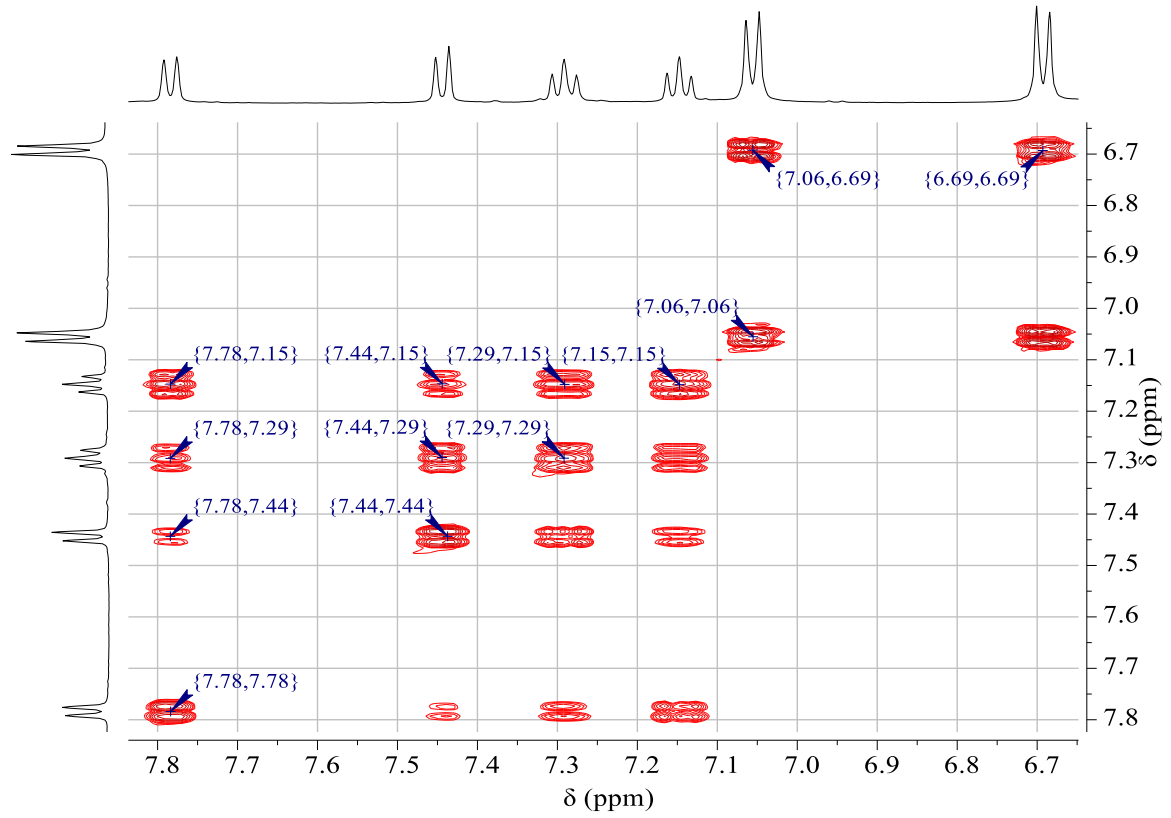


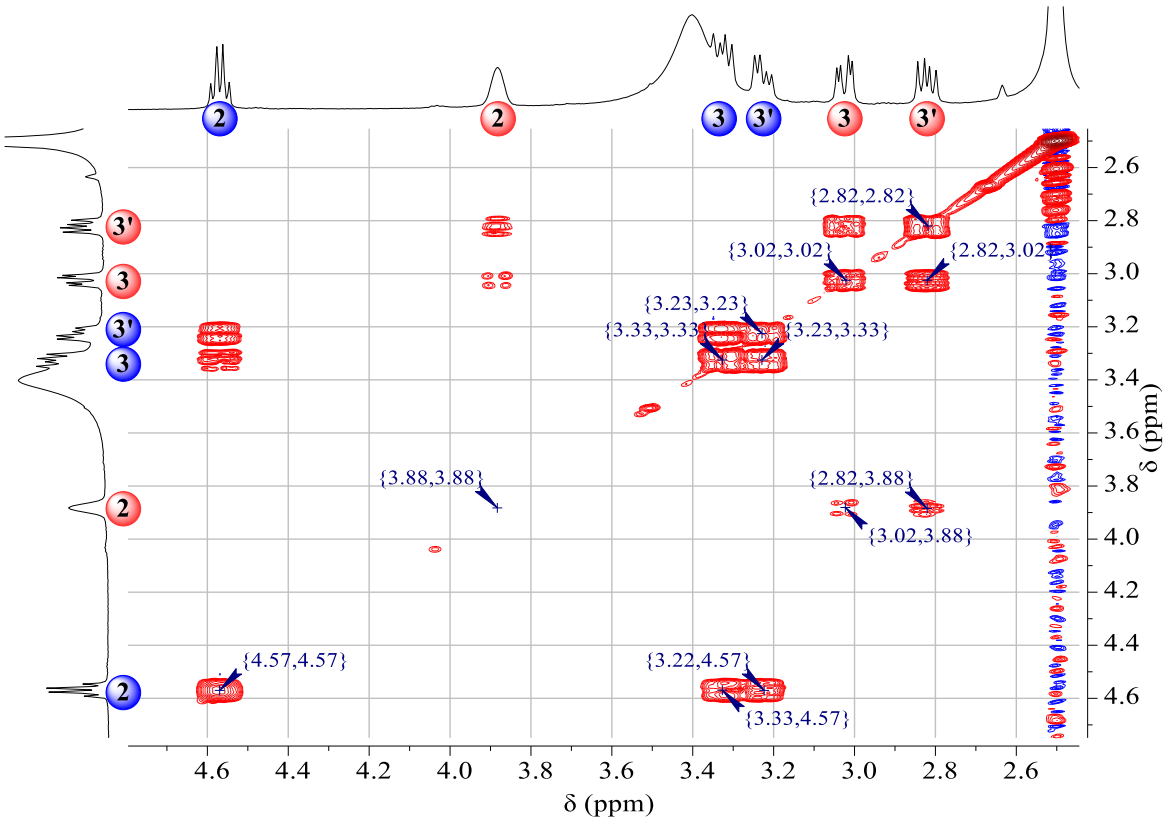
To a mixture of Tyr-Trp (18.4 mg, 0.05 mmol), sodium trifluoromethanesulfinate (7.8 mg, 0.05 mmol), and iron(III) nitrate nonahydrate (20.2 mg, 0.05 mmol) in 1:9 AcOH:25 mM aqueous NH_4HCO_2 (0.5 mL) was added *tert*-butyl hydroperoxide solution (13.8 μL, 0.1 mmol, 70% in H_2O) before stirring at 40 ºC for 20 min. The solution was taken up in H_2O (10 mL) and added to an Oasis HLB Plus cartridge (Waters, part # 186000132, activated with 2 mL MeOH, 10 mL H_2O) before eluting the crude product with MeOH (5 mL). The MeOH was evaporated, the desired product was isolated using reverse phase preparative HPLC and lyophilised to obtain a white solid (9.6 mg, 0.0175 mmol, 35%). **Reverse phase HPLC details**: Phenomenex Synergi^{TM} 4 μm Hydro RP 80 Å, 250 x 10 mm; Flow rate = 4 mL/min; Column temperature = 40 °C, eluent = 15% MeCN (0.1% TFA) and 85% H_2O (0.1% TFA) for 3 min then increase linearly to 49% MeCN (0.1% TFA) at 25 min; Retention time = 16.3 min; **^{1}H NMR** (500 MHz, DMSO-d_6): δ 12.95 (s, 1H), 12.06 (s, 1H), 9.36 (s, 1H), 9.01 (d, *J* = 8.1 Hz, 1H), 8.04 (s, 3H), 7.78 (d, *J* = 8.1 Hz, 1H), 7.44 (d, *J* = 8.2 Hz, 1H), 7.31 – 7.28 (m, 1H), 7.16 – 7.13 (m, 1H), 7.06 (d, *J* = 8.4 Hz, 2H), 6.69 (d, *J* = 8.4 Hz, 2H), 4.57 (q, *J* = 7.6 Hz, 1H), 3.91 – 3.86 (m, 1H), 3.33 (dd, *J* = 14.3, 8.3 Hz, 1H), 3.23 (dd, *J* = 14.3, 6.6 Hz, 1H), 3.02 (dd, *J* = 14.3, 4.8 Hz, 1H), 2.82 (dd, *J* = 14.3, 8.3 Hz, 1H); **^{13}C NMR** (126 MHz, DMSO-d_6): δ 172.10, 168.11, 156.62, 135.67, 130.54, 126.73, 124.56, 124.36,

123.22 (q, *J* = 269.3 Hz), 121.66 (q, *J* = 36.1 Hz), 120.11, 120.00, 115.36, 112.38, 112.04 (q, *J* = 2.9 Hz), 53.58, 53.37, 36.01, 26.62; **^{19}F NMR** (376 MHz, DMSO-d_6): δ -57.70, -74.95; **HRMS** (ESI$^+$): for $C_{21}H_{21}O_4N_3F_3$ $[M+H]^+$ requires *m/z* = 436.1479, found 436.1480; **[α]$_D^{25\,°C}$** = +29 ± 5° (*c* 0.071, H_2O).

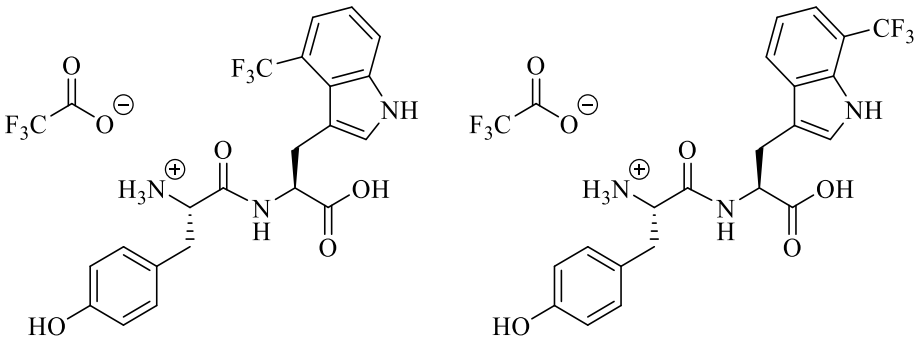
COSY NMR




{7.06,6.69}
{6.69,6.69}
{7.06,7.06}
{7.78,7.15}
{7.44,7.15}
{7.29,7.15}
{7.15,7.15}
{7.78,7.29}
{7.44,7.29}
{7.29,7.29}
{7.78,7.44}
{7.44,7.44}
{7.78,7.78}
δ (ppm)
δ (ppm)


2
2
3
3'
3
3'
3'
3
3
2
2
{2.82,2.82}
{3.02,3.02}
{2.82,3.02}
{3.23,3.23}
{3.33,3.33}
{3.23,3.33}
{3.88,3.88}
{2.82,3.88}
{3.02,3.88}
{4.57,4.57}
{3.22,4.57}
{3.33,4.57}
δ (ppm)
δ (ppm)

(*S*)-1-(((*S*)-1-Carboxy-2-(7-(trifluoromethyl)-1H-indol-3-yl)ethyl)amino)-3-(4-hydroxyphenyl)-1-oxopropan-2-aminium 2,2,2-trifluoroacetate and (*S*)-1-(((*S*)-1-carboxy-2-(4-(trifluoromethyl)-1H-indol-3-yl)ethyl)amino)-3-(4-hydroxyphenyl)-1-oxopropan-2-aminium 2,2,2-trifluoroacetate



Tyr-Trp(4-CF 3) **Tyr-Trp(7-CF 3)**

To a mixture of Tyr-Trp (18.4 mg, 0.05 mmol), sodium trifluoromethanesulfinate (7.8 mg, 0.05 mmol), and iron(III) nitrate nonahydrate (20.2 mg, 0.05 mmol) in 1:9 AcOH:25 mM aqueous NH_4HCO_2 (0.5 mL) was added *tert*-butyl hydroperoxide solution (13.8 μL, 0.1 mmol, 70% in H_2O) before stirring at 40 ºC for 20 min. The solution was taken up in H_2O (10 mL) and added to an Oasis HLB Plus cartridge (Waters, part # 186000132, activated with 2 mL MeOH, 10 mL H_2O) before eluting the crude with MeOH (5 mL). The MeOH was evaporated, the crude was purified using reverse phase preparative HPLC and lyophilised to obtain a mixture of products in a ratio of 2:1 Tyr-Trp(4-CF_3):Tyr-Trp(7-CF_3):. **Reverse phase HPLC details**: Phenomenex Synergi^{TM} 4 μm Hydro RP 80 Å, 250 x 10 mm, flow rate = 4 mL/min, column temperature = 40 °C, eluent = 15% MeCN (0.1% TFA) and 85% H_2O (0.1% TFA) for 3 min then increase linearly to 49% MeCN (0.1% TFA) at 25 min, retention time = 19.1 min**.**

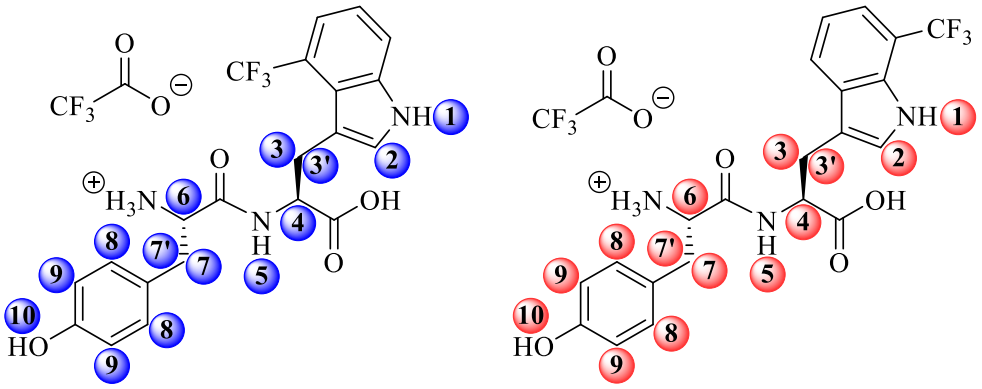
Tyr-Trp(4-CF_3):

^{1}H NMR (500 MHz, DMSO-d_6): δ 11.59 (d, *J* = 2.3 Hz, 1H), 9.34 (s, 1H), 8.93 (d, *J* = 7.4 Hz, 1H), 7.95 (s, 3H), 7.71 (d, *J* = 8.2 Hz, 1H), 7.45 – 7.43 (m, 1H), 7.42 (d, *J* = 2.3 Hz, 1H), 7.25 – 7.22 (m, 1H), 7.08 (d, *J* = 8.6 Hz, 2H), 6.69 (d, *J* = 8.6 Hz, 2H), 4.64 – 4.58 (m, 1H), 3.91 – 3.89 (m, 1H), 3.11 – 2.99 (m, 2H), 2.81 (dd, *J* = 14.6, 8.4 Hz, 1H), *observed indirectly from COSY since obscured by solvent peak*: 3.21, *carboxylic acid OH was not observed*; **^{19}F NMR** (471 MHz, DMSO-d_6): δ -57.63, -74.95; **HRMS** (ESI^+): for $C_{21}H_{21}O_4N_3F_3$ $[M+H]^+$ requires *m*/*z* = 436.1479, found 436.1489.

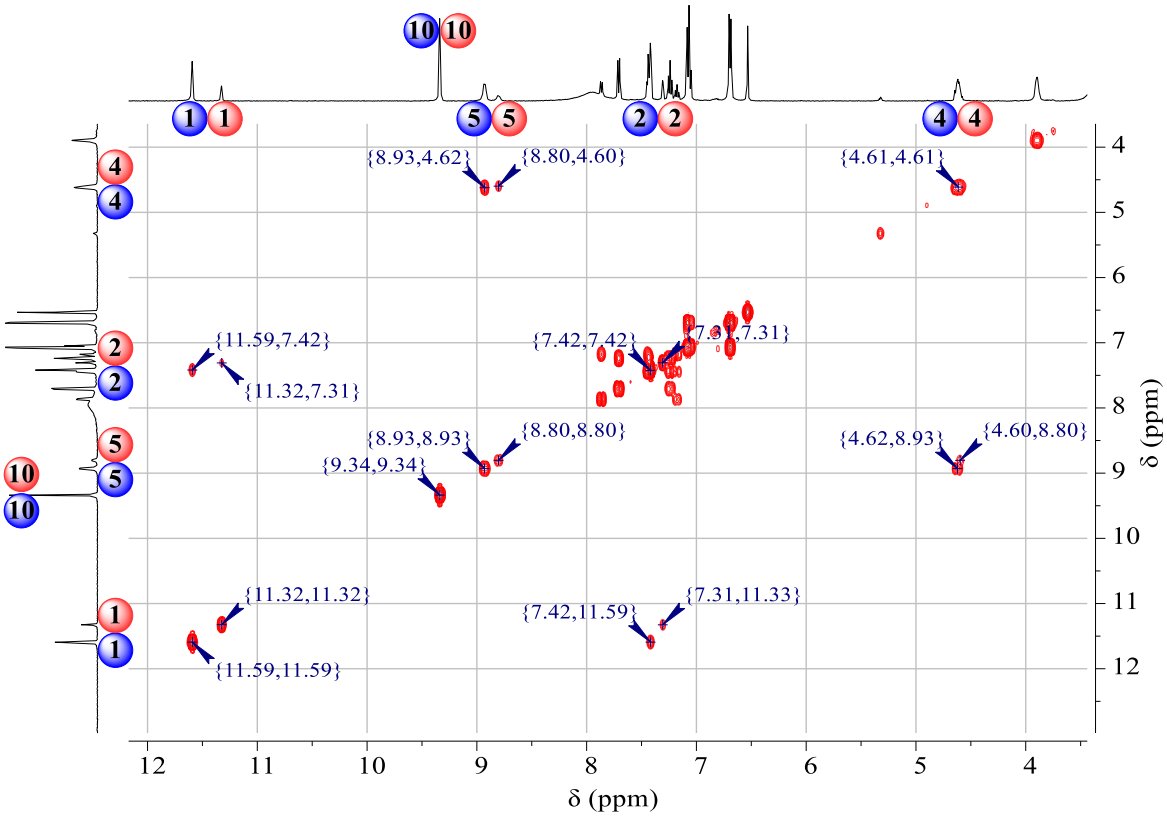
Tyr-Trp(7-CF_3):

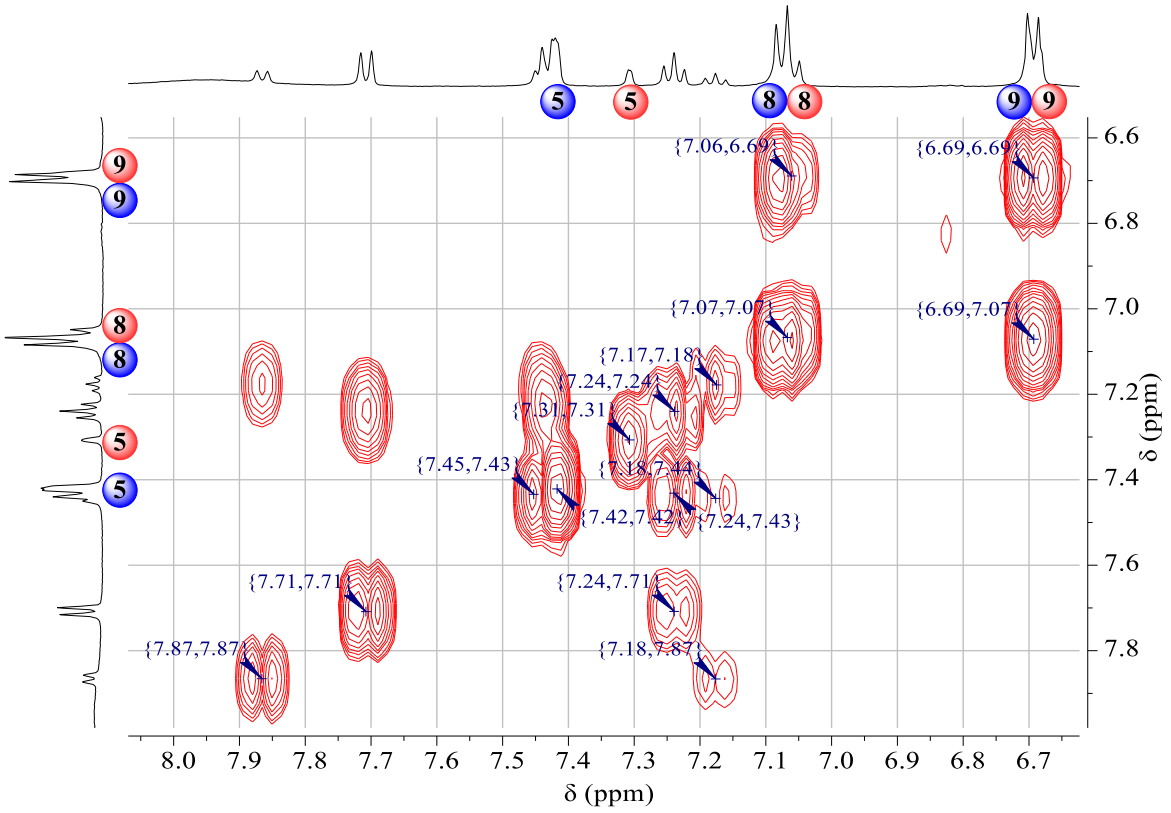
^{1}H NMR (500 MHz, DMSO-d_6): δ 11.32 (d, *J* = 2.2 Hz, 1H), 9.33 (s, 1H), 8.81 (d, *J* = 7.0, 1H), 7.95 (s, 3H), 7.87 (d, *J* = 8.0 Hz, 1H), 7.45 – 7.43 (m, 1H), 7.31 (d, *J* = 2.2 Hz, 1H), 7.19 – 7.16 (m, 1H), 7.06 (d, *J* = 8.6 Hz, 2H), 6.69 (d, *J* = 8.6 Hz, 2H), 4.64 – 4.58 (m, 1H), 3.91 – 3.89 (m, 1H), 3.11 – 2.99 (m, 2H), *observed indirectly from COSY since obscured by solvent peak*: 3.21, 3.30, *carboxylic acid OH was not observed*; **^{19}F NMR** (471 MHz, DMSO-d_6): δ -61.22, -74.95; **HRMS** (ESI^+): for $C_{21}H_{21}O_4N_3F_3$ $[M+H]^+$ requires *m*/*z* = 436.1479, found 436.1489.

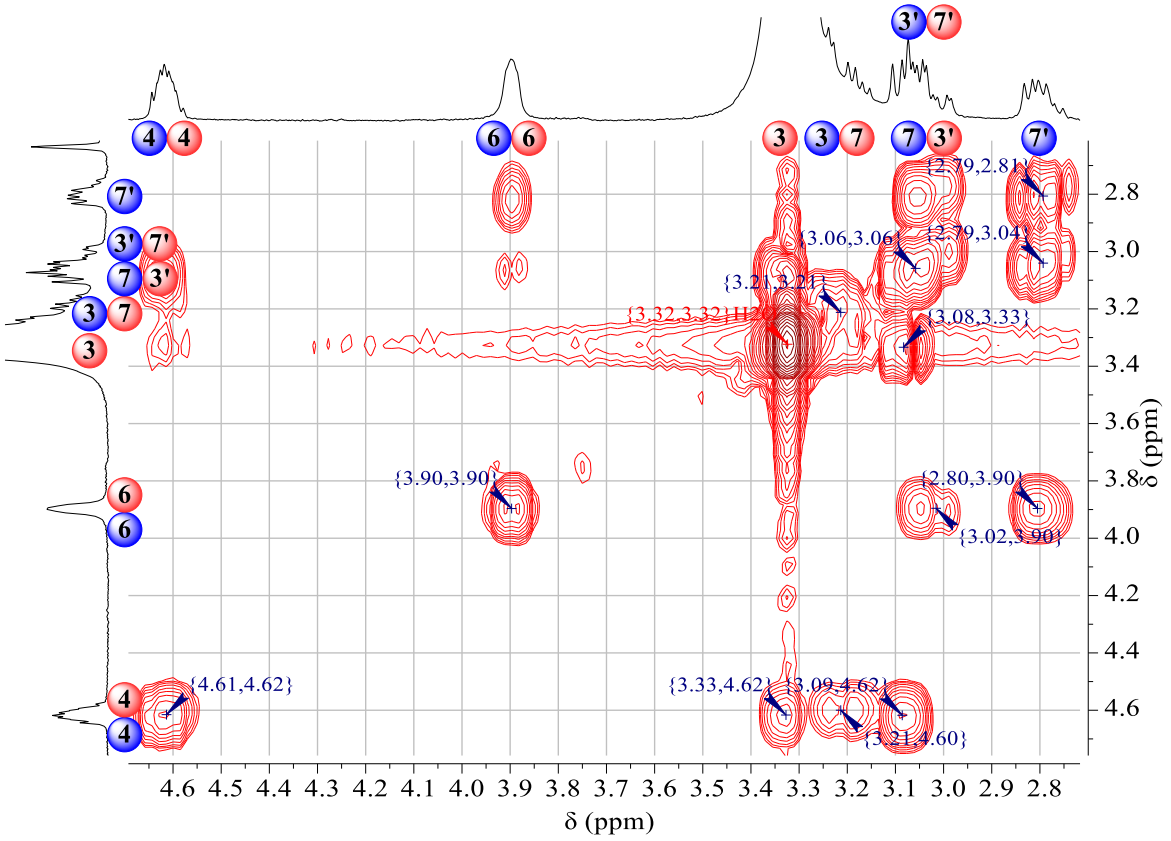
COSY NMR



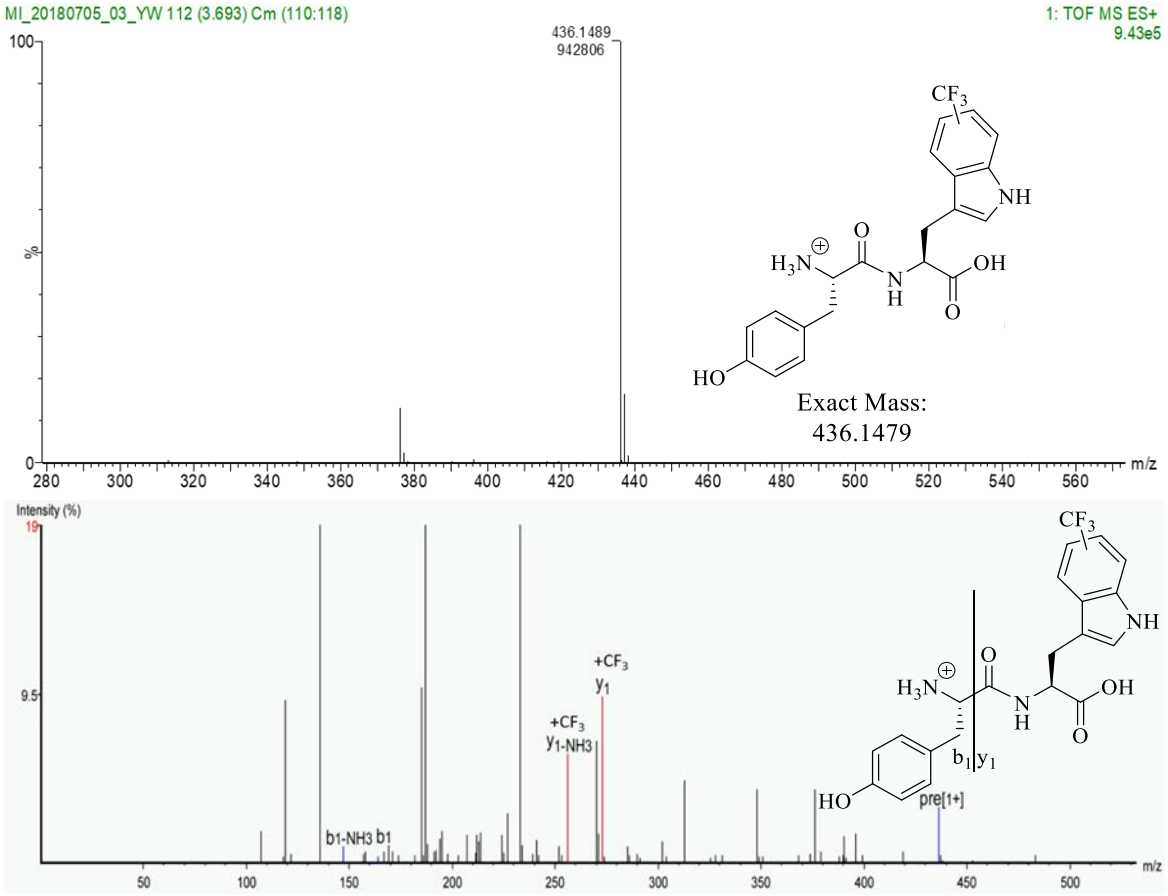
Tyr-Trp(4-CF 3) **Tyr-Trp(7-CF 3)**



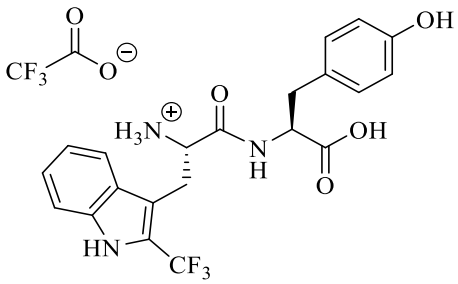

{7.06,6.69}
{6.69,6.69}
{7.07,7.07}
{6.69,7.07}
{7.17,7.18}
{7.24,7.24}
{7.31,7.31}
{7.45,7.43}
{7.18,7.44}
{7.42,7.42}
{7.24,7.43}
{7.71,7.71}
{7.24,7.71}
{7.87,7.87}
{7.18,7.87}
δ (ppm)
δ (ppm)


{2.79,2.81}
{3.06,3.06}
{2.79,3.04}
{3.21,3.21}
{3.32,3.32}
{3.08,3.33}
{3.90,3.90}
{2.80,3.90}
{3.02,3.90}
{4.61,4.62}
{3.33,4.62}
{3.09,4.62}
{3.21,4.60}
δ (ppm)
δ (ppm)

MS/MS Analysis



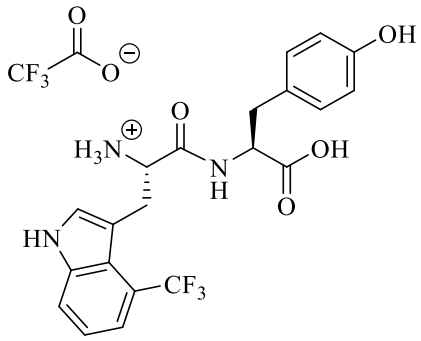
(*S*)-1-(((*S*)-1-Carboxy-2-(4-hydroxyphenyl)ethyl)amino)-1-oxo-3-(2-(trifluoromethyl)-1H-indol-3-yl)propan-2-aminium 2,2,2-trifluoroacetate



To a mixture of Trp-Tyr (36.7 mg, 0.1 mmol), sodium trifluoromethanesulfinate (15.6 mg, 0.1 mmol), and iron(III) nitrate nonahydrate (40.4 mg, 0.1 mmol) in 1:9 AcOH:25 mM aqueous NH_4HCO_2 (1 mL) was added *tert*-butyl hydroperoxide solution (27.7 μL, 0.2 mmol,

70% in H_2O) before stirring at 40 ºC for 20 min. The solution was taken up in H_2O (10 mL) and added to an Oasis HLB Plus cartridge (Waters, part # 186000132, activated with 2 mL MeOH, 10 mL H_2O) before eluting the crude product with MeOH (5 mL). The MeOH was evaporated, the desired product was isolated using reverse phase preparative HPLC and lyophilised to obtain a white solid (11.0 mg, 0.02 mmol, 20%). **Reverse phase HPLC details**: Phenomenex C18(2) Luna 5 µm 100 Å, 250 x 10 mm, flow rate = 4 mL/min, column temperature = 25 °C, eluent = 19% MeCN (0.1% TFA) in 81% water (0.1% TFA), retention time = 17 min; **^{1}H NMR** (500 MHz, DMSO-d_6): δ 12.73 (s, 1H), 12.09 (s, 1H), 9.21 (s, 1H), 8.62 (d, *J* = 7.8 Hz, 1H), 8.27 (s, 3H), 7.79 (d, *J* = 8.2 Hz, 1H), 7.44 (d, *J* = 8.3 Hz, 1H), 7.31 – 7.28 (m, 1H), 7.17 – 7.14 (m, 1H), 6.95 (d, *J* = 8.5 Hz, 2H), 6.63 (d, *J* = 8.5 Hz, 2H), 4.39 – 4.35 (m, 1H), 4.13 – 4.10 (m, 1H), 3.33 (dd, *J* = 14.7, 5.9 Hz, 1H), 3.17 (dd, *J* = 14.7, 6.6 Hz, 1H), 2.88 (dd, *J* = 13.9, 5.9 Hz, 1H), 2.82 (dd, *J* = 13.9, 6.6 Hz, 1H); **^{13}C NMR** (126 MHz, DMSO-d_6): δ 171.58, 167.64, 156.06, 135.77, 130.23, 126.78, 126.61, 124.38, 122.63 (q, *J* = 36.0 Hz), 121.89 (q, *J* = 269.2 Hz), 120.12, 120.00, 114.98, 112.38, 109.21 (q, *J* = 2.6 Hz), 54.01, 52.41, 36.31, 26.28;**^{19}F NMR** (471 MHz, DMSO-d_6): δ -57.59, -74.95; **HRMS** (ESI$^+$): for $C_{21}H_{21}O_4N_3F_3$ $[M+H]^+$ requires *m*/*z* = 436.1479, found 436.1476; $[\boldsymbol{\alpha}]_{\boldsymbol{D}}^{\mathbf{25}}$ = +53 ± 1° (*c* 0.065, H_2O).

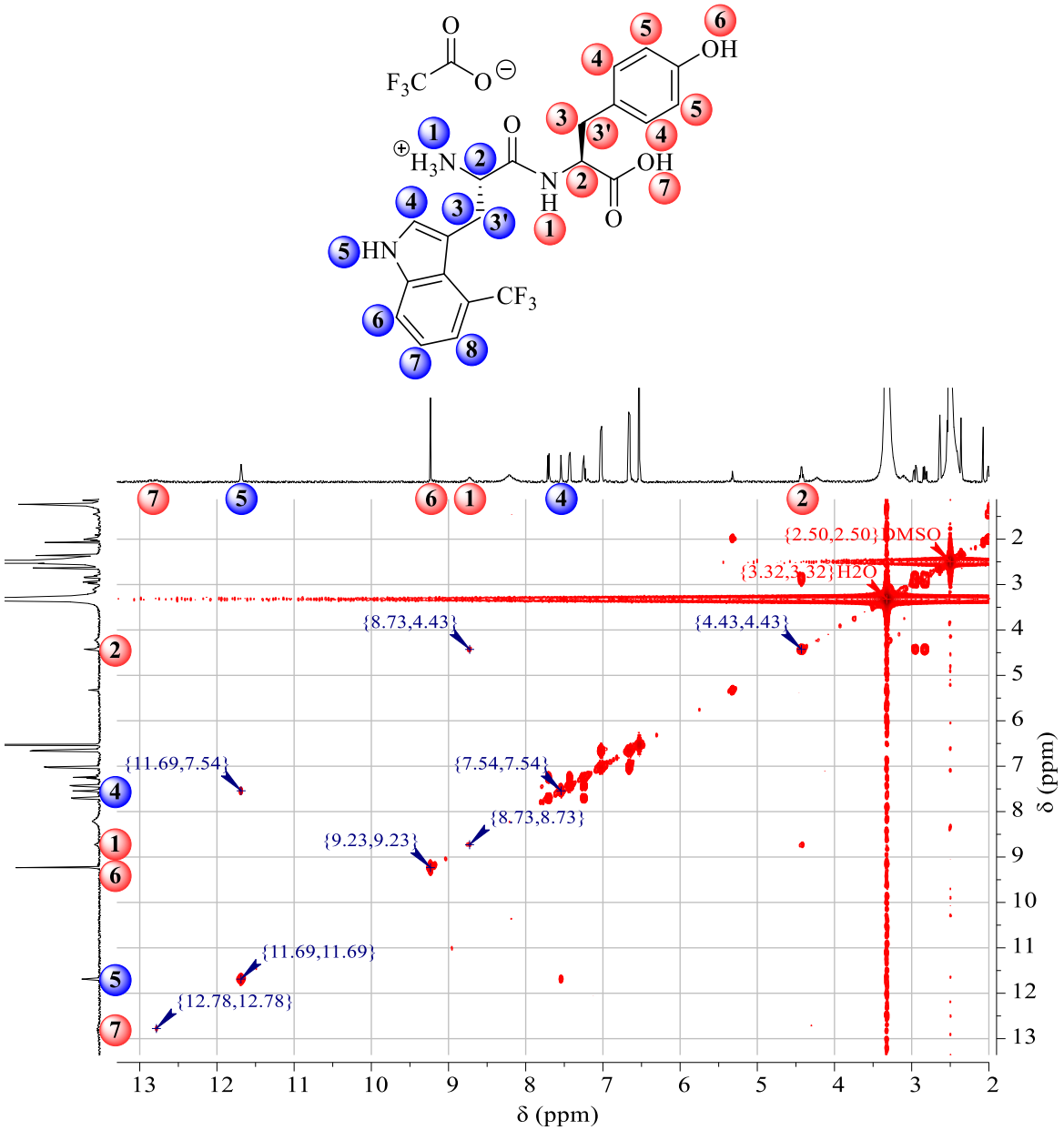
(*S*)-1-(((*S*)-1-Carboxy-2-(4-hydroxyphenyl)ethyl)amino)-1-oxo-3-(4-(trifluoromethyl)-1H-indol-3-yl)propan-2-aminium 2,2,2-trifluoroacetate

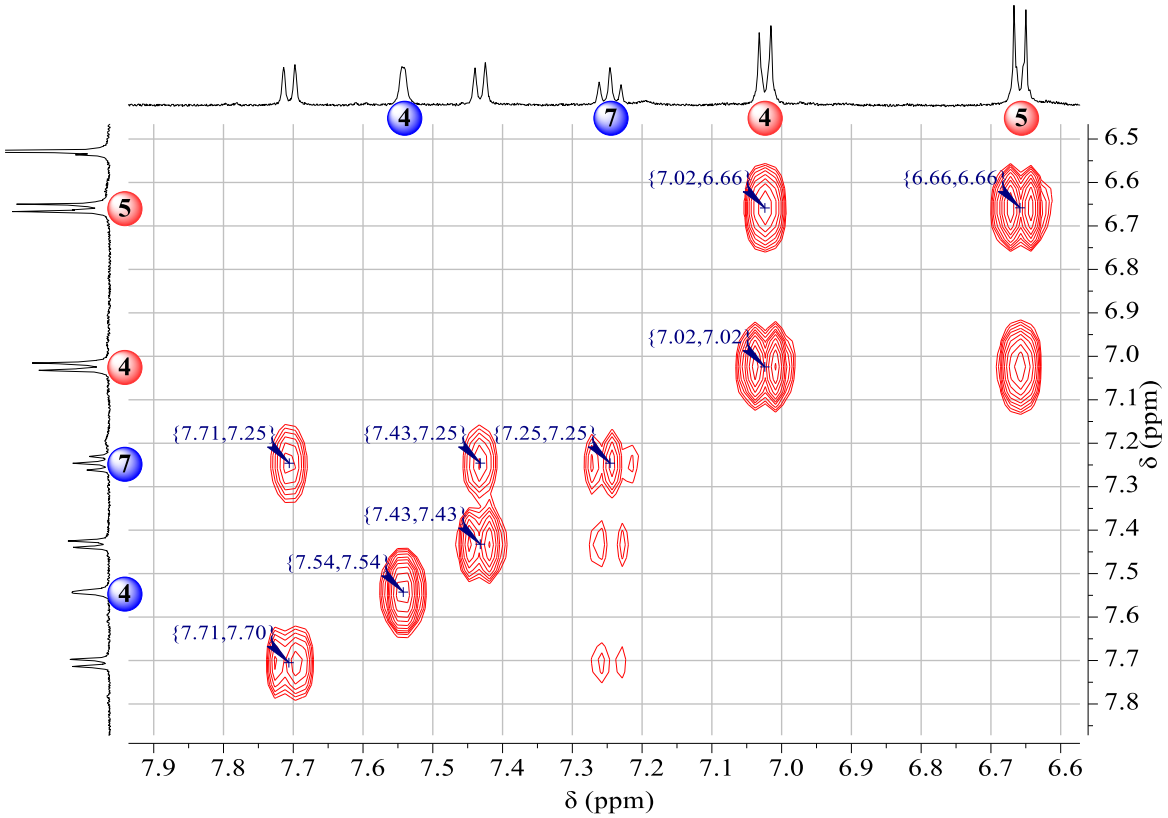


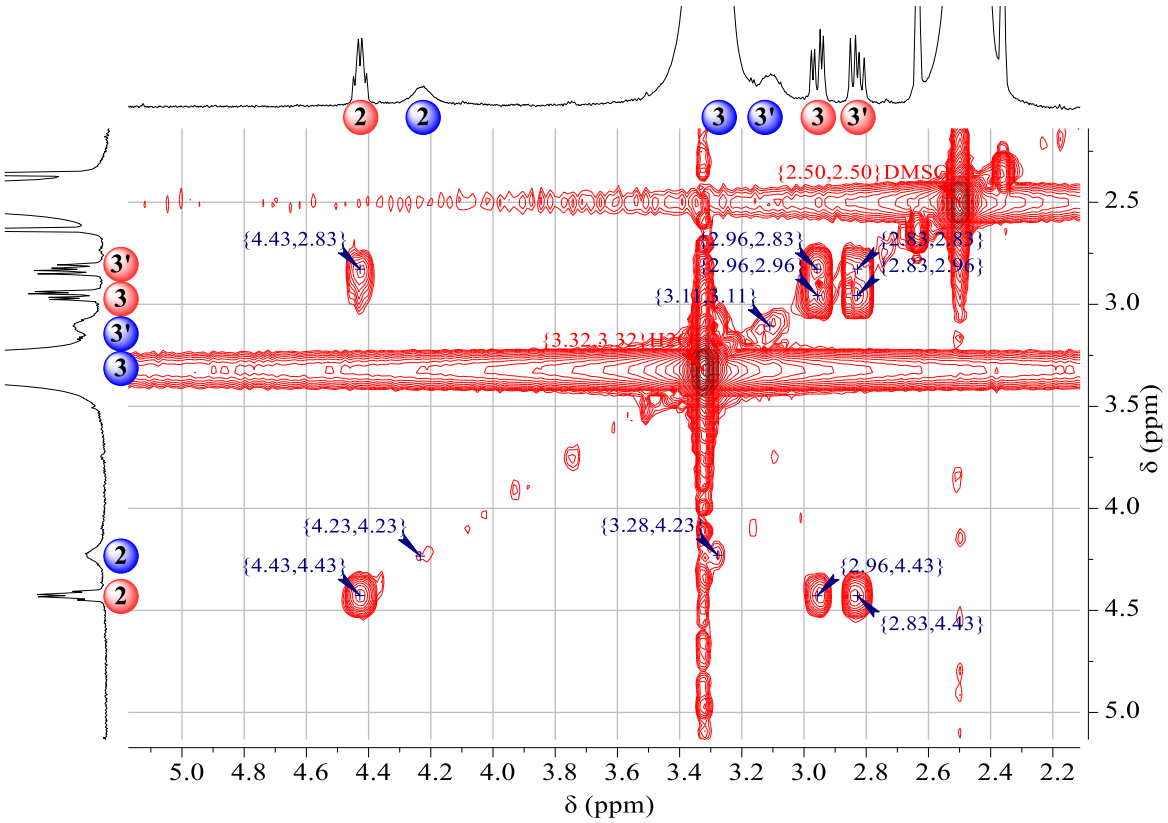
To a mixture of Trp-Tyr (36.7 mg, 0.1 mmol), sodium trifluoromethanesulfinate (15.6 mg, 0.1 mmol), and iron(III) nitrate nonahydrate (40.4 mg, 0.1 mmol) in 1:9 AcOH:25 mM aqueous NH_4HCO_2 (1 mL) was added *tert*-butyl hydroperoxide solution (27.7 μL, 0.2 mmol, 70% in H_2O) before stirring at 40 ºC for 20 min. The solution was taken up in H_2O (10 mL) and added to an Oasis HLB Plus cartridge (Waters, part # 186000132, activated with 2 mL MeOH, 10 mL H_2O) before eluting the crude product with MeOH (5 mL). The MeOH was evaporated, the desired product was isolated using reverse phase preparative HPLC and lyophilised. **Reverse phase HPLC details**: Phenomenex Synergi^{TM} 4 μm Hydro RP 80 Å, 250 x 10 mm, flow rate = 4 mL/min, column temperature = 40 °C, eluent = 17% MeCN (0.1% TFA) and 83% H_2O (0.1% TFA) for 3 min then increase linearly to 32% MeCN at 25 min then another linear increase to 36% MeCN (0.1% TFA) at 27 min, retention time = 21.6. min; **^{1}H NMR** (500 MHz, DMSO-d_6): δ 12.83 (s, 1H), 11.69 (d, *J* = 2.0 Hz, 1H), 9.23 (s, 1H), 8.73 (s, 1H), 8.21 (s, 3H), 7.71 (d, *J* = 8.1 Hz, 1H), 7.54 (d, *J* = 2.0 Hz, 1H), 7.43 (d, *J* = 7.5 Hz, 1H), 7.26 – 7.23 (m, 1H), 7.03, (d, *J* = 8.5 Hz, 2H), 6.66 (d, *J* = 8.5 Hz, 2H), 4.45 – 4.41 (m, 1H), 4.29 – 4.18 (m, 1H), 3.14 – 3.07 (m, 1H), 2.96 (dd, *J* = 13.8, 5.3 Hz, 1H), 2.83 (dd, *J* = 14.0, 8.3 Hz, 1H), *observed indirectly from COSY since obscured by solvent*

peak: 3.30*;* **^{19}F NMR** (471 MHz, DMSO-d_6): δ -57.29, -74.95; **HRMS** (ESI$^+$): for $C_{21}H_{21}O_4N_3F_3$ $[M+H]^+$ requires *m/z* = 436.1479, found 436.1507.

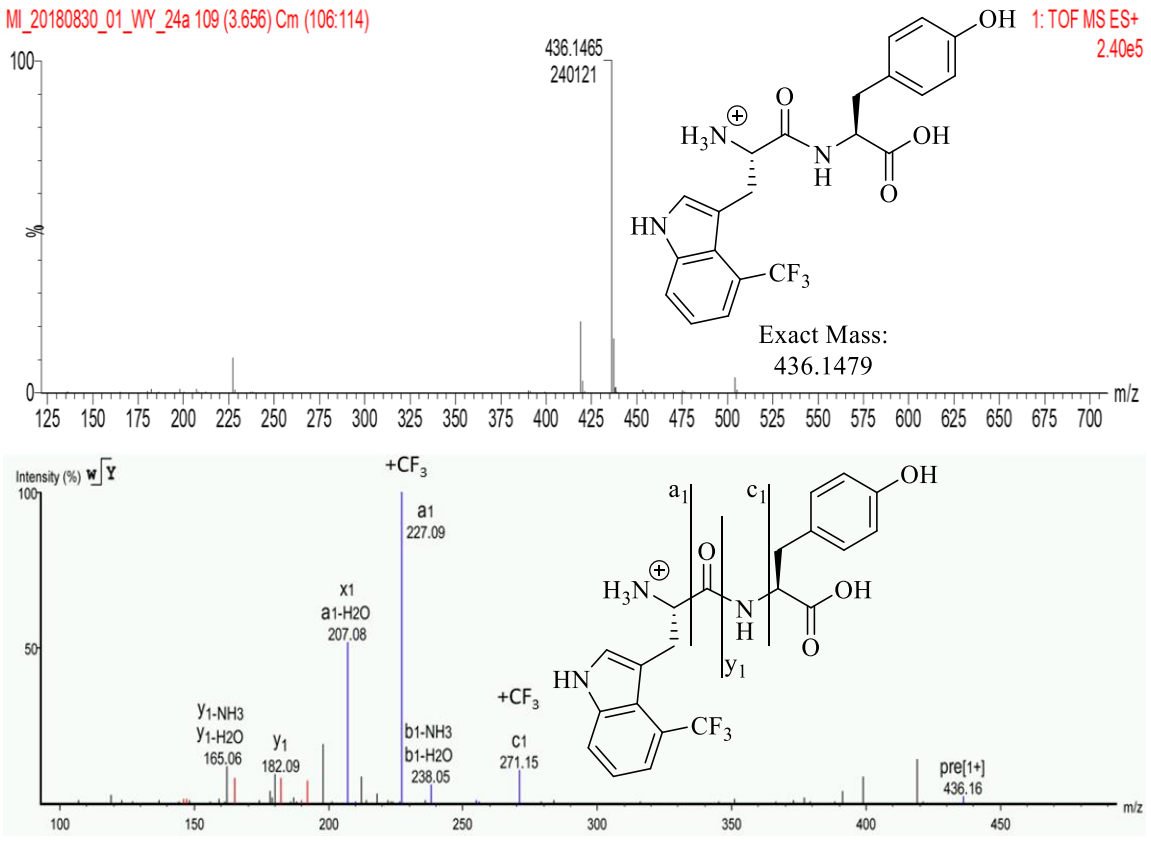
COSY Assignment



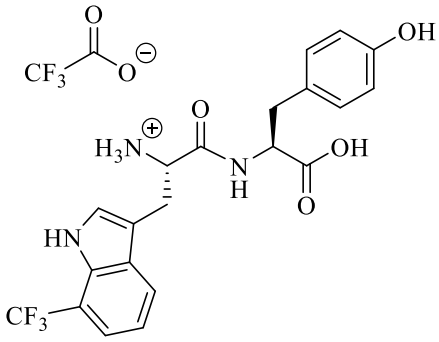

{7.02,6.66}
{6.66,6.66}
{7.02,7.02}
{7.71,7.25}
{7.43,7.25}
{7.25,7.25}
{7.43,7.43}
{7.54,7.54}
{7.71,7.70}
δ (ppm)
δ (ppm)


{2.50,2.50}DMSO
{4.43,2.83}
{2.96,2.83}
{2.96,2.96}
{2.83,2.83}
{2.83,2.96}
{3.11,3.11}
{4.23,4.23}
{4.43,4.43}
{3.28,4.23}
{2.96,4.43}
{2.83,4.43}
δ (ppm)
δ (ppm)

MS/MS Analysis



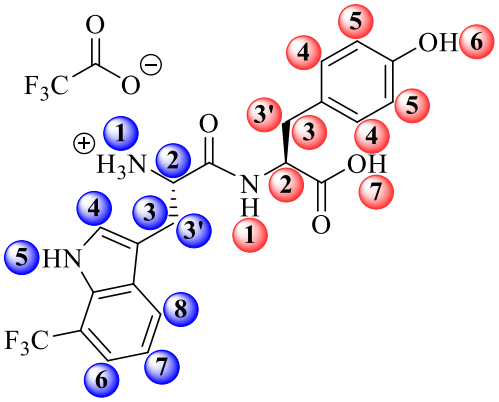
(*S*)-1-(((*S*)-1-Carboxy-2-(4-hydroxyphenyl)ethyl)amino)-1-oxo-3-(7-(trifluoromethyl)-1H-indol-3-yl)propan-2-aminium 2,2,2-trifluoroacetate

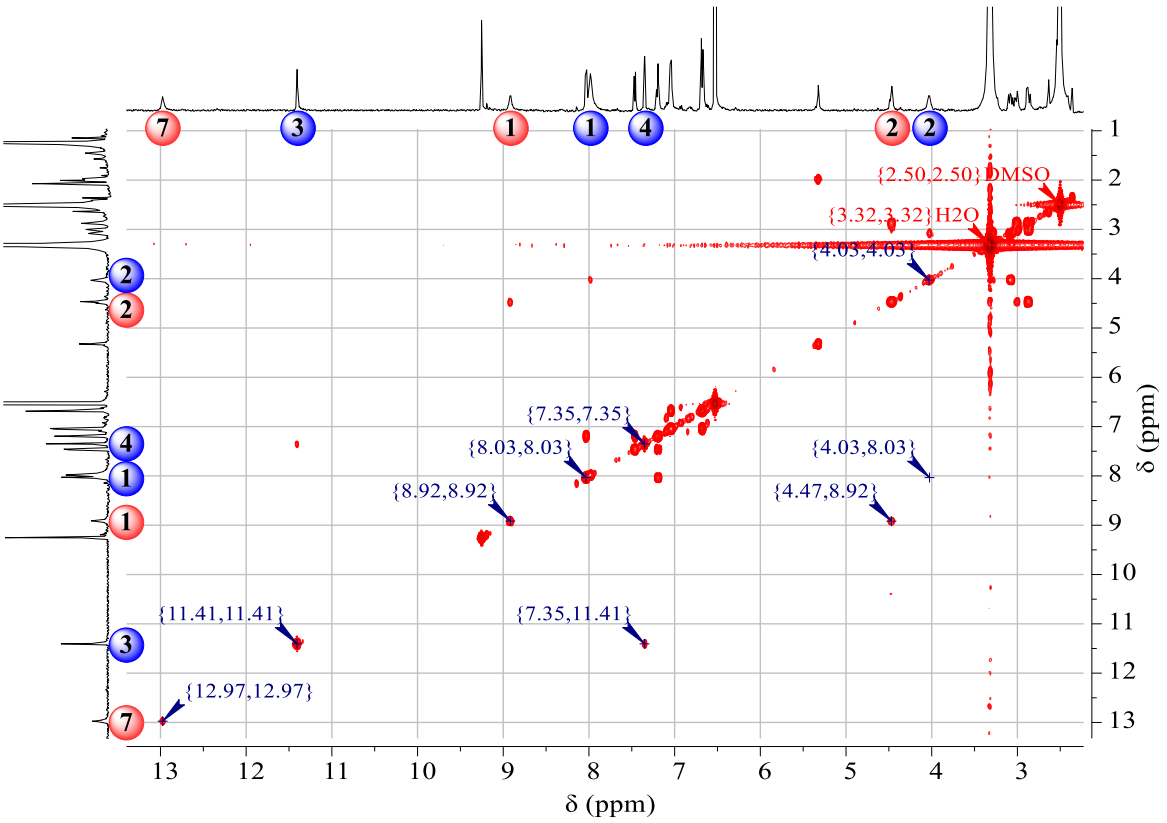


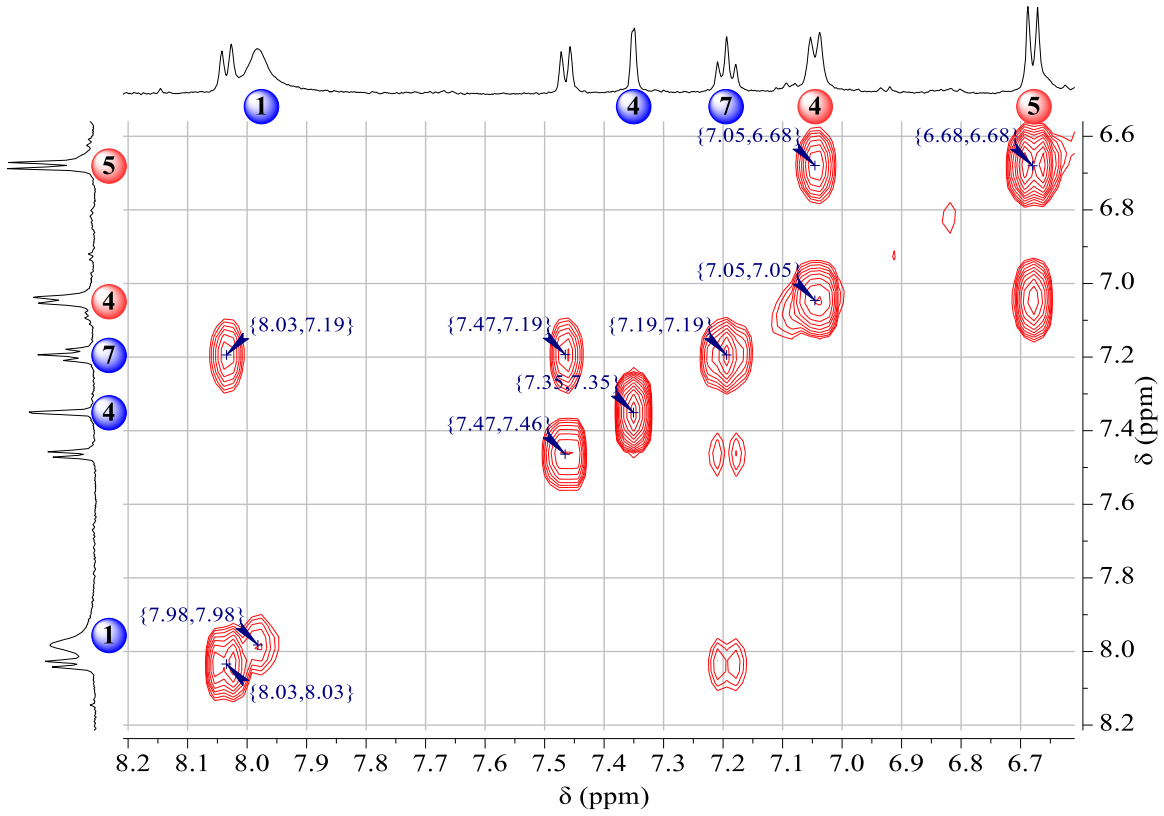
To a mixture of Trp-Tyr (36.7 mg, 0.1 mmol), sodium trifluoromethanesulfinate (15.6 mg, 0.1 mmol), and iron(III) nitrate nonahydrate (40.4 mg, 0.1 mmol) in 1:9 AcOH:25 mM aqueous NH_4HCO_2 (1 mL) was added *tert*-butyl hydroperoxide solution (27.7 μL, 0.2 mmol,

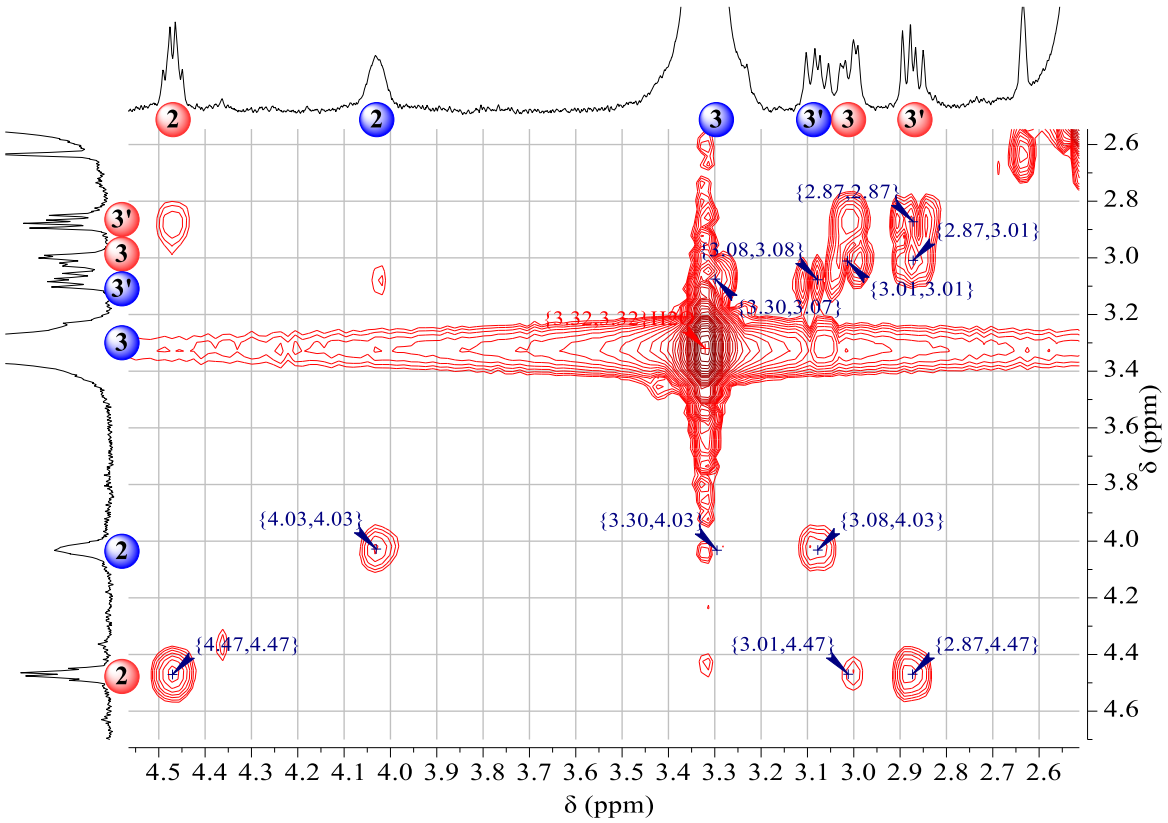
70% in H_2O) before stirring at 40 ºC for 20 min. The solution was taken up in H_2O (10 mL) and added to an Oasis HLB Plus cartridge (Waters, part # 186000132, activated with 2 mL MeOH, 10 mL H_2O) before eluting the crude product with MeOH (5 mL). The MeOH was evaporated, the desired product was isolated using reverse phase preparative HPLC and lyophilised. **Reverse phase HPLC details**: Phenomenex Synergi^{TM} 4 µm Hydro RP 80 Å, 250 x 10 mm, flow rate = 4 mL/min, column temperature = 40 °C, eluent = 17% MeCN (0.1% TFA) and 83% H_2O (0.1% TFA) for 3 min then increase linearly to 32% MeCN (0.1% TFA) at 25 min then another linear increase to 36% MeCN at 27 min, retention time = 24.0. min; **^{1}H NMR** (500 MHz, DMSO-d_6): δ 12.98 (s, 1H), 11.41 (s, 1H), 9.25 (s, 1H), 8.92 (d, *J* = 7.9 Hz, 1H), 8.03 (d, *J* = 8.1 Hz, 1H), 7.98 (s, 3H), 7.46 (d, *J* = 7.5 Hz, 1H), 7.35 (d, *J* = 2.5 Hz, 1H), 7.21 – 7.18 (m, 1H), 7.05 (d, *J* = 8.4 Hz, 2H), 6.68 (d, *J* = 8.4 Hz, 2H), 4.48 – 4.45 (m, 1H), 4.06 – 4.00 (m, 1H), 3.08 (dd, *J* = 15.0, 9.4 Hz, 1H), 3.01 (dd, *J* = 14.2, 5.1 Hz, 1H) 2.87 (dd, *J* = 13.8, 8.3 Hz, 1H), *observed indirectly from COSY since obscured by solvent peak*: 3.30; **^{19}F NMR** (471 MHz, DMSO-d_6): δ -61.18, -74.95; **HRMS** (ESI$^+$): for $C_{21}H_{21}O_4N_3F_3$ $[M+H]^+$ requires *m/z* = 436.1479, found 436.1465.

COSY Assignment

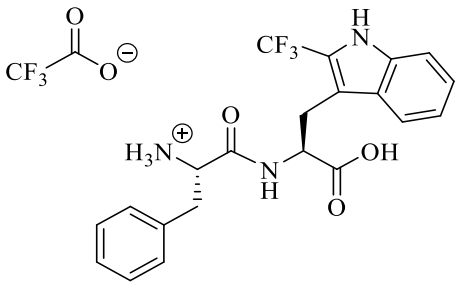



{2.50,2.50}DMSO
{3.32,3.32}H2O
{4.03,4.03}
{7.35,7.35}
{8.03,8.03}
{8.92,8.92}
{4.03,8.03}
{4.47,8.92}
{11.41,11.41}
{7.35,11.41}
{12.97,12.97}
δ (ppm)
δ (ppm)


{7.05,6.68}
{6.68,6.68}
{7.05,7.05}
{8.03,7.19}
{7.47,7.19}
{7.19,7.19}
{7.35,7.35}
{7.47,7.46}
{7.98,7.98}
{8.03,8.03}
δ (ppm)
δ (ppm)



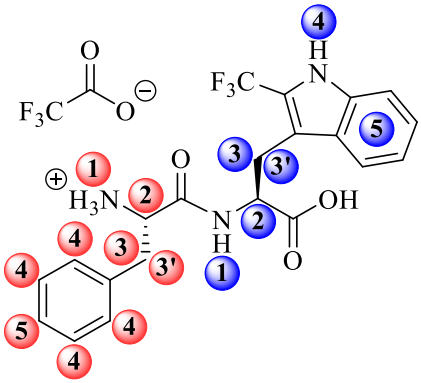
(*S*)-1-(((*S*)-1-Carboxy-2-(2-(trifluoromethyl)-1H-indol-3-yl)ethyl)amino)-1-oxo-3-phenylpropan-2-aminium 2,2,2-trifluoroacetate

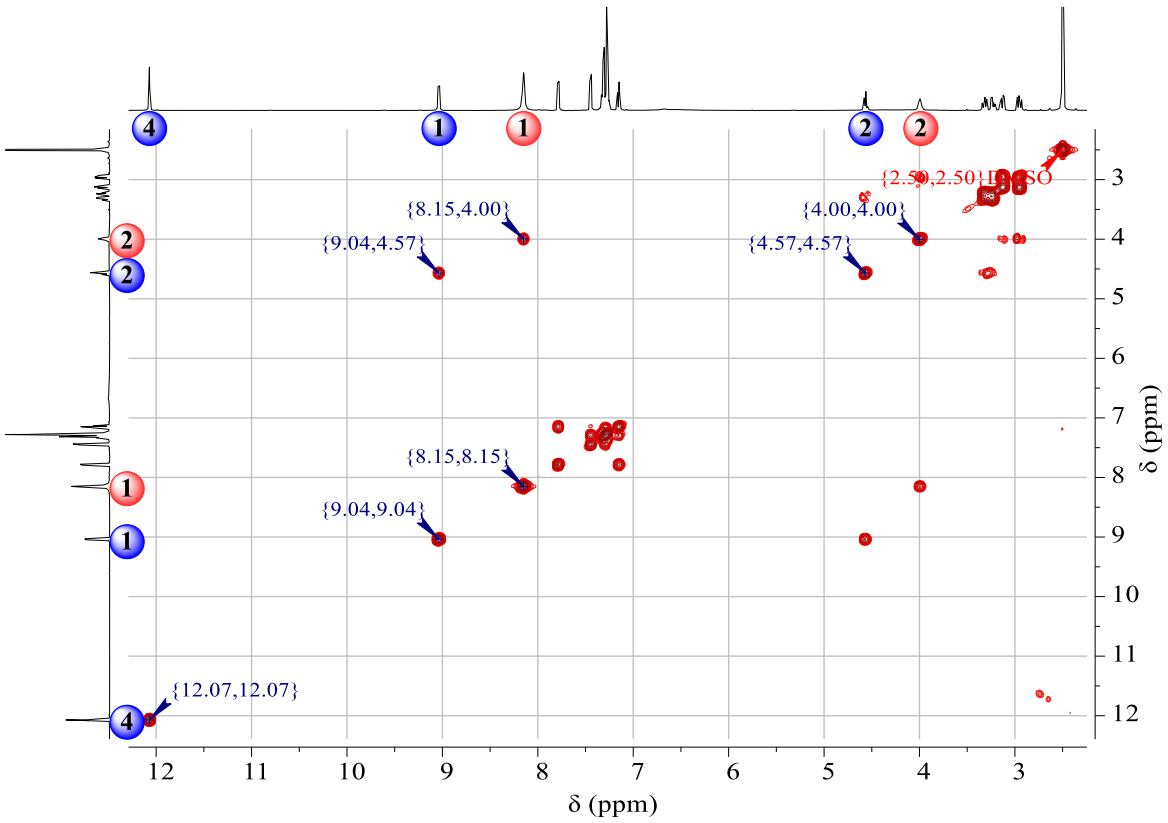


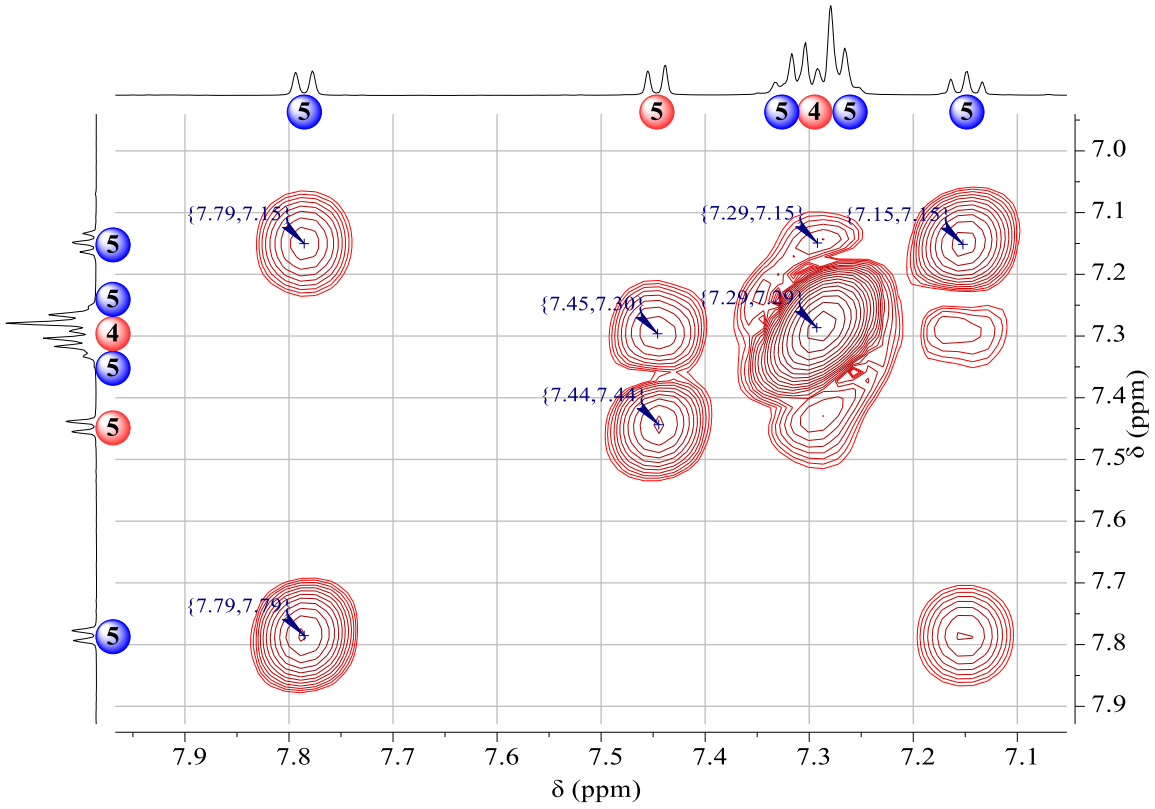
To a mixture of Phe-Trp (35.1 mg, 0.1 mmol), sodium trifluoromethanesulfinate (15.6 mg, 0.1 mmol), and iron(III) nitrate nonahydrate (40.4 mg, 0.1 mmol) in 1:9 AcOH:25 mM aqueous NH_4HCO_2 (1 mL) was added *tert*-butyl hydroperoxide solution (27.7 µL, 0.2 mmol, 70% in H_2O) before stirring at 40 ºC for 20 min. The solution was taken up in H_2O (10 mL) and added to an Oasis HLB Plus cartridge (Waters, part # 186000132, activated with 2 mL MeOH, 10 mL H_2O) before eluting the crude product with MeOH (5 mL). The MeOH was

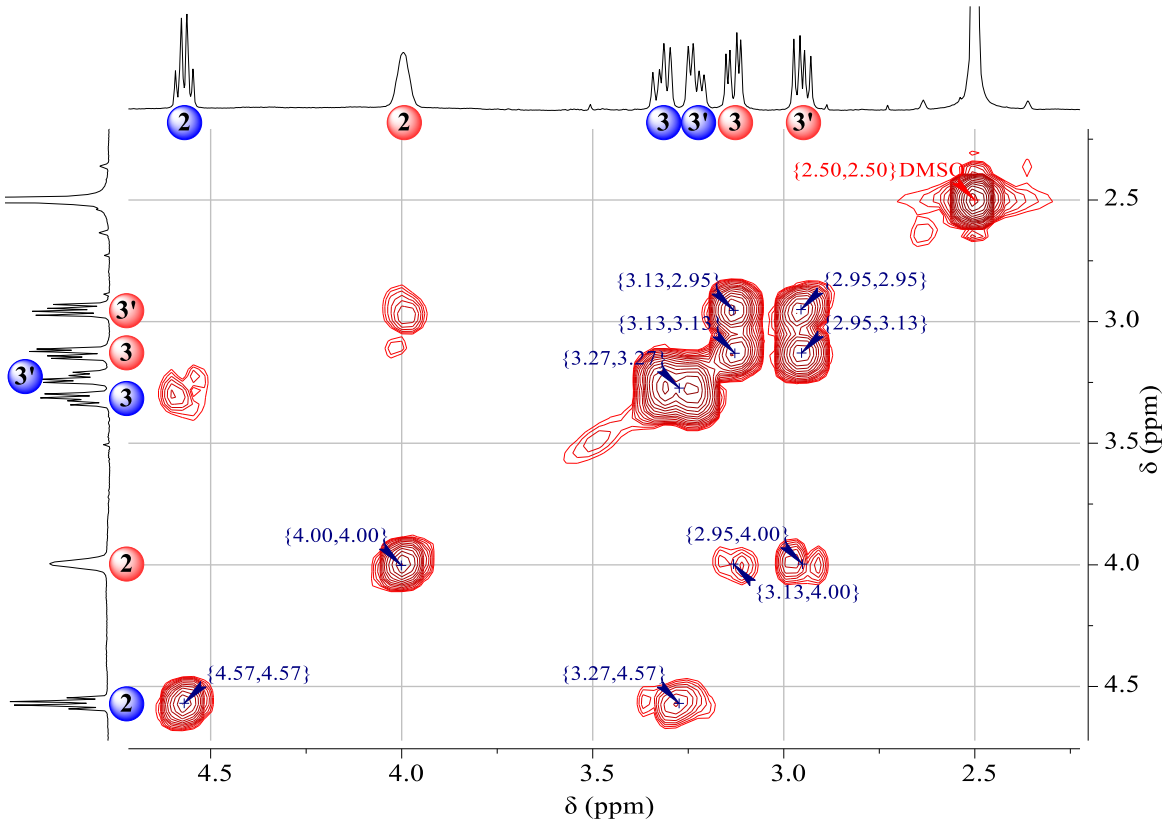
evaporated, the desired product was isolated using reverse phase preparative HPLC and lyophilised to obtain a white solid (9.5 mg, 0.0178 mmol, 18%). **Reverse phase HPLC details**: Phenomenex Synergi^{TM} 4 µm Hydro RP 80 Å, 250 x 10 mm, flow rate = 4 mL/min, column temperature = 40 °C, eluent = 15% MeCN (0.1% TFA) and 85% H_2O (0.1% TFA) for 3 min then increase linearly to 49% MeCN (0.1% TFA) at 25 min, retention time = 18.8 min; **^{1}H NMR** (500 MHz, DMSO-d_6): δ 12.94 (s, 1H), 12.07 (s, 1H), 9.04 (d, *J* = 8.1 Hz, 1H), 8.15 (s, 3H), 7.79 (d, *J* = 8.1 Hz, 1H), 7.45 (d, *J* = 8.2 Hz, 1H), 7.33 – 7.27 (m, 6H), 7.16 – 7.13 (m, 1H), 4.59 – 4.55 (m, 1H), 4.02 – 3.97 (m, 1H), 3.36 – 3.28 (ddd, *J* = 14.3, 8.3, 0.9 Hz, 1H), 3.23 (ddd, *J* = 14.3, 6.6, 0.9 Hz, 1H), 3.13 (dd, *J* = 14.2, 5.2 Hz, 1H), 2.95 (dd, *J* = 14.1, 8.1 Hz, 1H); **^{13}C NMR** (126 MHz, DMSO-d_6): δ 172.04, 167.98, 135.68, 134.72, 129.54, 128.56, 127.22, 126.73, 124.36, 122.16 (q, *J* = 269.1 Hz), 121.68 (q, *J* = 36.1 Hz), 120.11, 120.00, 112.40, 112.00 (q, *J* = 2.8 Hz), 53.38, 53.32, 36.81, 26.67; **^{19}F NMR** (471 MHz, DMSO-d_6): δ -57.48, -74.95; **HRMS** (ESI^{+}): for $C_{21}H_{21}F_3N_3O_3$ $[M+H]^+$ requires *m*/*z* = 420.1530, found 420.1527; $[\boldsymbol{\alpha}]_{\boldsymbol{D}}^{\mathbf{25}}$ = -71 ± 3° (*c* 0.051, H_2O).

COSY NMR

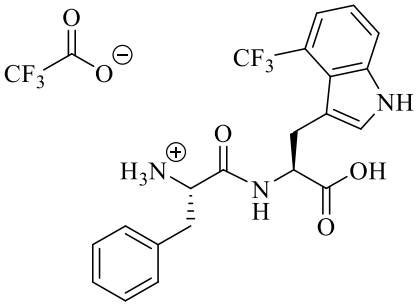



{8.15,4.00}
{9.04,4.57}
{4.00,4.00}
{4.57,4.57}
{8.15,8.15}
{9.04,9.04}
{12.07,12.07}
δ (ppm)
δ (ppm)


{7.79,7.15}
{7.29,7.15}
{7.15,7.15}
{7.45,7.30}
{7.44,7.44}
{7.79,7.79}
δ (ppm)
δ (ppm)



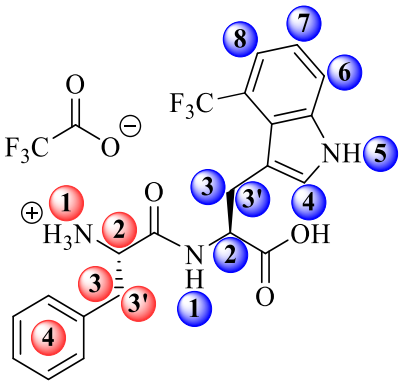
(*S*)-1-(((*S*)-1-Carboxy-2-(4-(trifluoromethyl)-1H-indol-3-yl)ethyl)amino)-1-oxo-3-phenylpropan-2-aminium 2,2,2-trifluoroacetate

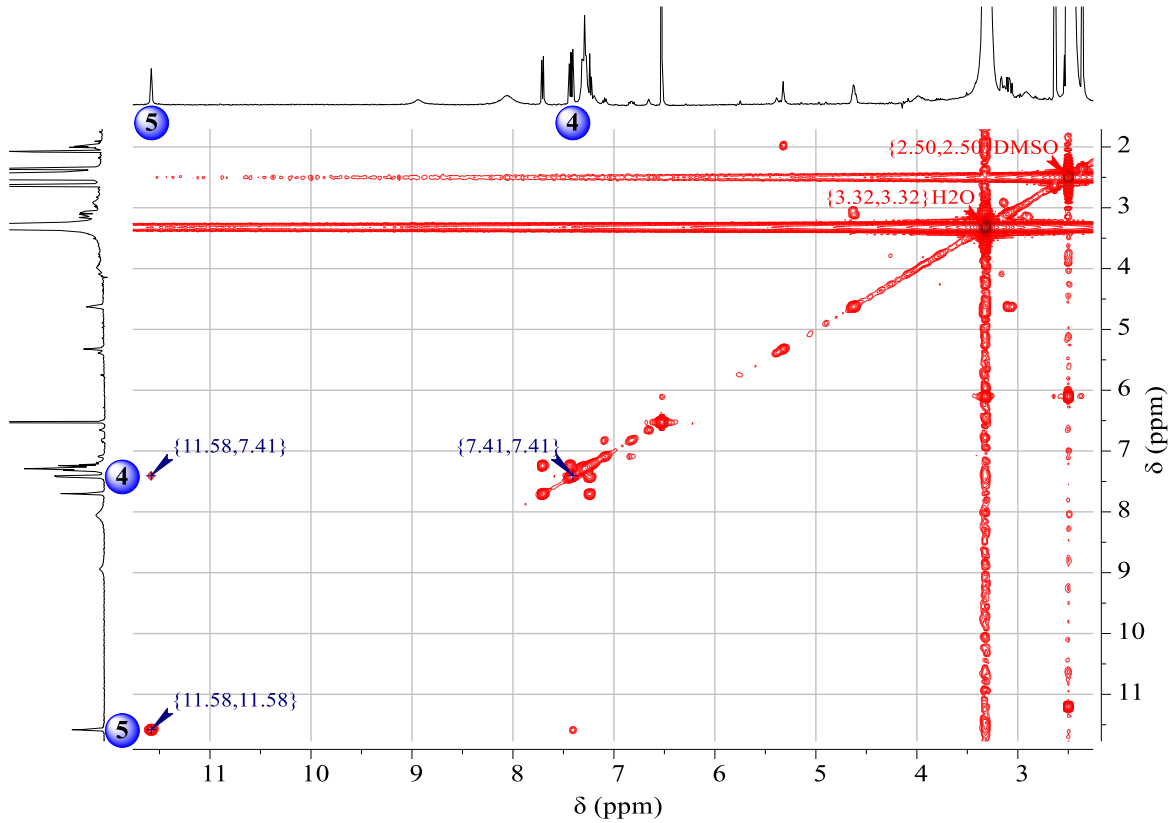


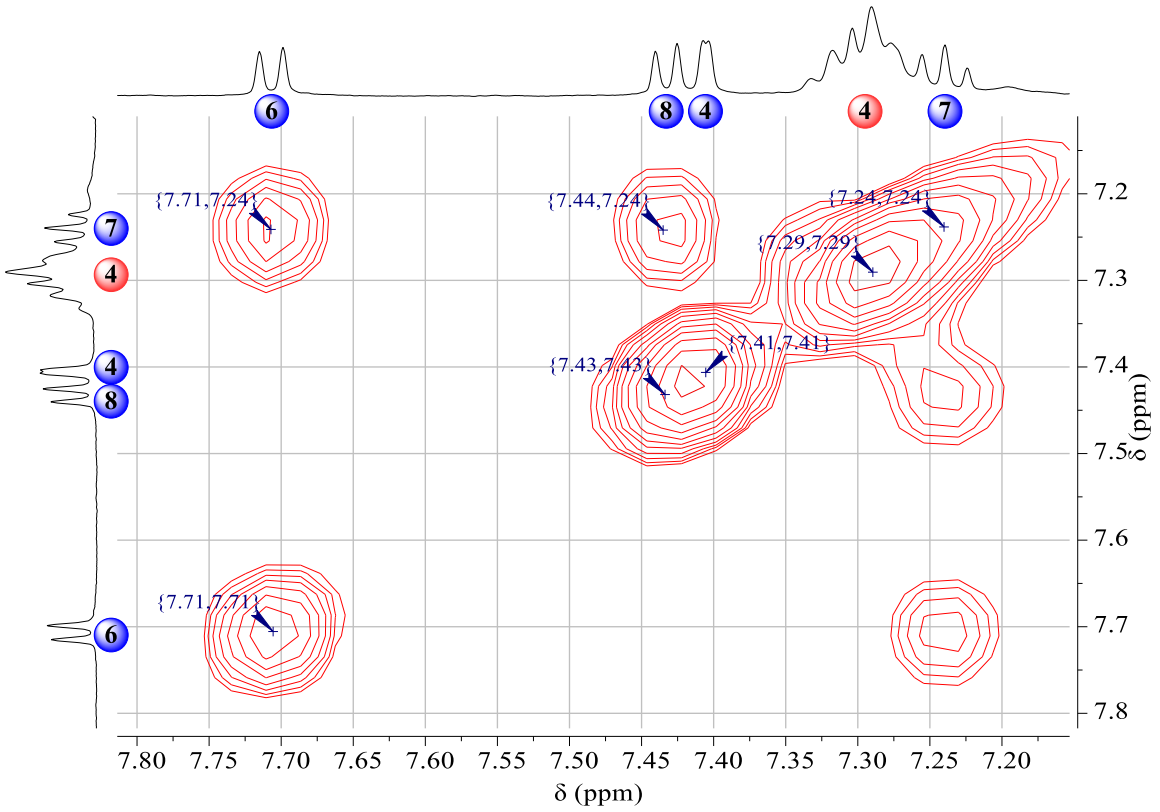
To a mixture of Phe-Trp (35.1 mg, 0.1 mmol), sodium trifluoromethanesulfinate (15.6 mg, 0.1 mmol), and iron(III) nitrate nonahydrate (40.4 mg, 0.1 mmol) in 1:9 AcOH:25 mM aqueous NH_4HCO_2 (1 mL) was added *tert*-butyl hydroperoxide solution (27.7 µL, 0.2 mmol, 70% in H_2O) before stirring at 40 ºC for 20 min. The solution was taken up in H_2O (10 mL) and added to an Oasis HLB Plus cartridge (Waters, part # 186000132, activated with 2 mL

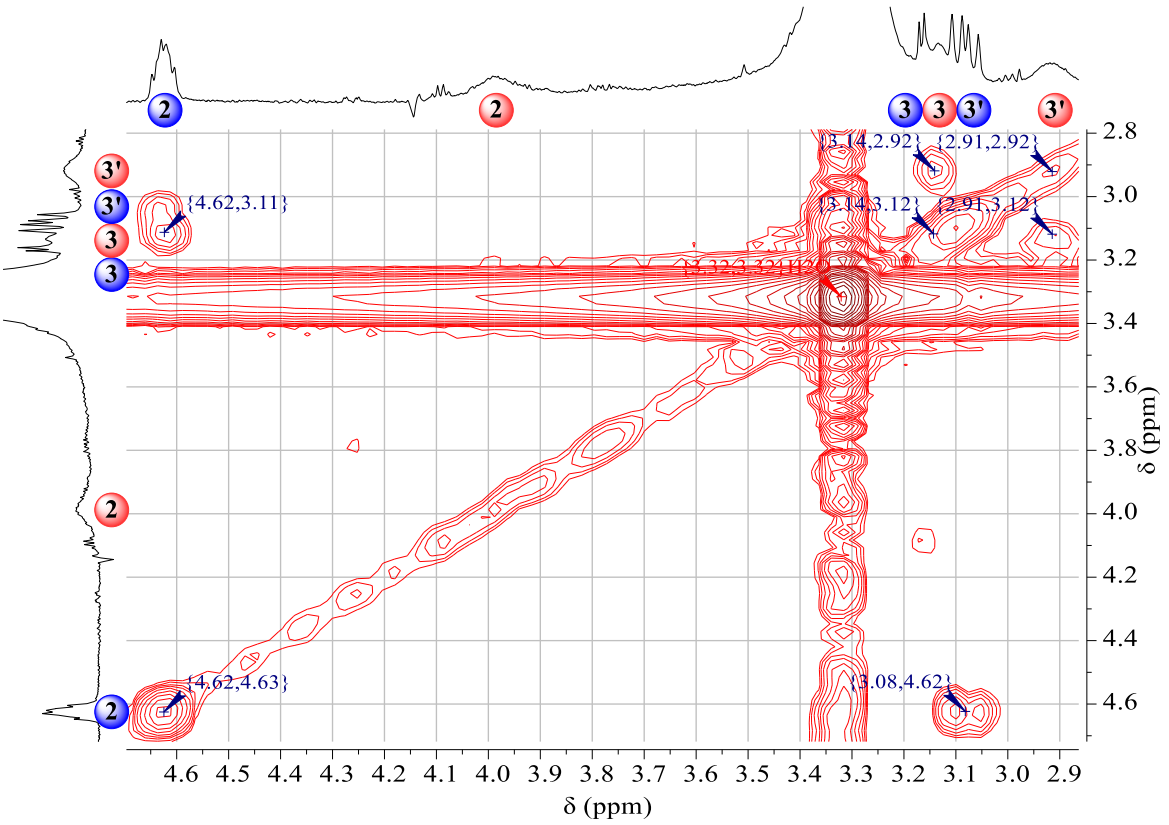
MeOH, 10 mL H_2O) before eluting the crude product with MeOH (5 mL). The MeOH was evaporated, the desired product was isolated using reverse phase preparative HPLC and lyophilised to obtain a white solid. **Reverse phase HPLC details**: Phenomenex Synergi™ 4 µm Hydro RP 80 Å, 250 x 10 mm, flow rate = 4 mL/min, column temperature = 40 °C, eluent = 15% MeCN (0.1% TFA) and 85% H_2O (0.1% TFA) for 3 min then increase linearly to 49% MeCN (0.1% TFA) at 25 min, retention time = 21.5 min; **^{1}H NMR** (500 MHz, DMSO-d_6): δ 12.92 (s, 1H), 11.58 (d, *J* = 2.2 Hz, 1H), 8.94 (s, 1H), 8.06 (s, 3H), 7.71 (d, *J* = 8.1 Hz, 1H), 7.43 (d, *J* = 7.5 Hz, 1H), 7.41 (d, *J* = 2.2 Hz, 1H),7.33 – 7.22 (m, 6H), 4.65 4.60 (m, 1H), 4.03 – 3.94 (m, 1H), 3.17 – 3.06 (m, 3H), 2.96 – 2.89 (m, 1H); **^{19}F NMR** (470 MHz, DMSO-d_6): δ -57.62, -74.95; **MS** (ESI^+): for $C_{21}H_{21}F_3N_3O_3$ $[M+H]^+$ requires *m/z* = 420.15, found 420.16.

COSY NMR

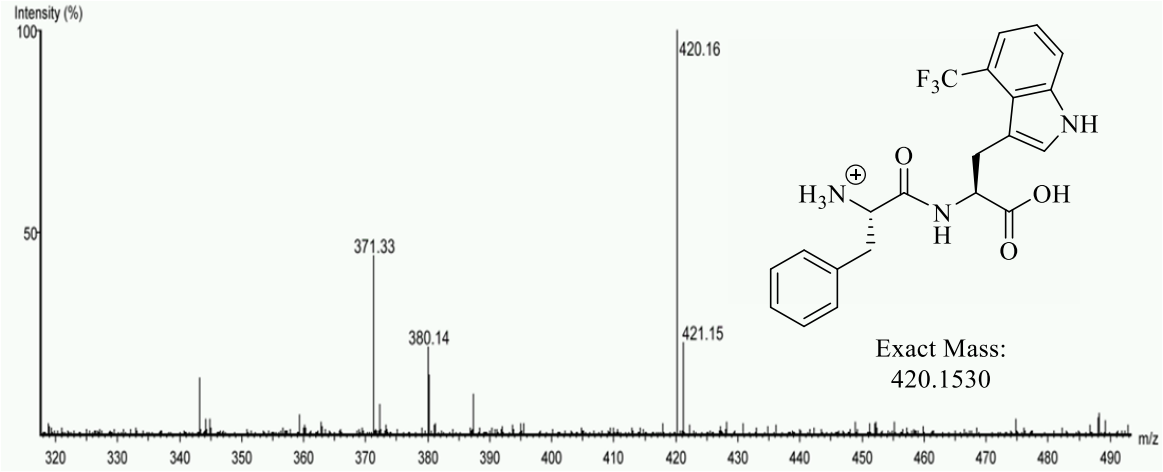


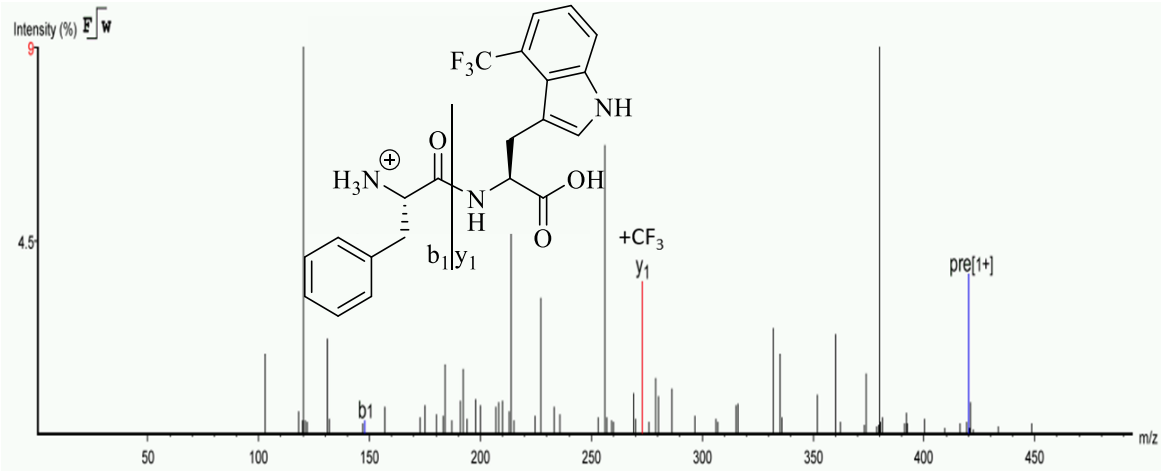

5
4
{2.50,2.50}DMSO
{3.32,3.32}H2O
{11.58,7.41}
{7.41,7.41}
{11.58,11.58}
δ (ppm)
δ (ppm)


6
8
4
4
7
{7.71,7.24}
{7.44,7.24}
{7.24,7.24}
{7.29,7.29}
{7.41,7.41}
{7.43,7.43}
{7.71,7.71}
δ (ppm)
δ (ppm)

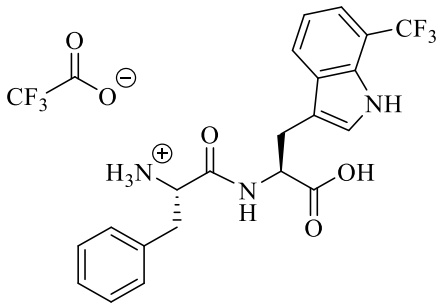


MS/MS Analysis





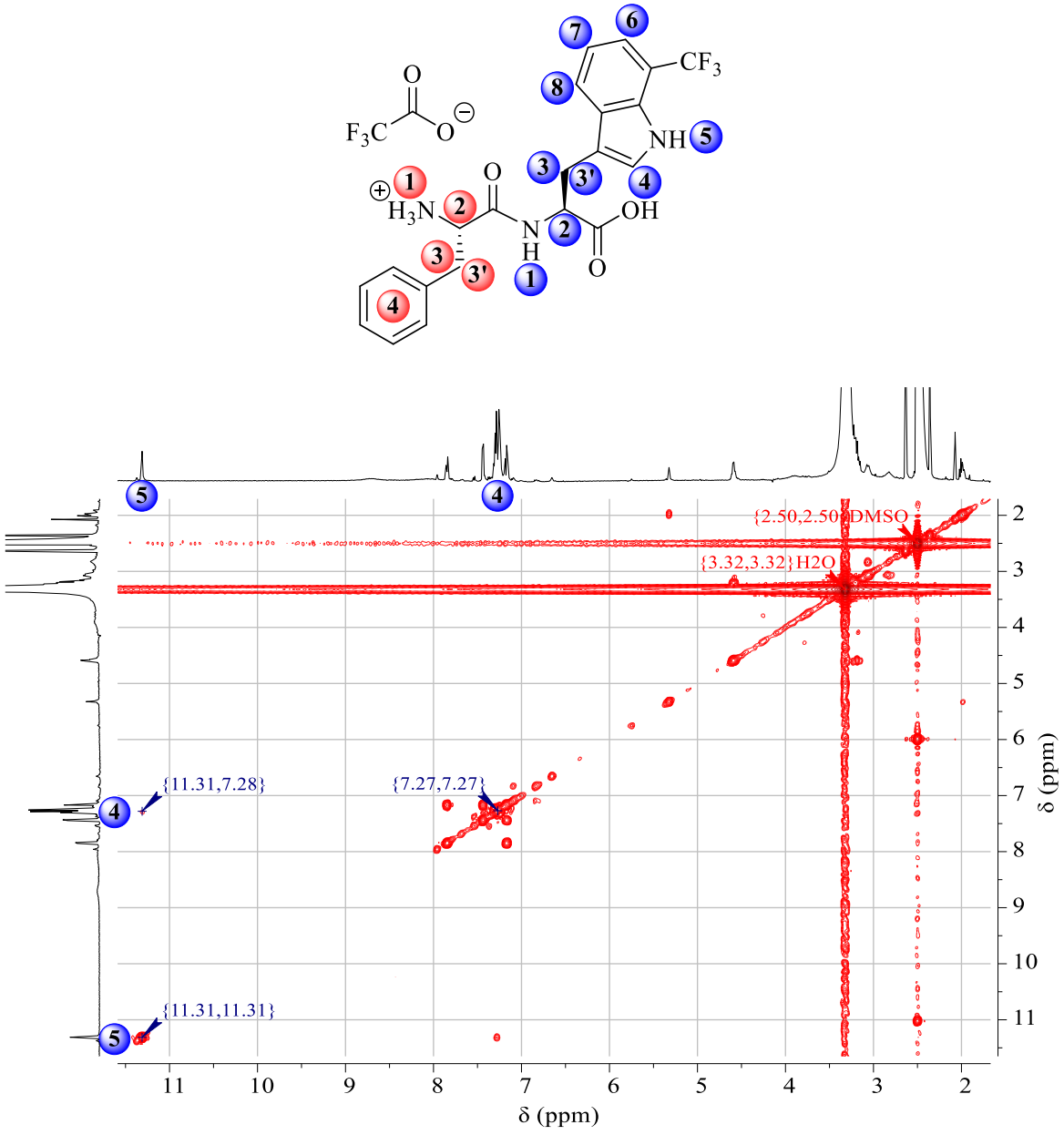
(*S*)-1-(((*S*)-1-Carboxy-2-(7-(trifluoromethyl)-1H-indol-3-yl)ethyl)amino)-1-oxo-3-phenylpropan-2-aminium 2,2,2-trifluoroacetate

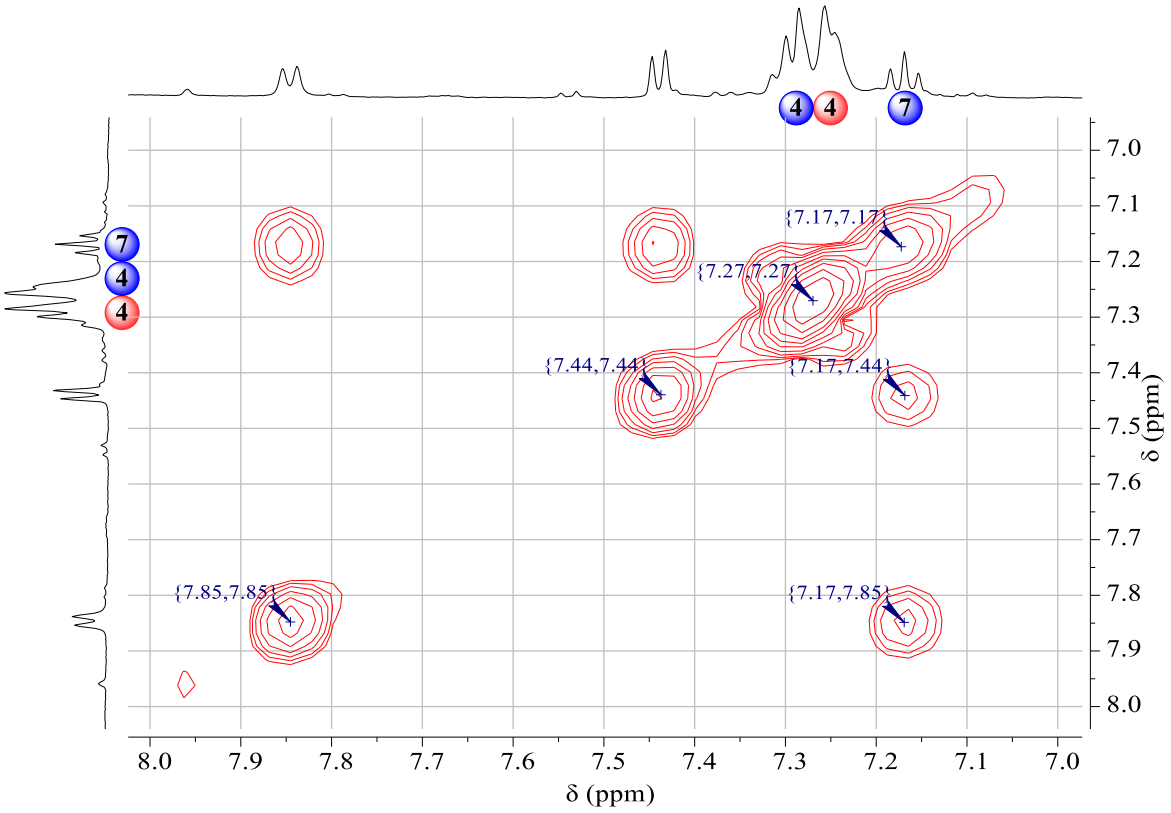


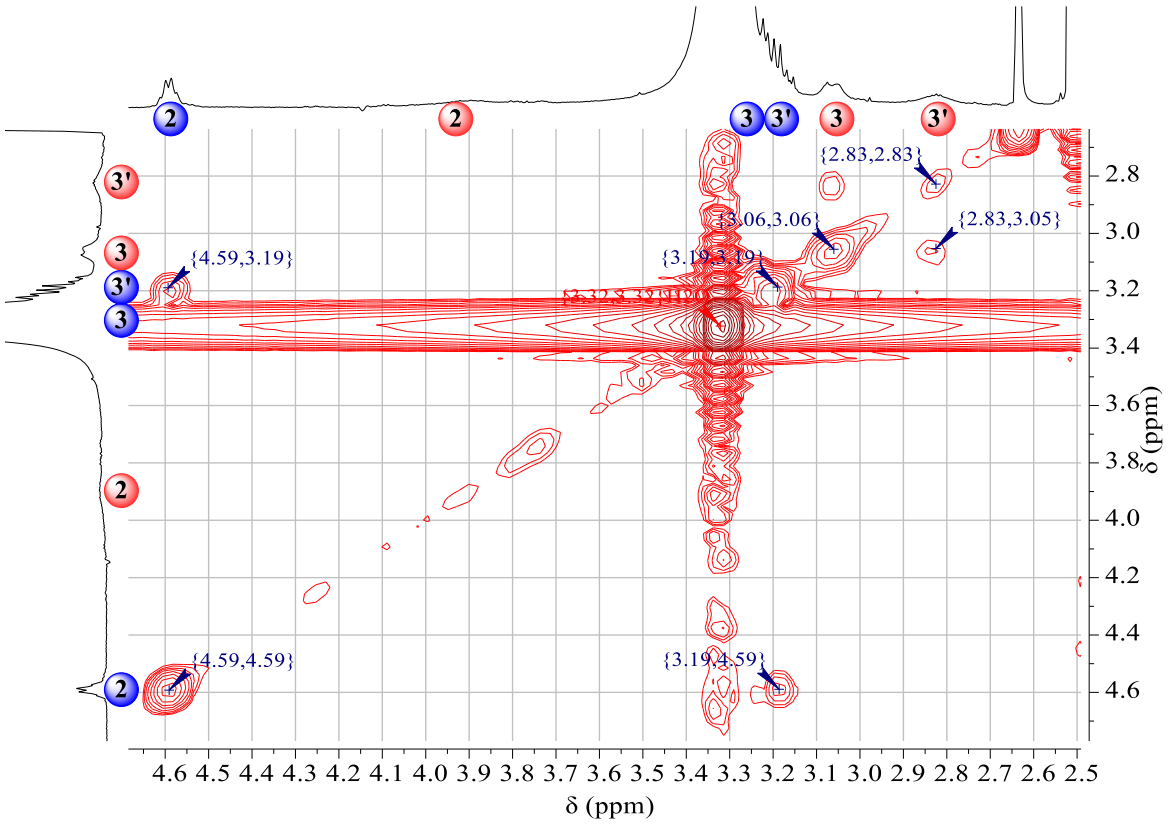
To a mixture of Phe-Trp (35.1 mg, 0.1 mmol), sodium trifluoromethanesulfinate (15.6 mg, 0.1 mmol), and iron(III) nitrate nonahydrate (40.4 mg, 0.1 mmol) in 1:9 AcOH:25 mM aqueous NH_4HCO_2 (1 mL) was added *tert*-butyl hydroperoxide solution (27.7 µL, 0.2 mmol, 70% in H_2O) before stirring at 40 ºC for 20 min. The solution was taken up in H_2O (10 mL) and added to an Oasis HLB Plus cartridge (Waters, part # 186000132, activated with 2 mL MeOH, 10 mL H_2O) before eluting the crude product with MeOH (5 mL). The MeOH was evaporated, the desired product was isolated using reverse phase preparative HPLC and lyophilised to obtain a white solid. **Reverse phase HPLC details**: Phenomenex Synergi™ 4 µm Hydro RP 80 Å, 250 x 10 mm, flow rate = 4 mL/min, column temperature = 40 °C, eluent = 15% MeCN (0.1% TFA) and 85% H_2O (0.1% TFA) for 3 min then increase linearly

to 49% MeCN (0.1% TFA) at 25 min, retention time = 21.1 min; **^{1}H NMR** (500 MHz, DMSO-d_6): δ 11.31 (s, 1H), 8.72 (s, 1H), 8.07 (s, 3H) 7.85 (d, J = 8.0 Hz, 1H), 7.44 (d, J = 7.4 Hz, 1H), 7.32 – 7.25 (m, 6H), 7.18 – 7.15 (m, 1H), 4.61 – 4.57 (m, 1H), 3.95 – 3.83 (m, 1H), 3.08 – 3.05 (m, 1H), 2.88 – 2.78 (m, 1H), *observed indirectly from COSY since obscured by solvent peak*: 3.19*;* **^{19}F NMR** (470 MHz, DMSO-d_6): δ -61.23, -74.95; **MS** (ESI$^+$): for $C_{21}H_{21}F_3N_3O_3$ $[M+H]^+$ requires m/z = 420.15, found 420.15.

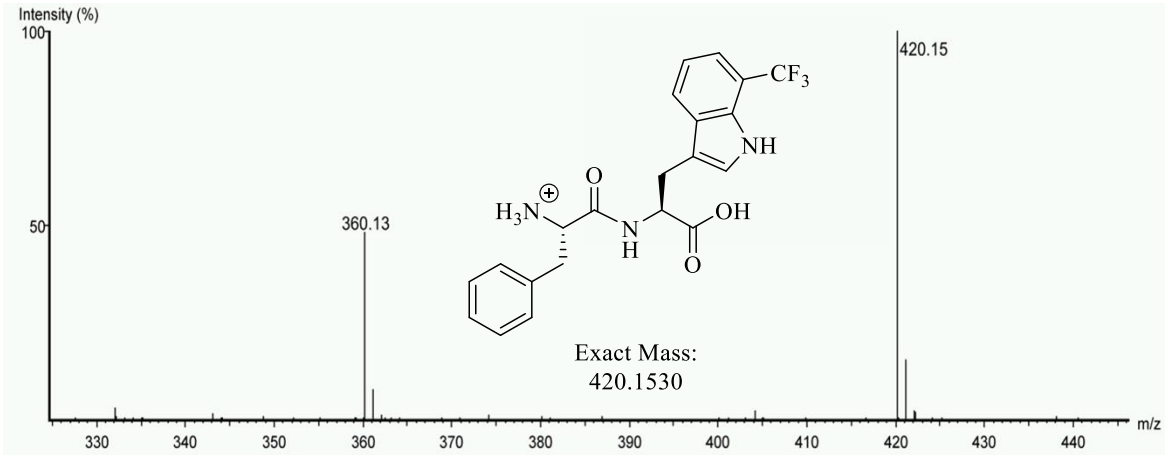
COSY NMR

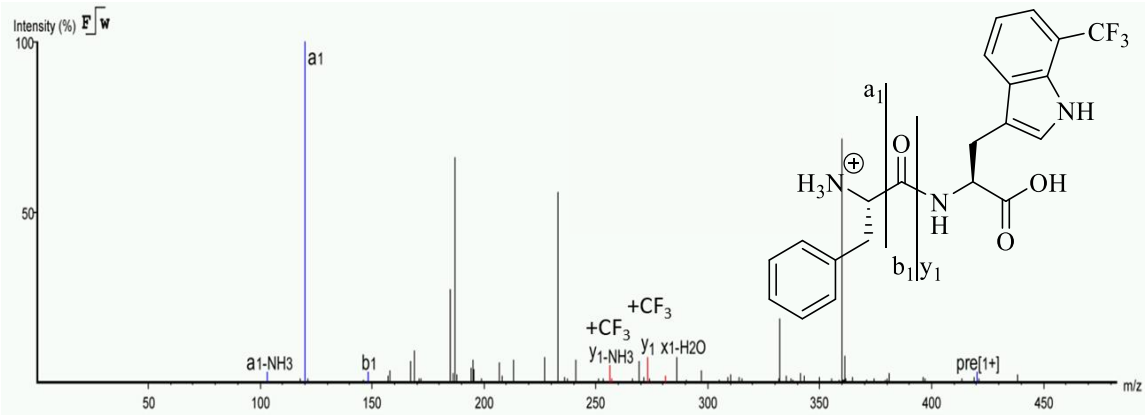



4
4
7
7
4
4
{7.17,7.17}
{7.27,7.27}
{7.44,7.44}
{7.17,7.44}
{7.85,7.85}
{7.17,7.85}
8.0 7.9 7.8 7.7 7.6 7.5 7.4 7.3 7.2 7.1 7.0
δ (ppm)
7.0 7.1 7.2 7.3 7.4 7.5 7.6 7.7 7.8 7.9 8.0
δ (ppm)

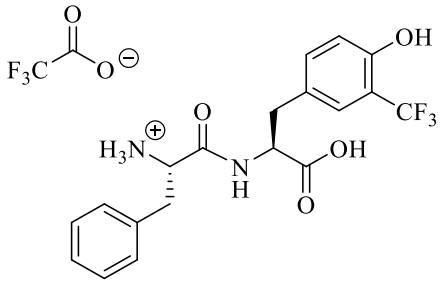

2
2
3
3'
3
3'
3'
3
3'
3
{2.83,2.83}
{3.06,3.06}
{2.83,3.05}
{4.59,3.19}
{3.19,3.19}
2
2
{4.59,4.59}
{3.19,4.59}
4.6 4.5 4.4 4.3 4.2 4.1 4.0 3.9 3.8 3.7 3.6 3.5 3.4 3.3 3.2 3.1 3.0 2.9 2.8 2.7 2.6 2.5
δ (ppm)
2.8 3.0 3.2 3.4 3.6 3.8 4.0 4.2 4.4 4.6
δ (ppm)

MS/MS Analysis





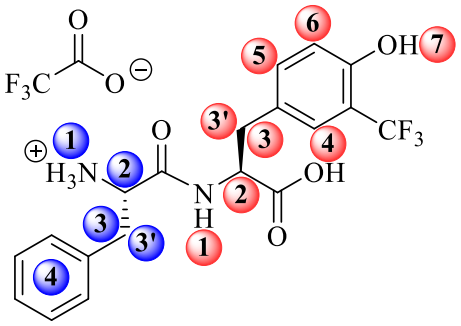
(*S*)-1-(((*S*)-1-Carboxy-2-(4-hydroxy-3-(trifluoromethyl)phenyl)ethyl)amino)-1-oxo-3-phenylpropan-2-aminium 2,2,2-trifluoroacetate

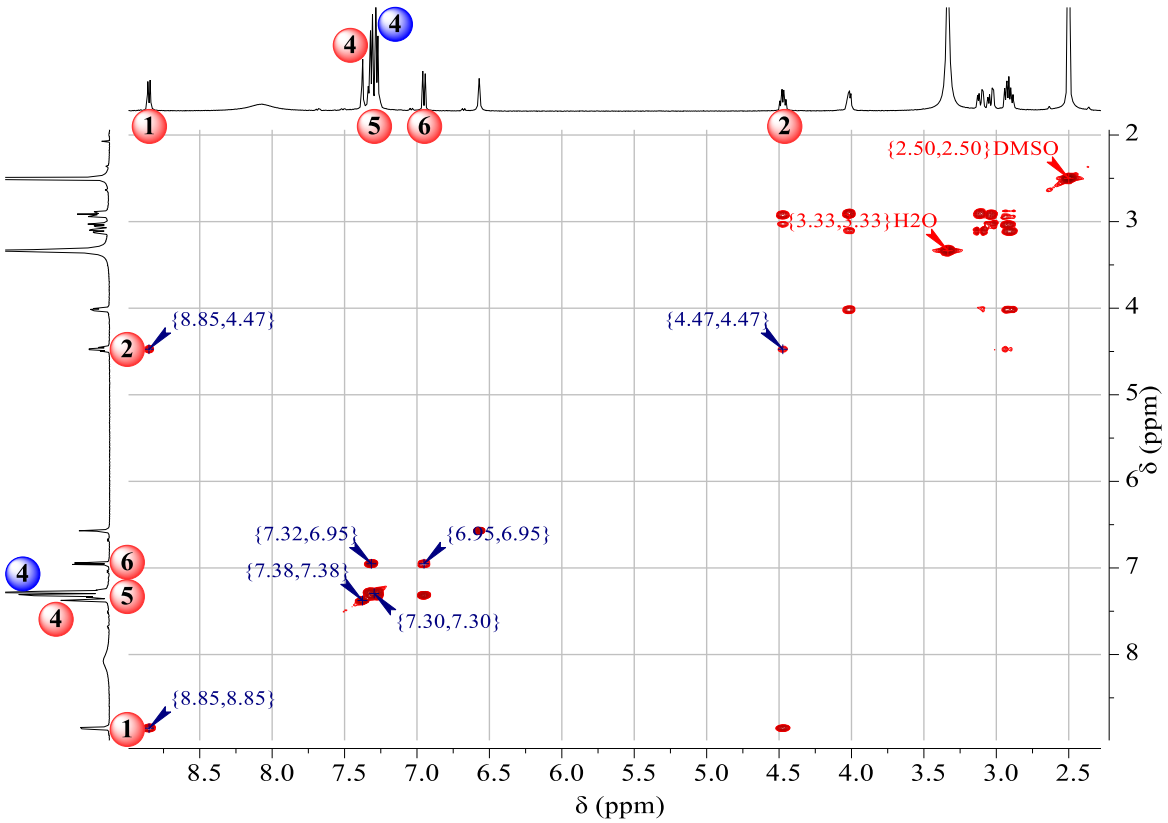


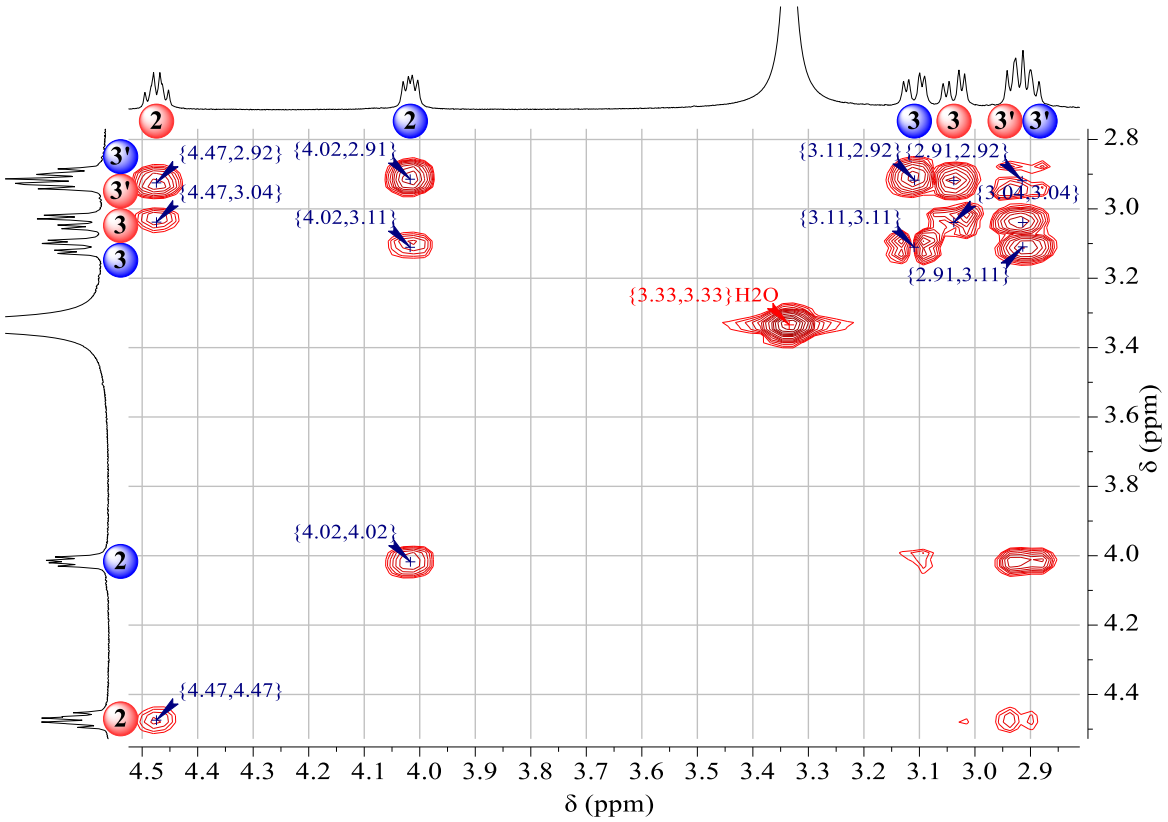
To a mixture of Phe-Tyr (32.8 mg, 0.1 mmol), sodium trifluoromethanesulfinate (15.6 mg, 0.1 mmol), and iron(III) nitrate nonahydrate (40.4 mg, 0.1 mmol) in 1:9 AcOH:25 mM

aqueous NH_4HCO_2 (1 mL) was added *tert*-butyl hydroperoxide solution (27.7 µL, 0.2 mmol, 70% in H_2O) before stirring at 40 ºC for 20 min. The solution was taken up in H_2O (10 mL) and added to an Oasis HLB Plus cartridge (Waters, part # 186000132, activated with 2 mL MeOH, 10 mL H_2O) before eluting the crude product with MeOH (5 mL). The MeOH was evaporated, the desired product was isolated using reverse phase preparative HPLC and lyophilised to obtain a white solid (34.7 mg, 0.0680 mmol, 68%). **Reverse phase HPLC details**: Phenomenex Synergi^{TM} 4 µm Hydro RP 80 Å, 250 x 10 mm, flow rate = 4 mL/min, column temperature = 40 °C, eluent = 28% MeCN (0.1% TFA) and 72% H_2O (0.1% TFA), retention time = 10.0 min; **^{1}H NMR** (500 MHz, DMSO-d_6) δ 13.05 (s, 1H), 10.50 (s, 1H), 8.85 (d, *J* = 7.9 Hz, 1H), 8.08 (s, 3H), 7.38 (d, *J* = 1.7 Hz, 1H), 7.34 – 7.27 (m, 6H), 6.95 (d, *J* = 8.4 Hz, 1H), 4.49 – 4.45 (m, 1H), 4.03 – 4.00 (m, 1H), 3.11 (dd, *J* = 14.3, 4.6 Hz, 1H), 3.04 (dd, *J* = 14.1, 5.2 Hz, 1H), 2.94 – 2.88 (m, 2H). *Carboxylic acid -OH is not observed.* **^{13}C NMR** (126 MHz, DMSO-d_6) δ 172.10, 168.20, 157.96, 157.71, 154.58, 134.71, 134.47, 129.56, 128.55, 127.20, 127.16, 127.12, 124.06 (q, *J* = 272.7 Hz), 116.91, 115.09 (q, *J* = 29 Hz), 53.84, 53.16, 36.98, 35.60. **^{19}F NMR** (470 MHz, DMSO-d_6) δ -62.25, -74.95. **HRMS** (ESI^+): for $C_{19}H_{20}O_4N_2F_3$ $[M+H]^+$ requires 397.1370 found 397.1371. **$[\alpha]_D^{25}$** = +28 ± 2° (*c* 0.044, H_2O).

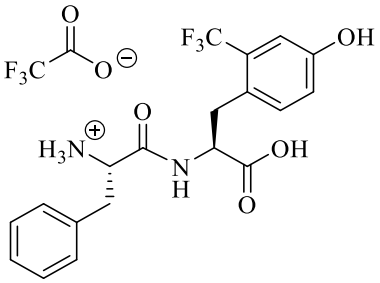
COSY NMR



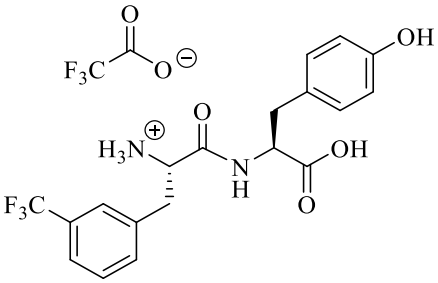

{2.50,2.50}DMSO
{3.33,3.33}H2O
{8.85,4.47}
{4.47,4.47}
{7.32,6.95}
{6.95,6.95}
{7.38,7.38}
{7.30,7.30}
{8.85,8.85}
δ (ppm)
δ (ppm)


{4.47,2.92}
{4.02,2.91}
{4.47,3.04}
{4.02,3.11}
{3.11,2.92}
{2.91,2.92}
{3.04,3.04}
{3.11,3.11}
{2.91,3.11}
{3.33,3.33}H2O
{4.02,4.02}
{4.47,4.47}
δ (ppm)
δ (ppm)

(*S*)-1-(((*S*)-1-Carboxy-2-(4-hydroxy-2-(trifluoromethyl)phenyl)ethyl)amino)-1-oxo-3-phenylpropan-2-aminium 2,2,2-trifluoroacetate and (*S*)-1-(((*S*)-1-carboxy-2-(4-hydroxyphenyl)ethyl)amino)-1-oxo-3-(3-(trifluoromethyl)phenyl)propan-2-aminium 2,2,2-trifluoroacetate



Phe-Tyr(2-CF_3)



Phe(3-CF_3)-Tyr

To a mixture of Phe-Tyr (32.8 mg, 0.1 mmol), sodium trifluoromethanesulfinate (15.6 mg, 0.1 mmol), and iron(III) nitrate nonahydrate (40.4 mg, 0.1 mmol) in 1:9 AcOH:25 mM aqueous NH_4HCO_2 (1 mL) was added *tert*-butyl hydroperoxide solution (27.7 μL, 0.2 mmol, 70% in H_2O) before stirring at 40 ºC for 20 min. The solution was taken up in H_2O (10 mL) and added to an Oasis HLB Plus cartridge (Waters, part # 186000132, activated with 2 mL MeOH, 10 mL H_2O) before eluting the crude product with MeOH (5 mL). The MeOH was evaporated, the desired product was isolated using reverse phase preparative HPLC and lyophilised to obtain a white solid (34.7 mg, 0.0680 mmol, 68%). **Reverse phase HPLC details**: Phenomenex Synergi^{TM} 4 μm Hydro RP 80 Å, 250 x 10 mm, flow rate = 4 mL/min, column temperature = 40 °C, eluent = 20% MeCN (0.1% TFA) and 80% H_2O (0.1% TFA) then increase linearly to 30% MeCN (0.1% TFA) and 70% H_2O (0.1% TFA), retention time = 18.6 min.

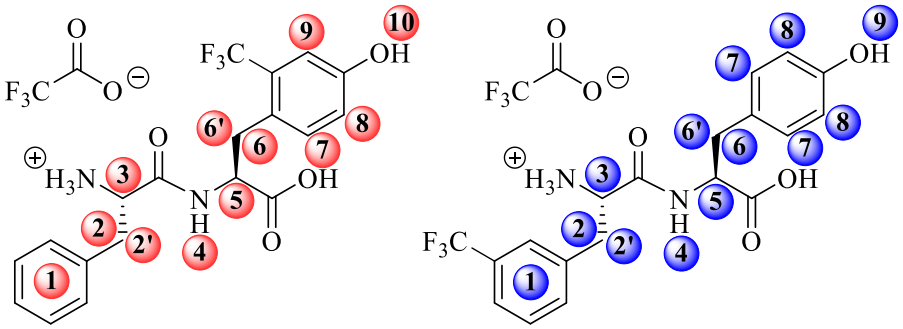
Phe-Tyr(2-CF_3)

^{1}H NMR (500 MHz, DMSO-d_6) δ 10.04 (s, 1H), 8.98 (d, *J* = 8.3 Hz, 1H), 8.07 (s, 3H), 7.36 – 7.28 (m, 6H), 7.06 (d, *J* = 2.6 Hz, 1H), 6.98 (dd, *J* = 8.5, 2.6 Hz, 1H), 4.51 – 4.45 (m, 1H), 4.02 – 4.00 (m, 1H), 3.23 – 3.14 (m, 2H), 2.98 – 2.93 (m, 2H), *carboxylic acid OH was not observed.* **^{19}F NMR** (470 MHz, DMSO-d_6) δ -59.96, -74.95. **MS** (ESI^+): for $C_{19}H_{20}O_4N_2F_3$ $[M+H]^+$ requires 397.14 found 397.15.

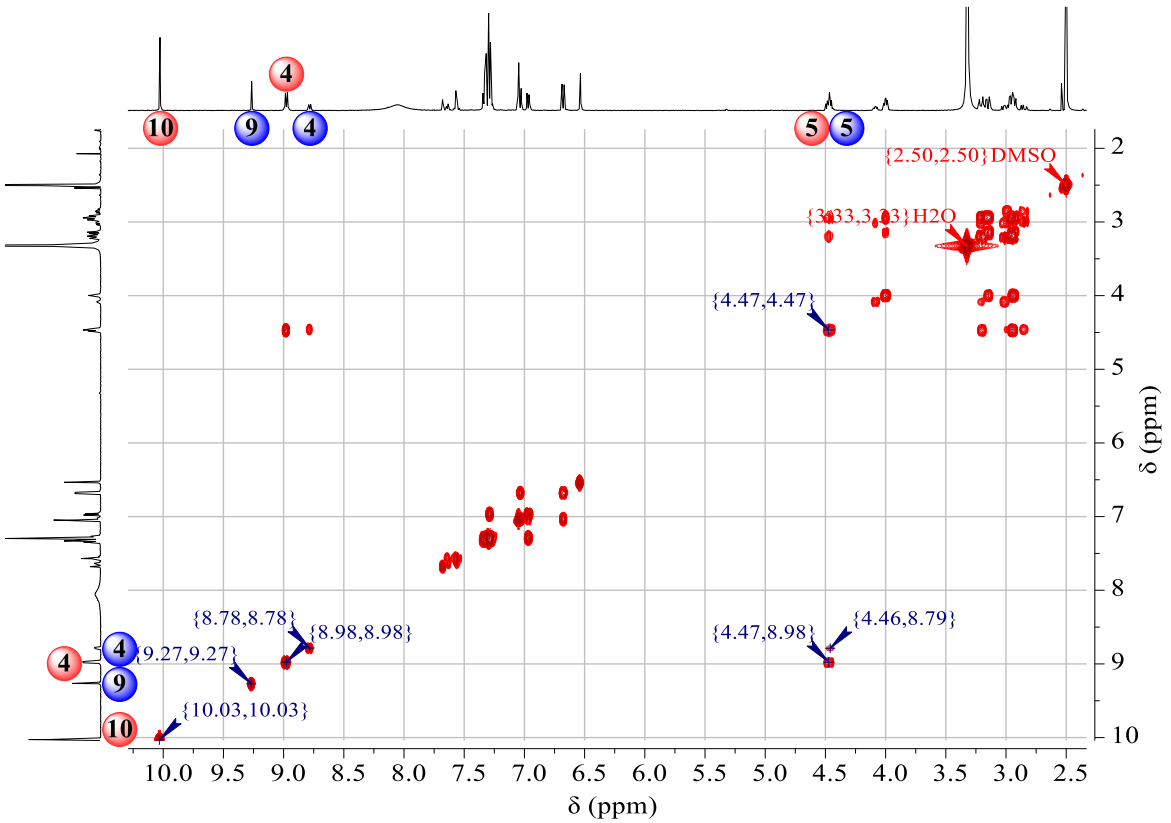
Phe(3-CF_3)-Tyr

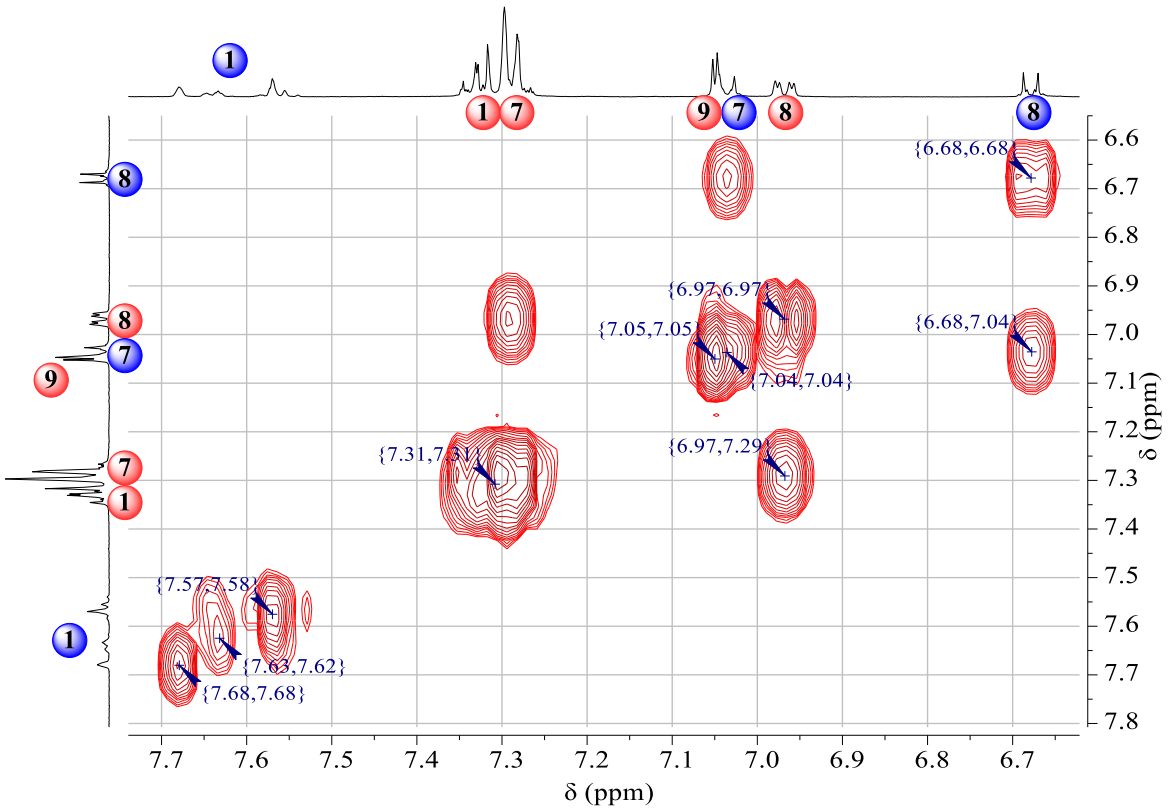
^{1}H NMR (500 MHz, DMSO-d_6) δ 9.27 (s, 1H), 8.79 (d, *J* = 7.9 Hz, 1H), 8.07 (s, 3H), 7.69 (s, 1H), 7.66 – 7.4 (m, 1H), 7.61 – 7.51 (m, 1H), 7.59 – 7.55 (m, 2H), 7.05 (d, *J* = 8.6 Hz, 2H), 6.69 (d, *J* = 8.6 Hz, 2H), 4.51 – 4.45 (m, 1H), 4.11 – 4.08 (m, 1H), 3.23 – 3.14 (m, 1H), 3.04 – 2.99 (m, 2H), 2.88 – 2.84 (m, 1H), *carboxylic acid OH was not observed.* **^{19}F NMR** (470 MHz, DMSO-d_6) δ -62.48, -74.95; **MS** (ESI^+): for $C_{19}H_{20}O_4N_2F_3$ $[M+H]^+$ requires 397.14 found 397.15.

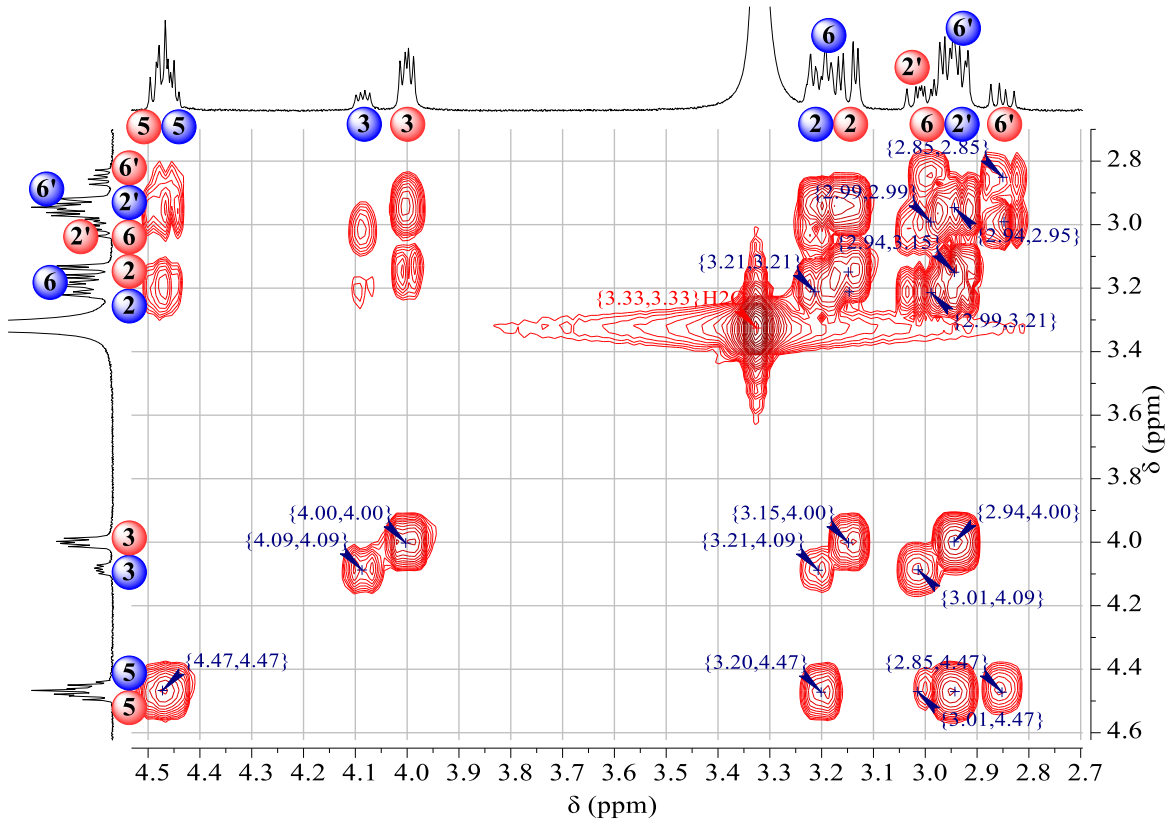
COSY NMR



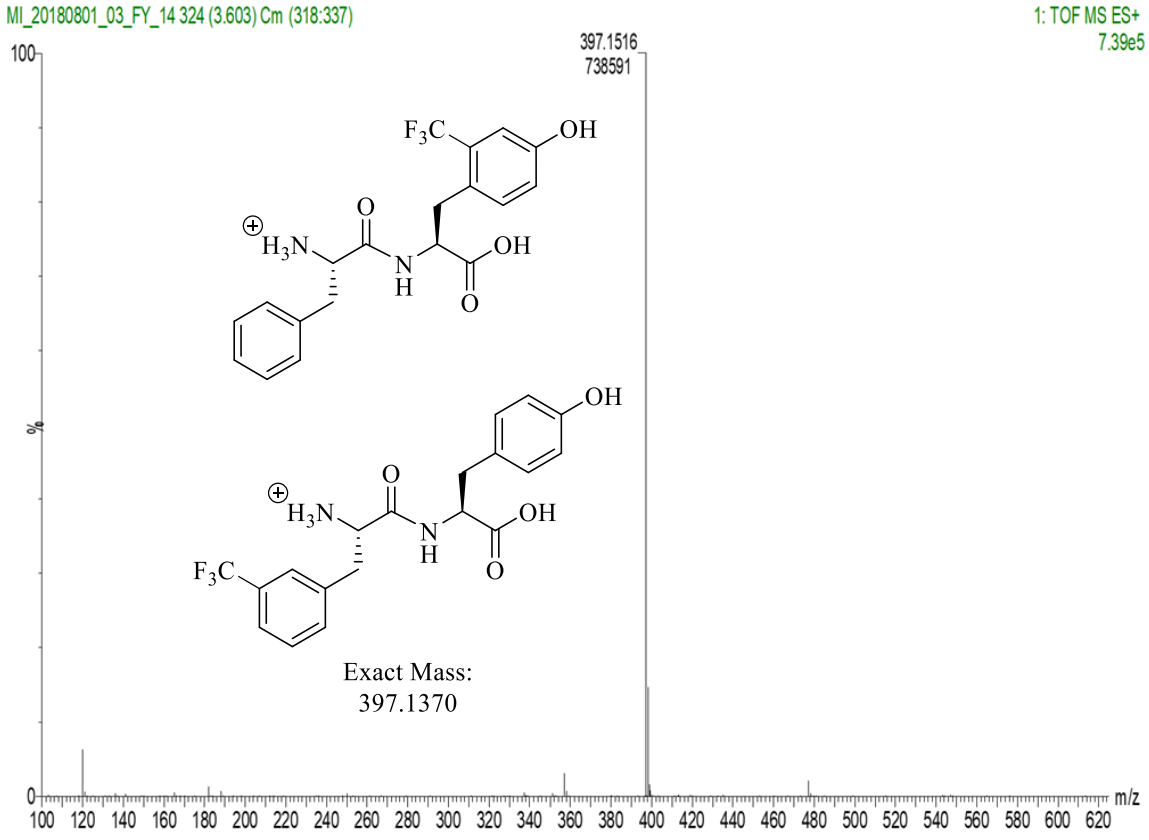
Phe-Tyr(2-CF_3) **Phe(3-CF_3)-Tyr**

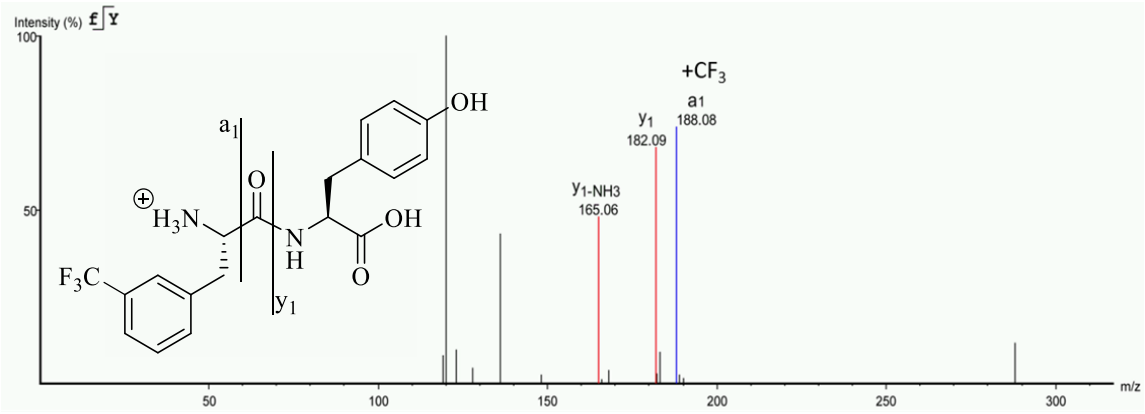

{2.50,2.50}DMSO
{3.33,3.33}H2O
{4.47,4.47}
{8.78,8.78}
{8.98,8.98}
{9.27,9.27}
{10.03,10.03}
{4.47,8.98}
{4.46,8.79}
δ (ppm)
δ (ppm)

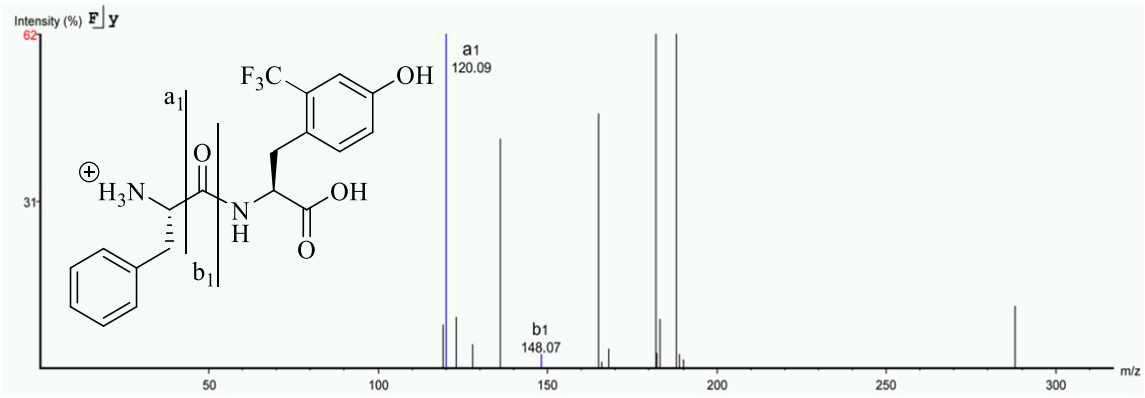

{6.68,6.68}
{6.97,6.97}
{7.05,7.05}
{7.04,7.04}
{6.68,7.04}
{7.31,7.31}
{6.97,7.29}
{7.57,7.58}
{7.63,7.62}
{7.68,7.68}
δ (ppm)
δ (ppm)



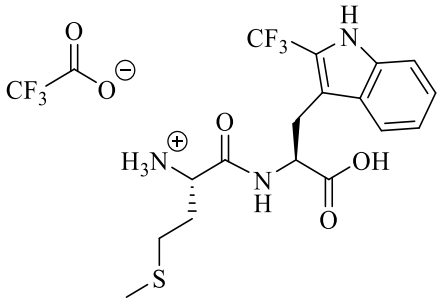
MS/MS Analysis







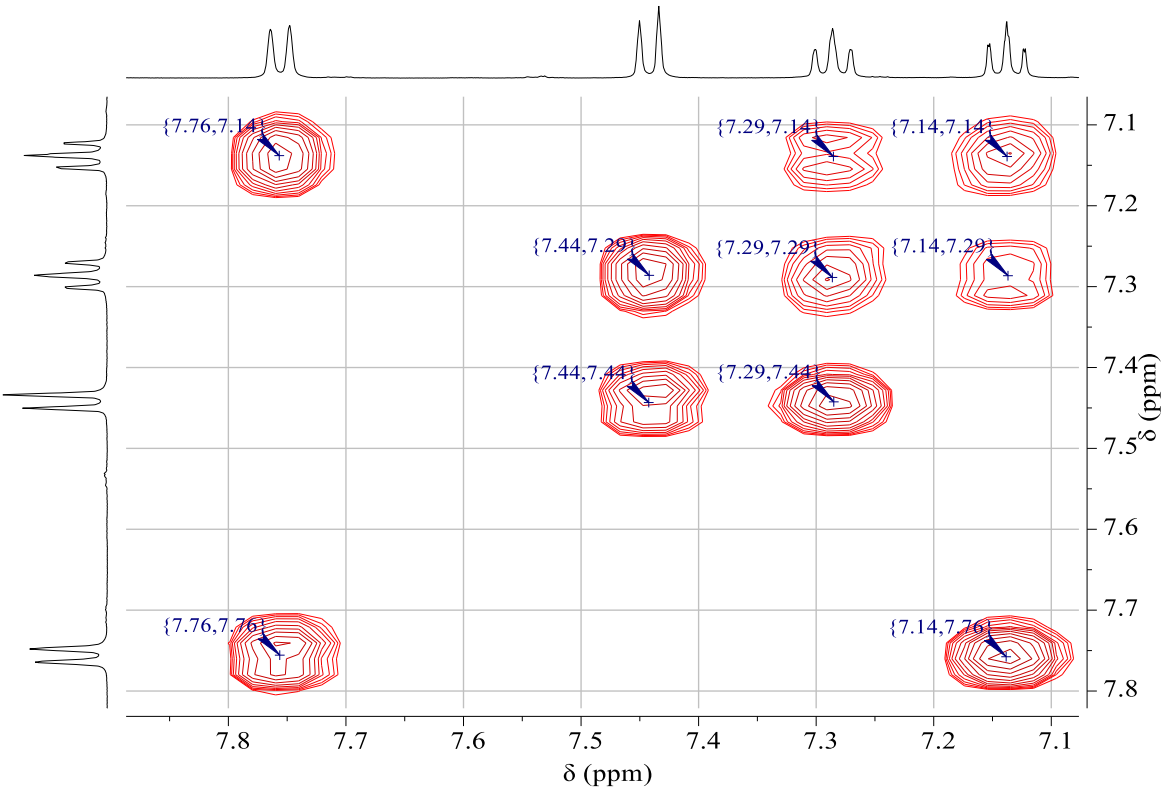
(*S*)-1-(((*S*)-1-Carboxy-2-(2-(trifluoromethyl)-1H-indol-3-yl)ethyl)amino)-4-(methylthio)-1-oxobutan-2-aminium 2,2,2-trifluoroacetate



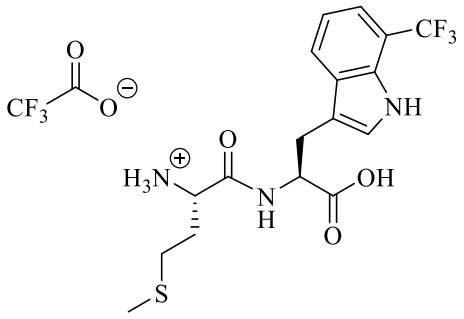
To a mixture of Met-Trp (33.5 mg, 0.1 mmol), sodium trifluoromethanesulfinate (15.6 mg, 0.1 mmol), and iron(III) nitrate nonahydrate (40.4 mg, 0.1 mmol) in 1:9 AcOH:25 mM aqueous NH_4HCO_2 (1 mL) was added *tert*-butyl hydroperoxide solution (27.7 μL, 0.2 mmol, 70% in H_2O) before stirring at 40 ºC for 20 min. The solution was taken up in H_2O (10 mL) and added to an Oasis HLB Plus cartridge (Waters, part # 186000132, activated with 2 mL

MeOH, 10 mL H_2O) before eluting the crude product with MeOH (5 mL). The MeOH was evaporated, the desired product was isolated using reverse phase preparative HPLC and lyophilised to obtain a white solid (5.1 mg, 0.00986 mmol, 10%). **Reverse phase HPLC details**: Phenomenex Synergi^{TM} 4 μm Hydro RP 80 Å, 250 x 10 mm, flow rate = 4 mL/min, column temperature = 40 °C, eluent = 5% MeCN (0.1% TFA) and 95% H_2O (0.1% TFA) for 3 min then increase linearly to 40% MeCN (0.1% TFA) at 25 min, retention time = 23.0 min; **^{1}H NMR** (500 MHz, DMSO-d_6): δ 12.82 (s, 1H), 12.07 (s, 1H), 8.96 (d, *J* = 8.0 Hz, 1H), 8.20 (s, 3H), 7.76 (d, *J* = 8.1 Hz, 1H), 7.44 (dd, *J* = 8.3, 1.0 Hz, 1H), 7.30 – 7.27 (m, 1H), 7.15 – 7.12 (m, 1H), 4.54 (q, *J* = 7.6 Hz, 1H), 3.82 – 3.80 (m, 1H), 3.24 – 3.20 (m, 1H), 2.05 (s, 3H), 2.03 – 1.98 (m, 2H), *observed indirectly from COSY and HSQC since obscured by solvent peak*: 2.50, 3.35; **^{13}C NMR** (126 MHz, DMSO-d_6): δ 172.19, 168.15, 135.65, 126.75, 124.34, 122.17 (q, *J* = 269.1 Hz), 121.63 (q, *J* = 36.2 Hz), 120.11, 119.98, 112.38, 112.20 (q, *J* = 2.9 Hz), 53.51, 51.51, 30.89, 27.88, 26.07, 14.43; **^{19}F NMR** (470 MHz, DMSO-d_6): δ -57.71, -74.95; **HRMS** (ESI^+): for $C_{17}H_{21}F_3N_3O_3{}^{32}S$ $[M+H]^+$ requires *m*/*z* = 404.1250, found 404.1253; $[\boldsymbol{\alpha}]_{\boldsymbol{D}}^{\mathbf{25}}$ = +18 ± 1° (*c* 0.076, H_2O).

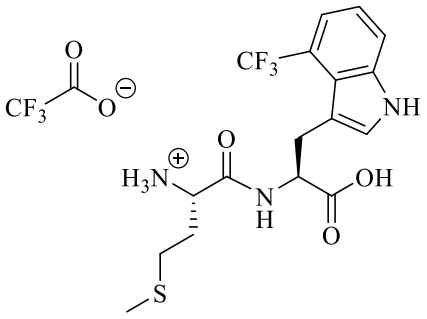
COSY NMR



(*S*)-1-(((*S*)-1-Carboxy-2-(7-(trifluoromethyl)-1H-indol-3-yl)ethyl)amino)-4-(methylthio)-1-oxobutan-2-aminium 2,2,2-trifluoroacetate and (*S*)-1-(((*S*)-1-Carboxy-2-(4-(trifluoromethyl)-1H-indol-3-yl)ethyl)amino)-4-(methylthio)-1-oxobutan-2-aminium 2,2,2-trifluoroacetate



Met-Trp(7-CF_3)



Met-Trp(4-CF_3)

To a mixture of Met-Trp (33.5 mg, 0.1 mmol), sodium trifluoromethanesulfinate (15.6 mg,

0.1 mmol), and iron(III) nitrate nonahydrate (40.4 mg, 0.1 mmol) in 1:9 AcOH:25 mM aqueous NH_4HCO_2 (1 mL) was added *tert*-butyl hydroperoxide solution (27.7 μL, 0.2 mmol, 70% in H_2O) before stirring at 40 ºC for 20 min. The solution was taken up in H_2O (10 mL) and added to an Oasis HLB Plus cartridge (Waters, part # 186000132, activated with 2 mL MeOH, 10 mL H_2O) before eluting the crude with MeOH (5 mL). The MeOH was evaporated, the crude was purified using reverse phase preparative HPLC and lyophilised to obtain a mixture of products in a ratio of 2:1 Met-Trp(4-CF_3):Met-Trp(7-CF_3). **Reverse phase HPLC details**: Phenomenex Synergi^{TM} 4 μm Hydro RP 80 Å, 250 x 10 mm, flow rate = 4 mL/min, column temperature = 40 °C, eluent = 5% MeCN (0.1% TFA) and 95% H_2O (0.1% TFA) for 3 min then increase linearly to 40% MeCN (0.1% TFA) at 25 min, retention time = 25.6 min.

Met-Trp(4-CF_3):

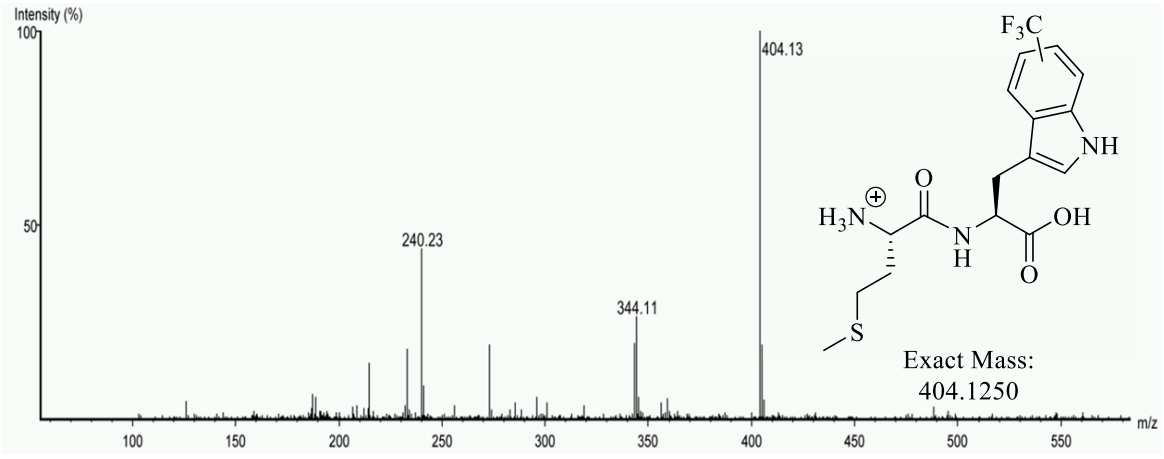
^{1}H NMR (500 MHz, DMSO-d_6): δ 12.89 (s, 1H), 11.59 (d, *J* = 2.6 Hz, 1H), 8.87 (d, *J* = 7.8 Hz, 1H), 8.10 (s, 3H), 7.71 (d, *J* = 8.1 Hz, 1H), 7.43 (d, *J* = 7.2 Hz, 1H), 7.40 (d, *J* = 2.6 Hz, 1H), 7.26 – 7.22 (m, 1H), 4.62 – 4.56 (m, 1H), 3.88 – 3.82 (m, 1H), 3.08 (dd, *J* = 15.7, 10.0 Hz, 1H), 2.06 (s, 3H) 2.02 – 1.95 (m, 2H), *observed indirectly from COSY since obscured by solvent peak*: 3.35, 2.53; **^{19}F NMR** (376 MHz, DMSO-d_6): δ -57.61, -74.95; **MS** (ESI^+): for $C_{17}H_{21}F_3N_3O_3{}^{32}S$ $[M+H]^+$ requires *m*/*z* = 404.13, found 404.13.

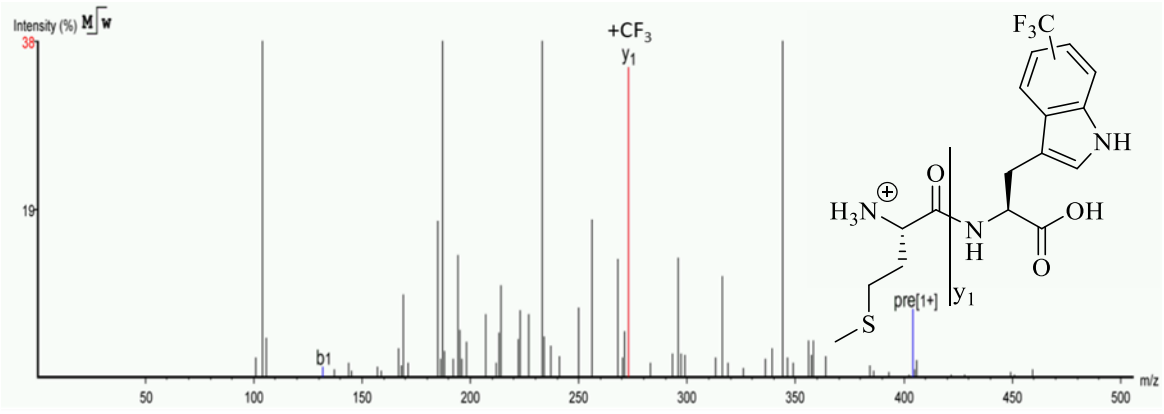
Met-Trp(7-CF_3):

^{1}H NMR (500 MHz, DMSO-d_6): δ 12.97 (s, 1H), 11.32 (d, *J* = 2.6 Hz, 1H), 8.75 (d, *J* = 7.5 Hz, 1H), 8.10 (s, 3H), 7.87 (d, *J* = 8.0 Hz, 1H), 7.45 (d, *J* = 7.0 Hz, 1H), 7.32 (d, *J* = 2.5 Hz, 1H), 7.20 – 7.17 (m, 1H), 4.62 – 4.56 (m, 1H), 3.88 – 3.82 (m, 1H), 3.16 (dd, *J* = 14.8, 8.8, 1H), 2.04 (s, 3H) 2.02 – 1.95 (m, 2H), *observed indirectly from COSY since obscured by*

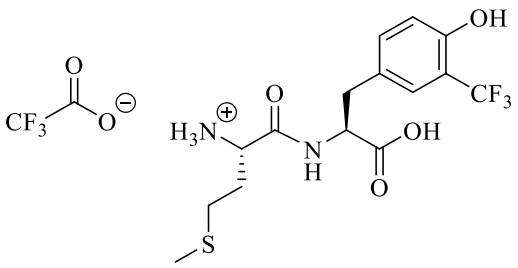
solvent peak: 3.26, 2.53; **^{19}F NMR** (376 MHz, DMSO-d_6): δ -61.20, -74.95; **MS** (ESI$^+$): for $C_{17}H_{21}F_3N_3O_3{}^{32}S$ $[M+H]^+$ requires *m/z* = 404.13, found 404.13.

MS/MS Analysis



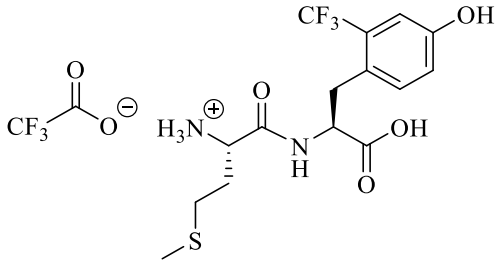


(1*S*)-1-(((*S*)-1-Carboxy-2-(4-hydroxy-3-(trifluoromethyl)phenyl)ethyl)amino)-4-(methylthio)-1-oxobutan-2-aminium 2,2,2-trifluoroacetate



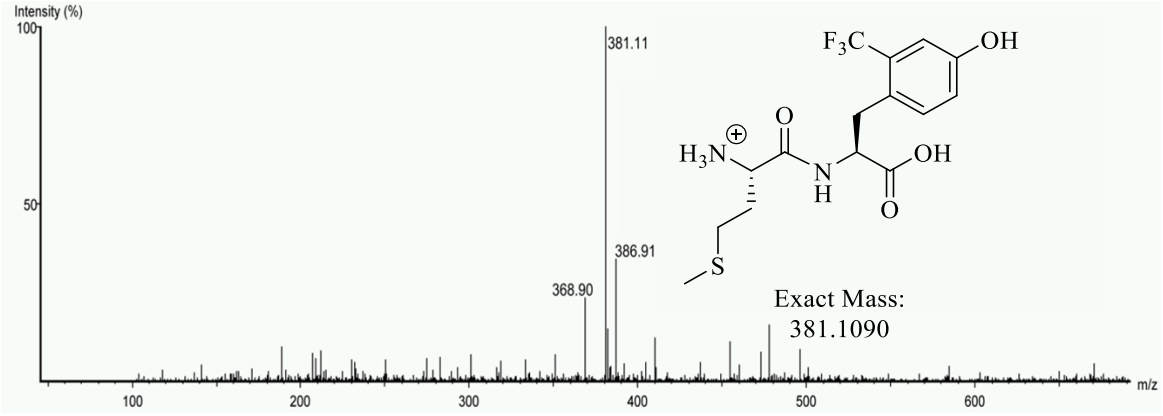
To a mixture of Met-Tyr (32.1 mg, 0.1 mmol), sodium trifluoromethanesulfinate (15.6 mg, 0.1 mmol), and iron(III) nitrate nonahydrate (40.4 mg, 0.1 mmol) in 1:9 AcOH:25 mM aqueous NH_4HCO_2 (1 mL) was added *tert*-butyl hydroperoxide solution (27.7 μL, 0.2 mmol, 70% in H_2O) before stirring at 40 ºC for 20 min. The solution was taken up in H_2O (10 mL) and added to an Oasis HLB Plus cartridge (Waters, part # 186000132, activated with 2 mL MeOH, 10 mL H_2O) before eluting the crude product with MeOH (5 mL). The MeOH was evaporated, the desired product was isolated using reverse phase preparative HPLC and lyophilised to obtain a green solid (4.9 mg, 0.00981 mmol, 10%). **Reverse phase HPLC details**: Phenomenex Synergi^{TM} 4 μm Hydro RP 80 Å, 250 x 10 mm, flow rate = 4 mL/min, column temperature = 40 °C, eluent = 5% MeCN (0.1% TFA) and 85% H_2O (0.1% TFA) for 3 min then increase linearly to 30% MeCN (0.1% TFA) at 30 min, retention time = 24.9 min; **^{1}H NMR** (500 MHz, DMSO-d_6): δ 13.02 (s, 1H), 10.52 (s, 1H), 8.76 (d, *J* = 7.6 Hz, 1H), 8.16 (s, 3H), 7.39 (d, *J* = 2.2 Hz, 1H), 7.33 (dd, *J* = 8.5, 2.2 Hz, 1H), 6.95 (d, *J* = 8.3 Hz, 1H), 4.46 – 4.42 (m, 1H), 3.86 – 3.81 (m, 1H), 3.05 (dd, *J* = 14.2, 4.9 Hz, 1H), 2.89 (dd, *J* = 14.2, 9.1 Hz, 1H), 2.04 (s, 3H), 2.02 – 1.92 (m, 2H), *observed indirectly from COSY and HSQC since obscured by solvent peak*: 2.49; **^{13}C NMR** (126 MHz, DMSO-d_6): δ 172.27, 168.32, 154.56, 134.35, 127.33, 127.09 (q, *J* = 4.7 Hz), 124.09 (q, *J* = 272.0 Hz), 116.92, 115.10 (q, *J* = 29.7 Hz), 53.98, 51.45, 35.18, 31.10, 27.81, 14.42; **^{19}F NMR** (470 MHz, DMSO-d_6): δ -62.34, -74.95; **HRMS** (ESI^+): for $C_{15}H_{20}F_3N_2O_4{}^{32}S$ $[M+H]^+$ requires *m*/*z* = 381.1090 found 381.1088; $[\boldsymbol{\alpha}]_{\boldsymbol{D}}^{\mathbf{25}}$= -48 ± 3° (*c* 0.073, H_2O).

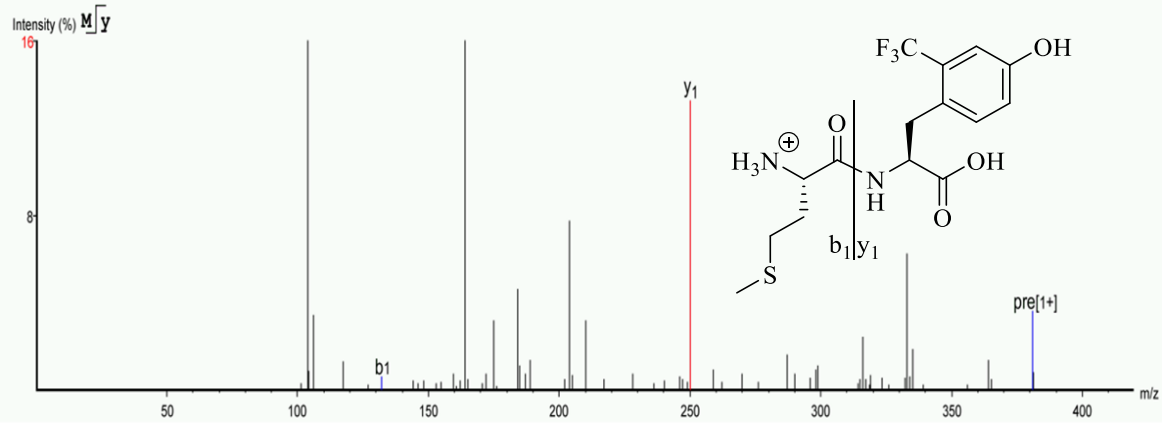
(*S*)-1-(((*S*)-1-Carboxy-2-(4-hydroxy-2-(trifluoromethyl)phenyl)ethyl)amino)-4-(methylthio)-1-oxobutan-2-aminium 2,2,2-trifluoroacetate



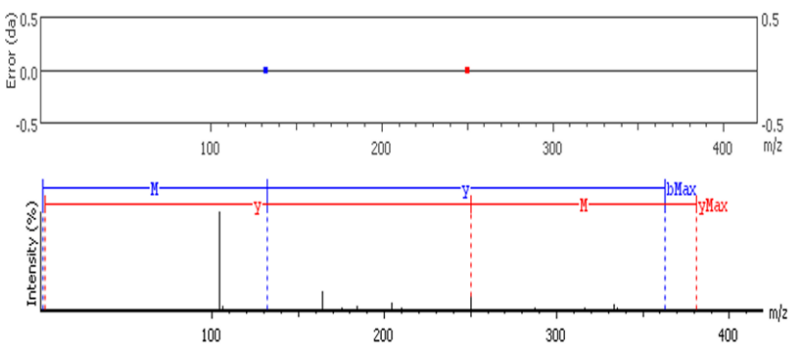
To a mixture of Met-Tyr (32.1 mg, 0.1 mmol), sodium trifluoromethanesulfinate (15.6 mg, 0.1 mmol), and iron(III) nitrate nonahydrate (40.4 mg, 0.1 mmol) in 1:9 AcOH:25 mM aqueous NH_4HCO_2 (1 mL) was added *tert*-butyl hydroperoxide solution (27.7 μL, 0.2 mmol, 70% in H_2O) before stirring at 40 ºC for 20 min. The solution was taken up in H_2O (10 mL) and added to an Oasis HLB Plus cartridge (Waters, part # 186000132, activated with 2 mL MeOH, 10 mL H_2O) before eluting the crude product with MeOH (5 mL). The MeOH was evaporated, the desired product was isolated using reverse phase preparative HPLC and lyophilised. **Reverse phase HPLC details**: Phenomenex Synergi™ 4 μm Hydro RP 80 Å, 250 x 10 mm, flow rate = 4 mL/min, column temperature = 40 °C, eluent = 5% MeCN (0.1% TFA) and 95% H_2O (0.1% TFA) for 3 min then increase linearly to 30% MeCN (0.1% TFA) at 30 min, retention time = 24.3 min; **^{1}H NMR** (500 MHz, DMSO-d_6): δ 12.98 (s, 1H), 10.00 (s, 1H), 8.86 (d, *J* = 8.2 Hz, 1H), 8.12 – 8.02 (m, 3H), 7.30 (d, *J* = 8.4 Hz, 1H), 7.05 (d, *J* = 2.6 Hz, 1H), 6.96 (dd, *J* = 8.5, 2.7 Hz, 1H), 4.47 – 4.43 (m, 1H), 3.85 – 3.82 (m, 1H), 3.22 (dd, *J* = 15.0, 5.5 Hz, 1H), 2.94 (dd, *J* = 14.7, 9.8 Hz, 1H), 2.06 (s, 3H), 2.05 – 1.94 (m, 2H), *observed indirectly from COSY since obscured by solvent peak*: 2.51; **^{19}F NMR** (470 MHz, DMSO-d_6): δ -59.95, -74.95; **MS** (ESI$^+$): for $C_{15}H_{20}F_3N_2O_4{}^{32}S$ $[M+H]^+$ requires *m*/*z* = 381.11, found 381.11.

MS/MS Analysis

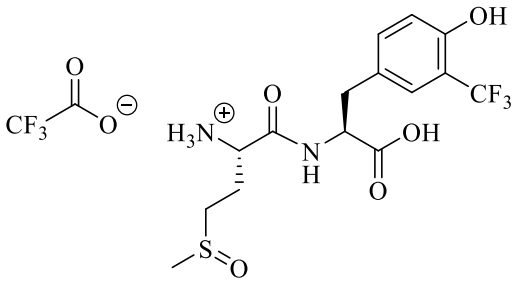




#	b	b (2+)	Seq	y	y (2+)	#
1	132.05	66.52	M			2
2			Y(+67.99)	250.07	125.53	1

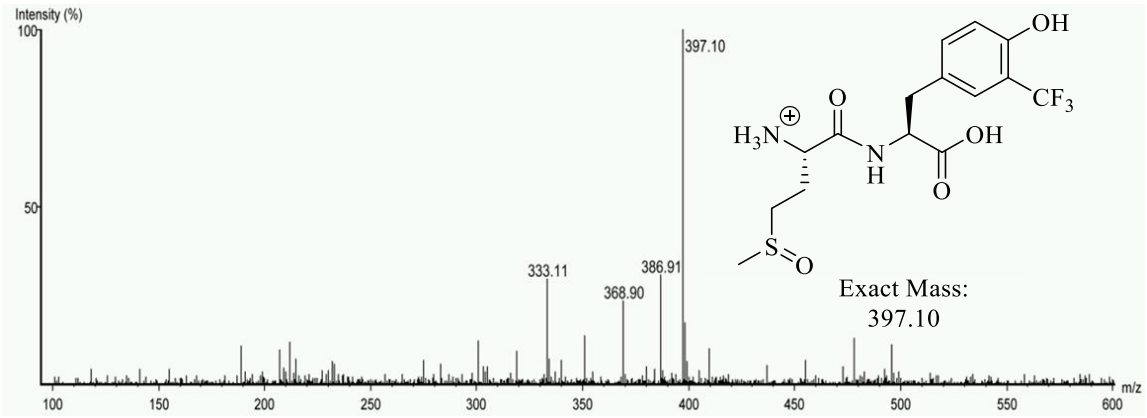


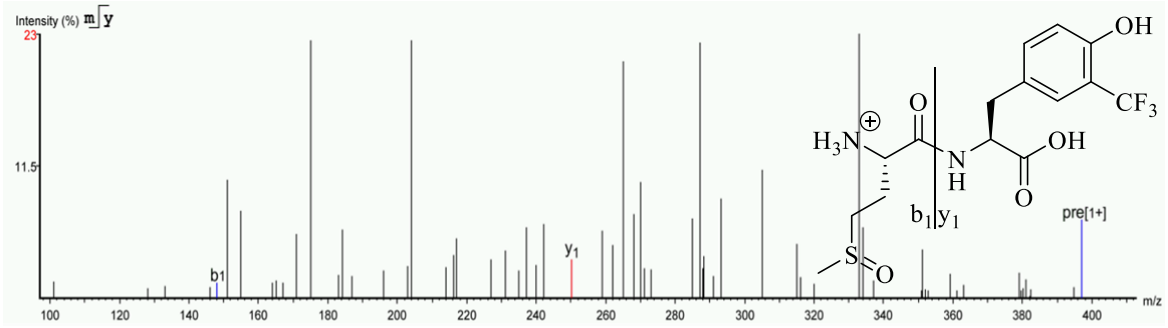
(2*S*)-1-(((*S*)-1-Carboxy-2-(4-hydroxy-3-(trifluoromethyl)phenyl)ethyl)amino)-4-(methylsulfinyl)-1-oxobutan-2-aminium 2,2,2-trifluoroacetate



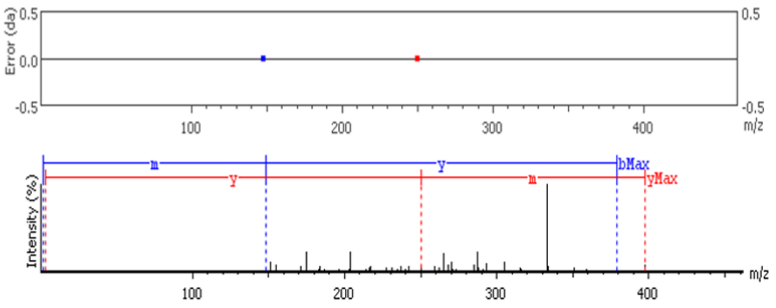
To a mixture of Met-Tyr (32.1 mg, 0.1 mmol), sodium trifluoromethanesulfinate (15.6 mg, 0.1 mmol), and iron(III) nitrate nonahydrate (40.4 mg, 0.1 mmol) in 1:9 AcOH:25 mM aqueous NH_4HCO_2 (1 mL) was added *tert*-butyl hydroperoxide solution (27.7 μL, 0.2 mmol, 70% in H_2O) before stirring at 40 ºC for 20 min. The solution was taken up in H_2O (10 mL) and added to an Oasis HLB Plus cartridge (Waters, part # 186000132, activated with 2 mL MeOH, 10 mL H_2O) before eluting the crude product with MeOH (5 mL). The MeOH was evaporated, the desired product was isolated using reverse phase preparative HPLC and lyophilised. **Reverse phase HPLC details**: Phenomenex Synergi^{TM} 4 μm Hydro RP 80 Å, 250 x 10 mm, flow rate = 4 mL/min, column temperature = 40 °C, eluent = 5% MeCN (0.1% TFA) and 95% H_2O (0.1% TFA) for 3 min then increase linearly to 30% MeCN (0.1% TFA) at 30 min, retention time = 21.3 min; **^{1}H NMR** (500 MHz, DMSO-d_6): δ 10.41 (s, 1H), 8.77 (s, 1H), 8.15 (s, 3H), 7.40 (d, *J* = 1.6 Hz, 1H), 7.33 (dd, *J* = 8.3, 1.6 Hz, 1H), 6.94 (d, *J* = 8.4 Hz, 1H), 4.49 – 4.45 (m, 1H), 3.94 – 3.86 (m, 1H), 3.06 (dd, *J* = 14.2, 4.9 Hz, 1H), 2.92 – 2.74 (m, 3H), 2.55 (s, 3H), 2.03 – 1.97 (m, 2H), *carboxylic acid OH was not observed*; **^{19}F NMR** (471 MHz, DMSO-d_6): δ -62.32, -62.33, -74.95; **MS** (ESI$^+$): for $C_{15}H_{20}F_3N_2O_5{}^{32}S$ $[M+H]^+$ requires *m*/*z* = 397.10, found 397.10.

MS/MS Analysis

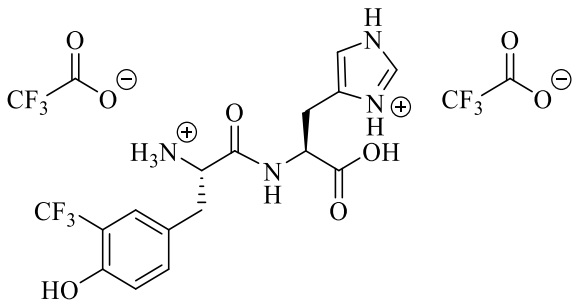




#	b	b (2+)	Seq	y	y (2+)	#
1	148.04	74.52	M(+15.99)			2
2			Y(+67.99)	250.07	125.53	1

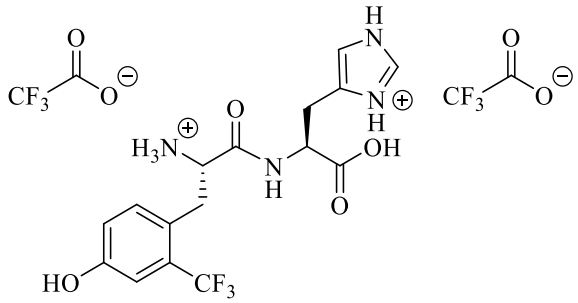


4-((*S*)-2-((*S*)-2-Ammonio-3-(4-hydroxy-3-(trifluoromethyl)phenyl)propanamido)-2-carboxyethyl)-1H-imidazol-3-ium 2,2,2-trifluoroacetate



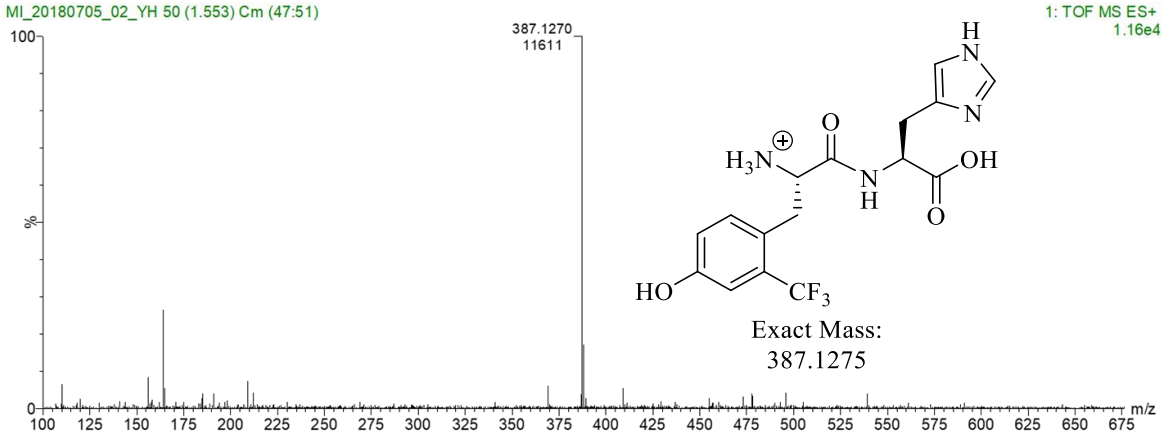
To a mixture of Tyr-His (32.8 mg, 0.1 mmol), sodium trifluoromethanesulfinate (15.6 mg, 0.1 mmol), and iron(III) nitrate nonahydrate (40.4 mg, 0.1 mmol) in 1:9 AcOH:25 mM aqueous NH_4HCO_2 (1 mL) was added *tert*-butyl hydroperoxide solution (27.7 μL, 0.2 mmol, 70% in H_2O) before stirring at 40 ºC for 20 min. The solution was taken up in H_2O (10 mL) and added to an Oasis HLB Plus cartridge (Waters, part # 186000132, activated with 2 mL MeOH, 10 mL H_2O) before eluting the crude product with MeOH (5 mL). The MeOH was evaporated, the desired product was isolated using reverse phase preparative HPLC and lyophilised to obtain a white solid (7.0 mg, 0.0114 mmol, 11%). **Reverse phase HPLC details**: Phenomenex Synergi^{TM} 4 μm Hydro RP 80 Å, 250 x 10 mm, flow rate = 4 mL/min, column temperature = 40 °C, eluent = 5% MeCN (0.1% TFA) and 95% H_2O (0.1% TFA) for 3 min then increase linearly to 25% MeCN (0.1% TFA) at 25 min, retention time = 17.3 min; **^{1}H NMR** (500 MHz, DMSO-d_6): δ 14.41 (s, 1H), 10.58 (s, 1H), 9.02 – 9.00 (m, 2H), 8.10 (s, 3H), 7.44 – 7.43 (m, 2H), 7.32 (dd, *J* = 8.5, 2.2 Hz, 1H), 6.95 (d, *J* = 8.4 Hz, 1H), 4.68 – 4.63 (m, 1H), 4.04 – 4.01 (m, 1H), 3.22 – 3.19 (m, 1H), 3.10 – 3.04 (m, 2H), 2.90 – 2.86 (m, 1H); **^{13}C NMR** (126 MHz, DMSO-d_6): δ 171.38, 168.22, 155.08, 134.89, 134.04, 128.94, 127.65 (q, *J* = 4.3, 3.8 Hz), 124.62, 124.05 (q, *J* = 272.5 Hz), 117.12, 117.03, 115.42 (q, *J* = 30.0 Hz), 53.33, 51.36, 35.73, 26.32; **^{19}F NMR** (470 MHz, DMSO-d_6): δ -62.22, -74.95; **HRMS** (ESI^+): for $C_{16}H_{18}O_4N_4F_3$ $[M+H]^+$ requires *m*/*z* = 387.1275, found 387.1278; $[\boldsymbol{\alpha}]_{\boldsymbol{D}}^{\mathbf{25}}$ = +28 ± 1° (*c* 0.073, H_2O).

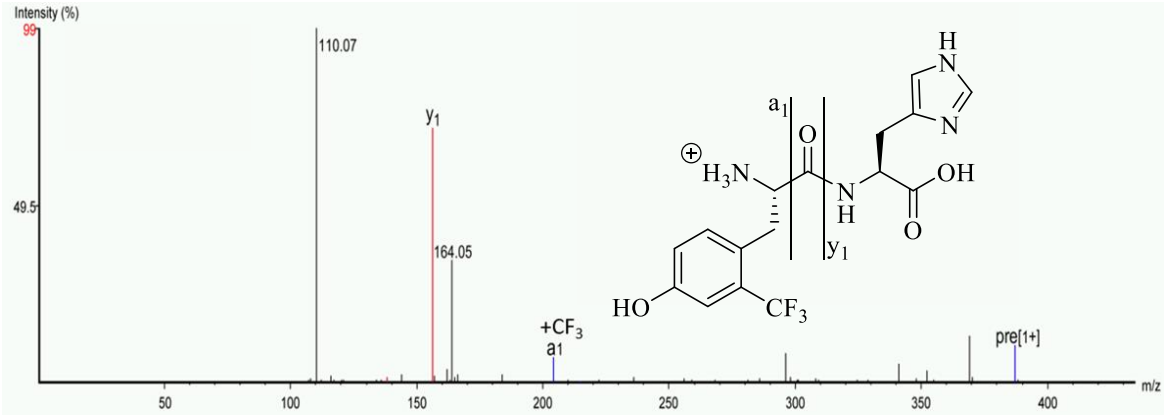
4-((*S*)-2-((*S*)-2-Ammonio-3-(4-hydroxy-2-(trifluoromethyl)phenyl)propanamido)-2-carboxyethyl)-1H-imidazol-3-ium 2,2,2-trifluoroacetate



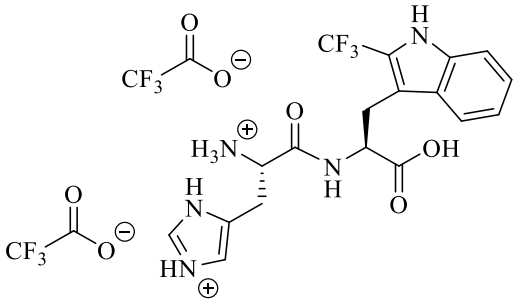
To a mixture of Tyr-His (32.8 mg, 0.1 mmol), sodium trifluoromethanesulfinate (15.6 mg, 0.1 mmol), and iron(III) nitrate nonahydrate (40.4 mg, 0.1 mmol) in 1:9 AcOH:25 mM aqueous NH_4HCO_2 (1 mL) was added *tert*-butyl hydroperoxide solution (27.7 μL, 0.2 mmol, 70% in H_2O) before stirring at 40 ºC for 20 min. The solution was taken up in H_2O (10 mL) and added to an Oasis HLB Plus cartridge (Waters, part # 186000132, activated with 2 mL MeOH, 10 mL H_2O) before eluting the crude product with MeOH (5 mL). The MeOH was evaporated, the desired product was isolated using reverse phase preparative HPLC and lyophilised. **Reverse phase HPLC details**: Phenomenex Synergi^{TM} 4 μm Hydro RP 80 Å, 250 x 10 mm, flow rate = 4 mL/min, column temperature = 40 °C, eluent = 5% MeCN (0.1% TFA) and 95% H_2O (0.1% TFA) for 3 min then increase linearly to 25% MeCN (0.1% TFA) at 25 min, retention time = 16.1 min; **^{1}H NMR** (500 MHz, DMSO-d_6): δ 10.08 (s, 1H), 9.06 – 8.94 (m, 1H), 8.76 (d, *J* = 7.9 Hz, 1H), 8.29 (s, 3H), 7.40 – 7.33 (m, 1H), 7.26 (d, *J* = 8.5 Hz, 1H), 7.07 (d, *J* = 2.6 Hz, 1H), 6.97 (dd, *J* = 8.4, 2.6 Hz, 1H), 4.63 – 4.59 (m, 1H), 4.00 – 3.97 (m, 1H) 3.15 – 2.96 (m, 4H), *carboxylic acid OH was not observed*; **^{19}F NMR** (471 MHz, DMSO-d_6): δ -59.68, -74.95; **HRMS** (ESI^+): for $C_{16}H_{18}O_4N_4F_3$ $[M+H]^+$ requires *m*/*z* = 387.1275, found 387.1270.

MS/MS Analysis





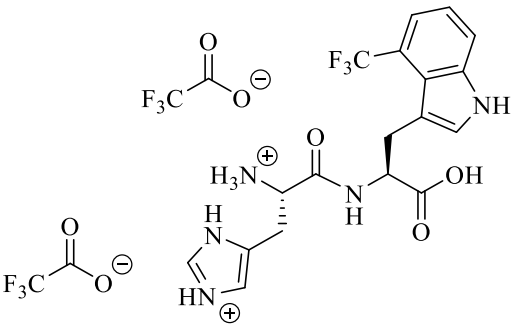
5-((*S*)-2-Ammonio-3-(((*S*)-1-carboxy-2-(2-(trifluoromethyl)-1H-indol-3-yl)ethyl)amino)-3-oxopropyl)-1H-imidazol-3-ium 2,2,2-trifluoroacetate



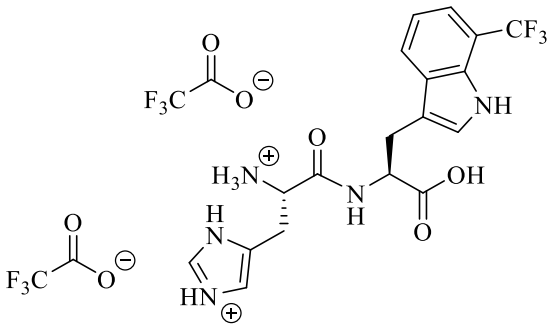
To a mixture of His-Trp (34.1 mg, 0.1 mmol), sodium trifluoromethanesulfinate (15.6 mg, 0.1 mmol), and iron(III) nitrate nonahydrate (40.4 mg, 0.1 mmol) in 1:9 AcOH:25 mM aqueous NH_4HCO_2 (1 mL) was added *tert*-butyl hydroperoxide solution (27.7 μL, 0.2 mmol,

70% in H_2O) before stirring at 40 ºC for 20 min. The solution was taken up in H_2O (10 mL) and added to an Oasis HLB Plus cartridge (Waters, part # 186000132, activated with 2 mL MeOH, 10 mL H_2O) before eluting the crude product with MeOH (5 mL). The MeOH was evaporated, the desired product was isolated using reverse phase preparative HPLC and lyophilised to obtain a white solid (7.4 mg, 0.0116 mmol, 12%). **Reverse phase HPLC details**: Phenomenex Synergi^{TM} 4 μm Hydro RP 80 Å, 250 x 10 mm, flow rate = 4 mL/min, column temperature = 40 °C, eluent = 11% MeCN (0.1% TFA) and 89% H_2O (0.1% TFA) for 3 min then increase linearly to 25% MeCN (0.1% TFA) at 25 min, then another linear increase to 40% at 30 min, retention time = 20.6 min; **^{1}H NMR** (500 MHz, DMSO-d_6): δ 14.38 (s, 1H), 12.07 (s, 1H), 9.00– 8.99 (m, 2H), 8.35 (m, 3H), 7.77 (d, *J* = 8.1 Hz, 1H), 7.45 (d, *J* = 8.3 Hz, 1H), 7.42 (s, 1H), 7.31 – 7.28 (m, 1H), 7.16 – 7.13 (m, 1H), 4.58 – 4.54 (m, 1H), 4.15 – 4.12 (m, 1H), 3.31 (dd, *J* = 14.6, 8.3 Hz, 1H), 3.25 – 3.14 (m, 3H); **^{13}C NMR** (126 MHz, DMSO-d_6): δ 172.10, 167.29, 135.69, 134.45, 126.71, 126.69, 124.39, 122.17 (q, *J* = 268.9 Hz), 121.70 (q, *J* = 36.1 Hz), 120.14, 119.94, 118.00, 112.43, 112.01 (q, *J* = 2.9 Hz), 53.59, 51.22, 26.45, 26.37; **^{19}F NMR** (470 MHz, DMSO-d_6): δ -57.37, -74.95; **HRMS** (ESI$^+$): for $C_{18}H_{19}F_3N_5O_3$ $[M+H]^+$ requires *m*/*z* = 410.1440, found 410.1429$[\boldsymbol{\alpha}]_{\boldsymbol{D}}^{\mathbf{25}}$ = +10 ± 2° (*c* 0.119, H_2O).

5-((*S*)-2-Ammonio-3-(((*S*)-1-carboxy-2-(4-(trifluoromethyl)-1H-indol-3-yl)ethyl)amino)-3-oxopropyl)-1H-imidazol-3-ium 2,2,2-trifluoroacetate and 5-((*S*)-2-ammonio-3-(((*S*)-1-carboxy-2-(7-(trifluoromethyl)-1H-indol-3-yl)ethyl)amino)-3-oxopropyl)-1H-imidazol-3-ium 2,2,2-trifluoroacetate



His-Trp(4-CF_3)



His-Trp(7-CF_3)

To a mixture of His-Trp (34.1 mg, 0.1 mmol), sodium trifluoromethanesulfinate (15.6 mg, 0.1 mmol), and iron(III) nitrate nonahydrate (40.4 mg, 0.1 mmol) in 1:9 AcOH:25 mM aqueous NH_4HCO_2 (1 mL) was added *tert*-butyl hydroperoxide solution (27.7 μL, 0.2 mmol, 70% in H_2O) before stirring at 40 ºC for 20 min. The solution was taken up in H_2O (10 mL) and added to an Oasis HLB Plus cartridge (Waters, part # 186000132, activated with 2 mL MeOH, 10 mL H_2O) before eluting the crude with MeOH (5 mL). The MeOH was evaporated, the crude was purified using reverse phase preparative HPLC and lyophilised to obtain a mixture of products in a ratio of 3:1 His-Trp(4-CF_3):His-Trp(7-CF_3). **Reverse phase HPLC details**: Phenomenex Synergi^{TM} 4 μm Hydro RP 80 Å, 250 x 10 mm, flow rate = 4 mL/min, column temperature = 40 °C, eluent = 11% MeCN (0.1% TFA) and 89% H_2O (0.1% TFA) for 3 min then increase linearly to 25% MeCN (0.1% TFA) at 25 min, then another linear increase to 40% at 30 min, retention time = 28.1 min.

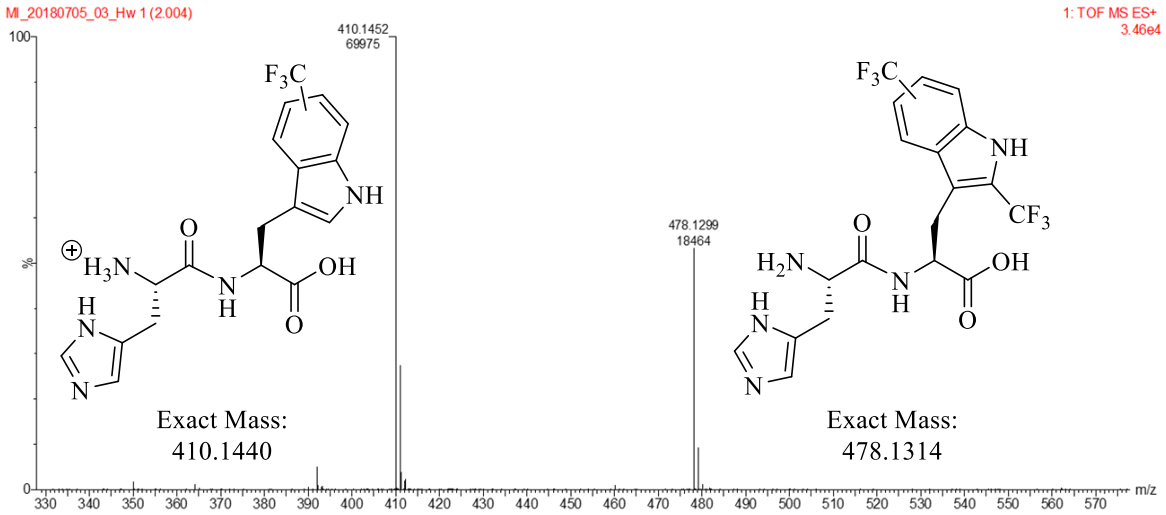
His-Trp(4-CF_3):

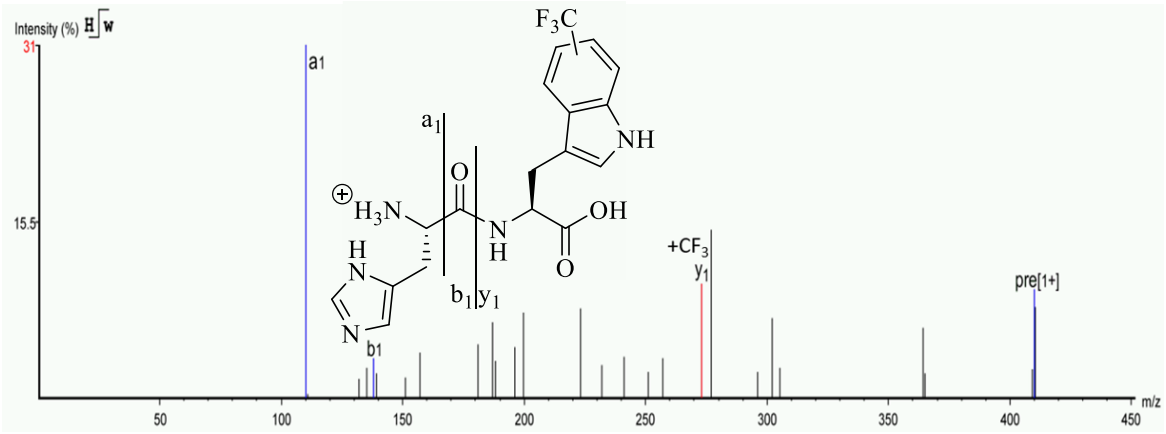
^{1}H NMR (500 MHz, DMSO-d_6): δ 11.58 (d, *J* = 2.7 Hz, 1H), 9.01 (s, 1H), 8.18 (s, 3H), 7.71 (d, *J* = 8.2 Hz, 1H), 7.43 (d, *J* = 7.3 Hz, 1H), 7.40 (d, *J* = 2.6 Hz, 1H), 7.25 –7.22 (m, 1H), 4.63 – 4.58 (m, 1H), 4.11 – 4.02 (m, 1H), 3.18 – 2.98 (m, 4H), *carboxylic acid OH was not observed*; **^{19}F NMR** (470 MHz, DMSO-d_6): δ -57.59, -74.95; **HRMS** (ESI^+): for $C_{18}H_{19}F_3N_5O_3$ $[M+H]^+$ requires *m/z* = 410.1440, found 410.1452.

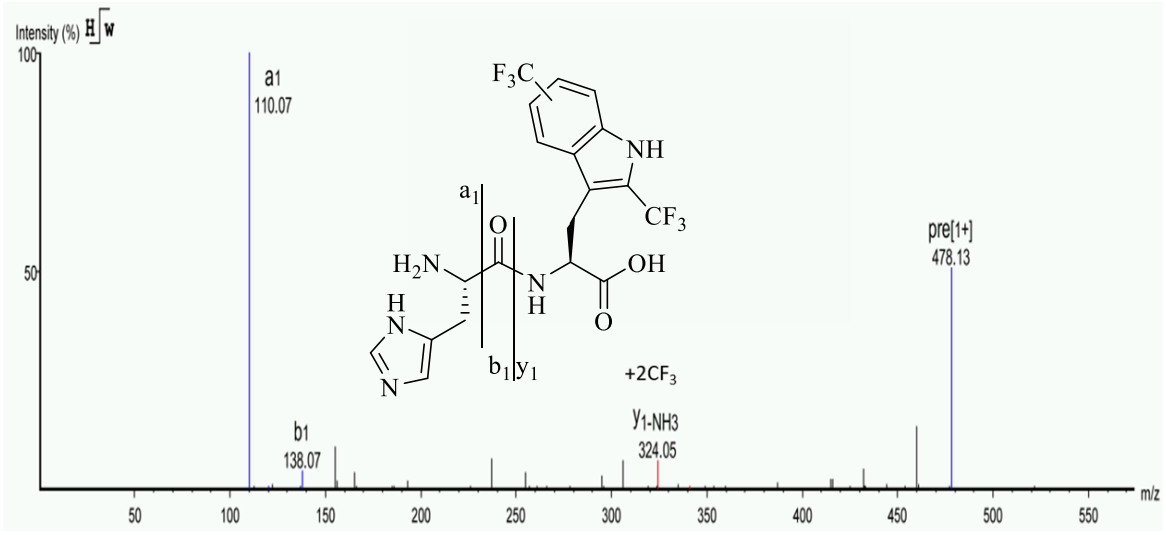
His-Trp(7-CF_3):

^{1}H NMR (500 MHz, DMSO-d_6): δ 11.37 – 11.26 (m, 1H), 8.89 (s, 1H), 8.18 (s, 3H), 7.87 (d, *J* = 8.0 Hz, 1H), 7.44 (d, *J* = 6.9 Hz, 1H), 7.31 (d, *J* = 2.5 Hz, 1H), 7.19 – 7.16 (m, 1H), 4.63 – 4.58 (m, 1H), 4.11 – 4.02 (m, 1H), 3.18 – 2.98 (m, 4H), *carboxylic acid OH was not observed*; **^{19}F NMR** (470 MHz, DMSO-d_6): δ -61.18, -74.95; **HRMS** (ESI^+): for $C_{18}H_{19}F_3N_5O_3$ $[M+H]^+$ requires *m/z* = 410.1440, found 410.1452.

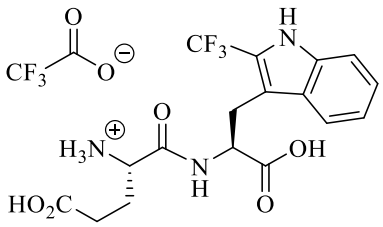
MS/MS Analysis







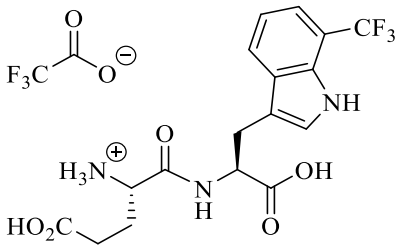
Thymogen[Trp(2-CF_3)]



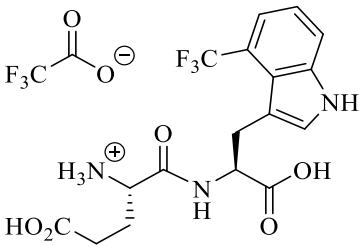
To Glu-Trp (10.4 mg, 0.031 mmol) in a 3 mL V-vial was added DMSO (90 µL), iron(III) chloride (5.5 mg, 0.034 mmol), sodium trifluoromethanesulfinate solution (45 µL of 1.0 M solution in 25 mM aqueous NH_4HCO_2, 0.045 mmol), and *tert*-butyl hydroperoxide solution (45 µL of 1.87 M solution in 25 mM aqueous NH_4HCO_2, 0.084 mmol) before stirring at 40

°C for 30 min. The solution was taken up in TFA:MeCN:H_2O 0.1:4.9:95 (2 mL), purified by reverse phase preparative HPLC, and lyophilised to obtain a white solid (4.6 mg, 3.4 μmol mol, 11%). **Reverse phase HPLC details**: Phenomenex Synergi^{TM} 4 μm Hydro RP 80 Å, 250 x 10 mm, flow rate = 4 mL/min, column temperature = 40 °C, eluent = 12% MeCN (0.1% TFA) and 88% H_2O (0.1% TFA) for 3 min then increase linearly to 40% MeCN (0.1% TFA) at 25 min, retention time = 17.7 min; **^{1}H NMR** (500 MHz, DMSO-d_6): δ 12.90 (s, 1H), 12.36 (s, 1H), 12.05 (s, 1H), 8.94 (d, *J* = 8.0 Hz, 1H), 8.12 (d, *J* = 5.3 Hz, 3H), 7.76 (d, *J* = 8.1 Hz, 1H), 7.44 (d, *J* = 8.3 Hz, 1H), 7.31 – 7.28 (m, 1H), 7.17 – 7.14 (m, 1H), 4.57 – 4.52 (m, 1H), 3.79 – 3.76 (m, 1H), 3.34 (dd, *J* = 14.3, 8.0 Hz, 1H), 3.22 (dd, *J* = 14.3, 7.0 Hz, 1H), 2.37 – 2.34 (m, 2H), 2.01 – 1.97 (m, 2H); **^{13}C NMR** (126 MHz, DMSO-d_6): δ 173.38, 172.18, 168.29, 135.63, 126.73, 124.35, 122.15 (q, *J* = 268.7 Hz), 121.62 (q, *J* = 36.1 Hz), 120.12, 119.97, 112.36, 112.15 (q, *J* = 2.7 Hz), 53.50, 51.45, 28.84, 26.33, 26.15; **^{19}F NMR** (471 MHz, DMSO-d_6): δ -57.32, -74.95; **HRMS** (ESI^+): for $C_{17}H_{19}O_5N_3F_3$ $[M+H]^+$ requires *m*/*z* = 402.1271, found 402.1268; $[\boldsymbol{\alpha}]_{\boldsymbol{D}}^{\mathbf{25}}$ = +14 ± 2° (*c* 0.040, H_2O).

Thymogen[Trp(7-CF_3)] and Thymogen[Trp(4-CF_3)]



Thymogen[Trp(7-CF_3)]



Thymogen[Trp(4-CF_3)]

To Glu-Trp (10.4 mg, 0.031 mmol) in a 3 mL V-vial was added DMSO (90 μL), iron(III) chloride (5.5 mg, 0.034 mmol), sodium trifluoromethanesulfinate solution (45 μL of 1.0 M solution in 25 mM aqueous NH_4HCO_2, 0.045 mmol), and *tert*-butyl hydroperoxide solution (45 μL of 1.87 M solution in 25 mM aqueous NH_4HCO_2, 0.084 mmol) before stirring at

40 °C for 30 min. The solution was taken up in TFA:MeCN:H_2O 0.1:4.9:95 (2 mL), purified by reverse phase preparative HPLC, and lyophilised to obtain a mixture of products. **Reverse phase HPLC details**: Phenomenex Synergi^{TM} 4 μm Hydro RP 80 Å, 250 x 10 mm, flow rate = 4 mL/min, column temperature = 40 °C, eluent = 12% MeCN (0.1% TFA) and 88% H_2O (0.1% TFA) for 3 min then increase linearly to 40% MeCN (0.1% TFA) at 25 min, retention time 21.4 min.

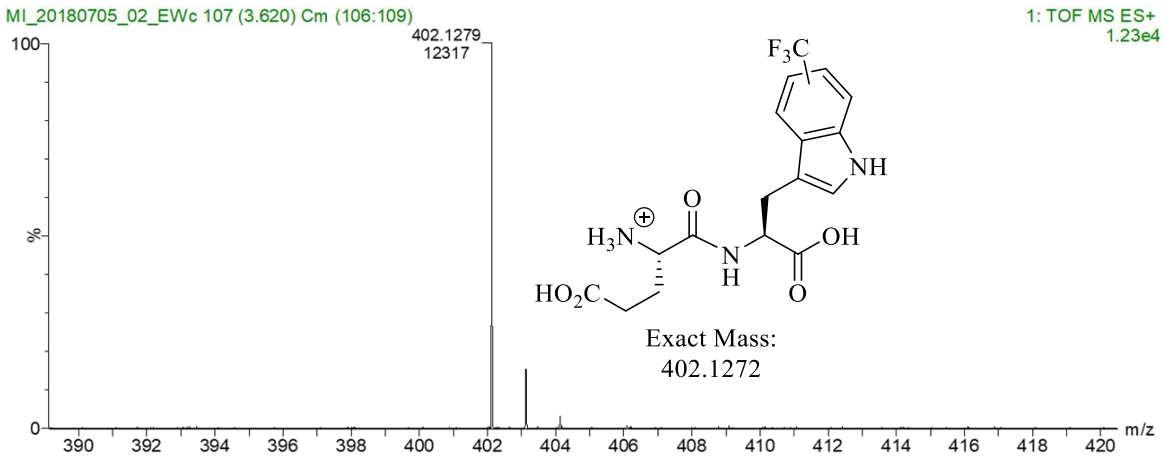
Thymogen[Trp(4-CF_3)]:

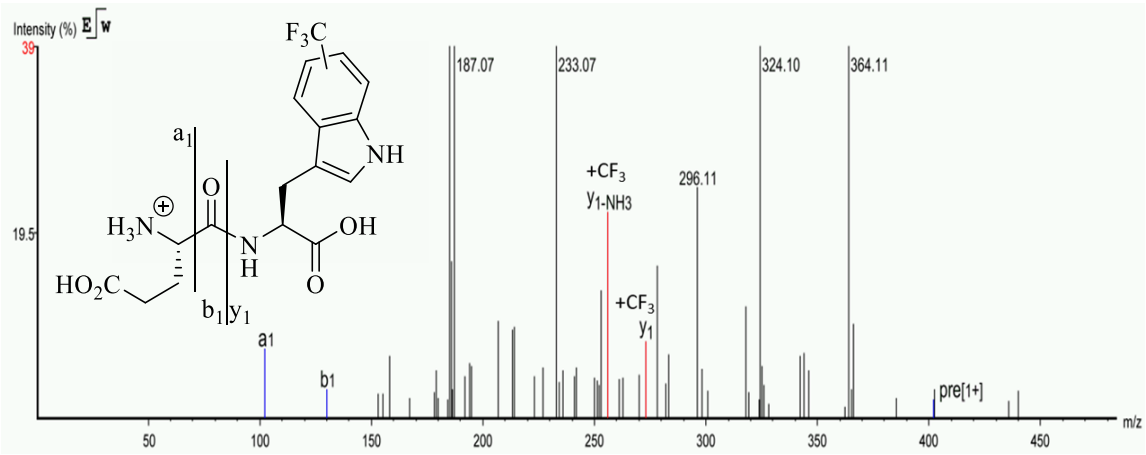
^{1}H NMR (500 MHz, DMSO-d_6): δ 12.88 (s, 1H), 12.33 (s, 1H), 11.59 (s, 1H), 8.87 (d, *J* = 7.7 Hz, 1H), 8.09 (s, 3H), 7.71 (d, *J* = 8.1 Hz, 1H), 7.43 (d, *J* = 7.3 Hz, 1H), 7.41 (d, *J* = 2.6 Hz, 1H), 7.25 – 7.22 (m, 1H), 4.61 – 4.55 (m, 1H), 3.84 – 3.79 (m, 1H), 3.07 (dd, *J* = 15.6, 9.9 Hz, 1H), 2.02 – 1.96 (m, 3H), *observed indirectly from COSY since obscured by solvent peak*: 3.24, 2.39; **^{19}F NMR** (471 MHz, DMSO-d_6): δ -57.66, -74.95; *Insufficient quantity for ^{13}C NMR*; **HRMS** (ESI$^+$): for $C_{17}H_{19}O_5N_3F_3$ $[M+H]^+$ requires *m*/*z* = 402.1271, found 402.1279.

Thymogen[Trp(7-CF_3)]:

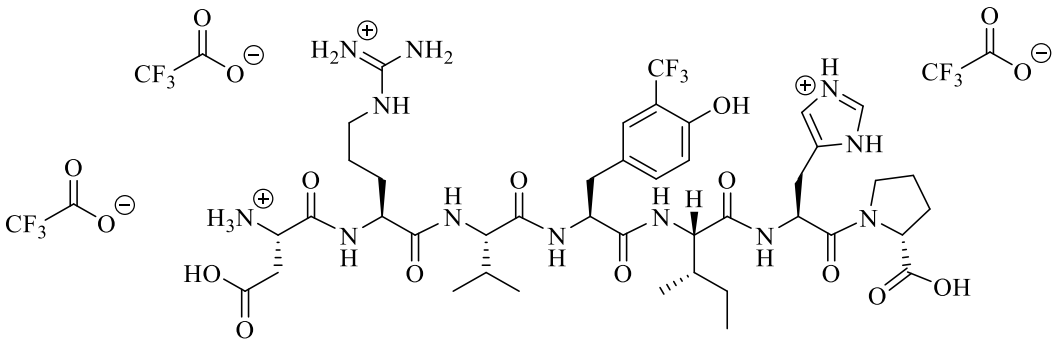
^{1}H NMR (500 MHz, DMSO-d_6): δ 12.97 (s, 1H), 12.33 (s, 1H), 11.32 (d, *J* = 2.1 Hz, 1H), 8.76 (d, *J* = 7.7 Hz, 1H), 8.09 (s, 3H), 7.87 (d, *J* = 7.9 Hz, 1H), 7.45 (d, *J* = 6.8 Hz, 1H), 7.32 (d, *J* = 2.1 Hz, 1H), 7.20 – 7.17 (m, 1H), 4.61 – 4.55 (m, 1H), 3.84 – 3.79 (m, 1H), 3.17 – 3.12 (m, 2H), 2.02 – 1.96 (m, 2H), *observed indirectly from COSY since obscured by solvent peak*: 3.24, 2.39; **^{19}F NMR** (471 MHz, DMSO-d_6): δ -61.23, -74.95; **HRMS** (ESI$^+$): for $C_{17}H_{19}O_5N_3F_3$ $[M+H]^+$ requires *m*/*z* = 402.1272, found 402.1279.

MS/MS Analysis



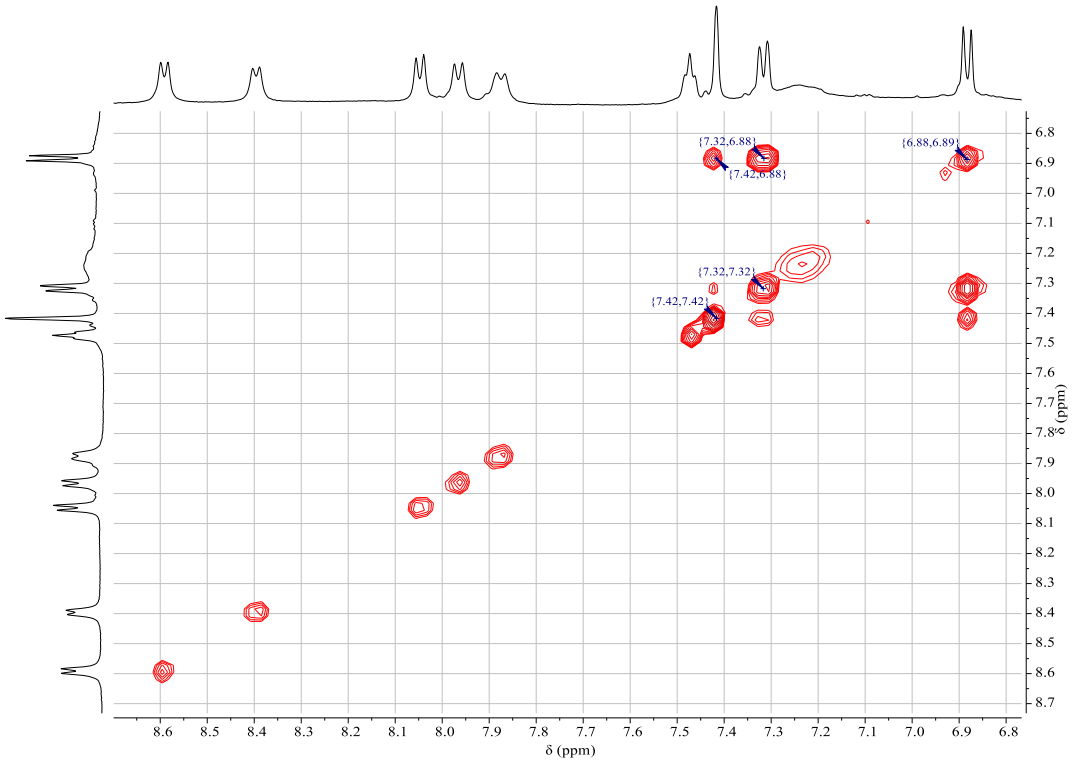


Angiotensin I/II (1-7)[Tyr(3-CF_3)]

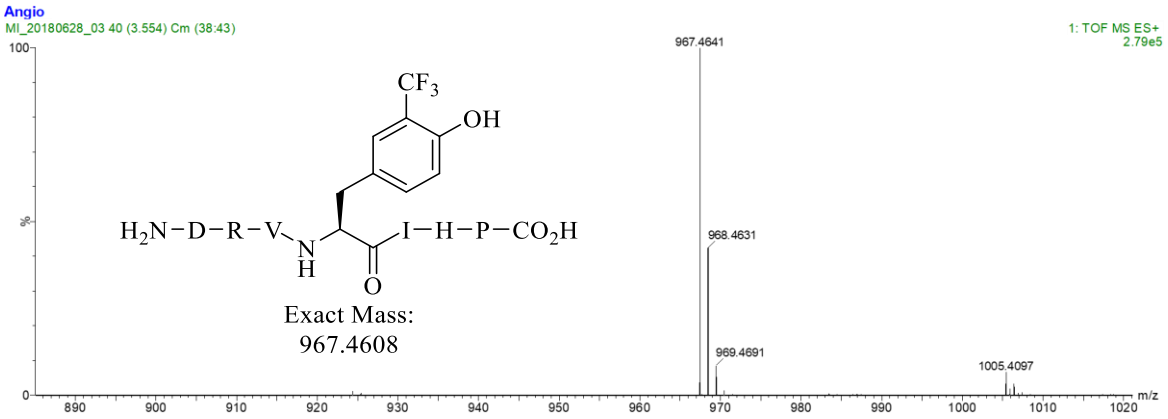


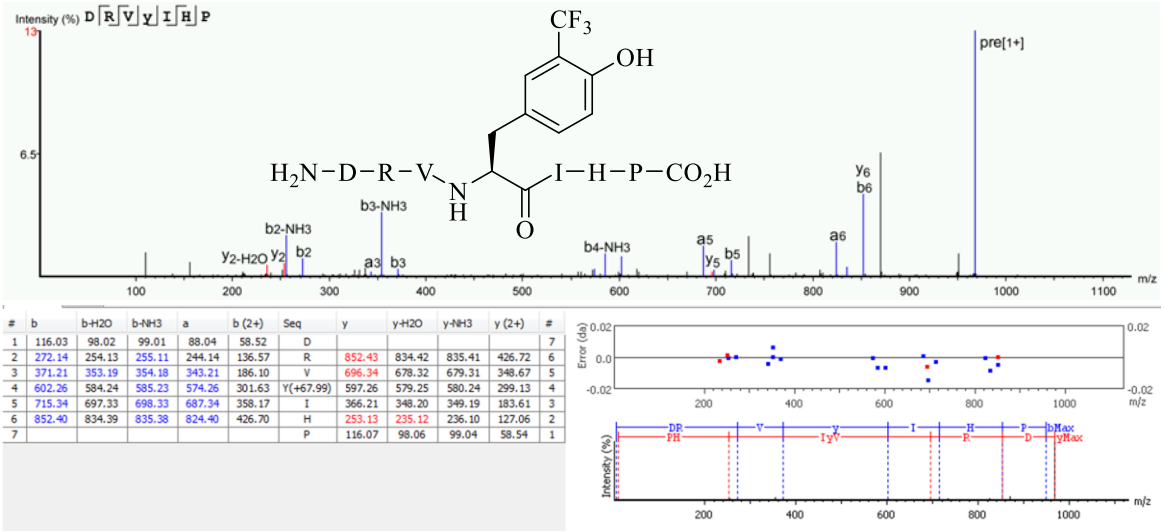
To Angiotensin I/II (1-7) (6.3 mg) in a 3 mL V-vial was added DMSO (20 µL), iron(III) chloride (4.4 mg, 0.027 mmol), sodium trifluoromethanesulfinate solution (10 µL of 1.0 M solution in 25 mM aqueous NH_4HCO_2, 0.010 mmol), and *tert*-butyl hydroperoxide solution (10 µL of 1.87 M solution in 25 mM aqueous NH_4HCO_2, 0.019 mmol) before stirring at 40 °C for 50 min. The solution was taken up in TFA:MeCN:H_2O 0.1:9.9:90 (1 mL), purified by reverse phase preparative HPLC, and lyophilised to obtain a white solid (2.4 mg, 1.8 µmol, 36%). **Reverse phase HPLC details**: Phenomenex Synergi^{TM} 4 µm Hydro RP 80 Å, 250 x 10 mm, flow rate = 4 mL/min, column temperature = 40 °C, eluent = 8% MeCN (0.1% TFA) and 92% H_2O (0.1% TFA) for 3 min then increase linearly to 30% MeCN (0.1% TFA) at 30 min, retention time 25.9 min; **^{1}H NMR** (500 MHz, DMSO-d_6): *only tyrosine residue protons are listed* δ 7.42 (d, *J* = 1.3 Hz, 1H), 7.32 (d, *J* = 8.5, 1.3 Hz, 1H), 6.88 (d, *J* = 8.5 Hz, 1H); **^{19}F NMR** (471 MHz, DMSO-d_6): δ -62.17, -74.95; **HRMS** (ESI$^+$): for $C_{42}H_{62}O_{11}N_{12}F_3$ $[M+H]^+$ requires *m*/*z* = 967.4608, found 967.4606.

COSY NMR



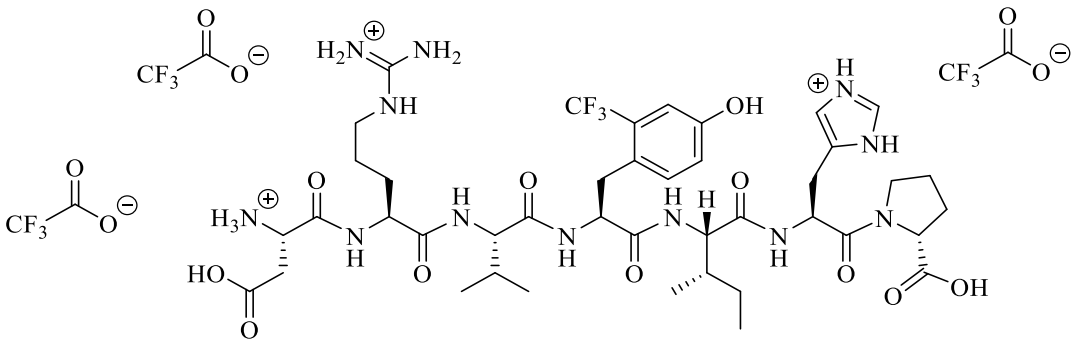
MS/MS Analysis





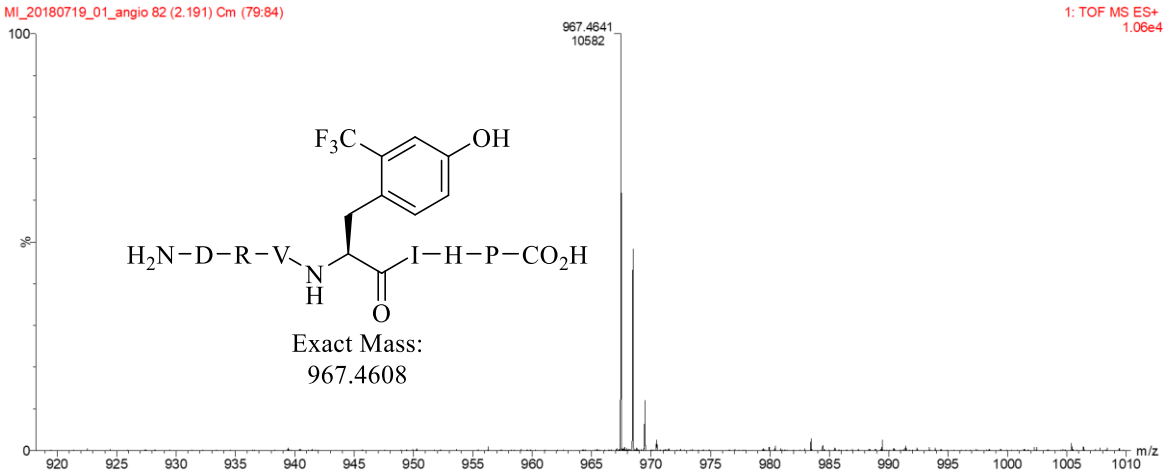
#	b	b-H2O	b-NH3	a	b (2+)	Seq	y	y-H2O	y-NH3	y (2+)	#
1	116.03	98.02	99.01	88.04	58.52	D					7
2	272.14	254.13	255.11	244.14	136.57	R	852.43	834.42	835.41	426.72	6
3	371.21	353.19	354.18	343.21	186.10	V	696.34	678.32	679.31	348.67	5
4	602.26	584.24	585.23	574.26	301.63	Y(+67.99)	597.26	579.25	580.24	299.13	4
5	715.34	697.33	698.33	687.34	358.17	I	366.21	348.20	349.19	183.61	3
6	852.40	834.39	835.38	824.40	426.70	H	253.13	235.12	236.10	127.06	2
7						P	116.07	98.06	99.04	58.54	1

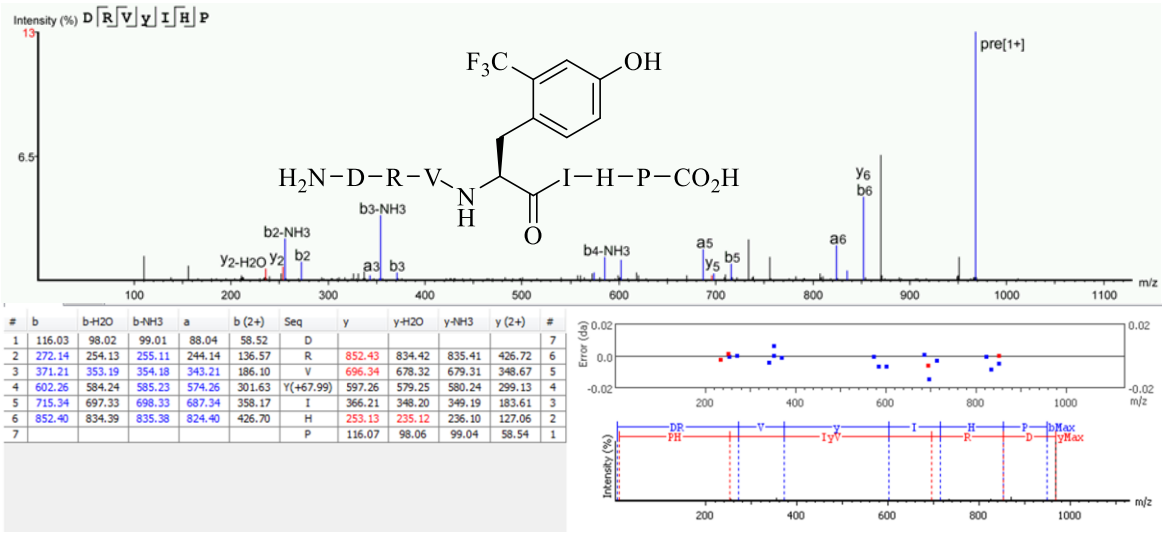
Angiotensin I/II (1-7)[Tyr(2-CF_3)]



To Angiotensin I/II (1-7) (6.3 mg) in a 3 mL V-vial was added DMSO (20 µL), iron(III) chloride (4.4 mg, 0.027 mmol), sodium trifluoromethanesulfinate solution (10 µL of 1.0 M solution in 25 mM aqueous NH_4HCO_2, 0.010 mmol), and *tert*-butyl hydroperoxide solution (10 µL of 1.87 M solution in 25 mM aqueous NH_4HCO_2, 0.019 mmol) before stirring at 40 °C for 50 min. The solution was taken up in TFA:MeCN:H_2O 0.1:9.9:90 (1 mL), purified by reverse phase preparative HPLC, and lyophilised to obtain a mixture of products. **Reverse phase HPLC details**: Phenomenex Synergi^{TM} 4 µm Hydro RP 80 Å, 250 x 10 mm, flow rate = 4 mL/min, column temperature = 40 °C, eluent = 8% MeCN (0.1% TFA) and 92% H_2O (0.1% TFA) for 3 min then increase linearly to 30% MeCN (0.1% TFA) at 30 min, retention time 25.9 min; **^{19}F NMR** (471 MHz, DMSO-d_6): δ -60.03, -74.95; **HRMS** (ESI^+): for $C_{42}H_{62}O_{11}N_{12}F_3$ $[M+H]^+$ requires *m*/*z* = 967.4608, found 967.4641.

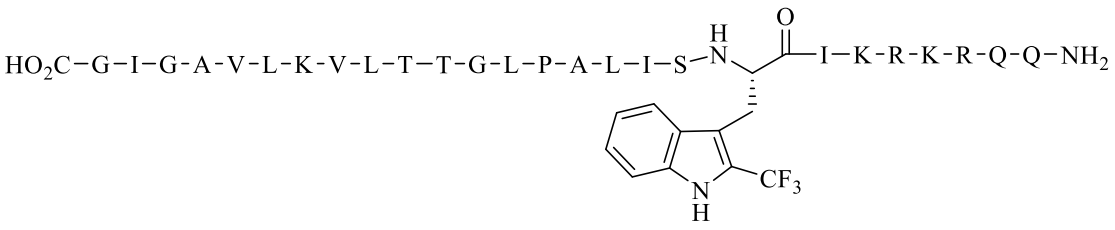
MS/MS Analysis





#	b	b-H2O	b-NH3	a	b (2+)	Seq	y	y-H2O	y-NH3	y (2+)	#
1	116.03	98.02	99.01	88.04	58.52	D					7
2	272.14	254.13	255.11	244.14	136.57	R	852.43	834.42	835.41	426.72	6
3	371.21	353.19	354.18	343.21	186.10	V	696.34	678.32	679.31	348.67	5
4	602.26	584.24	585.23	574.26	301.63	Y(+67.99)	597.26	579.25	580.24	299.13	4
5	715.34	697.33	698.33	687.34	358.17	I	366.21	348.20	349.19	183.61	3
6	852.40	834.39	835.38	824.40	426.70	H	253.13	235.12	236.10	127.06	2
7						P	116.07	98.06	99.04	58.54	1

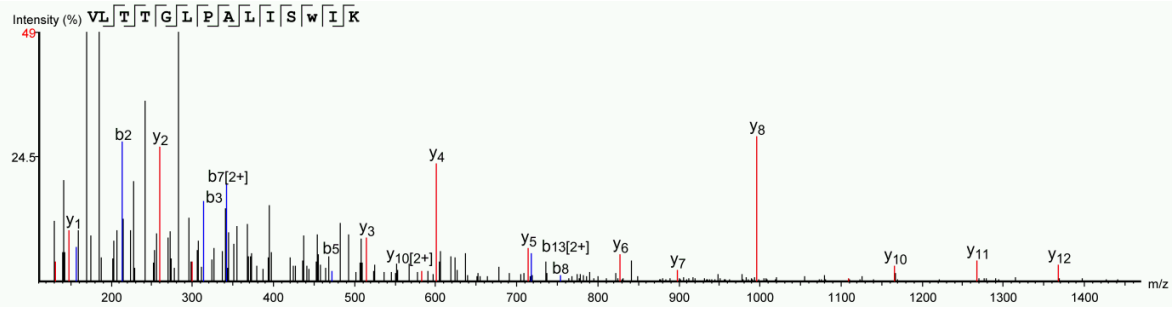
Melittin[Trp(2-CF_3)]



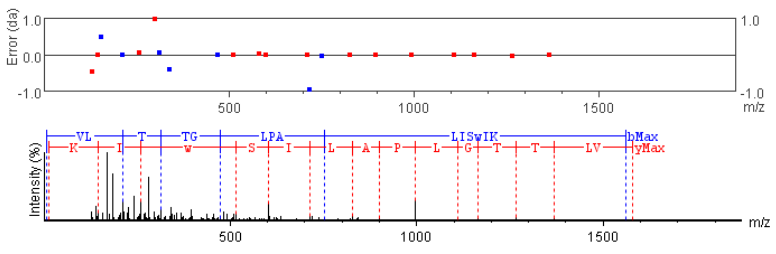
To melittin (0.7 mg) in a 3 mL V-vial was added DMSO (25 µL), iron(III) chloride solution (5 µL of 0.76 M solution in 25 mM aqueous NH_4HCO_2, 0.0038 mmol), sodium

trifluoromethanesulfinate solution (5 µL of 0.38 M solution in 25 mM aqueous NH_4HCO_2, 0.0019 mmol), *tert*-butyl hydroperoxide solution (5 µL of 0.64 M solution in 25 mM aqueous NH_4HCO_2, 0.0032 mmol), and NH_4HCO_2 solution (10 µL, 25 mM in H_2O) and before stirring at 40 °C for 20 min. The solution was taken up in TFA:MeCN:H_2O 0.1:14.9:85 (1 mL), purified by reverse phase preparative HPLC, and lyophilised. **Reverse phase HPLC details**: Zorbax 300SB-C18 5 µ 300 Å, 9.4 x 250 mm, flow rate = 4 mL/min, column temperature = 40 °C, eluent = 17.5% MeCN (0.1% TFA) and 82.5% H_2O (0.1% TFA) for 6 min then increase linearly to 55% MeCN (0.1% TFA) at 25 min, retention time = 23.3 min; **^{1}H NMR** (500 MHz, D_2O with 0.1% CF_3CO_2D): *only tryptophan residue protons are listed*, δ 7.74 (d, *J* = 8.0 Hz, 1H), 7.53 (d, *J* = 8.6 Hz, 1H), 7.31 – 7.26 (m, 1H), 7.15 – 7.12 (m, 1H); **^{19}F NMR** (470 MHz, D_2O with 0.1% CF_3CO_2D): δ -57.87, -75.50; **HRMS** (ESI^+): for $C_{132}H_{232}O_{31}N_{39}F_3$ $[M+4H]^{4+}$ requires *m/z* = 729.1927, found 729.1926.

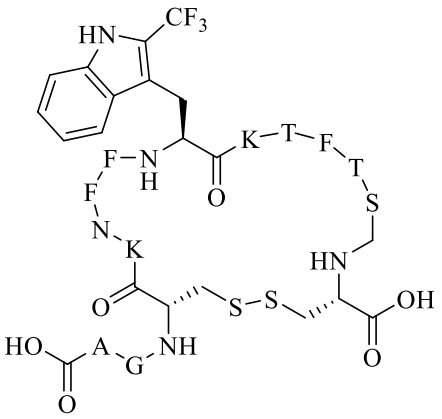
MS/MS Analysis after Trypsin Digestion



#	b	b (2+)	Seq	y	y (2+)	#
1	100.08	50.54	V			14
2	213.17	107.08	L	1480.84	740.92	13
3	314.12	157.10	T	1367.76	684.38	12
4	415.26	208.13	T	1266.74	633.85	11
5	472.29	236.64	G	1165.68	583.29	10
6	585.36	293.18	L	1108.66	554.82	9
7	682.41	342.11	P	995.58	498.28	8
8	753.48	377.23	A	898.53	449.75	7
9	866.54	433.77	L	827.48	414.23	6
10	979.62	490.31	I	714.40	357.69	5
11	1066.65	533.83	S	601.31	300.15	4
12	1320.72	660.86	W(+67.99)	514.28	257.63	3
13	1433.80	718.37	I	260.13	131.09	2
14			K	147.12	74.06	1

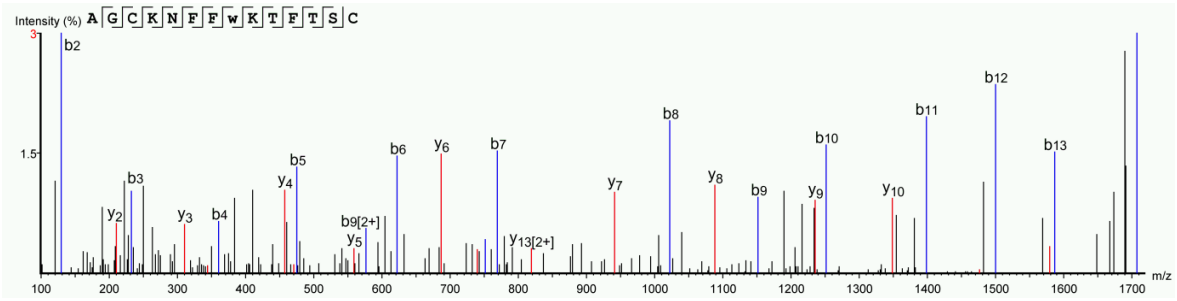


Somatostatin-14[Trp(2-CF_3)]

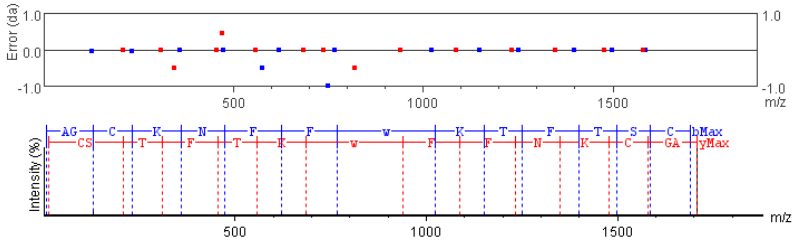


To Somatostatin-14 (2.4 mg) in a 3 mL V-vial was added DMSO (40 µL), iron(III) chloride solution (10 µL of 0.76 M solution in 25 mM aqueous NH_4HCO_2, 0.0076 mmol), sodium trifluoromethanesulfinate solution (15 µL of 0.38 M solution in 25 mM aqueous NH_4HCO_2, 0.0057 mmol), and *tert*-butyl hydroperoxide solution (10 µL of 0.64 M solution in 25 mM aqueous NH_4HCO_2, 0.0064 mmol) before stirring at 40 °C for 25 min. The solution was taken up in TFA:MeCN:H_2O 0.1:14.9:85 (1.1 mL), purified by reverse phase preparative HPLC, and lyophilised. **Reverse phase HPLC details**: Zorbax 300SB-C18 5 µ 300 Å, 9.4 x 250 mm, flow rate = 4 mL/min, column temperature = 40 °C, eluent = 17.5% MeCN (0.1% TFA) and 82.5% H_2O (0.1% TFA) for 6 min then increase linearly to 47% MeCN (0.1% TFA) at 25 min, retention time = 19.4 min; **^{19}F NMR** (470 MHz, DMSO-d_6): δ -57.58, -74.95; **HRMS** (ESI^+): for $C_{77}H_{104}O_{19}N_{18}F_3{}^{32}S_2$ $[M+H]^+$ requires *m*/*z* = 1705.7113, found 1705.7086.

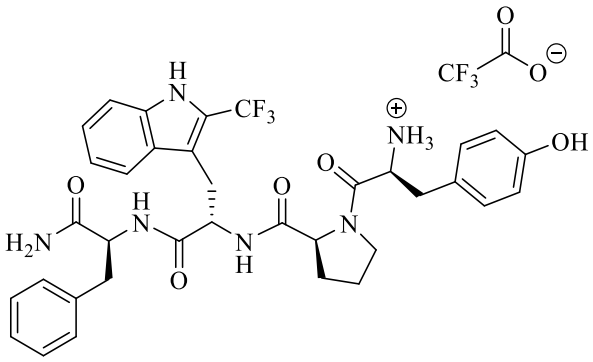
MS/MS Analysis



#	b	b (2+)	Seq	y	y (2+)	#
1	72.04	36.52	A			14
2	129.10	65.03	G	1636.69	819.36	13
3	232.11	116.54	C	1579.67	790.33	12
4	360.17	180.59	K	1476.66	738.83	11
5	474.21	237.61	N	1348.56	674.78	10
6	621.28	311.14	F	1234.52	617.76	9
7	768.35	384.68	F	1087.45	544.23	8
8	1022.42	511.71	W(+67.99)	940.38	470.22	7
9	1150.51	576.26	K	686.32	344.16	6
10	1251.56	626.28	T	558.22	279.61	5
11	1398.63	699.81	F	457.18	229.09	4
12	1499.67	751.33	T	310.11	155.55	3
13	1586.71	793.85	S	209.06	105.03	2
14			C	122.03	61.51	1



Endomorphin-1[Trp(2-CF_3)]



To endomorphin-1 (7.8 mg) in a 3 mL V-vial was added DMSO (52 µL), iron(III) chloride solution (26 µL of 1.0 M solution in 25 mM aqueous NH_4HCO_2, 0.026 mmol), sodium trifluoromethanesulfinate solution (20 µL of 1.0 M solution in 25 mM aqueous NH_4HCO_2, 0.020 mmol), and *tert*-butyl hydroperoxide solution (20 µL of 1.87 M solution in 25 mM aqueous NH_4HCO_2, 0.037 mmol) before stirring at 40 °C for 35 min. The solution was taken up in TFA:MeCN:H_2O 0.1:4.9:95 (1.1 mL), purified by reverse phase preparative HPLC, and lyophilised to obtain a white solid (0.59 mg, 0.743 µmol, 6%). **Reverse phase HPLC**

details: Phenomenex Synergi^{TM} 4 μm Hydro RP 80 Å, 250 x 10 mm, column temperature = 40 °C, flow rate = 4 mL/min, eluent = 17% MeCN (0.1% TFA) and 83% H_2O (0.1% TFA) for 3 min then increase linearly to 48% MeCN (0.1% TFA) at 25 min, retention time = 19.8 min.

Presence of *cis*- and *trans*- conformers was observed in the ^{1}H NMR spectra in a ratio of 25:75. This observation is consistent with that observed in the literature (*cis*- and *trans*-conformers of endomorphin-1 were reported in a ratio of 25:75 by Podlogar *et al*).[6]

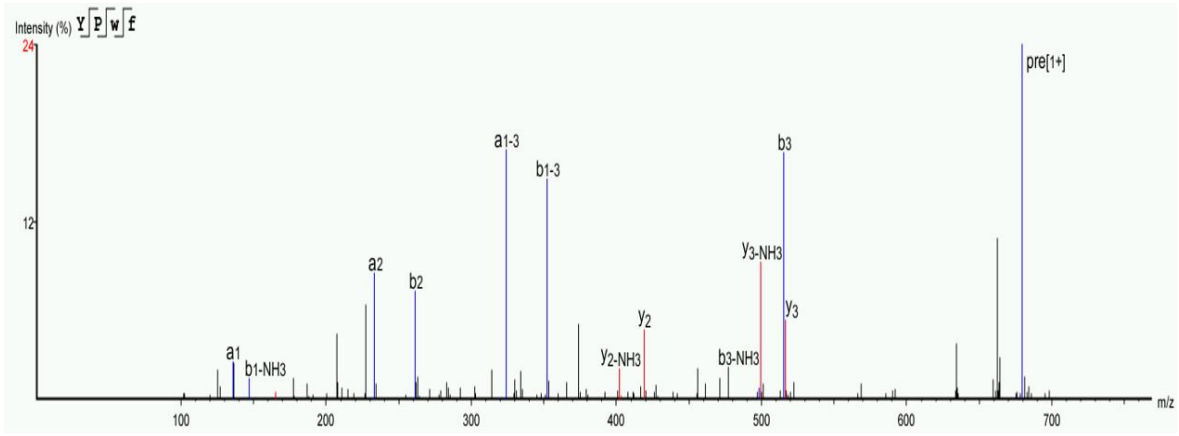
cis-endomorphin-1[Trp(2-CF_3)] isomer:

^{1}H NMR (500 MHz, DMSO-d_6): δ 11.91 (s, 1H), 9.42 (s, 1H), 8.23 (d, *J* = 8.6, 1H), 8.16 (s, 3H), 7.86 (d, *J* = 8.2 Hz, 1H), 7.79 (d, *J* = 8.1 Hz, 1H), 7.41 (d, *J* = 8.1 Hz, 1H), 7.29 – 7.05 (m, 10H), 7.05 (s, 1H), 6.68 (d, *J* = 8.2 Hz, 2H), 4.56 (q, *J* = 7.6 Hz, 1H), 4.45 – 4.42 (m, 1H), 3.72 – 3.70 (m, 1H), 3.63 – 3.53 (3.70 – 3.50, 2H), 3.28 – 2.75 (m, 7H), 2.02 – 1.94 (m, 1H), 1.67 – 1.61 (m, 2H); **^{19}F NMR** (470 MHz, DMSO-d_6): δ -57.60, -74.95; **HRMS** (ESI^+): for $C_{35}H_{38}O_5N_6F_3[M+H]^+$ requires *m*/*z* = 679.2850, found 679.2847.

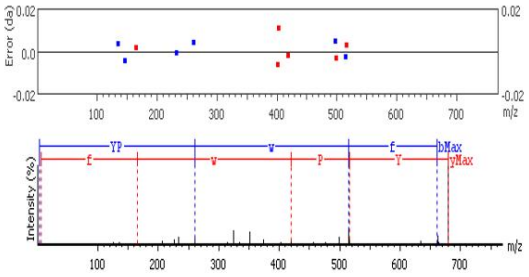
trans-endomorphin-1[Trp(2-CF_3)] isomer:

^{1}H NMR (500 MHz, DMSO-d_6): δ 11.91 (s, 1H), 9.33 (s, 1H), 8.08 (d, *J* = 8.1 Hz, 1H), 7.99 (s, 3H), 7.83 (d, *J* = 8.1 Hz, 1H), 7.74 (d, *J* = 8.1 Hz, 1H), 7.40 (d, *J* = 8.1, 1H), 7.29 – 7.05 (m, 10H), 6.99 (s, 1H), 6.68 (d, *J* = 8.2 Hz, 2H), 4.50 (q, *J* = 7.4 Hz, 1H), 4.41 – 4.34 (m, 2H), 4.22 (s, 1H), 3.63 – 3.53 (3.70 – 3.50, 1H), 3.28 – 2.75 (m, 7H), 2.02 – 1.94 (m, 1H), 1.82 – 1.71 (m, 2H); **^{19}F NMR** (470 MHz, DMSO-d_6): δ -57.57, -74.95; **HRMS** (ESI^+): for $C_{35}H_{38}O_5N_6F_3[M+H]^+$ requires *m*/*z* = 679.2850, found 679.2847.

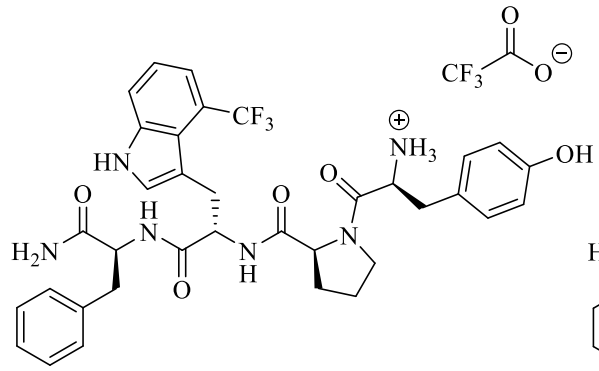
MS/MS Analysis



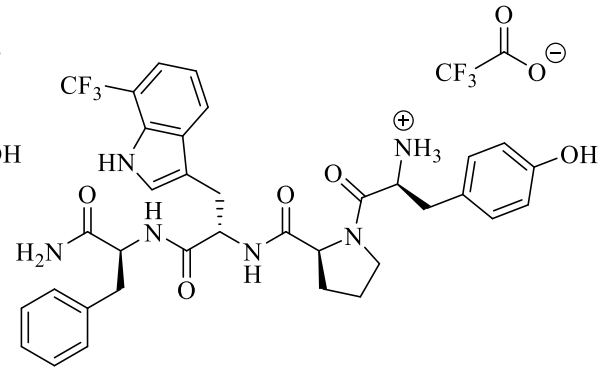
#	b	b-NH3	a	a-NH3	c	c-NH3	Seq	x	x-H2O	y	y-NH3	z	z'	#
1	164.07	147.05	136.07	119.05	181.10	164.07	Y							4
2	261.12	244.10	233.13	216.10	278.15	261.12	P	542.20	524.19	516.22	499.20	499.20	500.20	3
3	515.19	498.16	487.20	470.17	532.22	515.19	W(+67.99)	445.15	427.14	419.17	402.15	402.15	403.14	2
4							F(-.98)	191.08	173.07	165.10	148.08	148.08	149.08	1



Endomorphin-1[Trp(7-CF_3)] and Endomorphin-1[Trp(4-CF_3)]



Endomorphin-1[Trp(4-CF_3)]



Endomorphin-1[Trp(7-CF_3)]

To endomorphin-1 (7.8 mg) in a 3 mL V-vial was added DMSO (52 µL), iron(III) chloride solution (26 µL of 1.0 M solution in 25 mM aqueous NH_4HCO_2, 0.026 mmol), sodium trifluoromethanesulfinate solution (20 µL of 1.0 M solution in 25 mM aqueous NH_4HCO_2,

0.020 mmol), and *tert*-butyl hydroperoxide solution (20 µL of 1.87 M solution in 25 mM aqueous NH_4HCO_2, 0.037 mmol) before stirring at 40 °C for 35 min. The solution was taken up in TFA:MeCN:H_2O 0.1:4.9:95 (1.1 mL), purified by reverse phase preparative HPLC, and lyophilised to obtain a mixture of products. **Reverse phase HPLC details**: Phenomenex Synergi^{TM} 4 µm Hydro RP 80 Å, 250 x 10 mm, column temperature = 40 °C, flow rate = 4 mL/min, eluent = 20% MeCN (0.1% TFA) in H_2O (0.1% TFA) for 3 min then increase linearly to 48% MeCN (0.1% TFA) at 27 min, retention time = 22.4 min; **^{19}F NMR** (470 MHz, DMSO-d_6): δ -57.22, -57.24, -61.08, -61.10, -74.95; **MS** (ESI^+): for $C_{35}H_{38}O_5N_6F_3$ $[M+H]^+$ requires *m*/*z* = 679.29, found 679.31.

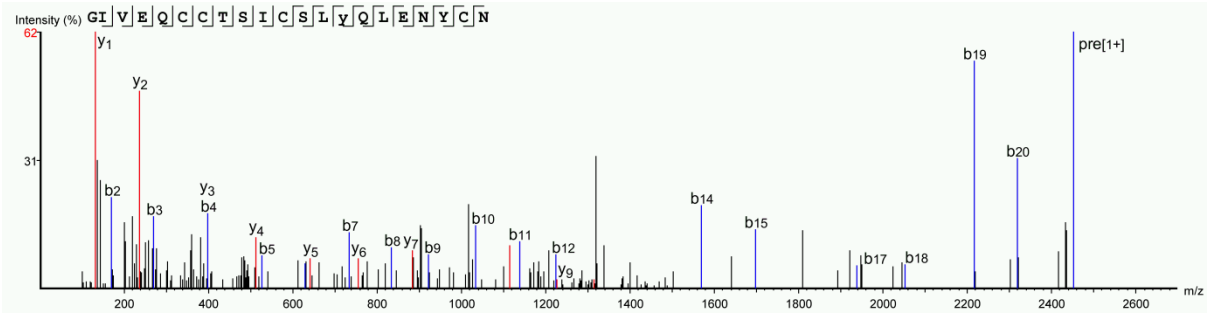
Trifluoromethylation of Insulin

To recombinant human insulin (20.7 mg) in a 3 mL V-vial was added sodium trifluoromethanesulfinate (14.6 mg, 0.94 mmol), DMSO (320 µL), AcOH (59 µL), H_2O (59 µL), and *tert*-butyl hydroperoxide (24 µL, 0.17 mmol) before stirring at 30 °C for 15 min. The solution was taken up in TFA:MeCN:H_2O 0.1:14.9:85 (1 mL), the products were purified by reverse phase preparative HPLC, and lyophilised. **Reverse phase HPLC details**: Zorbax 300SB-C18, 9.4 x 250 mm 5 µ 300 Å, flow rate = 4 mL/min, column temperature = 40 °C, eluent = 24% MeCN (0.1% TFA) and 76% H_2O (0.1% TFA) for 3 min then increase linearly to 42% MeCN (0.1% TFA) at 25 min.

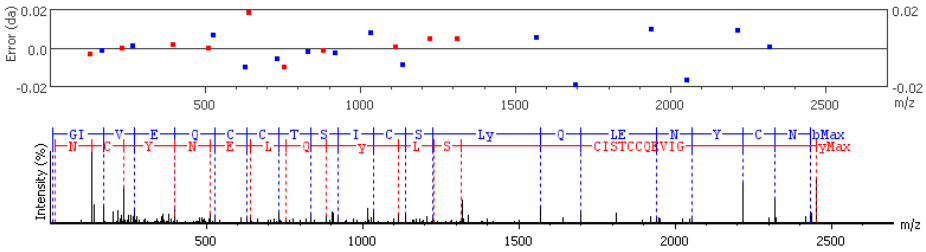
Insulin Chain A Y14[CF_3]

2.9 mg of white solid was obtained after lyophilisation, retention time = 19.1 min. **^{19}F NMR** (471 MHz, D_2O with 0.1% CF_3CO_2D) δ -61.50, -74.95.

MS/MS Analysis

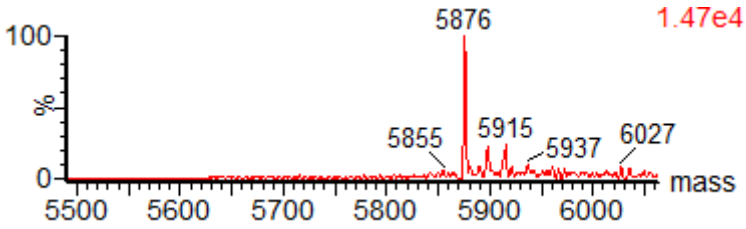


#	b	Seq	y	#
1	58.03	G		21
2	171.12	I	2393.97	20
3	270.18	V	2280.89	19
4	399.22	E	2181.82	18
5	527.28	Q	2052.78	17
6	630.30	C	1924.72	16
7	733.31	C	1821.71	15
8	834.35	T	1718.70	14
9	921.38	S	1617.65	13
10	1034.46	I	1530.62	12
11	1137.48	C	1417.54	11
12	1224.50	S	1314.52	10
13	1337.59	L	1227.49	9
14	1568.64	Y(+67.99)	1114.41	8
15	1696.72	Q	883.36	7
16	1809.78	L	755.31	6
17	1938.82	E	642.20	5
18	2052.89	N	513.18	4
19	2215.92	Y	399.13	3
20	2318.94	C	236.07	2
21		N	133.06	1

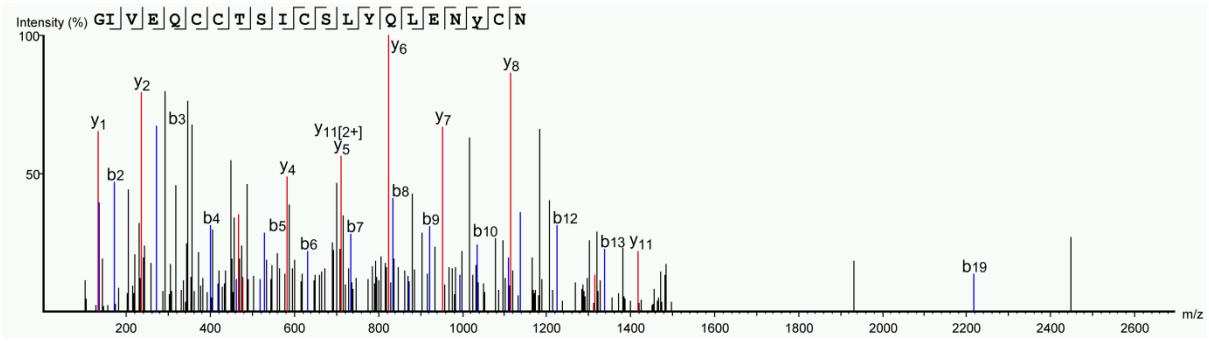


Insulin Chain A Y19[CF_3]

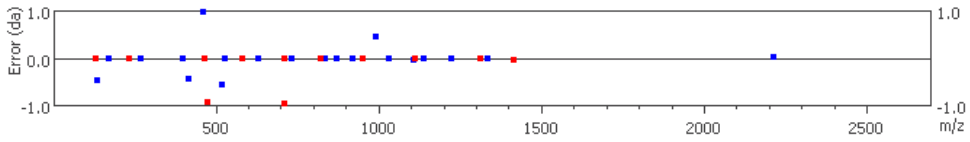
2.9 mg of white solid was obtained after lyophilisation, retention time = 18.0 min. **^{19}F NMR** (471 MHz, D_2O with 0.1% CF_3CO_2D) δ -60.31, -74.95.

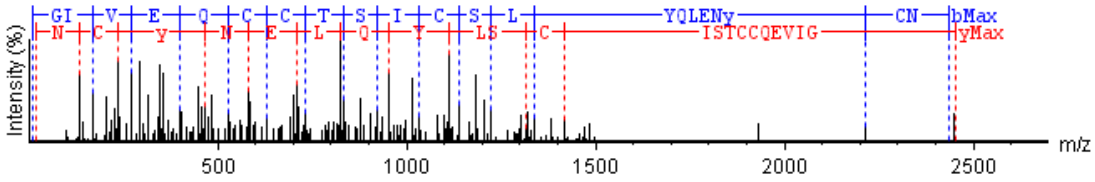


MS/MS Analysis



#	b	b (2+)	Seq	y	y (2+)	#
1	58.03	29.51	G			21
2	171.12	86.06	I	2393.97	1197.49	20
3	270.19	136.08	V	2280.89	1140.94	19
4	399.23	200.11	E	2181.82	1091.41	18
5	527.29	264.14	Q	2052.78	1026.89	17
6	630.31	315.65	C	1924.72	962.86	16
7	733.32	367.15	C	1821.71	911.36	15
8	834.36	418.14	T	1718.70	859.85	14
9	921.39	460.19	S	1617.65	809.33	13
10	1034.48	518.31	I	1530.62	765.81	12
11	1137.50	569.24	C	1417.57	710.22	11
12	1224.54	612.75	S	1314.54	657.76	10
13	1337.60	669.30	L	1227.50	614.25	9
14	1500.65	750.83	Y	1114.43	557.71	8
15	1628.71	814.86	Q	951.37	477.11	7
16	1741.80	871.40	L	823.30	412.15	6
17	1870.84	935.92	E	710.22	355.60	5
18	1984.88	992.46	N	581.17	291.08	4
19	2215.87	1108.51	Y(+67.99)	467.13	234.06	3
20	2318.94	1159.97	C	236.08	118.53	2
21			N	133.07	67.03	1





Chain B unmodified

Insulin Chain B Y16[CF_3] and Insulin Chain B Y26[CF_3]

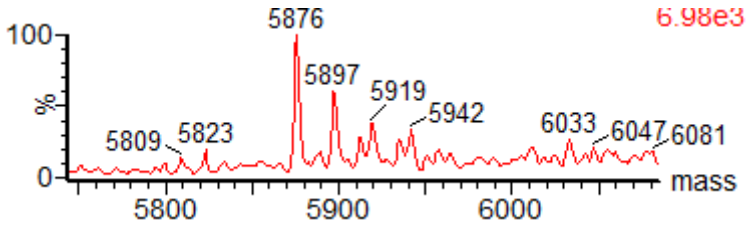
1.7 mg of white solid was obtained after lyophilisation. Both products are separable to a certain extent, however, they were collected together for NMR measurement. The two

products were separated for LC-MS/MS. **^{19}F NMR** (471 MHz, D_2O with 0.1% CF_3CO_2D) δ -61.36, -61.39, -74.95.

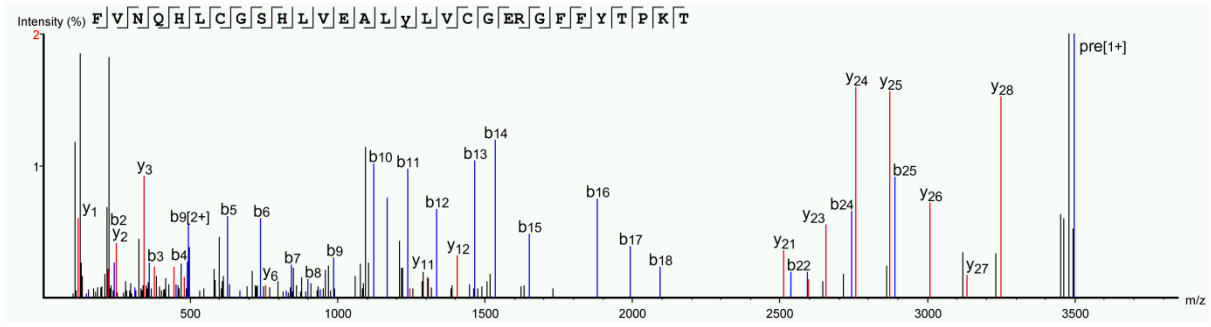
Insulin Chain B Y16[CF_3]

MS/MS Analysis

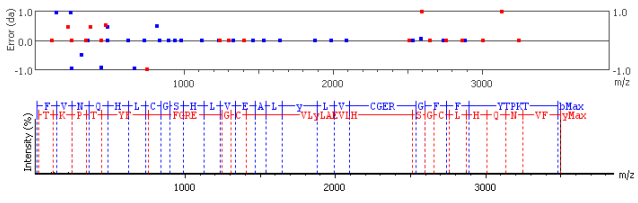
Retention time = 18.4 min.



MS/MS under optimised conditionsindicated chain B as the position of modification.



#	b	b (2+)	Seq	y	y (2+)	#
1	147.12	74.54	F			30
2	248.11	124.07	V	3349.61	1675.31	29
3	361.19	181.09	N	3250.53	1625.77	28
4	489.24	244.17	Q	3135.51	1568.75	27
5	626.31	314.17	H	3008.43	1504.72	26
6	739.39	370.19	L	2871.38	1436.19	25
7	842.40	421.70	C	2758.30	1379.65	24
8	899.42	451.16	G	2655.28	1328.14	23
9	986.45	493.25	S	2597.27	1299.63	22
10	1123.51	562.26	H	2511.24	1256.12	21
11	1236.58	618.80	L	2374.18	1187.59	20
12	1335.65	669.29	V	2261.09	1131.05	19
13	1464.70	732.85	E	2162.02	1081.51	18
14	1535.74	768.37	A	2032.98	1016.99	17
15	1648.82	824.40	L	1961.94	981.47	16
16	1879.87	940.44	Y(+67.99)	1848.86	924.93	15
17	1992.96	996.98	L	1617.81	809.40	14
18	2092.01	1046.52	V	1504.73	752.86	13
19	2195.04	1098.02	C	1405.65	703.33	12
20	2252.06	1126.53	G	1302.63	651.82	11
21	2381.10	1191.05	E	1245.60	623.31	10
22	2537.19	1269.10	R	1116.58	558.79	9
23	2594.16	1297.61	G	960.48	480.20	8
24	2741.29	1371.15	F	903.46	452.23	7
25	2888.36	1444.68	F	757.38	378.21	6
26	3051.43	1526.21	Y	609.32	305.16	5
27	3152.47	1576.74	T	446.26	223.16	4
28	3249.53	1625.26	P	345.21	173.11	3
29	3377.62	1689.31	K	248.16	124.58	2
30			T	120.08	60.53	1

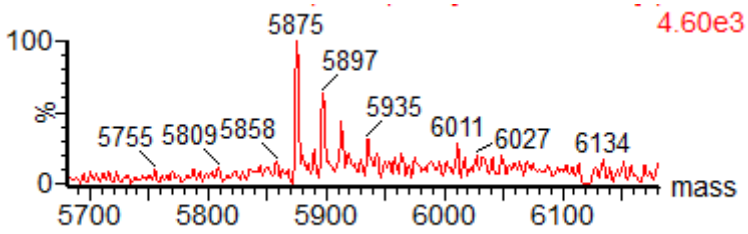


Chain A was unmodified.

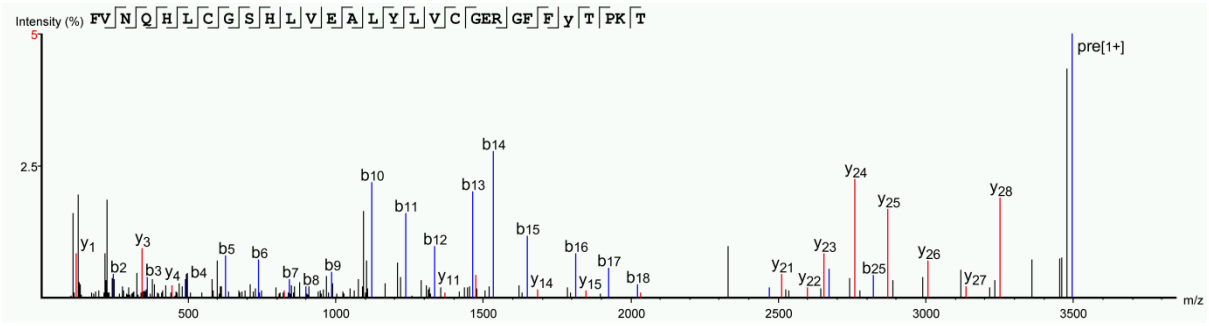
Insulin Chain B Y26[CF_3]

MS/MS Analysis

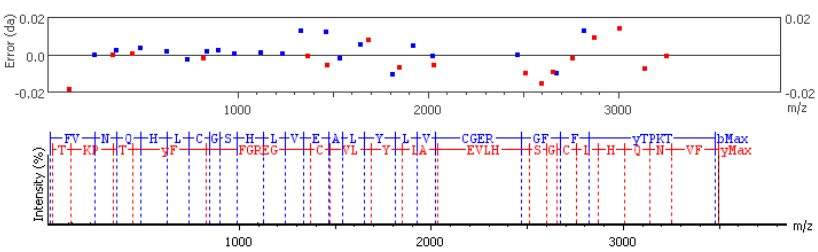
Retention time = 18.6 min.



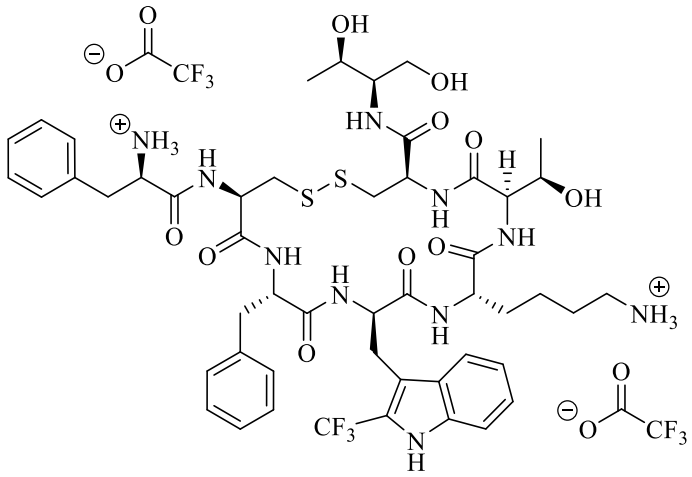
MS/MS under optimised conditions indicated Y26 as the position of modification.



#	b	b (2+)	Seq	y	y (2+)	#
1	148.08	74.54	F			30
2	247.15	124.07	V	3349.61	1675.31	29
3	361.18	181.09	N	3250.54	1625.77	28
4	489.24	245.12	Q	3136.51	1568.75	27
5	626.30	313.65	H	3008.43	1504.72	26
6	739.39	370.19	L	2871.37	1436.19	25
7	842.40	421.70	C	2758.30	1379.65	24
8	899.42	450.21	G	2655.30	1328.14	23
9	986.45	493.73	S	2598.28	1299.63	22
10	1123.51	562.26	H	2511.25	1256.12	21
11	1236.59	618.80	L	2374.18	1187.59	20
12	1335.65	668.33	V	2261.09	1131.05	19
13	1464.69	732.85	E	2162.02	1081.51	18
14	1535.74	768.37	A	2032.99	1016.99	17
15	1648.82	824.91	L	1961.94	981.47	16
16	1811.90	906.45	Y	1848.87	924.93	15
17	1924.97	962.99	L	1685.79	843.40	14
18	2024.04	1012.52	V	1572.71	786.86	13
19	2127.05	1064.03	C	1473.65	737.32	12
20	2184.07	1092.54	G	1370.64	685.82	11
21	2313.12	1157.06	E	1313.61	657.31	10
22	2469.22	1235.11	R	1184.57	592.79	9
23	2526.24	1263.62	G	1028.47	514.73	8
24	2673.32	1337.15	F	971.45	486.22	7
25	2820.36	1410.69	F	824.38	412.69	6
26	3051.43	1526.21	Y(+67.99)	677.31	339.16	5
27	3152.47	1576.74	T	446.26	223.63	4
28	3249.53	1625.26	P	345.21	173.11	3
29	3377.62	1689.31	K	248.16	124.58	2
30			T	120.08	60.53	1



Octreotide[Trp(2-CF_3)]

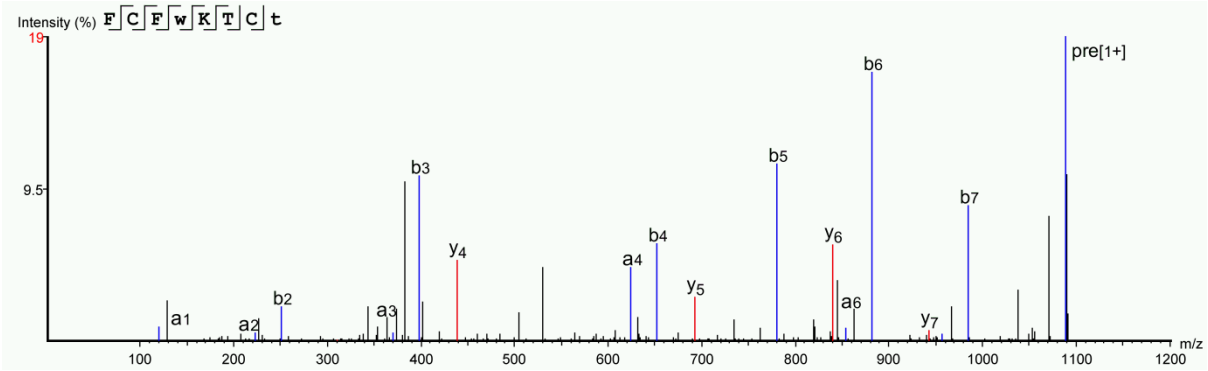


To octreotide acetate salt (2.0 mg, 0.00185 mmol) in a vial was added DMSO (40 µL), iron(III) nitrate solution (10 µL of 0.76 M solution in 25 mM aqueous NH_4HCO_2, 0.0076 mmol), sodium trifluoromethanesulfinate solution (15 µL of 0.38 M solution in 25 mM aqueous NH_4HCO_2, 0.0057 mmol), and *tert*-butyl hydroperoxide solution (10 µL of 0.64 M solution in 25 mM aqueous NH_4HCO_2, 0.0064 mmol) before stirring at 40 °C for 10 min. The solution was taken up in H_2O (2.0 mL), purified by reverse phase preparative HPLC, and lyophilised to obtain a white solid (0.85 mg, 0.71 µmol, 40%). **Reverse phase HPLC**

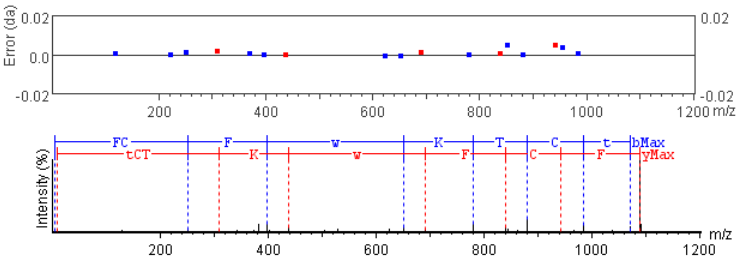
details: Phenomenex Synergi^{TM} 4 μm Hydro RP 80 Å, 250 x 10 mm, flow rate = 4 mL/min, column temperature = 25 °C, eluent = 20% MeCN (0.1% TFA) and 80% H_2O (0.1% TFA) for 6 min then increase linearly to 37% MeCN (0.1% TFA) at 23 min, retention time = 22.4 min; **^{1}H NMR** (500 MHz, DMSO-d_6): δ 11.99 (s, 1H), 8.98 – 8.95 (m, 1H), 8.85 – 8.83 (m, 1H), 8.41 – 8.32 (m, 2H), 8.24 – 8.20 (m, 1H), 8.10 (s, 3H), 7.71 – 7.68 (m, 1H), 7.57 – 7.55 (m, 3H), 7.47 – 7.43 (m, 1H), 7.40 – 7.23 (m, 10H), 7.16 – 7.15 (m, 2H), 7.08 (t, *J* = 7.6 Hz, 1H), 5.19 – 5.17 (m, 1H), 4.96 – 4.87 (m, 1H), 4.80 – 4.78 (m, 1H), 4.70 – 4.63 (m, 2H), 4.38 – 4.26 (m, 2H), 4.15 – 4.11 (m, 1H), 4.09 – 4.04 (m, 2H), 3.96 – 3.92 (m, 1H), 3.66 – 3.59 (m, 2H), 3.48 – 3.43 (m, 1H), 3.15 – 2.78 (m, 12H), 1.23 – 1.03 (m, 13H); **^{19}F NMR** (470 MHz, DMSO-d_6): δ -57.93, -74.95; **HRMS** (ESI$^+$): for $C_{50}H_{66}F_3N_{10}O_{10}S_2$ $[M+H]^+$ requires 1087.4351, found 1087.4349.

MS/MS Analysis

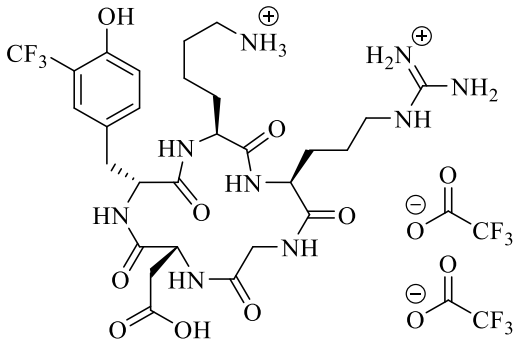
Sample treated with 5 mM DTT before analysis



#	b	a	b (2+)	Seq	y	y (2+)	#
1	148.08	120.08	74.54	F			8
2	251.08	223.09	126.04	C	942.38	471.69	7
3	398.15	370.16	199.58	F	839.37	420.19	6
4	652.22	624.23	326.61	W(+67.99)	692.30	346.65	5
5	780.32	752.32	390.66	K	438.24	219.62	4
6	881.36	853.36	441.18	T	310.14	155.57	3
7	984.37	956.37	492.69	C	209.10	105.05	2
8				T(-13.98)	106.09	53.54	1



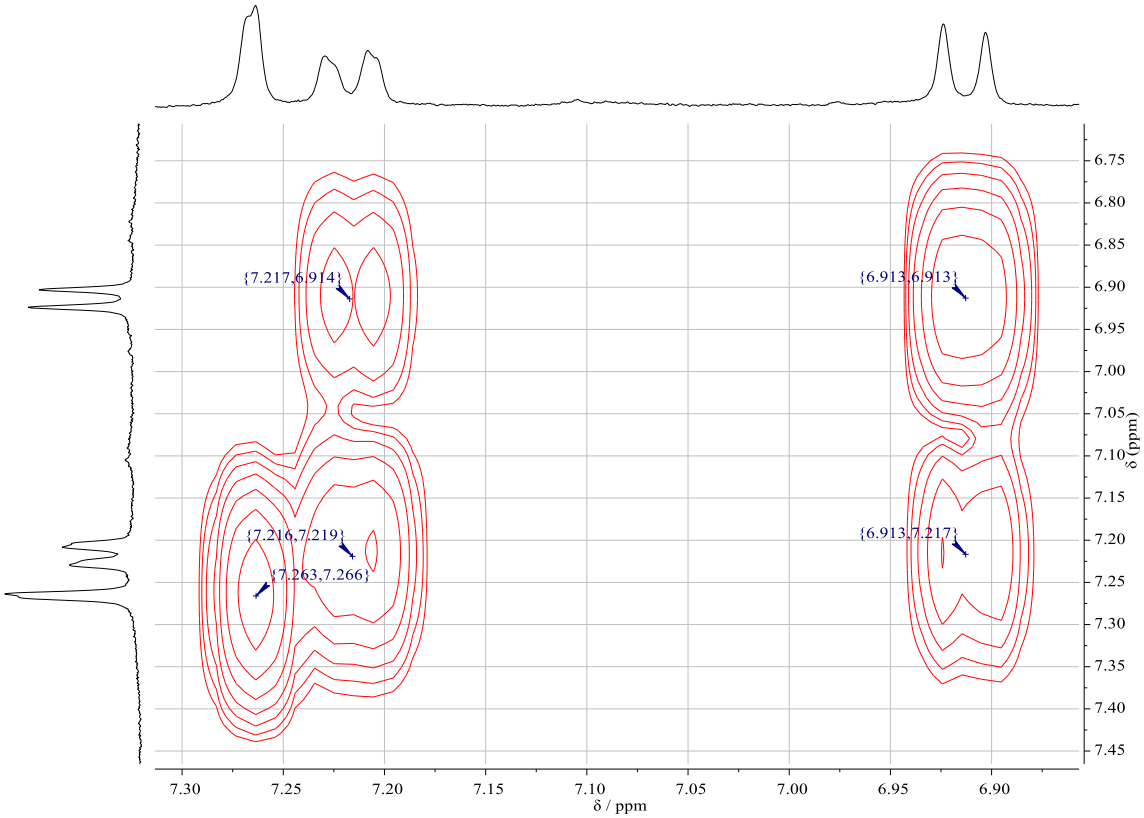
Cyclo(-Arg-Gly-Asp-D-Tyr-Lys)[Tyr(3-CF_3)]



To cyclo(-Arg-Gly-Asp-D-Tyr-Lys) trifluoroacetate salt (5.0 mg, 0.00807 mmol) in a vial was added DMSO (150 µL), iron(III) nitrate solution (50 µL of 0.12 M solution in 25 mM aqueous NH_4HCO_2, 0.00621 mmol), sodium trifluoromethanesulfinate solution (50 µL of 0.46 M solution in 25 mM aqueous NH_4HCO_2, 0.0230 mmol), and *tert*-butyl hydroperoxide solution (50 µL of 0.44 M solution in 25 mM aqueous NH_4HCO_2, 0.0219 mmol) before stirring at 40 °C for 10 min. The solution was taken up in H_2O (2.0 mL), purified by reverse phase preparative HPLC, and lyophilised to obtain a white solid. **Reverse phase HPLC details**: Phenomenex Synergi^{TM} 4 µm Hydro RP 80 Å, 250 x 10 mm, flow rate = 4 mL/min, column temperature = 25 °C, eluent = 17% MeCN (0.1% TFA) and 83% H_2O (0.1% TFA) for 15 min then increase linearly to 37% MeCN (0.1% TFA) at 23 min, retention time = 11.5 min; **^{1}H NMR** (600 MHz, DMSO-d_6): δ 10.37 (s, 1H), 8.47 (dd, *J* = 7.5, 4.6 Hz, 1H), 8.11 (t, *J* = 7.6 Hz, 2H), 8.02 (d, *J* = 7.2 Hz, 1H), 7.66 (s, 3H), 7.54 (d, *J* = 7.9 Hz, 1H), 7.50 (t, *J* = 5.9 Hz, 1H), 7.26 (d, *J* = 2.1 Hz, 1H), 7.21 (dd, *J* = 8.5, 2.1 Hz, 1H), 6.91 (d, *J* = 8.4 Hz, 1H), 4.63 (td, *J* = 8.3, 6.1 Hz, 1H), 4.37 (q, *J* = 7.2 Hz, 1H), 4.14 (q, *J* = 7.5 Hz, 1H), 4.02 (dd, *J* = 14.9, 7.5 Hz, 1H), 3.87 – 3.93 (m, 1H), 3.08 (q, *J* = 6.7 Hz, 2H), 2.81 (ddd, *J* = 42.7, 13.6, 7.1 Hz, 2H), 2.69 (dt, *J* = 14.3, 8.5 Hz, 3H), 2.36 – 2.41 (m, 1H), 1.65 – 1.74 (m, 1H), 1.53 – 1.60 (m, 1H), 1.31 – 1.50 (m, 7H), 1.01 – 1.09 (m, 2H) *carboxylic acid OH was not*

observed; observed indirectly from COSY since obscured by solvent peak: 3.23 – 3.28 (m); **^{19}F NMR** (565 MHz, DMSO-d_6): δ -62.14; **HRMS** (ESI$^+$): for $C_{28}H_{41}F_3N_9O_8$ $[M+H]^+$ requires 688.3025, found 688.2985.

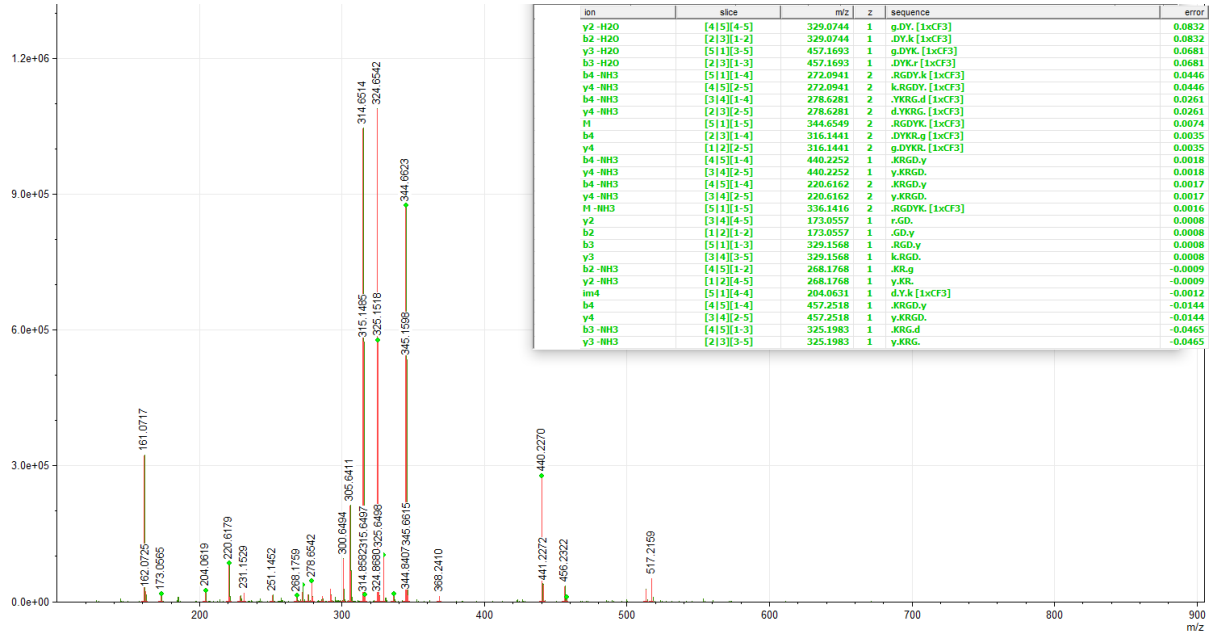
COSY NMR



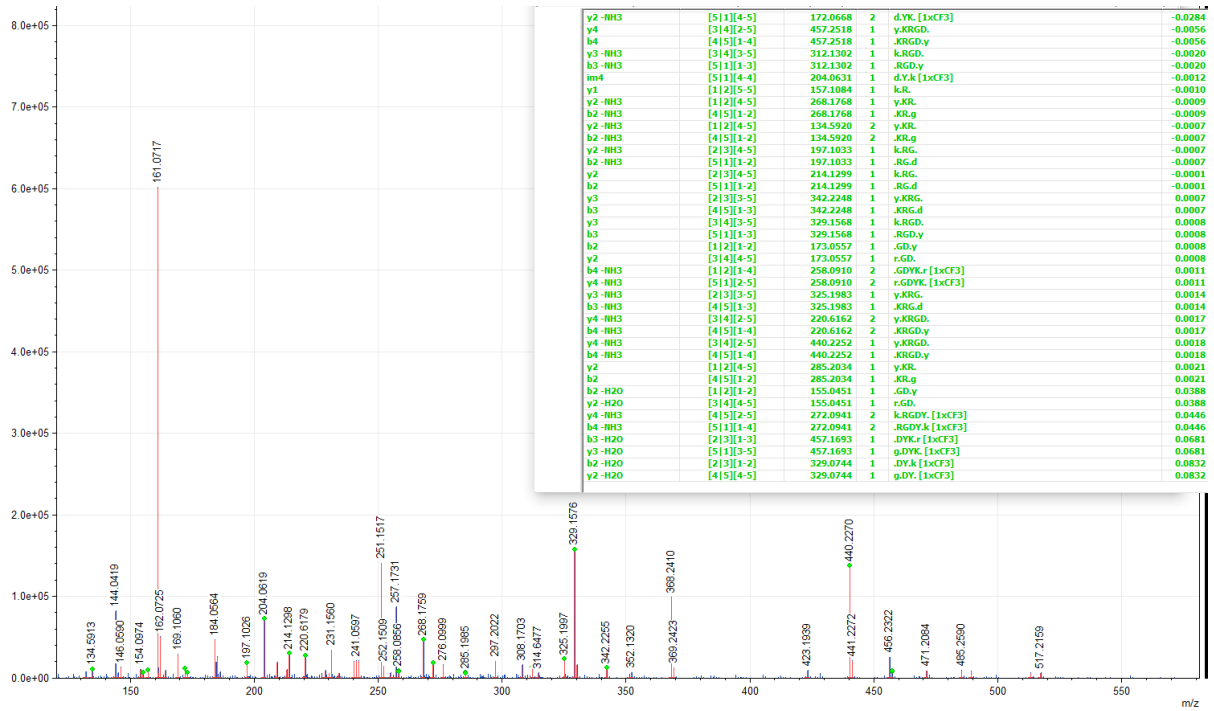
MS/MS Analysis

Peaks annotated in green matched with cyclo(-Arg-Gly-Asp-D-Tyr-Lys)[Tyr(3-CF_3)] fragmentation spectrum

Collision energy: 15V



Collision energy: 30V



4.3 Reaction Screening for Synthesis of the Langlois Reagent

General Procedure

A 10 mL vial with magnetic follower was purged with argon before adding potassium fluoride (5.8 mg, 0.1 mmol) and Kryptofix (37.7 mg, 0.1 mmol). MeCN (1.5 mL) was added before concentrating *in vacuo* for 1 h. SO_2 source (0.2 mmol), difluorocarbene reagent (0.2 mmol), and anhydrous DMF (0.5 ml) were added before flushing the vial with argon and stirring at 100 ºC for 15 min. The vial was cooled to room temperature.

For NMR analysis of the crude: Deuterated DMSO (2.0 mL) and α,α,α-trifluorotoluene (0.1 mmol) was added before ^{19}F NMR analysis.

For purification using WAX cartridges: The mixture was taken up in aqueous 2% formic acid (6 mL) and passed over a WAX cartridge. The cartridge was washed with EtOH (6 mL) before eluting with 0.7% NH_3 in EtOH (5 mL). Deuterated DMSO (2.0 mL) and α,α,α-trifluorotoluene (0.1 mmol) was added before ^{19}F NMR analysis.

For isolation using semi-preparative HPLC: The solvent was evaporated and the residue was dissolved in H_2O (1 mL) before purifying by reverse phase preparative HPLC. **Reverse phase HPLC details**: Phenomenex Synergi^{TM} 4 μm Hydro RP 80 Å, 250 x 10 mm, flow rate = 4 mL/min, column temperature = 25 °C, eluent = 5% MeCN and 95% H_2O for 5 min then increase linearly to 100% MeCN at 16 min, retention time = 3.6 min.

Procedure for Testing Stability of Langlois Reagent

A 10 mL vial with magnetic follower was purged with argon before adding Langlois reagent (15.6 mg, 0.1 mmol) and triphenylphosphine (52.4 mg, 0.2 mmol) in solvent (0.5 mL) at 100

ºC for 20 min. The vial was cooled to room temperature, deuterated DMSO (2.0 mL) and α,α,α-trifluorotoluene (0.1 mmol) was added before ^{19}F NMR analysis.

4.4 Radiochemistry at the University of Oxford

4.4.1 General Experimental Details

[^{18}F]Fluoride was produced by Alliance Medical (UK) via the $^{18}O(p,n)^{18}F$ reaction and delivered as [^{18}F]fluoride in [^{18}O]water. Radiosynthesis and azeotropic drying were performed on a NanoTek® automated microfluidic device (Advion). HPLC analysis was performed with a Dionex Ultimate 3000 dual channel HPLC system equipped with shared autosampler, parallel UV detectors and LabLogic NaI/PMT radiodetectors with Flowram analog output. Due to the separation of modules, the radiosignal was offset by 0.1 – 0.3 min from the UV signal. Mass spec analysis (ESI) was performed by diverting part of the HPLC flow, after passing through the radiodetector, to the inlet of an Advion CMS (see Figure S1). Only nonradioactive compounds were observed since the concentration of ^{18}F-compounds was below the limit of detection.

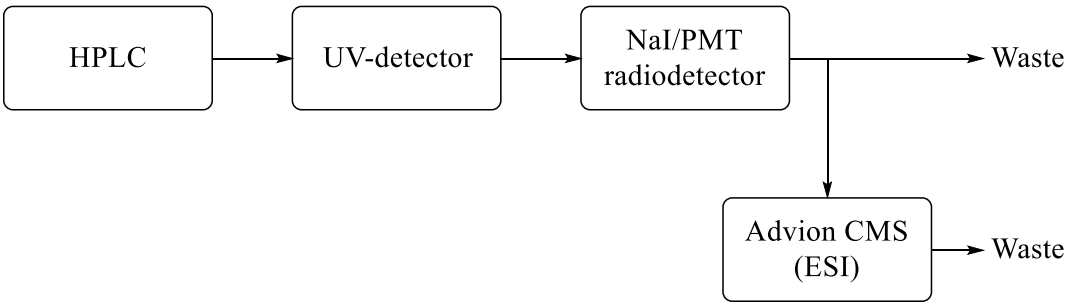


Figure S1: Flow diagram for UV, activity and mass measurement.

All Chromafix PSHCO_3 ^{18}F separation cartridges (45 mg) were activated by slowly adding H_2O (1 mL). All Waters Sep-Pak Accell Plus QMA Carbonate Plus Light cartridges (46 mg)

(Product Number: 186004540) were activated by slowly adding H_2O (2 mL). All Waters Sep-Pak Accell Plus QMA Plus Light cartridges (130 mg) (Product Number: WAT023525) were activated by slowly adding EtOH (10 mL), Na_2SO_4 solution (10 mL, 0.5 M in H_2O), and H_2O (10 mL). All Oasis Plus Weak Anion Exchange (WAX) short cartridges (Product Number: 186003519) were activated with water (3 mL) and 2% formic acid in water (3 mL). All procedures using WAX cartridges were carried out as efficiently as possible and flow rate was maintained at 3 mL/min.

For radiochemical reactions carried out using aliquots of [^{18}F]fluoride, the efficiency of labelling the desired product starting from [^{18}F]fluoride is calculated as the Radiochemical Yield (RCY). This can be measured by radio-HPLC using an aliquot of the crude reaction quenched with an aqueous solution to dissolve unreacted [^{18}F]fluoride. The RCY is the measured activity of labelled product as a percentage of the unreacted [^{18}F]fluoride and other labelled side products. The RCY is decay corrected which takes into account activity lost from decay over time thus giving a sense of chemical efficiency.

Activity Yield (AY) is calculated by comparing the starting activity with the activity of the purified product, after taking into account Radiochemical Purity (RCP) as determined by radio-HPLC. AY is not corrected for decay and is used to analyse overall synthesis efficiency by including purification and isolation steps of the final compound.

All ^{18}F-labeled compounds were characterised by comparing the radio-HPLC spectrum with a UV-HPLC spectrum of an authentic reference.

4.4.2 Radiosynthesis of [^{18}F]Langlois Reagent

20 – 30 MBq Reaction Screening using Aliquots of [^{18}F]Fluoride

[^{18}F]Fluoride (3.0 – 10.0 GBq) was separated from [^{18}O]water using a Chromafix PSHCO_3 ^{18}F separation cartridge (45 mg) and subsequently released using a solution of Kryptofix (15.0 mg) and K_2CO_3 (3.0 mg) in MeCN:H_2O 4:1 (900 μL in 6 x 150 μL portions) into a 5 mL V-vial containing a magnetic stirrer bar in a concentrator. The solution was azeotropically dried with anhydrous MeCN (1000 μL in 5 x 200 μL portions) under a flow of N_2 at 105 °C. The dried [^{18}F]KF/K_{222} residue was re-dissolved in anhydrous DMF (1000 μL).

The solution of [^{18}F]KF/K_{222} in DMF (20 – 30 MBq, 10 – 50 μL) was dispensed into a 3 mL V-vial containing the reagents and a magnetic stirrer bar. Anhydrous solvent was added before stirring at the specified temperature and time using a block heater. The reaction was quenched with 10% EtOH in H_2O (200 μL). An aliquot was removed for analysis by radio-HPLC. Analysis was performed using a Phenomenex Synergi^{TM} 4 μm Hydro RP 80 Å, 150 x 4.6 mm, column with the following gradient:

Flow rate = 1.0 mL/min, temperature = 25 °C

Time (min)	MeCN (%)	25 mM NH_4HCO_2 in H_2O (%)
0	1	95
5	1	95
12	95	5
16	95	5
17	1	95
19	1	95

For purification using WAX cartridges: The reaction mixture was cooled, taken up in 2% formic acid in H_2O (6 mL) and added to an Oasis Plus WAX short cartridge. The reaction vial was rinsed with EtOH (2 mL) and added to the WAX cartridge before adding EtOH (4 mL) to the cartridge. [^{18}F]$CF_3SO_2NH_4$ was eluted into a 5 mL vial using 0.7% NH_3 in EtOH (3 mL) followed by a stream of N_2. An aliquot was removed for analysis by radio-HPLC.

0.1 – 8.0 GBq Single Batch Reaction Screening

[^{18}F]Fluoride (3.0 – 10.0 GBq) was separated from [^{18}O]water using a Waters Sep-Pak Accell Plus QMA Carbonate Plus Light Cartridge (46 mg) and subsequently released using a solution of Kryptofix (6.3 mg) and K_2CO_3 (1.0 mg) in MeCN:H_2O 4:1 (900 μL in 3 x 300 μL portions), followed by MeCN (500 μL) into a 5 mL V-vial containing a magnetic stirrer bar in a concentrator. The solution was azeotropically dried with anhydrous MeCN (1000 μL in 5 x 200 μL portions) under a flow of N_2 at 105 °C.

The dried [^{18}F]KF/K_{222} residue was re-dissolved in anhydrous solvent (300 μL), stirred at 100 ºC for 2 min, and transferred into a 3 mL V-vial containing the reagents and a magnetic

stirrer bar. Anhydrous solvent was added before stirring at the specified temperature and time using a block heater.

The reaction mixture was cooled, taken up in 2% formic acid in H_2O (6 mL) and added to an Oasis Plus WAX short cartridge. The reaction vial was rinsed with EtOH (2 mL) and added to the WAX cartridge before adding EtOH (4 mL) to the cartridge. [^{18}F]$CF_3SO_2NH_4$ was eluted into a 5 mL vial using 0.7% NH_3 in EtOH (3 mL) followed by a stream of N_2.

An aliquot was removed for analysis by radio-HPLC. Analysis was performed using a Phenomenex Synergi^{TM} 4 μm Hydro RP 80 Å, 150 x 4.6 mm, column with the following gradient:

Flow rate = 1.0 mL/min, temperature = 25 °C

Time (min)	**MeCN (%)**	**25 mM NH_4HCO_2 in H_2O (%)**
0	1	95
5	1	95
12	95	5
16	95	5
17	1	95
19	1	95

0.1 – 8.0 GBq Single Batch Reaction Screening by Charging the Reaction Vial with Phosphine

[^{18}F]Fluoride (0.2 – 1.0 GBq) was separated from [^{18}O]water using a Waters Sep-Pak Accell Plus QMA Carbonate Plus Light Cartridge (46 mg) and subsequently released using a

solution of Kryptofix (6.3 mg) and K_2CO_3 (1.0 mg) in MeCN:H_2O 4:1 (900 μL in 3 x 300 μL portions), followed by MeCN (500 μL), into a 3 mL V-vial containing a magnetic stirrer bar and phosphine. The mixture was azeotropically dried with anhydrous MeCN (900 μL in 3 x 300 μL portions) under a flow of N_2 at 105 °C. NMM-SO_2 and the difluorocarbene reagent were dissolved in anhydrous solvent (PDFA was suspended using a vortex mixer for 5 seconds) and added to the V-vial before stirring at the specified temperature and time using a block heater.

The reaction mixture was cooled, taken up in 2% formic acid in H_2O (6 mL) and added to an Oasis Plus WAX short cartridge. The reaction vial was rinsed with EtOH (2 mL) and added to the WAX cartridge before adding EtOH (4 mL) to the cartridge. [^{18}F]$CF_3SO_2NH_4$ was eluted into a 5 mL vial using 0.7% NH_3 in EtOH (3 mL) followed by a stream of N_2.

An aliquot was removed for analysis by radio-HPLC. Analysis was performed using a Phenomenex Synergi^{TM} 4 μm Hydro RP 80 Å, 150 x 4.6 mm, column with the following gradient:

Flow rate = 1.0 mL/min, temperature = 25 °C

Time (min)	**MeCN (%)**	**25 mM NH_4HCO_2 in H_2O (%)**
0	1	95
5	1	95
12	95	5
16	95	5
17	1	95
19	1	95

2.0 – 10.0 GBq Single Batch Radiosynthesis and Isolation Procedure

[^{18}F]Fluoride (2.0 – 1.0 GBq) was separated from [^{18}O]water using a Waters Sep-Pak Accell Plus QMA Carbonate Plus Light Cartridge (46 mg) and subsequently released using a solution of Kryptofix (6.3 mg) and K_2CO_3 (1.0 mg) in MeCN:H_2O 4:1 (900 μL in 6 x 150 μL portions) into a 3 mL V-vial containing a magnetic stirrer bar. The mixture was azeotropically dried with anhydrous MeCN (1000 μL in 5 x 200 μL portions) under a flow of N_2 at 105 °C.

NMM-SO_2 (10.0 mg, 0.0605 mmol) and PDFA (57.0 mg, 0.160 mmol) were suspended in DMF:propylene carbonate 1:6 (350 μL) using a vortex mixer for 5 seconds before adding to the V-vial containing azeotropically dried [^{18}F]KF/K_{222}. The reaction mixture was stirred at 110 ºC for 20 min.

The reaction mixture was cooled, taken up in 2% formic acid in H_2O (6 mL) and added to an Oasis Plus WAX short cartridge. The reaction vial was rinsed with EtOH (2 mL) and added to the WAX cartridge before adding EtOH (4 mL) to the cartridge. [^{18}F]$CF_3SO_2NH_4$ was eluted into a 5 mL vial using 0.7% NH_3 in EtOH (3 mL) followed by a stream of N_2.

Solvent was removed under a stream of N_2 at 120 °C, the V-vial was cooled, 25 mM aqueous HCO_2NH_4 (<1 mL) was added, the V-vial was shaken vigorously, and the solution was loaded directly onto a 2 mL HPLC loop before injecting onto a semi-preparative column and eluting the product into a V-vial. **Semi-preparative HPLC details**: Phenomenex Synergi^{TM} 4 μm Hydro RP 80 Å, 250 x 10 mm, flow rate = 4 mL/min, column temperature = rt, eluent = 100% 25 mM NH_4HCO_2 in H_2O, retention time = 5.5 min.

A more concentrated solution was obtained by evaporating part of the HPLC eluent under a

stream of N_2 at 120 °C.

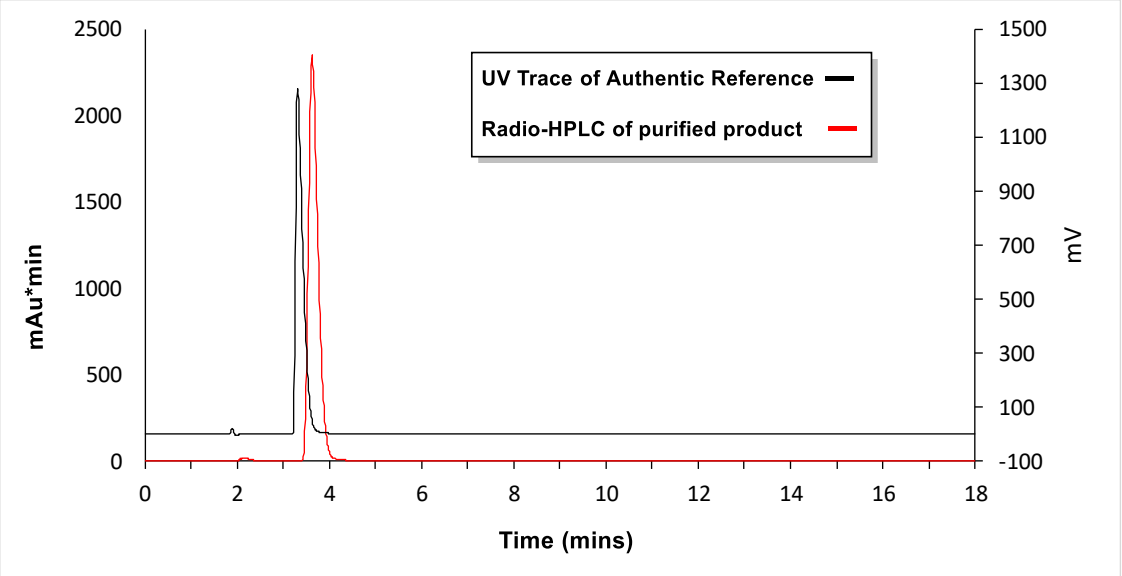
Additional Notes

All procedures using WAX cartridges were carried out as efficiently as possible and flow rate was maintained at 3 mL/min.

The presence of small quantities of EtOH after WAX purification affects the retention time during isolation by semi-preparative HPLC. All EtOH must be evaporated from the 5 mL vial prior to semi-preparative HPLC loading.

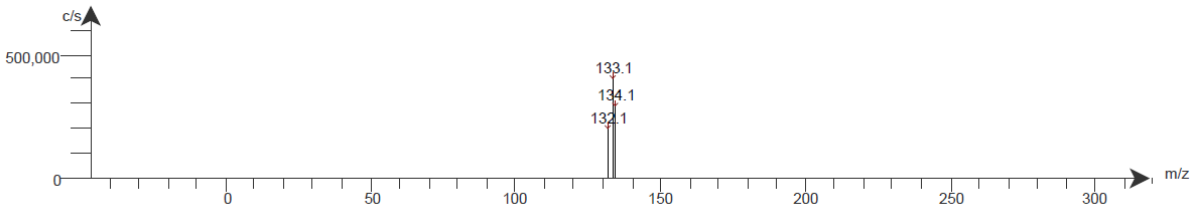
$[^{18}F]CF_3SO_2NH_4$ was loaded onto semi-preparative HPLC in no more 1 mL of 25 mM aqueous HCO_2NH_4 in order to minimise band width.

Radio-HPLC of Isolated [^{18}F]Langlois Reagent with UV Trace Overlay of an Authentic Reference



ESI-Mass Spectrometry of Ammonium ^{19}F-Trifluoromethanesulfinate

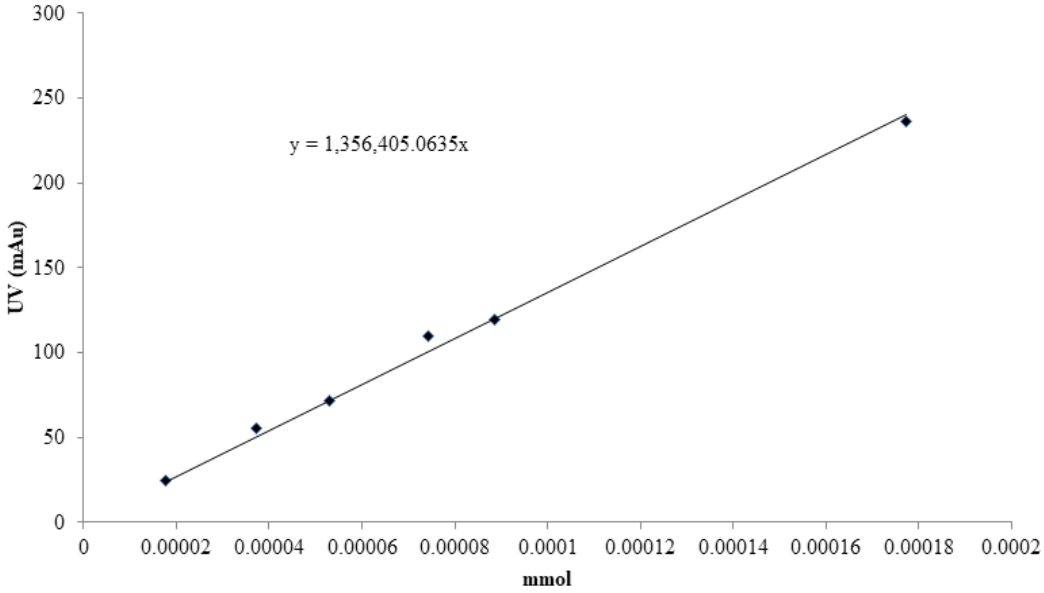
Required for $CF_3O_2{}^{32}S$ $[M\text{-}H]^-$ 133.0, found 133.1.



Molar Activity Determination of [^{18}F]Langlois Reagent

The molar activity of [^{18}F]$NH_4SO_2CF_3$ was assessed by radio-HPLC, using an analytical Phenomenex Synergi^{TM} 4 µm Hydro RP 80 Å, 150 x 4.6 mm, flow rate = 1 mL/min, column temperature = 25 °C, eluent = 1% MeCN and 99% 25 mM NH_4HCO_2 in H_2O.

Calibration Curve



Area (mAu)	$CF_3SO_2NH_4$ (mmol)	Activity (MBq)	Molar Activity (GBq µmol^{-1})
59.49	4.01x10^{-5}	0.6	0.01

4.4.3 [^{18}F]Trifluoromethylation of Amino Acids and Peptides

HPLC Eluent Systems

HPLC columns used**:** Phenomenex Synergi^{TM} 4 μm Hydro RP 80Å 150 x 4.6 mm column, Agilent Zorbax 300 Extended C-18 4 μm 300 Å 150 x 4.6 mm column or Agilent Zorbax 300SB CN 4 μm 300 Å 150 x 4.6 mm column.

Eluent A: ***Flow rate = 1.0 mL/min, temperature = 40 °C***

Time (min)	**MeCN with 0.1% TFA (%)**	**H_2O with 0.1% TFA (%)**
0	24	76
1.8	24	76
15	38	62
17	95	5
19	95	5
21	24	76

Eluent B: ***Flow rate = 1.0 mL/min, temperature = 40 °C***

Time (min)	**MeCN with 0.1% TFA (%)**	**H_2O with 0.1% TFA (%)**
0	8	92
1.8	8	92
18	30	70
21	95	5
24	95	5
25	8	92

Eluent C: ***Flow rate = 1.0 mL/min, temperature = 40 °C***

Time (min)	**MeCN with 0.1% TFA (%)**	**H_2O with 0.1% TFA (%)**
0	5	95
2	5	95
15	27.5	72.5
17	95	5
19	5	95

Eluent D: ***Flow rate = 1.0 mL/min, temperature = 40 °C***

Time (min)	**MeCN with 0.1% TFA (%)**	**H_2O with 0.1% TFA (%)**
0	5	95
2	5	95
15	45	55
17.5	95	5
20	95	5
22	5	95

Eluent E: ***Flow rate = 1.0 mL/min, temperature = 40 °C***

Time (min)	**MeCN with 0.1% TFA (%)**	**H_2O with 0.1% TFA (%)**
0	5	95
2	5	95
10	35	65
13	95	5

17	95	5
19	5	95

Eluent F: ***Flow rate = 1.0 mL/min, temperature = 40 °C***

Time (min)	**MeCN with 0.1% TFA (%)**	**H_2O with 0.1% TFA (%)**
0	15	85
2	15	85
15	60	40
17.5	95	5
20	95	5
22	15	85

Eluent G: ***Flow rate = 1.0 mL/min, temperature = 40 °C***

Time (min)	**MeCN with 0.1% TFA (%)**	**H_2O with 0.1% TFA (%)**
0	15	85
2	15	85
17.5	45	55
20	95	5
22	15	85

Eluent H: ***Flow rate = 1.0 mL/min, temperature = 40 °C***

Time (min)	**MeCN with 0.1% TFA (%)**	**H_2O with 0.1% TFA (%)**
0	15	85

2	15	85
20	60	40
22	15	85

Eluent I: ***Flow rate = 1.0 mL/min, temperature = 40 °C***

Time (min)	**MeCN with 0.1% TFA (%)**	**H_2O with 0.1% TFA (%)**
0	5	95
2	5	95
3	20	80
14	55	45
17	95	5
22	95	5
23	5	95

Eluent J: ***Flow rate = 1.0 mL/min, temperature = 30 °C***

Time (min)	**MeCN with 0.1% TFA (%)**	**H_2O with 0.1% TFA (%)**
0	15	85
2	15	85
20	60	40
22	15	85

Eluent K: ***Flow rate = 1.0 mL/min, temperature = 25 °C***

Time (min)	MeCN with 0.1% TFA (%)	H_2O with 0.1% TFA (%)
0	20	80
3	20	80
19	50	50

Eluent L: ***Flow rate = 4.0 mL/min, temperature = 25 °C***

Time (min)	MeCN with 0.1% TFA (%)	H_2O with 0.1% TFA (%)
0	5	95
2	5	95
20	50	50
22	50	50
23	85	15

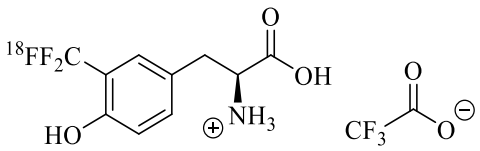
HPLC Eluent System for Isolation of Radiolabeled Peptides

For the isolation of radio-labeled peptides a Phenomenex Onyx Monolithic Semi-PREP C18 100 x 10 mm column was used.

Time (min)	MeCN with 0.1% TFA (%)	H_2O with 0.1% TFA (%)	Flow Rate (mL/min)
0	5	95	4
1	5	95	10
2	5	95	10
15	35	65	10

16	80	20	10
18	5	95	6
20	5	95	4

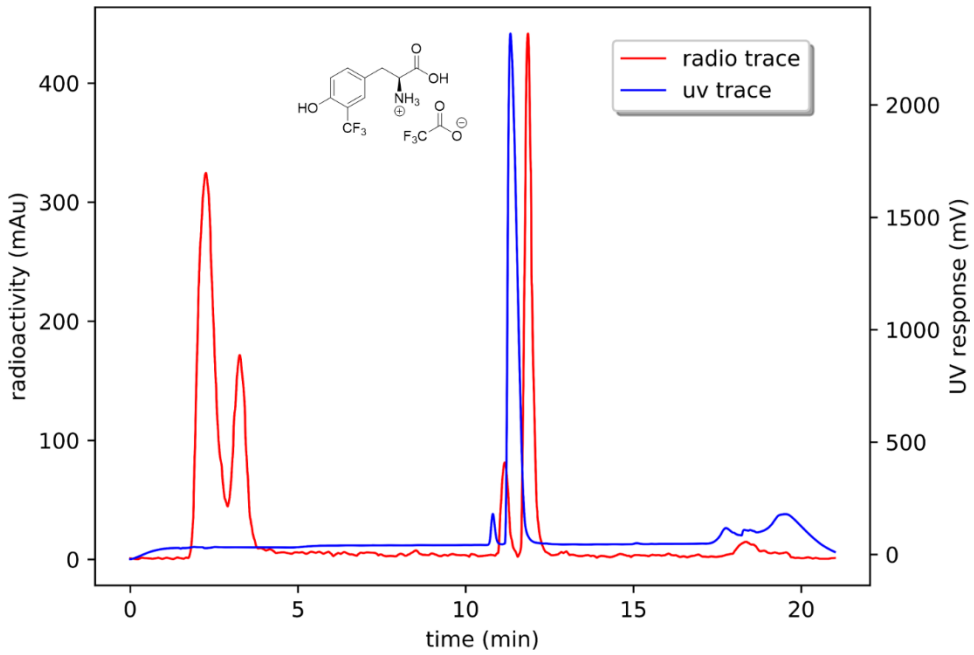
L-Tyr(3-$CF_2{}^{18}F$)

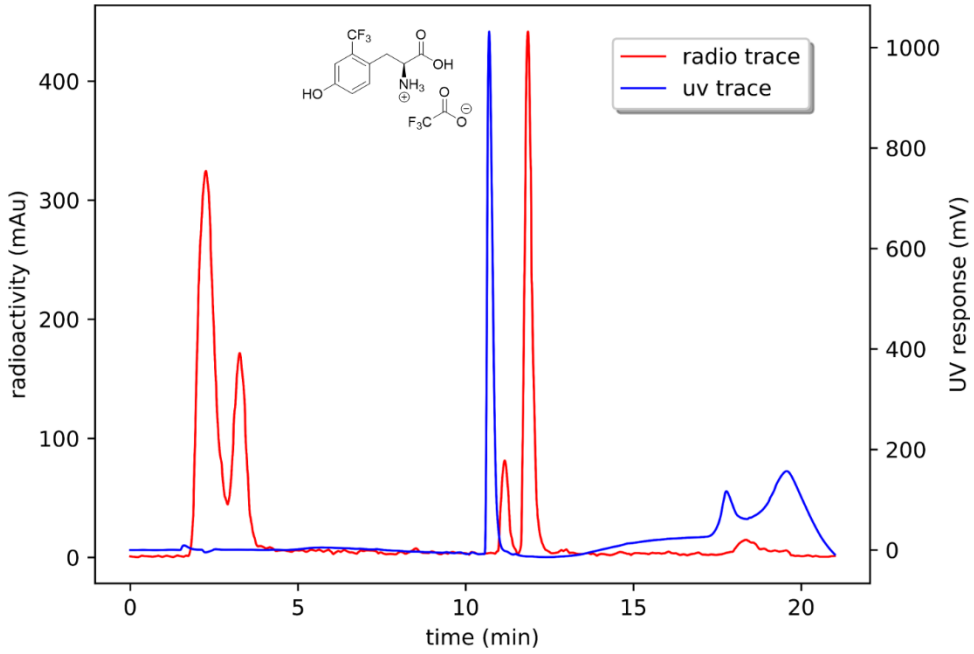


To L-tyrosine (5.4 mg, 0.03 mmol) and iron(III) nitrate nonahydrate (24.2 mg, 0.06 mmol) in a 3 mL V-vial was added [^{18}F]$NH_4SO_2CF_3$ in aqueous NH_4HCO_2 solution (10 – 100 MBq) followed by *tert*-butyl hydroperoxide solution (16.48 μL, 0.12 mmol, 70% in H_2O) in DMSO to give a total reaction solvent of 75% DMSO in aqueous NH_4HCO_2 (200 μL) before stirring at 40 ºC for 20 min. An aliquot was removed for analysis by radio-HPLC to give a RCY. **Reverse phase HPLC details**: Eluent C on a Phenomenex Synergi^{TM} 4 μm Hydro RP 80 Å 150 x 4.6 mm column.

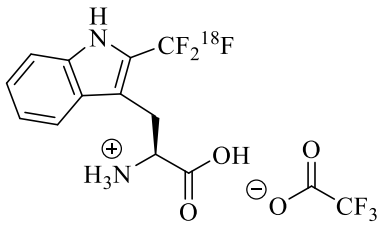
Run	**1**	**2**	**Average**	**Standard Deviation**
RCY for L-Tyr(3-$CF_2{}^{18}F$) (%)	17.4	10.6	14	5
RCY for L-Tyr(2-$CF_2{}^{18}F$) (%)	2.4	1.0	2	1

Radio-HPLC Analysis





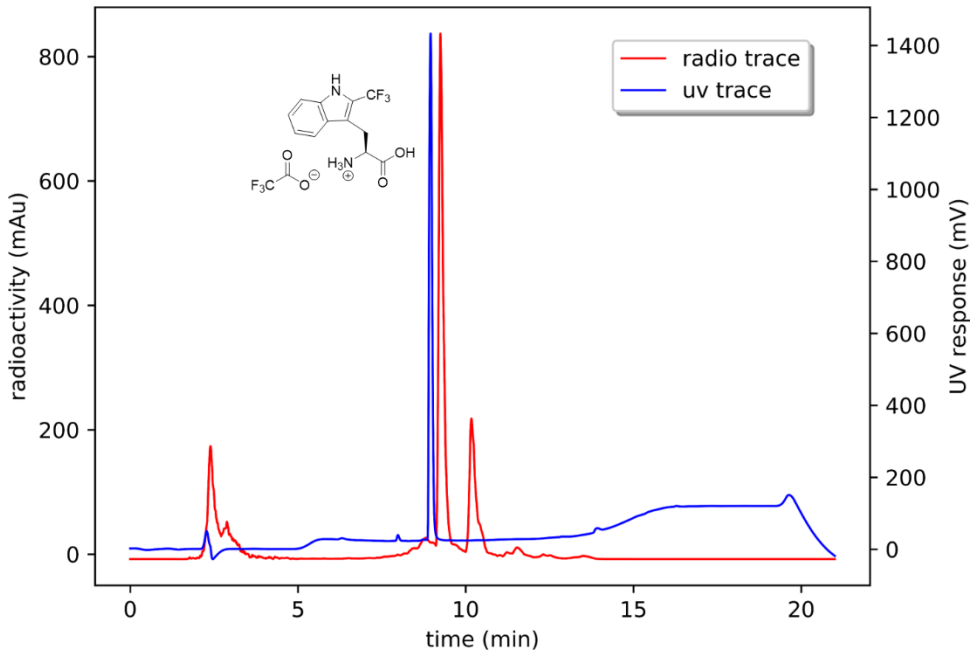
L-Trp(2-$CF_2{}^{18}F$)

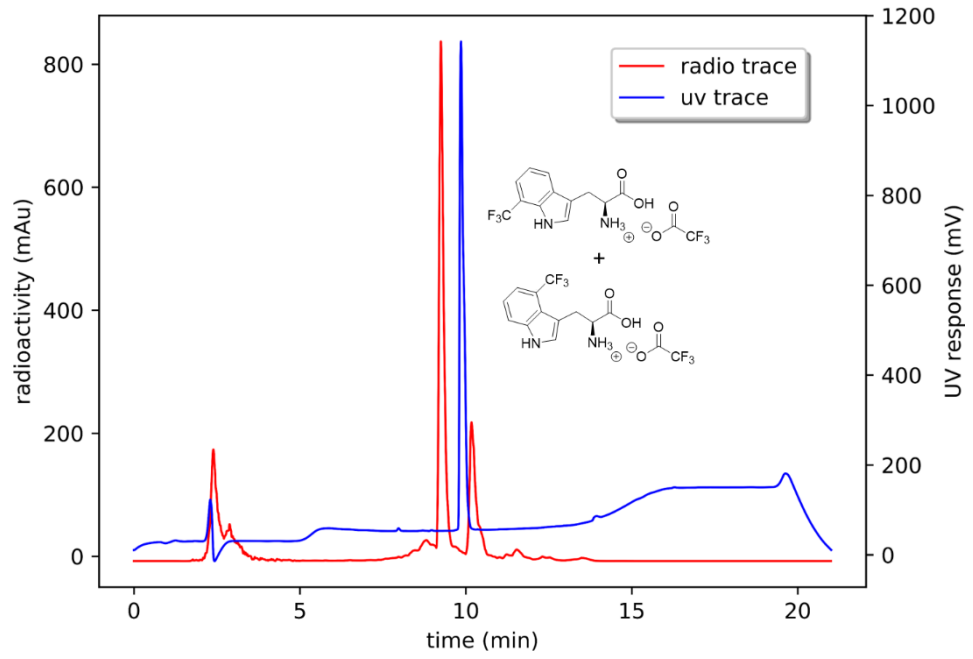


To L-tryptophan (6.1 mg, 0.03 mmol) and iron(III) nitrate nonahydrate (24.2 mg, 0.06 mmol) in a 3 mL V-vial was added [^{18}F]$NH_4SO_2CF_3$ in aqueous NH_4HCO_2 solution (10 – 100 MBq) followed by *tert*-butyl hydroperoxide solution (16.48 μL, 0.12 mmol, 70% in H_2O) in DMSO to give a total reaction solvent of 50% DMSO in aqueous NH_4HCO_2 (300 μL) before stirring at 40 ºC for 20 min. An aliquot was removed for analysis by radio-HPLC to give a RCY. **Reverse phase HPLC details**: Eluent D on a Phenomenex Synergi^{TM} 4 μm Hydro RP 80 Å 150 x 4.6 mm column.

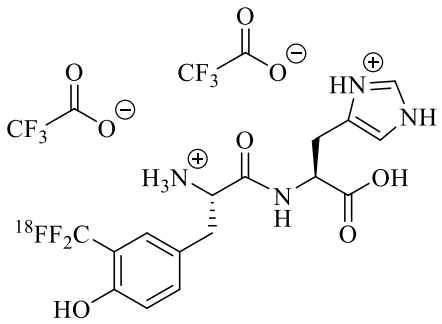
Run	1	2	Average	Standard Deviation
RCY for L-Trp(2-$CF_2{}^{18}F$) (%)	21.0	22.7	22	1
RCY for L-Trp(4-$CF_2{}^{18}F$) and L-Trp(7-$CF_2{}^{18}F$) (%)	9.4	11.1	10	1

Radio-HPLC Analysis





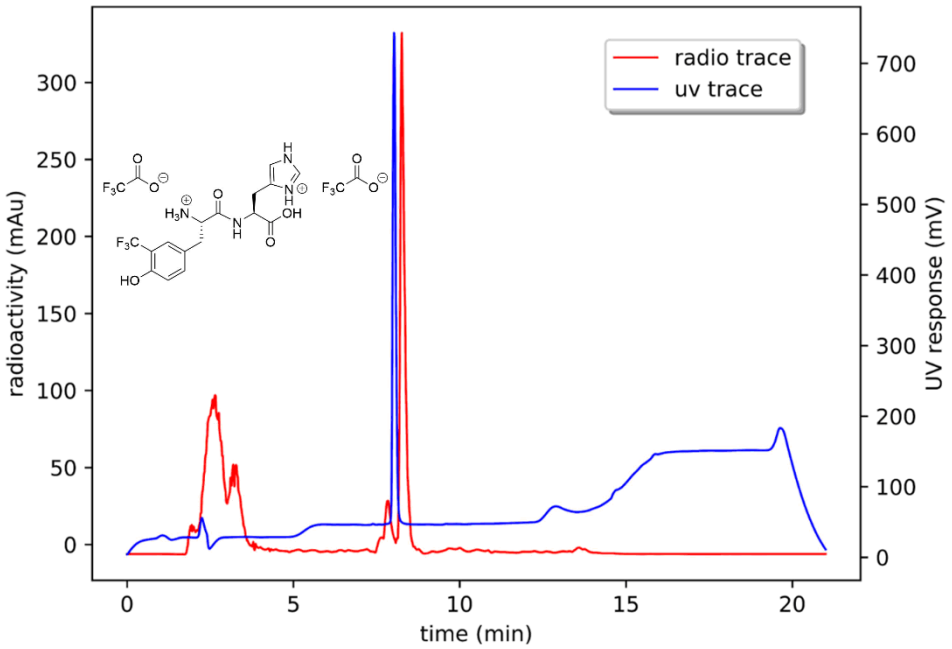
Tyr(3-CF_2^{18}F)-His

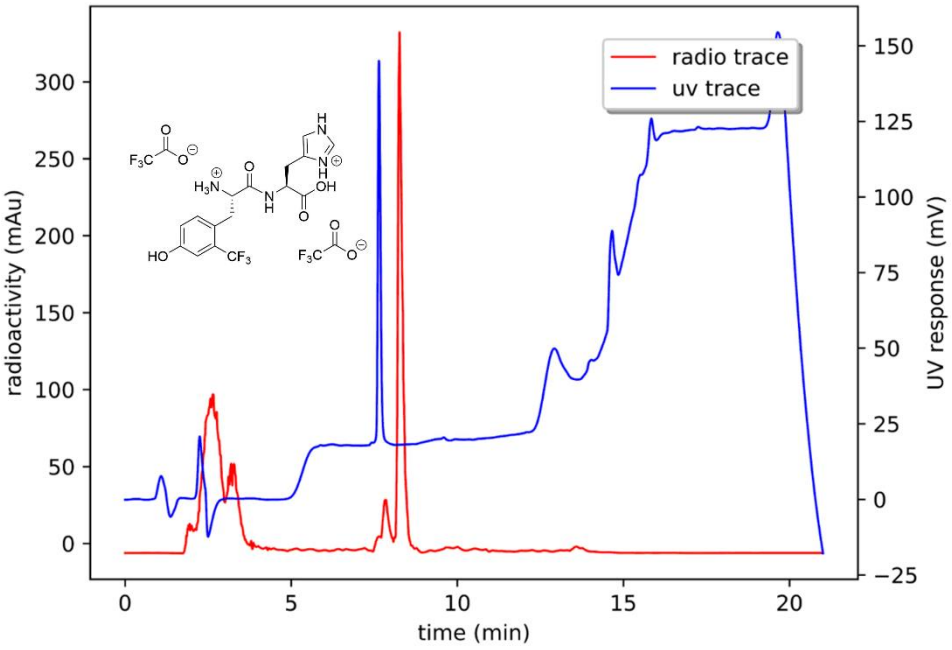


To Tyr-His (9.6 mg, 0.03 mmol) and iron(III) nitrate nonahydrate (24.2 mg, 0.06 mmol) in a 3 mL V-vial was added [^{18}F]$NH_4SO_2CF_3$ in aqueous NH_4HCO_2 solution (10 – 100 MBq) followed by *tert*-butyl hydroperoxide solution (16.48 μL, 0.12 mmol, 70% in H_2O) in DMSO to give a total reaction solvent of 40% – 60% DMSO in aqueous NH_4HCO_2 (250 μL) before stirring at 40 ºC for 20 min. An aliquot was removed for analysis by radio-HPLC to give a RCY. **Reverse phase HPLC details**: Eluent E on a Phenomenex Synergi^{TM} 4 μm Hydro RP 80 Å 150 x 4.6 mm column.

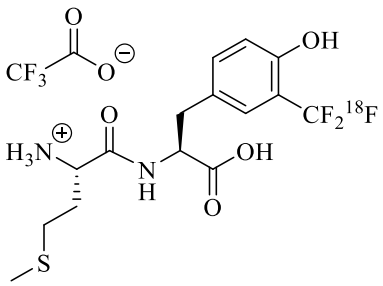
Run	1	2	3	4	Average	Standard Deviation
RCY for Tyr(3-CF_2^{18}F)-His (%)	30.8	30.2	28.6	14.1	26	8
RCY for Tyr(2-CF_2^{18}F)-His (%)	4.6	4.8	4.7	1.8	4	1

Radio-HPLC Analysis





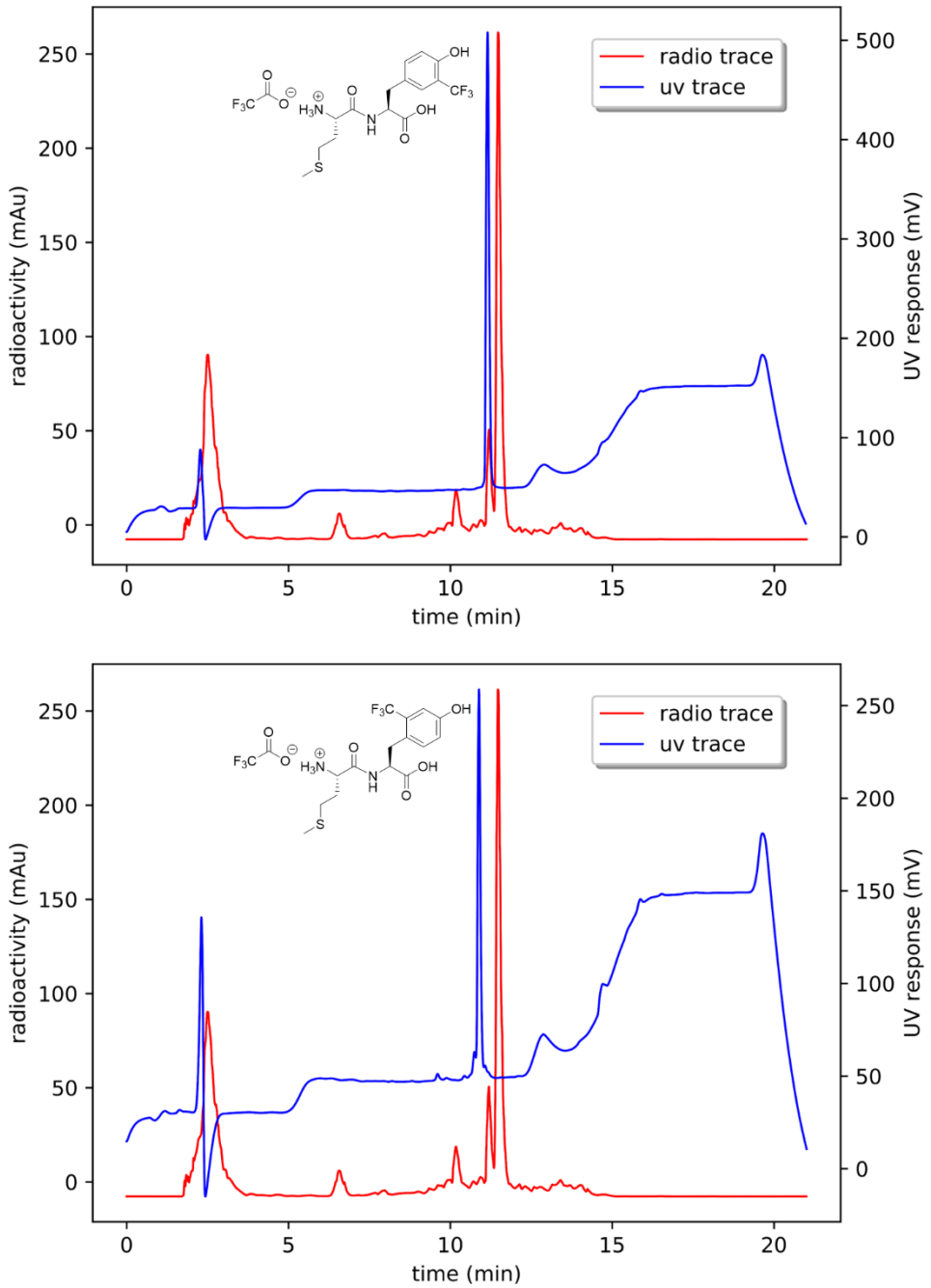
Met-Tyr(3-$CF_2{}^{18}F$)

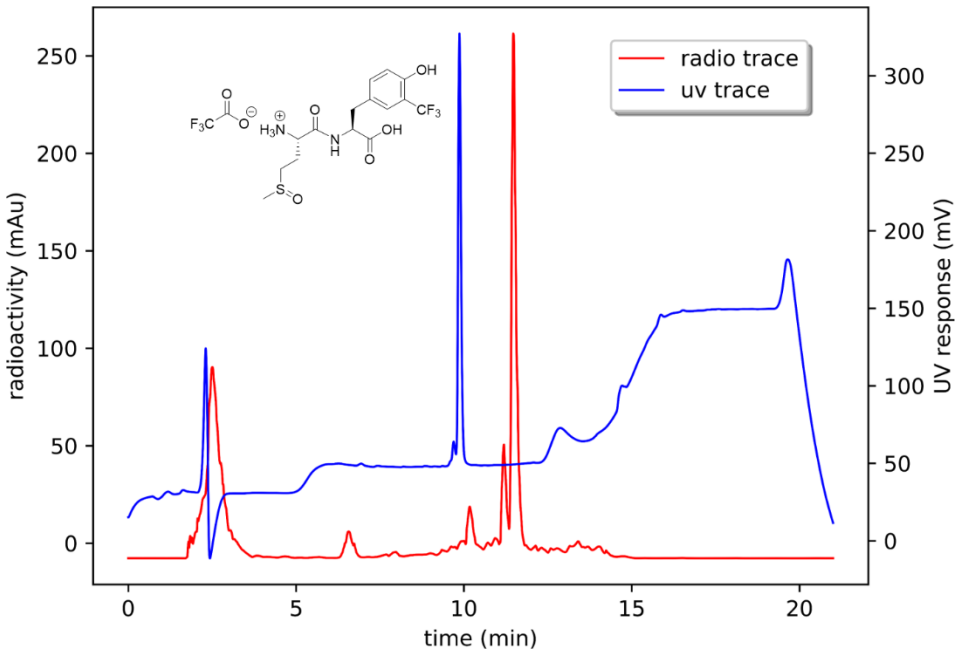


To Met-Tyr (9.4 mg, 0.03 mmol) and iron(III) nitrate nonahydrate (24.2 mg, 0.06 mmol) in a 3 mL V-vial was added [^{18}F]$NH_4SO_2CF_3$ in aqueous NH_4HCO_2 solution (10 – 100 MBq) followed by *tert*-butyl hydroperoxide solution (8.24 μL, 0.06 mmol, 70% in H_2O) in DMSO to give a total reaction solvent of 40% – 50% DMSO in aqueous NH_4HCO_2 (250 – 300 μL) before stirring at 40 ºC for 20 min. An aliquot was removed for analysis by radio-HPLC to give a RCY. **Reverse phase HPLC details**: Eluent E on a Phenomenex Synergi^{TM} 4 μm Hydro RP 80 Å 150 x 4.6 mm column.

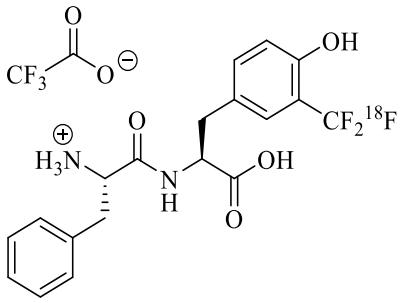
Run	1	2	3	4	Average	Standard Deviation
RCY for Met-Tyr(3-$CF_2{}^{18}F$) (%)	30.2	36.7	29.6	19.6	29	7
RCY for Met-Tyr(2-$CF_2{}^{18}F$) (%)	6.0	9.1	6.2	3.2	6	2
RCY for Met(oxidised)-Tyr(3-$CF_2{}^{18}F$) (%)	7.3	8.4	3.2	6.1	6	2

Radio-HPLC Analysis





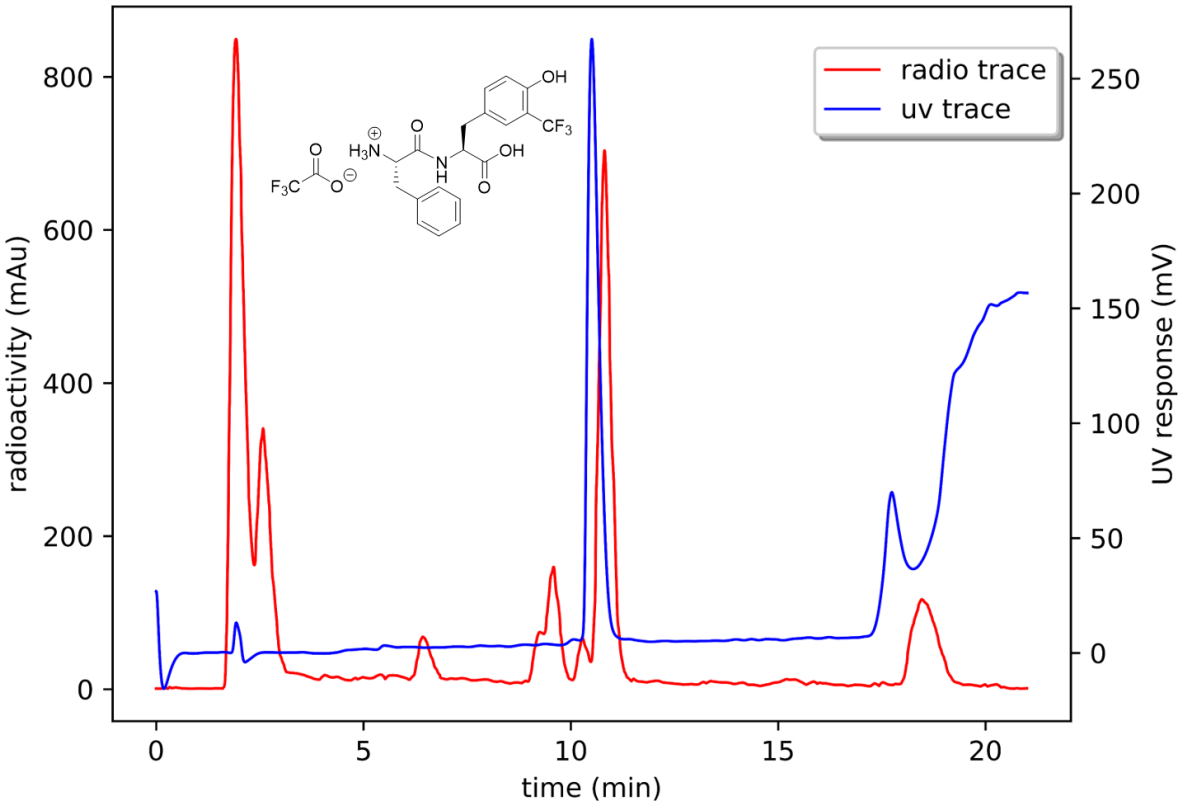
Phe-Tyr(3-$CF_2{}^{18}F$)

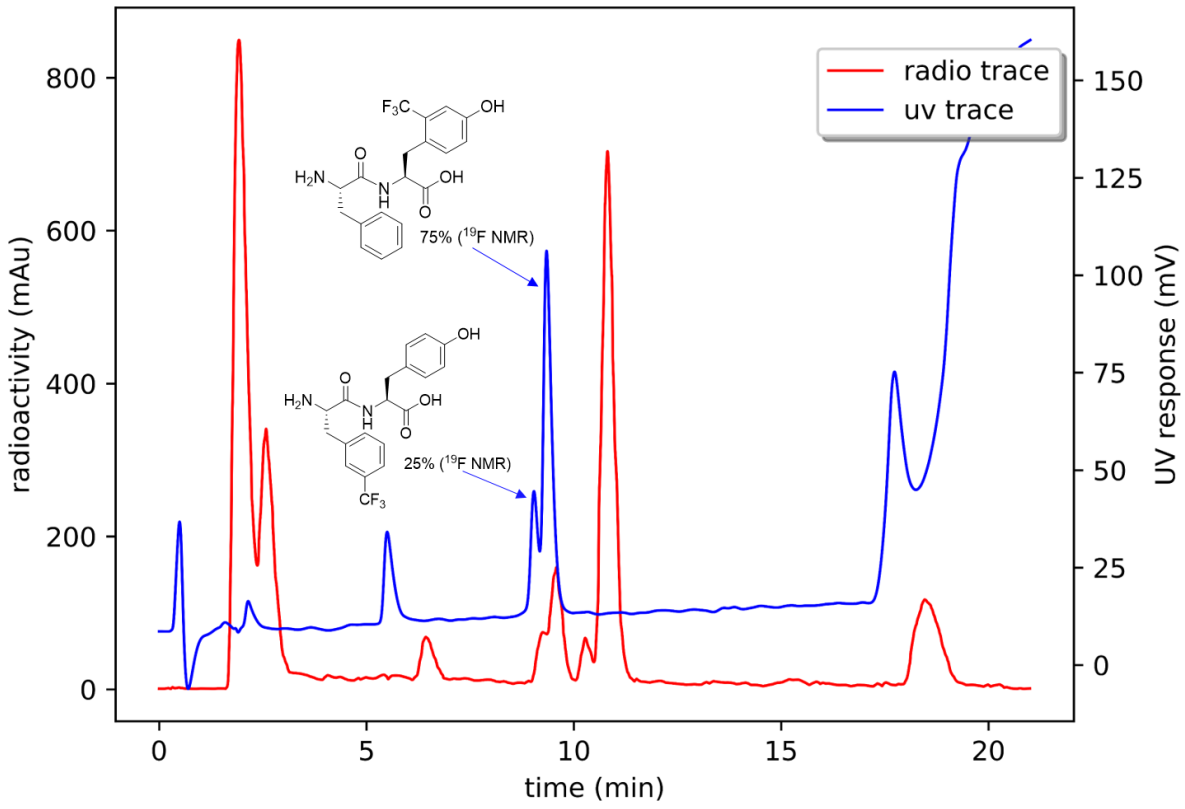


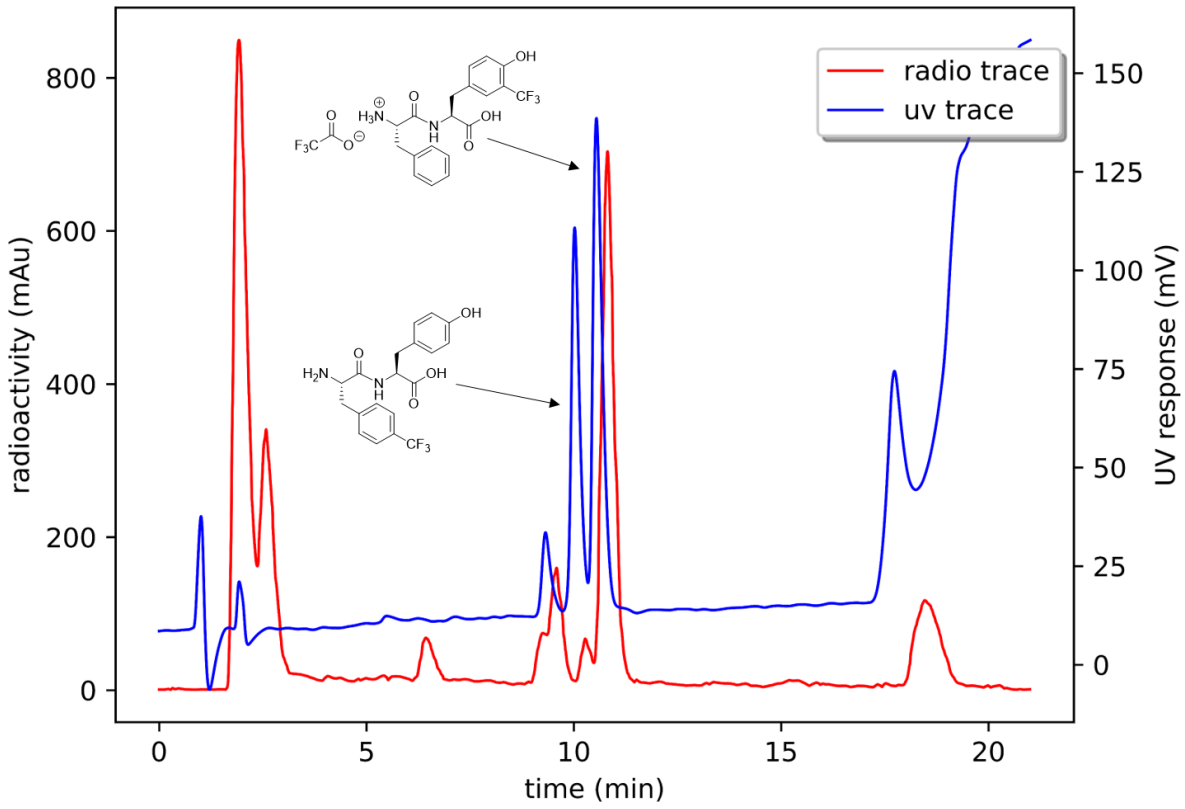
To Phe-Tyr (9.9 mg, 0.03 mmol) and iron(III) nitrate nonahydrate (24.2 mg, 0.06 mmol) in a 3 mL V-vial was added [^{18}F]$NH_4SO_2CF_3$ in aqueous NH_4HCO_2 solution (10 – 100 MBq) followed by *tert*-butyl hydroperoxide solution (16.48 µL, 0.12 mmol, 70% in H_2O) in aqueous AcOH to give a total reaction solvent of 8% AcOH in aqueous NH_4HCO_2 (300 µL) before stirring at 40 ºC for 20 min. An aliquot was removed for analysis by radio-HPLC to give a RCY. **Reverse phase HPLC details**: Eluent A on a Phenomenex Synergi^{TM} 4 µm Hydro RP 80 Å 150 x 4.6 mm column.

Run	1
RCY for Phe-Tyr(3-$CF_2{}^{18}F$) (%)	24
RCY for Phe-Tyr(2-$CF_2{}^{18}F$) (%)	1.5
RCY for Phe(3-$CF_2{}^{18}F$)-Tyr and Phe(4-$CF_2{}^{18}F$)-Tyr (%)	7.1

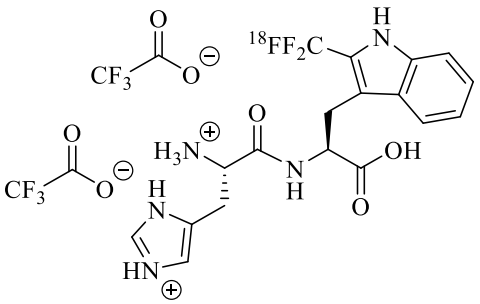
Radio-HPLC *Analysis*




radio trace
uv trace
radioactivity (mAu)
UV response (mV)
time (min)
75% (^{19}F NMR)
25% (^{19}F NMR)


radio trace
uv trace
radioactivity (mAu)
UV response (mV)
time (min)

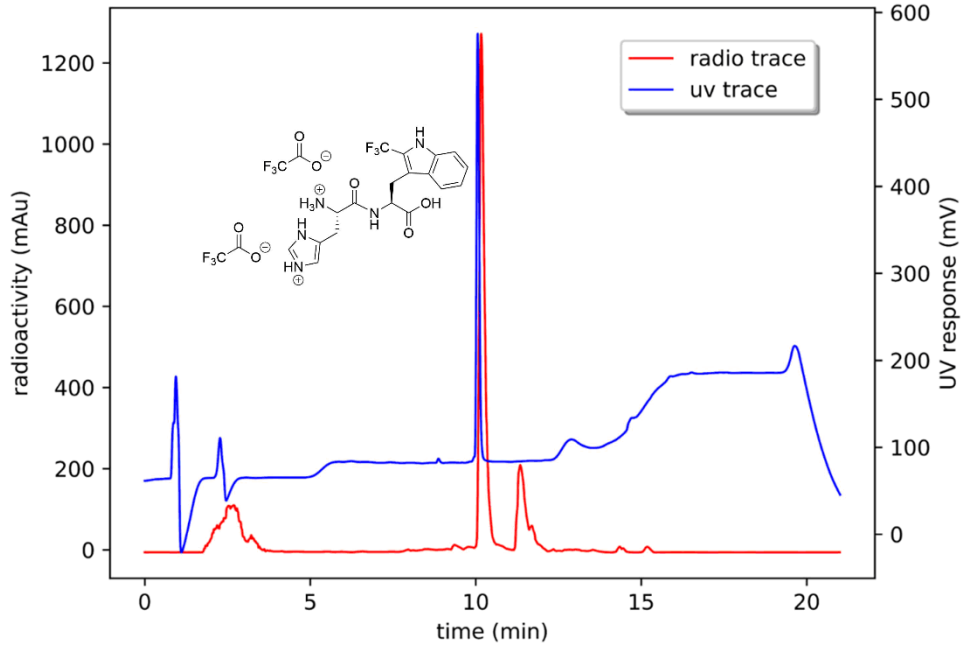
His-Trp(2-$CF_2{}^{18}F$)

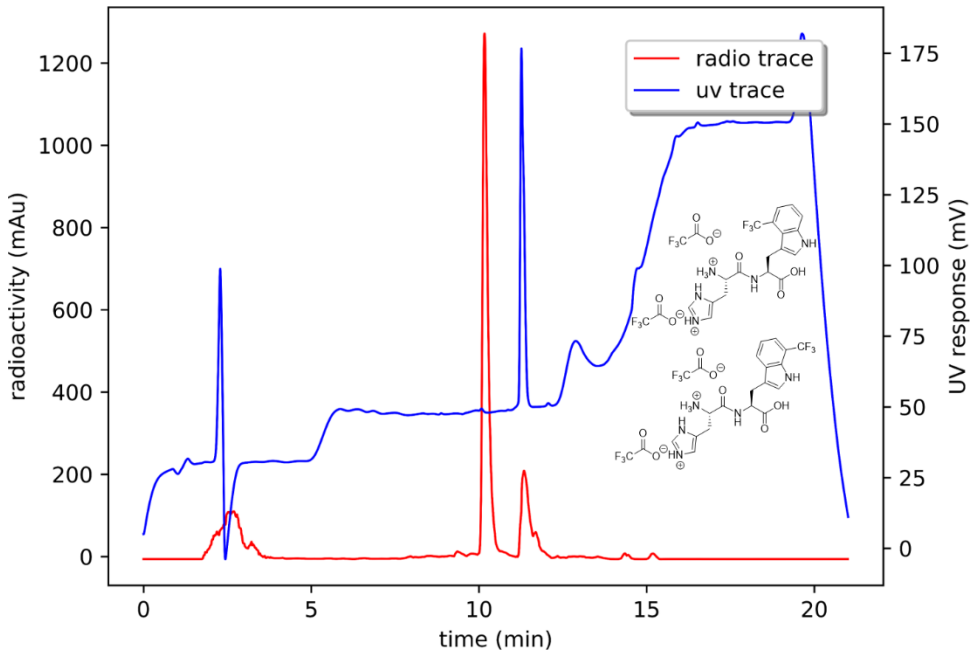


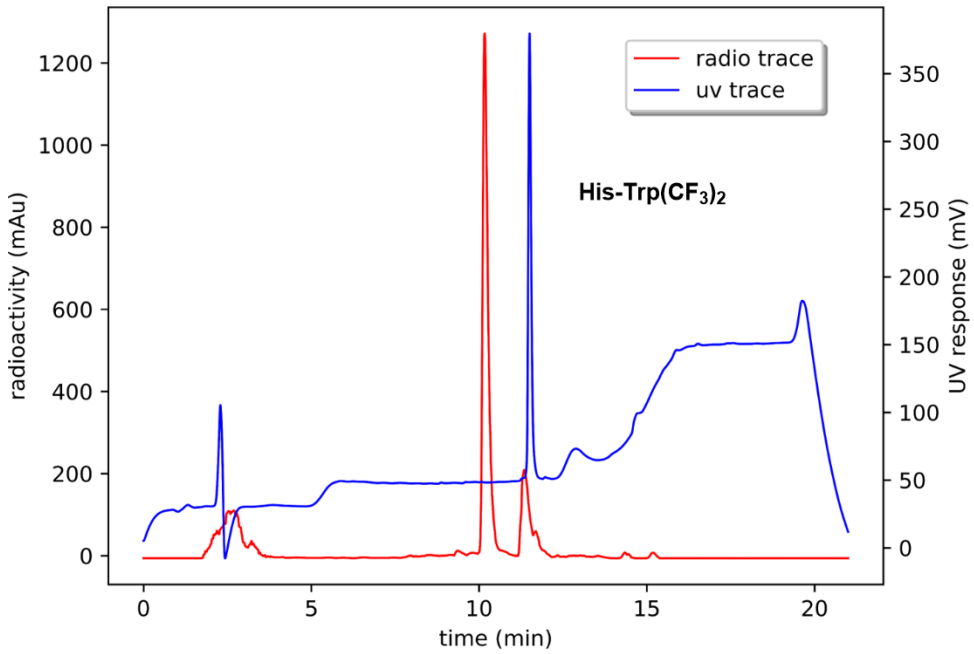
To His-Trp (5.1 mg, 0.015 mmol) and iron(III) nitrate nonahydrate (12.1 mg, 0.03 mmol) in a 3 mL V-vial was added [^{18}F]$NH_4SO_2CF_3$ in aqueous NH_4HCO_2 solution (10 – 100 MBq) followed by *tert*-butyl hydroperoxide solution (8.24 μL, 0.06 mmol, 70% in H_2O) in DMSO to give a total reaction solvent of 38% – 50% DMSO in aqueous NH_4HCO_2 (120 – 130 μL) before stirring at 40 ºC for 20 min. An aliquot was removed for analysis by radio-HPLC to give a RCY. **Reverse phase HPLC details**: Eluent E on a Phenomenex Synergi^{TM} 4 μm Hydro RP 80 Å 150 x 4.6 mm column.

Run	1	2	3	Average	Standard Deviation
RCY for His-Trp(2-$CF_2{}^{18}F$) (%)	51.8	56.7	58.9	56	4
RCY for His-Trp(4-$CF_2{}^{18}F$), His-Trp(7-$CF_2{}^{18}F$) and His-Trp($CF_2{}^{18}F$)(CF_3) (%)	15.4	16.8	16.3	16	1

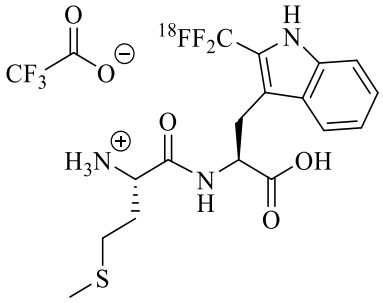
Radio-HPLC Analysis







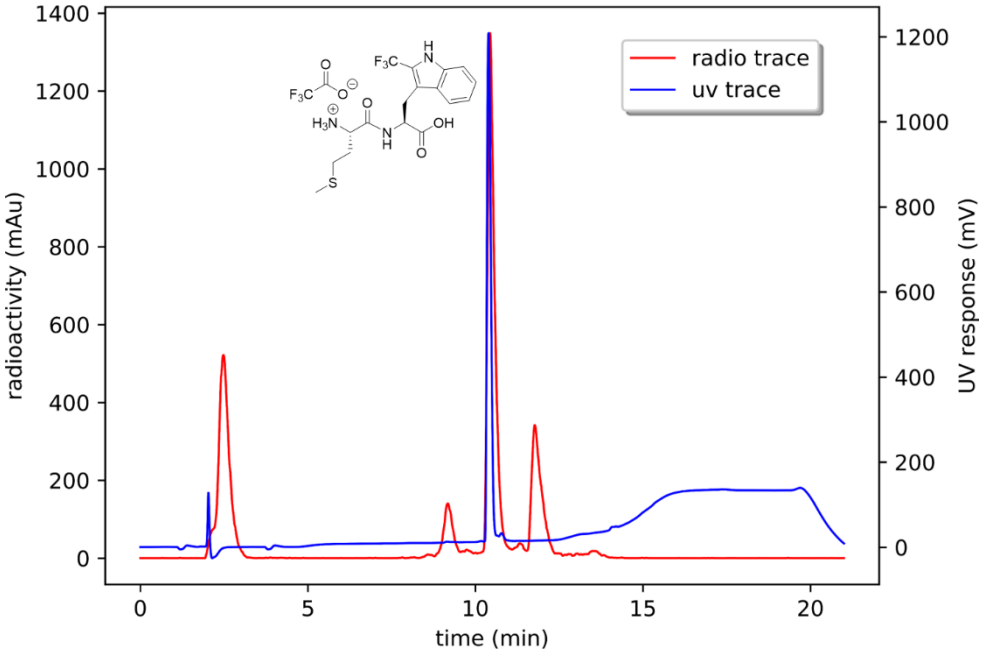
Met-Trp(2-$CF_2{}^{18}F$)

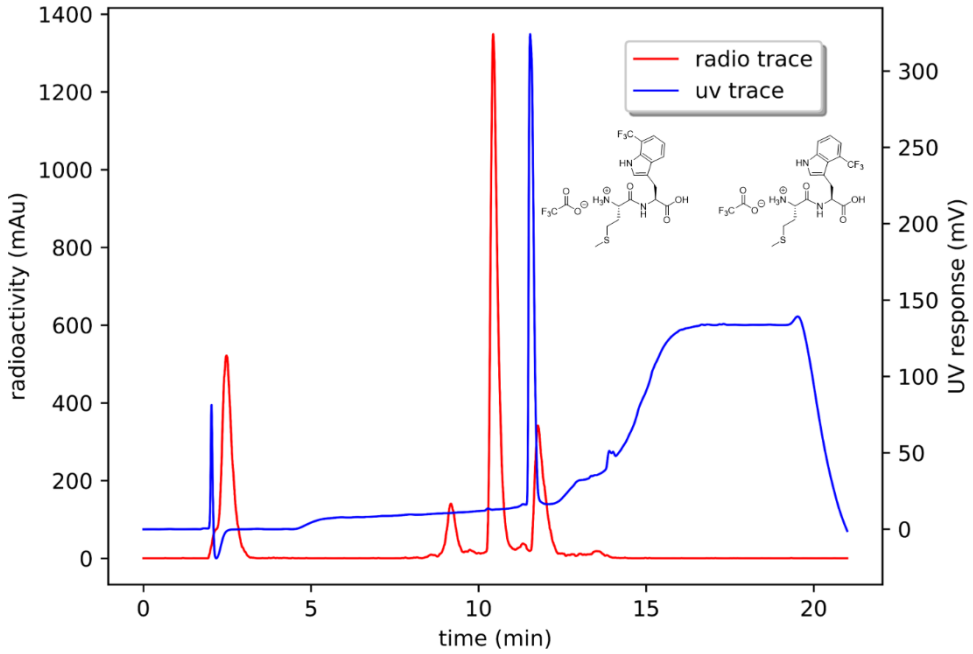


To Met-Trp (10.1 mg, 0.03 mmol) and iron(III) nitrate nonahydrate (24.2 mg, 0.06 mmol) in a 3 mL V-vial was added [^{18}F]$NH_4SO_2CF_3$ in aqueous NH_4HCO_2 solution (10 – 100 MBq) followed by *tert*-butyl hydroperoxide solution (8.24 µL, 0.06 mmol, 70% in H_2O) in DMSO to give a total reaction solvent of 40% – 50% DMSO in aqueous NH_4HCO_2 (250 µL) before stirring at 40 ºC for 20 min. An aliquot was removed for analysis by radio-HPLC to give a RCY. **Reverse phase HPLC details**: Eluent E on a Phenomenex Synergi™ 4 µm Hydro RP 80 Å 150 x 4.6 mm column.

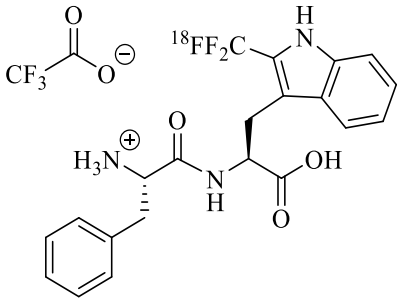
Run	1	2	3	Average	Standard Deviation
RCY for Met-Trp(2-$CF_2{}^{18}F$) (%)	45.1	38.8	34.0	39	6
RCY for His-Trp(4-$CF_2{}^{18}F$) and His-Trp(7-$CF_2{}^{18}F$) (%)	15.7	14.0	13.6	14	1

Radio-HPLC Analysis





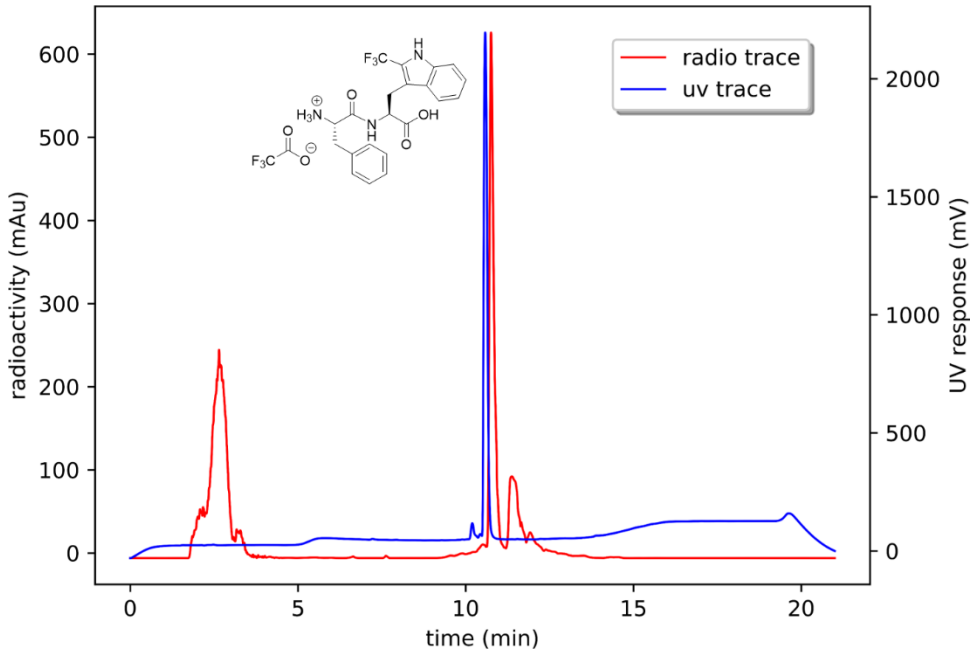
Phe-Trp(2-$CF_2{}^{18}F$)

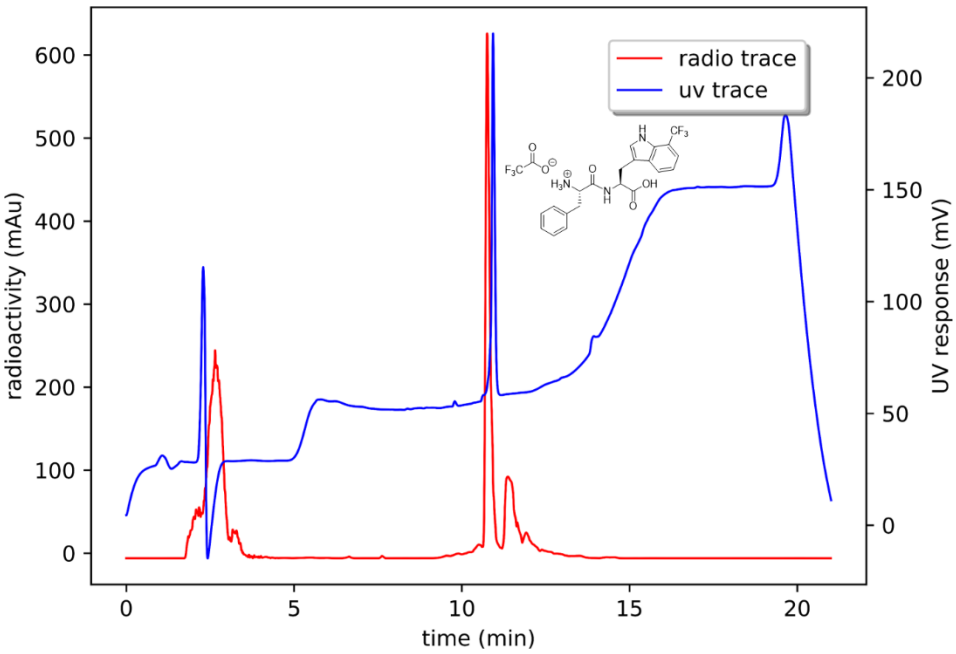


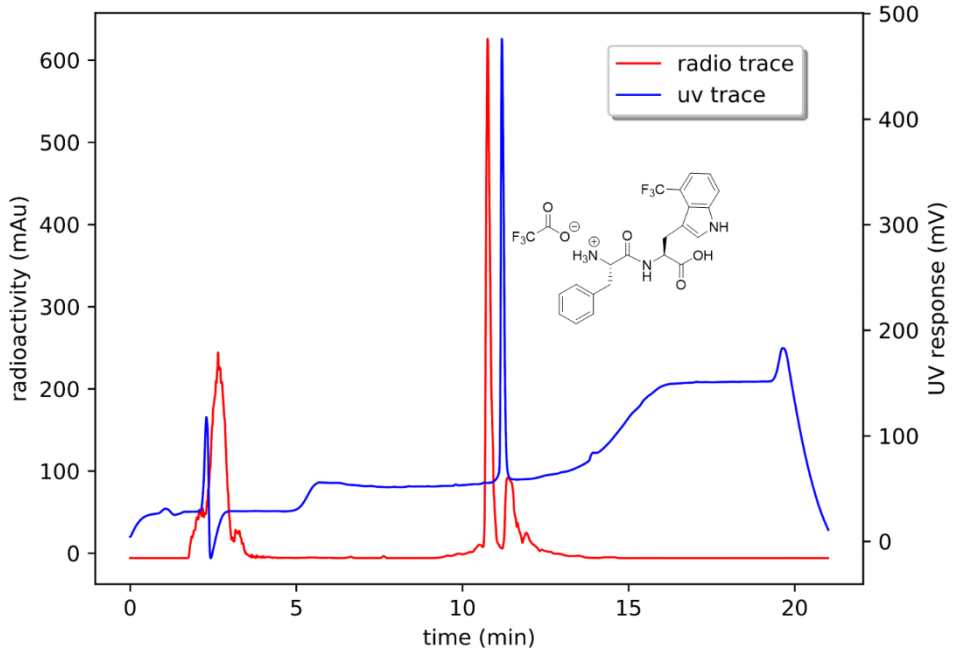
To Phe-Trp (5.3 mg, 0.015 mmol) and iron(III) nitrate nonahydrate (12.1 mg, 0.03 mmol) in a 3 mL V-vial was added [^{18}F]$NH_4SO_2CF_3$ in aqueous NH_4HCO_2 solution (10 – 100 MBq) followed by *tert*-butyl hydroperoxide solution (8.24 µL, 0.06 mmol, 70% in H_2O) in DMSO to give a total reaction solvent of 42% – 50% DMSO in aqueous NH_4HCO_2 (120 µL) before stirring at 40 ºC for 20 min. An aliquot was removed for analysis by radio-HPLC to give a RCY. **Reverse phase HPLC details**: Eluent I on a Phenomenex Synergi™ 4 µm Hydro RP 80 Å 150 x 4.6 mm column.

Run	1	2	3	Average	Standard Deviation
RCY for Phe-Trp(2-$CF_2{}^{18}F$) (%)	31.8	46.2	49.8	43	10
RCY for Phe-Trp(4-$CF_2{}^{18}F$) and Phe-Trp(7-$CF_2{}^{18}F$) (%)	15.1	16.4	17.2	16	1

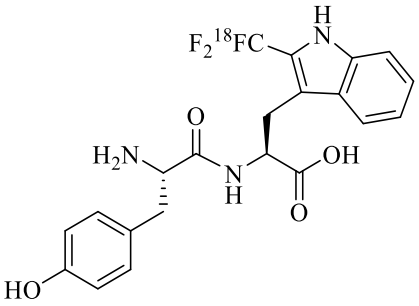
Radio-HPLC Analysis




radio trace
uv trace
radioactivity (mAu)
UV response (mV)
time (min)
0
100
200
300
400
500
600
0
50
100
150
200
0
5
10
15
20


radio trace
uv trace
radioactivity (mAu)
UV response (mV)
time (min)
0
100
200
300
400
500
600
0
100
200
300
400
500
0
5
10
15
20

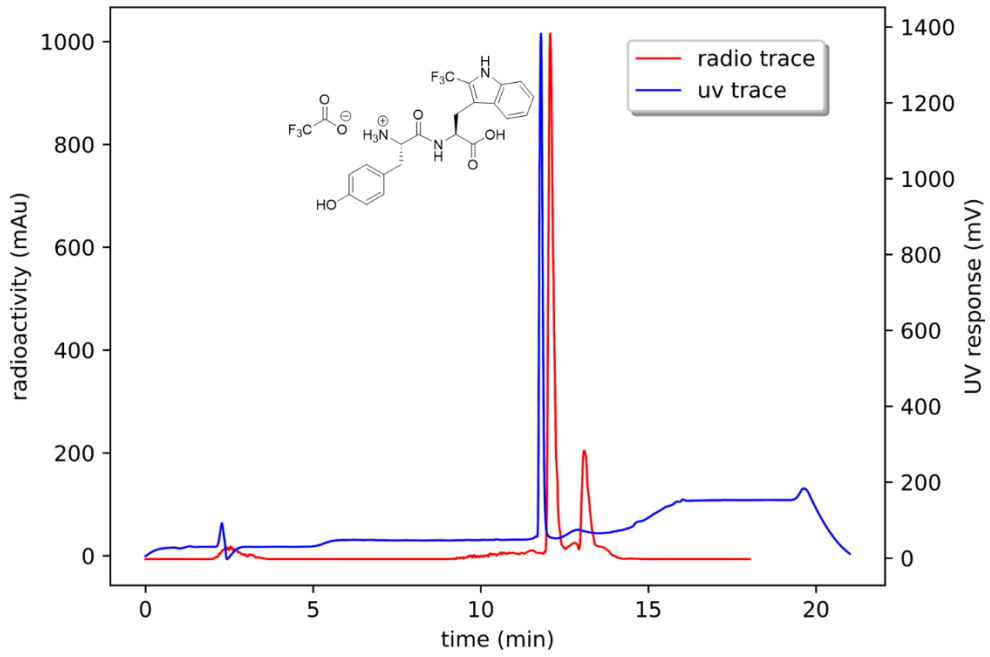
Tyr-Trp(2-$^{18}FF_2$)

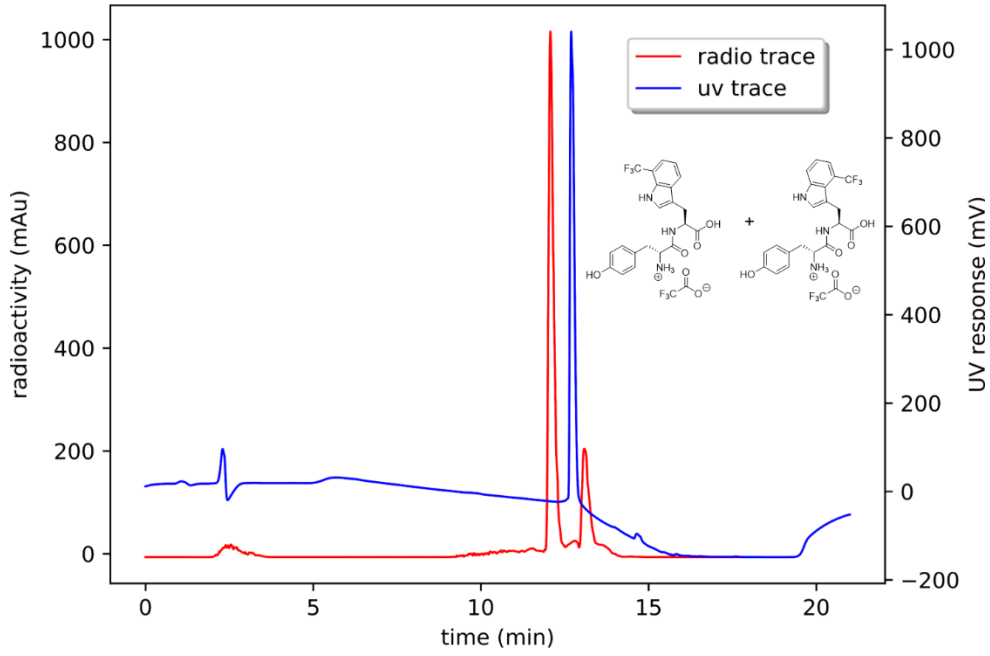


To Tyr-Trp (5.5 mg, 0.015 mmol) and iron(III) chloride solution (3 μL of 10 M solution in aqueous 25 mM NH_4HCO_2, 0.03 mmol) in a 3 mL V-vial was added [^{18}F]$NH_4SO_2CF_3$ in aqueous NH_4HCO_2 solution (10 – 100 MBq) followed by *tert*-butyl hydroperoxide solution (8.24 μL, 0.06 mmol, 70% in H_2O) in DMSO to give a total reaction solvent of 40% – 60% DMSO in aqueous NH_4HCO_2 (125 μL) before stirring at 40 ºC for 20 min. An aliquot was removed for analysis by radio-HPLC to give a RCC. **Reverse phase HPLC details**: Eluent J on an Agilent Zorbax 300 Extended C-18 4 μm 300 Å 150 x 4.6 mm column.

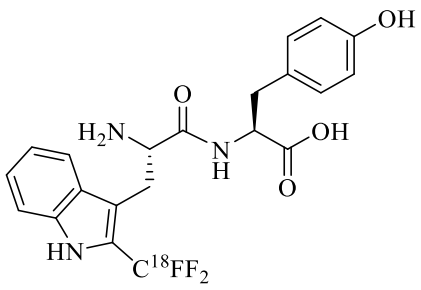
Run	1	2	3	Average	Standard Deviation
RCY for Tyr-Trp(2-$CF_2{}^{18}F$) (%)	59.8	52.7	51.9	55	4
RCY for Tyr-Trp(4-$CF_2{}^{18}F$) and Tyr-Trp(7-$CF_2{}^{18}F$) (%)	18.7	18.7	20.5	19	1

Radio-HPLC Analysis





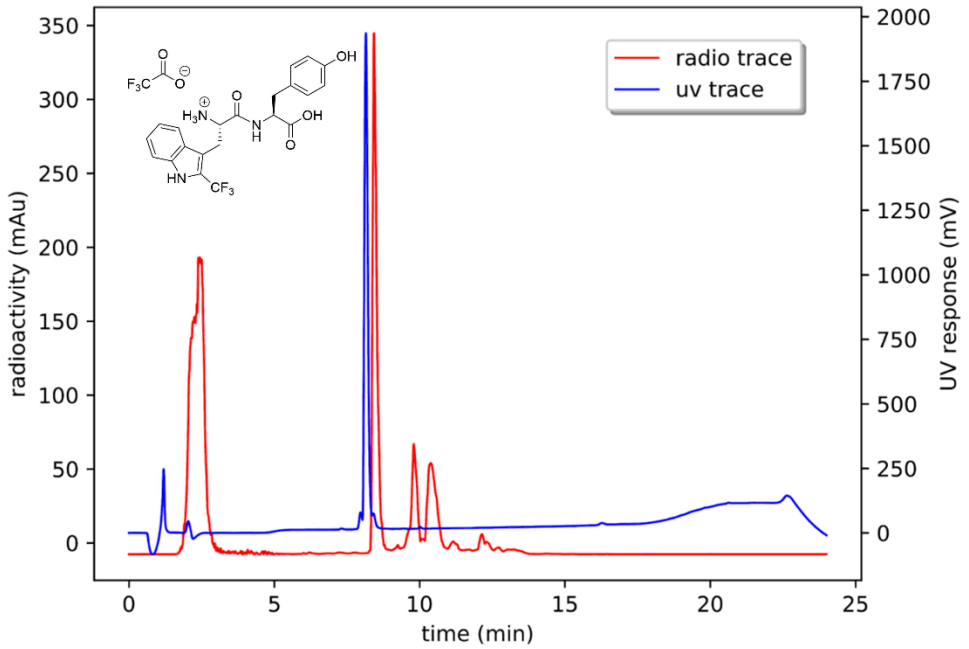
Trp(2-$^{18}FF_2$)-Tyr

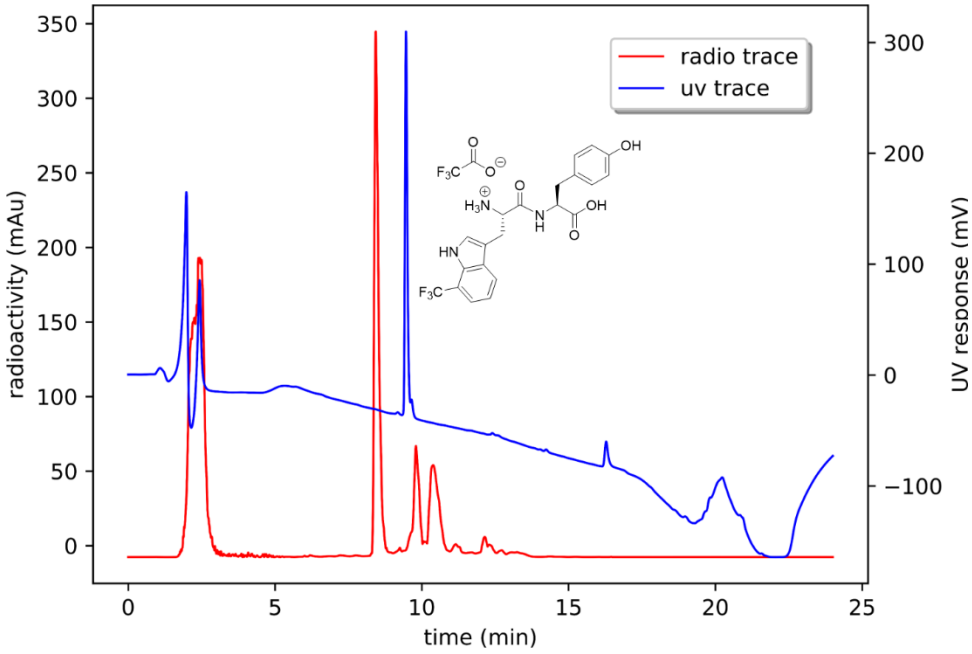


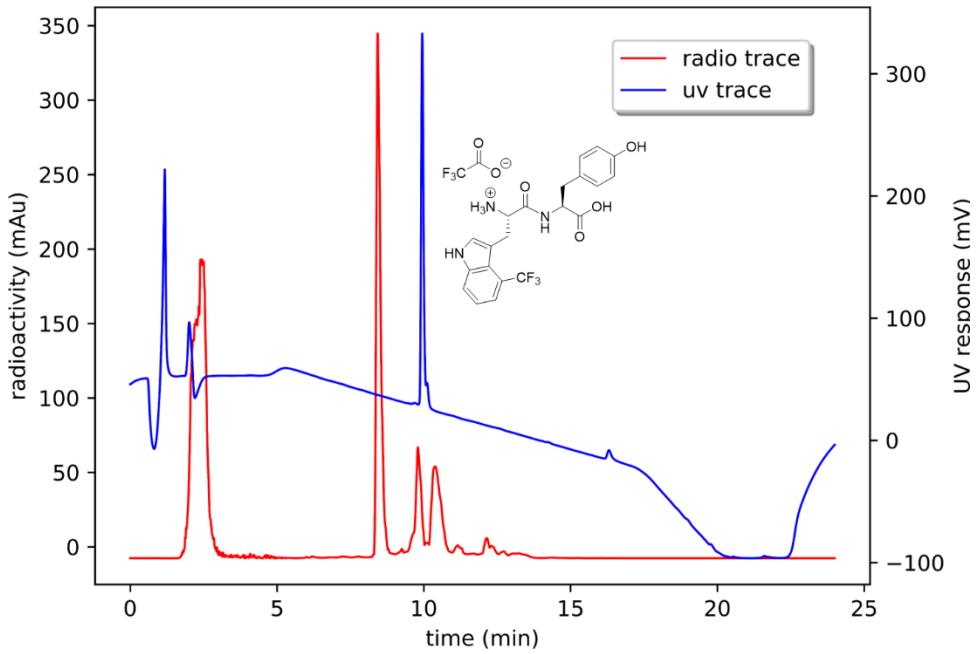
To Trp-Tyr (5.5 mg, 0.015 mmol) and iron(III) nitrate nonahydrate (12.1 mg, 0.03 mmol) in a 3 mL V-vial was added [^{18}F]$NH_4SO_2CF_3$ in aqueous NH_4HCO_2 solution (10 – 100 MBq) followed by *tert*-butyl hydroperoxide solution (8.24 μL, 0.06 mmol, 70% in H_2O) in DMSO to give a total reaction solvent of 50% DMSO in aqueous NH_4HCO_2 (150 μL) before stirring at 40 ºC for 20 min. An aliquot was removed for analysis by radio-HPLC to give a RCC. **Reverse phase HPLC details**: Eluent E on an Agilent Zorbax 300 Extended C-18 4 μm 300 Å 150 x 4.6 mm column.

Run	1	2	Average	Standard Deviation
RCY for Trp(2-$CF_2{}^{18}F$)-Tyr (%)	25.7	22.2	24	3
RCY for Trp(4-$CF_2{}^{18}F$)-Tyr (%)	10.8	10.8	11	0
RCY for Trp(7-$CF_2{}^{18}F$)-Tyr (%)	8.5	7.1	8	1

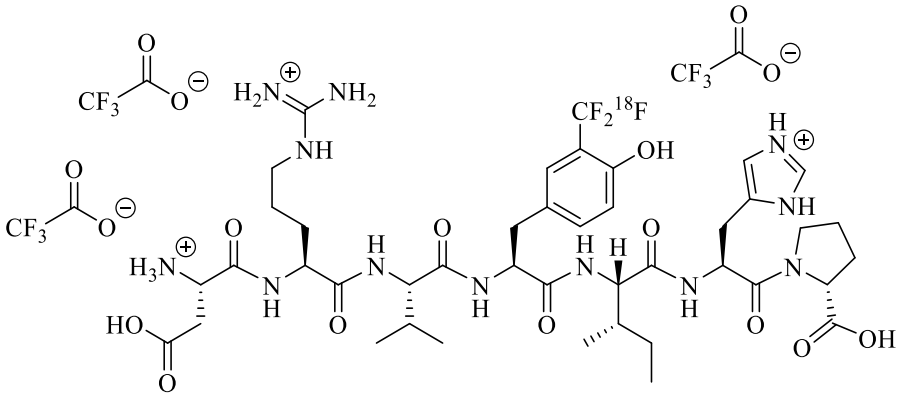
Radio-HPLC Analysis







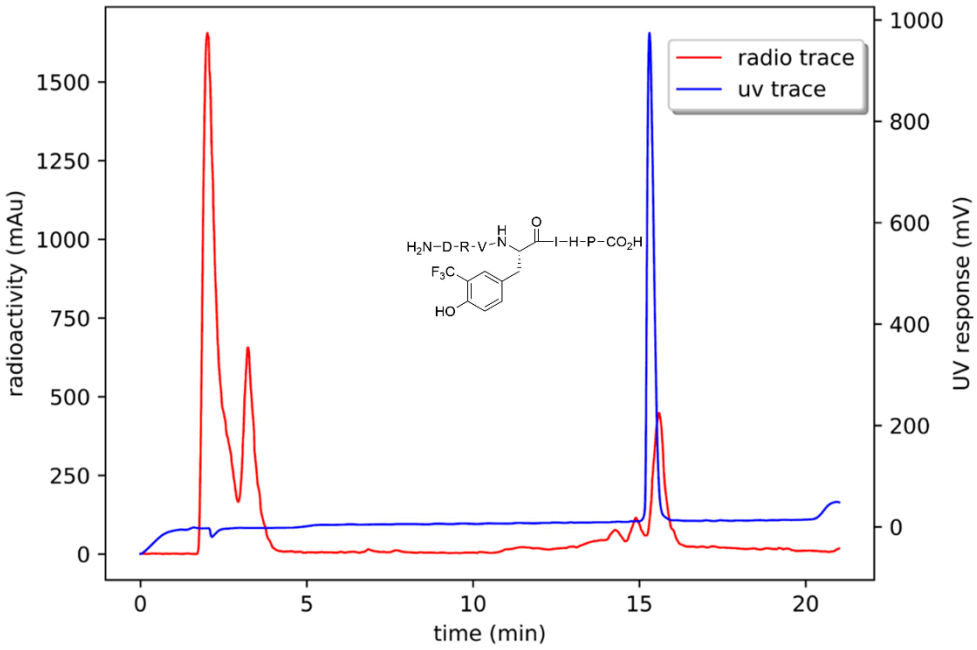
Angiotensin I/II (1-7)[Tyr(3-$CF_2{}^{18}F$)]

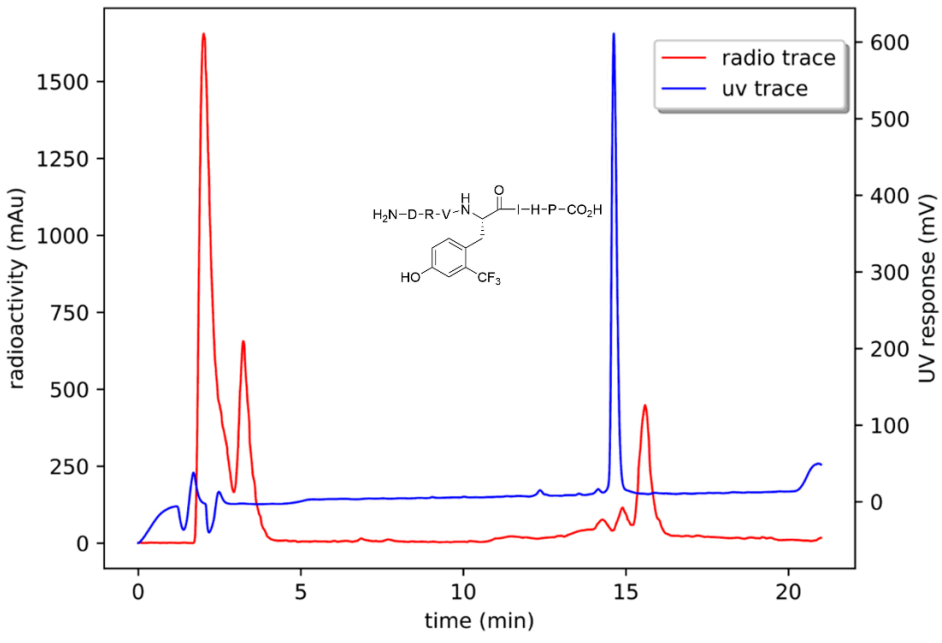


To angiotensin I/II (1-7) (12.0 mg) and iron(III) nitrate nonahydrate (24.2 mg, 0.06 mmol) in a 3 mL V-vial was added [^{18}F]$NH_4SO_2CF_3$ in aqueous NH_4HCO_2 solution (10 – 100 MBq) followed by *tert*-butyl hydroperoxide solution (8.24 µL, 0.06 mmol, 70% in H_2O) in DMSO to give a total reaction solvent of 50% DMSO in aqueous NH_4HCO_2 (100 µL) before stirring at 40 ºC for 20 min. An aliquot was removed for analysis by radio-HPLC to give a RCY. **Reverse phase HPLC details**: Eluent B on a Phenomenex Synergi™ 4 µm Hydro RP 80 Å 150 x 4.6 mm column.

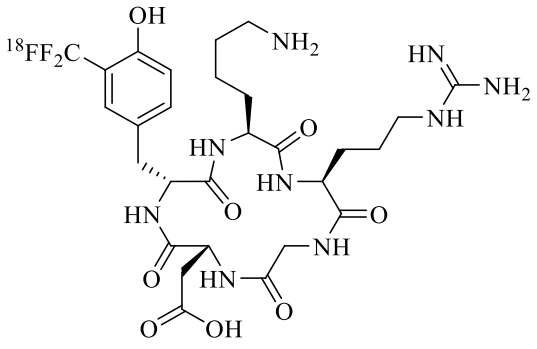
Run	1	2	3	Average	Standard Deviation
RCY for angiotensin I/II (1-7)[Tyr(3-$CF_2{}^{18}F$)] (%)	12.7	19.8	15.5	16	4
RCY for angiotensin I/II (1-7)[Tyr(2-$CF_2{}^{18}F$)] (%)	2.8	3.7	3.4	3	0

Radio-HPLC Analysis





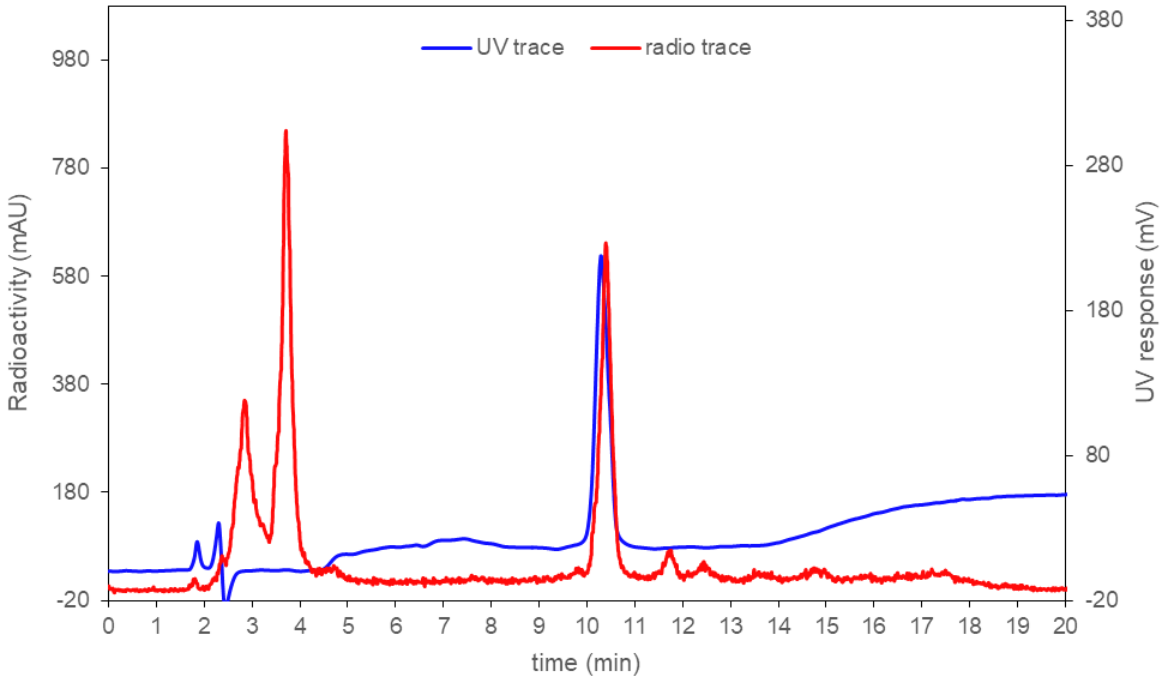
Cyclo(-Arg-Gly-Asp-D-Tyr-Lys)[Tyr(3-$CF_2{}^{18}F$)]



8

To a 5 mL V-vial containing dried [^{18}F]$CF_3SO_2NH_4$ (10 – 100 MBq) was added cyclo(-Arg-Gly-Asp-D-Tyr-Lys) trifluoroacetate salt (5.0 mg, 0.00807 mmol) and iron(III) chloride hexahydrate (8.8 mg, 0.0326 mmol) in H_2O (150 μL) followed by *tert*-butyl hydroperoxide solution (8.00 μL, 0.0597 mmol, 70% in H_2O) in DMSO (100 μL) before stirring at 60 ºC for 20 min. An aliquot was removed for analysis by radio-HPLC to give 34% RCY. **Reverse phase HPLC details**: Eluent L on a Phenomenex Synergi^{TM} 4 μm Hydro RP 80 Å 150 x 4.6 mm column.

Radio-HPLC Analysis

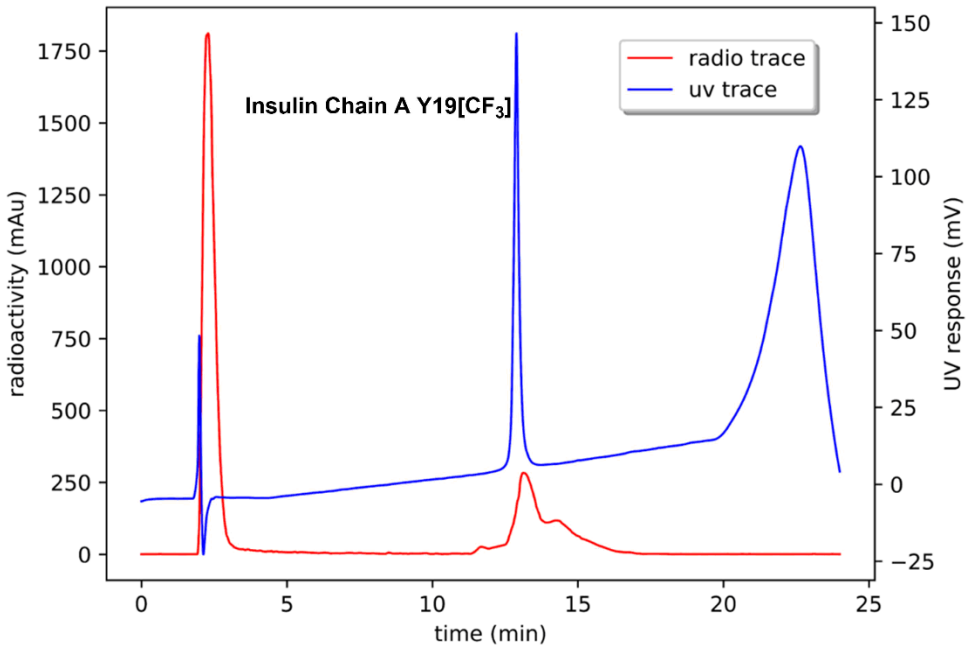


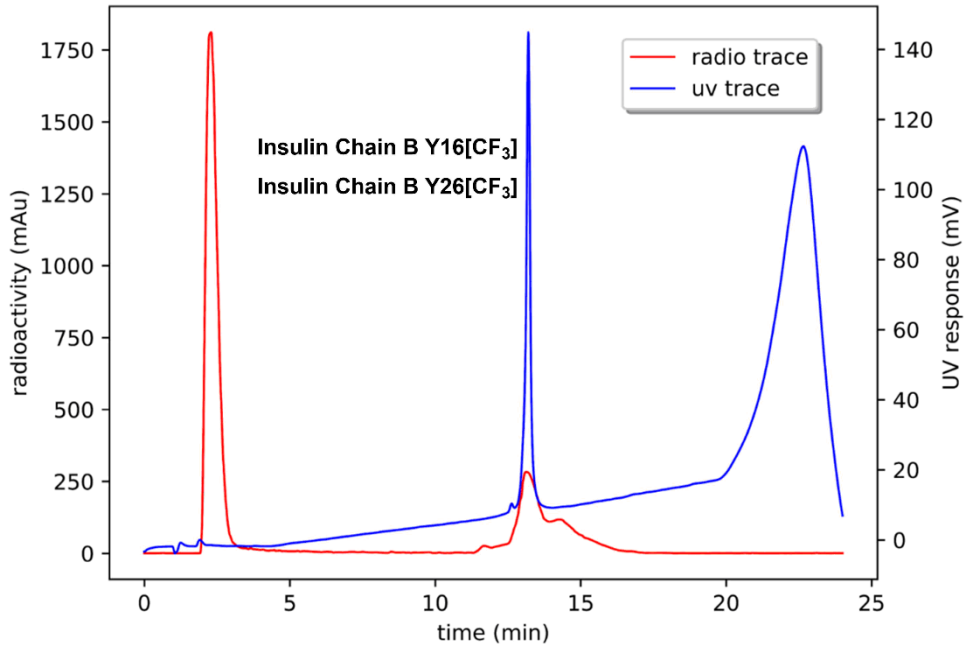
Insulin[Tyr(CF_2^{18}F)]

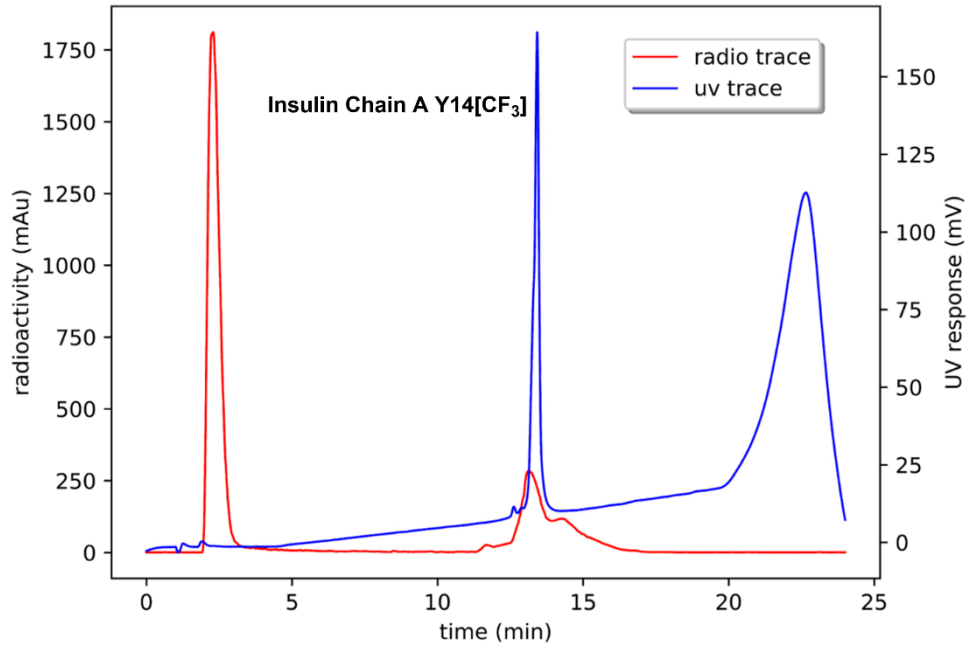
To recombinant human insulin (30.0 mg, 0.052 mmol) and iron(III) nitrate nonahydrate (12.1 mg, 0.03 mmol) in a 3 mL V-vial was added [^{18}F]$NH_4SO_2CF_3$ (0.03 – 0.2 μmol of [^{18}F/^{19}F]$CF_3SO_2NH_4$ (20 – 30 MBq)) in aqueous NH_4HCO_2 solution followed by *tert*-butyl hydroperoxide solution (8.24 μL, 0.06 mmol, 70% in H_2O) in DMSO to give a total reaction solvent of 47% – 74% DMSO in aqueous NH_4HCO_2 (150 μL) before heating at 40 ºC for 20 min without stirring. An aliquot was removed for analysis by radio-HPLC to give a RCY. Eluent A on an Agilent Zorbax 300SB CN 4 μm 300 Å 150 x 4.6 mm column.

Run	1	2	3	4	5	6	7	Average	Standard Deviation
RCY for insulin[Tyr(CF_2^{18}F)] (%)	24.7	34.0	22.3	38.7	39.4	30.3	46.5	34	9

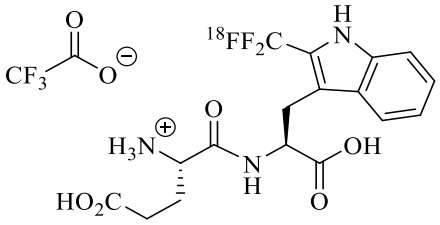
Radio-HPLC Analysis







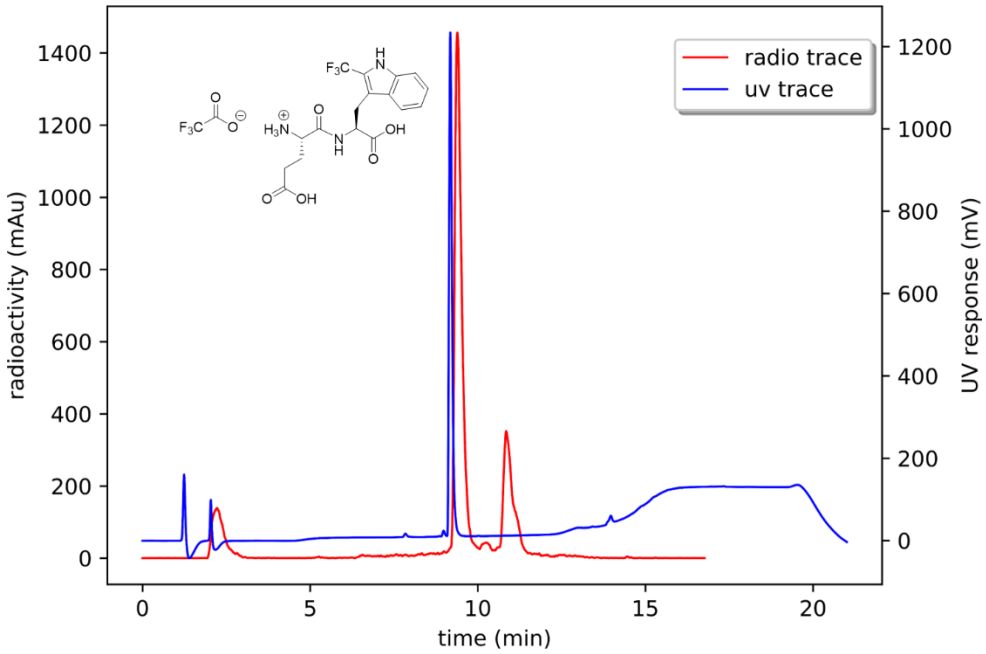
Thymogen[Trp(2-$CF_2{}^{18}F$)]

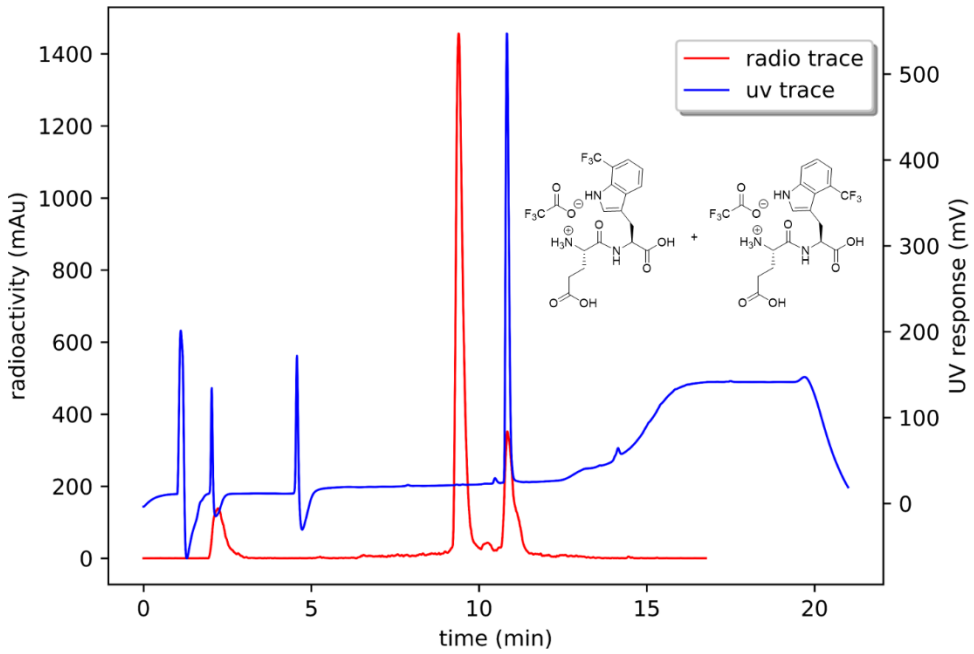


To thymogen (10.0 mg, 0.03 mmol) and iron(III) chloride solution (6 µL of 10 M solution in aqueous 25 mM NH_4HCO_2, 0.06 mmol) in a 3 mL V-vial was added [^{18}F]$NH_4SO_2CF_3$ in aqueous NH_4HCO_2 solution (10 – 100 MBq) followed by *tert*-butyl hydroperoxide solution (8.24 µL, 0.06 mmol, 70% in H_2O) in DMSO to give a total reaction solvent of 40% – 50% DMSO in aqueous NH_4HCO_2 (250 µL) before stirring at 40 ºC for 20 min. An aliquot was removed for analysis by radio-HPLC to give a RCY. **Reverse phase HPLC details**: Eluent E on an Agilent Zorbax 300 Extended C-18 4 µm 300 Å 150 x 4.6 mm column.

Run	1	2	3	4	5	Average	Standard Deviation
RCY for thymogen[Trp(2-$CF_2{}^{18}F$)] (%)	59.2	36.5	33.1	62.6	65.2	51	15
RCY for thymogen[Trp(4-$CF_2{}^{18}F$)] and thymogen[Trp(7-$CF_2{}^{18}F$)] (%)	19.4	12.7	12.6	21.0	23.1	18	5

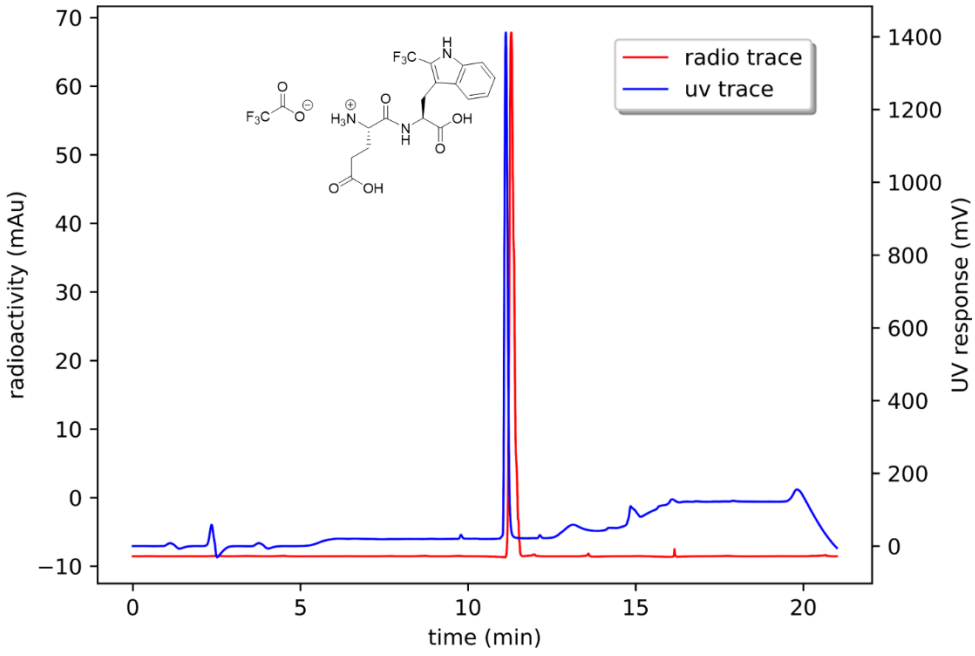
Radio-HPLC Analysis



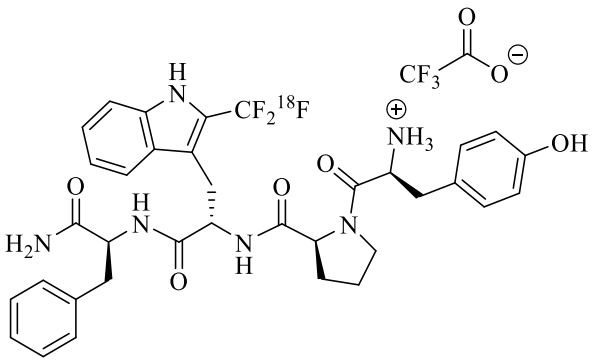


Isolation of thymogen[Trp(2-$CF_2{}^{18}F$)]

Run	1	2	3	Average	Standard Deviation
AY for thymogen[Trp(2-$CF_2{}^{18}F$)] (%)	38.4	37.1	42.0	39	3



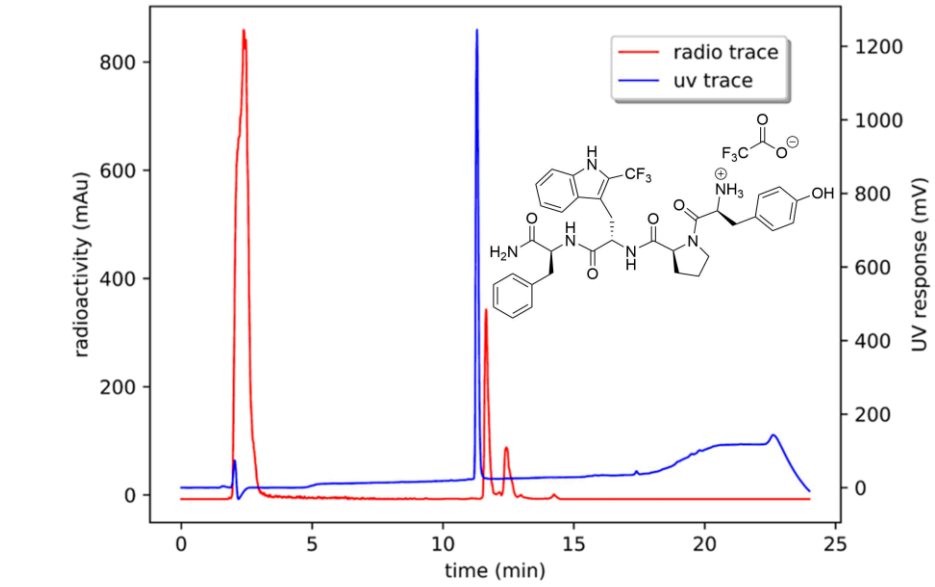
Endomorphin-1[Trp(2-$CF_2{}^{18}F$)]

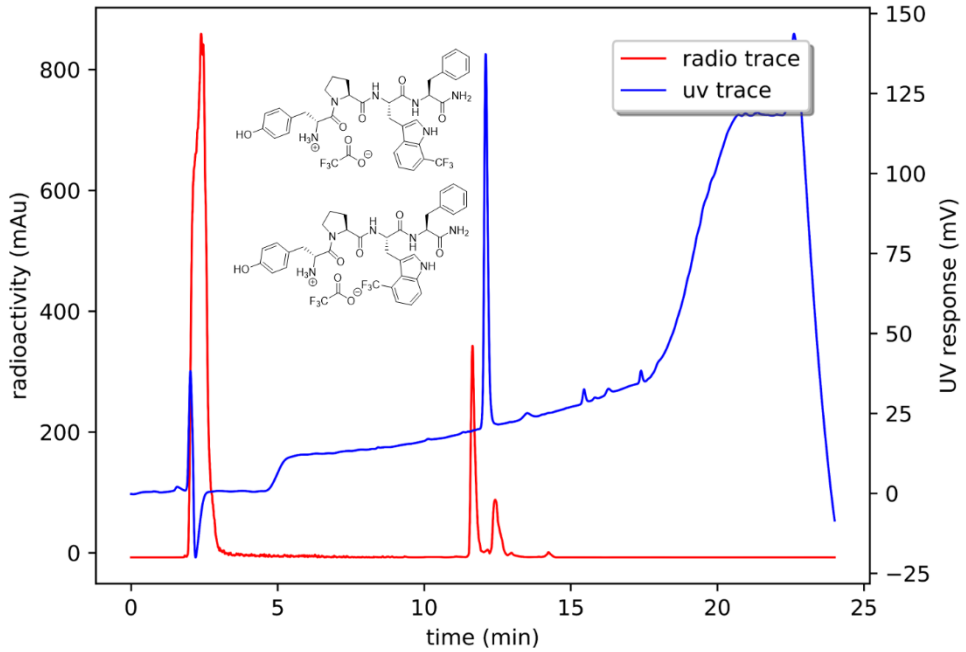


To endomorphin-1 (3.0 mg) and iron(III) chloride solution (2 μL of 10 M solution in aqueous 25 mM NH_4HCO_2, 0.02 mmol) in a 3 mL V-vial was added [^{18}F]$NH_4SO_2CF_3$ in aqueous NH_4HCO_2 solution (10 – 100 MBq) followed by *tert*-butyl hydroperoxide solution (1.37 μL, 0.02 mmol, 70% in H_2O) in DMSO to give a total reaction solvent of 40 – 50% DMSO in aqueous NH_4HCO_2 (100 μL) before stirring at 40 ºC for 20 min. An aliquot was removed for analysis by radio-HPLC to give a RCY. **Reverse phase HPLC details**: Eluent F on a Phenomenex Synergi^{TM} 4 μm Hydro RP 80 Å 150 x 4.6 mm column.

Run	1	2	3	4	Average	Standard Deviation
RCY for endomorphin-1[Trp(2-$CF_2{}^{18}F$)] (%)	10.9	15.3	8.6	10.1	11	3
RCY for endomorphin-1[Trp(4-$CF_2{}^{18}F$)] and endomorphin-1[Trp(7-$CF_2{}^{18}F$)] (%)	4.7	6.6	3.7	4.6	5	1

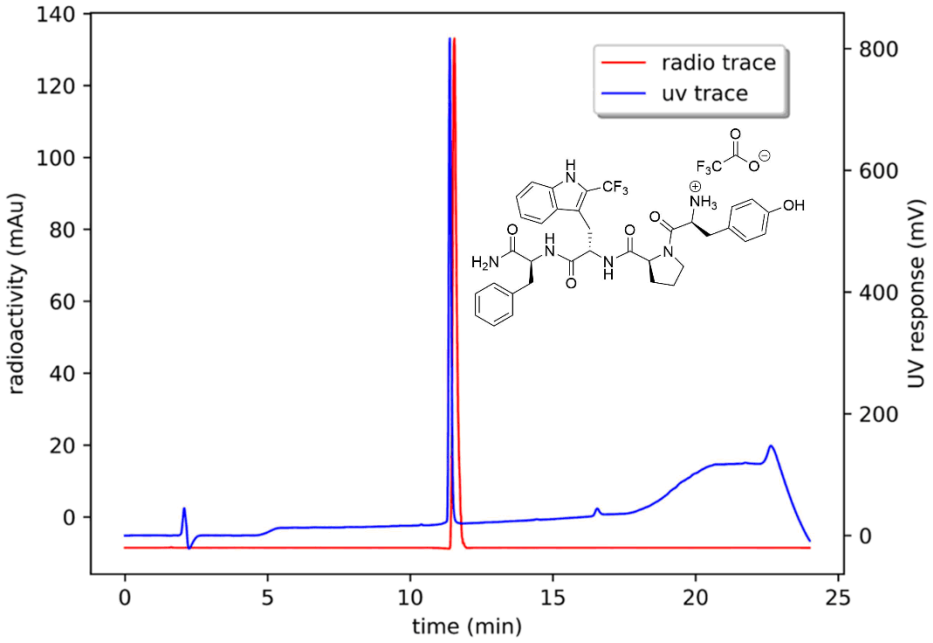
Radio-HPLC Analysis



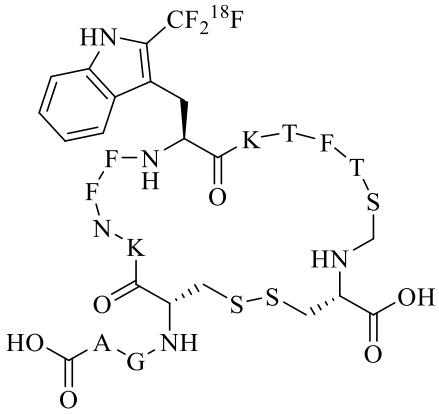


Isolation of endomorphin-1[Trp(2-$CF_2{}^{18}F$)]

Run	1
AY for endomorphin-1[Trp(2-$CF_2{}^{18}F$)] (%)	22.5



Somatostatin-14[Trp(2-$CF_2{}^{18}F$)]

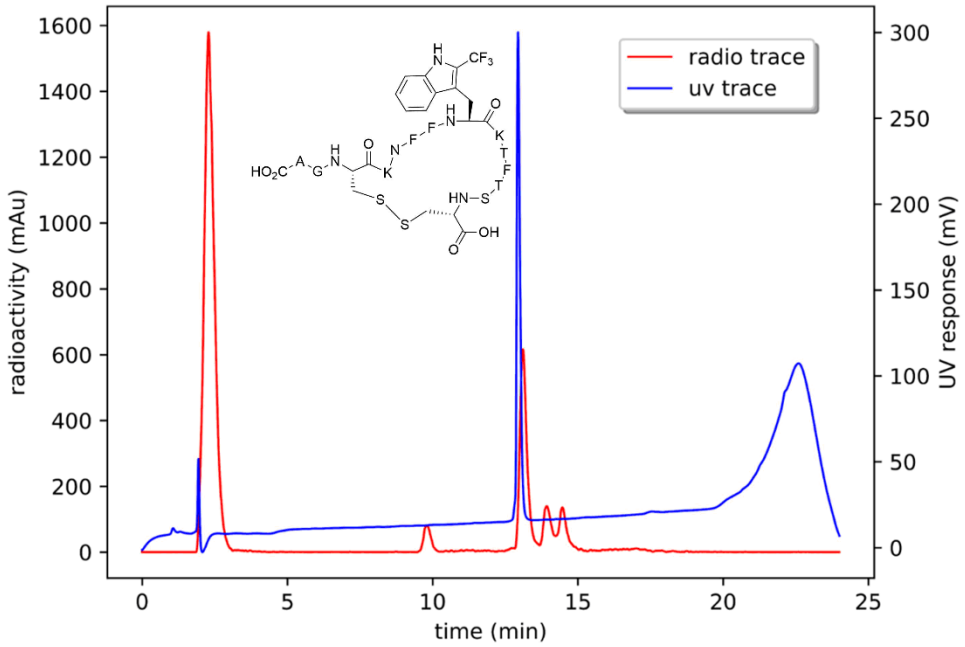


To somatostatin-14 (10.0 mg) and iron(III) chloride solution (8 µL of 10 M solution in aqueous 25 mM NH_4HCO_2, 0.08 mmol) in a 3 mL V-vial was added [^{18}F]$NH_4SO_2CF_3$ in

aqueous NH_4HCO_2 solution (10 – 100 MBq) followed by *tert*-butyl hydroperoxide solution (11.00 µL, 0.08 mmol, 70% in H_2O) in DMSO to give a total reaction solvent of 50% – 67% DMSO in aqueous NH_4HCO_2 (150 µL) before stirring at 40 ºC for 20 min. An aliquot was removed for analysis by radio-HPLC to give a RCY. **Reverse phase HPLC details**: Eluent G on an Agilent Zorbax 300 Extended C-18 4 µm 300 Å 150 x 4.6mm column.

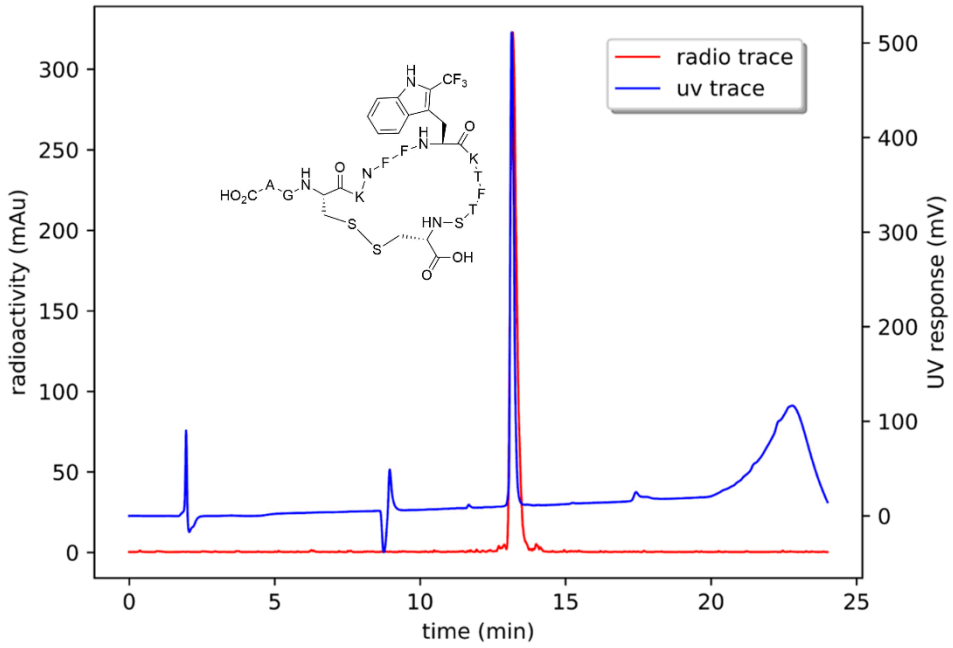
Run	1	2	3	Average	Standard Deviation
RCY for somatostatin-14[Trp(2-$CF_2{}^{18}F$)] (%)	18.1	8.4	8.4	12	6

Radio-HPLC Analysis

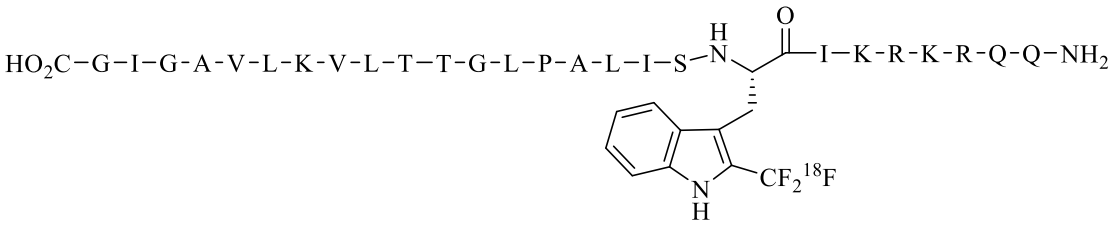


Isolation of somatostatin-14[Trp(2-$CF_2{}^{18}F$)]

Run	1	2	Average	Standard Deviation
AY for somatostatin-14[Trp(2-$CF_2{}^{18}F$)] (%)	23.5	16.4	20	5



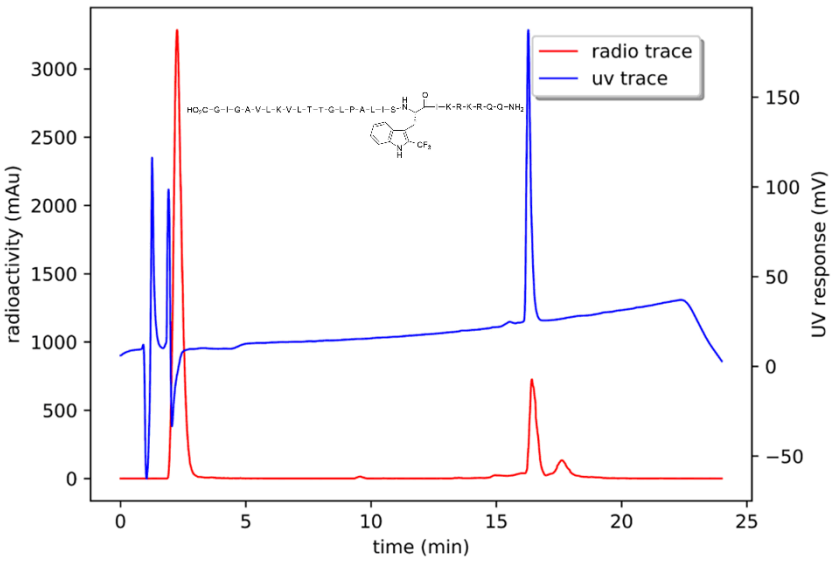
Melittin[Trp(2-$CF_2{}^{18}F$)]



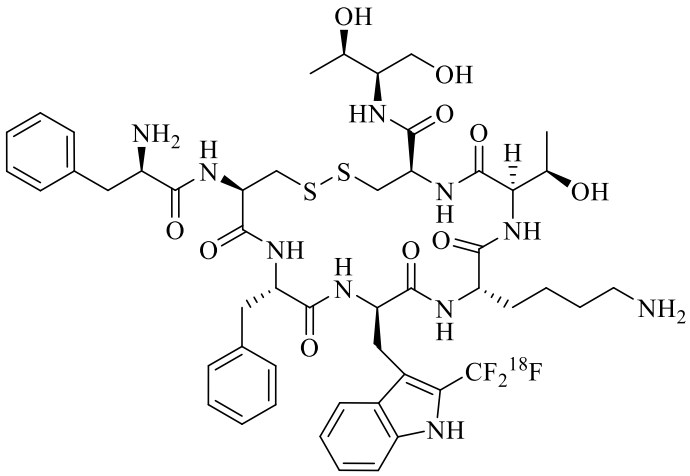
To melittin (2.0 mg) and iron(III) chloride solution (2 µL of 10 M solution in aqueous 25 mM NH_4HCO_2, 0.02 mmol) in a 3 mL V-vial was added [^{18}F]$NH_4SO_2CF_3$ in aqueous NH_4HCO_2 solution (10 – 100 MBq) followed by *tert*-butyl hydroperoxide solution (2.76 µL, 0.02 mmol, 70% in H_2O) in DMSO to give a total reaction solvent of 33% – 50% DMSO in aqueous NH_4HCO_2 (50 – 55 µL) before stirring at 40 ºC for 20 min. An aliquot was removed for analysis by radio-HPLC to give a RCY. **Reverse phase HPLC details**: Eluent H on an Agilent Zorbax 300 Extended C-18 4 µm 300 Å 150 x 4.6 mm column.

Run	1	2	3	4	Average	Standard Deviation
RCY for melittin[Trp(2-$CF_2{}^{18}F$)] (%)	16.9	15.0	15.1	9.4	14	3

Radio-HPLC Analysis



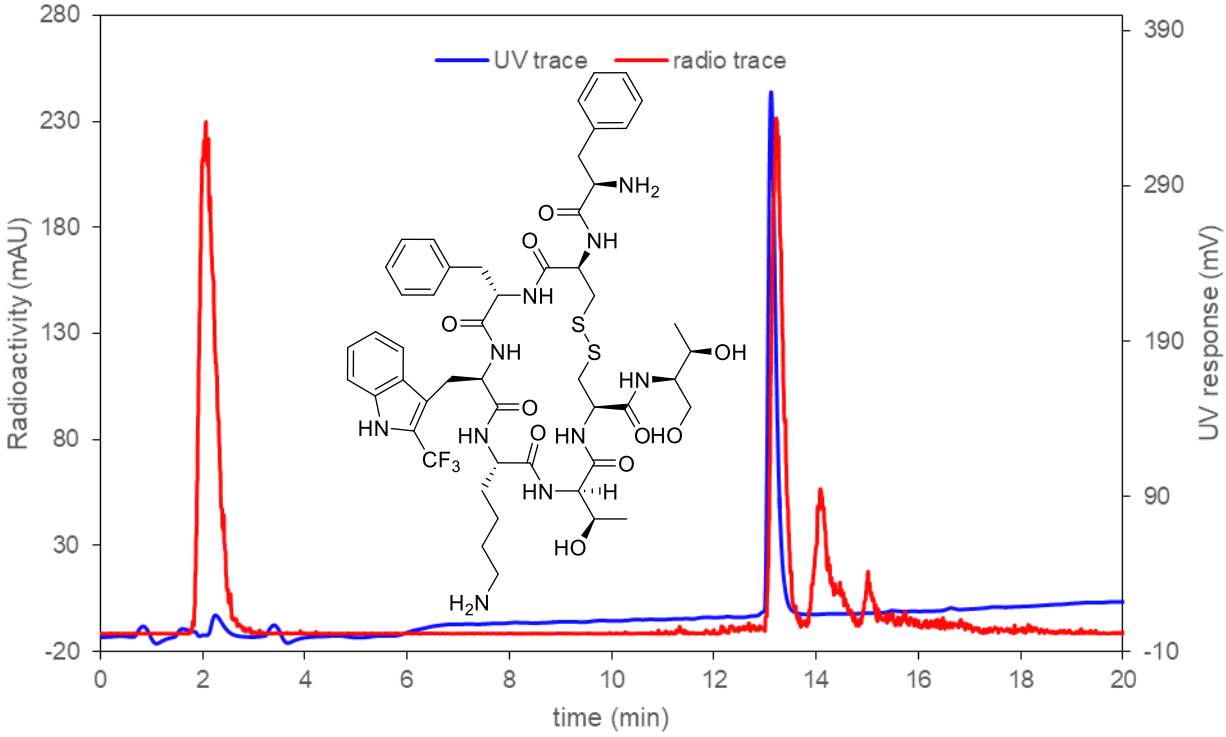
Octreotide[Trp(2-$CF_2{}^{18}F$)]



To a 5 mL V-vial containing dried [^{18}F]$CF_3SO_2NH_4$ (10 – 100 MBq) was added octreotide acetate (3.0 mg, 0.00278 mmol) in H_2O (75 µL) and iron(III) nitrate nonahydrate (4.5 mg, 0.0111 mmol) in H_2O (5 µL) followed by *tert*-butyl hydroperoxide solution (1.52 µL, 0.0111 mmol, 70% in H_2O) in DMSO (75 µL) to give a total reaction solvent of 48% DMSO in aqueous NH_4HCO_2 (155 µL) before stirring at 40 ºC for 10 min. An aliquot was removed

for analysis by radio-HPLC to give 33% RCY. **Reverse phase HPLC details**: Eluent K on a Phenomenex Synergi^{TM} 4 µm Hydro RP 80 Å 150 x 4.6 mm column.

Radio-HPLC Analysis



4.5 Automated Radiosynthesis at Invicro

4.5.1 General Experimental Details

[^{18}F]Fluoride was produced using a Siemens RDS-111 Eclipse cyclotron equipped with a fluoride target loaded with [^{18}O]water *via* the ^{18}O(p,n)^{18}F reaction. The [^{18}F]fluoride in [^{18}O]water was transferred with a sweep of argon gas from the cyclotron target to the hotcell containing a NanoTek® automated microfluidic device (Advion). All manipulations were carried out using remotely controlled syringes on the automated system unless use of gas flow is stated. HPLC analysis was performed on a 1100 series Agilent HPLC system equipped with a binary pump, diode array detector, shared autosampler, parallel UV

detectors and LabLogic NaI/PMT radiodetectors with Flowram analog output.

All SepPak Accell Plus QMA Carbonate Plus Light cartridges (46 mg) (Waters part # 186004540), Sep-Pak tC18 Plus Light Cartridge 145 mg Sorbent per Cartridge 37-55 µm (Waters part # WAT036805) and SepPak Plus C18 cartridges (Waters part # WAT020515) were conditioned with MeOH (2 mL) and H_2O (5 mL) before use. All Oasis Plus Weak Anion Exchange (WAX) short cartridges (product # 186003519) were activated with water (3 mL) and 2% formic acid in water (3 mL). All Phenomenex Strata-X 33 µm Polymeric Reversed Phase 1 mL tubes (30 mg) were used as received.

For radiochemical reactions carried out using aliquots of [^{18}F]fluoride, the efficiency of labelling the desired product starting from [^{18}F]fluoride is calculated as the Radiochemical Yield (RCY). This can be measured by radio-HPLC using an aliquot of the crude reaction quenched with an aqueous solution to dissolve unreacted [^{18}F]fluoride. The RCY is the measured activity of labelled product as a percentage of the unreacted [^{18}F]fluoride and other labelled side products. The RCY is decay corrected which takes into account activity lost from decay over time thus giving a sense of chemical efficiency.

Activity Yield (AY) is calculated by comparing the starting activity with the activity of the purified product, after taking into account Radiochemical Purity (RCP) as determined by radio-HPLC. AY is not corrected for decay and is used to analyse overall synthesis efficiency by including purification and isolation steps of the final compound.

All ^{18}F-labeled compounds were characterised by comparing the radio-HPLC spectrum with a UV-HPLC spectrum of an authentic reference.

4.5.2 Automated Radiosynthesis of [^{18}F]Langlois Reagent and Octreotide[Trp(2-$CF_2{}^{18}F$)]

[^{18}F]Fluoride (30 – 45 GBq) was separated from [^{18}O]water using a Waters Sep-Pak Accell Plus QMA Carbonate Plus Light cartridge (46 mg) (Waters part # 186004540) and subsequently eluted off using a solution of Kryptofix (6.3 mg) and K_2CO_3 (1.0 mg) in MeCN:H_2O 4:1 (6 x 50 µL portions added over 4 min) into a 5 mL V-vial heated at 95 ºC under a flow of Ar. Anhydrous MeCN (3 x 100 µL portions over 6 min) was passed through the QMA before heating at 115 ºC for 3 min.

NMM-SO_2 (4.6 mg, 27.7 µmol), JohnPhos (20.9 mg, 70.0 µmol) and methyl chlorodifluoroacetate (6.86 µl, 65.0 µmol) in DMA (150 µL) was added to the V-vial containing azeotropically dried [^{18}F]KF/K_{222} before heating at 115 ºC for 10 min.

50 mM aqueous HCO_2NH_4 (1.5 mL) was added to the reactor and the mixture was left to stand for 30 seconds before it was taken up into a 2 mL HPLC loop and injected onto a semi-preparative HPLC column. **Semi-preparative HPLC details**: Phenomenex Synergi^{TM} 4 µm Hydro RP 80 Å, 250 x 10 mm, flow rate = 3.5 mL/min, column temperature = rt, eluent = 100% 50 mM NH_4HCO_2 in H_2O, retention time = 6.9 – 8.0 min.

The product fraction was collected into a 20 mL V-vial containing 2% formic acid in H_2O (10 mL) and the diluted passed slowly through an Oasis Plus WAX short cartridge using a flow of He. H_2O (4 mL) was added to the 20 mL V-vial and was passed through the WAX cartridge. The cartridge was dried for 30 seconds using He flow before 1.4% ammonium hydroxide in MeCN (2 mL) was added to the 20 mL V-vial and used to elute off the [^{18}F]$CF_3SO_2NH_4$ product from the WAX cartridge slowly into a 5 mL V-vial heated at 70 ºC.

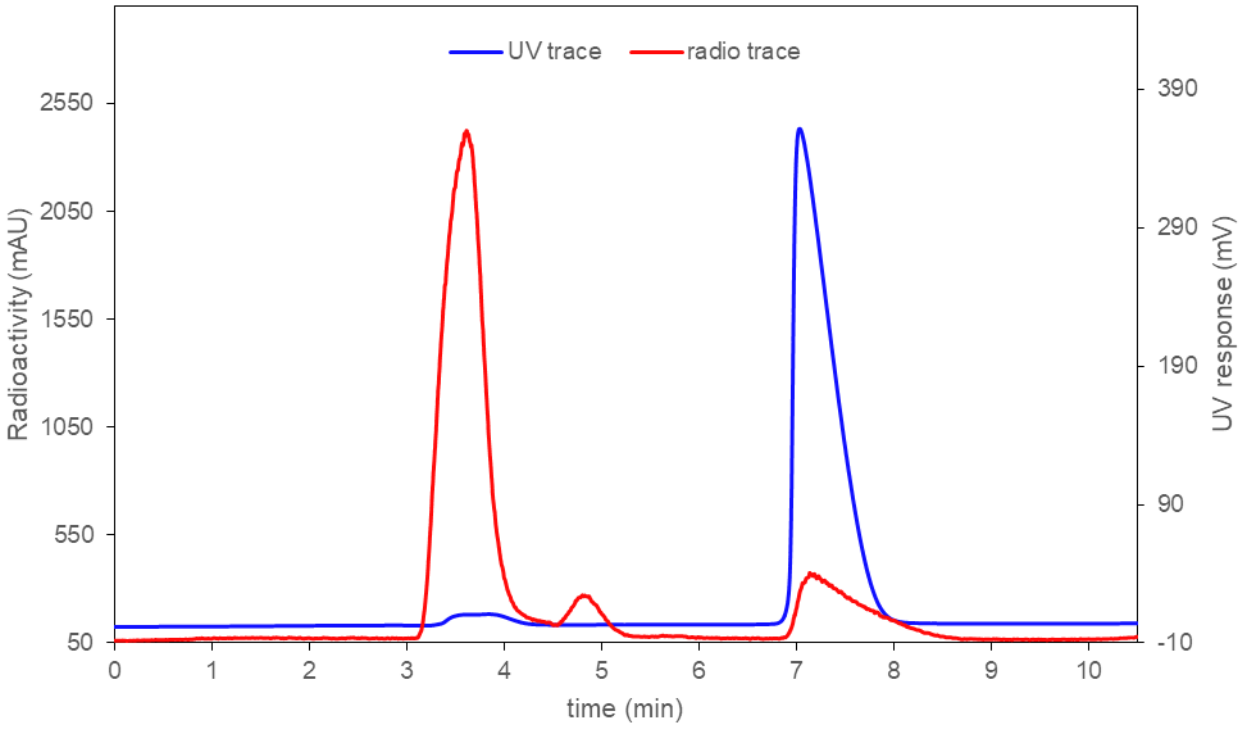
The solution of heated [^{18}F]$CF_3SO_2NH_4$ was added in 200 μL portions over 15 min to a 5 mL V-vial heated to 90°C under air flow. The lines connected to the V-vial were emptied and cleaned before heating the V-vial for a further 3 min at 100 ºC before cooling to 40 ºC.

Octreotide acetate (3.0 mg, 2.78 μmol) in 50 mM aqueous HCO_2NH_4 (65 μL) was added to iron nitrate nonahydrate (4.5 mg, 11.1 μmol) in H_2O (10 μL) before being added to the V-vial containing dried [^{18}F]$CF_3SO_2NH_4$. *Tert*-butyl hydroperoxide solution (3.04 μL, 22.2 μmol, 70% in H_2O) in DMSO (75 μL) was added before heating at 40 ºC for 10 min.

At the end of the reaction, 0.1% TFA in H_2O (1.5 mL) was added to the reactor before the mixture was taken up and loaded into a 2 mL HPLC loop for injection onto a semi-preparative HPLC column. **Semi-preparative HPLC details**: Phenomenex Synergi^{TM} 4 μm Hydro RP 80 Å, 250 x 10 mm, flow rate = 4 mL/min, column temperature = rt, eluent = 100% H_2O (0.1% TFA) for 5 min then increase linearly to 30% MeCN (0.1% TFA) at 6 min, then increase linearly to 50% MeCN (0.1% TFA) at 25 min, retention time = 19.0 min.

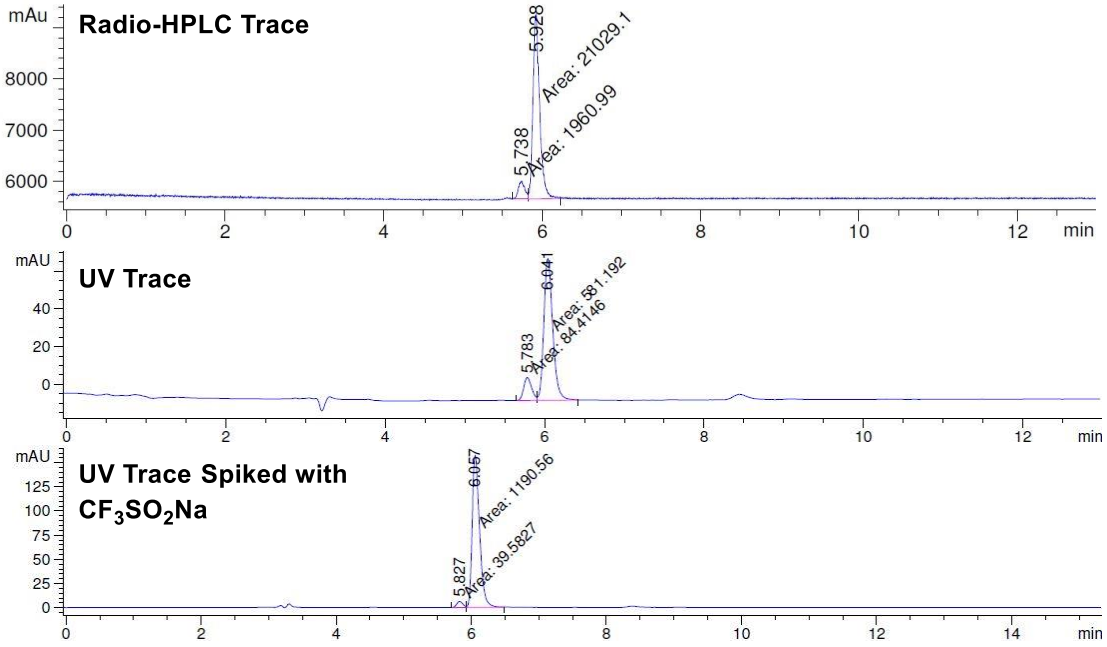
The product fraction was eluted into a large flask containing H_2O (40 mL) before being added to a Phenomenex Strata-X 33 μm Polymeric Reversed Phase 1 mL tube (30 mg) using a flow of N_2. H_2O (5 mL) was passed through the cartridge followed by drying with N_2 flow for 30 seconds before eluting the octreotide[Trp(2-$CF_2{}^{18}F$)] slowly with EtOH (0.7 mL) using N_2 flow.

Semi-Preparative Radio-HPLC of Reaction forming [^{18}F]Langlois Reagent with UV Trace Overlay of an Authentic Reference



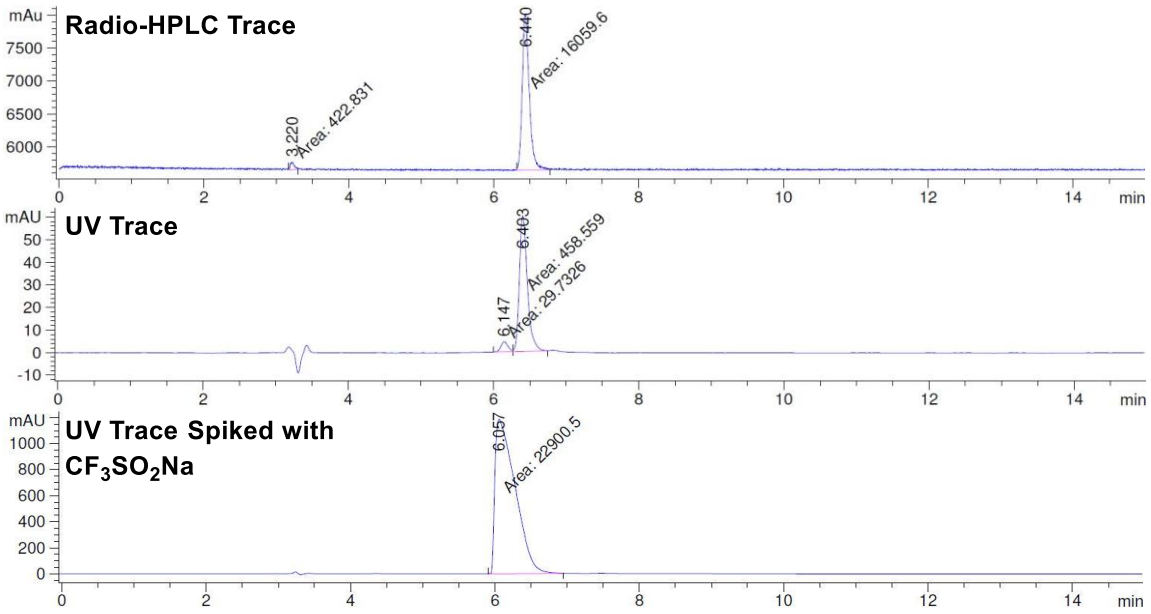
Radio-HPLC of Isolated [^{18}F]Langlois Reagent with UV Trace Spiked with an Authentic Reference

Reverse phase HPLC details: Phenomenex Gemini 5 µm NX-C18 110 Å, 250 x 10 mm, flow rate = 3.5 mL/min, column temperature = rt, eluent = 100% 50 mM NH_4HCO_2 in H_2O, retention time = 6.0 min.



Radio-HPLC of [^{18}F]Langlois Reagent after WAX cartridge with UV Trace Spiked with an Authentic Reference

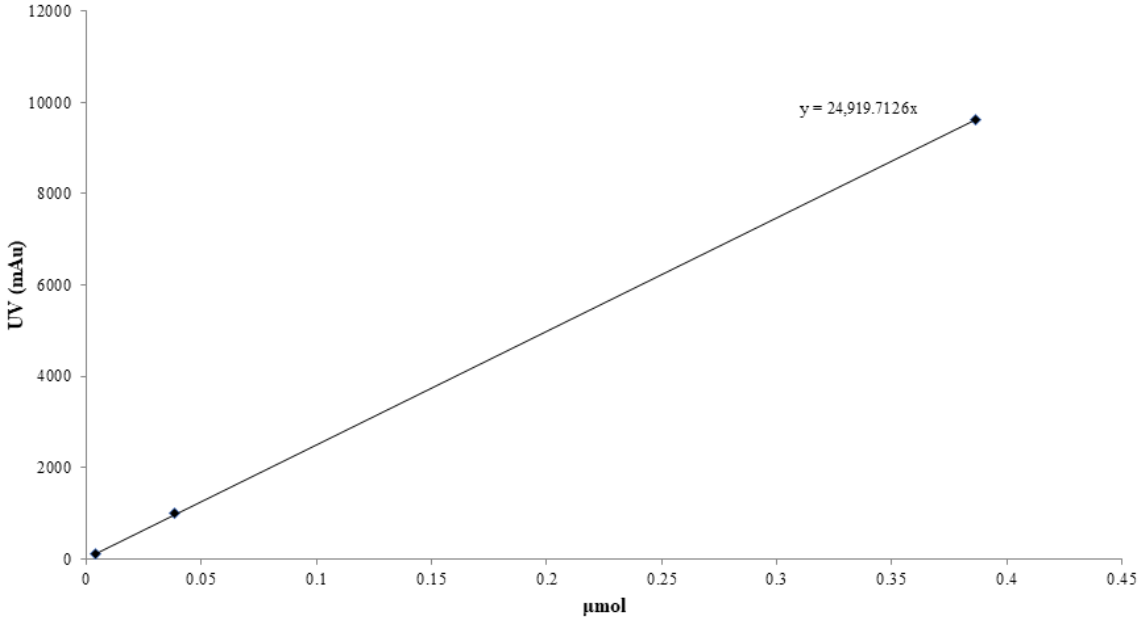
Reverse phase HPLC details: Phenomenex Gemini 5 μm NX-C18 110 Å, 250 x 10 mm, flow rate = 3.5 mL/min, column temperature = rt, eluent = 100% 50 mM NH_4HCO_2 in H_2O, retention time = 6.4 min.



Molar Activity Determination of [^{18}F]Langlois Reagent

The molar activity of [^{18}F]$NH_4SO_2CF_3$ was assessed by radio-HPLC, using a Phenomenex Gemini 5 μm NX-C18 110 Å, 250 x 10 mm, flow rate = 3.5 mL/min, column temperature = rt, eluent = 100% 50 mM NH_4HCO_2 in H_2O, retention time = 6.4 min.

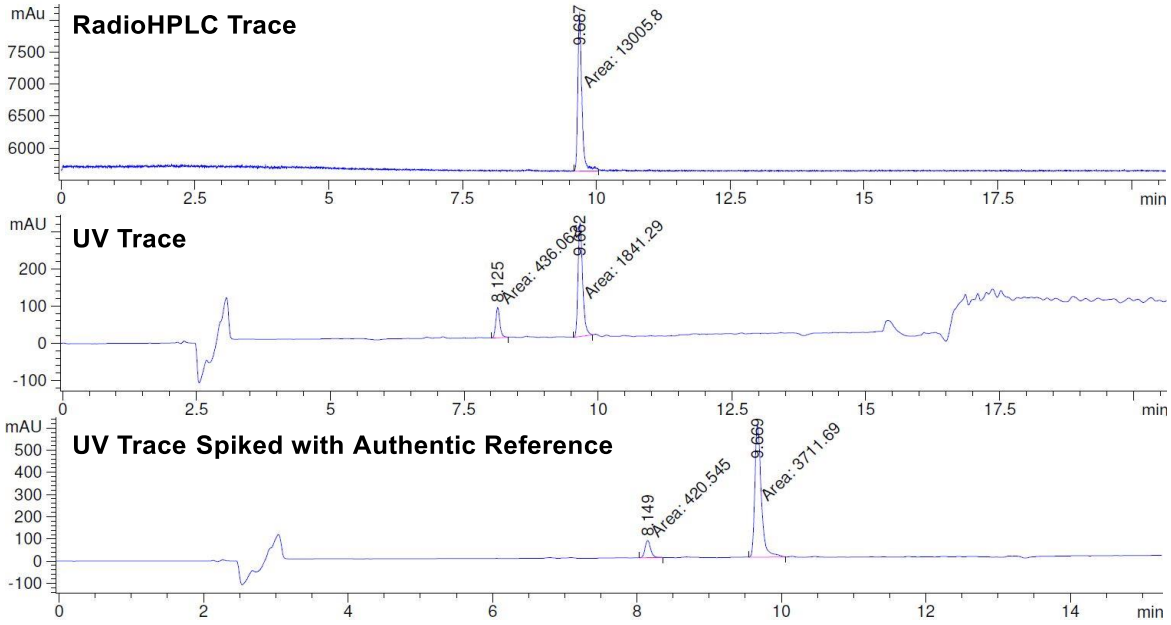
Calibration Curve



Area (mAu)	$CF_3SO_2NH_4$ (µmol)	Activity (MBq)	Molar Activity (GBq μmol^{-1})
320	0.016	18.0	1.13

Radio-HPLC of Isolated Octreotide[Trp(2-CF_2^{18}F)] with UV Trace Spiked with an Authentic Reference

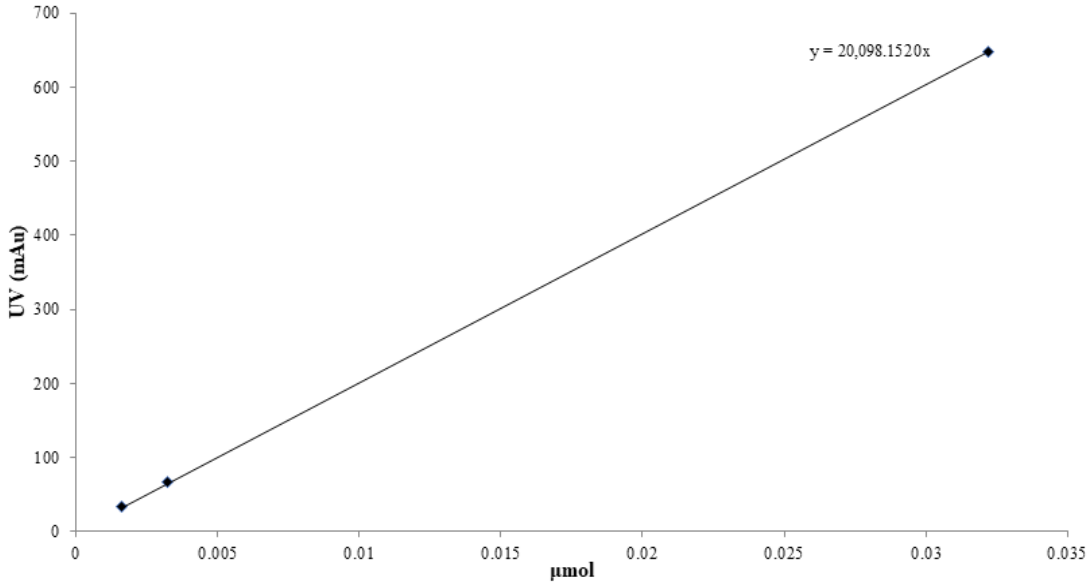
Reverse phase HPLC details: Phenomenex Gemini 5 μm NX-C18 110 Å, 250 x 10 mm, flow rate = 5 mL/min, column temperature = rt, eluent = 20% MeCN (0.1% TFA) and 80% H_2O (0.1% TFA) then increase linearly to 55% MeCN (0.1% TFA) at 13 min, retention time = 9.7 min.



Molar Activity Determination of octreotide[Trp(2-CF_2^{18}F)]

The molar activity of octreotide[Trp(2-CF_2^{18}F)] was assessed by radio-HPLC, using a Phenomenex Gemini 5 μm NX-C18 110 Å, 250 x 10 mm, flow rate = 5 mL/min, column temperature = rt, eluent = 20% MeCN (0.1% TFA) and 80% H_2O (0.1% TFA) then increase linearly to 55% MeCN (0.1% TFA) at 13 min, retention time = 9.7 min.

Calibration Curve



Area (mAu)	Octreotide[Trp(2-CF_3)] (µmol)	Activity (MBq)	Molar Activity (GBq µmol^{-1})
47	0.0024	0.60	0.25

4.5.3 Automated Radiosynthesis of [^{18}F]Langlois Reagent and c(RGDyK)[Tyr(3-$CF_2{}^{18}$F)]

[^{18}F]Fluoride (30 – 45 GBq) was separated from [^{18}O]water using a Waters Sep-Pak Accell Plus QMA Carbonate Plus Light cartridge (46 mg) (Waters part # 186004540) and subsequently eluted off using a solution of Kryptofix (6.3 mg) and K_2CO_3 (1.0 mg) in MeCN:H_2O 4:1 (6 x 50 µL portions added over 4 min) into a 5 mL V-vial heated at 95 ºC under a flow of Ar. Anhydrous MeCN (3 x 100 µL portions over 6 min) was passed through the QMA before heating at 115 ºC for 3 min.

NMM-SO_2 (4.6 mg, 27.7 μmol), JohnPhos (20.9 mg, 70.0 μmol) and methyl chlorodifluoroacetate (6.86 μl, 65.0 μmol) in DMA (150 μL) was added to the V-vial containing azeotropically dried [^{18}F]KF/K_{222} before heating at 115 ºC for 10 min.

50 mM aqueous HCO_2NH_4 (1.5 mL) was added to the reactor and the mixture was left to stand for 30 seconds before it was taken up into a 2 mL HPLC loop and injected onto a semi-preparative HPLC column. **Semi-preparative HPLC details**: Phenomenex Synergi^{TM} 4 μm Hydro RP 80 Å, 250 x 10 mm, flow rate = 3.5 mL/min, column temperature = rt, eluent = 100% 50 mM NH_4HCO_2 in H_2O, retention time = 6.9 – 8.0 min.

The product fraction was collected into a 20 mL V-vial containing 2% formic acid in H_2O (10 mL) and the diluted passed slowly through an Oasis Plus WAX short cartridge using a flow of He. H_2O (4 mL) was added to the 20 mL V-vial and was passed through the WAX cartridge. The cartridge was dried for 30 seconds using He flow before 1.4% ammonium hydroxide in MeCN (2 mL) was added to the 20 mL V-vial and used to elute off the [^{18}F]$CF_3SO_2NH_4$ product from the WAX cartridge slowly into a 5 mL V-vial heated at 70 ºC.

The solution of heated [^{18}F]$CF_3SO_2NH_4$ was added in 200 μL portions over 15 min to a 5 mL V-vial heated to 90°C under air flow. The lines connected to the V-vial were emptied and cleaned before heating the V-vial for a further 3 min at 100 ºC before cooling to 40 ºC.

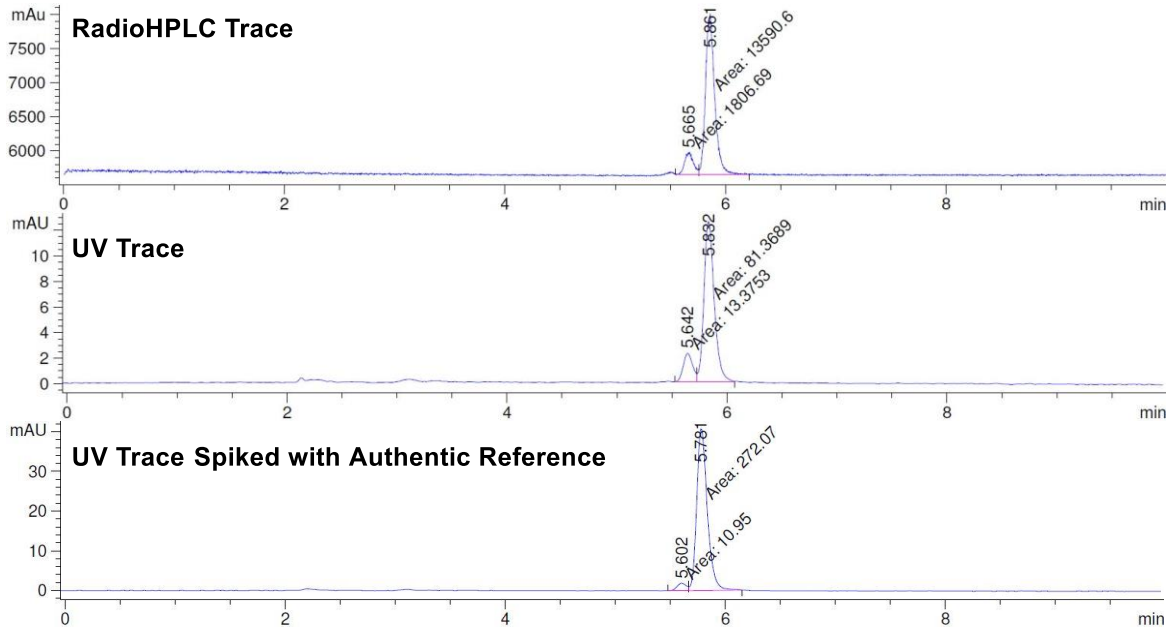
Cyclo(-Arg-Gly-Asp-D-Tyr-Lys) trifluoroacetate salt (2.5 mg, 40.4 μmol) in 50 mM aqueous HCO_2NH_4 (60 μL) was added to iron nitrate nonahydrate (10.96 mg, 27.1 μmol) in H_2O (10 μL) before being added to the V-vial containing dried [^{18}F]$CF_3SO_2NH_4$. *Tert*-butyl hydroperoxide solution (6.08 μL, 44.4 μmol, 70% in H_2O) in DMSO (70 μL) was added before heating at 40 ºC for 10 min.

At the end of the reaction, 0.1% TFA in H_2O (1.5 mL) was added to the reactor before the mixture was taken up and loaded into a 2 mL HPLC loop for injection onto a semi-preparative HPLC column. **Semi-preparative HPLC details**: Phenomenex Synergi^{TM} 4 μm Hydro RP 80 Å, 250 x 10 mm, flow rate = 4 mL/min, column temperature = rt, eluent = 100% H_2O (0.1% TFA) for 5 min then increase linearly to 30% MeCN (0.1% TFA) at 6 min, then increase linearly to 50% MeCN (0.1% TFA) at 25 min, retention time = 19.0 min.

The product fraction was eluted into a large flask containing H_2O (40 mL) before being added to a SepPak Plus C18 cartridge (Waters part # WAT020515) using a flow of N_2. H_2O (5 mL) was passed through the cartridge followed by drying with N_2 flow for 30 seconds before eluting the c(RGDyK)[Tyr(3-$CF_2{}^{18}F$)] slowly with MeCN (3 mL) using N_2 flow.

Radio-HPLC of Isolated c(RGDyK)[Tyr(3-$CF_2{}^{18}F$)] with UV Trace Spiked with an Authentic Reference

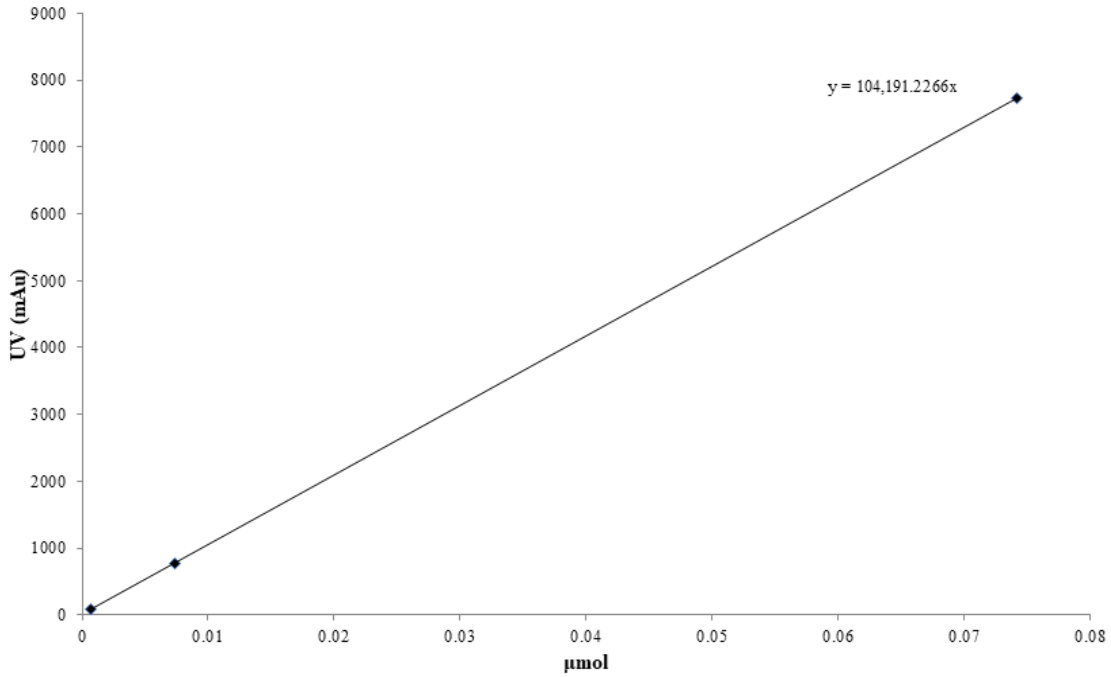
Reverse phase HPLC details: Phenomenex Gemini 5 μm NX-C18 110 Å, 250 x 10 mm, flow rate = 5 mL/min, column temperature = rt, eluent = 20% MeCN (0.1% TFA) and 80% H_2O (0.1% TFA) then increase linearly to 55% MeCN (0.1% TFA) at 13 min, retention time = 5.8 min.



Molar Activity Determination of c(RGDyK)[Tyr(3-$CF_2{}^{18}F$)]

The molar activity of c(RGDyK)[Tyr(3-$CF_2{}^{18}F$)] was assessed by radio-HPLC, using a Phenomenex Gemini 5 μm NX-C18 110 Å, 250 x 10 mm, flow rate = 5 mL/min, column temperature = rt, eluent = 20% MeCN (0.1% TFA) and 80% H_2O (0.1% TFA) then increase linearly to 55% MeCN (0.1% TFA) at 13 min, retention time = 5.8 min.

Calibration Curve



Area (mAu)	c(RGDyK)[Tyr(3-CF_3)] (µmol)	Activity (MBq)	Molar Activity (GBq μmol^{-1})
520	0.0044	3.0	0.68

4.6 Cell Uptake Experiments

Cells

AR42J cells were cultured in DMEM (Gibco, ThermoFisher Scientific) supplemented with 10% FBS (Gibco) in a 37°C humidified incubator with 5% CO_2.

Preparation and purification of ^{125}I-DOTA-TATE radioligand

DOTA-TATE acetate (GMP) (ABX, Radeberg, Germany) was radioiodinated using I-125 in 0.1 M NaOH (Perkin Elmer) *via* the chloramine-T method, reacted at room temperature

for 10 min. The reaction was quenched with sodium metabisulphite. Radiochemical purity was determined by iTLC-SG (Varian) run in 0.2 M phosphate buffer with radiolabelled peptide remaining at the origin (Rf = 0) and free iodide eluting to the solvent front (Rf = 1). ^{125}I-DOTA-TATE was purified from unlabelled DOTA-TATE by RP-HPLC using a Beckman system gold 128 solvent module and a 166 UV detector module (monitoring at 220 nm). Compounds were separated on an Agilent Eclipse XDB-C18 4.6x150 mm internal diameter column, with the following mobile phases: Solvent A, 0.1% TFA in water; solvent B, 0.1% TFA in acetonitrile. The elution gradient used was as follows: 5% B to 22% B over 1 min, then held at 22% B for 20 min, then increased to 50% over 10 min and back to 5% B over 2 min (flow rate of 1 mL/min). In this system DOTA-TATE elutes at 12 min and major ^{125}I-DOTA-TATE peaks between 21 and 24 min. The labelling efficiency of DOTA-TATE radioiodination was found to be 82.8% on iTLC (See Fig.S2). ^{125}I-DOTA-TATE (major radiolabelled peptide component retention time 21-24 min) was purified from non-labelled DOTA-TATE (retention time 16 min) *via* RP-HPLC (see Figures S3 & S4). 1 mL fractions of ^{125}I-DOTA-TATE were collected and fraction 23 containing the highest activity was selected for downstream experiments. The purity was confirmed via RP-HPLC and iTLC (Figure S4).

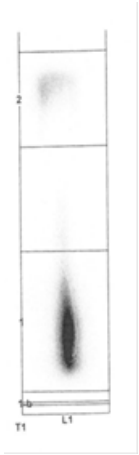


Figure S2. iTLC of radiolabelled ^{125}I -DOTA-TATE run in 0.2 M phosphate buffer. ^{125}I-DOTA-TATE remains at the origin and free ^{125}I-iodide travels to the solvent front.

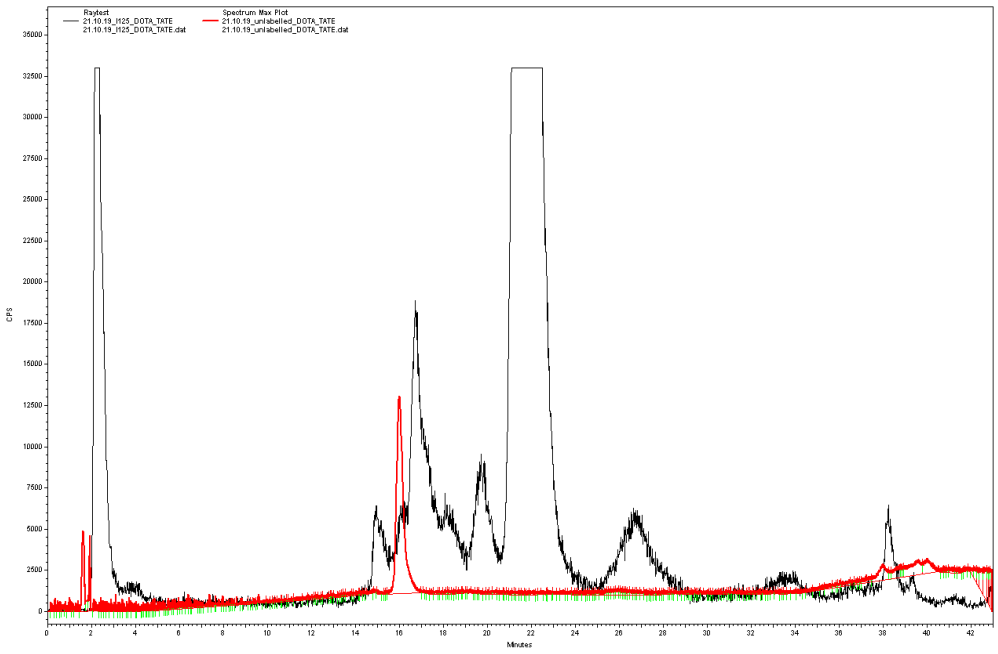


Figure S3: Radiochromatogram of the labelled ^{125}I-DOTA-TATE (black) overlaid with the UV trace of the unlabelled DOTA-TATE (red).

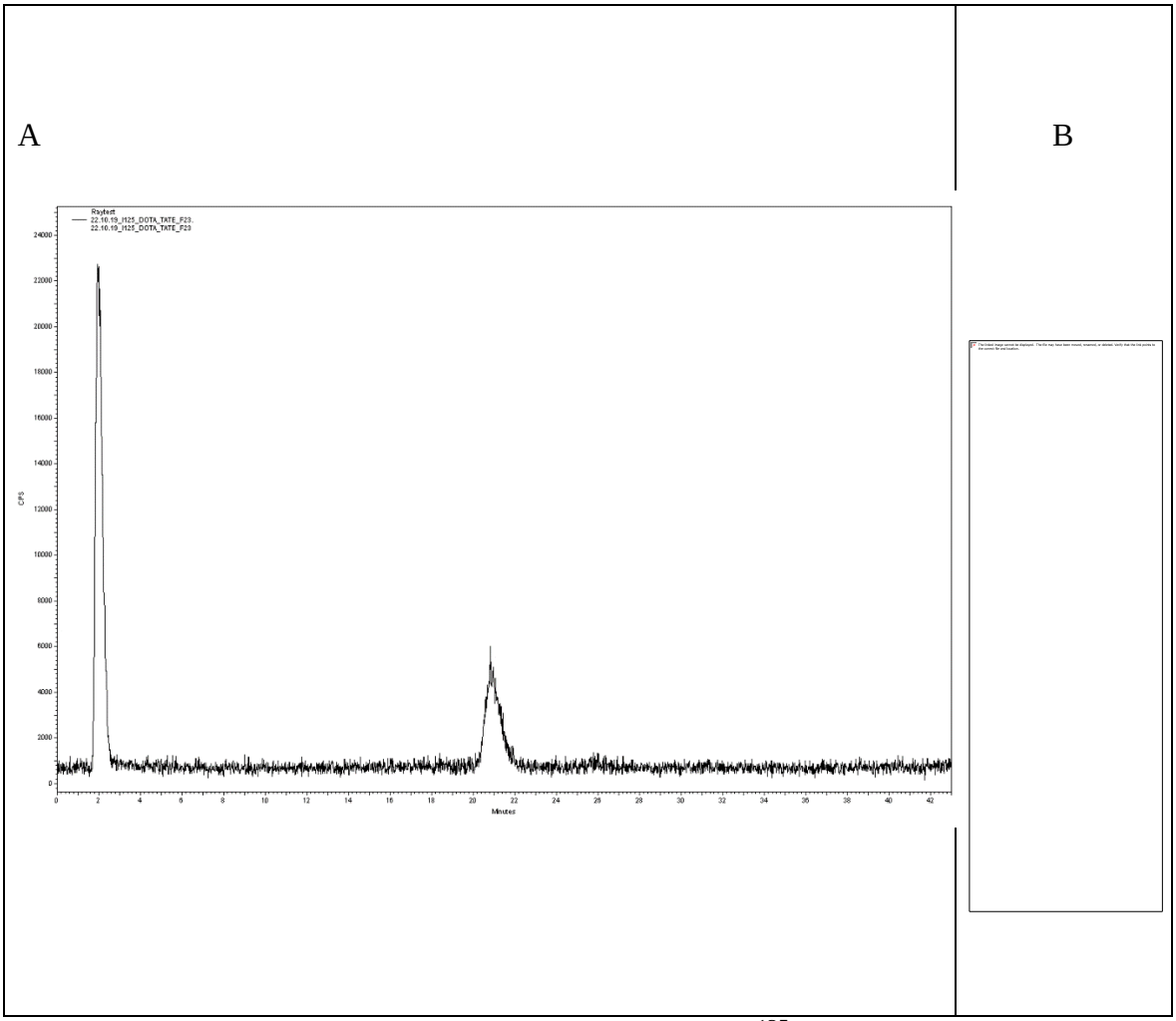
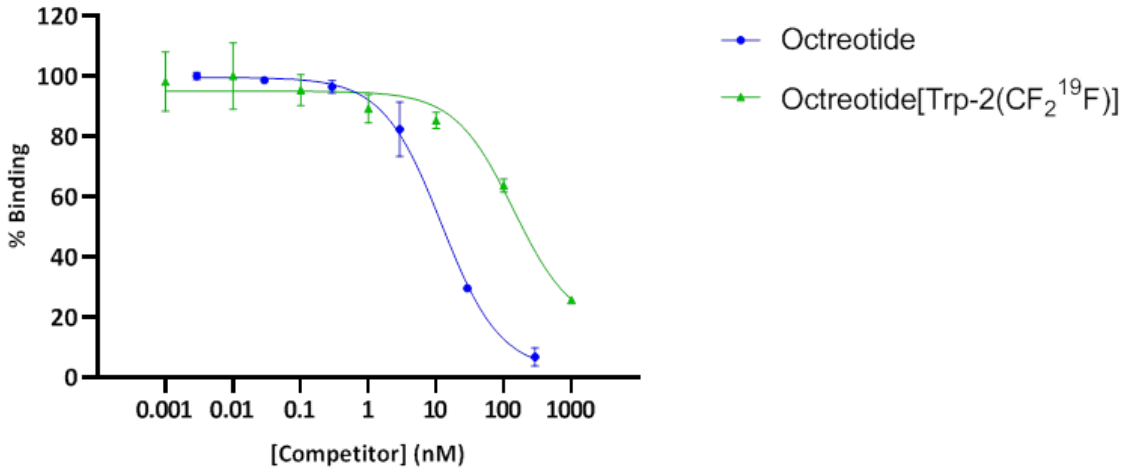


Figure S4. (A): Radiochromatogram of HPLC-purified ^{125}I-DOTA-TATE (fraction 23) eluting at 20.5 mins. No peak is seen in the UV chromatogram at 16 minutes (retention time of octreotide). The peak at the solvent front is not seen in the iTLC (B) where free ^{125}I-iodide would have appeared at the top of the strip.

Competition binding assay

AR42J cells were detached using versene (Gibco) and transferred to DMEM supplemented with 1% FBS. Increasing amounts of competitor (octreotide or octreotideCF_3) corresponding to final concentrations between 0.001 and 1000 nM were added to 1 x 10^6 AR42J cells in triplicate along with a constant amount of ^{125}I-DOTA-TATE in a final volume of 1.5 mL and incubated for 1 hour at room temperature with constant agitation. The samples were

washed twice by centrifugation in PBS (Gibco) containing 1% BSA (Sigma Aldrich). The activity remaining in the cell pellets was measured on a gamma counter (1282 Compugamma CS, LKB Wallac) and the % of total bound radioactivity (average ± SD) plotted vs log concentration (nM) used to determine the IC_{50} values. IC_{50} analysis was performed using GraphPad Prism version 8.2.0 (GraphPad Software) non-linear regression for one site fit logIC50 (Figure S5). Results show that ^{18}F-trifluoromethylation at tryptophan affects binding by a factor of 11.7 (IC_{50} octreotide[Trp-2($CF_2{}^{18}F$)]/octreotide = 140 nM/12nM).



	Octreotide	**Octreotide[Trp(2-$CF_2{}^{19}F$)]**
IC_{50}	12.08	140.1

Figure S5. *In vitro* competition binding assay of [^{125}I]DOTA-TATE in AR42J cells comparing octreotide to octreotide[Trp-2($CF_2{}^{19}F$)]. In contrast to [^{18}F]CF_3-insulin, binding studies undertaken with octreotide[Trp(2-$CF_2{}^{18}F$)] suggest that tryptophan C-H ^{18}F-trifluoromethylation affects binding by a factor of ~10 (CF_3-octreotide/native octreotide: IC_{50} = 140 nM/12 nM). These two examples clearly indicate that no general conclusion can be extrapolated on how attachment of a ^{18}F-prosthetic including the minimally-size [^{18}F]CF_3 group affects peptide's function.

4.7 *In Vivo* Naïve Rat Model

All animal procedures were performed in accordance with the United Kingdom Home Office Animals (Scientific Procedures) Act 1986 and the EU directive 2010/63/EU. The procedures were reviewed by independent ethics committees (Imperial College London and King's College London). All animals were sourced from Charles River. A rat was anaesthetised under isoflurane anaesthesia (2-3% isoflurane, 1 L/min O_2) with scavenging throughout the experimental period. An angiocath was inserted in the tail vein. The body temperature was maintained with a heating mat and warming lamp, and monitored using a rectal probe. The body was placed in the field of view of a scanner (Siemens Inveon DPET with docked multi-modality CT) and a CT scan collected for attenuation correction and structural information. Octreotide[Trp-2($CF_2{}^{18}F$)] was dried under vacuum and Ar flow before reformulating in saline (1 mL). A dynamic PET scan of up to 60 min was performed after the intravenous (i.v.) administration of 9.5 MBq of octreotide[Trp-2($CF_2{}^{18}F$)]. At the end of the scan, or 60 mins after tracer injection, the subject was killed by exsanguination with cervical dislocation. The tissues (heart, liver, small intestine, large intestine, brain, kidney, lung, muscle, bone and pancreas) were dissected, weighed and counted for radioactivity using a gamma-counter (Figure S6). Image processing and data analysis were performed using MIAKAT - an in-house computational pipeline implemented in MATLAB™. The native PET format images were converted into NIfTI format and quality checked. The PET images were re-aligned to the CT images using VivoQuant (Figure S7).

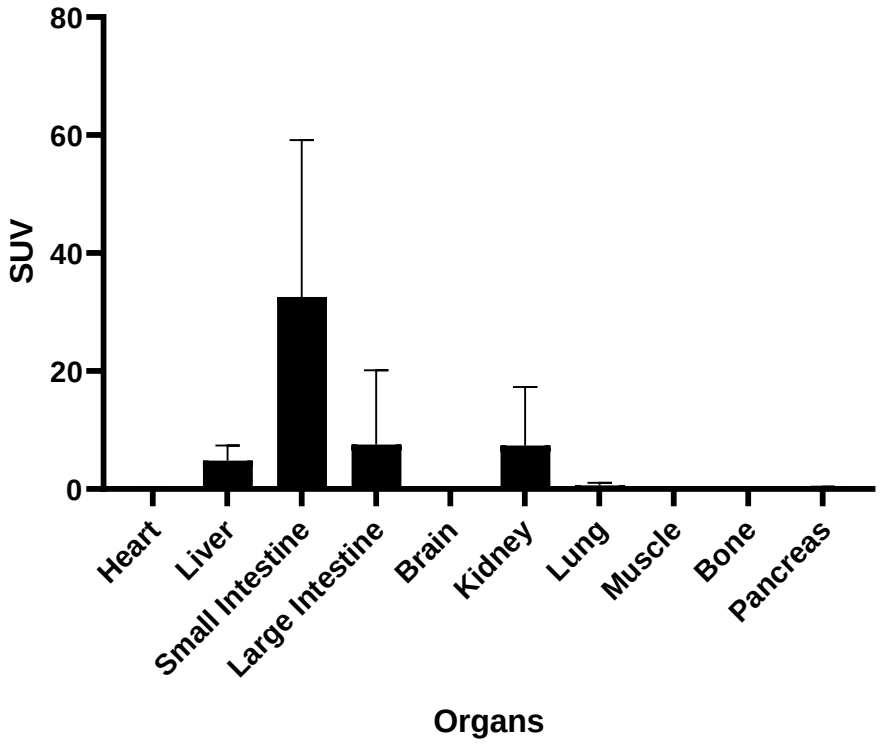


Figure S6. Biodistribution profile in selected organs of octreotide[Trp-2(CF_2^{18}F)] 60 minutes post injection in Sprague Dawley rats (n = 3).

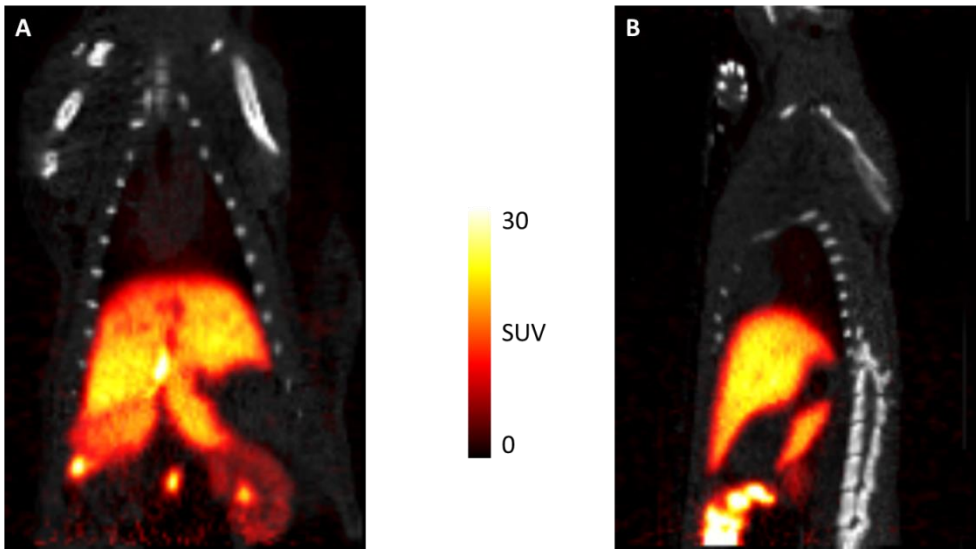


Fig S7. Summed (0 – 60 mins) PET/CT images of a Sprague Dawley rat after iv injection (9.5 MBq) of octreotide[Trp-2(CF_2^{18}F)]. (A) Transverse view; (B) Sagittal view.

4.8 References

[1] H. E. Gottlieb, V. Kotlyar & A. Nudelman *J. Org. Chem.* **1997**, 62, 7512 – 7515.

[2] C. P. Rosenau *et al. Angew. Chem. Int. Ed.* **2018**, 57, 9528 – 9533.

[3] T. H. J. Niedermeyer & M. Strohalm *PLoS One* **2012**, 7 (9), e44913.

[4] J. Zheng *et al. Chem. Commun.* **2013**, 49, 7513 – 7515.

[5] M. Imiołek *et al. J. Am. Chem. Soc.* **2018**, 140, 1568 – 1571.

[6] B. L. Podlogar *et al. FEBS Lett.* **1998**, 439, 13 – 20.